

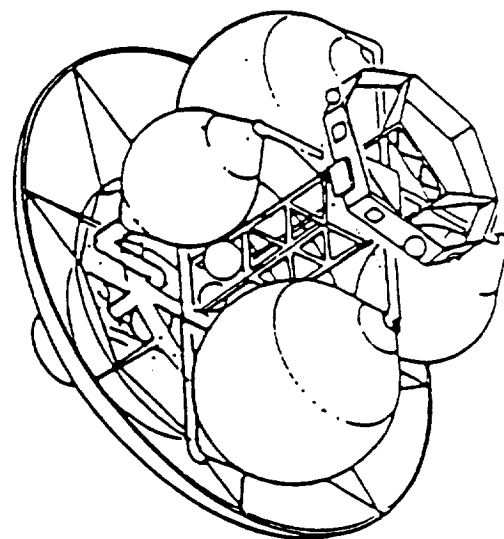
MCR-86-2601
NAS8-36108

Volume II, Book 3

**OTV Concept Definition
And Evaluation -
Subsystem Trade Studies**

**Orbital Transfer Vehicle
Concept Definition and
System Analysis Study**

1985



(NASA-CR-183544) ORBITAL TRANSFER VEHICLE
CONCEPT DEFINITION AND SYSTEM ANALYSIS
STUDY. VOLUME 2: OTV CONCEPT DEFINITION AND
EVALUATION. BOOK 3: SUBSYSTEM TRADE STUDIES
(Martin Marietta Aerospace) 431 p CSCL 22B G3/18

N89-13458

Unclas
0134684

MCR-86-2601
NAS8-36108

**ORBITAL TRANSFER VEHICLE
CONCEPT DEFINITION AND SYSTEM ANALYSIS STUDY**

**VOLUME II
OTV CONCEPT DEFINITION AND EVALUATION
BOOK 3
SUBSYSTEM TRADE STUDIES**

**October 1985
Rev 1 - July 1987**

Prepared By:

Glen J. Dickman
Glen J. Dickman
Cryogenics Manager

Approved By:

J. T. Keeley
J. T. Keeley
Program Manager
Initial Phase

**MARTIN MARIETTA
ASTRONAUTICS GROUP
P.O. BOX 179
DENVER, COLORADO 80201**

445



FOREWORD

This final report, Volume II, Book 2 — OTV Concept Definition, was prepared by Martin Marietta Denver Aerospace for NASA/MSFC in accordance with contract NAS8-36108. The study was conducted under the direction of NASA OTV Study Manager, Mr. Donald R. Saxton, during the period from July 1984 to October 1985. This final report is one of nine documents arranged as follows:

Volume I	Executive Summary
Volume II	OTV Concept Definition and Evaluation
	Book 1 Mission and System Requirements
	Book 2 OTV Concept Definition
	Book 3 Subsystem Trade Studies
	Book 4 Operations
Volume III	System and Program Trades
Volume IV	Space Station Accommodations
Volume V	Work Breakdown Structure and Dictionary
Volume VI	Cost Estimates
Volume VII	Integrated Technology Development Plan
Volume VIII	Environmental Analyses
Volume IX	Study Extension Results

The following personnel were key contributors during the July 1984 to October 1985 period in the identified disciplines:

Study Manager	J.T. Keeley (March 1985–October 1985) R.B. Demoret (July 1984–February 1985)
Project Managers	G.J. Dickman (Cryogenic Systems) A.E. Inman (Storable Systems)
Task Leads	J.H. Nelson (Missions, Trades & Programmatics) T.K. Stanker (Design) J.C. Mitchell (Operations) R.M. Randall (Accommodations)

Denver Engineering Support

Aerothermodynamics	G.W. Heckel
Avionics	R.B. Schroer, J.S. Schmidt
Flight Operations	L.A. Jenkins
GN&C Analyses	W.H. Willcockson
Ground Operations	J.S. Hostetler, C.D. Garner
Mission Analyses	S.G. Carson
Propulsion	E.C. Fox, T.J. Rudman, D.H. Beekman
Sp. Base Accommod.	D.L. Kelley, K.E. Falkner, N.E. Lefebvre
Systems Engineering	G.W. Mohrman

Michoud Engineering Support

Engineering Manager	W.P. Haese
Cost Analyses	R.A. Ernst, D.R. Callan
Ground Operations	C.D. Diloreto
Structural Analyses	G.S. Kovacevic, R. Pequet
Structural Design	J. Hamilton, F.W. Houte, G. Shanks, D. Stanley
Weight Analyses	G.A. Edmonson

TABLE OF CONTENTS

	<u>Page</u>
1.0 Introduction	1
2.0 Subsystem Trades	2
2.1 Avionics Trade Studies and Analyses	2
2.1.1 Guidance, Navigation and Control Trade Studies and Analyses	2
2.1.1.1 State Vector Update	2
2.1.1.2 Space Sextant Data	3
2.1.1.3 GPS for State Vector Update	3
2.1.1.4 GPS Beam Patterns	3
2.1.1.5 GPS Acquisition	4
2.1.1.6 GPS Summary	5
2.1.1.7 On-Orbit Calibration / Alignment	6
2.1.1.8 Midcourse Analysis	8
2.1.1.9 Aeroentry Error Analysis	8
2.1.1.10 Aeropass Navigation Errors	10
2.1.1.11 OTV Minor Burns	10
2.1.1.12 Control Corridor Definition	12
2.1.1.13 Aeromaneuver Control Modes	13
2.1.1.14 Aerospike Fuel Requirements	13
2.1.1.15 Velocity Savings from Inclination Control in Aeropass	13
2.1.1.16 Deorbit Overview	16
2.1.1.17 Aerophase Overview	17
2.1.1.18 Aeroentry Overview - Space-Based	18
2.1.1.19 Aeroentry Overview	19
2.1.1.20 OTV Aerostabilization	20
2.1.1.21 L/D Versus Control Corridor	21
2.1.1.22 Aerothermodynamic Environment	21
2.1.1.23 Flow Regime Transition Criteria Based on Viking Flight and Wind Tunnel Data	23
2.1.1.24 Free Molecular Flow Impact on L/D	23
2.1.1.25 Aeropass Simulation Data	25
2.1.1.26 Aeroguidance	25
2.1.1.27 Lift Vector Targeting	26
2.1.1.28 Guidance Update Cycle	26
2.1.1.29 Roll Control Algorithm	28
2.1.1.30 Atmospheric Feedback	29
2.1.1.31 Aeropass Parametrics	29
2.1.1.32 Circularization Velocity and Phasing Shift	29
2.1.1.33 Deceleration and Airloads	31
2.1.1.34 Stagnation Heating	32
2.1.1.35 Aeroguidance Dispersions: Single Parametrics	34
2.1.1.36 Aeroguidance Dispersions: Coupled Parametrics	34
2.1.1.37 Aerosimulation Summary	35
2.1.1.38 STS Atmospheric Profiles	38
2.1.1.39 Atmospheric Density Feedback	39

TABLE OF CONTENTS (Continued)

	<u>Page</u>
2.1.1.40 CG Uncertainty Assessment	40
2.1.1.41 Relative Control Capability	40
2.1.1.42 Aeroguidance Highlights	41
2.1.1.43 Long Duration Attitude Control Options	42
2.1.1.44 RCS Configuration	43
2.1.1.45 Cryo ACS Usage	44
2.1.2 Avionics Hardware Trade Studies	46
2.1.2.1 Centralized versus Distributed Data Management	46
2.1.2.2 Fuel Cells versus Solar Array Power	77
2.1.2.3 Built-In versus Multiple Unit Redundancy	83
2.1.2.4 Microprocessor Technology	91
2.1.2.5 On-Board Checkout versus Ground Processing	96
2.1.2.6 Gyro Technology	100
2.1.2.7 Electro-Optical Navigation Sensors	109
2.2 Aeroassist Trade Studies and Analyses	116
2.2.1 Aeroassist Concepts Evaluation and Selection . .	116
2.2.1.1 All Propulsive versus Aeroassist	116
2.2.1.2 Candidate Aeroassist Techniques	118
2.2.1.3 Aerothermal Protection for Space-based Aeroassist Device	120
2.2.1.4 Aeroassist Low versus Medium L/D Selection	135
2.2.1.5 Vehicle Lift versus Drag Aeroassist Maneuvering	137
2.2.1.6 Aeropass Environment and L/D Selection . .	143
2.2.1.7 Evolution and Space-Basing Accommodations	152
2.2.2 Definition of Selected Aeroassist Concept	158
2.2.2.1 Design Philosophy and Concept Overview . .	158
2.2.2.2 Aerodynamic Characterizations	168
2.2.2.3 Aerothermodynamic Heating and Thermal Protection	172
2.2.2.4 OTV Aerobrake Sizing	180
2.2.2.6 References	186
2.3 Propulsion Trade Studies and Analyses	188
2.3.1 Man-rating and Mission Reliability	188
2.3.2 Main Engine Analysis	196
2.3.3 LH ₂ /LO ₂ Engine Selection	217
2.3.4 Space Maintenance of Propulsion System	221
2.3.5 Pressurization System	224
2.3.6 MPS Retrieval Considerations	230
2.3.7 Reaction Control System Selection (RCS)	233
2.3.8 References	245

TABLE OF CONTENTS (Continued)

	<u>Page</u>
2.4 Structure Trade Studies and Analyses	246
2.4.1 OTV/ACC Weight Vs ACC Beam Stiffness	246
2.4.2 9 DOF vs 10DOF OTV to ACC Attachment Weight Impact	251
2.4.3 Trade Study of Umbilical Locations for Ground Based Cryo OTV	255
2.4.4 Composite Material Trade Study	267
2.4.5 Material Selection for Metal Tanks and Air Frame	272
2.4.6 Transportation and Assembly of Space-Based Cryo OTV	279
2.4.7 Growth of Ground-Based 55K Cryo OTV to 94K Space-Based OTV	282
2.4.8 Space Based Drop Tank Configurations	284
2.4.9 Meteoroid Protection System	288
2.4.10 References	293
2.5 Thermal Control Trade Studies and Analyses	294
2.5.1 Prelaunch Considerations and STS Ascent Environments	294
2.5.1.1 Thermal Analysis to Determine ACC/OTV (Ground-Based Cryo) Purge System Requirements	294
2.5.1.2 Thermal Analysis to Determine ACC/OTV (Ground-Based Storable) Purge System Requirements	298
2.5.1.3 Compartment Temperature of ACC/OTV (Ground-Based) During Prelaunch and Ascent	301
2.5.1.4 Post-Shroud Separation Thermal Analysis of Ground-Based OTV	305
2.5.2 AOTV Flight Phase Thermal Control Aspects . . .	307
 Appendices	
Appendix A - 1962 std. stmos., angle of attack error - +1.5°	
Appendix B - STS 2 atmosphere	
Appendix C - STS 4 atmosphere	
Appendix D - STS 6 atmosphere	
Appendix E - STS 6 atmos., angle of attack error - + 1°	
Appendix F - STS 6 atmos., perigee aimpoint error - +.2 nm	
Appendix G - STS 6 atmos, bulk density shift (equivalently ballistic coefficient shift) = +22%	
Appendix H- STS 6 atmos, navigation error: 2000 ft. position and 14 fps. velocity	
Appendix I - STS 6 atmosphere, space-based OTV	

List of Figures

<u>Figure</u>		<u>Page</u>
2.1.1.4-1	GPS Acquisition - Transmitting Beam Patterns . . .	4
2.1.1.5-1	GPS Acquisition - GEO Downleg	5
2.1.1.5-2	GPS Acquisition - Geosynchronous Orbit	6
2.1.1.12-1	Control Corridor Definition	12
2.1.1.13-1	Aeromaneuver Control Modes	14
2.1.1.14-1	Aerospike Fuel Requirements	14
2.1.1.15-1	Velocity Savings from Inclination Control in Aeropass	15
2.1.1.16-1	Deorbit Overview - Option #1	16
2.1.1.16-2	Deorbit Overview - Option #2	17
2.1.1.17-1	Aerophase Overview - Ground-Based	18
2.1.1.18-1	Aerophase Overview - Space-Based	19
2.1.1.19-1	Aeroentry Overview	20
2.1.1.20-1	OTV Aerostabilization	21
2.1.1.21-1	L/D vs Control Corridor	22
2.1.1.22-1	Aerothermodynamic Environment	22
2.1.1.23-1	Flow Regime Transition Criteria Based on Viking Flight and Wind Tunnel Data	23
2.1.1.24-1	Free Molecular Flow Impact on L/D	24
2.1.1.27-1	Lift Vector Targeting	26
2.1.1.28-1	Guidance Update Cycle	27
2.1.1.29-1	Roll Control Algorithm	28
2.1.1.30-1	Atmospheric Feedback	29
2.1.1.32-1	Circularization Velocity and Phasing Shift - All W/C _D A's	30
2.1.1.33-1	Deceleration and Airloads - Low L/D	31
2.1.1.33-2	Deceleration and Airloads - High W/C _D A	32
2.1.1.34-1	Stagnation Heating - Low W/C _D A	33
2.1.1.34-2	Stagnation Heating - High W/C _D A	33
2.1.1.38-1	STS Atmospheric Profiles	38
2.1.1.39-1	Atmospheric Density Feedback	39
2.1.1.41-1	Relative Control Capability	41
2.1.2.1-1	Core Architecture for OTV Avionics Data Management System	49
2.1.2.1-2	Interconnection Subsystem Schematic Representation	49
2.1.2.1-3	OTV Interconnection Subsystem Hierarchy	58
2.1.2.1-4	Generalized Structure (internal) of Primary and Secondary Memories	59
2.1.2.1-5	Generalized Internal Structure of a Single Microprocessor with I/O Processor	61
2.1.2.1-6	Usage and LCCs for HOL/LOLs in Spacecraft Avionics Systems	63
2.1.2.1-7	Interconnection Subsystem Schematic Representation	73
2.1.2.1-8	Estimates for Available Memory Utilization by Avionics Function	75

List of Figures (cont)

<u>Figure</u>		<u>Page</u>
2.1.2.2-1	Baseline Fuel Cell System	78
2.1.2.2-2	Photovoltaic Baseline System	79
2.1.2.3-1	Reliability vs time for Simplex, Deplex, and Triple System Partitioned into 10, 30, and 100 Independent Pieces (Lowries Figure 11) .	90
2.1.2.6-1	Fiber Optic Principle	104
2.1.2.6-2	Principal Components of the HRG	105
2.2.1.1-1	All Propulsive vs Aeroassist Analysis	117
2.2.1.2-1	Aeroassist Configuration Options	118
2.2.1.3-1	Developed Heat Shields	122
2.2.1.3-2	Pressure/Temperature Distributions - Raked Brake	124
2.2.1.3-3	Present Technology Configurations	125
2.2.1.3-4	Future Technology Requirements	127
2.2.1.3-5	Compositional Heat Stability	131
2.2.1.3-6	Nextel Emittance Data	132
2.2.1.3-7	Tailorable Advanced Blanket Insulation (TABI) . .	133
2.2.1.4-1	Low vs Mid L/D Performance Trade	136
2.2.1.5-1	Low L/D Aero - Configuration Concepts	137
2.2.1.5-2	Space Based Cryogenic OTV - 55K Propellant - 44 Foot Ballute	141
2.2.1.5-3	53K Space Based Storable OTV - 32 and 41 Foot Ballute	142
2.2.1.5-4	Fixed vs Inflatable Flex TPS Lifting Brake . . .	143
2.2.1.6-1	Aerothermodynamic Environment	144
2.2.1.6-2	Aero-entry Overview	145
2.2.1.6-3	Heat Flux Correlation With Ballistics Coefficient and Lift to Drag Ratio	146
2.2.1.6-4	Typical AOTV Flight Trajectories	147
2.2.1.6-5	Vehicle L/D and Heating Environment Set by Angle of Attack	148
2.2.1.6-6	Heating Environment vs L/D	149
2.2.1.6-7	Impact of Edge Radius on Aerobrake Size, Surface Area, and Weight Stability Margin	150
2.2.1.6-8	Heat Flux Distribution vs L/D	151
2.2.1.6-9	L/D vs Control Corridor	152
2.2.1.7-1	SBOTV Folding Aerobrake	153
2.2.1.7-2	Initial Delivery of the Space-Based Foldable Aerobrake	154
2.2.1.7-3	Aerobrake Ring Interface Mechanism for On-Orbit Changeout	156
2.2.1.7-4	SBOTV Aerobrake Deployment/Retractable Interface Mechanism	157
2.2.2.1-1	Aerobrake Configuration and Characteristics . . .	160
2.2.2.1-2	OTV Rigid/Flex TPS Aerobrake	161
2.2.2.1-3	Flexible TPS Selection and Construction - Tailorable Advanced Blanket Insulation (TABI)	162
2.2.2.1-4	Nose Region and Engine Doors TPS Detail	163

List of Figures (cont)

<u>Figure</u>		<u>Page</u>
2.2.2.1-5	Aerobrake TPS and Engine Cover Mechanism	164
2.2.2.1-6	Space Based Folding Aerobrake	165
2.2.2.1-7	Ground Based Aerobrake Deployment	166
2.2.2.1-8	Aerobrake Design Detail	166
2.2.2.1-9	Aerobrake Heating Design Margin	167
2.2.2.1-10	Space Based Aerobrake Rib Reflection	168
2.2.2.2-1	Aerocharacteristics vs Angle of Attack	169
2.2.2.2-2	Force and Moment Coefficients for Free Molecular Flow	170
2.2.2.2-3	Flow Regime Transition Criteria Based on Viking Flight and Wind Tunnel Data	171
2.2.2.3-1	Aerobrake Analytical Heating Model	172
2.2.2.3-2	Aerobrake TPS Heat Transfer Models	173
2.2.2.3-3	Heating Rate Distribution on Models of the NASA-MMC Viking Mars Entry Aeroshell	174
2.2.2.3-4	Typical AOTV Heating Environments	176
2.2.2.3-5	Aerobrake Heat Transfer Distribution	177
2.2.2.3-6	Aerobrake Peak Temperature Profile	178
2.2.2.3-7	Correlation of Peak Heat Flux and Temperature with Ballistic Coefficient and Brake Diameter	179
2.2.2.3-8	Correlation of Aerobrake Face Pressure Distribution with Ballistic Coefficient for L/D=0.12	180
2.2.2.4-1	Aerobrake Sizing Criteria	181
2.2.2.4-2	OTV Impingement Heating	182
2.2.2.4-3	Aeroassist Flight Experiment OTV Payload Impingement Summary	183
2.2.2.4-4	Integrated Heat Load Correlation with Ballistic Coefficient and Insulation Thickness	184
2.3-1	Propulsion System Reliability	190
2.3-2	MPS Parametric Data for Trade Studies	190
2.3-3	MPS Parametric Data for Trade Studies	191
2.3-4	Thrust vs Propellant Weight for Cryo 20K Delivery Mission	192
2.3-5	Preliminary Storable Engine/Stage Data	193
2.3-6	RL-10 With Redundant Turbopumps	194
2.3-7	MPS Redundancy Cost Trade	195
2.3-8	GEO Mission Finite Burn Velocity Losses	197
2.3-9	MPS Engine Cycles	198
2.3-10	Ground-Based MMH/N ₂ O ₄ Engine Selection	200
2.3-11	Optimum Expansion Ratio-Storable	201
2.3-12	AOTV Thrust Level MMH/N ₂ O ₄	202
2.3-13	AOTV Thrust Level MMH/N ₂ O ₄	203
2.3-14	MMH/N ₂ O ₄ Throttling Performance	203

List of Figures (cont)

<u>Figure</u>		<u>Page</u>
2.3-15	Engine Throttling (Rocketdyne)	204
2.3-16	XLR-132 Throttling Conditions (Rocketdyne)	204
2.3-17	Ground-Based LH ₂ /O ₂ Engine Selection	207
2.3-18	AOTV Thrust Level LH ₂ /LO ₂	208
2.3-19	AOTV Thrust Level LH ₂ /LO ₂	209
2.3-20	AOTV Thrust Level LH ₂ /LO ₂	210
2.3-21	AOTV Thrust Level LH ₂ /LO ₂	211
2.3-22	Multiple Burn Cost Trade	212
2.3-23	Multiple Perigee Burn Cost Trade	213
2.3-24	OTV Planetary Mission Thrust	214
2.3-25	LH ₂ /LO ₂ Engine Step Throttling	215
2.3-26	Extendable Nozzle Trade	216
2.3-27	Engine Payback for Various OTV Engines	218
2.3-29	Main Engine Recommendation	221
2.3-30	Engine Modularity Trade	223
2.3-31	MPS Candidate Engines Interfaces	225
2.3-32	Tank Pressure Trade	227
2.3-33	Pressurization and Propellant Dump System Trade	230
2.3-34	Ground Based Cryo - LH ₂ Tank Retrieval	232
2.3-35	Removable Cryo Tank Concept	233
2.3-36	RCS Configuration - All Vehicles	235
2.3-37	OTV RCS Parametrics	236
2.3-38	Heating Rate Required for H ₂ Conditioning at Constant Volume	237
2.3-39	Conditioning Energy for GH ₂ /GO ₂ RCS	237
2.3-40	RCS Resupply Trade	238
2.3-41	Film Cooling Sensitivity (Rocketdyne)	240
2.3-42	T/C Performance Regen-Radiation Cooled Concept (Rocketdyne)	241
2.3-43	Predicted Performance High Temperature GO ₂ /GH ₂ Rhenium Thruster (JPL Data)	242
2.3-44	MPS vs RCS	243
2.3-45	Boiling Increases Heat Transfer Causing Oxidizer (Pratt and Whitney)	244
2.4-1	OTV Rack Weight vs Interface Out-of-Plane Deflection	247
2.4-2	Basic ACC Beam Geometry and Simplified Loading	248
2.4-3	Beam Deflections vs Slope of Top Cap for Various Beam Depths	249
2.4-4	ACC Beam Weight vs Beam Depth (for Various Tapering Beams)	250
2.4-6	Degree-of-Freedom Attachment Restraints	252
2.4-7	OTV Structural Members	254
2.4-8	Member Cap Loads (KIPS) for 9 and 10 DOF Attachment	255
2.4-9	View Looking Forward with Tanks Removed Showing Area Under Consideration for Umbilical Locations	256

List of Figures (cont)

<u>Figure</u>		<u>Page</u>
2.4-10	ACC/OTV LO ₂ Disconnect Panel	257
2.4-11	ACC/OTV LH ₂ Disconnect Panel	258
2.4-12	Tail Service Mast Concept	260
2.4-13	ACC/OTV Disconnect Panels, Forward View, Baseline	261
2.4-14	ACC/OTV Disconnect Panel, Forward View, Option 1	262
2.4-15	ACC/OTV Disconnect Panel, Forward View, Option 2	263
2.4-16	ACC/OTV Disconnect Panel, Forward View, Option 3	264
2.4-17	ACC/OTV Disconnect Panel, Forward View, Option 4	265
2.4-18	Ground-Based Cryo OTV Umbilical - Conclusions . .	266
2.4-19	Major Material Concerns for Truss Structure . . .	267
2.4-20	Major Material Concerns for Aerobrake Structure .	268
2.4-21	Space-Based Cryo OTV Transportation - Orbiter 1 .	280
2.4-22	Space-Based Cryo OTV Transportation - Orbiter 2 . . .	281
2.4-23	2-Engine, 55K, GB, Cryo OTV Ground Rules	283
2.4-24	2-Engine, 55K, G/B, Cryo OTV Configuration	283
2.4-25	GB to SB Cryo OTV Configurations	284
2.4-26	Cryo Droptank OTV Weight Trade	285
2.4-27	Cryo Droptank OTV - Reference Configuration	
	Baseline	286
2.4-28	Cryo Droptank OTV - Reference Configuration	286
2.4-29	Cryo Droptank OTV - Tandem Stage	287
2.4-30	Cryo Droptank OTV Summary	288
2.4-31	Meteoroid Environment	289
2.4-32	Meteoroid Protection - Method 1 (Solid Barrier) .	290
2.4-33	Meteoroid Protection - Method 2 (Bumper/Gap/ Backing)	290
2.4-34	Baseline Protection System - Method 2	291
2.4-35	Penalty of No Bumper	292
2.4-36	Penalty of No Gap	292
2.5-1	ACC/OTV Cryo Configuration	294
2.5-2	GN ₂ Purge Requirement for ACC/OTV Compartment Temperature Control Prior to Cryo Loading .	297
2.5-3	GHe Purge Requirement for ACC/Cryo OTV Compartment Temperature Control	297
2.5-4	ACC/Storable OTV Configuration	298
2.5-5	GN ₂ Purge Requirement for ACC/Storable OTV Compartment Temperature Control	300
2.5-6	GNe Purge Requirement for ACC/Storable OTV Compartment Temperature Control	300
2.5-7	ACC/OTV Compartment Transient Pressure and Mass Flow	302
2.5-8	ACC/Cryo OTV Transient Compartment Gas Temperature	303
2.5-9	Transient Boiloff in Cryo Tanks of ACC/OTV	303
2.5-10	ACC/Storable OTV Transient Compartment Gas Temperature	304

List of Figures (cont)

<u>Figure</u>		<u>Page</u>
2.5-11	ACC/Storable OTV Transient Boiloff in Propellant Tanks	304
2.5-12	Thermal Math Model for ACC/OTV After Shroud Separation	305
2.5-13	Convective Environment to Cold Surfaces	306
2.5-14	Incident SSME Plume Radiation Rates for Altitudes Above 150,000 Feet (Directions Shown Are Surface Normals)	308
2.5-15	Incident SSME Plume Radiation Rates for Altitudes Above 150,000 Feet (Directions Shown Are Normals)	309
2.5-16	Convective Environment to Cold Surfaces	310
2.5-17	ACC/OTV Insulation Temperature During Ascent	311
2.5-18	Heat Leak to ACC/OTV Tanks After Shroud Separation	312
2.5-19	Boiloff in ACC/OTV Tanks After Shroud Separation	313
2.5-20	Radiator Sizing of Fuel Cells and Avionics (Hot Cases)	314
2.5-21	Fuel Cell/Radiator System Weight Breakdown	315
2.5-22	F.C./Radiator System Weight With Propellant Requirements for Various Mission Times	316

List of Tables

<u>Table</u>		<u>Page</u>
2.1.1.10-1	Aeropass Navigation Analysis	10
2.1.1.11-1	OTV Minor Burns	11
2.1.1.37-1	Aerosimulation Summary: Single Parameters	36
2.1.1.37-2	Aerosimulation Summary: Coupled Parameters	37
2.1.1.45-1	Cryo Attitude Control Usage	44
2.1.1.45-2	Cryo Attitude Control Usage	45
2.1.2.1-1	Preferred Candidate Architecture Summary-OTV Data Management System	47
2.1.2.1-2	Comparison of Centralized and Distributed Processing Approaches	48
2.1.2.1-3	Centralized Avionics Computer Architecture	51
2.1.2.1-4	Distributed Avionics Computer Architecture	51
2.1.2.1-5	OTV Baseline Configurations for Avionics Data Management Designs	53
2.1.2.1-6	OTV Data Management System Functional Responsibilities	54
2.1.2.1-7	Applicability of AIPS Architecture Building Blocks to OTV Avionics	56
2.1.2.1-8	General Criteria for Measuring Avionics Subsystem Hardware	57
2.1.2.1-9	Interprocessor Candidate Topologies	64
2.1.2.1-10	Comparison of Fiber Optics with Other Transmission Media	65
2.1.2.1-11	Candidate Scoring Summary	69
2.1.2.1-12	Comparison of Interconnection Candidates	70
2.1.2.1-13	Reported Shuttle Data Bus Rates (Kbps) (Centralized System Design)	71
2.1.2.1-14	Memory Technology Candidates	74
2.1.2.1-15	Executive Computer Candidates	76
2.1.2.2-1	Battery Comparison	77
2.1.2.2-2	Selection Criteria Weights	80
2.1.2.2-3	Configuration/Mission: Ground Based Storable Cargo Bay	81
2.1.2.2-4	Configuration/Mission: Ground Based Storable ACC Perigee	81
2.1.2.2-5	Configuration/Mission: Space Based Storable Perigee (97 & 51K)	81
2.1.2.2-6	Configuration/Mission: Space Based Storable Apogee (57K & 27K)	82
2.1.2.2-7	Configuration/Mission: Ground Based Cryo (43K & 57K)	82
2.1.2.2-8	Configuration/Mission: Space Based Cryo (94K & 57K)	82
2.1.2.2-9	Configuration/Mission: Space Based Cryo (84K)	83
2.1.2.2-10	OTV Fuel Cell Breakdown	84
2.1.2.3-1	Summary of Avionics Functional Unit Equipment Redundancy and Mean	85

List of Tables (cont.)

<u>Table</u>		<u>Page</u>
2.1.2.3-2	Gate Logic Level Redundancy Comparison	87
2.1.2.3-3	Functional Module Level Redundancy Comparisons	87
2.1.2.3-4	Box (Computer) Level Redundancy Comparisons	88
2.1.2.3-5	Simplex Redundancy Method	88
2.1.2.3-6	Duplex Redundancy Method	88
2.1.2.3-7	Triplex Redundancy Method	89
2.1.2.5-1	Checkout Requirements Summary	97
2.1.2.5-2	Ground vs Onboard Checkout Summary	99
2.1.2.6-1	DTG vs RLG Gyro Comparison	107
2.1.2.6-2	Gyro Weighting and Rating	107
2.1.2.7-1	Scanner/Tracker Factor Weights	111
2.1.2.7-2	Scanner/Tracker Comparison	114
2.1.2.7-3	Scanner/Tracker Evaluation	115
2.2.1.2-1	Aeroassist Characteristics - Configuration vs Weight	119
2.2.1.3-1	Classes of Heat Shield Materials	122
2.2.1.3-2	Material Properties	126
2.2.1.3-3	Fabric/Filament Data	129
2.2.1.3-4	Tailorable Advanced Ceramic Materials	130
2.2.1.4-1	Low vs Mid L/D Aeroassist	136
2.2.1.5-1	Aerobrake Concept Comparison	138
2.2.1.5-2	Aeroassist Decision Logic and Selection	140
2.2.2.1-1	Aerobrake Design Philosophy	158
2.2.2.1-2	Aerobrake Weights	167
2.2.2.4-1	Aerobrake Design Requirements (Cryogenic OTV)	185
2.3-1	Evaluation of Backup Concepts	189
2.3-2	MPS Candidate Engines	197
2.3-3	H ₂ O ₄ /MMH Engine Technology Assessment	199
2.3-4	LO ₂ /LH ₂ Engine Technology Assessment	205
2.3-5	Engine Data Summary	206
2.3-5a	Martin Marietta Cost Estimates	217
2.3-6	Recommended IOC Engine Requirements	220
2.3-7	Modular Turbopump for New Engine	222
2.3-8	MPS Candidate Engines Interfaces	226
2.3-9	System Comparison of MMH/N ₂ O ₄ Pressurization Candidates	228
2.3-10	RCS Ground Rules and Assumptions	234
2.4-1	Composite Material Properties	269
2.4-2	Composite Material Properties	269
2.4-3	Preliminary Tank Metal Selection	275
2.4-4	Preliminary OTV Structural Metal Selection	278
2.5-1	ACC Purge Scenario	296
2.5-2	Separate Radiator Trade	315

1.0 Introduction

The technical trade studies and analyses reported in this book represent the accumulated work of the technical staff for the contract period. The general disciplines covered here are: 1) GN&C, 2) Avionics Hardware, 3) Aeroassist Technology, 4) Propulsion, 5) Structures and Materials, and 6) Thermal Control Technology. The objectives in each of these areas were to develop the latest data, information, and analyses in support of the vehicle design effort.

2.0 SUBSYSTEM TRADES

2.1 AVIONICS TRADE STUDIES AND ANALYSES

2.1.1 Guidance, Navigation and Control Trade Studies and Analyses - Work in the area of guidance, navigation and control established a number of critical vehicle parameters in the course of the OTV Phase A Study. These include sizing of L/D requirements for the lifting aerobrake, characterization of navigation errors for the various critical flight phases, estimation of midcourse and post-aero burn magnitudes, as well as ACS fuel usage for various flight phases. A critical element in the evaluation of the aeropass was the development of a closed loop trajectory simulation which was used to generate parametrics for various control options and evaluate dispersed capabilities for the final configurations.

NAVIGATION - The primary tasks which were studied in the area of navigation were an evaluation of potential systems for performing state vector updates, characterization of navigation errors for critical mission phases and sizing of midcourse and other "minor burns" for various baseline missions.

2.1.1.1 - State Vector Update - Because of the lengthy mission durations involved the OTV must have a means of correcting inevitable state vector drift.

The methods our study considered were ground tracking (or TDRSS tracking) with state vector uplink and GPS (Global Positioning System) and the Space Sextant onboard navigation systems.

Current ground tracking accuracies are on the order of a few thousand feet. Ground processing is required followed by uplink of results to the spacecraft. This operation typically has a turnaround time of several hours. Visibility problems exist with low earth orbits which can be overcome through use of the TDRSS system. In general, the process requires a team of support personnel on the ground which represents a cost and scheduling burden.

GPS, on the other hand, represents a highly accurate and autonomous method for state vector update. Accuracies on the order of tens of meters are possible for low earth orbits. Turnaround times are measured in seconds once the initial acquisition phase of less than 15 minutes is complete. The system is available on-demand and requires no special ground support for the user.

However, a significant problem with GPS is its use at high altitude. The system was tailored for earthbound users and has acquisition problems for users above an altitude of approximately 8000 nm.

Space sextant represents a completely autonomous update system which takes sightings on the lunar limb plus a star to derive spatial position, similar to the method used on Apollo. A flight demonstration unit was flown on Shuttle. Accuracies on the order of 800 ft. are achievable anywhere in the earth-moon system. However, this level of accuracy requires 24 hours to achieve. The system is completely autonomous and requires no ground support. The system is fairly mechanism intensive which could be a problem for space basing.

The most attractive system appears to be GPS. Solutions to the high altitude acquisition problem will be presented following a more detailed discussion of the Space Sextant system.

2.1.1.2 - Space Sextant Data - The space sextant (ANARS) represents flight proven hardware for providing autonomous state vector and attitude updates. The technique is similar to that used in Apollo with multiple sightings on the lunar limb and a set of reference stars.

The flight demonstration unit had a weight of 120 pounds and required 125 watts to operate, for an operational unit these parameters could be reduced to 65 lbs. and 50 w., respectively. Accuracies on the order of 800 feet are achievable, however, 24 hours is required to converge to this level of accuracy. The system is less sensitive than GPS to large distances from the earth, being able to function accurately anywhere in the earth-moon system. In addition, because the package performs high accuracy star shots it would eliminate the need for a separate star tracker.

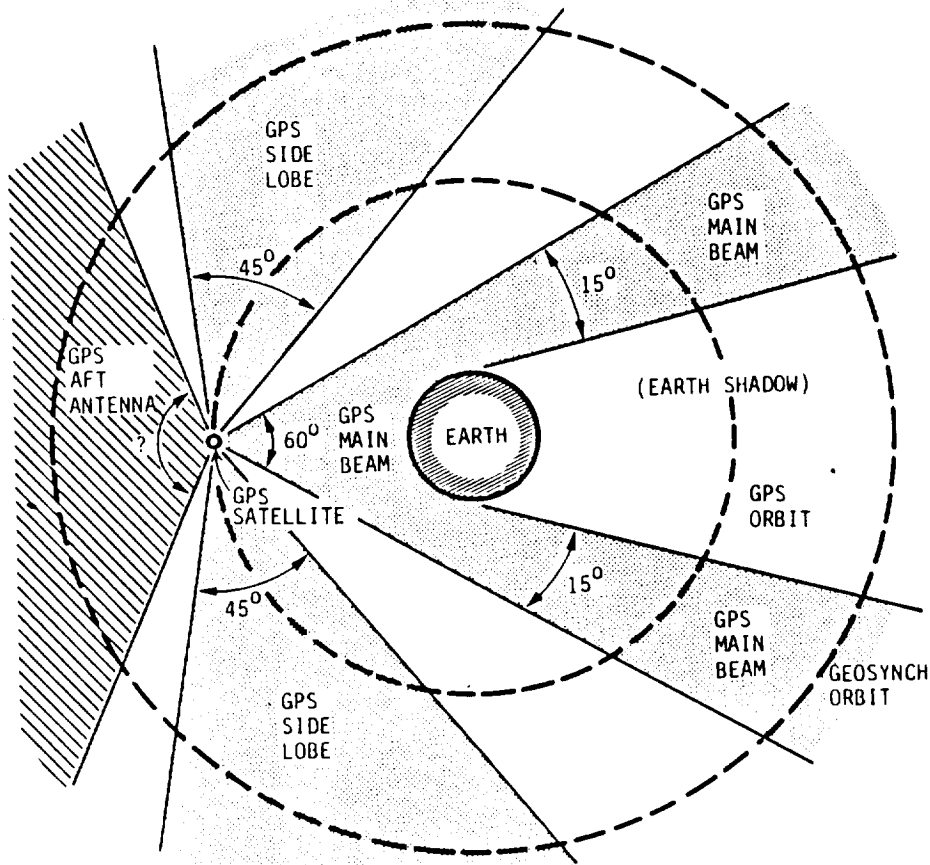
In the final analysis the high accuracy and speed of update for the GPS system results in its being superior to the sextant for a vehicle undergoing the large orbit maneuvers of the OTV. An additional complication is that the sextant is not currently planned for production.

2.1.1.3 - GPS For State Vector Update - The Global Positioning System (GPS) is far and away the most attractive method for navigation state vector updates because of its high accuracy, speed and autonomy. State vector accuracies of 40 ft. and 0.07 fps will be achievable when the system becomes operational. The major problem with the system is acquisition at high altitudes. GPS was designed primarily for earth surface usage with a main beam that is fairly tightly focused on the planet. Above an altitude of about 8000 nmi. the normal omnidirectional acquisition technique becomes marginal due to space losses. In the discussion that follows, approaches to overcome this problem are elaborated upon.

2.1.1.4 - GPS Beam Patterns - Three options are presented for acquiring the GPS signal (Figure 2.1.1.4-1).

- 1) The GPS main beam. This beam has significantly higher power than the side lobes. However, a large portion of it is lost by earth blocking. The resulting beam is a nested cone in appearance with a thickness of 15°.
- 2) The GPS side lobes. While these are relatively low power beams, they have wide extent when mapped into the geosynchronous orbit. They can be represent as a nested cone with a thickness of 45°.
- 3) GPS Aft Antenna. This is a potential GPS hardware modification which would be tailored to geosynchronous users. However, its status is currently uncertain and may not be implemented. Because of its indeterminate status, we will present an alternate solution.

The most attractive option in terms of coverage and availability is the side lobe approach. This approach does require the use of medium gain antenna.



- 3 POTENTIAL GPS BEAMS
- GPS MAIN BEAM 15° WIDE AFTER EARTH OBSCURATION
- GPS SIDE LOBES 45° WIDE
- GPS AFT ANTENNA NOT ON CURRENT DESIGNS STATUS INDETERMINATE
- MOST PROMISING APPROACH IS TO USE SIDE LOBES BECAUSE OF WIDER COVERAGE

Figure 2.1.1.4-1 GPS Acquisition - Transmitting Beam Patterns

2.1.1.5 - GPS Acquisition - Satellite acquisition plots are shown in Figures 2.1.1.5-1,5-2 for an OTV deorbiting from geosynchronous orbit as well as for a vehicle orbiting at GEO. Shown here are total number of GPS satellites visible to the OTV that are transmitting along the designated beams (main beam or side lobe). These total numbers are plotted as a function of time.

To overcome the space losses as well as increasing the effective main beam widths requires about 20 dB worth of antenna gain. For the purpose of producing the plots, this 20 dB gain was assumed to apply in an omni-directional fashion. When one looks at actual antenna characteristics, the use of 4 20° horn antennas gives the required gain as well as reasonable coverage. Using these horns to acquire the GPS results in the following corrections to the plots shown: 1) for main beam acquisition a reduction of about 10% in the numbers shown is required to account for masking, 2) for side lobe acquisition this reduction is about 35%.

It should be pointed out that these two modes are mutually exclusive. Both types of transmitted signals cannot be acquired simultaneously due to geometry. To obtain a normal update, four to six GPS satellites must be acquired simultaneously.

Figure 2.1.1.5-1 shows that the use of the GPS side lobes allows for an adequate number of satellites to be acquired through the first 3.5 hours of transfer, even when allowing for 35% masking. This is not the case for main beam tracking. In addition, the triangulation geometry is more favorable for this case because of wider spacing of the satellites.

Shortly after the midcourse, sufficient numbers of main beam satellites become visible to obtain normal updates. Because the OTV has crossed the GPS constellation at this point, sufficient gain exists in the GPS omni-antenna for it to acquire the signals. This low orbit mode is used throughout the rest of the mission.

In the case of the OTV in geosynchronous orbit, (Figure 2.1.1.5-2) it may again be seen that the use of the GPS side lobes gives adequate numbers of visible satellites even when masking effects are considered.

2.1.1.6 - GPS Summary - The GPS system appears to be the optimum solution to the OTV state vector update problem. The accuracies achievable are better than any other system (40 feet and 0.07 fps in low orbit, 1020 feet and 0.1 fps at GEO). This can be put to good use in reducing the aeroentry system impacts. The updates can be obtained without special ground support and are available quickly and at a relatively high frequency. An additional plus is that GPS is being actively pursued by other space systems which will result in a number of space qualified hardware elements being available when the OTV flies.

The only problem with the system is its acquisition at high altitudes. For low altitude operations, the standard GPS omni antenna give good coverage, allowing updates at any time, and at almost any vehicle attitude.

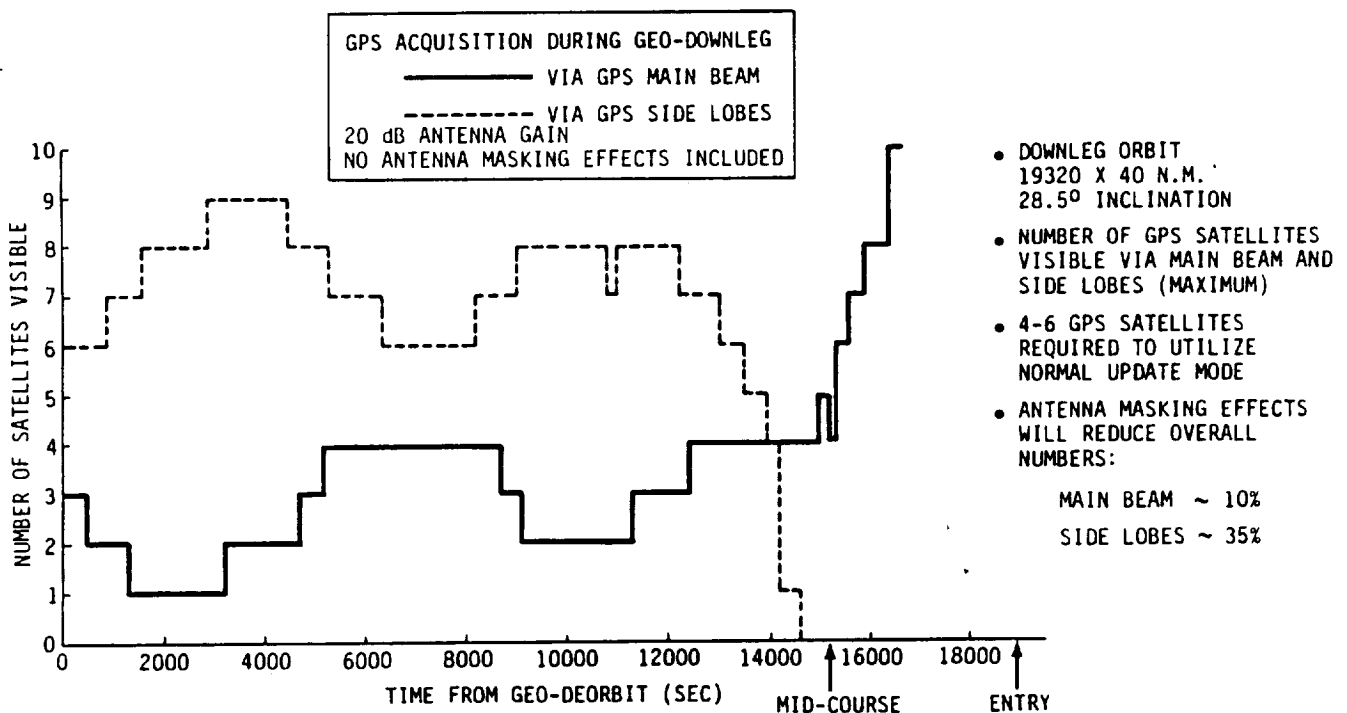


Figure 2.1.1.5-1 GPS Acquisition - GEO Downleg

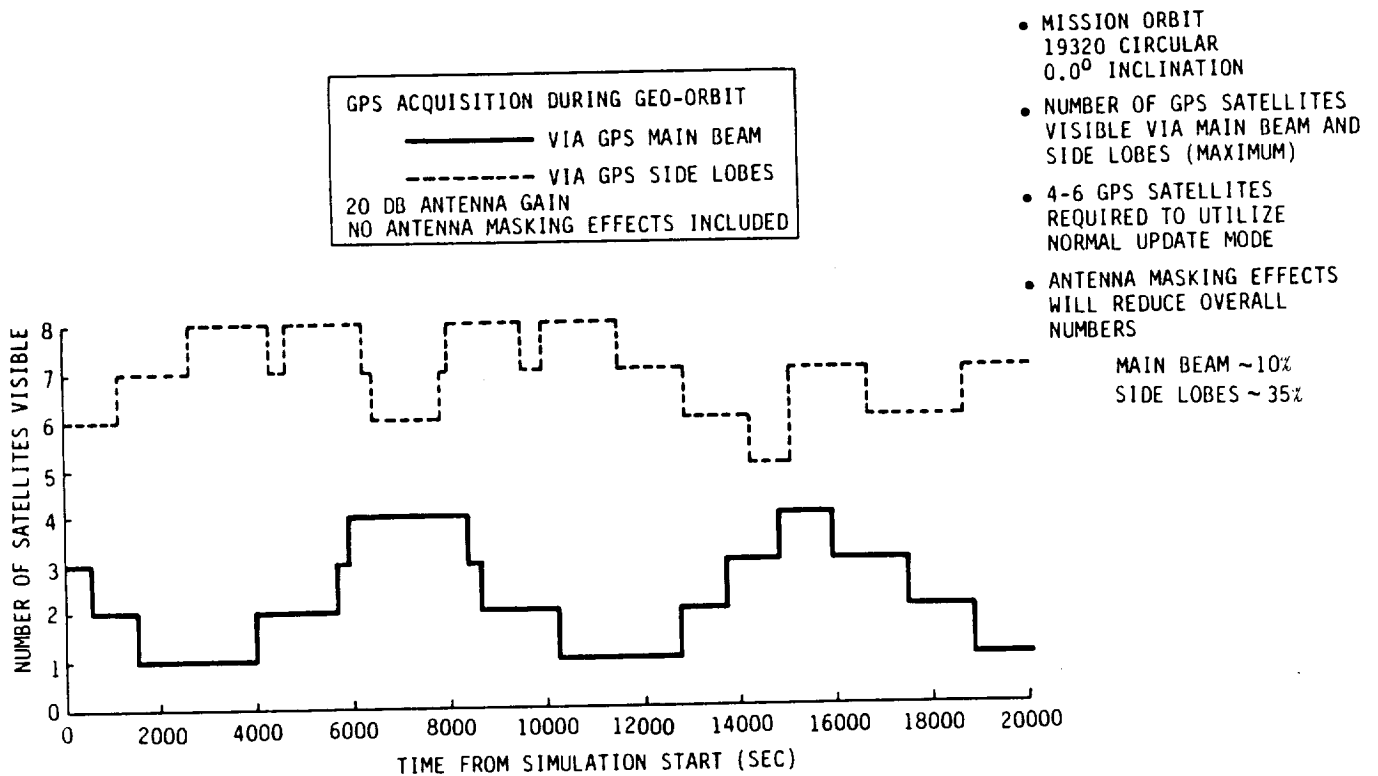


Figure 2.1.1.5-2 GPS Acquisition - Geosynchronous Orbit

For high altitude operations a workable solution appears to be the use of the four fixed 20 degree horns. The OTV periodically slews to an update attitude which requires less than 15 minutes to obtain. On board navigation hardware and software propagates the resulting state vector forward to the next update opportunity. For the downleg trajectory, use of the horns results in about three hours of unambiguous state vector update opportunities. This time can be extended to about four hours if a repositioning system is included in the horns. This would be a single worm drive motor which would slew one of the two horn sets out as a function of deorbit time to capture the enlarging GPS constellation.

Recommendation: GPS consider incorporation of an aft pointing antenna in the next block change which would minimize impact on OTV. Failing this, the above described horn system will give the required accuracies and operational flexibility though at a cost of some 20 Lbs. of additional antenna hardware.

2.1.1.7 - On Orbit Calibration/Alignment - An evaluation of the recalibration and alignment of the inertial systems for space-based OTV's was performed. The calibration analysis concentrated on compensation terms for the gyros and accelerometers. The star tracker was not included because it is a solid state device (inherently stable) which is hard mounted directly to the IMU package. The entire package is assembled/aligned on the ground and is replaceable on

orbit only as a complete unit, hence no subsequent star tracker to IMU realignment is required. Relatively large (a few tenths of a degree) misalignments of OTV to IMU are tolerable, so IMU changeout activities are not tightly constrained.

The selection of the laser gyro for space basing results in part from the elimination of g-sensitive recalibration (difficult to provide at the space station). The only calibration required is on the drift and scale factors which is accomplished in a coarse fashion while attached to the space station. Final calibration is accomplished in-flight via stellar updates.

Recalibration of the accelerometers is done entirely at the station. The low-g environment is ideal for calibrating bias terms so this activity can proceed during any station quiescent periods. The accelerometer scale factor calibration is accomplished by internal test torquers (equipment which is present on some of today's accelerometers). An alternative approach is to look at changes in GPS sensed velocities, though this would require more software on the vehicle.

This recalibration of the internal instruments does not create a special impact to the space station, only a tie-in to the station's inertial reference unit is required to implement the above strategies. In addition, a properly designed orbit-replaceable IMU package can be changed out with less than 1 arc minute alignment disruption. This means that no box realignment is required for space maintenance since all vehicle-relative measurements (pitch, yaw, roll jet separation; aero lift & drag, thermal attitude computations, etc.) can tolerate an arc min. error.

The result of all this is that space based maintenance can be accomplished without special calibration/alignment fixtures.

NAVIGATION ERROR MODEL

The Navigation error model provides the base for orbit accuracy analysis. In most cases the accuracies are achievable with today's instruments and thus demonstrate the practicality of the OTV system. The following summarizes the basic data for the navigation error model:

Effective gyro drift	0.03 deg/hr
Stellar update accuracy	4 arc min
Accelerometer model	200 ppm scale factor; 100 micro-g bias
GPS state vector	40 ft., 0.07 FPS (Low Earth Orbit) 1020 Ft., 0.1 FPS (Geosynchronous Orbit)
Attitude alignment	0.074 deg. 15 minutes after stellar update; 0.17 deg. G.B. pad align 1 deg. space station alignment

Although the characteristics quoted often correspond to real hardware, this should not be construed as representing a selection process, only a realistic bounding of desired capabilities.

2.1.1.8 - Midcourse Analysis - An analysis was performed to establish midcourse burn requirements for the downleg portion of the OTV geosynchronous mission. This midcourse is performed an hour before atmospheric entry. Various errors in the deorbit burn were considered and mapped into an equivalent aeropass perigee variation and inclination error by performing covariance analysis of worst-case error sensitivities.

- 1) A burn attitude pointing error of 0.074 deg. results from star tracker misalignments and gyro drift over 15 minutes of time. This results in 59200 ft. perigee and 0.052 deg. inclination error.
- 2) Accelerometer errors on the 6080 fps deorbit burn amount to 1.22 fps in longitudinal delta-V and 0.003° of burn misalignment due to lateral accelerometer bias. The RSS total of the longitudinal and lateral effects results in 7470 ft. perigee and 0.011 deg. inclination errors.
- 3) An RCS vernier trim burn is used for precision cutoff of the main engine burn. The shutdown uncertainty on the two RCS engines is 2 lb-sec. which results in a 55 ft. perigee error.
- 4) GPS state vector error causes targeting errors by the onboard guidance system. GPS position uncertainty is estimated to be 1020 feet and velocity uncertainty is 0.1 fps at this point in mission. These result in 650 ft. perigee and 0.001 deg. inclination errors.

The RSS total of all errors is \pm 9.82 nm on perigee and .052° on inclination.

A midcourse of 20.0 fps performed approximately four hours after deorbit is sufficient to cover errors in perigee altitude. The inclination error will be corrected by out of plane steering in the aerophase.

2.1.1.9 - Aeroentry Error Analysis - In order to minimize aerobrake TPS weight, it is desirable for the dynamic range of the aeroentry maneuver to be as small as possible. This is accomplished by reducing the aeroentry control corridor to the minimum required for covering expected entry variations. The following analysis was used to define the baseline variations.

A series of error sources were considered with their impacts being normalized to an equivalent variation in vacuum perigee. The RSS total of these effects was then used to size the aerocontrol corridor and the L/D of the vehicle. The sources were grouped into two categories: 1) targeting errors which cause OTV to miss its desired atmospheric aiming point and 2) aerodynamic variations which cause the vehicle to fly a different atmospheric trajectory than expected.

- 1) Targeting Errors - The last opportunity to correct the OTV's downleg trajectory occurs one hour before entry with a midcourse correction burn. This burn is nominally performed with the RCS system which results in a very accurate injection. All errors prior to this point are nulled out and only those factors that disturb the burn and subsequent trajectory are considered.

- a) Guidance Errors - Experience indicates an error of about 200 ft. for this parameter.
- b) Pointing Errors - Midcourse burn attitude errors due to IMU misalignment (after stellar update) and cg trim errors amount to about 0.1 deg. which equates to 130 ft. variation in vacuum perigee.
- c) Cutoff Errors - Accelerometer errors and a 10 millisecond shutdown uncertainty results in a 490 ft. error.
- d) GPS Error - originally, estimates of state vector errors for GPS at this stage of flight (at a relatively high altitude of 9000 n.m.) were 1500 ft. in position and 2 fps. in velocity which results in a net perigee error of 9514 ft. This state error has subsequently been greatly reduced to 1020 ft. position and 0.1 fps. velocity uncertainty (based on recent GPS simulation work conducted at the Aerospace Corporation) which results in a perigee error of only 745 ft. The old uncertainties were used to derive the basic control requirements and will be carried here. Subsequent testing with our closed loop aeropass simulation has shown that the extra margin this provides is required to overcome system response lags for the case of fluctuating atmospheric dispersions.
- e) Onboard Clock Error - Very accurate time comes with the use of GPS - not a significant effect.
- f) Nongravitational Effects - Nonbalanced configuration of the RCS jets produces unbalanced torques (see controls section for a layout). This is estimated to result in a 320 ft. perigee miss.

2) Aerodynamic Variations - No two aeroentries will be quite the same. The impact of variations in the atmosphere and the vehicle are accounted for here.

- a) Atmospheric Uncertainty - Current best estimates of atmospheric prediction accuracies for the 1990s are plus or minus 30% in density. This figure is primarily based on observed density fluctuations in Shuttle reentry data. This results in a 5700 ft. uncertainty in perigee altitude.
- b) L/D Uncertainty - An angle-of-attack variation of 1° is due to variations in the entry cg location consistent with Viking entry data and OTV c.g. analysis. The impact on perigee is 4500 ft.
- c) Ballistic Uncertainty - Weight uncertainty = 150 lbs. (propellant residual uncertainty), coefficient of drag (C_d) variation = 10% (Shuttle and Viking experience), and brake area variation = 5% (to cover uncertainties in the flex of the support ribs and Nextel cloth). The RSS effect of these factors on ballistic coefficient is 12%.

RSS'ing of all the above factors yields a net variation in perigee of + 2.01 nm. A control corridor of + 2.5 nm was chosen to cover this uncertainty with a 25% margin. The key contributors to this variation are the uncertainties in atmospheric density and angle of attack. Better atmospheric prediction capabilities (through real-time remote sensing and improved dynamic modeling) as well as reduced aerodynamic uncertainties (better computational fluid dynamics codes plus a vigorous pre-flight test program) could greatly reduce the perigee variation.

Conclusion: We conclude that ± 2.5 n.m. worth of control capability must be in the OTV aerodesign.

2.1.1.10 - Aeropass Navigation Errors - Table 2.1.1.10-1 summarizes the analysis undertaken to establish errors in the aeroexit orbit due to aeropass uncertainties.

Table 2.1.1.10-1 Aeropass Navigation Analysis

- o GEO DEORBIT ERRORS
 - 20 FPS MIDCOURSE AT ENTRY MINUS 1 HOUR REQUIRED TO CORRECT DEORBIT PERIGEE ERROR OF 8.91 NM
 - 0.047° INCLINATION ERROR CORRECTED IN AEROPASS
- o MIDCOURSE ERRORS
 - 0.16 NM UNCERTAINTY IN PERIGEE ALTITUDE
 - 0.0019° VARIATION IN AERENTRY FLIGHT PATH ANGLE
- o AEROPASS ERRORS
 - MIDCOURSE RESIDUALS PLUS AERODYNAMIC UNCERTAINTIES REQUIRE A 5 NM CONTROL CORRIDOR (L/D - 0.116)
 - 1.47 NM APOGEE AND 0.021° INCLINATION ERRORS REMAIN IN AEROEXIT ORBIT

2.1.1.11 - OTV Minor Burns - An analysis was conducted to establish OTV requirements for burns other than those for major transfers. These include midcourse maneuvers, separation burns, post-aero circularization and trim delta-v's, as well as ACC OTV boost requirements. These so called "minor burns" are summarized in Table 2.1.1.11-1

Use was made of GN&C error analysis as well as simulations to derive results for selected missions. The mission profiles may be found in the flight operations section.

This burn information was incorporated into the performance analysis used to size OTV propellant requirements.

Table 2.1.1.11-1 OTV Minor Burns

	GROUND-BASED ACC			SPACE-BASED			
	GEO	PERIGEE		GEO	GEO	MANNED	
	DEL	PLAN.	KICK	DEL	SERV.	GEO	PLANETARY
ET/SS SEP	366	366	366	8 (OMV)	8(OMV)	8(OMV)	8 (OMV)
UPLEG MIDCOURSE	---	---	---	---	20	20	---
PL SEP/EVADE	5	20	20	5	--	--	20
DOWNLEG PHASING	165	---	378	165	165	165	---
DOWNLEG MIDCOURSE	20	40	20	20	20	20	40
POST AERO TRIM	350	350	350	450	450	450	450
SPACE STA. XFER	---	---	---	85	85	85	85

ALL QUANTITIES IN F.P.S.

Aeromaneuver Control Options - Flight through an atmosphere requires that a vehicle have some method for altering its trajectory to correct for inevitable variations in targeting and aerodynamic performance. Two basic options exist to accomplish this control:

Drag control alters the trajectory by direct variation of the vehicle's ballistic coefficient. This can be accomplished either by area variation (with devices such as drag brakes) or drag coefficient (with streamline modification techniques such as Aerospike) or by a combination of the two (such as with the Ballute concept which simultaneously alters its volume and shape by pressurizing and depressurizing an aerodynamic gas bag). Drag control can be used to control exit apogee only since no out of plane control is possible. Desired exit inclination relies on accurate pre-entry targeting.

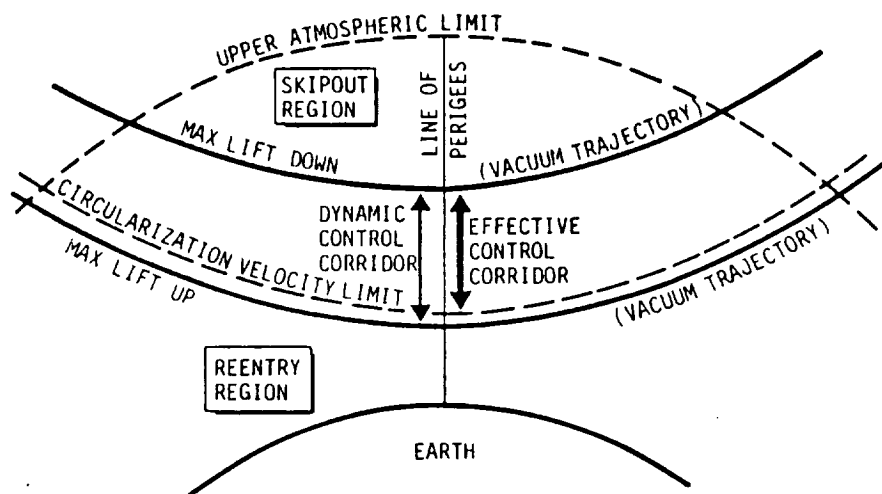
The second option is lift control which utilizes the pointing of a lift vector to directly alter the vehicle's flight path. This lift vector arises from a non-zero trim angle of attack in the entering vehicle and represents a technique which has been used by the Apollo, Viking and Shuttle Programs. Use of this technique allows out-of-plane corrections to be made which means that both apogee and inclination errors can be corrected in the Aeropass. With a mid to high lifting device, larger amounts of Aeropass inclination turn can be executed which reduces the rocket burn which would otherwise be required.

Based on our studies of the aero-entry process we recommend the use of a low L/D lifting device. The rationale for this selection will be presented in the following paragraphs.

2.1.1.12 - Control Corridor Definition - Safe flight through the atmosphere is restricted to a region which can be controlled by the OTV. For example, if the OTV uses lift vector pointing to modulate its trajectory, the limits of this control are continuous lift vector up and continuous lift vector down. Trajectories run with these two conditions define lower and upper (respectively) boundaries (Fig. 2.1.1.12-1) for vehicle flight. Conditions which exceed these boundaries will result in either skip-out or reenter.

For the purposes of establishing a working concept, these boundary profiles are characterized by their (preentry) vacuum perigee altitudes. The difference in the perigee altitudes for the two limiting conditions is known as the dynamic control corridor. This corridor represents the zone within which an orbital targeting routine must aim the OTV for a successful aeropass.

As will be seen later, the bottom portion of the control corridor has penalties associated with it in the form of larger post-aero circularization burns. This is due to the decay of the exit perigee with steeper exit angles-of-attack. Because of this penalty, the lower portion of the corridor is removed leaving an effective control corridor as the target window.



- CONTROL CORRIDOR BOUNDED BY:
 - CONTINUOUS LIFT UP CASE (LOWER BOUNDARY)
 - CONTINUOUS LIFT DOWN CASE (UPPER BOUNDARY)
- LOWER BOUNDARY MODIFIED BY RAPID GROWTH OF POST-AERO CIRCULARIZATION VELOCITY (DUE TO PERIGEE ALTITUDE DECAY).
- RESULTING CORRIDOR IS EXPRESSED AS THE PERIGEE ALTITUDE SEPARATION OF THE VACUUM TRAJECTORIES. USE OF VACUUM ORBITS EASES ORBITAL GUIDANCE TARGETING.

Figure 2.1.1.12-1 Control Corridor Definition

2.1.1.13 - Aeromaneuver Control Modes - Our trajectory simulation was used to compare three basic approaches to aerobraking: aerospike; drag modulation; and lift modulation. Control corridor parametrics were generated for varying levels of aerospike thrust, drag modulation ratio, and L/D. All trajectories are for a ground-based OTV configuration returning from a geosynchronous mission orbit. All the parametrics were normalized to show impact of the various approaches on the aerodynamic control corridor.

For the case of aerospike control, it may be seen from Figure 2.1.1.13-1 that the control authority is limited to an approximately 6 mile wide corridor (with correspondingly high propellant usage (see Figure 2.1.1.14-1)).

The geometric constraints of mechanical drag modulation appear to limit its area variation to less than 3:1. From the chart one can see that this corresponds to a control corridor of 3 nm or less. This represents a somewhat marginal control situation, when compared with the 5 nm control corridor resulting from our aeroentry error analysis work.

The offset C.G. approach (lift control) appears to offer the largest amount of control for the smallest vehicle impact. For example, L/D values of 0.25 are easily achievable with the 70 degree Viking aeroshell and result in control corridor widths on the order of 12 nm. This is more than adequate to cover trajectory dispersions.

Our conclusion is that lift control is the most promising method of controlling the OTV through the aeropass.

2.1.1.14 - Aerospike Fuel Requirements - Trajectory simulations of the OTV aeropass were used to generate various parameters. In this case simulation of the aerospike dynamics was used to derive the aerocontrol corridor for various maximum thrust levels. The control corridor is obtained by differencing the perigee altitude obtained with no control from that with maximum control, both with proper exit conditions. Basically then, a vehicle whose vacuum perigee lies within the control corridor can be steered by guidance to a proper exit orbit. In the case of aerospike, minimum control is the no thrust condition and maximum control is full thrust (within the atmosphere).

Figure 2.1.1.14-1 shows control corridors resulting from thrust levels up to 1200 lbs., where the effectiveness decays due to dominance of the rocket effect over drag reduction. All cases are for a geosynchronous return with the ground-based OTV configuration. It may be seen from Figure 2.1.1.14-1 that Aerospike is fairly propellant expensive (420 lb. propellant for a five mile corridor).

Based on its high propellant usage (which is not offset by weight savings elsewhere) and large uncertainties in the dynamics of the process we conclude that Aerospike is not an attractive option for the OTV Aeropass.

2.1.1.15 - Velocity Savings From Inclination Control in Aeropass - Lift can be used to trim out-of-plane (inclination control) as well as the in-plane (apogee control) errors in the aero-maneuver. Converged trajectories were generated with maximum out-of-plane lift for various L/D configurations to evaluate how much inclination change is achievable. Figure 2.1.1.15-1 shows deorbit from geosynchronous orbit to a Shuttle recovery orbit of 28.5° inclination and 140 nmi altitude.

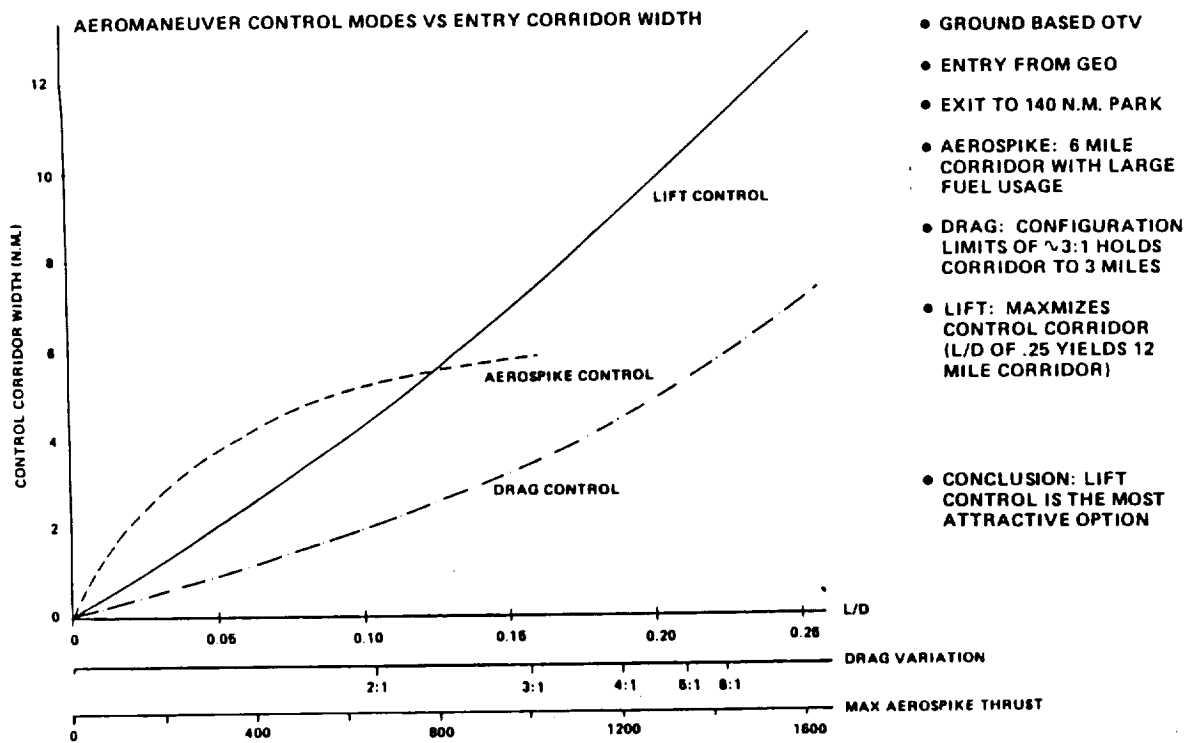


Figure 2.1.1.13-1 Aeromaneuver Control Modes

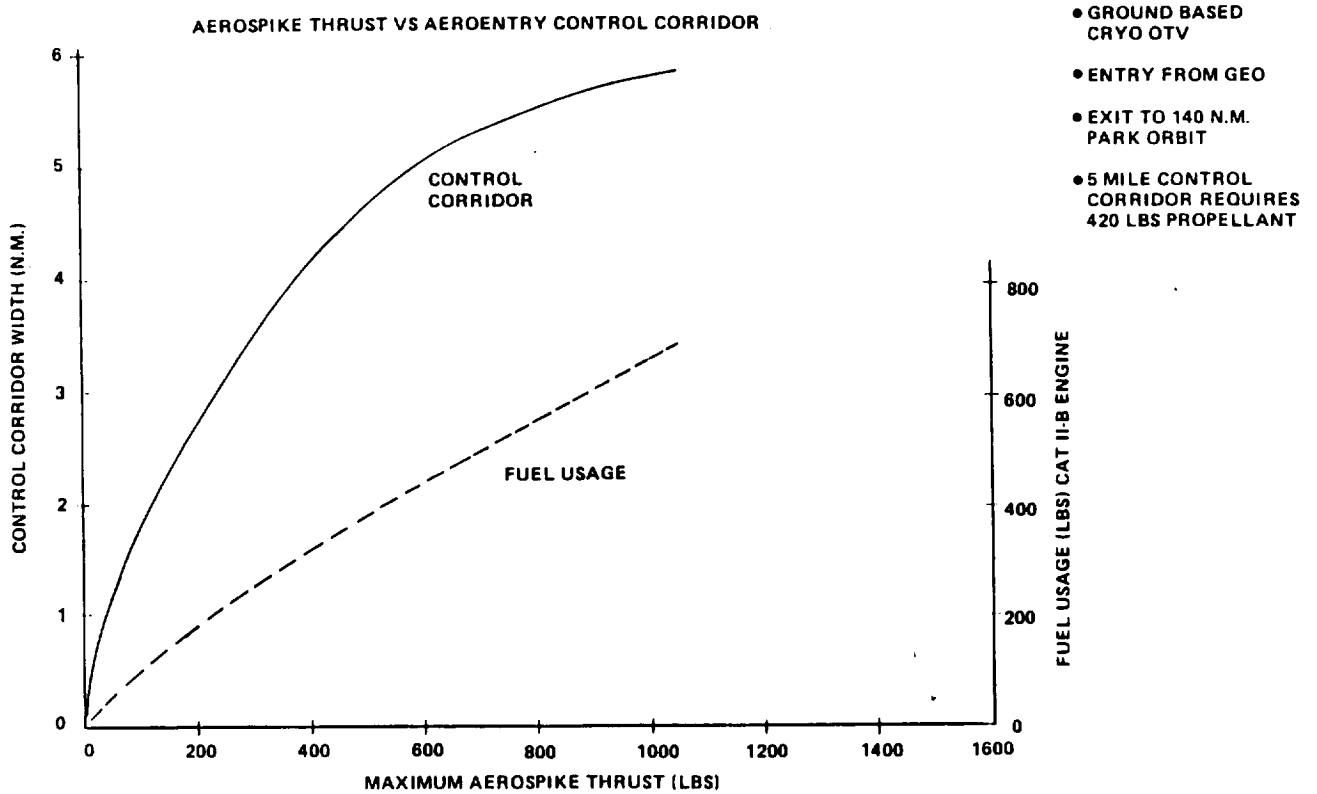


Figure 2.1.1.14-1 Aerospike Fuel Requirements

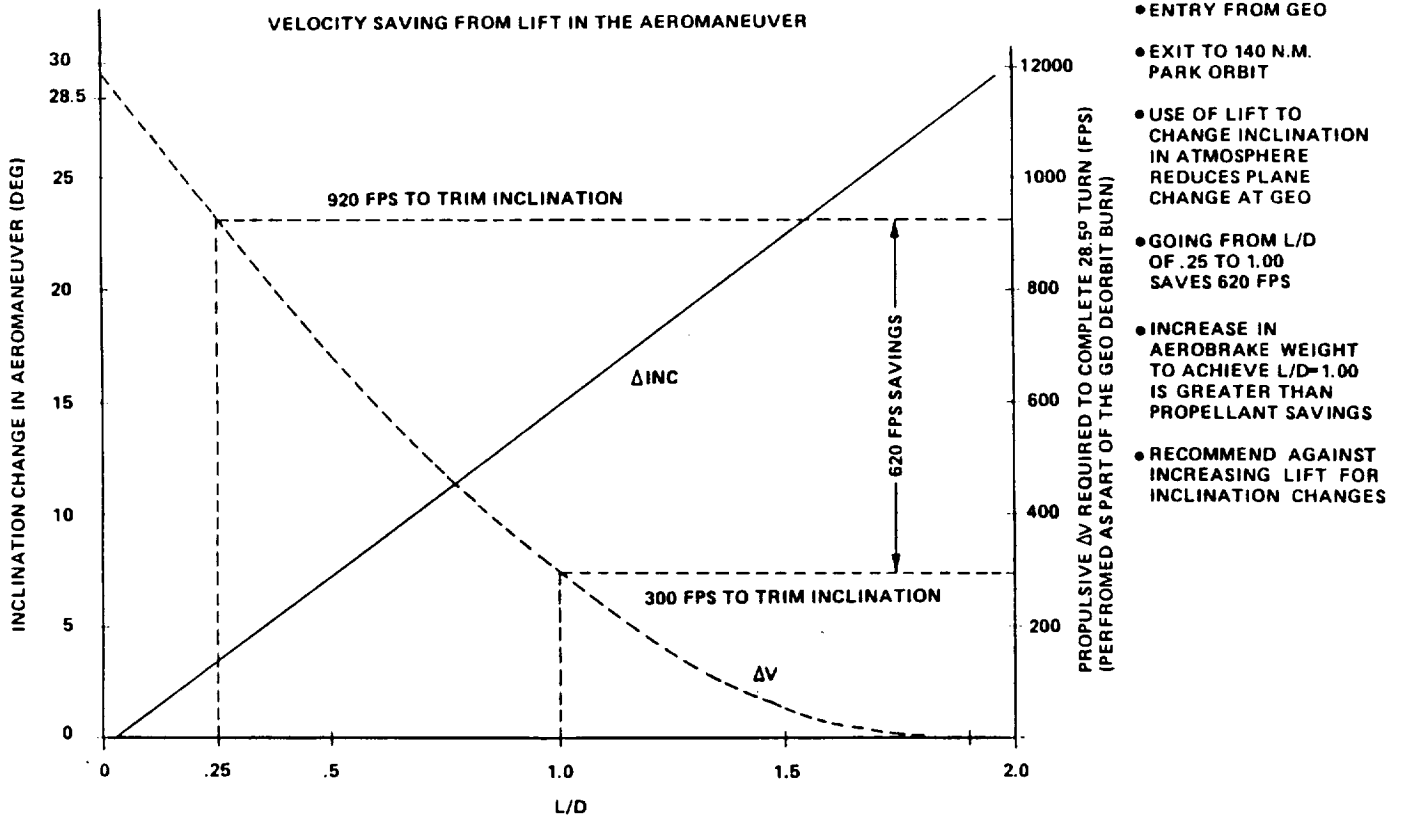


Figure 2.1.1.15-1 Velocity Savings from Inclination Control in Aeropass

It may be seen that for an L/D of 1.8 the entire 28.5° plane change can be accomplished in the aeropass.

A comparison is made of the velocity savings to be gained by going from an L/D of .25 to 1.00. This represents an additional inclination change capability of 11.5° (increasing from 3.5° to 15° delta inclination) which corresponds to a velocity savings of 620 fps.

This velocity savings at the apogee burn can be equated to the following propellant savings at the end of the mission:

	<u>Return Empty</u>	<u>14K Return</u>
Storable Stage (I _{sp} = 342 sec)	350 lb	1160 lb
Cryogenic (I _{sp} = 470 sec)	250 lb	840 lb

The increase in dry weight necessary to produce the L/D of 1.0 must be less than these propellant savings to realize a net performance benefit. The hypersonic sled aeroassist configuration which accomplishes this L/D (detailed in Section 2.2.1) weighs 6000 lb more than the equivalent low L/D storable vehicle with 14 K return capability. In this case, a benefit from mid l/D of 1160 lb of propellant savings is overwhelmed by a structural penalty of 6000 lb.

We conclude that adding lift to significantly alter inclination in the aeropass results in an inefficient OTV. Our design approach is to use only enough lift to control trajectory errors.

2.1.1.16 - Deorbit Overview - Figures 2.1.1.16-1 and -2 show two basic strategies for deorbiting the OTV from GEO. The basic problem is controlling the OTV phase relative to the pick-up vehicle since the deorbit point is fixed by the orbit intersection of the two spacecraft.

Figure 2.1.1.16-1 shows a direct descent where the size of the downleg orbit is varied to change the time of aeroentry. To accommodate the full range of relative phasing requires this orbit's timing shift be adjustable between +.8 to -.7 hr. This requires an additional velocity penalty of up to 170 FPS on the deorbit burn.

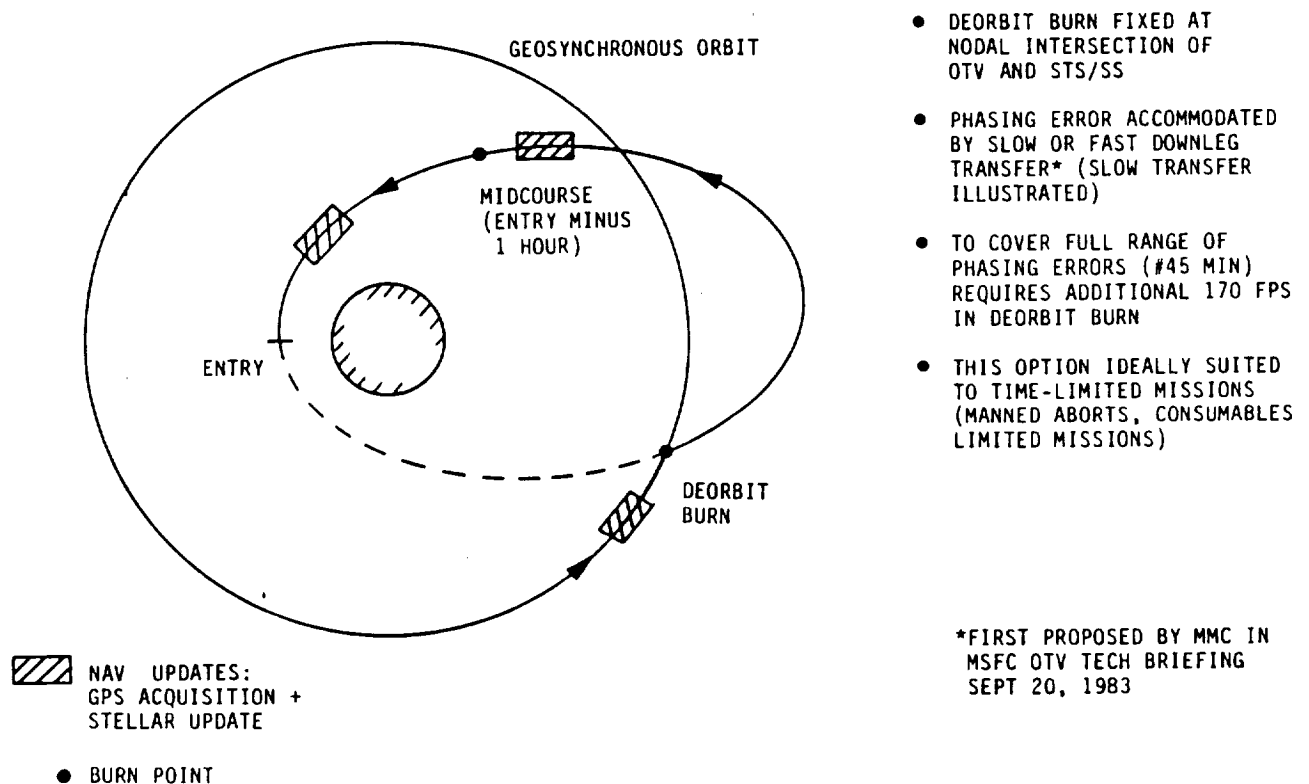
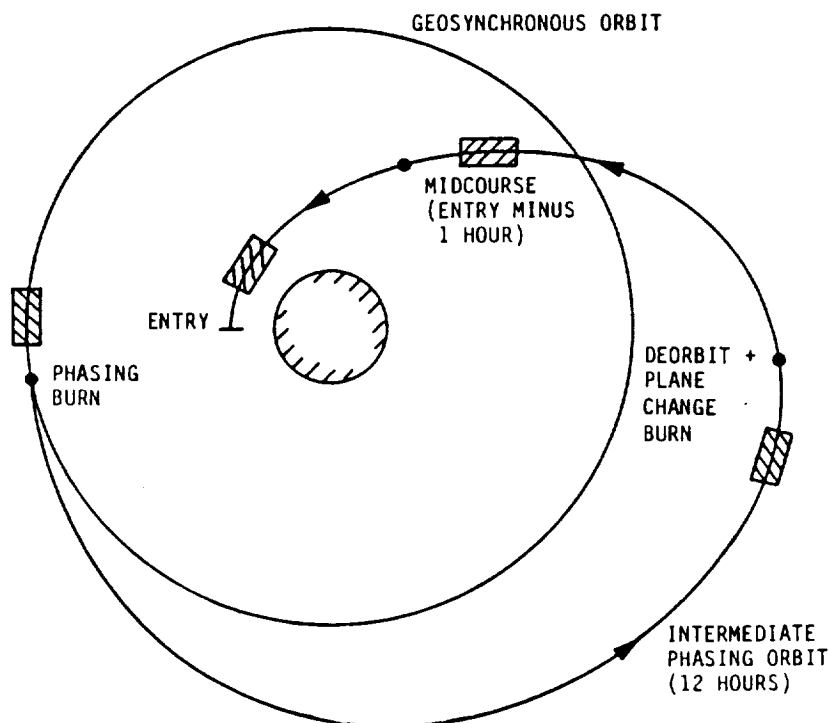


Figure 2.1.1.16-1 Deorbit Overview - Option #1

Figure 2.1.1.16-2 shows an alternate approach where phasing is accomplished by first raising the apogee of the geo-orbit half a revolution prior to the deorbit point. A Hohman transfer is used for the downleg to the atmosphere. Since both segments require more time to traverse, a net delay in the entry time is accomplished which produces the required phasing shift. Since the deorbit burn occurs at a higher altitude (about 2000 N.M. higher than GEO for the 90 minute delay case) less velocity is required to accomplish it. The maximum delay situation of 90 minutes actually requires 129 FPS less overall than a normal deorbit.



- DEORBIT BURN FIXED AT NODAL INTERSECTION OF OTV AND STS/SS
- PHASING ERROR ACCOMMODATED BY COMBINATION OF THE BURNS:
 - 1) PHASING BURN TO RAISE APOGEE
 - 2) DEORBIT BURN AT RESULTING APOGEE
 (THE COMBINATION DELAYS TIME OF ENTRY WHICH ADJUSTS RELATIVE PHASE)
- DEORBIT BURN AT HIGHER ALTITUDE ACTUALLY SAVES FUEL OVERALL (+90 MIN ADJUST USES 129 FPS LESS THAN NOMINAL)
- INTERMEDIATE PHASING ORBIT REQUIRES 12 HOURS ADDITIONAL TIME AT GEO
- THIS OPTION IDEALLY SUITED TO PERFORMANCE CRITICAL MISSIONS


 NAV UPDATES:
 GPS ACQUISITION +
 STELLAR UPDATE
 ● BURN POINT

Figure 2.1.1.16-2 Deorbit Overview - Option #2

Thus, Deorbit Option #2 is more optimum than option #1 from a propellant standpoint (12 hours worth of additional consumables is outweighed by the velocity reduction). However, missions which cannot afford the additional 12 hrs at GEO will find Option #1 more attractive. This would include such time critical modes as a manned abort from GEO.

2.1.1.17 - Aerophase Overview - The aerobrake trajectory and subsequent orbital maneuvers are shown in Figure 2.1.1.17-1. Upon leaving the atmosphere, the OTV is in a suborbital trajectory whose perigee must be raised to at least 100 nm to provide a stable orbit. In order to correct for

relative phasing shifts, a single pass in a postaero phasing orbit is undertaken. By varying the perigee between 100 nm and 140 nm (circularization) results in a phasing shift of 3.01° . This is more than adequate to correct the atmospheric dispersion.

Subsequently, an inclination trim burn is accomplished at the intersection of the nodes, followed by a final circularization at the Shuttle rendezvous altitude of 140 nm.

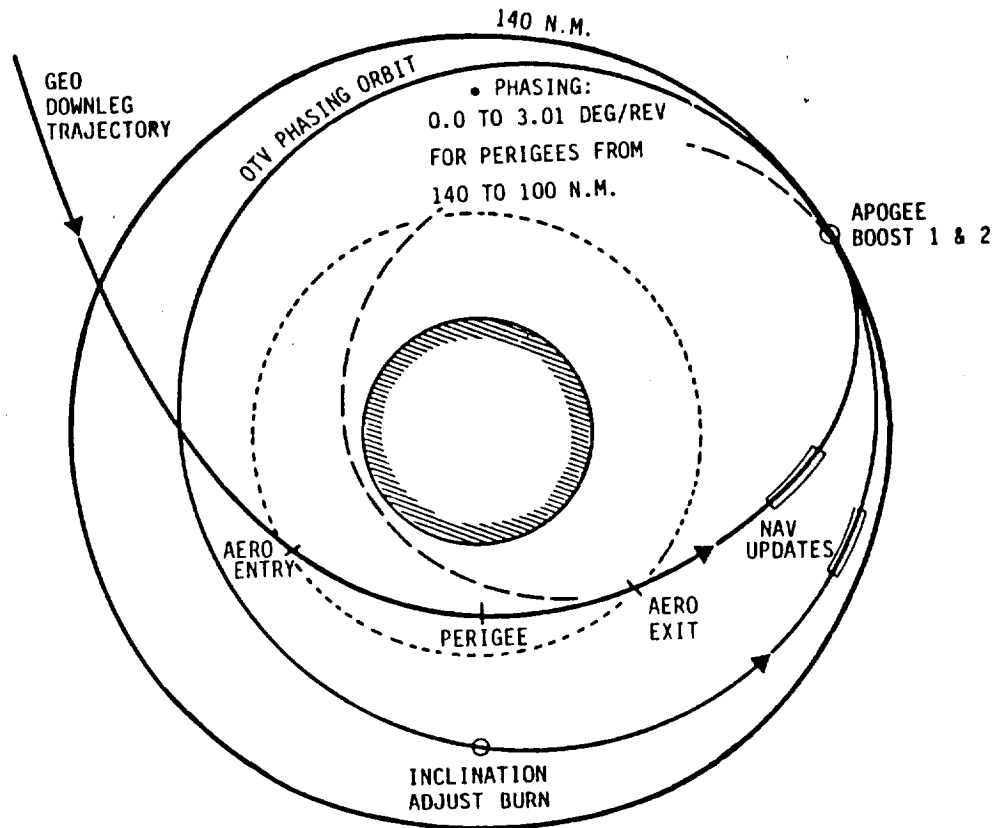


Figure 2.1.1.17-1 Aerophase Overview - Ground-Based

2.1.1.18 - Aeroentry Overview - SPACE-BASED - The space-based aerophase (Figure 2.1.1.8-1) is very similar to that for the ground-based. Because of the higher Space Station altitude the postaero targeted apogee is correspondingly higher. To avoid interference with the defined Space Station control zones, this apogee target has been set 25 miles below the 270 nm station orbit.

The range of OTV phasing orbits achievable can adjust for 3.63 to 14.08 deg/rev between the OTV and Space Station.

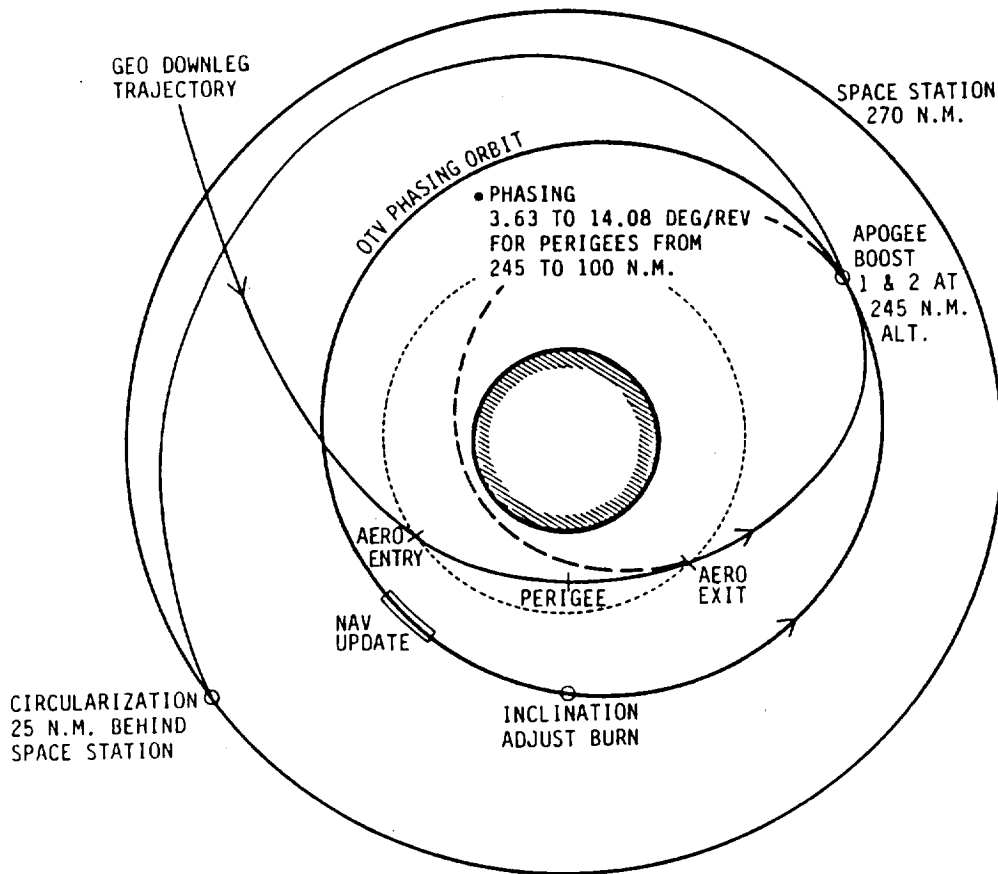


Figure 2.1.1.18-1 Aerophase Overview - Space-Based

2.1.1.19 Aeroentry Overview - Figure 2.1.1.19-1 presents an overview of the aeroentry process. The control corridor forms a tunnel within the atmosphere which defines where the vehicle can successfully fly. Note that the bottom of the control corridor is defined by an operational boundary rather than a dynamic one. This is because flying at the bottom of the dynamic corridor causes very depressed perigees in the post-aero orbit which requires a large amount of fuel to correct.

Just prior to entry the OTV performs a final midcourse correction (entry minus 1 hour), Stellar and GPS updates, and a preentry guidance update. After accomplishing these tasks, the OTV establishes an entry attitude which it holds until entry begins at a sensed acceleration of .03 g's.

GEO DOWNLEG

MIDCOURSE
FINAL STELLAR UPDATE
CONTINUOUS GPS UPDATES
PRE-ENTRY GUIDANCE UPDATE

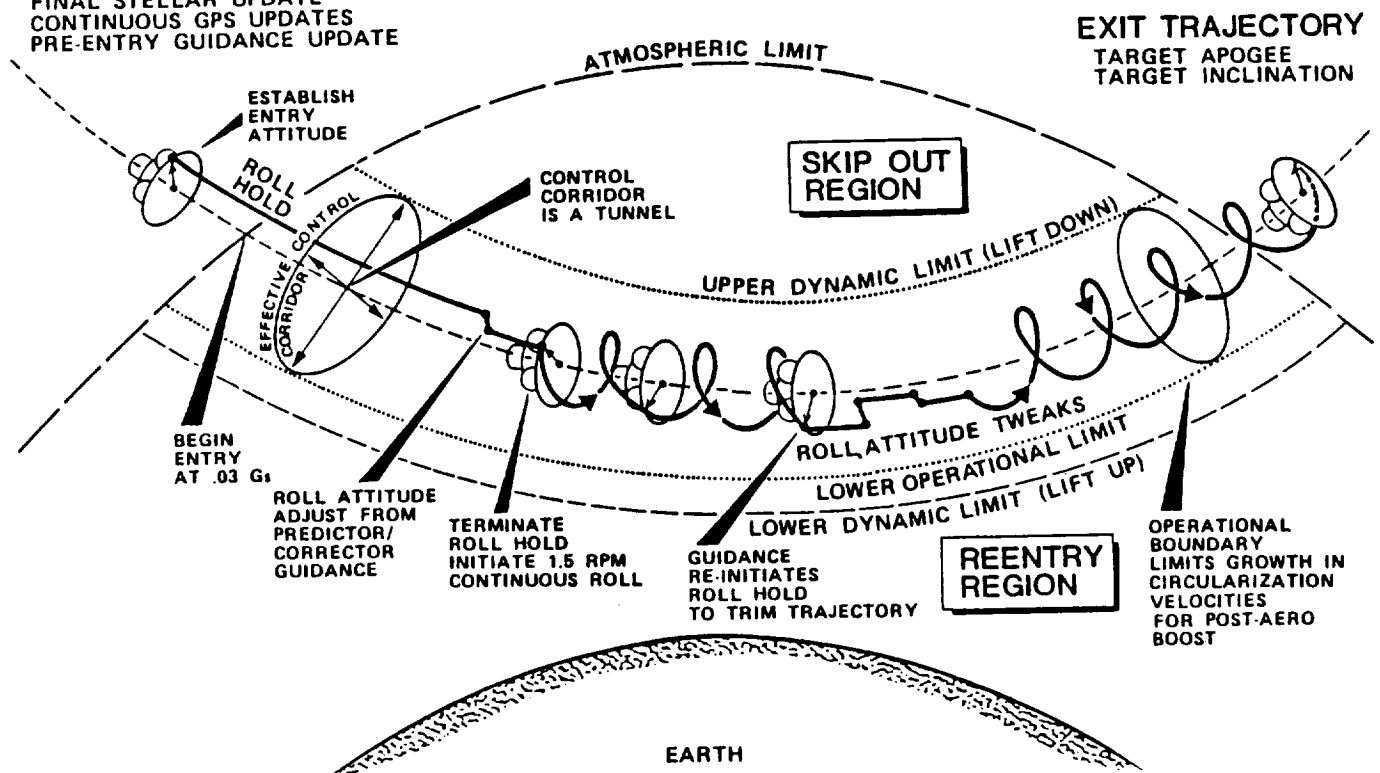


Figure 2.1.1.19-1 Aeroentry Overview

As the entry proceeds, guidance updates (every 10 seconds) refine the desired pointing of the vehicle lift vector. Upon achieving sensed velocity targets, the vehicle initiates a continuous roll at 1.5 RPM to null the fixed lift vector. In a typical trajectory, subsequent roll holds are required to tweak the trajectory. This process continues until the vehicle exits the atmosphere, at which time the apogee and inclination targets for the post-aero orbit have been achieved.

2.1.1.20 - OTV Aerostabilization - Figure 2.1.1.20-1 shows the OTV in its 7.2° aeroentry attitude required for adequate lift. A fundamental point shown is that the aeroroll maneuvers are performed about the vehicle's trim angle of attack rather than its axis of symmetry. Because the aerodynamic torques are larger than the offset inertia effects the vehicle can be rolled about this axis with smaller RCS jet consumption.

The attitude control algorithm uses rate damping about the pitch and yaw axes and an attitude/rate deadband for the roll axis.

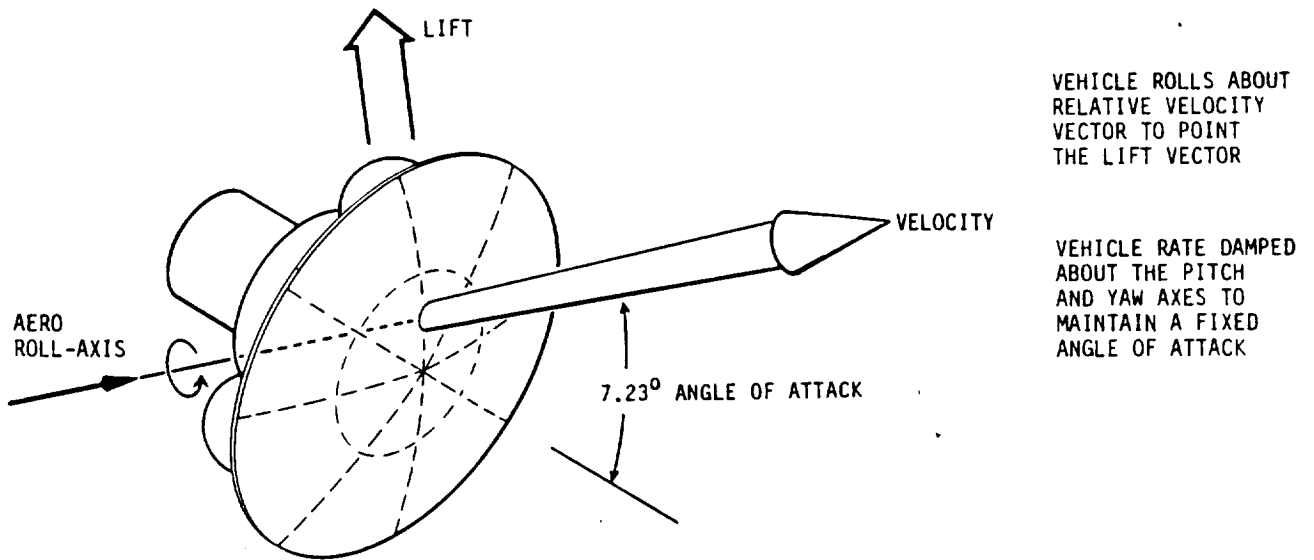
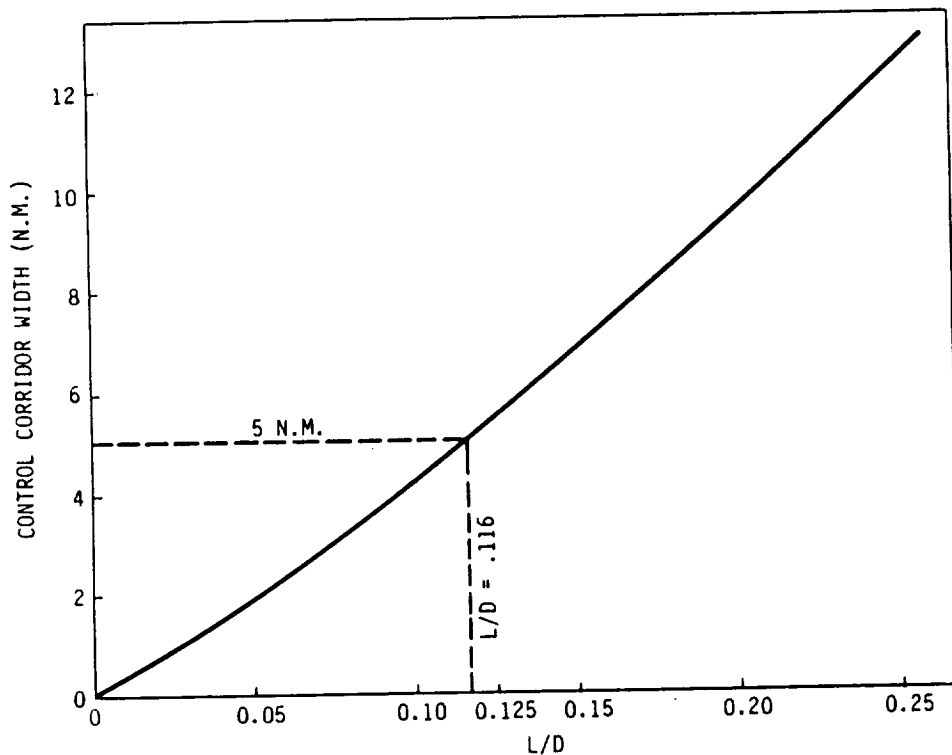


Figure 2.1.1.20-1 OTV Aerostabilization

2.1.1.21 - L/D Versus Control Corridor - Using the 5 nm control corridor width that results from the aeroentry error analysis it is possible to specify the L/D requirements for the OTV. A series of continuous lift-up and lift-down geosynchronous return trajectories were generated for various L/D's to define corridor boundaries. The resulting control corridor widths are plotted on Figure 2.1.1.21-1. This data shows that an L/D of 0.116 gives the desired 5 nm corridor. This L/D is achieved via an angle-of-attack of 7.2 degrees based on Viking data for this type of aerobrake shape. (Reference: Viking Aerodynamic Data Book, NASA TR-3709014)

An analysis of free molecular flow effects shows no significant impact to this angle of attack as will be discussed in the following paragraphs

2.1.1.22 - Aerothermodynamic Environment - The aerothermodynamic flight domain of an AOTV is shown in Figure 2.1.1.22-1. A STS trajectory is shown for comparison. The AOTV decelerates at a much higher altitude than STS and makes its aeropass in a very energetic environment of the upper atmosphere. STS peak heating occurs in a dissociated oxygen dominated convective heating environment. The AOTV's entry into the atmosphere is almost twice as energetic as STS. The environment associated with the passage of the OTV through this high altitude consists of radiation from chemically relaxing air (also known as nonequilibrium radiation) and convection from dissociated, ionized air. It has been shown (Reference AIAA paper 83-04060 that a regime exists for blunt bodies where continuum theory applies although a slip condition may occur. The limit of applicability of continuum theory for a blunt body is termed the quasi continuum limit.



- 5 N.M. CONTROL CORRIDOR REQUIRES L/D OF 0.116
 - USE OF VIKING CONTINUUM FLOW DATA RESULTS IN AN ANGLE OF ATTACK = 7.23° (REF: VIKING AERODYNAMIC DATA BOOK, NASA TR-3709014)
 - FREE MOLECULAR FLOW ANALYSIS RESULTS IN NO SIGNIFICANT IMPACT TO ANGLE OF ATTACK
- OTV DESIGN ATTITUDE FOR ENTRY IS 7.23° DEG

Figure 2.1.1.21-1 L/D vs Control Corridor

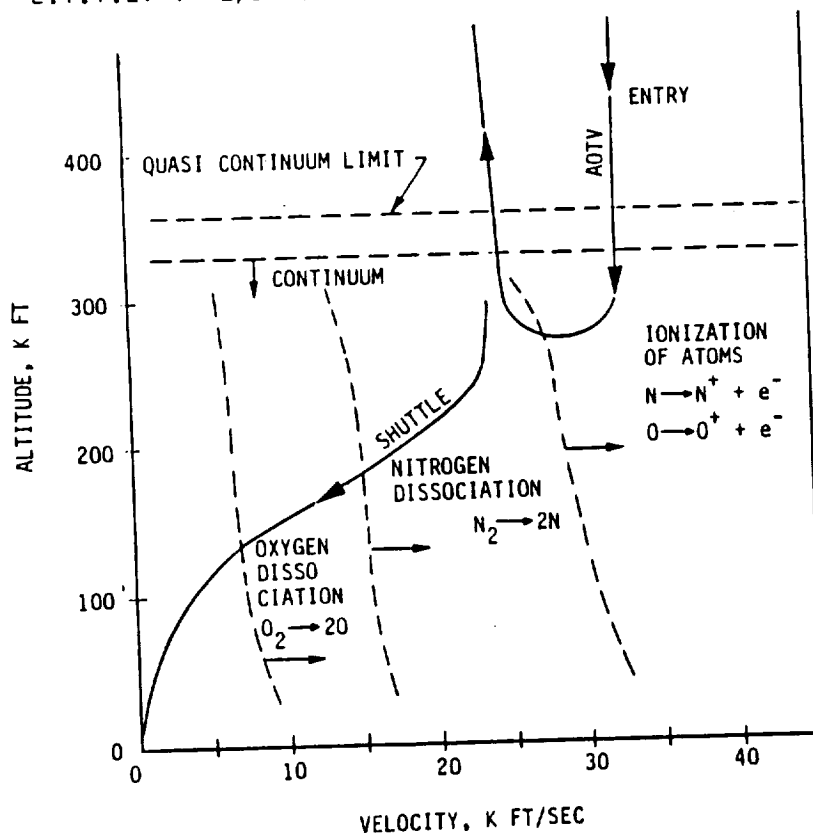


Figure 2.1.1.22-1 Aerothermodynamic Environment

2.1.1.23 - Flow Regime Transition Criteria Based on Viking Flight and Wind Tunnel Data - Over the high Reynolds number flight regime, the drag coefficient (C_D) is nearly constant at a value of 1.6. Just below a Reynolds number of 10^5 , a decrease in C_D has been observed. This is due to a transition from equilibrium to nonequilibrium flow in the shock layer. Based on Viking flight data, C_D is reduced to approximately 1.55 at $Re = 10^4$ (wind tunnel data indicates a decrease in C_D to 1.48). Then as the Reynolds number becomes lower, an increase in C_D occurs as transitional and then free-molecule flow are obtained. A simplified bridging technique for use in trajectory simulations is illustrated in Figure 2.1.1.23-1.

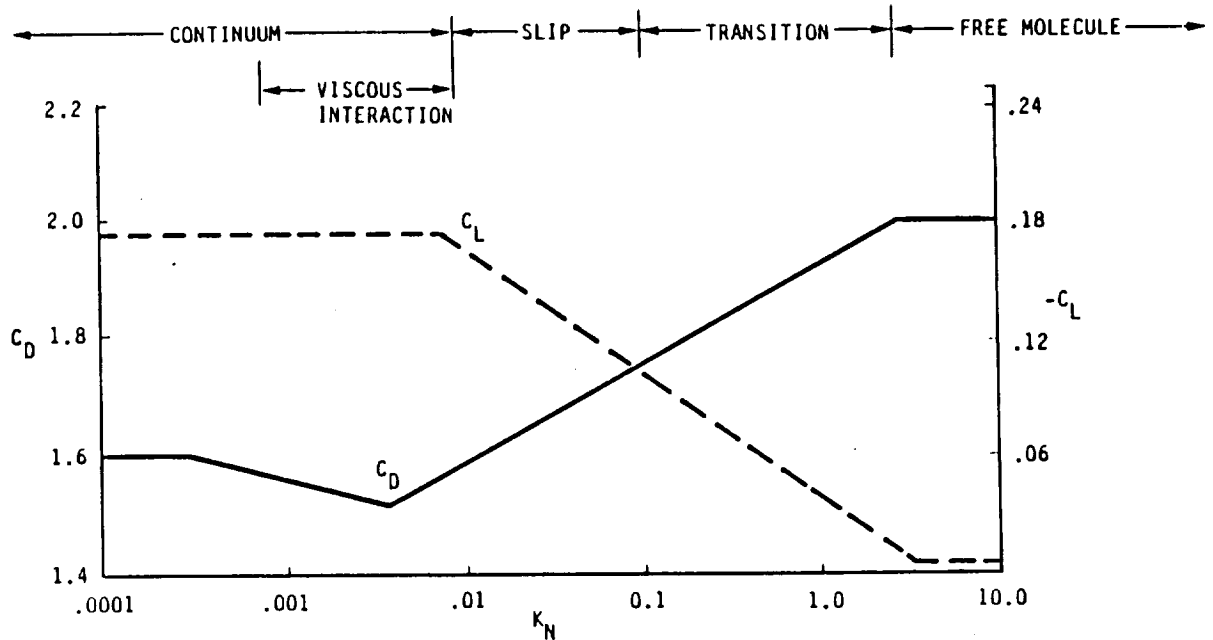


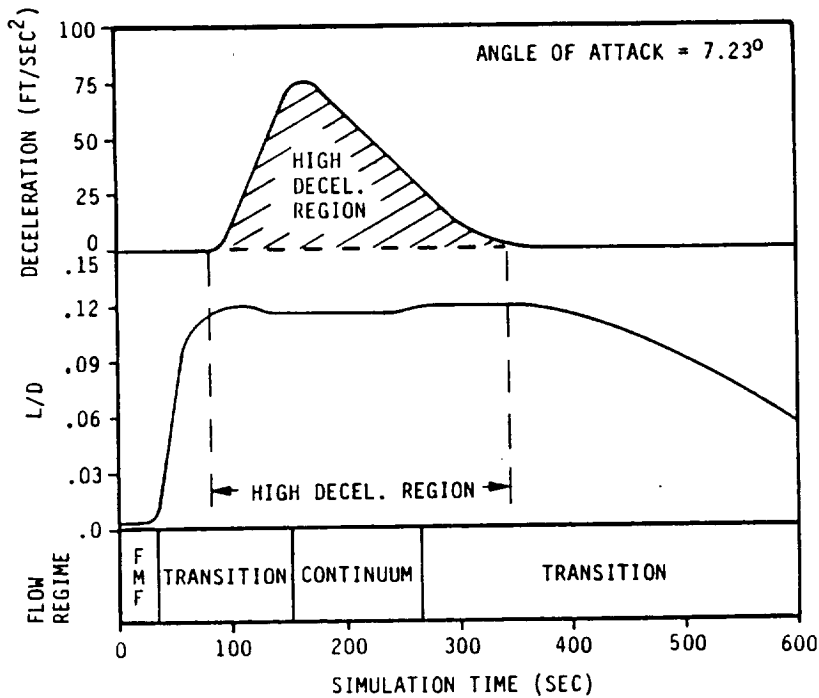
Figure 2.1.1.23-1 Flow Regime Transition Criteria Based on Viking Flight and Wind Tunnel Data

The most commonly accepted criteria for division of the flow regimes is the Knudsen number, Kn . The Knudsen number can be related to more familiar parameters of fluid mechanics, the Mach number (Mn) and the Reynolds number (Re), by the following equation: $Kn = 1.49085 * Mn/Re$. Using this equation, the boundaries of the various regimes can be defined.

2.1.1.24 - Free Molecular Flow Impact on L/D - After implementing the above model for lift and drag vs. flow regime, an analysis was undertaken to evaluate free molecular flow impacts. Typical results are shown in the time history profiles of acceleration and L/D shown in Figure 2.1.1.24-1. It can be seen from the data that the region of significant L/D decay is restricted to the extremely low acceleration regions of the aeropass, and thus has no impact on the aero trajectory. In addition, similar data for attitude control shows that the region of perturbed trim attitude is easily overcome by RCS jet firings.

One significant impact has been the incorporation of a free molecular flow predictor in guidance. Without this the guidance density feedback function is incorrectly biased in early and late entry.

We conclude that the free molecular flow effects have no significant trajectory impacts for the OTV.



- FREE MOLECULAR FLOW (FMF) REGIME DEGRADES LIFT CAPABILITY
 - LIFT DEGRADATION IS ONLY SIGNIFICANT IN THE LOW DECELERATION PORTIONS (PROFILES LEFT)
 - ACS HAS NO PROBLEM MAINTAINING DESIGN ATTITUDE IN FREE MOLECULAR AND TRANSITION FLOW REGIMES
 - IMPLEMENT FMF PREDICTOR IN GUIDANCE TO IMPROVE AERO DENSITY FEEDBACK
- CONCLUSION: FMF LIFT DEGRADATION HAS NO SIGNIFICANT TRAJECTORY IMPACT FOR OTV

Figure 2.1.1.24-1 Free Molecular Flow Impact on L/D

2.1.1.25 Aeropass Simulation Data

The following table summarizes key data used to drive the closed-loop Aeropass simulation. Ground-based and space-based OTV data are separated where appropriate.

ALL VEHICLES

L/D	= 0.116
ANGLE OF ATTACK	= 7.23°
MAX ROLL RATE	= 90°/SEC
ROLL DEADBAND	= 0.2°
TARGET INCLINATION	= 28.5°
GRAVITY MODEL	= ROTATING OBLATE (J ₂)
ATMOSPHERIC MODEL	= ROTATING OBLATE, 1962 STANDARD AND STS PROFILES

VEHICLE UNIQUE

GROUND BASED

BALLISTIC COEF.	= 3.78 LB/FT ²	= 6.52 LB/FT ²
RCS THRUST	= 25 LB EACH (3 JETS*)	= 100 LB EACH (3 JETS*)
RCS ISP	= 230 SEC	= 378 SEC
RCS LEVER ARM	= 7.75 FT	= 8.92
ROLL INERTIA	= 13200 SLUG-FT ²	= 23300 SLUG-FT ²
TARGET APOGEE	= 140 NM	= 245 N.M. (25 N.M. BELOW STATION)
ROLL ACCEL.	= 2.52 DEG/SEC ²	= 6.58 DEG/SEC ²

(NOTE; ONE RCS ROLL JET ASSUMED FAILED OFF)

2.1.1.26 Aeroguidance

The basic aeroguidance scheme is a predictor-corrector algorithm which targets to an exit orbit apogee and inclination. Guidance steers the vehicle by pointing the body-fixed lift vector in a direction which nulls apogee and inclination simultaneously. After the targets are met the lift vector is nulled via a continuous roll. It should be noted that the lift vector is never perfectly nulled out by this roll; however, guidance accounts for this by detecting its effect in the prediction process. The actual roll hold duration is controlled via a lateral velocity target which is the net sensed velocity in the lift direction accumulated during a roll hold. The use of this targeting method reduces the impact of L/D dispersions.

An important feature of the predictor-corrector approach is that it enables a preentry prediction to be made. This update bootstraps an initial control set while there are large timing margins. It also establishes a nominal entry attitude which reduces the roll response lags by pre-aiming the vehicle.

Because of density dispersions that will always occur in the atmosphere, a feedback routine is included which utilizes sensed accelerations from the navigation package to correct the onboard atmospheric model.

2.1.1.27 Lift Vector Targeting

Figure 2.1.1.27-1 illustrates the technique utilized to determine the OTV lift vector pointing. The inclination and apogee guidance algorithms produce desired vertical and horizontal velocity targets required to produce the desired exit trajectory. These two targets are added vectorally to produce a net required velocity target. The direction of this vector is the required pointing for the lift vector. The magnitude of the vector is the "velocity-to-go" target for the lateral accelerometers to use as a cutoff value for the roll hold.

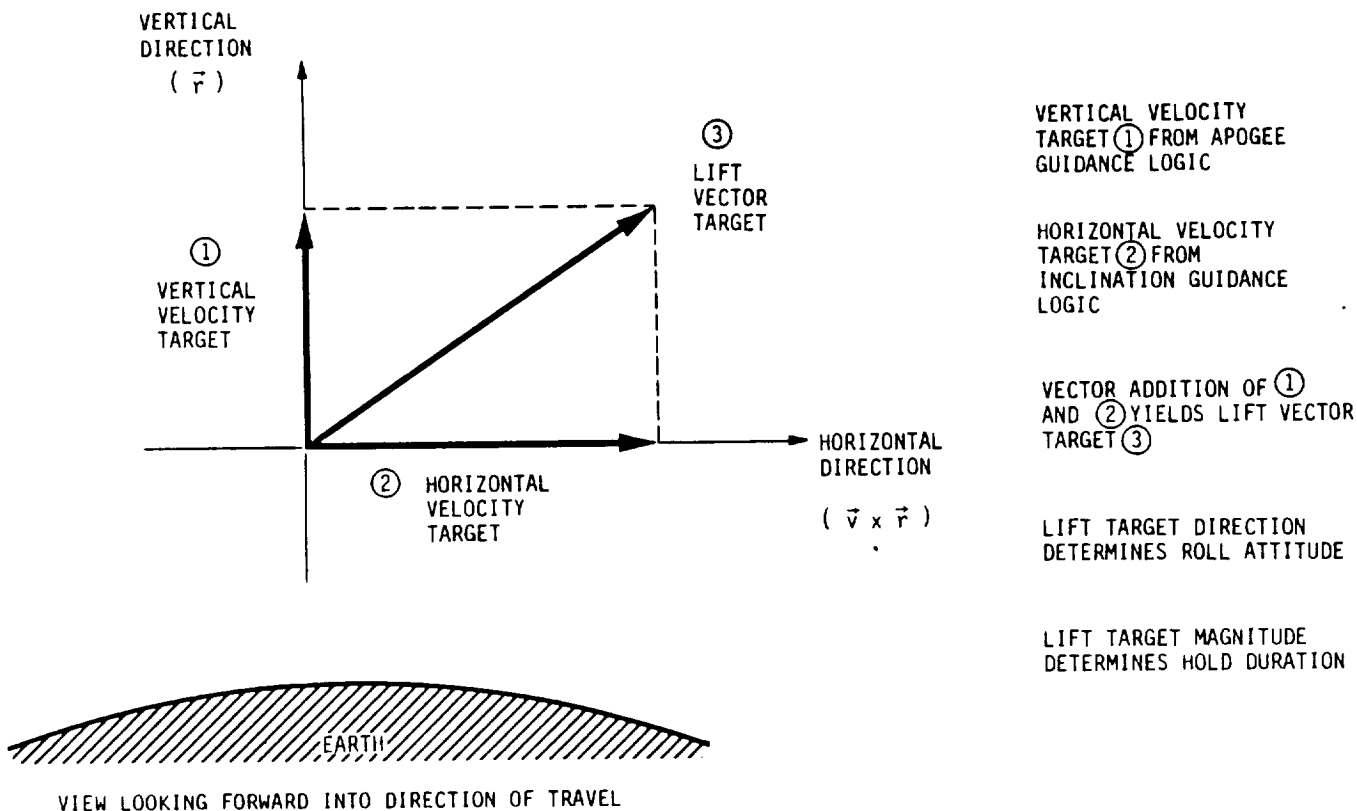


Figure 2.1.1.27-1 Lift Vector Targeting

2.1.1.28 Guidance Update Cycle

Figure 2.1.1.28-1 shows the functional flow of an aeroguidance update. Beginning at the left, the guidance function starts with the current navigation state vector plus commanded roll attitude and commanded lateral velocity from the previous update cycle. The navigation state plus sensed decelerations are fed into an atmospheric feedback function which acts to correct the onboard density model for observed fluctuations. The state vector and commanded controls are then fed into the trajectory prediction routine which produces estimated postero errors in inclination and apogee.

ORIGINAL PAGE IS
OF POOR QUALITY

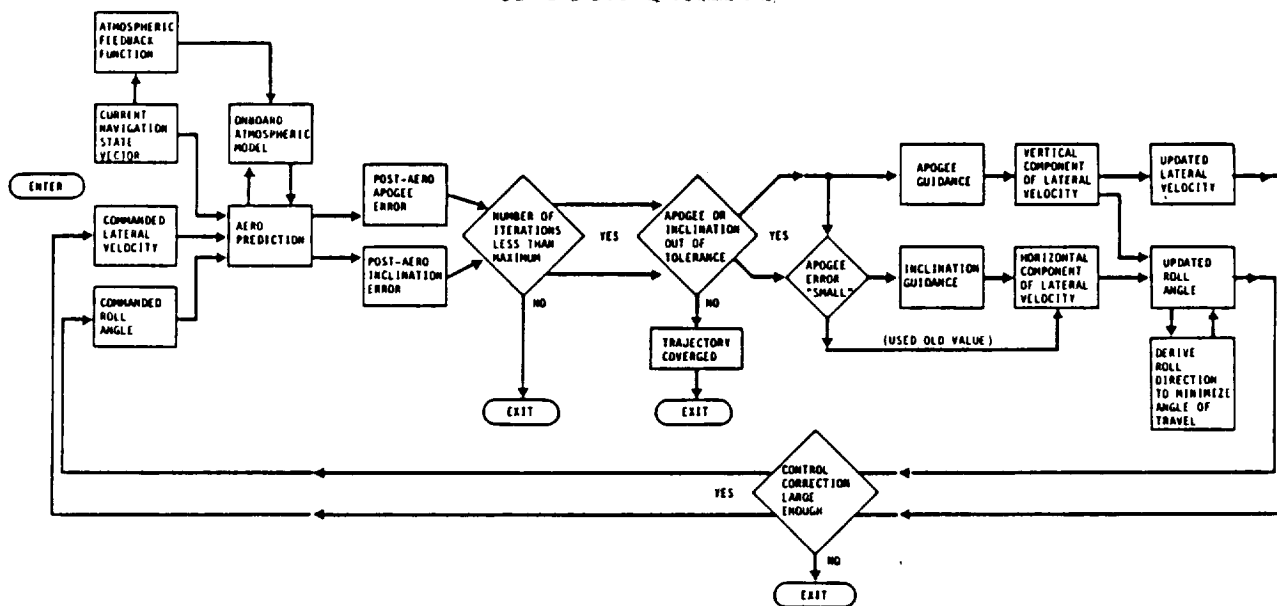


Figure 2.1.1.28-1 Guidance Update Cycle

If the maximum number of iterations for this update has been exceeded, execution is halted until the next update to avoid exceeding the vehicle's computational timing limits. If the estimated errors are both small enough, guidance has converged and the update function is exited. On the other hand, if either or both errors exceed a specified tolerance and the maximum iterations is not exceeded, the correction portion of the algorithm is entered. When performing corrections, the apogee routine is always executed. However, the inclination correction logic is only performed when apogee errors fall within an error band. The reason for this is that trajectory predictions with large apogee errors have false inclination values that will corrupt the inclination steering. If the inclination correction logic is so disabled, a previous output is used instead.

The apogee and inclination guidance functions produce vertical and horizontal components of lateral "velocity to be gained". These two components, when taken together, produce a new target roll attitude for the vehicle. The duration of the new roll hold is determined by the amount of time it takes to accumulate the vertical component of lateral velocity.

These new control variables are compared with the old ones to see if the changes are large enough to be realistically implemented. If not, the update function terminates; if so, processing continues and the new control variables are fed back into the prediction routine to start a new guidance iteration.

2.1.1.29 Roll Control Algorithm

The roll control function determines when roll attitude holds are to be initiated and terminated. It is a fast control function, operating at the same frequency as the basic attitude control function (10 millisecond frequency). The function implements the two control outputs of the aeroguidance update routine: commanded roll attitude and commanded lateral velocity.

The Figure 2.1.1.29-1 is entered from the left with a comparison of the commanded and actual roll attitudes. If the difference between the two is within the attitude deadband, then a roll hold is commanded. Otherwise the active roll is continued to acquire the commanded roll attitude.

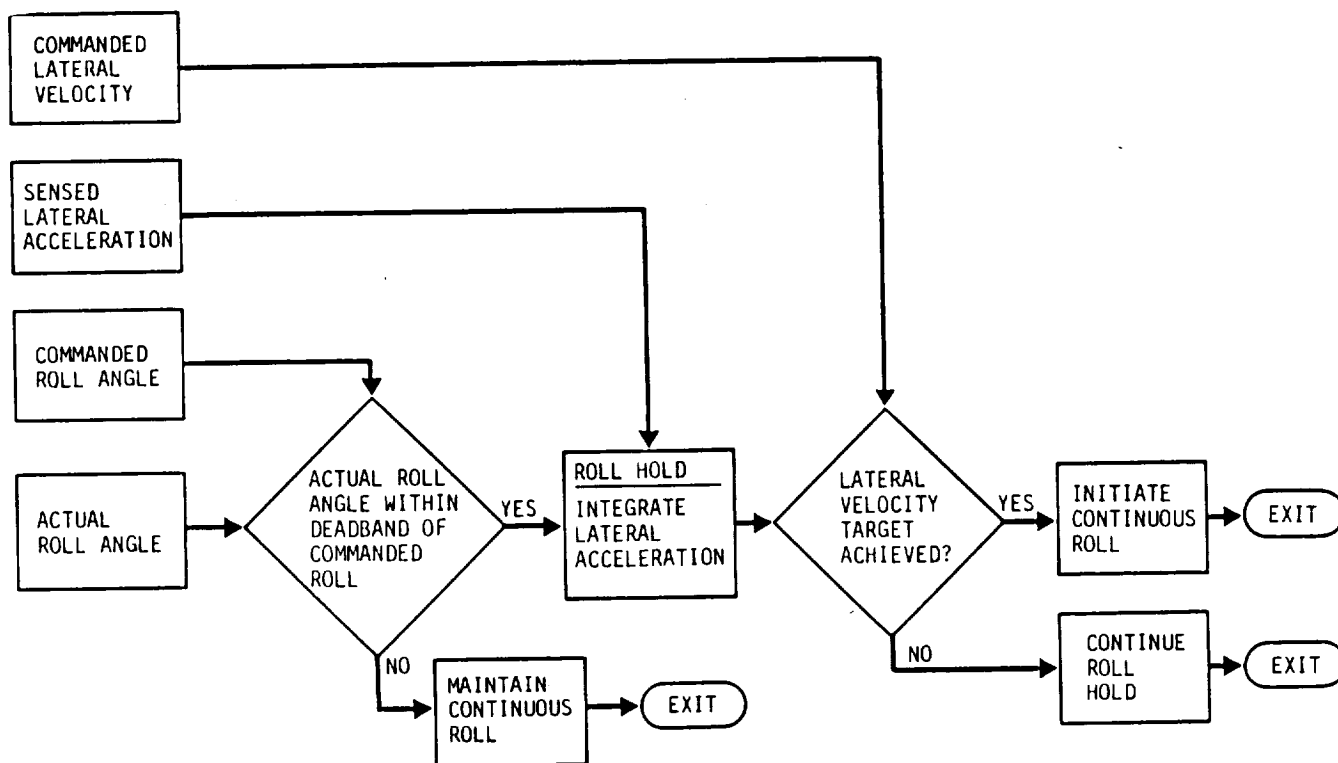


Figure 2.1.1.29-1 Roll Control Algorithm

If the vehicle is in a roll hold period, the output of the accelerometers is integrated in the lateral plane to produce the lateral sensed velocity. This velocity is compared with the commanded "velocity to go" to determine if the roll hold should continue. Once the sensed lateral velocity exceeds the commanded velocity, the roll hold is terminated and a continuous roll initiated.

2.1.1.30 Atmospheric Feedback--The atmospheric feedback function acts to correct the onboard atmospheric model for observed density shifts. This can be due to changes in vehicle aerodynamic properties and navigation errors as well as atmospheric shifts. The function is executed once at the beginning of each guidance update.

The functional block diagram (Figure 2.1.1.30-1) begins on the left with the current navigation state vector and the current sensed deceleration. The state vector is fed into the onboard atmospheric model which produces an expected deceleration level. This predicted deceleration is differenced with the measured value. The result is combined with previous deltas in an averaging technique which is then used to produce corrections to the onboard atmospheric model.

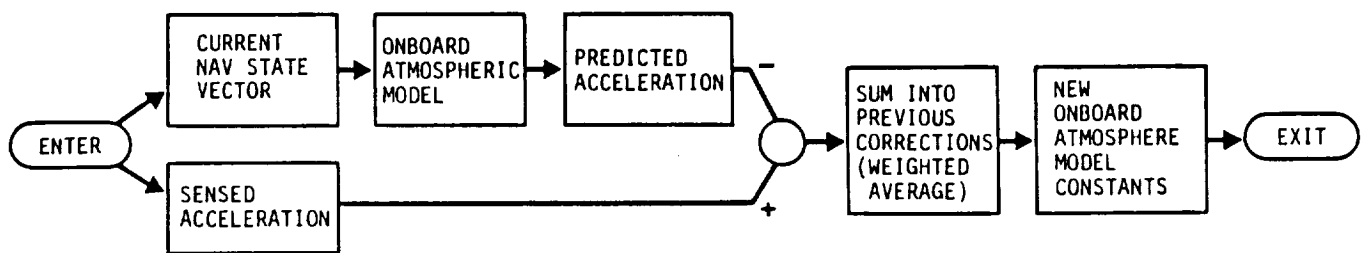


Figure 2.1.1.30-1 Atmospheric Feedback

2.1.1.31 Aeropass Parametrics

The following three sections present aeroassist parametric data derived from closed loop simulations. This data was generated for two ballistic coefficients ($W/C_D A = 3.78$ and 9.00 LB/FT^2). The parameters covered are post-aero circularization and phasing requirements, aeropass peak deceleration and airloads, and stagnation heating data. This information is used for post-aero orbit and operations design, structural load sizing and aerobrake thermal analysis.

The basic approach was to span the dynamic control corridor with entry trajectories flown through a 1962 standard atmosphere. By this means all possible entry conditions are covered.

2.1.1.32 Circularization Velocity and Phasing Shift

Figure 2.1.1.32-1 shows post-aero circularization requirements and phasing shifts. It is applicable to all ballistic coefficients considered. The circularization velocity is defined to be the delta-V required to circularize the exit condition orbit at its target apogee. It may be seen that this velocity is fairly constant across the corridor with a fairly sharp rise near the lower boundary. The increase in delta-V is due to the decay of the exit

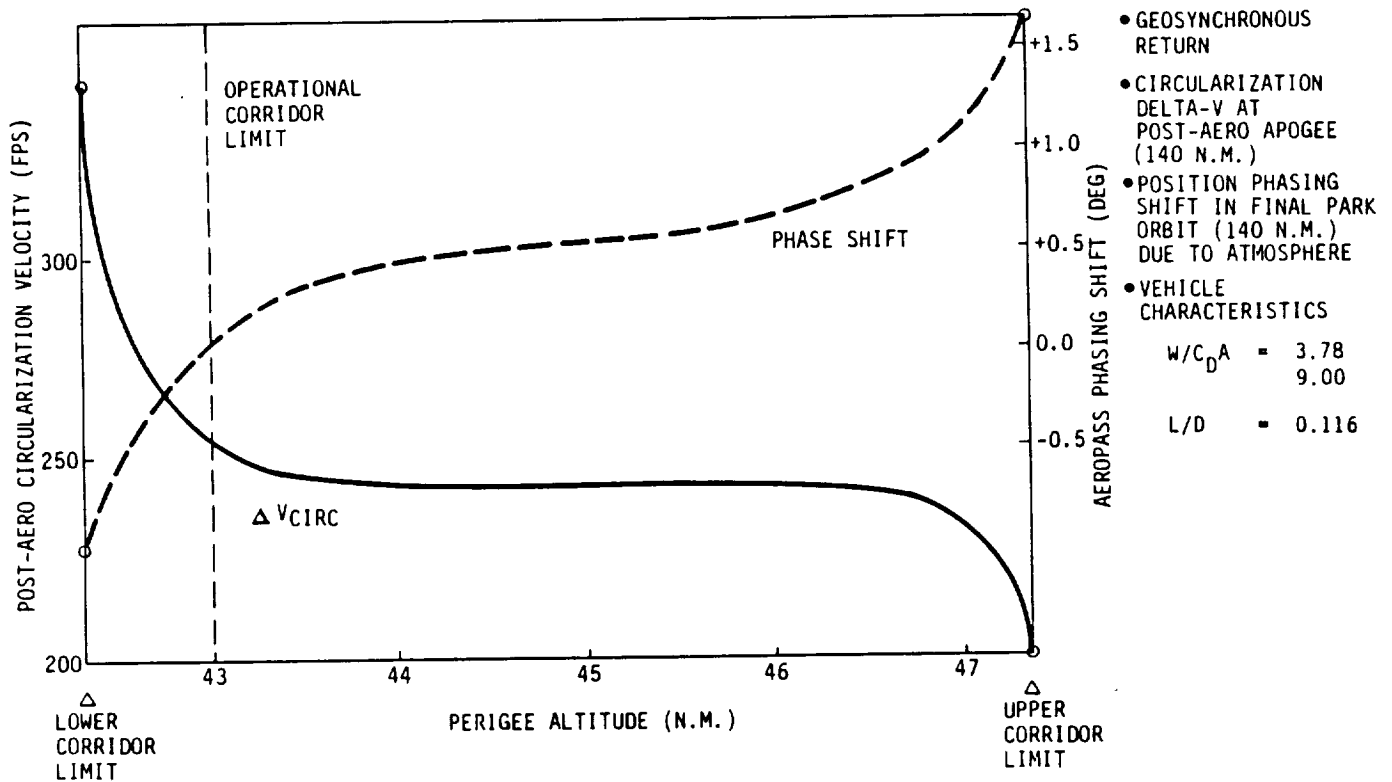


Figure 2.1.1.32-1 Circularization Velocity and Phasing Shift - All $W/C_D A$'s

orbit's perigee. As aeropasses are flown lower and lower in the control corridor, the vehicle is forced into steeper and steeper relative flight path angle trajectories in order to get quickly through the higher atmospheric densities at perigee. Because the exit apogees are fixed by guidance at the desired target altitudes, the perigee must decrease in the face of increasing exit flight path angles.

In order to avoid the performance penalty associated with this increase in delta-V, the lower 0.7 nm of the control corridor is eliminated. This leaves a resulting corridor width of 4.3 nm which is still adequate to cover the error budget of 4.01 nm. The post-aero circularization requirement is 250 fps.

The varying exit conditions also bring about relative phasing shifts, with respect to nominal, upon reaching final circular orbit. These relative alignment shifts must be nulled out for a successful rendezvous. From the chart it may be seen that the total phasing change from the bottom to the top of the control corridor amounts to about 1.6 degrees. To accommodate this, a single pass phasing orbit has been baselined for the first orbit after aerobraking.

Due to the interaction of the control system with the aerodynamic fluctuations presented by STS atmosphere profiles, trajectories flown with these dispersed atmospheres resulted in circularization burns and phase shifts which are slightly larger than the parametric results (Table 2.1.1.37-1). These dynamic variations are relatively small and do not represent a major mission impact. The parametric envelope for airloads and heating presented in the next two sections is not affected by these STS profiles.

2.1.1.33 Deceleration and Airloads

The peak deceleration and airloads are shown in Figure 2.1.1.33-1 over the range of the control corridor. The first graph (Figure 2.1.1.33-1) shows data for the low ballistic case ($W/C_D A = 3.78 \text{ lb/ft}^2$) while the second (Figure 2.1.1.33-2) shows the same information for a high ballistic number ($W/C_D A = 9.0$). The curves are identical because the two parameters are related by the constants of OTV weight and aerobrake area. Observed peak deceleration of 3 g's was used to size aerobrake support structure. The peak dynamic pressure of 15 psf (plus a shock modification factor) was used to derive required aerobrake shield strength.

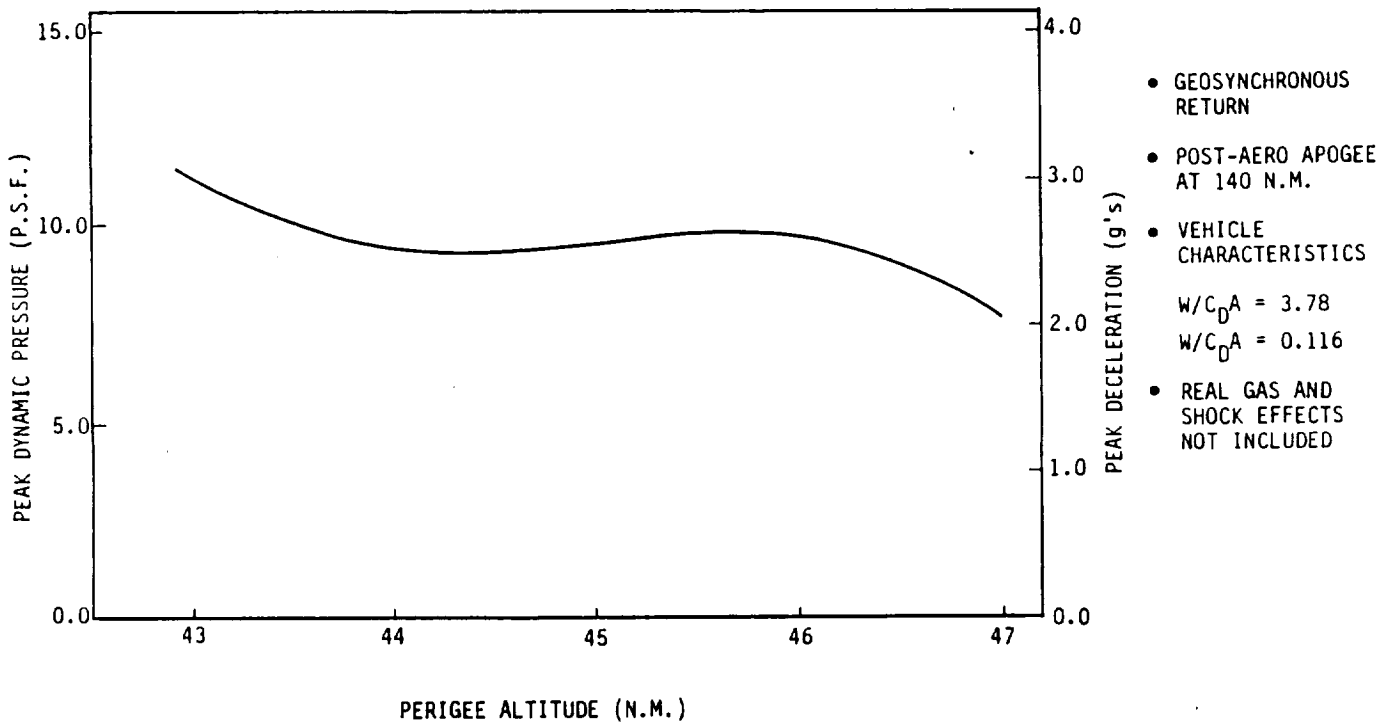


Figure 2.1.1.33-1 Deceleration and Airloads - Low L/D

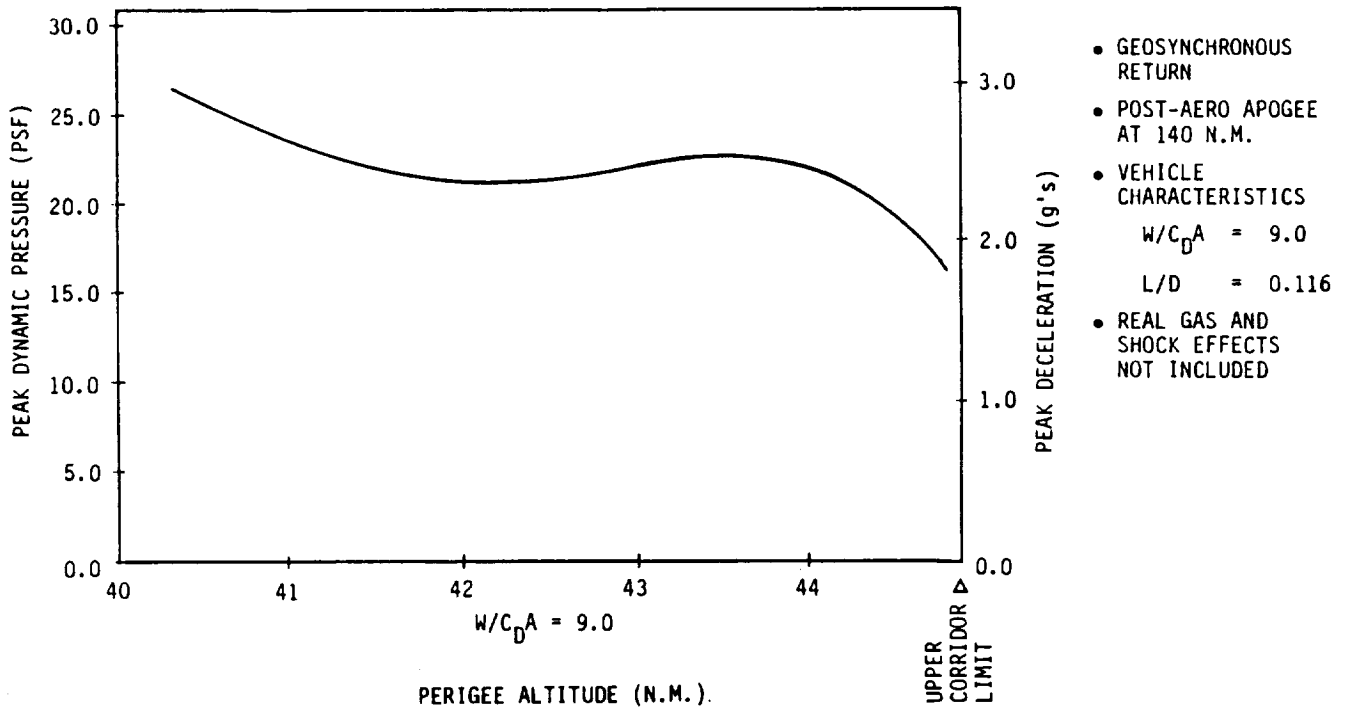


Figure 2.1.1.33-2 Deceleration and Airloads - High $W/C_D A$

2.1.1.34 Stagnation Heating

Peak thermal flux and integrated heat load (normalized to a one ft. nose radius) are shown for trajectories spanning the control corridor. The first graph (Figure 2.1.1.34-1) shows data for the low ballistic case ($W/C_D A = 3.78$ ($W/C_D A = 9.0 \text{ lb/ft}^2$)), while the second (Figure 2.1.1.34-2) shows the same information for a high ballistic number. Note that for aerobasses that travel deep in the atmosphere (short duration, high deceleration) the peak thermal flux is high while the integrated heat load is low, while for trajectories high in the corridor (long duration, low deceleration) the opposite is true.

This data is used as input for the aerothermal analysis which must also include real gas effects and radiant shock heating, not included there. Aerobrake TPS thicknesses were sized by the corridor extremes which represent the worst-case conditions.

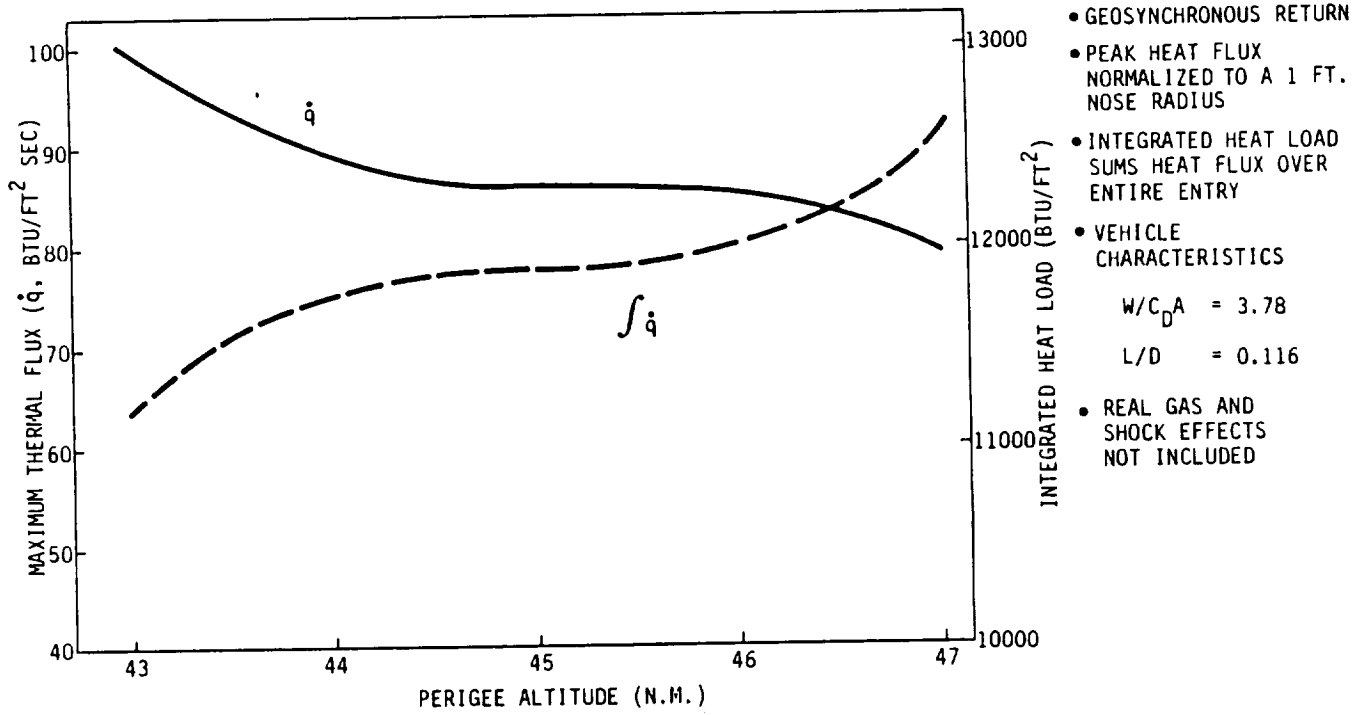


Figure 2.1.1.34-1 Stagnation Heating - Low $W/C_D A$

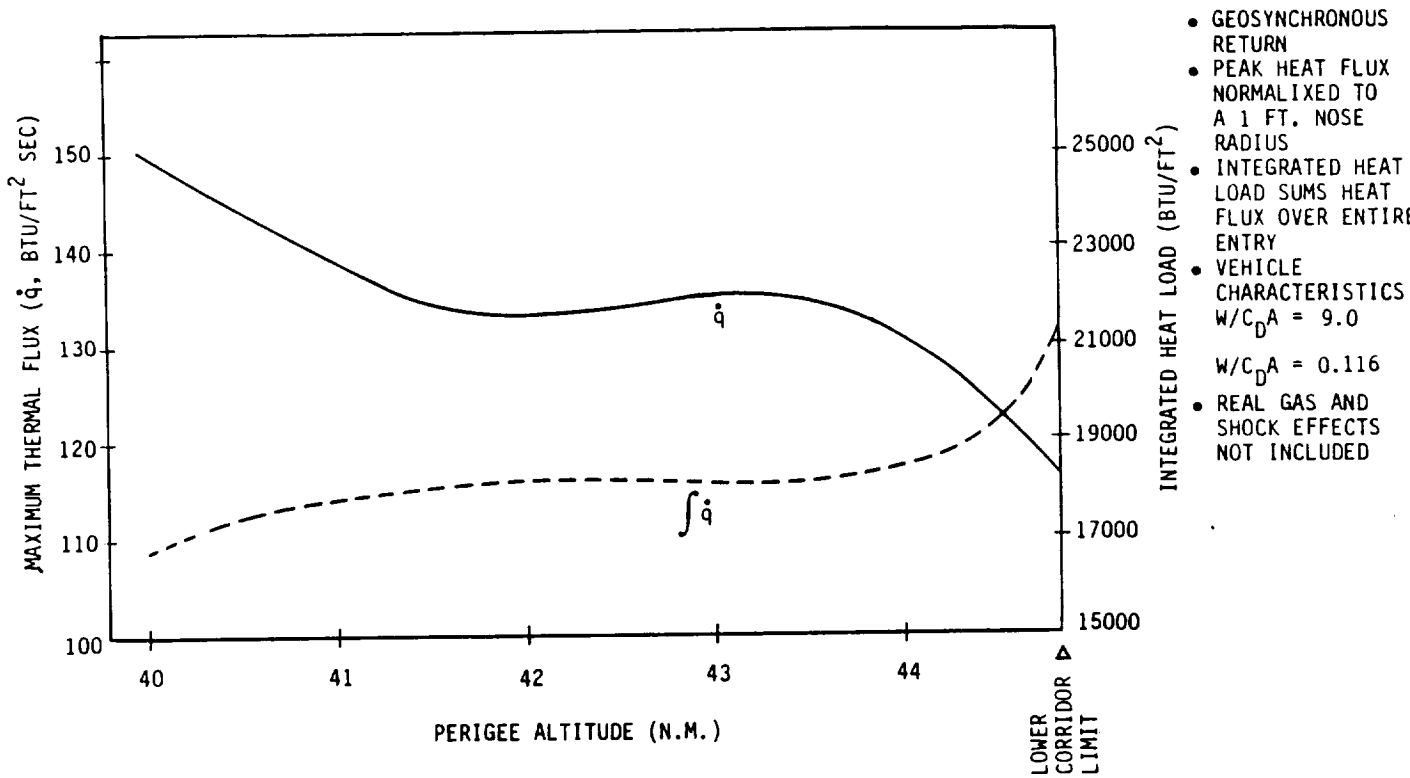


Figure 2.1.1.34-2 Stagnation Heating - High $W/C_D A$

2.1.1.35 Aeroguidance Dispersions: Single Parameters

A variety of dispersions were simulated one at a time to test the robustness of the guidance technique. Where applicable, these dispersions are at three sigma levels. The dispersions are as follows:

- 1) Perigee Altitude Errors - Entry trajectories which spanned the control corridor were generated. This represents a variation in the vacuum perigee altitude of plus or minus 2.2 nm.
- 2) Inclination Errors - Dispersions of plus or minus 0.5 deg. were utilized to test the inclination targeting logic. This greatly exceeds the entry error estimate of 0.048 deg.
- 3) STS Observed Fluctuations - In the course of Shuttle reentries measurements have been taken which have allowed plots of density variations to be produced. The data set which has been used is from STS-2, 4, and 6. These profiles establish high frequency density variations in the atmosphere.
- 4) Global Density Shifts - A density multiplier is applied to the entire 1962 standard atmosphere. Variations of $\pm 15\%$ and $\pm 40\%$ have been tested.
- 5) Angle-of-Attack Errors - Because of cg uncertainties, the vehicle will trim out at a different angle-of-attack than expected. Based on cg analysis and Viking experience a value of ± 1.5 degree has been used.
- 6) Entry flight path angle - the net effect of this dispersion is similar to a perigee altitude error, however a corresponding apogee increase occurs to keep the entry velocity constant. The dispersion value of $\pm .23$ deg. greatly exceeds the expected variation.

2.1.1.36 Aeroguidance Dispersions: Coupled Parameters--In order to evaluate performance of the OTV in a more strenuous environment, the single parameter dispersions mentioned previously were each rerun simultaneously with a shuttle density profile (STS-6). In most cases the dispersion values had to be reduced, but in all cases, they lie within the maximum values set by error analysis.

It should be noted that some of the dispersions were found to be skewed (density and angle of attack). This represents a failing in the simple method of nominal vacuum perigee targeting which is currently set at the midpoint of the control corridor. In actuality, the corridor does not have a linear nature, and nominal targeting must be biased off-center. How much this bias is, must be deferred to a more detailed performance optimization.

An added dispersion parameter is a worst case navigation error of 2000 ft. position and 14 fps. velocity. These coupled dispersions are summarized as follows:

o PERIGEE ALTITUDE ERRORS	<u>±</u> .2 NM
o INCLINATION ENTRY ERRORS	<u>±</u> .5 DEG
o GLOBAL DENSITY OR BALLISTIC COEFFICIENT SHIFT	+22%, -15%
o ANGLE OF ATTACK ERRORS	+2 DEG, -1 DEG
o ENTRY FLIGHT PATH ANGLE	<u>±</u> .02 DEG
o NAVIGATION ERROR	2000 FT 14 FPS

2.1.1.37 Aerosimulation Summary

Table 2.1.1.37-1 summarizes the results of these singly dispersed aeropass simulations. For each of the previously discussed dispersion parameters, the following information is displayed:

- 1) Apogee error in nautical miles.
- 2) Absolute perigee in nautical miles.
- 3) Inclination error in degrees.
- 4) Ascending node shift in degrees.
- 5) Net plane change due to combined effect of inclination and ascending node error (deg).
- 6) Phase shift of OTV after circularizing at target altitude (deg). This is computed with respect to the nominal (undispersed) profile and is a measure of the amount of phase adjustment required in the postaero phasing orbit.
- 7) Circularizing Delta-V (FPS). This is the net velocity required to perform a Hohmann transfer from the exit orbit to the circular target orbit (140 n.m. for these ground based missions)
- 8) Inclination trim Delta-V is the amount of velocity to correct the net plane error (FPS).
- 9) Net Delta-V is the sum of 7) & 8).
- 10) Net propellant is the pounds of MPS propellant required to perform the net Delta-V of 9).
- 11) Roll RCS usage is the pounds of propellant required to perform all the aeroroll maneuvers. This quantity does not include pitch and yaw damping requirements. Based on independent simulation results this is estimated to be less than 10% of the roll propellant requirement.
- 12) Peak heat flux. This is the largest observed value of the reference stagnation point convective heat flux referenced to a one ft. sphere (BTU/ft.² sec.).

Highlights of the single parameter dispersions are as follows:

Table 2.1.1.37-1 Aerosimulation Summary: Single Parameters

DESCRIPTION	EXIT CONDITIONS						POSTAERO TRIM BURNS				ROLL RCS USAGE	PEAK HEAT FLUX
	APOGEE ERROR	PERIGEE ALTITUDE	INCLIN. ERROR	ASCEND NODE SHIFT	NET PLANE CHANGE	PHASE SHIFT	CIRCULARIZI ΔV	INCLIN TRIM ΔV	HET ΔV	NET PROP.*		
	(N.M.)	(N.M.)	(DEG)	(DEG)	(DEG)	(DEG)	(FPS)	(FPS)	(FPS)	(LB)		
UNDISPERSED	.00	6.53	-.0033*	-.0219*	.0109*	0.0*	241.05	4.04	245.89	125.65	2.94	86.74
PERIGEE ERROR												
+2.20 NM	-.03	9.83	-.0005*	-.0504*	.0241*	+.5004*	235.07	10.68	245.75	125.75	3.49	79.39
-2.20 NM	.00	-8.46	-.0040*	-.0002*	.0056*	-.0238*	268.61	2.46	271.07	138.63	1.61	98.66
INCLINATION ERROR												
+.5°	.02	6.66	+.0002*	+.0146*	.0070*	-.0422*	240.71	3.09	243.80	124.57	3.48	87.04
-.5°	.06	5.39	-.0007*	-.0707*	.0375*	-.0303*	243.12	16.66	259.78	132.81	5.81	89.47
DENSITY SHIFT OR BALLISTIC SHIFT												
+40%	.05	3.57	-.0117*	-.0201*	.0151*	-.2025*	245.53	6.72	252.25	128.92	12.72	90.32
-40%	.01	6.28	-.0070*	-.0250*	.0139*	+.2901*	242.22	6.15	248.37	126.92	12.49	85.50
TRIM ANGLE ERROR												
+1.5	-.02	0.81	-.0043*	-.0252*	.0127*	-.0974*	251.51	5.65	257.16	131.46	13.14	88.17
-1.5	.00	5.69	-.0029*	-.0248*	.0155*	-.0324*	242.49	6.86	249.35	127.43	10.43	86.11
FLIGHT PATH ANGLE												
+.233°	.04	-2.57	-.0032*	-.0112*	.0062*	-.6503*	257.72	2.76	260.48	133.17	1.77	97.30
-.233°	.19	0.79	-.0091*	-.0409*	.0215*	+.3880*	237.24	9.56	246.79	126.11	10.45	82.88
SHUTTLE ATMOS.												
STS-2	2.06	2.21	+.0036*	-.0440*	.0213*	+.3779*	252.39	9.45	261.84	133.87	22.57	78.14
STS-4	2.57	10.58	+.0024*	-.0723*	.0346*	+.4127*	238.06	15.36	253.42	129.53	25.57	83.73
SIS-6	.01	12.76	+.0181*	-.0056*	.0183*	+.4207*	229.41	8.12	237.53	121.34	21.31	78.25

(NOTE: RESULTS ARE FOR GROUND-BASED GEO-RETURN MISSION. TARGET APOGEE = 140 NM)
 (* PROPELLANT REQUIRED FOR 7500 LB VEHICLE, ISP = 460 SEC)
 (** STAGNATION POINT CONVECTIVE HEAT FLUX,
 BTU/FT²-SEC. REFERENCED TO A 1 FT SPHERE)

Errors in apogee and inclination are quite small (the largest apogee error is 2.57 nm for STS 4 and the largest inclination error is .0181° for STS 6). Phase shift errors span a total range of 1.4042° which is easily accommodated by a single pass postaero phasing orbit. Total correction Delta-V ranges from 243.80 to 271.07 fps which translates to an MPS propellant requirement of 124.57 to 138.63 lb. This represents a fairly small variation of only 14 lbs.

Peak RCS roll usage is 25.57 lb. (for STS 4). Peak heat flux values range from 78.14 to 98.66 BTU/ft² sec. This range lies within the two limiting profiles used for aerobrake TPS design which are the cases were flown at the dynamic top and bottom of the aerocontrol corridor. These limiting cases had peak heat fluxes ranging from 75.33 to 100.58 BTU/ft² sec. Not shown is the integrated heat flux which also was bounded by the limiting cases for aerobrake design.

See Appendix 2.1.1 for detailed profiles of selected trajectories.

Table 2.1.1.37-2 gives the results of this coupled parameter dispersion analysis as follows:

ORIGINAL PAGE IS
CONTAINED IN
REF ID: A68100

Table 2.1.1.37-2 Aerosimulation Summary: Coupled Parameters

DESCRIPTION	EXIT CONDITIONS						POSTAERO TRIM BURNS				ROLL RCS	PEAK HEAT FLUX	
	APOGEE ERROR	PERIGEE ALTITUDE ERROR	INCLIN. ERROR	ASCEND. NODE SHIFT	NET PLANE CHANGE	PHASE SHIFT	CIRCULARIZ. ΔV	INCLIN. TRIM ΔV	NET ΔV	NET PROP. USAGE			
THE FOLLOWING:	(N.M.)	(N.M.)	(DEG)	(DEG)	(DEG)	(DEG)	(FPS)	(FPS)	(FPS)	(LB)	(LB)	**	
UNDISPERSED	+ .08	6.53	- .0033*	- .0219*	.0109*	0.0*	241.05	4.84	245.89	125.65	2.94	86.74	
PERIGEE FLT PATH ERROR													
+0.2M	+ .023*	-6.40	+6.69	+ .0166*	- .0004*	.0166*	+0.8521*	251.91	7.36	259.27	132.54	25.43	77.40
-0.2M	- .023*	-15.70	-4.72	- .0093*	- .0343*	.0188*	+1.0954*	289.27	8.35	297.62	152.35	18.29	78.47
INCLIN ENTRY ERROR													
+ .5°	-15.34	-7.22	- .0005*	+ .0015*	.0009*	+1.0483*	293.24	0.40	293.64	150.29	28.61	80.24	
- .5°	-6.66	-0.58	- .0055*	- .1731*	.0028*	+ .7268*	264.57	36.74	301.31	154.26	38.59	81.93	
DENSITY, W/C _D A													
+22%	-2.77	10.95	- .0030*	- .0687*	.0329*	+ .4908*	237.20	14.60	251.80	128.69	30.34	80.61	
-15%	-22.05	4.98	- .0162*	- .0722*	.0381*	+1.7556*	301.85	16.89	318.74	163.28	25.12	77.18	
ANGLE OF ATTACK													
+2°	-10.98	-7.61	- .0009*	- .0296*	.0141*	+ .8400*	286.32	6.27	292.59	149.75	20.52	80.07	
-1°	-11.36	-0.57	- .0001*	- .0289*	.0138*	+ .9516*	273.98	6.12	280.10	143.29	23.26	77.82	
NAVIGATION													
2000 FT	+1.88	11.13	+ .0161*	- .0371*	.0239*	+ .4275*	235.85	10.60	246.45	125.94	34.31	76.55	
14 EPS													

(NOTE: RESULTS ARE FOR GROUND-BASED GEO-RETURN MISSION. TARGET APOGEE = 140 NM)
 (* PROPELLANT REQUIRED FOR 7500 LB VEHICLE, ISP = 460 SEC)
 (** STAGNATION POINT CONVECTIVE HEAT FLUX, BTU/FT²-SEC, REFERENCED TO A 1 FT SPHERE)

Apogee errors are larger than with the single parameter set (largest value = 22.05 nm). Further work with optimizing the nominal aim point of the OTV would probably greatly reduce this quantity (notice that most of the results have a skew to them). However, this relatively large apogee error does not significantly impact the overall OTV performance as will be seen.

Inclination errors are very manageable. The largest one is only .0166°. The largest resulting net plane change is .0828° which requires 36.74 FPS (and 19 lbs of propellant) to correct.

The total range of phasing errors is 1.7556°. This slightly exceeds the results of the parametric analysis presented earlier (1.6° shift) However, the single pass phasing orbit illustrated previously can completely correct this.

The maximum correction Delta-V required is 318.74 FPS which results in an MPS propellant usage of 163.28 lb. When contrasted with the minimum usage from the previous chart of 121.34 lb, we see that even with a relatively large apogee error, the total variation in OTV MPS propellant is only 42 lb.

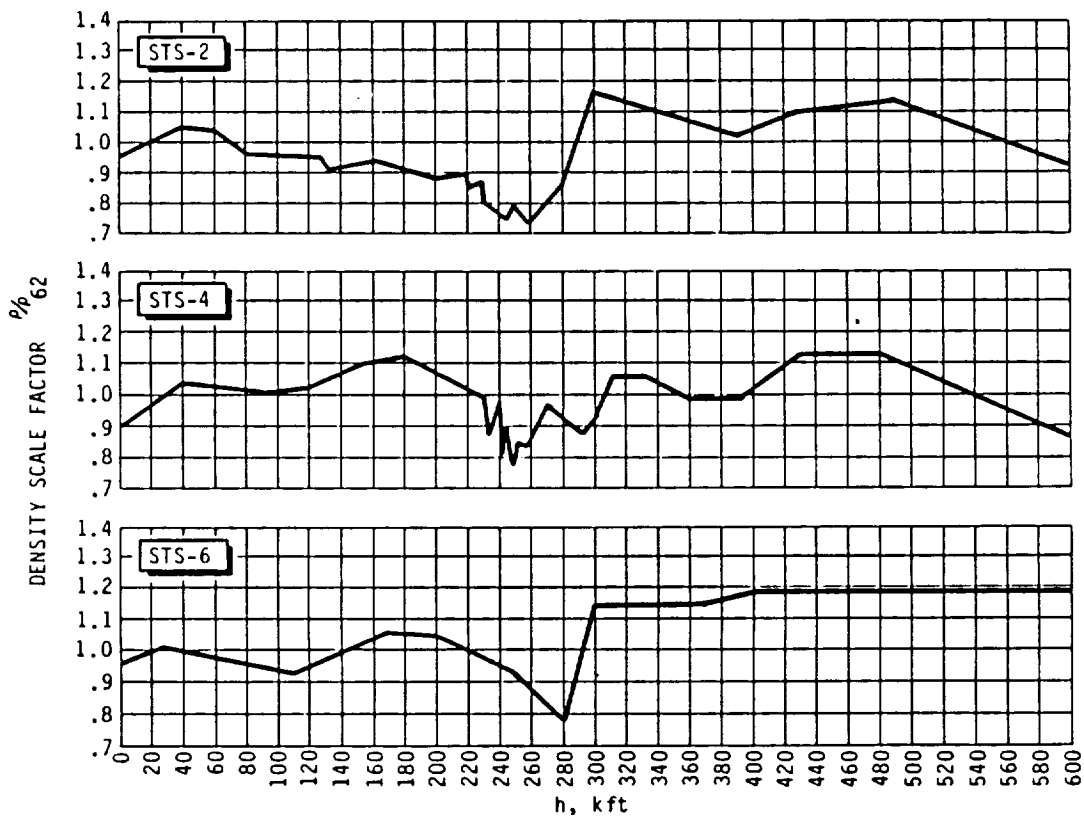
The maximum roll RCS usage is 38.60 lb.

The peak heat flux ranges between 76.55 and 81.93 BTU/ft²-sec. This peak heat flux (as well as the integrated heat flux, not shown) lies within the thermal limits used to size the aerobrake.

In conclusion, a relatively severe range of dispersions has not violated any of the system constraints of the OTV aero-pass operation. All of the dispersions equal or exceed 3 sigma limits established by error analysis. Thus, a comfortable operational envelope has been verified for our OTV configuration. Further optimization of the nominal targeting could certainly improve these results. This is left to a later effort.

2.1.1.38 STS Atmospheric Profiles

The most severe dispersions for the aeropass guidance system are STS-derived fluctuating atmospheric density profiles because of the way these fluctuations can couple into the control response time. Figure 2.1.1.38-1 shows the basic atmospheric profiles used for STS-2, 4, 6 density dispersions. The data is expressed as variations with respect to the 1962 standard atmospheric model.



DATA COURTESY OF J. GAMBLE & C. CERIMELE, JSC

Figure 2.1.1.38-1 STS Atmospheric Profiles

2.1.1.39 Atmospheric Density Feedback

The Figure 2.1.1.39-1 shows the response of the onboard atmospheric model to shifts in the density environment. The heavy line shows the density profile derived from STS-4 reentry, displayed as a function of altitude, which is used as the environmental model in the simulation. As the vehicle flies through the changing atmosphere, estimates of the density are generated onboard from information supplied by the accelerometer package. These density feedback measurements are averaged together to give the response denoted by the dotted line. The averaging process acts to damp out response transients which would otherwise result from the sharp fluctuations. At each point that the feedback routine is executed, the new estimate of the global density is applied uniformly to the entire atmospheric model.

Once the OTV has started onto its outbound leg (as indicated by its velocity falling below 27600 fps.), the averaging of feedback data is dropped and direct measurements used instead.

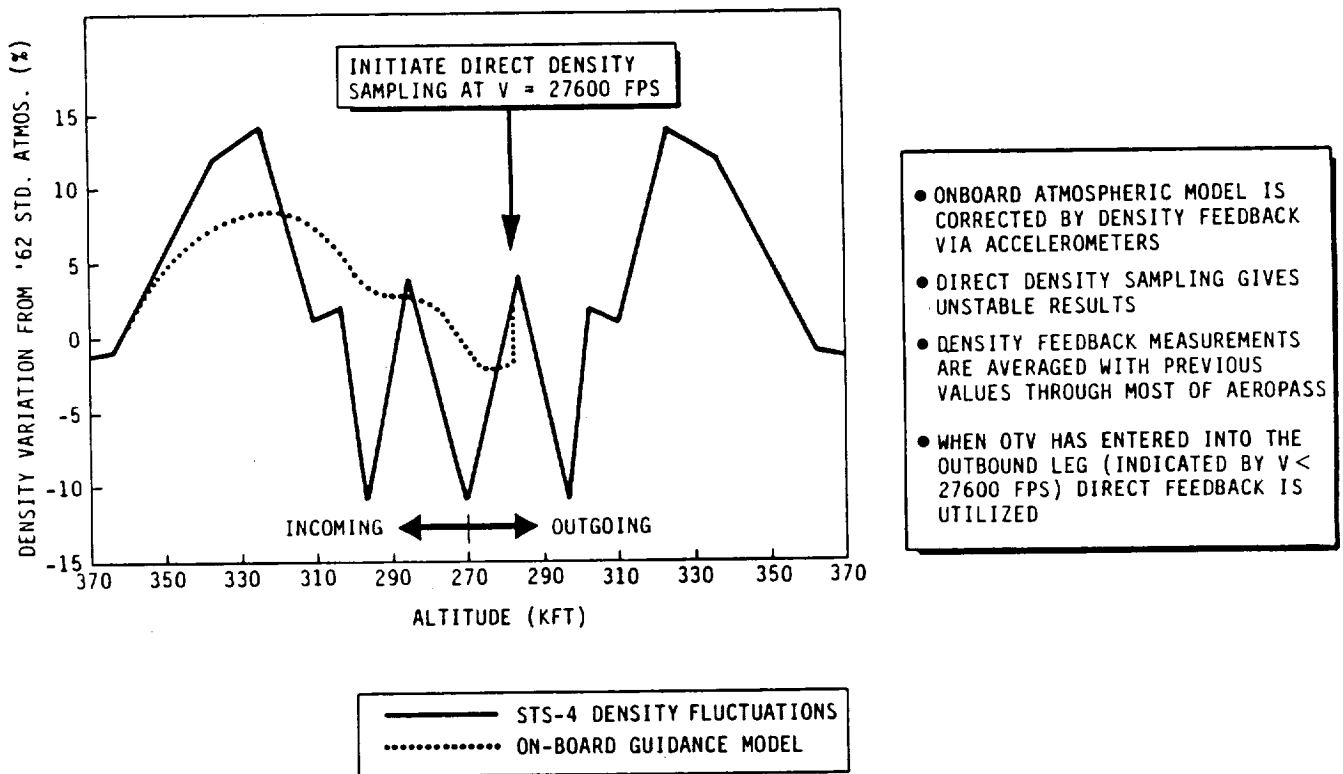


Figure 2.1.1.39-1 Atmospheric Density Feedback

2.1.1.40 CG Uncertainty Assessment

A preliminary cg analysis for our ground and space based vehicles was undertaken to assess aero trim attitude shifts. The primary sources of uncertainty are the vehicle and aerobrake's dry weight cg uncertainty, and propellant imbalances between the twin lox and LH₂ tanks. This latter effect is minimized through the use of point sensors in the bottom of the tanks which, when coupled with the P.U. system, act to accurately balance the residuals (to within 16 lb./tank for lox, 3 lb./tank for LH₂).

Because the greater mass uncertainty is in the lox tanks, these are aligned perpendicular to the pitch plane which acts to minimize dispersions in angle of attack. This results in the rectangular cg envelope shown in the diagram. The worst case trim attitude impact is obtained by placing the vehicle cg in one of the corners furthest from the vehicle centerline. Upon doing this the following shifts are obtained:

	TRIM ATTITUDE SHIFT	LIFT DIRECTION SHIFT
Ground-Based OTV	.76°	6.17°
Space-Based OTV (7.5K P/L)	1.12°	7.75°

These results are an acceptable impact to the vehicle. The trim attitude shift is detected by the aeroguidance which compensates its targeting. The lift direction shift is detected by the IMU package and biases the vehicle roll pointing accordingly.

One requirement from this analysis is that an active payload adapter will be required to adjust a returned payload's cg location prior to aeroentry.

2.1.1.41 Relative Control Capability

Using parametric data generated by our aeroentry computer simulation, we have normalized the control corridor capabilities of three major OTV concepts.

Figure 2.1.1.41-1 illustrates the JSC Raked Brake (L/D = 0.3), the Martin Low Lift Fabric Brake (L/D = 0.12), and two Boeing Ballutes (turn down ratios of 2.2 and 1.5). Also shown is our evaluation of the control capability required to perform the aeropass successfully.

Both the lifting brake and raked cone meet the required capability. Of concern is the fact that the ballute falls short in its trajectory control ability.

Because our concept meets the required capability without overexceeding it, we feel that the Low Lift Brake will be the most efficient aerobrake design.

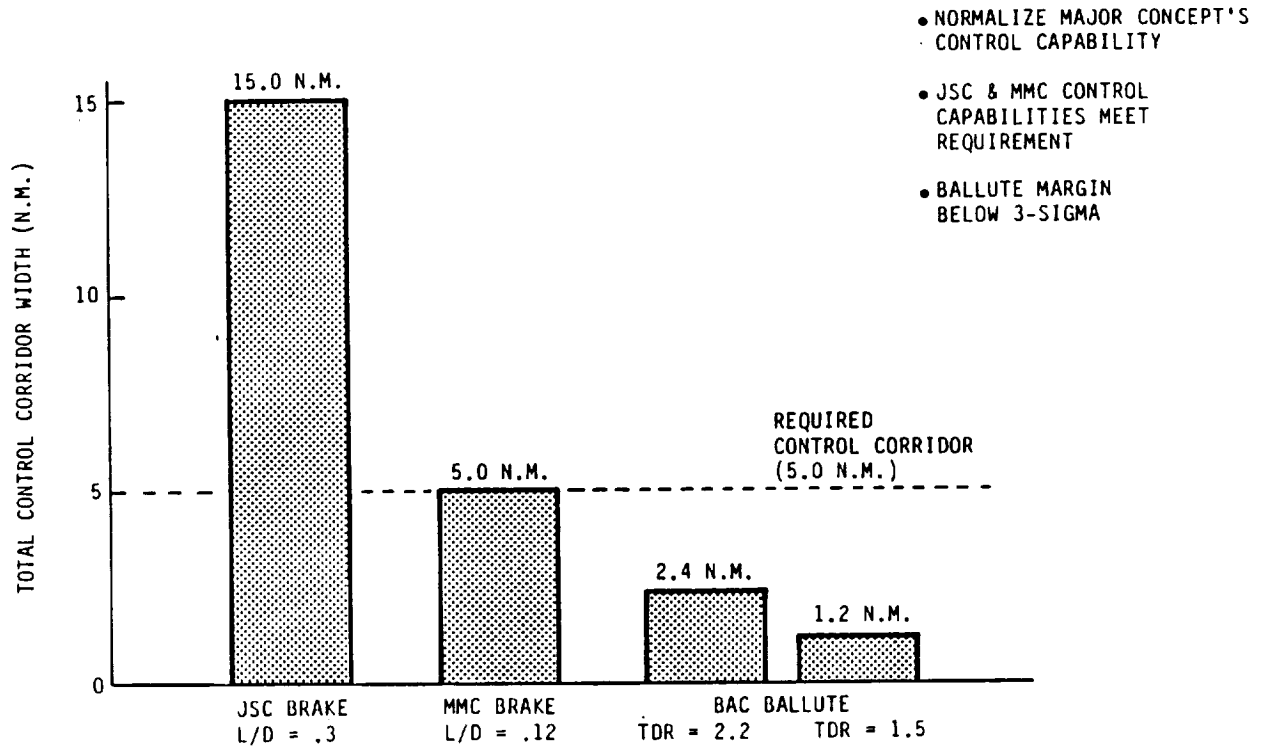


Figure 2.1.1.41-1 Relative Control Capability

2.1.1.42 Aeroguidance Highlights

The aeroguidance technique utilizes a predictor corrector technique for steering the vehicle through the aerobraking phase. Some of the algorithm highlights are as follows.

Because it is a predictive method, an update can be performed before the atmosphere is actually reached. This allows preaiming of the vehicle lift vector to reduce system response time to off-nominal aerodynamic conditions.

The use of a predictor-corrector minimizes integration difference with the onorbit guidance since this package is envisioned to also be a predictor-corrector technique (similar to algorithms used on Centaur and IUS). Since many of the software modules would be shared (such as the integrator, gravity model, etc.) the size of the overall guidance package would be minimized. This type of technique also does not require as many gain constants as fly-by-wire systems and thus requires less pre-mission support.

Our design implementation results in a self-starting algorithm which does not require a nominal trajectory base to start with. In addition, the same data load can be used for a variety of trajectories without modification.

Because the continuous roll nulls out the body-fixed lift vector, the attitude hold phases target the precise attitude required for apogee and inclination correction simultaneously, eliminating the need for bank reversals. This minimizes the number of start/stop transients which reduces the attitude fuel requirements. In addition, a fairly low roll rate of 1.5 rpm (90°/sec) provides adequate control response time.

Because of expected transients in the atmospheric density, an acceleration feedback algorithm is critical to maintaining the correct exit conditions. This feedback routine requires no special instrumentation, only the normal outputs of the accelerometer package.

The attitude hold duration is determined by lateral velocity targets rather than start and stop times which minimizes the impact of lift variations.

2.1.1.43 Long Duration Attitude Control Options

The long duration of the manned servicing mission prompted an evaluation of alternate means of controlling the vehicle attitude. Momentum exchange devices have been used with good success on such programs as Skylab where conservation of RCS propellant was important over a lengthy flight duration. Three momentum exchange systems were considered for OTV: 1) a reaction wheel assembly (RWA), 2) single gimbled control moment gyro (CMG), and 3) double gimbled control moment gyro (DGCMG). All configurations required a despun table mount to accommodate the 0.5°/sec thermal roll which is required for most of the on-station operation.

Utilizing the space-based cryo OTV (midterm configuration) the momentum capability required of such a system is 291 FT-LB-SEC per axis. When candidate systems are sized to accommodate this, the following results are obtained:

	<u>Hardware (lb.)</u>	<u>Power (Watts)</u>
RCS (Baseline)	202 (fuel)	--0
RWA (3 units)	415	335
CMG (4 skewed units)	580	200
DGCMG (2 units)	440	100

It is readily seen that based on hardware weight alone the RCS option is most attractive. Other factors which contribute to this conclusion are its reduced complexity and reduced dry weight (the momentum devices cannot completely replace the RCS system). Based on this study all vehicles were equipped with RCS systems only.

Based on the use of error analysis we have sized a lifting brake with control margin adequate to perform the aeropass with 3-sigma confidence. By minimizing the required control we have also minimized the weight of the aerobrake. Our design has been verified through the use of a variety of closed-loop aeropass simulations.

2.1.1.44 RCS Configuration

The primary driver for the jet arrangement of the RCS system is that no six degree of freedom (attitude plus translation) requirements exist for our baseline missions. The current philosophy is for payloads to provide their own translation and docking capability after the OTV has brought them within rendezvous range.

Three degrees of freedom (pitch, yaw, and roll) is provided by six basic force vectors. Two RCS jets are associated with each attitude force direction for redundancy, resulting in a total of 12 attitude control engines. In addition, two +X translation jets are provided to perform vernier trim burns and propellant dump settling. This function becomes very important when the vehicle is nearly empty, as the shutdown uncertainties of the main engine can result in velocity errors of as much as 2 FPS in this state (based on RL-10 data). This level of uncertainty would have a large impact on the aero-entry accuracies. Redundancy in translation is not provided since failure of a translation jet can be corrected for by utilizing an appropriate pitch engine to balance torques.

The RCS engines are packaged into two clusters mounted in the aft of the vehicle. A forward location was considered early in the design process; however, this position is extremely sensitive to cg shifts with propellant usage (attitude control is lost completely when the cg lies on a line between the jet clusters). This sensitivity is due to the fact that these jets must fire laterally (perpendicular to the vehicle longitudinal axis) to avoid impinging on the aerobrake or the payload. Additionally, forward jet locations cannot supply aft pointing thrust (for +X translation) because of aerobrake impingement.

The aft mounting of the RCS jets requires that they fire through the aerobrake. This is accomplished by scarfing the nozzles into the brake such that their exit planes are parallel with the local brake surface.

This type of jet configuration raises the concern of plume interaction with the free stream flow during aeropass. Since practically no data exists on this type of configuration an extensive test program would be required to validate the concept. It is presented here as the most weight efficient solution to the RCS problem for the OTV. Many alternate solutions were looked at in the early design process but they all required doubling the number of RCS thrust chambers with the attendant rise in dead weight. These configurations could be utilized, however, if the plume interaction unknowns loom too large.

The thrust sizing of the RCS system is driven by the roll requirements of the aeropass. The rate of 90°/sec is achieved with 30 lb. thrusters for the ground-based systems and 100 lb. thrusters for the space-based vehicle with 14000 lb. manned capsule return capability.

2.1.1.45 Cryo ACS Usage

Attitude control propellant usage estimates (Tables 2.1.1.45-1, -2) were generated for the ground and space-based cryogenic OTVs. Mass property estimates for the two stages and associated payloads were used in conjunction with mission profiles (see midterm flight operations report for profile data). All estimates are reported in pounds and include a 10% margin.

Table 2.1.1.45-1 Cryo Attitude Control Usage

MISSION PHASE	GND BASED PLANETARY (4D RETURN ORB)	GND BASED GEO DELIVERY	20K GEO DEL (1D @ GEO)	4.51K UNMANNED GEO SERVICE (10D @ GEO)
PRIOR TO 1ST MAJOR BURN	70	70	20	17
DURING ASCENT	N/A	55	34	32
ON MISSION ORBIT	N/A	22	23	176
DURING RETURN (PRIOR TO CIRC. MANEUVER)	78	32	41	74
END MISSION USE	3	3	12	12
TOTAL	151	182	130	311

ALL QUANTITIES IN LBS (INCLUDES A 10% MARGIN)

Table 2.1.1.45-2 Cryo Attitude Control Usage

MISSION PHASE	7.5K RND TRP MANNED GEO SERVICE (18d @ GEO)	SB PLANETARY (4d RETURN)	LUNAR DELIVERY (5K P/L) (7d @ MOON)	LUNAR LOGISTICS (80K UP/15K DN) (16d @ MOON)
PRIOR TO 1ST MAJOR BURN	17	20	16	STA I: 89 STA II: 85
DURING ASCENT	32	N/A	61	STA II: 165
ON MISSION ORBIT	270	N/A	92	STA II: 96
DURING RETURN (PRIOR TO CIRC. MANEUVER)	74	80	89	STA I: 57 STA II: 132
END MISSION USE	12	12	12	STA I: 12 STA II: 12
TOTAL	405	112	270	STA I: 158 STA II: 490

ALL QUANTITIES IN LBS (INCLUDES A 10% MARGIN)

2.1.2 Avionics Hardware Trade Studies and Analyses

2.1.2.1 Centralized Versus Distributed Data Management

PURPOSE--Technology advances in microprocessors, memories, interconnection methods and in avionics subsystems as a whole have matured rapidly with the introduction of LSI and VLSI components. Spacecraft avionics to be built in the late 1980s will be able to take advantage of the considerable leaps in sophistication offered by these latest devices.

Avionics systems have traditionally, for the most part, relied on a central computer for all data management activities. This does not necessarily have to continue given the above mentioned advances. It is possible to apply distributed processing technology to spacecraft avionics in order to achieve attributes of increased modularity, reliability, and general mission capability. Performing the specific processing chores in the individual functional units (e.g., IMU, C&DH, etc.) moves the software development closer to the cognizant designer, reduces the computational load on any one unit and therefore reduces overall total software development cost.

This trade will compare traditional avionics design (centralized processing) with that of the distributed processing type for the OTV "family" of spacecraft.

SUMMARY--The central vs distributed processing trade involved a number of related issues. Five technology areas were surveyed with respect to spacecraft avionics subsystem applications:

- 1) Interconnection technology
- 2) Memory technology
- 3) Executive computer technology
- 4) Fault-tolerance technology
- 5) Modularity/Commonality/Growth ability

No new technology requirements were found necessary to meet the demands of the OTV avionics subsystems. Possible use of CRAM, fiber optic, and GaAs devices in the space-based OTV would require maturation of present-day products and production economics. These are not truly new technology requirements as these devices are in limited use now and need only to be space-rated to be suitable for OTV.

The VHSIC technology is being pursued vigorously by many of the major semiconductor vendors. Though the goals of the VHSIC will be realized in ground-based applications first, they will eventually be integrated into spacecraft systems. The small feature size of these microcircuits is particularly sensitive to radiation effects. Hardening processes generally drive up the feature size or increase weight through shielding. With respect

to OTV's data management requirements, it is felt that sufficient throughput and processing power is available in VLSI equipment when used in a distributed environment. VHSIC is therefore not considered to be a significant evaluation factor. Should later requirements in OTV's data management function dictate VHSIC class performance, it is desirable that equipment selected for OTV be easily upgradable to VHSIC technology.

Because of advances in LSI and VLSI components spacecraft avionics manufacturers are beginning to embed microprocessors, memories, and related integrated circuits within their products so that a truly centralized data management system is no longer necessary.

Table 2.1.2.1-1 shows the preferred candidate architectures summary for the OTV data management subsystem.

Table 2.1.2.1-2 summarizes the principle advantages and disadvantages of the centralized and distributed architectures.

Figure 2.1.2.1-1 illustrates the core architecture selected for the data management system. Figure 2.1.2.1-2 shows the interconnection subsystem schematic representaiton.

Table 2.1.2.1-1 Preferred Candidate Architecture Summary-OTV Data Management System

Design Components	Executive Computer		Memory		Interconnection		General		
	Throughput	Weight	Technology	Technology	Primary	Secondary	General	Modularity/	
Configuration	Processor	Power	Volume	Max.			Fault-Tolerance	Commonality/Expandability	
	ISA	Quantity	Technology	Primary	Secondary				
Ground-Based	850 KOPS	9 lbs							
Perigee Stage	Dual Processor	1	60 w	CMOS/SOS	Bubble	Shared	Global Bus	Moderate	Very Good
Cargo Bay Delivered	1750A		CMOS	128 Kw	12 Mw	Memory	Coax	to High	
Storable	Magic V					3 Mfps	5 Mbps		
Ground-Based & Space-Based	850 KOPS	20 lbs		CMOS/SOS	Bubble	Shared	Global Bus		
Perigee & Apogee	Dual Processor	2	120 w	128 Kw	12 Mw	Memory	Coax or	High	Excellent
Storable & Cryogenic	1750A		CMOS			3 Mfps	Fiber-Optic		
							120 Mfps		

ORIGINAL PAGE IS
OF POOR QUALITY

Table 2.1.2.1-2 Comparison of Centralized and Distributed Processing Approaches

Advantages	Disadvantages
<u>Centralized</u>	
<ul style="list-style-type: none"> o Less complex operating system o Less complex hardware architecture 	<ul style="list-style-type: none"> o Catastrophic system failure more probable o Software LCCs higher o Processing load at central computer requires a single, very high performance unit o Tendency to underutilize available processing power o Reconfiguration is costly o Poorly adapted to HOL applications
<u>Distributed</u>	
<ul style="list-style-type: none"> o Emphasizes modularity of hardware and software by functional partitioning o Takes advantage of intelligent sensors, peripherals, and support equipment o Excess processing capability is minimized o Allows system reconfiguration with minimal cost o More adaptable to HOL implementations 	<ul style="list-style-type: none"> o More complex hardware architecture o More complex operating system o Increased number of interfaces

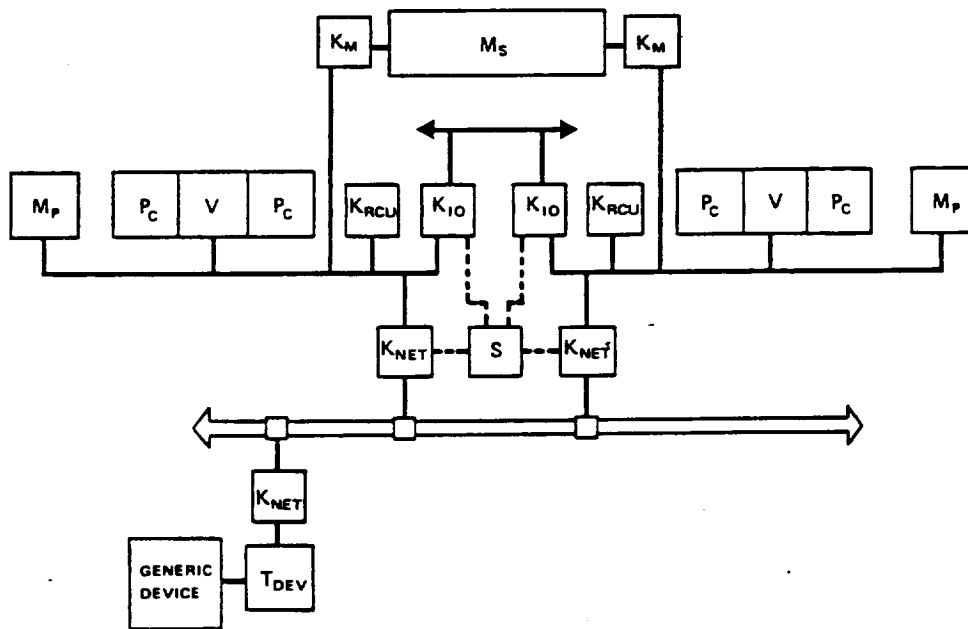


Figure 2.1.2.1-1 Core Architecture for OTV Avionics Data Management System

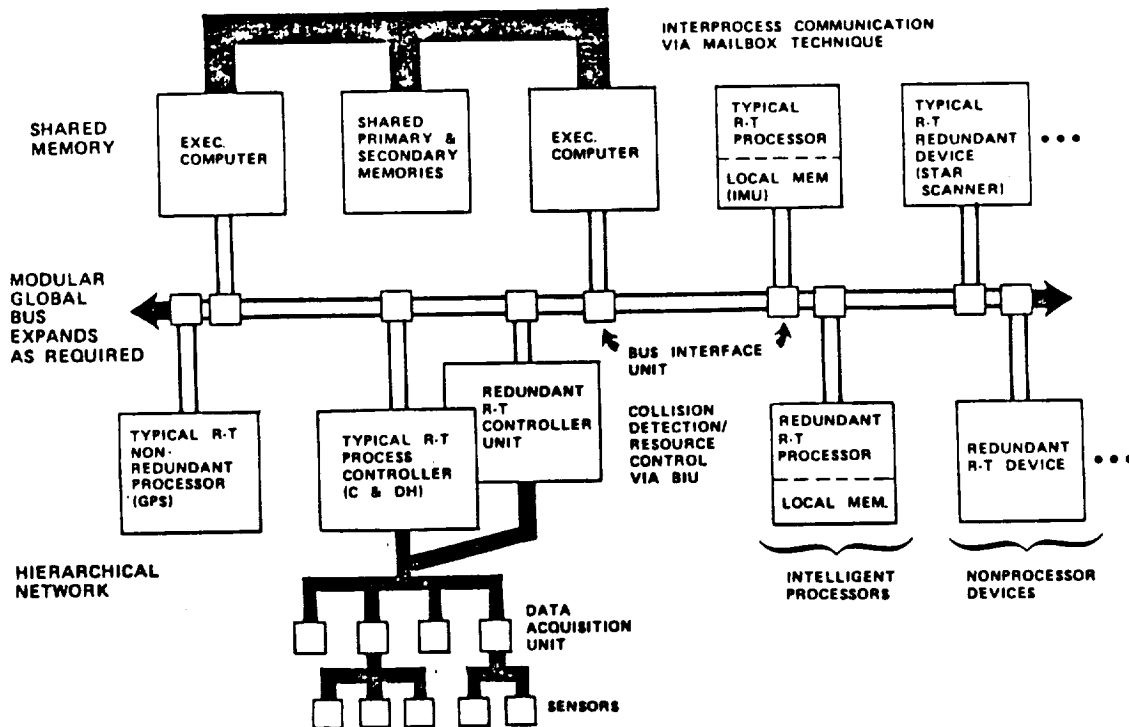


Figure 2.1.2.1-2 Interconnection Subsystem Schematic Representation

STATEMENT OF PROBLEM--Is a centralized data management design preferred for the OTV avionics hardware environment or is a distributed processing architecture more suitable?

ANCILLARY PROBLEMS--Which processor interconnecting topology will best support OTV? What memory technology is preferred for main memories? What memory technology is preferred for secondary memories for OTV? What combination of processor, memories, and interconnection paths is preferred for each OTV configuration. What are the sizing and timing parametrics for the interconnect, memory, and executive processor subsystems? What level of single-event-upset is acceptable for the data management system? What level of radiation hardness, measured by total dose, is adequate for the data management system?

ASSUMPTIONS--It is possible to build an avionics system using either a centralized or distributed architectural morphology for both ground and space-based OTV configurations.

Technological advances in processors, memories, and all avionics subsystems usable on an OTV lend themselves to a distributed processing environment.

The basic data management architecture is indifferent to the propulsion type or man-rating attributes of the OTV.

Tables 2.1.2.1-3 and -4 state the assumptions implied by the terms "centralized" and "distributed" within the context of this study.

Avionics hardware architecture candidate designs must be compatible with the following five OTV configuration options:

- 1) Propulsion type (storable or cryogenic)
- 2) Basing mode (ground or space)
- 3) Man-rating (manned or unmanned)
- 4) Mission duration (short or long)
- 5) Type-of-stage (perigee or apogee)

Table 2.1.2.1-3 Centralized Avionics Computer Architecture

Centralization of processing implies the following primary ideas:

- * A single, large, powerful computer handles all computational and general data processing chores on behalf of all avionics subsystems.
- * All avionics subsystems are considered peripheral equipment with respect to the central computer and are interfaced to it via the peripheral data/control bus.
- * The central computer supervises both data and control/status buses to which all peripherals are attached.
- * Peripheral equipment communicates with only the central computer and not with other peripheral devices.
- * Peripheral devices which may themselves actually be computers appear to the central computer as "dumb" or "semi-intelligent" devices.
- * Centralization of processing requires a single-threaded, real-time operating system running on the central computer to achieve total system control and coordination.
- * Redundancy within any or all of the subsystems and the central computer in no way alters any of the above conditions.

Table 2.1.2.1-4 Distributed Avionics Computer Architecture

Distribution of processing implies the following:

- * Multiple computer systems exist within the various avionics subsystems.
- * Each avionics subsystem is considered individually with respect to its processing requirements and therefore would not necessarily be considered as a peripheral to a specific computer within the system.
- * Computers are interconnected with the data/control/status buses which respect computer-computer protocol without a bus supervisor necessarily present.
- * Subsystems communicate with any or all other subsystems attached to the bus as required by function or condition of the system.
- * Subsystems which are themselves actually computers conduct themselves as such, thereby providing (potentially) multiprocessor capability to the avionics system.
- * Distribution of processing requires a multithreaded, real-time operating system run on a specified computer at any give moment (global computer).
- * The operating system can, under predefined conditions, shift to operating from another computer within the system in the event of a fault.

INITIAL CONDITIONS--The centralized avionics design uses the guidance and navigation computer as the central point of system and process control as well as for flight executive software operations. The distributed avionics design uses multiple computers for data processing, but at any given moment a single computer is in overall charge of coordinating the avionics environment. Five technology areas embrace all of the tradable attributes of the data management system:

- 1) Processor interconnection technology
- 2) Memory technology
- 3) Executive computer technology
- 4) Fault-tolerance technology
 - 4a) Reliability
 - 4b) Availability
- 5) Modularity/Commonality/Expandability

The interconnection subsystem has two forms:

- 1) Primary - The interconnection path between major subsystem processors and peripheral devices which are actually processors themselves.
- 2) Secondary- The interconnection path between a subsystem processor and its sensors, actuators, or the like. This form may be replicated in a hierarchical fashion to any practical level.

The memory subsystem has two forms:

- 1) Primary memory - That random access store used by the operating system. This is the fastest, nonvolatile memory available to the executive computer(s).
- 2) Secondary memory - Memory which is used as scratch space, software storage, and data retention store for all processors in the avionics system. This is often used to hold programs when not executing, telemetry packets, and spacecraft state and status information for trend analysis in the post-flight period. This may be nonvolatile, random, or sequential media.

The executive computer is the central element of the data management system. Primary interconnection path supervision and memory are dependent upon this device's capabilities to manage a totally functioning entity. The computer's essential capabilities are dependent on its microcircuit technology, its instruction set, and the level of integration and packaging which establish its form factor characteristics.

Table 2.1.2.1-5 shows the three baseline OTV configurations to be used in developing data management design candidates. The general architecture of the data management system is constructed from preferred candidates selected from the interconnection, memory, and executive computer hardware categories.

Table 2.1.2.1-5 OTV Baseline Configurations for Avionics Data Management Designs

<u>Configuration</u>	<u>Remarks</u>
Ground-Based, Cargo Bay delivered, perigee stage	<ul style="list-style-type: none"> o Most minimal weight configuration o Unmanned only <ul style="list-style-type: none"> o Storable propellant only o Single executive computer
Ground-based, ACC delivered, perigee/apogee stage	<ul style="list-style-type: none"> o Unmanned only o Storable and cryogenic versions
Space-based, perigee/apogee stage	<ul style="list-style-type: none"> o Most frequently flown member of OTV family <ul style="list-style-type: none"> o Used in minor variations from basic model o Offloaded fuel versions o Manned and unmanned versions

APPLICABLE REQUIREMENTS AND CONSTRAINTS--All avionics designs must meet the general requirement which states:
 "No single credible failure shall prevent the safe return of the crew or of the OTV only, if unmanned." Table 2.1.2.1-6 shows the general functional requirements of the data management subsystem. Specific requirements items may or may not apply on specific missions; however, data management design must satisfy these requirements where applicable.

Table 2.1.2.1-6 OTV Data Management System Functional Responsibilities

Data Table Retention

Mission Load Data
Constraints
General scratch RAM

Executive Operating System

Scheduling/Process Control
Interrupt Processing
I/O Control
Recovery Management
Utility Services
 Memory Reconfiguration
 Garbage Collection
 Arithmetic
 Interprocess Communication

Attitude Management

Thrust Vector (Powered Flight) Control
Reaction (Coast Flight) Control
Thermal Control
Attitude Quaternion
Error Quaternion
Lateral Steering

Guidance Management

Rendezvous
Rotation/Translation
Velocity Control
Aeromaneuver

Engine Management

Thrust Control

Condition Monitoring

Navigation Management

Sensor Processing
 Inertial Measurement Unit
 Star Tracker/Scanner
GPS Processing

Table 2.1.2.1-6 (continued)

Telemetry Processing and Communications Management

Processor Self-Test
BITE
Ground Checkout
Redundancy Management Check
Interrupt Test
Initialization
Discretes Test
IMU Test
Command Fail Detect
Memory Exerciser
Telemetry and Command Unit Test
Process Synchronization
Clock/Time Test

Power Management

Power Application
Discrete Conditioning
Ordnance Firing

Data available from the Advanced Information Processing Study (AIPS) of the MIT/Draper Labs is used here as background guidance for OTV data management designs. The near-term development requirements of the ground-based OTV do not permit the inclusion of technologies called for in the AIPS. The space-based OTV has a longer lead time to design and thus can make fuller use of the AIPS recommendations. Table 2.1.2.1-7 gives a summary of the AIPS goals and the applicability of their architectural "building blocks" to the OTV.

The AIPS is a conceptually elegant design philosophy which may be beyond the cost boundary of most engineered systems. As a means to stimulate design issues it is outstanding. Triple module redundancies are not proven to be as necessary as implied by the AIPS. Sufficiently adequate fault-tolerance measures using dual-redundant, cross-strapped modules are more attractive for space data management systems.

Table 2.1.2.1-7 Applicability of AIPS Architecture Building Blocks to OTV Avionics

AIPS Building Block	Ground-based	Space-based
Fault-Tolerant Processors	Yes	Yes
Fault-Tolerant Multiprocessors	Possible	Yes
Data Communication Networks	Possible	Yes
Fault-Tolerant Mass Memory	Yes	Yes
Local Operating Systems	Yes	Yes
Network Operating System	Possible	Yes
Gateway Interface to other Systems	No	Possible for Space Station Operations
<u>AIPS Goals</u>		
Failure Probability (Manned)	10 ⁻² failures/20 yrs	
Throughput (Manned)	15 MOPS	
(Unmanned)	500 KOPS	
Memory	300 Kbytes to 400 Mbytes	
Multiple-parallel logic in software and hardware is necessary		

SELECTION CRITERIA--Table 2.1.2.1-8 shows the general criteria and scoring values to be used for all three hardware categories. Subscores are shown to document the emphasis of major contributing metrics within the principal criterion concept. Point values are assigned based upon comparative analysis within each category from published and proprietary literature.

The avionics hardware environment is composed of equipment from each of the three scored subsystems; i.e., interconnection, memory, and executive computer. Together with their related software (not fully handled here) these three core technology areas embrace the basis for an overall OTV avionics architecture design. The avionics design candidates are formed from combinations of the preferred candidate subsystems for each primary OTV configuration of Table 2.1.2.1-5.

Table 2.1.2.1-8 General Criteria for Measuring Avionics Subsystem Hardware

<u>Principal and Secondary Criteria</u>	<u>Minimize or Maximize</u>	<u>Point Range</u>	<u>Weight</u>	<u>Max Score</u>
Performance	Max	100	.8	80
Fault-Tolerance	Max	100	1.0	100
Reliability		(60)	(1.0)	
Availability		(40)	(1.0)	
Modularity	Max	50	.8	40
Commonality	Max	10	.4	4
Growth Ability	Max	40	.6	24
Form Factor	Min	100	.9	90
Power		(40)	(1.0)	
Weight		(40)	(1.0)	
Size		(20)	(1.0)	
Development Risk	Min	100	.7	70
Hardware		(20)	(1.0)	
Software		(80)	(1.0)	
Life Cycle Costs	Min	100	.8	80
Hardware		(10)	(1.0)	
Software		(90)	(1.0)	
				488

To develop a reasonable data management architecture for multiple OTV configurations we first determine the hardware technologies which are required for each subsystem. We then examine alternatives within these technologies which best meet the most general OTV data management requirements. Once preferred technologies are established we next size each subsystem according to the OTV configurations of Table 2.1.2.1-5. Finally we next construct overall candidate data management systems for each OTV configuration.

SELECTION RATIONALE--

INTERCONNECTION SUBSYSTEM--Figure 2.1.2.1-3 illustrates the interconnection subsystem of a generalized OTV avionics system. Selection of candidates will give preference to topologies which provide data flow rate capabilities adequate for primary level requirements as well as providing the hierarchical control supervision needed for secondary levels.

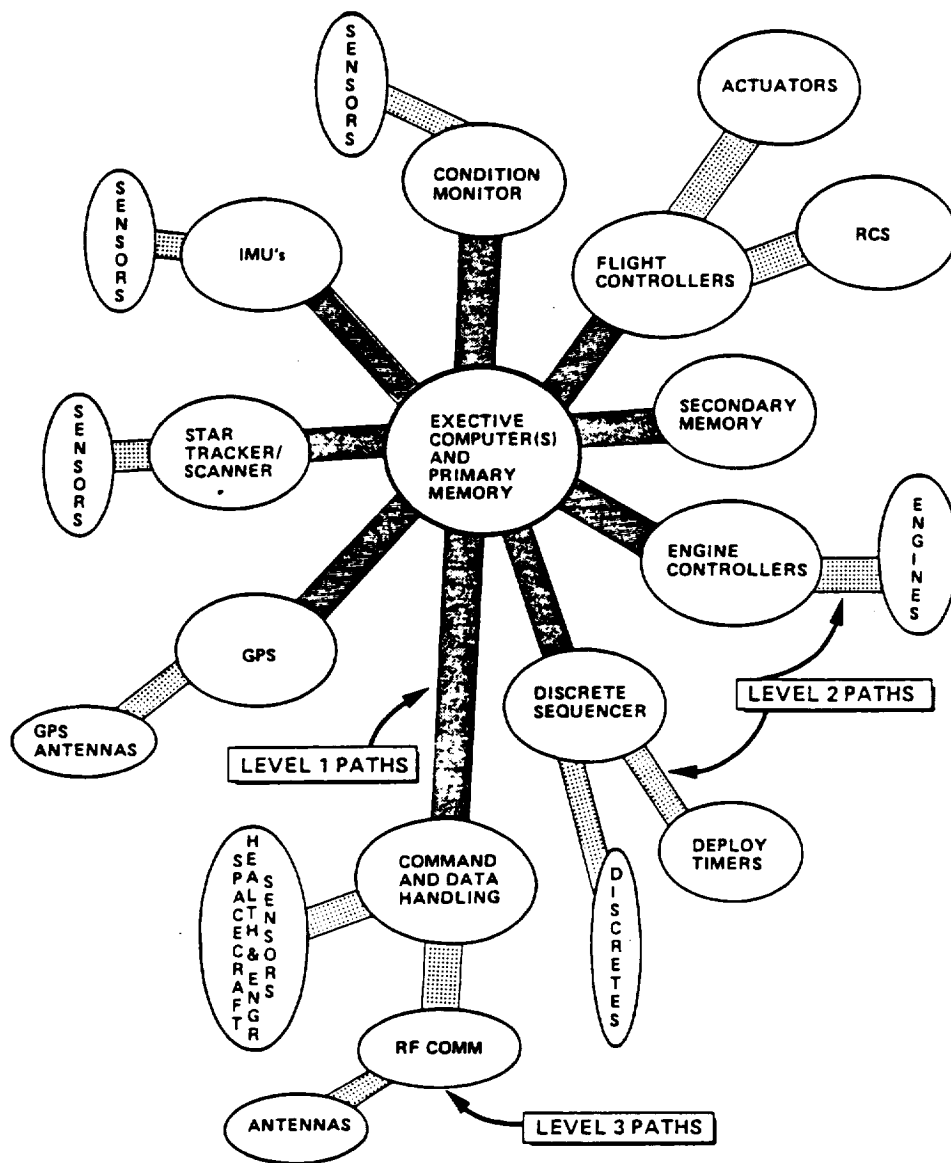
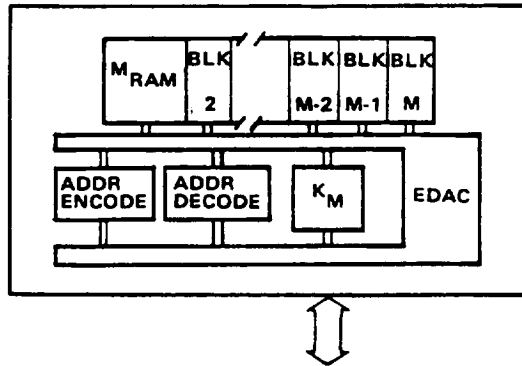


Figure 2.1.2.1-3 OTV Interconnection Subsystem Hierarchy

A simple linear bus structure is not considered here to be a responsive option given the assumption of "smart" peripheral device content within the avionics system as a whole. For this reason, all interconnection path topologies are of the networking type having the capability, if required, to support transmission of data and control in accordance with any supported protocol/rate combination suitable for the final system design requirements.

MEMORY SUBSYSTEM--Figure 2.1.2.1-4 illustrates the structural relationship of primary and secondary memories. In all designs bulk secondary memory will be necessary to accommodate the large operating system and flight executive software. Sufficient secondary memory volume coupled with a Level 1 interconnection path of moderate to high speed will permit a strong virtual operating system - a highly desirable feature.



M _{RAM}	Primary or Secondary Random Access Memory
ADDR ENCODE	Address Encoder
ADDR DECODE	Address Decoder
K _M	Memory Function Control
EDAC	Error Detection and Correction
BLK n	nth Addressable Block (bank)

Figure 2.1.2.1-4 Generalized Structure (internal) of Primary and Secondary Memories

The volume of both primary and secondary memory represents the major constraint on overall avionics system control sophistication. The key trade factors for selection here are memory chip density, which limits the amount of memory-per-container, and power consumption. Primary memory selection should focus on high density-per-chip and low power attributes.

EXECUTIVE COMPUTER SUBSYSTEM--The executive computer subsystem supports the guidance and navigation, attitude, power management and sequence control functions as well as any other general purpose processors not restricted in their programmability by virtue of a dedicated function. The principal characterizing feature of an executive computer is that it must be able to support the executive operating system software function. In a distributed processing design, multiple executive computers (not all necessarily alike)

would be available for such duty while only one at a time actually has the operating system active. A general purpose, space-rated computer is the logical choice for such a subsystem. The question of redundancy to meet reliability requirements directly affects the appropriateness of the distributed processing option.

In all designs, two complete executive computers are needed. Both computers are allocated part of the overall processing load while remaining fully able to resort to a single processor system should a critical failure occur (see Figure 2.1.2.1-5). This capability is gained by following four general design guidelines: 1) use "smart" peripheral instruments and controllers which are maximally autonomous or independent, 2) provide a large, sharable mass memory not associated with a particular executive processor, 3) design the information and control flow to follow a device-independent philosophy and 4) structure processing flow and specific algorithms to be stepwise separable while using the principle of information hiding. This latter point strongly implies the need for high-order language support. Strong HOL software development support is preferred.

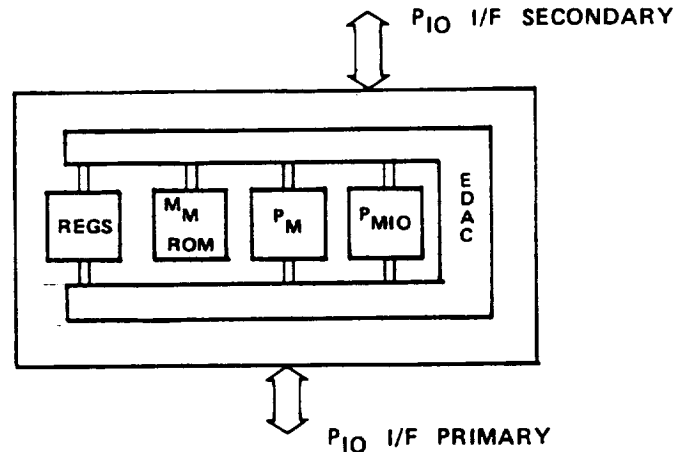
Modularity in executive computers is generally found in two forms: 1) modularity of function where a plug-in card or card-set performs a specific function, and 2) modularity of general hardware; here multifunction cards are common in order to reduce the number of cards, overall bulk, and get multiple use of common circuits or components. Either approach affects serviceability and logistics positively. The former, however, is preferred based upon reliability models.

Commonality in computers is reflected primarily in the genealogy of product lines. A totally new technology approach (e.g., VHSIC) will not have the heritage from which to draw strengths from previous generations. Preference, albeit small, is given to computers matured from proven designs, some part of which is common to the bloodline. We do not look here for the replacement part type of commonality, rather commonality of concept and, if possible, interface to external devices.

Growth ability is measured by control function extensibility; e.g., can we add more devices without overloading the interrupt system? Packaging is critical here since we do not want to have too many nor too few open "slots" on the main backplane. Some room to add functions is necessary and preference is given to those computers having adequate internal expansion capacity. Greater preference is given to computers providing both primary and large secondary store as well as CPU and control functions in a single package without excessive volume and weight.

Principal selection factors for executive computers are: 1) performance, which is itself a complex measure of hardware technology, instruction architecture, software organization, and primary memory/processor interaction; 2) fault-tolerance capabilities (addressed in next section); 3) form factor, a composite of power consumption, weight, and volume.

Preference will be given to computers which maximize performance and fault-tolerance while minimizing form. Development risk for space computers is only slightly greater today than for non-space-rated (aircraft) devices using LSI and VLSI technologies. VHSIC computers, however, are considered to be in the moderate-to-high risk class.



P_m	Microprocessor
M_m	ROM w/Microcode
P_{mIO}	I/O Control Processor
REGS	Read/Write Registers (RAM)
EDAC	Error Detection and Correction

Figure 2.1.2.1-5 Generalized Internal Structure of a Single Microprocessor with I/O Processor

FAULT-TOLERANCE--Fault-tolerance is measured here primarily by the general metrics of reliability and availability of a given subsystem. Each of the three hardware candidate categories must have some attributes of fault-tolerant behavior. Such behavior has three active forms: 1) detection, 2) diagnosis, and 3) correction. One or more of these activities must be available to each subsystem. The traditional definitions for reliability and availability are adopted here:

Reliability:

The reliability of a system as a function of time is the conditional probability that the system has survived the interval (0, t), given that it was operational at time t = 0.

Availability:

The availability of a system as a function of time is the probability that the system is operational at any instant of time.

In general, reliability is more difficult to achieve than availability due to its more restrictive definition. Preference is therefore given to subsystems providing higher reliability. Presumably, high availability will be obtained through incremental gains in reliability throughout the system as a whole.

Built-in-test (BIT) and evaluation (BITE) hardware is preferred wherever obtainable. Self-diagnosis is preferred over external fault detection and error correction capability is preferred even more. LSI devices tend not to have as much BITE as do VLSI's due in part to the need of the VLSI for such functionality as a consequence of its reduced scale and manufacturing processes. The degree to which BITE hardware is present in a device is considered a positive fault-tolerance attribute.

SINGLE EVENT UPSET--Specific requirements for OTV SEU levels have not been established as yet. Hardware candidates for executive computers and memories all cite some SEU performance value based upon laboratory testing. As a selection process general criteria for logic components, the following values are felt adequate and achievable goals given present manufacturing technology:

CPU logic 10^{-7} bit/day

Memory logic 10^{-9} bit/day

RADIATION HARDNESS--Specific requirements for OTV radiation hardness have not been set, but total dose rate (rads) should be in the range of 10^{-5} to 10^{-6} . Preference will be given for proven (not goal) hardness below 10^{-5} .

MEMORY CROSS-STRAPPED REDUNDANT MODULES (CSRM)--Memory units connected by a cross-strapping technique are preferred to non-cross-strapped arrangements. EDAC hardware using CSRMs has proven superior to other methods in previously flown space systems as well as through reliability modeling. Preference is given to CSRM designs in executive computer subsystems. No criteria addressing specific cross-strapping methodology is used here.

HIGH-ORDER LANGUAGE (HOL) SUPPORT/ISA--Selection of an executive computer cannot be solely based upon hardware parameters. The life-cycle costs for avionics computer systems are dominated by software, not hardware costs. Figure 2.1.2.1-6 illustrates the estimated LCCs for high-order and low-order languages (HOLs/LOLs) with respect to embedded avionics computer systems. Significant here is the time frame which finds OTV's software development period for the ground-based configurations coming at what will undoubtedly be a highly transitional time for HOL applications in avionic systems. Specifically, the rapid upswing of Ada-based applications in spacecraft avionics will be receiving much greater attention than is being generated today. Standardized software development environments (integrated hardware and software) could lower the early development, test, and integration costs for the ground-based OTV significantly. Preference is therefore given to space computers provided with an Ada support environment or at least a mature HOL development, test, and integration support system.

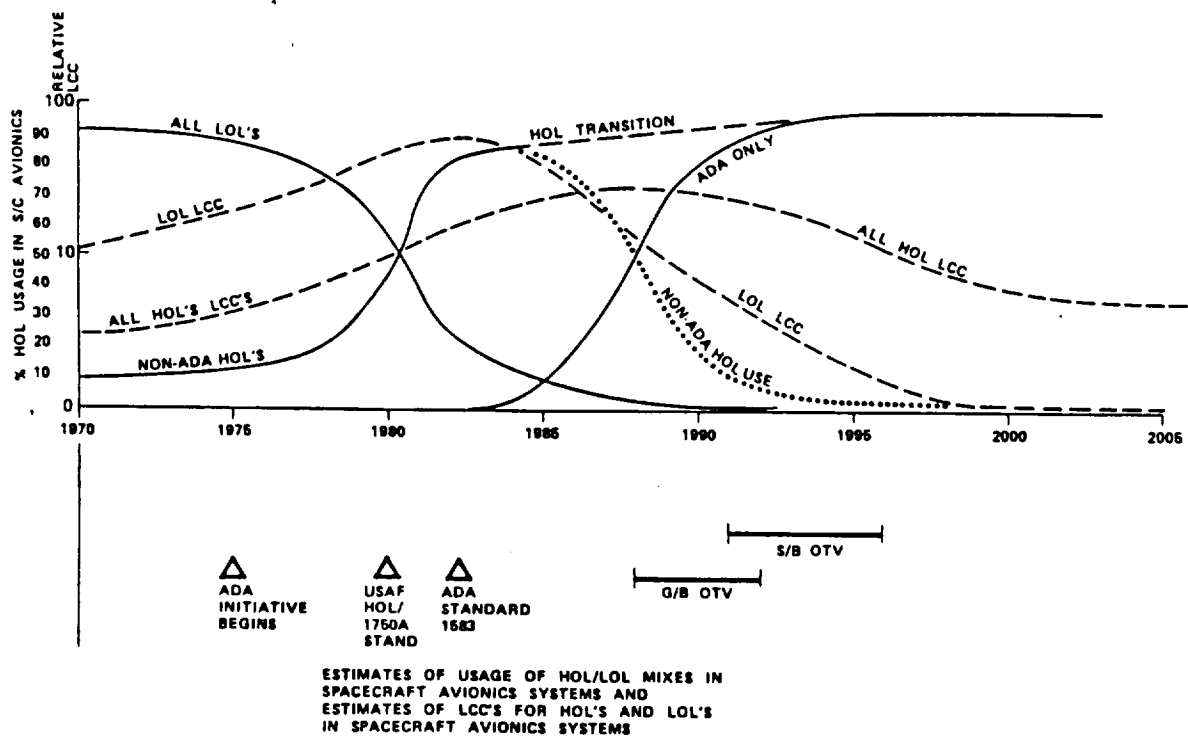


Figure 2.1.2.1-6 Usage and LCCs for HOL/LOLs in Spacecraft Avionics Systems

The instruction set architecture (ISA) of the executive computer is closely tied to the HOL compiler. They form a tightly coupled relationship which has ramifications in the recurring LCCs of the avionics system. No ISA requirement has been established for the OTV executive computer. Based upon a preponderance of manufacturer's stated development goals, the MIL-Spec-1750A, Notice 1, ISA is given preference in this study. An Ada-to-1750A compiler is being certified by several commercial firms and the 1750A ISA is the only type of processor being seriously developed by all credible sources today.

DESCRIPTION OF CANDIDATES--

INTERCONNECTION SUBSYSTEM--The processor interconnection subsystem acts as the data and control information path between processing nodes. Included here are the cabling and device interfacing hardware which permits the flow of data and responds to control exerted by either the sender or receiver. The conventional "bus" concept arises here; however, we are interested in interprocessor connection not internal (backplane) connection candidates. This is not to say that a processor's backplane bus architecture is unacceptable; on the contrary, it is entirely possible to have them coincident. Table 2.1.2.1-9 describes the seven interconnection candidates.

Table 2.1.2.1-9 Interprocessor Candidate Topologies

Total Interconnection

All processors are directly connected to all other processors. This is the simplest of all methodologies but incurs high cost and weight penalties as the number of processors increases. Control software for this method is generally complex and costly.

Irregular Network

There are no consistent neighbor relationships between processors. This is a commonly observed topology in spatially disbursed systems using multiple internodal communications methods. Control software tends to be simpler than above. Slower throughput can result from ill-defined processor relationships.

Hierarchical Network

This is the classic process-control topology. Strongly defined processor relationships reduce software costs. Throughput is moderate while reliability is generally good. Hardware protocol management reduces reliance on software.

Loop or Ring Network

This is a typical topology for a communications dominated system. Data and control may flow in one or both directions around the ring. Each processor is connected to its adjacent neighbors only. Control software is simple and maintenance is low.

Global Bus

This type of interconnection requires a predefined allocation scheme for message passing between processors. The bus may or may not be supervised.

Star Network

A central switch, which is generally not a network processor, is connected to each processor. All traffic passes through the switch in both directions. This is a common topology of fiber optic systems and has the obvious single-point failure of the central switch. Control software is complex, timing sensitive, and easily overloaded. Costs for software are generally moderate as are hardware costs.

Shared Memory

This is the most common of all interconnection topologies. Speed is highest as no cabling nor interfaces intervene. This is also the least reliable method when multiple processors must communicate over extended time. Control software complexity increases as does the need for memory protection hardware (not EDAC type, but address-spec-type). Memory substitutes for data path hardware. This is also the first choice for a centralized processing system.

Implementation of the selected interconnection topology produces a second order trade issue, namely whether or not to use fiber optics or conventional wiring approach as the transmission media. Table 2.1.2.1-10 shows basic data on fiber optic paths. This study found that, although MIL-Spec fiber optic systems are in active use, they would not be warranted for ground-based OTV systems due to technology immaturity. Space-based OTVs, however, may make use of fiber optics to interface with the Space Station.

Table 2.1.2.1-10 Comparison of Fiber Optics with Other Transmission Media

	TWISTED PAIR WIRES	BASEBAND COAXIAL CABLE	BROADBAND COAXIAL CABLE	FIBER OPTIC CABLE
Partial bandwidth	1.5Mbps	10Mbps	400MHz	Greater than 150Mbps
Media expense (\$/km)	300	1500-5000	1500-5000	300-6000
Coupler/terminal hardware expense	Low	Mod	Mod	High
Installation expense	Low	Mod	High	Low
Cable weight: (kg/km)	50	75-750	150-1500	30-170
RFI/EMI susceptibility	High	Mod	Low	None
Freedom from crosstalk, echoing, and ringing	Low	Mod	High	Very High
Spark hazard	High	High	High	None
Data transfer reliability	Low	High	High	Very High
Transmission security	Low	Low	Low	High

A negative point regarding use of fiber optics is their (present) tendency for the star network approach to processor interconnection. While being suitable for nonprimary paths (e.g., from flight controller to controlled actuators) it is seriously flawed in the primary path situation at this time.

MEMORY SUBSYSTEM--The memory subsystem includes the main dynamic memory of the executive computer(s), the secondary memory used by avionics processors granted memory privilege, and any cache or alternate memories required by the executive computer(s). A discussion of memory subsystem candidates follows. Selection of a memory technology for a particular application does not affect the address space capability of the executive computer. However, chip density limits of a memory technology, if too low, could increase component (chip) counts and thereby indirectly limit the amount of addressable space within an acceptable size container. Therefore the higher density memories are generally preferred for packaging considerations.

CMOS AND CMOS/SOS--Complementary-metal-oxide-semiconductor (CMOS) and CMOS/silicon-on-sapphire (CMOS/SOS) memories are used for dynamic, random access applications, are very low power, and have a very low cost-per-bit. CMOS/SOS is the rad-hardened, variant which is the clear industry choice for advanced, rad-hard, low power processors and their associated memories. Laboratory tests (PCA) indicate that CMOS/SOS is capable of operating without circumvention for dose rates near 10^{12} rads/s, or with total dose of 5×10^5 rads with shielding and neutron fluxes of 10^{15} N/cm². CMOS/SOS with these properties has a high SEU immunity.

MNOS--Metal-nitride-oxide-semiconductor (MNOS) is a nonvolatile, electrically alterable memory. This technology can be used for both RAM and ROM applications. It is a moderately well developed technology which is fairly fast and generally has low Chip density.

DYNAMIC RANDOM ACCESS MEMORY (DRAM)--Dynamic random access memory is a volatile, fast, inexpensive memory commonly found in nonspace applications. Its volatility precludes its use on OTV subsystems.

BUBBLE MEMORY--Bubble memory is considered for the secondary memory only, particularly for replacement of tape recorder functions in the command and data handling subsystem and as a large RAM disk for operating system and flight executive software storage. Present technology for bubble memories is 1-megabit chip densities with 4-megabit chips being in mass production within months. 32-megabit plug-in memory cards are available now in space-rated packages.

PLATED WIRE MEMORY--Plated wire memories are very slow, expensive, high cost devices which have seen space applications over the past decade. They are rad-hard and nonvolatile but exhibit very high power consumption.

MAGNETIC TAPE MEMORY--Magnetic tape memory is strictly used for secondary memory applications such as with the command and data handling subsystem. Bulk, cost, speed, power, and general mechanical nature bode poorly for these devices. Their very large storage capacity, however, is their redeeming virtue. Bubble memories are none the less displacing them in space applications.

CORE MEMORY--The traditional core memories have all of the drawbacks of the plated wire memories and are low in density per plane, thereby making them even less attractive than plated wire.

CROSS-TIE RAM (CRAM)--CRAM memories are very good prospects for space-based OTV applications, but are too new a technology to seriously consider at this time. It is likely that the OTV could eventually use CRAM for both main and/or secondary memories. They are rad-hard, low power, fast, and very dense in their packaging. This technology should be evaluated again in about three years.

GALLIUM ARSENIDE (GaAs)--Gallium-arsenide technology is just this year seeing the emergence of commercial ICs. Though very new, GaAs gives very fast, rad-hard, low-power service which spans the CMOS-bipolar gap. Its cost-per-bit today is excessive, but DoD pressure to have total GaAs systems by 1987 assures its future role in spacecraft systems of the 1990s. GaAs has particularly excellent radiation tolerance, 10^7 to 10^8 rads, compared to CMOS/SOS, 10^4 to 10^5 rads (total dose).

EXECUTIVE COMPUTER SYSTEM--Overall management of data flow and process control is vested in an Executive Computer. Major functional responsibilities include guidance, navigation and its supporting sensory device control/data management, attitude management, telemetry/command and communications management, discrete event supervision, and providing overall coordination, control, and services support for all resources connected to its primary bus system. An Executive Operating System capable of multiprocessing, asynchronous and synchronous task control, and complete redundancy management capability is required.

APPLIED TECHNOLOGY, ATAC-16MS--This computer is particularly fault-tolerant and has good throughput. Its design, however, is somewhat dated and is implemented in mid-70's technology for the Gallileo spacecraft. There are sufficient demands regarding autonomous operation placed on this device to make it a final candidate for OTV.

GENERAL MOTORS, DELCO M362/IUS--This space-rated computer is the most recent of the MAGIC III series and has proven itself on the IUS. Its technology is outdated so that its form factor is much worse than currently available computers and keeping it from serious consideration. It has, however, provided a technology development step for the subsequent "MAGIC IV and V series".

GENERAL MOTORS, DELCO MAGIC 572H--The 572H is a VLSI/CMOS/1750A class computer. It has much better throughput characteristics than earlier MAGIC III and IV versions and is targeted for spacecraft in the ground-based OTV time frame. Its radiation and SEU sensitive design make it an excellent candidate. It is HCL supported and has a good software development environment.

GENERAL MOTORS, DELCO MAGIC V--The Delco MAGIC V is the latest generation design of 1750A/VLSI/CMOS/SOS computers. Its rated 850 Kops throughput is probably a conservative value. Its very modular design, like the MAGIC 572H, is attractive from several angles. Should Delco's VHSIC work with TRW prove successful, this computer could see production in VHSIC rather than VLSI form. In the meantime the MAGIC V has an excellent VLSI implementation with particular features suitable for distributed, multiprocessor configuration designs. Its performance, form factor, and fault-tolerance features are excellent. It is now in final production for the F-20 in a six-computer, multiprocessor implementation (FY 85 delivery).

TELEDYNE TDY 750S--Teledyne's only candidate in this study is its TDY 750S advanced space computer. It is a highly compact, powerful processor (1750A) with excellent primary (CMOS/SOS) and secondary memory resources. One of the key features of the 750S is the very well crafted development support system which is highly versatile and reasonably priced (approx 175K). The heritage of the TDY 750S is long and well respected. Radiation and SEU characteristics are designed into this device based upon considerable research. The 750S is in brassboard development with production slated for 1986 for a high reliability, classified spacecraft.

RCA SCP-STAR DUAL CPU--RCA has several variations of the (1750A) STAR design. We consider here only the dual CPU configuration. This processor has good internal redundant CPUs with switching logic, CMOS/SOS primary memory, and a good expansion capability. Its packaging is in 1/2 ATR units. The CMOS/SOS STAR computers are designed to minimize form factors, tolerate nuclear events, and have very high reliability.

RCA SCP-STAR II--This is the VHSIC/CMOS/SOS upgrade of the SCP-STAR II. This high performance model is now reaching its early brassboard stage of development. All STAR processors have HOL support for their 1750A ISA which is very adequate.

LITTON LC-4516E OBC--This is a proven space computer of early 70s design. It is presented here for historical comparison only. Its form factor and performance are much less than its nearest competitor candidates.

LITTON LC-4750--Litton's serious candidate here is its most advanced 1750A ISA processor. Plans for an Ada HOL support system are an important feature of this computer as is the unusual non-VLSI nature of its technology. The wide range of throughput rates is a result of instruction mix and test algorithms.

IBM AP-101S--The information in Table 2.1.2.1-11 is based upon specifications, not an actual machine description. The AP-101S is to be the upgraded version of the Space Shuttle's AP-101 onboard computer.

IBM NSSC-I--This processor's data is provided for historical reference only. The NSSC-I has been used on numerous NASA spacecraft over the past decade. This was a benchmark device in its day.

ORIGINAL PAGE IS
OF POOR QUALITY

Table 2.1.2.1-11 Candidate Scoring Summary

	Interconnection Subsystem								Memory Subsystem				Executive Computer Subsystem																	
	Total Interconnection Network	Hierarchical Network	Loop/Ring Network	Global bus Network	Shared Memory	CMOS	CMOS/SOS	MMOS, BORAM	Magnetic Bubble	ITEK	ATAC-16MS	DELCO	MAGIC 572H	DELCO	MAGIC V	TELEDYNE	TDY 750S	RCA	SCP-STAR	DUAL OPU	RCA	SCP-STAR II	LITTON	LC-4750						
Performance	150	40	170	56	150	40	160	48	190	72	190	72	175	60	170	56	150	40	175	60	185	68	190	72	155	44	180	64	175	60
Fault-Tolerance	190	90	180	80	160	60	170	70	195	95	195	95	175	75	185	85	180	80	185	85	185	85	185	85	180	80	195	95	180	80
Reliability	158		150		140		140				155		140		150		150		150		150		150		150		157		155	
Availability	132		130		120		130				140		135		135		130		135		135		135		130		138		125	
Modularity	125	20	150	40	150	40	150	40	140	32	145	36	145	36	150	40	140	32	145	36	145	36	130	24	145	36	145	36	145	36
Commonality	110	4	110	4	110	4	110	4	110	4	110	4	110	4	110	4	110	4	110	4	110	4	110	4	110	4	110	4	110	4
Growth Ability	110	24	130	18	120	12	135	21	130	18	140	24	140	24	140	24	110	6	130	18	135	21	120	12	130	18	135	21	130	18
Form Factor	130	27	165	58.5	155	49.5	175	67.5	190	81	1100	90	190	81	170	63	135	31.5	165	58.5	190	81	165		175	67.5	175	67.5	180	72
Power	115		125		120		130		130		140		130		120		110		120		135		130		130		135		130	
Weight	110		130		125		130		140		140		140		135		115		130		135		125		135		135		135	
Size	15		110		110		115		120		120		120		120		110		115		120		110		110		115		115	
Development Risk	155	38.5	190	63	175	52.5	190	63	1100	70	1100	70	185	59.5	197	67.9	177	53.9	172	50.4	175	52.5	175	52.5	162	43.4	155	38.5	170	49
Hardware	15		120		115		120		120		120		15		117		117		112		115		115		112		110		110	
Software	150		170		160		170		180		180		180		180		160		160		160		160		160		150		150	
Life-Cycle-Costs	165	52	187	69.6	186	68.8	190	72	190	72	198	78.4	196	76.8	193	74.4	172	57.6	176	60.8	174	59.2	188	70.4	182	65.6	164	51.2	176	60.8
Hardware	15		17		16		18		110		118		116		118		117		116		114		118		117		114		116	
Software	160		180		180		182		180		190		185		165		170		170		170		170		175		160		170	
TOTALS	295.5		389.1		326.8		385.5		442.0		469.4		413.3		412.3		302.1		337.7		404.7		376.4		356.5		334.2		376.8	
Selected									*		*										*									

SINGER/KEARFCTT SKC-3121H--This computer was eliminated for the primary OBC of the Space Shuttle. Several problems with radiation hardening were encountered, but probably can be overcome by obtaining Sandia rad-hard chips. Its HOL support is a modified dialect of Fortran-68.

COARSE SCREENING--

PROCESSOR INTERCONNECTION CANDIDATES--The star network topology is rejected as it has only fair reliability and limits growth due to inherent switch saturation problems. The irregular network is also rejected as it is inconsistent with the structured design of avionics systems as well as difficult to supervise via software which would result in much higher development and maintenance costs.

MEMORY SUBSYSTEM--Cross-tie RAM is rejected as an immature technology. It may be sufficiently developed for space-based OTV designs; however, this is not clear at this time. Magnetic tape is rejected for weight, cost, bulk, and performance reasons. Core is rejected for cost and serviceability reasons. Plated wire technology is rejected for high cost and low performance reasons. GaAs is rejected for cost and immature technology reasons. However, this may be a viable candidate for technology insertion in post-1990 systems.

EXECUTIVE COMPUTER SUBSYSTEM--The NSSC-I is rejected for performance and memory technology reasons. The IBM-101S is rejected as being customized for Shuttle operations which differ substantially from OTV requirements. Both of the above are provided in the comparison charts for reference. The M362/IUS is rejected for high power consumption and its bipolar technology. The SKC-3121H is rejected due to its radiation susceptibility and construction. The LC-4316E is rejected for performance and processor technology reasons.

EVALUATION AND CANDIDATE SELECTION--The three selection categories are presented in comparison table form: interconnection topologies, memory technologies, and executive computers. Table 2.1.2.1-11 summarizes the weighted scores for all candidates which passed coarse screening. Table 2.1.2.1-12 gives a general comparison of the candidates. Table 2.1.2.1-13 is used for comparative evaluation of throughput values using Space Shuttle reported rates during various stages of flight. A discussion of each subsystem candidate's evaluation follows the summary.

Table 2.1.2.1-12 Comparison of Interconnection Candidates

<u>Topology</u>	<u>Reliability</u>	<u>Expandability</u>	<u>Performance</u>
Total Processor Interconnection	Maximal	Fair	2400-9600 bps 50 Kbps to 1 Mbps possible
Irregular Network	Excellent	Fair	3 to 5 Mbps
Hierarchical Network	Very Good	Good	2400 to 9600 bps; 1 to 10 Mbps possible
Loop / Ring Network	Good	Good to Fair	1.3 Mbps
Star Network	Fair	Good to Switch limit	1 - 3 Mbps 75 Mbps possible
Global Bus Network	Good	Very good	50 Kbps to 50 Mbps
Shared Memory	Minimal	Poor	Memory speed 3 Mwps possible

INTERCONNECTION SUBSYSTEM--The total processor connection approach would be bulky, limit growth severely, and is difficult to supervise. Through a very reliable approach it does not lend itself at all to spacecraft implementation. The hierarchical network is very well suited to spacecraft implementation. It has the range of throughput and reliability needed for the most ambitious OTV designs. This topology appears to give the best overall

Table 2.1.2.1-13 Reported Shuttle Data Bus Rates (Kbps)(Centralized System Design)

	Pre-flight	Boost Boost	On-Orbit	Descent & Landing	Post-Flight
Flight Computer/ DCM Computer	1 1	1 1	1 1	1 1	1
Attitude		16	16	16	
Aerosurface Control				5	
Multipurpose Displays	90	90	90	90	90
Electronic Displays	6	6	6	6	6
Telemetry Up/Down Link	1.4	1.4	1.4	1.4	
Ground Link	27.0				
Checkout	45	45	45	45	45
Sequential Control Reconfig.	5	5	5	5	5
Others	7	23	23	23	
Total	182.4	187.4	187.4	187.4	146

characteristics for processor interconnection throughout level 2 of the avionics system. The loop or ring network approach has the serious weaknesses of message overload potential and single-point failure of the ring decoder. The reliability is not sufficient for long duration missions. The global bus network is moderately reliable, and encourages system modularity by its very nature. It is closely related to the loop topology but does not suffer from its weaknesses. This topology is well suited to spacecraft avionics at the highest level of processor interconnection. It would be ill-suited for high speed and volume real-time data communications.

The shared memory approach is the highest ranked topology. This topology is easy to implement, inexpensive to software manage, and highly conducive to the use of virtual operating systems which have large secondary memories. Controlled access is managed through hardware and software and is relatively impervious to the device interconnection topology provided a direct memory access privilege is granted. Mailbox-type interprocessing communication is encouraged through this methodology.

INTERCONNECTION CANDIDATE SELECTION--Because the interconnection subsystem is the means by which all other subsystems are physically related, there is no single "best" candidate. In the same sense that there are several types of nerve pathways in the body, each level of body (system) control requires its own "best suited" interconnection approach. The pathway between executive processors and their respective primary memories is direct, very high speed, and isolated from approach by external devices. Here the shared memory topology is selected as most appropriate. The path to which the principal subsystems connect (GPS, IMUs, etc.) must be shareable, moderate in speed and capable of being supervised to limit contention/collision problems. Here, the global bus is selected as being most suitable. Pathways controlled by principal subsystems which conduct real-time process control functions (engine controller, flight controller, IMU, etc.) must exert absolute supervision in a tightly controlled subsystem environment. The hierarchical topology is selected as best suited for this level of the interconnection subsystem. Figure 2.1.2.1-7 illustrates the schematic relationship of the 3-level interconnection subsystem proposed here for the avionics system.

MEMORY SUBSYSTEM--CMOS/SOS is by far the preferred candidate owing to its high performance, low-power characteristics. The cost-per-bit is very low and the radiation hardness is good. Production sources are somewhat limited though this will change with increased demand.

MNOS is cost ineffective and not of sufficient radiation hardness to merit usage. Although its performance is good it will suffer if radiation hardening processes are applied.

Bubble memory is the preferred form for secondary memory storage. Its speed is very good as is its radiation hardness. Chip density is increasing rapidly and gives every indication of matching the VLSI circuits themselves, most favorably impacting large memory packaging. Power is a negative point here, though the increased memory volume easily offsets this. Of course, bubble memory is nonvolatile.

Cross-tie RAM could replace bubble memories by the late 1990s. Though it is too new for selection here it has distinct advantages and the technology should be closely monitored.

MEMORY SIZING--Assuming that a 1750A ISA processor is selected for the executive computer type, we immediately derive a 64 Kw directly addressable memory space and memory management capable of 1 Mw address space. All vendors offering 1750A processors provide a minimum of 64 Kw with each processor, typically 128 Kw is offered. The minimum memory included is 128 Kw but typically is 356 to 640 Kw.

Due to memory technology advances (see Table 2.1.2.1-14), sizing of the physical memory store is far more dependent on container limitations than on any estimate of lines-of-code. How, eventually, the actual memory resource is allocated to functional categories of the avionics system is only roughly estimated. Figure 2.1.2.1-8 illustrates estimates for primary and secondary memory allocation for centralized and a distributed avionics configuration. In both cases, the operating system is assumed to have virtual storage ability which requires secondary memory support. A very rough estimate of memory allocation for a fixed, nonvirtual configuration is also provided.

INTERPROCESS COMMUNICATION
VIA MAILBOX TECHNIQUE

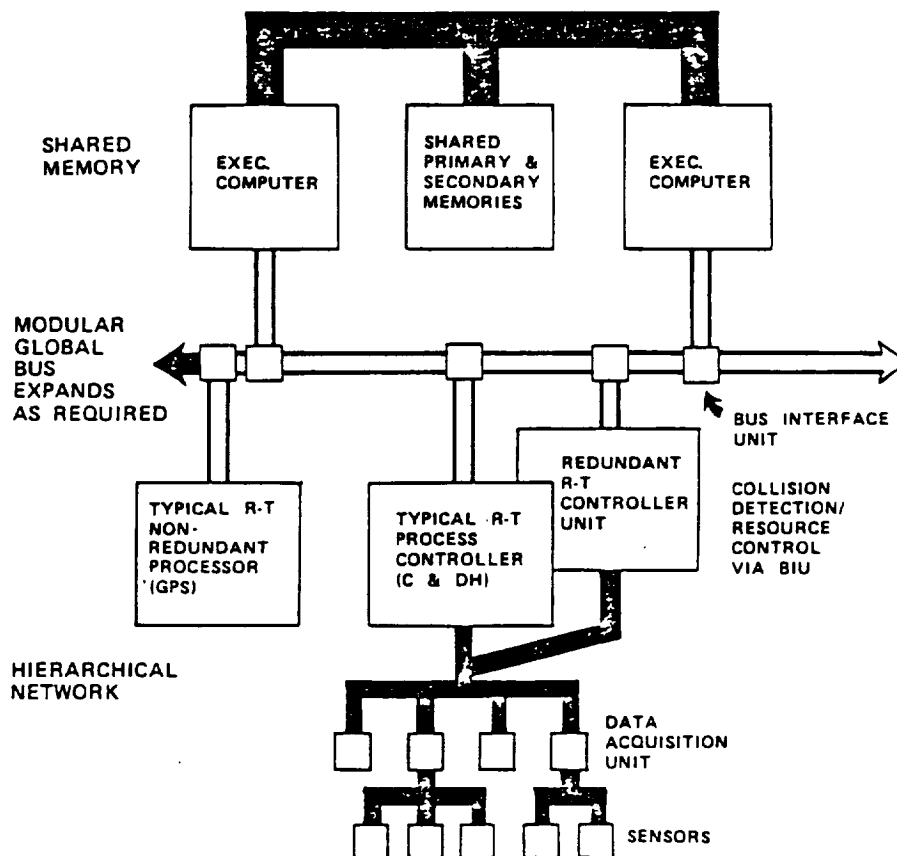


Figure 2.1.2.1-7 Interconnection Subsystem Schematic Representation

Physical memory volume for both primary and secondary memory is critically dependent upon the nature of the operating rather than the complexity of applications software. No less than 128 Kw is suitable for a virtual environment and preferably 256 Kw, which is Shuttle's new (minimum) requirement.

EXECUTIVE COMPUTER SUBSYSTEM--Based on ranked performance, design heritage, production potential, 1750A ISA, and high modularity/expandability, the DELCO MAGIC V is evaluated as the preferred candidate for the ground-based avionics data management executive computer. Its power/weight/volume and packaging factors also are significant positives in its favor. The F-20 multiprocessor version using the MAGIC V is in production for FY85 delivery.

Table 2.1.2.1-14 Memory Technology Candidates

Technology	Chip Density [Bits/Chip]	Rad [Hard]	Non- volatile [Yes]	Access [Time]	Cost [Per Bit in Cents]	Temp [Range]	Appli- cation [Areas]	1984 Matur- ity	Reli- abil- ity	Power	Comments
CMOS	64K	No	Yes	150-200ns	.12	0 to 70°C	Main Mem	Mod	High	V. Low	Good power, Cost Rel.
CMOS/SOS	16K	Yes	Yes	165ns	.01			Mod	High		
NMOS, BORAM	8K	No	Yes	500ns	.04	-55°C +125°C	Fixed Mem. Callb Tbits Cache	Mod	Mod	Low	Costly
Dynamic Ram	64K (256K) (1M)	No	No	250ns	.04	-55°C +125°C	Main Mem. Cache Mem.	Mod	High	Low to Mod	No Rad-Hard
Magnetic Bubble	1M (4M) (16M)	Yes	Yes	1.5ms per Mbit	.05	-40°C +85°C	Secondary Memory	Low to	Mod to	Mod to	Excellent Secondary Memory
Plated Wire	10 ⁶ Bits per plane	Yes	Yes	1 sec	2. to 11.	-55°C +85°C	Main Memory	High	Mod	Mod to High	V. High Cost; Limited Suppliers
Magnetic Tape	10 ⁸ to 10 ⁹ Bits per in. ²	Yes	Yes	10 ⁻¹ to 10 ⁻² sec	10 ⁻⁶ to 10 ⁻⁷	-55°C +85°C	Secondary Memory	High	Mod to Low	Very to High	Mechanical Slow, Bulk
Core	10 ⁵ per plane	Yes	Yes	350ns	1.5/Bit	-55°C +85°C	Main Memory	High	High	High Bulk	Mod. Cost High Power
Cross-Tie (CRAM)	16K	Yes	Yes	500ns	.06	-55°C +125°C	Main Mem Core Re- placement	Low	Unkn	Mod to Low	New Technology
(Projected) Gallium- Arsenide (GaAs)	256 bits 1K (4K)	Yes (Very)	Yes	1-5ns	.38	-200°C +200°C	Main Mem. Cache	Low	Unkn	Unkn	New Technology

Note 1: Values in parentheses are densities project to be available for space applications within OTV development time frame.

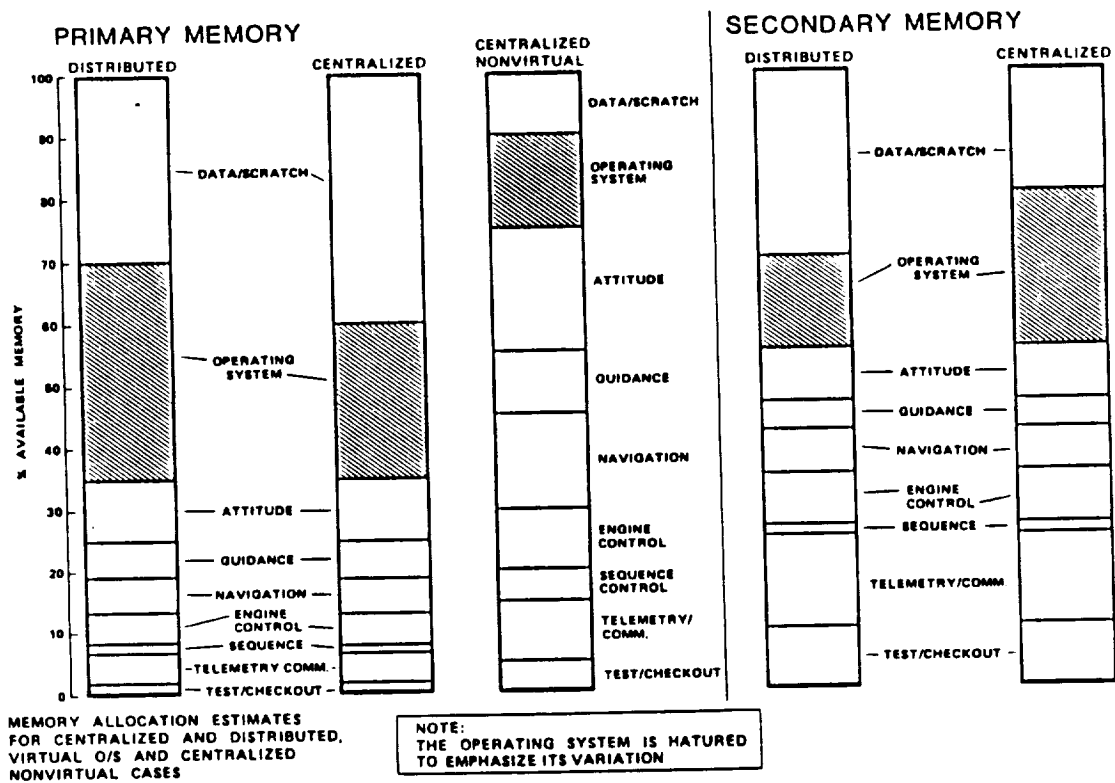


Figure 2.1.2.1-8 Estimates for Available Memory Utilization by Avionics Function

The Teledyne TDY 750S is a close second to the MAGIC V. Its performance metric is quite good as are the fault-tolerance features and its overall risk metric. The TDY 750S's growth ability is weaker than the MAGIC V, due in part to its very close ancestry to the MECA 43S (not used in this study). The same reason is cited for the weak rating of its form factor.

The remaining computers are lower in score value than the above units. Close examination of Table 2.1.2.1-11 shows the areas in which each excelled or fell short of the preferred candidate's benchmark. Table 2.1.2.1-15 summarizes the significant features of the candidate executive computers.

ORIGINAL PAGE IS
OF POOR QUALITY

Table 2.1.2.1-15 Executive Computer Candidates

	ITEK IATAC-16MS	DELCO MS62/1US	DELCO MAGIC 572H	DELCO MAGIC V	TELEDYNE TDY 750S	IRCA SCP-STAR DUAL CPU	IRCA SCP-STAR 111	LITTON ILC-4516E	LITTON ILC-4750	IBM AP-101S	IBM NSSC-1	SINGER SKC-3121H
Performance (KIPS)	1500	1718	1750	1850	1574	1536	12000	1300	1800/3000	1000	1135	1000
Word Size(s) (bits)	116/32	116/32	116/32	116/32	116/32	116/32	116/32	116/32	116/32	116/32	118	116/32
Processor Technology	Schottky 1bit slice	Bipolar Monolith	CMOS	CMOS/SOS	CMOS	CMOS/SOS	CMOS/SOS VHSIC	LSI bit slice	Standard LSI	MEM:CMOS	Hybrid;CMOS	CMOS
Power of xKw	160w @	1150w @	136w @	160w @	1135w @	123w @	CPU: 15w MEM: 10w	180w @	121w @	120A @ 28v	139w @	111.5w @
Memory Size	164Kw	164Kw	164Kw	11000Kw	1640Kw	1128Kw	1128Kw	148Kw	164Kw	1256Kw	164Kw	164Kw
Weight (lbs)	125	144	17.1 (Brass- board)	19.0	150	148 No Shield	1160 w/Shld board)	127	1160 w/Shld board)	70	140	
Radiation Hardened	Yes	15 E+3	1E+5 to E+6	Yes	Yes	Yes	Yes	12 E+4	Yes	Yes	Partial	Partial
Reliability at x yrs	1.998	1.99 @ 2 Yrs		1.96 @	1.9 @ 10 Yrs	1.927 @	1.98 @ 10 Yrs	2 Yrs	16Khr + 1MTBF			
Floot Pt. Available	Yes	Yes	Yes	Yes	Yes	Yes	Yes	Yes	Yes	Yes	Yes	Yes
Processor Instr. Set	Unique	Unique	11750A-1	11750A-1	11750A-1	11750A-1	11750A-1	Unique	11750A-1	11750A-1	Unique	Unique
High-Order Language Suppt	Fort 4 HAL/SI APL; IBM	Jovial J3B J371	J73; VAX	J73; VAX	J73; VAX	J73	J73	Fortran; VAX IBM	J73, Ada; VAX		HAL/S; PDP-11/70	SKC Fortran
Space-Rated	No	Yes	No	No	No	No	No	Yes	No	No	Yes	No
Heritage	Galileo	11US						Space Sextant, Others		Shuttle OBC Upgrade	Solar Max, Others	Shuttle Bidder

RECOMMENDATIONS--A shared memory approach is recommended for the OTV's primary interconnection path. A global network approach is recommended for interprocessor connection. A hierarchical approach is recommended for the OTV's secondary interconnection paths such as between controller and sensors/actuators. Prepare a trade study on fiber optic versus coaxial path methodologies and applicability to OTV primary and secondary interconnection subsystems. CMOS/SOS is recommended for all primary memory stores on OTV. Bubble memory is recommended for all secondary memory stores on OTV. The DELCO MAGIC V is recommended as the executive computer candidate. Conduct system reliability modeling on selected data management candidates using applicable Martin reliability analysis tools. Conduct a technology study regarding the nature of the executive operating system, its functional requirements, and whether or not custom-built system software is appropriate. Prepare recommendations for standards on computer ISA, internal data and control buses, external data/control interfaces with 1) Shuttle, 2) OMV, 3) Space Station, 4) Manned Capsule, and 5) generalized payload.

2.1.2.2 Fuel Cell Versus Solar Array Power

PURPOSE--Batteries, fuel cells and photovoltaic arrays are currently used to power spacecraft. Each imposes particular requirements upon the spacecraft configuration and operations. Technical improvements in batteries and solar cells make them attractive for use in the OTV. In particular, high energy density batteries such as lithium thionyl chloride batteries (LiSOCl₄) appear promising for short duration missions, while fuel cell systems and photovoltaic systems appear better suited to longer mission timelines such as manned GEO servicing. The objective of this study is to select a method of power generation based on the requirements of the various OTV missions.

PROBLEM STATEMENT--Several options exist for spacecraft power generation. High and low rate primary batteries, solar arrays and secondary batteries, and fuel cells were considered.

POWER SOURCE CANDIDATES--

PRIMARY BATTERIES--Primary battery systems utilize electrochemical energy storage to provide power to the spacecraft. Primary as opposed to secondary batteries are characterized by a moderate to high energy density. In addition, power conditioning is not required because of the voltage regulation of the battery. At the end of battery discharge the battery is expended with the electrodes mechanically degraded, and incapable of accepting a recharge. Two types of primary batteries were considered, Lithium Thionyl Chloride and Silver Zinc. Silver Zinc (Ag/Zn) batteries are characterized by moderate energy density (55 W-Hr/lb), low impedance, and a very high discharge rate capability. AgZn units have a long history of space operation and are well understood. Lithium Thionyl Chloride (LiSOCl₄) batteries are characterized by high energy density (100-200 W-Hr/lb), high impedance, and limited discharge rate capability. (See Table 2.1.2.2-1) A nominal discharge rate for a LiSOCl₄ battery is 150 hours. These batteries can be discharged at higher rates, however, up to 15 hours with modifications. The effect of a fast (15 hour) discharge is a decrease in energy density due to decreased capacity and added componentry in the battery. The effective energy density for a LiSOCl₄ battery at a 15 hour is approximately 100 W-Hr/lb. Battery self heating and internal pressure rise make it impractical to design the system for a higher than 15 hour rate.

Table 2.1.2.2-1 Battery Comparison

BATTERY	TYPE	SPECIFIC ENERGY W-HR/LB	SPECIFIC POWER W/LB	STATUS
Ag/Zn	PRI	80	240	QUALIFIED
Li SOCl ₄	PRI	150	10	NOT QUALIFIED
Ni/Cd	SEC	13	26	QUALIFIED
Ni/H ₂	SEC	18	35	QUALIFIED (GEO)

FUEL CELLS--Fuel cells convert the energy from reactants (H_2 , O_2) to electrical energy directly. A fuel cell is approximately 50% efficient. A high current density point design was selected for the fuel cell to minimize weight and development effort. This results in a slightly higher reactant consumption (approx. 1 lb/KW-H). The fuel cell assembly is designed for maximum power, voltage regulation and size. The OTV maximum power consumption is 2110 W for cryogenic propulsion and 1560 W for storable propulsion with a 20% design margin. This difference is due to the difference in engine power consumption between the cryogenic and storable stages. All other components in the Fuel Cell system are sized for average power consumption or mission energy usage. The resultant thermal load requires an active coolant loop with radiators. The baseline radiator design is sized to reject approximately 1.5 KW which represents a 47% design margin (see Figure 2.1.2.2-1).

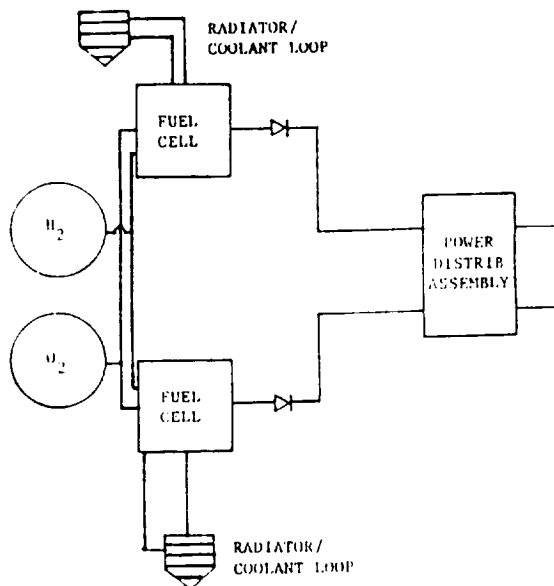


Figure 2.1.2.2-1 Baseline Fuel Cell System

PHOTOVOLTAIC--Photovoltaic systems consist of a photovoltaic solar array and secondary (rechargeable) batteries to supply power to the OTV during the eclipse period of the orbit. The OTV must be capable of operation at both LEO and GEO. The solar array size (power output) is driven by LEO operation, because of the relatively short period available for battery recharge (57 min). Capacity of the secondary batteries is driven by GEO operation due to the longer eclipse duration. Table 2.1.2.2-1 shows two space proven secondary batteries (Ni/Cd and Ni/ H_2). Solar array and battery sizing is based on a day and night time average power consumption of 888 W which includes a 20%

margin. In addition to batteries, solar systems also require active power conditioning to maintain buss regulation and recharge control. The OTV point design is a shunt regulated system. (See Fig. 2.1.2.2-2) Two types of solar array were considered; Gallium Arsenide (GaAs) and Silicon (Si). Gallium Arsenide was selected because of its higher efficiency, lower temperature coefficients, and resistance to radiation damage. These characteristics result in an array which is 23% smaller than the silicon array. The solar array is sized based on a $+10^\circ$ off sun pointing error. This would be accomplished with a two axis gimbal mechanism. The solar array would also be stowed during propulsive maneuvers. Orientation control and stowage are disadvantages of the solar array.

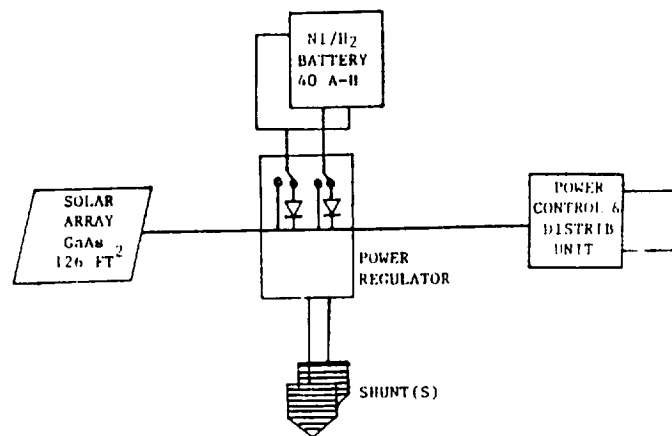


Figure 2.1.2.2-2 Photovoltaic Baseline System

SELECTION CRITERIA--The primary criteria for the selection of an OTV power source are; weight, cost, operational flexibility, development effort, evolution, complexity, and on orbit resupply. These parameters are important because they directly impact program Life Cycle Cost (LCC), vehicle performance, or acquisition cost. Weight, operational flexibility and complexity impact performance, while cost, weight, complexity, evolution, resupply and development effort drive LCC. Table 2.1.2.2-2 depicts the relative weights of these parameters in this trade study.

Table 2.1.2.2-2 Selection Criteria Weights

<u>Factor</u>	<u>Weight</u>
Weight	10
Cost	8
Flexibility	6
Development Effort	7
Resupply	5
Complexity	4
Evolution	10

Orbital resupply refers to the relative amount of effort required to change batteries or load fuel cell reactants at the end of a mission. Changing batteries appears to be limited to ground based designs. Because space-based power systems must be rechargeable, there are no viable candidates, because secondary batteries are too heavy. Operational flexibility refers to the relative number of constraints imposed on the OTV by the power system such as mission duration, maximum power consumption, orientation and deployment/retraction of solar arrays/radiators. Evolution is the relative effort required to utilize the OTV for longer missions.

POWER SOURCE TRADEOFF--A detailed load analysis was performed for each of the OTV design reference missions. These analyses were used in the conceptual design for each of the power source alternatives. These conceptual designs formed the basis for weight and cost estimates which were used to arrive at the relative rankings in Tables 2.1.2.2-3 through -9. Both mission timeline and OTV configuration influence the relative merits of the power source alternatives. Due to a wide variation in energy usage between DRM's the relative weights of the power sources change because of extra battery capacity and additional fuel cell reactant and tankage. Relative weights and costs also are affected by OTV configuration. This is particularly true of the fuel cell because use of cryogen boil off eliminates the need for reactant tankage, and simplifies on orbit resupply. Tables 2.1.2.2-6 and -7 indicate that it is technically infeasible to support a twenty-five day OTV mission with primary batteries. This is due to the excessive weight and volume that this would require. (11,000 lb Ag/Zn and 4300 lb Li SOCl₄). It should also be noted that in all cases the LiSOCl₄ system is heavier than the fuel cell system. This is due to the limited maximum power capability of the lithium battery. For short duration missions the battery size is driven by maximum steady state power consumption. Beyond this point, the added weight of fuel cell reactants (1000 W-Hr/lb) is much less than the added weight of battery capacity (105 W-Hr/lb).

Table 2.1.2.2-3 Configuration/Mission: Ground Based Storable Cargo Bay

FACTOR	WEIGHT	RANKING			
		AgZn	LiSOCl ₄	FUEL CELL	PHOTOVOLTAIC
Weight	10	5 (50)	8 (80)	10 (100)	7 (70)
Cost	8	10 (80)	6 (48)	5 (40)	4 (32)
Flexibility	6	10 (60)	10 (60)	10 (60)	8 (48)
Development	7	10 (70)	6 (42)	7 (49)	9 (63)
Resupply	5	N/A	N/A	N/A	N/A
Complexity	4	10 (40)	10 (40)	7 (28)	6 (24)
Evolution	10	1 (10)	3 (30)	9 (90)	10 (100)
TOTAL		310	300	367	337

Table 2.1.2.2-4 Configuration/Mission: Ground Based Storable ACC Perigee

FACTOR	WEIGHT	RANKING			
		AgZn	LiSOCl ₄	FUEL CELL	PHOTOVOLTAIC
Weight	10	3 (30)	7 (70)	10 (100)	9 (90)
Cost	8	10 (80)	7 (56)	6 (48)	5 (40)
Flexibility	6	10 (60)	10 (60)	10 (60)	8 (48)
Development	7	10 (70)	6 (42)	7 (49)	9 (63)
Resupply	5	N/A	N/A	N/A	N/A
Complexity	4	10 (40)	10 (40)	7 (28)	6 (24)
Evolution	10	1 (10)	3 (30)	9 (90)	10 (100)
TOTAL		281	298	375	365

Table 2.1.2.2-5 Configuration/Mission: Space Based Storable Perigee (97 & 51K)

FACTOR	WEIGHT	RANKING			
		AgZn	LiSOCl ₄	FUEL CELL	PHOTOVOLTAIC
Weight	10	5 (50)	7 (70)	10 (100)	6 (60)
Cost	8	10 (80)	9 (72)	6 (48)	5 (40)
Flexibility	6	10 (60)	10 (60)	10 (60)	8 (48)
Development	7	10 (70)	6 (42)	7 (49)	9 (63)
Resupply	5	3 (15)	3 (15)	6 (30)	10 (50)
Complexity	4	10 (40)	10 (40)	7 (28)	6 (24)
Evolution	10	1 (10)	3 (30)	8 (80)	10 (100)
TOTAL		325	329	395	385

Table 2.1.2.2-6 Configuration/Mission: Space Based Storable Apogee (57K & 27K)

FACTOR	WEIGHT	RANKING			
		AgZn	LiSOCl ₄	FUEL CELL	PHOTOVOLTAIC
Weight	10	Not Feasible		4 (40)	10 (100)
Cost	8			10 (80)	7 (56)
Flexibility	6	10 (60)	10 (60)	10 (60)	8 (48)
Development	7	10 (70)	6 (42)	7 (49)	9 (63)
Resupply	5	3 (15)	3 (15)	6 (30)	10 (50)
Complexity	4	10 (40)	10 (40)	7 (28)	6 (24)
Evolution	10	1 (10)	3 (30)	8 (80)	10 (100)
TOTAL		Not Feasible		367	441

Table 2.1.2.2-7 Configuration/Mission: Ground Based Cryo (43K & 57K)

FACTOR	WEIGHT	RANKING			
		AgZn	LiSOCl ₄	FUEL CELL	PHOTOVOLTAIC
Weight	10	3 (30)	6 (60)	10 (100)	8 (80)
Cost	8	10 (80)	10 (80)	6 (48)	4 (32)
Flexibility	6	10 (60)	10 (60)	10 (60)	8 (48)
Development	7	10 (70)	6 (42)	7 (49)	9 (63)
Resupply	5	N/A	N/A	N/A	N/A
Complexity	4	10 (40)	10 (40)	7 (28)	6 (24)
Evolution	10	1 (10)	3 (30)	8 (80)	10 (100)
TOTAL		290	312	365	347

Table 2.1.2.2-8 Configuration/Mission: Space Based Cryo (94K & 57K)

FACTOR	WEIGHT	RANKING			
		AgZn	LiSOCl ₄	FUEL CELL	PHOTOVOLTAIC
Weight	10	Not Feasible		5 (50)	10 (100)
Cost	8			10 (80)	7 (56)
Flexibility	6	10 (60)	10 (60)	10 (60)	8 (48)
Development	7	10 (70)	6 (42)	7 (49)	9 (63)
Resupply	5	4 (20)	4 (20)	9 (45)	10 (50)
Complexity	4	10 (40)	10 (40)	7 (28)	6 (24)
Evolution	10	1 (10)	3 (30)	8 (80)	10 (100)
TOTAL		Not Feasible		392	441

Table 2.1.2.2-9 Configuration/Mission: Space Based Cryo (84K)

FACTOR	WEIGHT	RANKING			
		AgZn	LiSOC14	FUEL CELL	PHOTOVOLTAIC
Weight	10	3 (30)	6 (60)	10 (100)	8 (80)
Cost	8	8 (80)	10 (80)	6 (48)	4 (32)
Flexibility	6	10 (60)	10 (60)	10 (60)	8 (48)
Development	7	10 (70)	6 (42)	7 (49)	9 (63)
Resupply	5	4 (20)	4 (20)	9 (45)	10 (50)
Complexity	4	10 (40)	10 (40)	7 (28)	6 (24)
Evolution	10	1 (10)	3 (30)	8 (80)	10 (100)
TOTAL		310	332	410	357

SUMMARY--The optimum power system configuration for OTV is dependent upon vehicle configuration and mission duration. Generally, a fuel cell system will be best for missions less than one hundred seventy hours, and a photovoltaic system will be best for missions greater than one hundred seventy hours. Lithium batteries are not a recommended power source because of their severely limited maximum power capability negates the weight savings that could be realized from the improved energy density (i.e., the maximum power consumptions of 1500 and 2100 watts drives battery size). These batteries would also require a significant development effort. Although Silver Zinc batteries offer no advantage in weight, they do represent a feasible approach to a cargo bay storable OTV. This is particularly true if a low cost, low risk limited capability OTV is begun early to prove the aerobraking concept.

The optimum approach to OTV electrical power generation is a fuel cell system for short duration missions, and a photovoltaic system for manned GEO sorties and lunar missions. This is because for long duration missions the fuel cell system, exhibits a weight penalty of 1000 lb for reactants and tankage. However, use of a power down mode for long term orbital storage (during GEO manned, GEO servicing or lunar missions) would reduce this weight penalty and make the fuel cell more attractive. To avoid the development of two separate electrical power systems it is recommended that power down be assumed and the fuel cell system be selected. The existing shuttle orbiter fuel cells can be downsized with little design risk and minimum cost and the remainder of the plumbing also derived from existing designs.

The basic characteristics of the OTV fuel cell system for both cryogenic and storable stage applications is shown in Table 2.1.2.2-10.

2.1.2.3 Built-In Versus Multiple Unit Redundancy

PURPOSE--This study presents issues concerned with determining the general level of redundancy to be used in packaging OTV avionics equipment. The trade is essentially between simplex, duplex and/or triplex redundancy given the "no single failure" criteria used throughout the OTV design.

Table 2.1.2.2-10 OTV Fuel Cell Breakdown

ORIGINAL PAGE IS
OF POOR QUALITY

	Storable					
	Ground-Based		Space-Based			
	Cargo Bay	ACC	Perigee		Apogee	
	Perigee	Perigee	97K/31 Hours	51K/31 Hours	58K/25 Days	27K/25 Days
	37.3K/23 Hours	37.3K/46 Hours				
Fuel Cells (2)	110 Lb	110 Lb	110 Lb	110 Lb	N/A	N/A
Plumbing	25 Lb	25 Lb	25 Lb	25 Lb	N/A	N/A
Radiators (2)	50 Lb	50 Lb	50 Lb	50 Lb	N/A	N/A
Coolant	15 Lb	15 Lb	15 Lb	15 Lb	N/A	N/A
H ₂ O Storage	15 Lb	15 Lb	15 Lb	15 Lb	N/A	N/A
Reactants	25 Lb	43 Lb	30 Lb	30 Lb	N/A	N/A
Tankage (Fuel)	60 Lb	87 Lb	68 Lb	68 Lb	N/A	N/A
Solar Array	N/A	N/A	N/A	N/A	175 Lb	175 Lb
Batteries (Ni/He)	N/A	N/A	N/A	N/A	123 Lb	123 Lb
Regulator	N/A	N/A	N/A	N/A	40 Lb	40 Lb
S.A. Controller	N/A	N/A	N/A	N/A	22 Lb	22 Lb
PCDU* (2)	54 Lb	54 Lb	54 Lb	54 Lb	54 Lb	54 Lb
Total EPS	354 Lb	399 Lb	367 Lb	367 Lb	414 Lb	414 Lb

*Includes: Sequencers
MDS
Diodes and Resistors

	Cryo				
	Ground-Based		Space-Based		
	ACC		Perigee/Apogee		
	Perigee/Apogee	Perigee/Apogee	84K/76 Hours	57K/25 Days	58K/25 Days
	42K/76 Hours	57K/76 Hours			
Fuel Cells (2)	110 Lb	110 Lb	110 Lb	N/A	N/A
Plumbing	25 Lb	25 Lb	25 Lb	N/A	N/A
Radiators (2)	50 Lb	50 Lb	50 Lb	N/A	N/A
Coolant	15 Lb	15 Lb	15 Lb	N/A	N/A
H ₂ O Storage	15 Lb	15 Lb	15 Lb	N/A	N/A
Reactants	71 Lb	71 Lb	71 Lb	N/A	N/A
Tankage (Fuel)	N/A	N/A	N/A	N/A	N/A
Solar Array	N/A	N/A	N/A	175 Lb	175 Lb
Batteries (Ni/He)	N/A	N/A	N/A	123 Lb	123 Lb
Regulator	N/A	N/A	N/A	40 Lb	40 Lb
S.A. Controller	N/A	N/A	N/A	22 Lb	22 Lb
PCDU* (2)	54 Lb	54 Lb	54 Lb	54 Lb	54 Lb
Total EPS	340 Lb	340 Lb	340 Lb	414 Lb	414 Lb

*Includes: Sequencers
MDS
Diodes and Resistors

SUMMARY-- Quite adequate reliability can be achieved using a functional modular duplex redundancy approach for OTV avionics subsystems. Triple modular redundancy is appropriate for cases where single failure diagnosis is not necessary or would seriously degrade system performance.

PROBLEM STATEMENT--Determine the appropriate level of redundancy (simplex, duplex, or triplex) to be used in packaging avionics functions.

ASSUMPTIONS--No more than triplex redundancy is appropriate for consideration given the "no single failure" requirement.

INITIAL CONDITIONS--Table 2.1.2.3-1 summarized the given levels of avionics equipment redundancy and mean failure rate (MFR) to be used in this study.

Table 2.1.2.3-1 Summary of Avionics Functional Unit Equipment Redundancy and Mean Failure Rate

<u>FUNCTIONAL UNIT</u>	<u>QUANTITY</u>	<u>FAILURE RATE (PER HOUR)</u>
Executive Computer	2	1 x 10 ⁻⁴
IMU	2	1 x 10 ⁻⁴
Star Tracker	2	2 x 10 ⁻⁵
Flight Controller	2	1 x 10 ⁻⁵
Command & Data HDLR	2	1 x 10 ⁻⁵
TLM PWR supply	2	2.5 x 10 ⁻⁶
Transponder	2	2.0 x 10 ⁻⁵
RF PWR AMP	2	1 x 10 ⁻⁵
GPS RCVR	1	1 x 10 ⁻⁵
GPS Antenna	2	9 x 10 ⁻⁸
Sequencer	2	1 x 10 ⁻⁵
Deploy Timer	2	1 x 10 ⁻⁵
Steerable Antenna	2	2.7 x 10 ⁻⁶
Duplexer	2	1 x 10 ⁻⁶
Motor Switches	6	1 x 10 ⁻⁵
Battery	2	1.43 x 10 ⁻⁵
Fuel Cell	2	1.05 x 10 ⁻⁵
Radiators	2	1 x 10 ⁻⁶
FC PWR Conditioning	2	1 x 10 ⁻⁵
Condition Monitor	1	1 x 10 ⁻⁴
Engine Controller	2	1 x 10 ⁻⁵
Power Control/Distrib	2	1 x 10 ⁻⁵

REQUIREMENT AND CONSTRAINTS--The overall requirement which established reliability states "that no single failure shall prevent the safe return of the crew or, if unmanned, the OTV alone."

SELECTION CRITERIA--The redundancy method which yields the greatest reliability over time is considered the preferred candidate.

DESCRIPTION OF CANDIDATES--The candidates and results presented here are those described by Snyder (1980). Three levels of redundancy are defined here: a. logic gate level b. functional module level c. box computer level.

GATE LEVEL REDUNDANCY--Logic gates are replicated or are added in circuits to mask failures. For example, triple modular redundancy (TMR), quadded logic and various error detection/correction (EDAC) codes are commonly observed in present-day devices. Combinations of these redundancy types within a device are also common. EDAC on each word of memory is a viable technique when single bit error masking is desired, for example.

FUNCTIONAL MODULE LEVEL REDUNDANCY--It is now common to produce a functional unit of a semiconductor-based device on a single, plug-in card or module. Memory cards, I/O controller cards, and CPU cards are examples of such functional units.

Functional partitioning (breakdown) of units is also common. For example, 4K or 16K memory cards plug in for a composite memory bank. Power supplies also are rendered in such form.

Two popular redundancy variations are observed at this level. These are a) Cross-strapping (duplex or triplex redundancy), and b) block sparing (n-plex).

BOX LEVEL (EXTERNAL) REDUNDANCY--This is the "black" box level or external redundancy. It is the use of independent, (usually) simplex devices that are interconnected into redundancy types such as duplex or triplex redundant. Here, the box is considered a subsystem and redundant interconnection to other subsystems is provided (cross-strapping).

COARSE SCREENING-- No coarse screening is appropriate for the three redundancy approaches considered here.

EVALUATION OF CANDIDATES--The three levels of redundancy are compared in Tables 2.1.2.3-2 thru -7 in terms of their advantages and disadvantages. It is clear that the functional module level of redundancy has superior attributes to those of either gate or box level redundancies. Hughes (1973) shows conclusively in the case of a PCM encoder that using functional module (duplex) redundancy significantly improves reliability (.7669 vs .9265 at 10 yrs.) over a (simplex) parallel standby configuration at an increase of only 7.5% in componentry.

With respect to the candidate redundancy approaches (simplex, duplex, and triplex), Lowrie (1963) demonstrated conclusively that for a partitioned computer (box) system, the duplex method achieved the best reliability over time. Figure 2.1.2.3-1 is a reproduction of Lowrie's Figure 11. Here it is seen that for a partitioning of the system into 10, 30, and 100 mutually independent pieces, the relationship of the simplex, duplex and triplex methods is maintained with duplex redundancy being superior in all cases.

Table 2.1.2.3-2 Gate Logic Level Redundancy Comparison

ADVANTAGES	DISADVANTAGES
<ul style="list-style-type: none"> o Errors are masked o No diagnostic overhead is incurred o Excellent for cases requiring safe operation over short time periods o Use of CMOS or other low power, high speed technology can counteract some of the negatives o Promotes the use of single bit error detection/correction code on memory words 	<ul style="list-style-type: none"> o To achieve triple modular redundancy for majority vote systems, three times the simplex number of gates are required o Increased gate numbers cause increased power drain and heat, which decreases reliability o Weight and volume are increased o TMR depends upon the reliability of the voting circuits, which themselves require more power and increase weight and volume o Voting circuit, in some cases, must be triplexed which further compounds these negative features

Table 2.1.2.3-3 Functional Module Level Redundancy Comparisons

ADVANTAGES	DISADVANTAGES
<ul style="list-style-type: none"> o Takes advantage of convenient, material partitions arising from manufacturing or other processes i.e. Memories partition into 2K, 4K, 8K, 16K, 64K and 256K bit or byte assemblies o Functional partitioning generally reduces power, size and cost of assemblies o Several redundancy techniques are available using functional module partitioning <ul style="list-style-type: none"> a) Triple redundant CPUs with S/W voting b) Two active, are spare CPU with S/W voting (pair and spare method) c) Cross-strapping d) Block sparing o Functional module level of redundancy is most suitable for software and H/W fault detection with recovery by S/W or external control o Easy to obtain using building blocks of systems 	<ul style="list-style-type: none"> o Recovery from faults may require significant time

Table 2.1.2.3-4 Box (Computer) Level Redundancy Comparisons

ADVANTAGES	DISADVANTAGES
<ul style="list-style-type: none"> o Off-the-shelf existing and previously qualified units can be used o During testing, S/W development or maintenance, a unit can be removed from the system without shutting down the entire system 	<ul style="list-style-type: none"> o Weight and volume is very large o Use of remote TMR circuits adds to system complexity o Synchronization problems are frequent o A failure in any one of a computer's functional units will fail the system o The failure rate is the sum of failure rates of its functional units; the computer's MTBF is lower than the MTBF of the individual functional units o Box level redundancy is less suitable for long life missions

Table 2.1.2.3-5 Simplex Redundancy Method

ADVANTAGES	DISADVANTAGES
<ul style="list-style-type: none"> o Uses minimum resources; parts, power, etc. o Minimum complexity factor (1.0) 	<ul style="list-style-type: none"> o Most susceptible to single point failure o Least reliable method

Table 2.1.2.3-6 Duplex Redundancy Method

ADVANTAGES	DISADVANTAGES
<ul style="list-style-type: none"> o Basic logic circuitry is doubled, not tripled (as required by triplex) o All errors are detected o Two units are required to fail the system which is the same as in a triplex design o The error detector is independent of the data, thus if the detector fails, no data is affected o The faulty unit can be identified uniquely 	<ul style="list-style-type: none"> o Additional time is required to diagnose and then correct a fault o Diagnostic circuits are introduced which can themselves be sources of failure o Intermittent errors are difficult to handle o A condition can exist which permits error detection but no correction

Table 2.1.2.3-7 Triplex Redundancy Method

ADVANTAGES	DISADVANTAGES
<ul style="list-style-type: none"> o Masks single failures without degrading system performance o Reliability better than simplex by a factor of 3 	<ul style="list-style-type: none"> o 3 to 3.2 times as complex as simplex method o Reliability less than duplex o Voting circuits must be 5 to 10 times as reliable as input circuitry - increases cost and complexity o Diagnosis of masked fault difficult, often impossible

RECOMMENDATION--Duplex method's functional module redundancy offers the best reliability versus time performance. Where system performance degradation cannot be tolerated, or in cases where single failure diagnosis is not a strong consideration, then triple module redundancy with voting is preferred. In any case, the simplex method is discouraged unless functional module partitioning produces a simplex train of very high reliability.

REFERENCES

Snyder, F. C., 1980, A Comparison of Redundant Computer Configurations, IEEE.

Hughes, R. J., Jr., 1973, Functional Redundancy Assures Greater System Reliability, Electronics, Mar. 15.

Lowrie, R. W., 1963, High-reliability Computers Using Duplex Redundancy, Electronics Industries, Aug., pp. 116-128.

ORIGINAL PAGE IS
OF POOR QUALITY

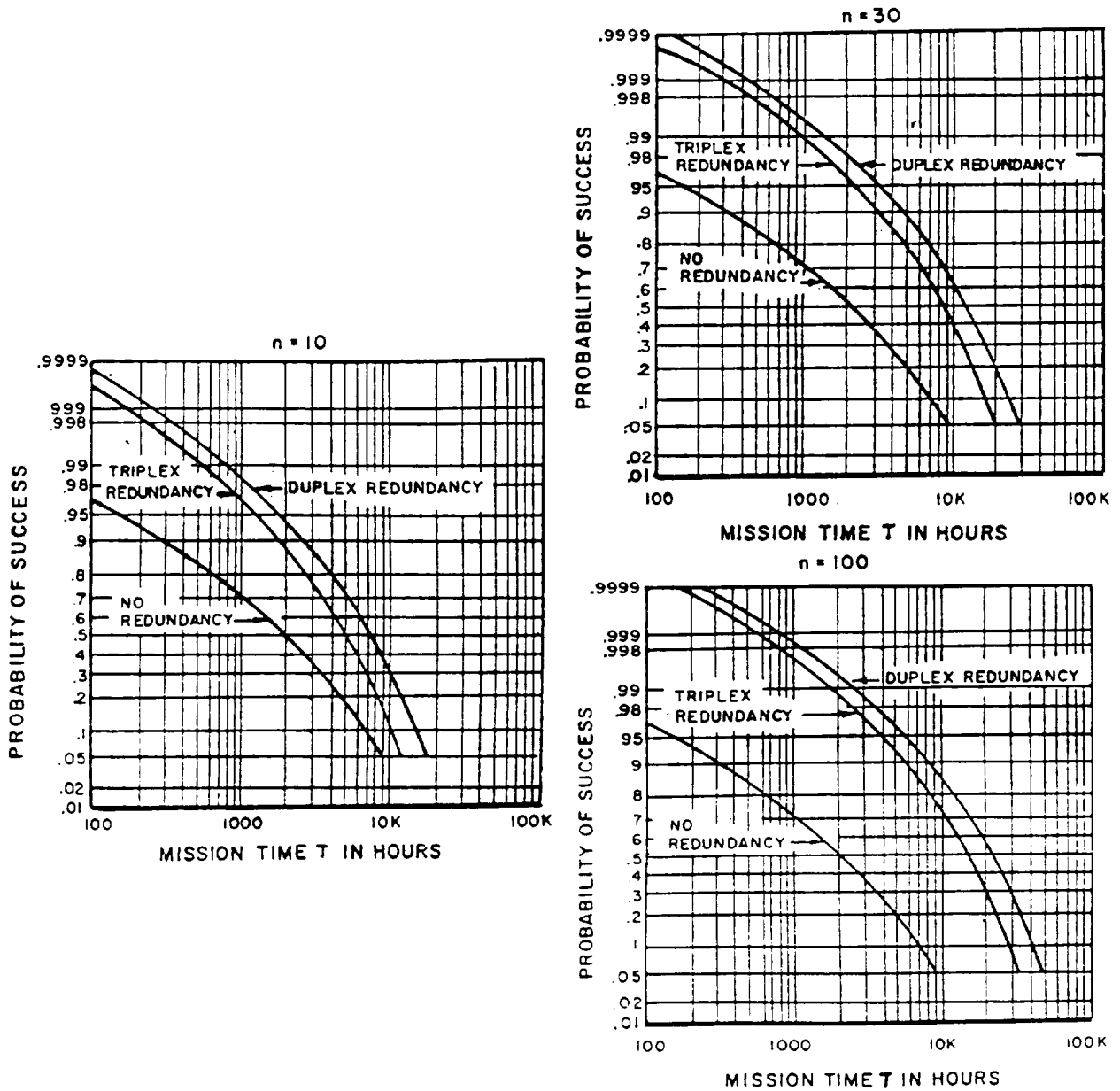


Figure 2.1.2.3-1 Reliability vs time for Simplex, Deplex, and Triple System Partitioned into 10, 30, and 100 Independent Pieces. (Lowrie's Figure 11)

2.1.2.4 Microprocessor Technology

PURPOSE--The objective of this study is to evaluate commercially available microprocessors to understand their performance capabilities, application history and limitations in order to compare them with the requirements of a new upper stage such as OTV. The selection will focus on the reliability, flexibility and cost effectiveness of the spaceborne system.

SUMMARY--Micros have evolved from four-bit through 32-bit devices beginning in the early 70's. Each device has its own unique capabilities primarily determined by word length and instruction set. Because there are numerous candidates, this study has considered only 16 and 32 bit devices. 9 devices were screened down to 5 for the final evaluation. Two manufacturers are presently developing micros with the MIL-STD 1750A architecture. These devices (9450 and MD281) can compete with the most sophisticated computers now flying and will certainly see use in future spaceborne computer systems.

STATEMENT OF PROBLEM--Use of spaceborne digital computers is rapidly increasing with typical applications including attitude control, sequencing, navigation, guidance, signal processing, digital filtering, command and control, and digital imaging. These applications have varying processing requirements, many of which can now be satisfied by the new more capable microprocessors. This study will focus on computation embedded in peripheral units such as the IMU not on the central computer.

Microprocessors are the central processing unit of a microcomputer. When combined with the appropriate memory and input/output they offer the substantial advantage of low power consumption, light weight, flexibility, and low cost (100's of dollars) for space applications. Some micros even have an integral memory. Devices have become available that vastly exceed the performance capability of early aerospace computers. However, obtaining parts that satisfy space qualification requirements presents a problem.

Space and military use constitutes only a small fraction of total production. Manufacturers prefer to design and produce thousands and tens of thousands of units and are not very interested in small runs of "S" - level parts for MIL spec applications. Devices of interest are available only to "B" - level quality controls so that additional screening is left up to the user. Only a few parts are available to MIL-M-38510 on the JAN QPL.

The shuttle PAM upperstage uses micros in a redundant configuration in their sequencer. The inertial upper stage (IUS) also uses micros in their signal conditioner unit (SCU) There are redundant SCU's. A number of orbiting spacecraft use micros with standby redundancy to allow ground controlled switchover. The use of microprocessors in an autonomous avionics system will require careful parts selection and attention to failure modes.

Microprocessors have succeeded in replacing many "mini" computers for ground applications. Their attributes of small size, light weight, low power consumption and ease of software design has contributed to their success. These same attributes readily support the requirements for space applications; however, the space environment includes radiation and must be given serious consideration.

Since microprocessors are very popular for ground applications, many hardware and software tools are available to aid in the design, development and testing of microprocessor software and hardware. These tools can reduce the overall cost and lead time in new spaceborne applications.

SELECTION CRITERIA--A selection criteria that compares the strengths and weaknesses of the various devices is defined in the following paragraphs. Only production microprocessors with good documentation, vendor support and that are available to satisfy the appropriate military standards were considered. Currently Air Force programs having embedded computers require the MIL STD 1750A standard architecture. Until such a device is readily available (Fairchild 9450 is in process) the AF is giving waivers for the TI 9989 and the Intel 8086.

a) SPEED

Requirements indicate that about 16K of 16 bit words of assembly instructions (including floating point) need to be executed in less than 20 ms or approximately 200 KIPS - This is the minimum acceptable speed. Faster processors which increase the time margin will be given relative merit in the weighting criteria.

b) MEMORY ACCESS

Requirements indicate that at least 64K bytes of memory should be accessed. This is the minimum acceptable memory size. Larger accessing processors will be graded accordingly.

c) DATA TYPE

Floating point processing is desirable for both efficiency and ease of coding. Floating point processing on the CPU gets highest merit, followed by co-processors, and last multichip floating point processors.

d) INTERRUPTS

Initial requirements indicate that 5 interrupts are required. Processors which have 5 interrupts are given highest merit, followed by family interrupt support.

e) QUAL LEVEL

Only parts available as 883-B or better will be considered.

f) RADIATION HARDENING

Total Dose - Total duration in space for OTV is limited because each mission is comparatively short (2-20 days). However, with reuse it could approach one year.

g) RADIATION IMMUNITY

Single Event Upset - Processors will be given relative merit according to actual test data or data from similar manufacturing technologies. Parts available as hardened versions will be given highest merit.

h) NOISE IMMUNITY

Parts with the greatest signal noise immunity will be given highest merit.

i) OPERATING TEMPERATURE RANGE

Parts shall operate from -55 to +125°.

j) SUPPORT HARDWARE

Availability of family support circuits will be given highest merit. Requirements for unusual circuits will be given low merit.

k) SOFTWARE DEVELOPMENT SUPPORT

Availability of software development tools and hardware emulators gives highest merit.

The above criteria are summarized in the following table with respective weighting factors. Cost is implicit in the last three factors.

<u>Factor</u>	<u>Weight</u>
Speed	2
Architecture	3
Immunity	4
Support Chips	4
Support Software	5
Development Status	5

DESCRIPTION OF CANDIDATE SOLUTIONS--The following candidate microprocessors have been identified as satisfying the minimum processing requirements and will be evaluated based on the above factors.

- a. 68000 - 16 bit uP - Motorola
- b. 8086 - 16 bit uP - Intel
- c. 80C86 - 16 bit uP - Harris
- d. 9445 - 16 bit uP - Fairchild
- e. 9450 - 16 bit floating point uP - Fairchild
- f. 9989 - 16 bit uP - Texas Instruments
- g. Z8002 - 16 bit uP - Zilog
- h. 32032 - 32 bit uP - National
- j. MD281/MD281E - 16 bit floating point uP - McDonnell Douglas

68000 MOTOROLA--The 68000 is very popular and has an instruction set that provides maximum computing power with simplicity. However, testing that was done for radiation/single event upset indicated that the 68000 would not be suitable.

8086 INTEL--The Intel 8086 is made from HMOS (NMOS) technology and uses dynamic storage techniques for the internal registers. Dynamic memory is extremely sensitive to single bit errors induced by radiation in space. No known testing data is available for single bit errors in this processor, however at least two companies are presently building computers using this up for space applications. SCI, Inc. is using redundant 8086's in their new DACS. Southwest Research Institute is using the 8086 for non-critical applications on SpaceLab experiments.

80C86 HARRIS--This microprocessor is a static CMOS version of the Intel 8086, pin compatible and can drive TTL loads. This is a new device and problems can be expected for about 1 year. Harris also markets a full line of CMOS family support chips. Only one version, a 5MHz version is available. CMOS devices can be operated at a voltage greater than 5v (7 volts for the 80C86) reducing noise induced problems and also reducing single bit error susceptibility. Power dissipation is lower about 50mA compared to 200mA for the 68000 or 300mA for the Z8000 series. Software development tools are available and are inexpensive. Actual radiation tolerance is unknown. The device is made of CMOS using a self-aligned silicon gate CMOS process. Memory made from this process proves to be suitable for the space environment. Southwest Research Institute is changing their SC-1 computer to use this CMOS version of the 8086.

9445 FAIRCHILD--Martin Marietta performed tests with this up. Although rated for 20 MHz only 16 MHz versions are available. Although this is a good microprocessor the architecture was designed for ground based business applications and software would be very expensive.

9450 Fairchild--The F9450 is the first microprocessor to implement the full MIL-SPEC-1750A instruction set architecture (ISA). This ISA is a requirement for all 16-bit embedded computers for the Air Force. The Air Force will only grant waivers until this processor is available. This particular implementation will execute about 700 KIPS DAIS Mix with floating point operations executed in on-chip microcode. Along with the F9450 are two support chips, a block protect unit and a memory management unit. The basic 9450 can access 64K words of memory, and with the memory management unit it can access 1 M words. The 9450 was designed to permit a number of these devices to be interconnected into one system with independent and shared memories. This allows building a redundant system in the same envelope as a single string computer. Multi-processor systems are possible with external arbitration. Piping is done so that DMA is possible between bus cycles. This micro has the support of many commercial companies as well as the Air Force. Software development tools are available at no cost from the Air Force Language Control Facility at Wright-Patterson AFB. The microprocessor should be rad-hard and not susceptible to single event upsets. Floating point data types are on-chip. The 9450 has the greatest processing capability of all the listed micro-processors.

9989 TEXAS INSTRUMENTS--The 9989 is a faster enhanced version of the discontinued 9900. Due to its poor total dose radiation performance, little single event upset testing has been done. Draper Labs has a large investment in equipment requiring the 9989 and is helping TI develop a more radiation resistant version. The 9989 is the slowest processor of this trade study so that timing margins could be a problem.

Z8002 ZILOG--The Z8002 is an NMOS dynamic device and its dynamic registers make this part unsuitable for OTV due to SEU.

32032 NATIONAL--The 32000 microprocessor was designed to be used in large data base systems or where multi-tasking is required. It is able to access 16 M bytes and has provisions for 4 billion bytes of logical addressing. This is divided into 32,768 pages with a fixed size of 512 bytes. This processor implements high order languages in an efficient manner. With a 6 MHz clock speed, the 32000 can execute 16 or 32 bit fixed point instructions at about 700 KIPS. Software development stations are available with in circuit emulators to allow software development.

A CMOS commercial version has just become available and the 883B qualification of the CMOS part will be in about one year.

This CMOS part is new and very little actual data on speed and performance is available. Part yield is low, therefore, the part is difficult to procure at the present time. This is a very promising processor for projects in the 1986 and later timeframe. It should prove to be the workhorse of many large database and graphics multi-user systems.

MD281/MD281E (McDonnell Douglas)--The MDAC MD281 is a 1750A general purpose 16 bit "Microprocessor Module". The CPU consists of three custom CMOS/SOS LSI circuits on one single pluggable assembly (hybrid). The CPU can perform 944 KIPS (DAIS Mix) with 167nS memory. The MD281E is an "Extended Processor Module" which includes the MD281 and memory management functions. The memory cycle is 200nS which gives 884KIPS (DAIS Mix) performance.

The processor was designed for space and aerospace applications and is available in the military temperature ranges although not a full 883B. Also the packaging is rated for only 70,000 ft. The CMOS/SOS technology is the hardest known for both total dose as well as SEU. The 1750A instruction set architecture is currently being supported in many areas of software design/development including compilers, debuggers and simulators/emulators. MCDAC has their own 1750A development system.

COARSE SCREENING--The Motorola 68000 and Zilog Z 8002 use the NMOS technology and were eliminated for their susceptibility to single event upset. The Intel 8086 was avoided for the same reason; however, it is presently available as the Harris 80C86 fabricated with CMOS. The 9445 was eliminated because its architecture and instruction set are oriented to business applications.

EVALUATION AND CANDIDATE SELECTION--Evaluation of the 5 remaining microprocessors is summarized below emphasizing the weighting factors described in selection criteria.

<u>Factor</u>	<u>WT</u>	<u>80C86</u>	<u>9450</u>	<u>9989</u>	<u>32032</u>	<u>MD281</u>
Speed	2	3 (6)	4 (8)	1 (2)	3 (6)	5 (10)
Architecture	3	3 (9)	5 (15)	3 (9)	4 (12)	5 (15)
Immunity	4	4 (16)	4 (16)	5 (20)	4 (16)	5 (20)
Support Chips	4	5 (20)	5 (20)	4 (16)	4 (16)	4 (16)
Support Software	5	4 (20)	5 (25)	3 (15)	1 (5)	5 (25)
Development Status	5	5 (25)	5 (25)	5 (25)	4 (20)	3 (15)
Overall Totals		96	109	87	75	101

The weighted results indicate that 3 processors are most attractive for the OTV, the Fairchild 9450, Harris 80C86, and MCDAC MD281/MD281E. The TI9989 is considered too slow and power consumptive. Production of the NSC 32032 is limited and it is available now only in small sample quantities at a 6 MHz version. The 10 MHz and 883 versions will be available later next year.

The 9450 is the most attractive processor at this time if one discounts its limited distribution. However, this part far exceeds the performance of the other micros with the exception of the MD281.

The 80C86 is currently available in 883B qual level. Its performance would be marginal and some risk would be involved with the timing margins.

The MD281 is the fastest processor of the group. It also provides the best radiation resistance. Special packaging for the space environment would be required because of the 70,000 ft. rating.

2.1.2.5 On-Board Check Out Versus Ground Processing

PURPOSE--This study compares the ground and onboard methods of OTV checkout for the ground-based class of OTVs.

SUMMARY--The onboard checkout method is the preferred approach due to the extensive data processing, built-in-test, and sensors aboard the OTV.

STATEMENT OF PROBLEM--OTV checkout consists of those activities which validate the functional integrity and operational readiness of the vehicle. Checkout prior to launch of the ground-based OTV will make use of our computerized checkout set such as the CCMS. Determining the degree to which checkout activities are conducted by the OTV itself using its onboard equipment as opposed to having CCMS type equipment bear the entire burden of checkout is the principal objective of this study (i.e., onboard vs ground checkout).

ASSUMPTIONS--Onboard checkout for a ground-based OTV is directly transferable to space-based operations. Space station support services for checkout are available. Neither approach to checkout may significantly modify the OTV design. The CCMS or equivalent is interfaceable with the OTV.

INITIAL CONDITIONS--None.

REQUIREMENTS AND CONSTRAINTS--Vehicle condition monitoring equipment is not available on the ground-based OTV. Table 2.1.2.5-1 summarizes the general checkout procedures required of the OTV.

SELECTION CRITERIA--Both ground and onboard methods for vehicle checkout are evaluated in terms of their ability to satisfactorily conduct all of the required procedures.

SELECTION RATIONALE--The preferred candidate method will be that which accomplishes all required checkout procedures and has minimal impact on the established vehicle configuration (both hardware and software).

Table 2.1.2.5-1 Checkout Requirements Summary

	CHECKOUT PROCEDURE PERFORMABLE ON	
	GROUND	ONBOARD
<u>Propulsion System</u>		
Leaks	Yes	No
Valves	Yes	No
Tubes/Plumbing	Yes	No
Turbopumps	Yes	No
Blockage	Yes	No
Cracks/Fatigue	Yes	No
Tanks	Yes	Yes
<u>Avionics System</u>		
Executive Computer	Yes	Yes
Executive Operating System	Yes	Yes
Global Network bus	Yes	Yes
Primary & Secondary Memory	Yes	Yes
IMUs	Yes	Yes
Star Scanners	Yes	Yes
Flight Controllers	Yes	Yes
Engine Controllers	Yes	Yes
GPS Receiver/Antennas	Yes	Yes
Command Subsystem	Yes	Yes
Telemetry Processing Subsys	Yes	Yes
C&DH Remote Units Equip List	Yes	Yes
C&DH I/O Control Units	Yes	Yes
Transponder	Yes	Yes
RF Subsystem	Yes	Yes
Deploy Timers	Yes	Yes
Sequencers	Yes	Yes
Power Generation	Yes	Yes
Power Control and Distrib	Yes	Yes

DESCRIPTION OF CANDIDATES--

GROUND CHECKOUT METHOD--The ground checkout method has all vehicle checkout procedures (Table 2.1.2.5-1) vested in CCMS type facilities and the launch control center. The OTV undergoes preflight checkout via ground data bus circuits between the CCMS and STS/OTV as necessary to certify that all systems are flight ready. After integration with the Shuttle on the launch pad, only cursory functional checks are performed.

Prior to deployment from the shuttle, checkout is conducted by the ground crew with participation via the telemetry and command link.

ONBOARD CHECKOUT METHOD--The onboard checkout method has almost all vehicle checkout procedures conducted under the supervision and control of the prime executive computer. All test procedure software and hardware is carried on the OTV such that the OTV performs in a maximally autonomous fashion. Refer to Table 2.1.2.5-1 for required checkout functions. Secondary memory requirements for checkout software residence are approximately 30% to 50% greater than for the ground checkout approach. Execution of the onboard checkout software would be by one of the two executive computers without posing any significant timing conflict to ongoing operational codes running on the prime computer. Prior to STS/OTV launch, checkout procedures are initiated by and results returned to the CCMS via the various ground links. Thereafter, the telemetry and command link is used by the OTV to advise ground controllers of the vehicles health and status.

COARSE SCREENING--No coarse screening is necessary.

EVALUATION--The distributed, multiprocessor design of the avionics data management subsystem fully supports the onboard checkout methodology. In no case could the OTV perform the totality of tests which are required to fully validate the vehicle's condition, however, a very large fraction of the checkout activities now foreseen are doable by the OTV. Certain operational conditions (which are as yet not specified) must exist for the OTV to conduct semiautonomous checkout. Table 2.1.2.5-2 summarizes the ground and onboard checkout method's advantages and disadvantages.

Table 2.1.2.5-2 Ground vs Onboard Checkout Summary

GROUND CHECKOUT METHOD

ADVANTAGES	DISADVANTAGES
<ul style="list-style-type: none"> o Larger computers on ground allow for more sophisticated diagnostics o Reduces onboard memory volume requirement o Reduces complexity of onboard software 	<ul style="list-style-type: none"> o Tests and diagnostics are lost after launch o Procedures developed for ground-based checkout are not transferable to Space Station o Increases complexity of ground software o Increases ground operations complexity and overhead since vehicle is less autonomous

ONBOARD CHECKOUT METHOD

ADVANTAGES	DISADVANTAGES
<ul style="list-style-type: none"> o Provides a greater degree of spacecraft autonomy o Tests and diagnostics are available after launch which increases the spacecraft survivability o Procedures developed for onboard checkout are transferable to Space Station o Increases autonomous character of vehicle Decreases ground operations or Space Station operations complexity and overhead as a consequence of increased autonomy 	<ul style="list-style-type: none"> o Increases memory requirement o Increases spacecraft software complexity

The primary requirement is for the CCMS to have the ability to hold, transmit, and validate correct reception of checkout software by the OTV. Once downloading of test software is complete, the CCMS can initiate the checkout without further intervention.

Control of external devices to the OTV by the OTV is possible if a suitable data path is established. Again, the CCMS can set up such a path, download the appropriate software and relinquish control to the OTV. This may or may not be necessary depending on whether the measurements being made would normally be retained by the OTV to assist in trend analysis/failure prediction or calibration operations.

The absence of a condition monitor and supporting sensors significantly limits the OTV's ability to checkout the propulsion system. Extensive Built-in-test-and-evaluation (BITE) hardware/firmware throughout all assemblies of the avionics system allows the OTV to thoroughly checkout its subsystems. The multiprocessor design further allows "jumping" across computers so as to repeat testing from the prime and backup (or redundant) processor. A checkout performed by the OTV will be as or more reliable than a checkout conducted by an external system.

Checkout software development for an onboard method would be less than for the ground method due to reuseability of codes and tools developed for the operational software, assuming a common HOL development environment is utilized.

Insofar as can be determined at this time, no modification to OTV avionics is necessary to accomplish onboard checkout. Stimuli to begin any test would be handled the same in either case. Responses would be monitored either by the ground or onboard so that only minor wiring changes would be required in the case of the test output points.

RECOMMENDATION--The ground-based OTV is well suited to perform a significant portion of its own checkout activities. It cannot, however, conduct a total checkout without some CCMS support. A semiautonomous onboard checkout approach is recommended for the ground-based OTV.

2.1.2.6 Gyro Technology

PURPOSE--Lightweight, low power gyros are required to maintain a precise OTV attitude during both powered and coasting flight. Use of these gyros in the strapdown mode is also required for onorbit alignment and initialization as required with the Orbiter and Space Station. Advances in the state-of-the-art gyro systems have included increased use of dry tuned (2 DOF) gyros, limited application of laser gyro in space, and laboratory demonstration of other new technology gyros. The objective of this investigation is to assess the development and production status of rate sensing instruments and systems in order to identify those units that hold the most promise for OTV application. The scope of this study is intentionally broad in order to project far enough into the future.

SUMMARY--A trade study was performed to evaluate gyro technologies that might apply to OTV. Four basic gyro technologies were considered: 1) spinning mass, 2) ring laser, 3) fiber optic, and 4) hemispheric resonant or sonic.

Single degree of freedom spinning mass units were eliminated for complexity, cost, and maintenance considerations. Dry tuned gyro (DTG) units are very attractive for their performance, inherent redundancy (two output axes from a single instrument) and space proven status. Ring laser gyros have distinct performance advantages and will be space proven on the transfer orbit stage (TOS) well before the first OTV usage. Fiber optic and hemispheric resonant gyros were determined to be too risky for serious consideration at this time.

A detailed comparison of DTGs and RLGs resulted in the selection of the RLG based on performance and stability. Some consideration should be given, however, to DTGs for early use in low cost light weight ground-based storable applications.

STATEMENT OF PROBLEM--Spinning mass rate sensing devices have been in production for many years. The primary spinning mass sensor is the proven single degree of freedom (SDOF) gyro. In a SDOF unit, the gyro element senses and provides outputs about a single axis. The electrically restrained rate integrating gyro is the fundamental inertial quality instrument. The basic difference between an electrically and a mechanically (spring) restrained rate gyro is that the spring restrained unit reacts against a physical torsion spring while the rate integrating unit uses electrical restraint via a electromagnetic feedback torquer. Damping in the rate integrating gyro is produced by shearing of fluid between the float and the case. A two degree of freedom 2DOF gyro simultaneously senses and provides outputs about two axes. These dynamically tuned (also called dry tuned) 2DOF gyros are much less complex, and provide performance equal to or better than SDOF units.

The ring laser gyro (RLG) is a totally different rate sensor that measures phase differences between counter rotating light beams to determine turning rate. The RLG uses CW and CCW light beams reflected within a resonant quartz cavity to produce a varying fringe pattern as a measure of rate.

The fiber optics gyro (FOG), currently under development, will allow much longer light paths. The interference pattern in the fiber optics unit is produced with multiple turns of an optical fiber.

An even newer instrument is the Hemispherical Resonator Gyro (HRG). This device uses the wineglass type vibration to detect and integrate vehicle rates. One supplier is known to have this technology in the laboratory.

SELECTION CRITERIA--The problem is to select an inertial measurement unit made up of gyros with the necessary performance and reliability and having minimum weight, cost and risk. Overall performance includes accuracy, reaction time, dynamic range, plus the ability to operate in severe environments. Gyro and hence IMU accuracy is fundamentally determined by low g and non-g sensitive drift.

Recurring unit cost is not a severe constraint because with reuse it is amortized. However, a device that requires substantial development will have high non-recurring costs and probably suffer in the area of reliability as well. Development status has a substantial impact on front end program cost and may be a key factor in whether a program is initiated.

Both weight and power are important because they influence stage delivery capability. Power consumption can also be translated into weight because it drives sizing of the electrical power generation subsystem. This is especially severe for longer missions where the higher power consumption requires more fuel cell reactant and penalizes payload delivery.

Reliability and fault tolerance are determined by number of instruments, their complexity, and available redundancy. The DTG design has inherent redundancy not available with other instruments. With this exception the other inertial instruments can be replicated and/or oriented as required to provide fault tolerance.

Maintainability is an important factor for space station operations because it is not practical to periodically remove gyros for calibration on orbit. Instrument stability is very important in minimizing this maintenance requirement.

The selection factors discussed above and their assigned weights are as follows:

Factor	Weight
Overall Performance	5
Weight	4
Power	3
Cost	3
Reliability/Fault Tolerance	4
Development Status	5
Maintainability	5

DESCRIPTION OF CANDIDATE SOLUTIONS---The approach taken for this study was to define gyro and inertial measurement unit (IMU) requirements, and request and evaluate data from viable suppliers of inertial quality instruments. The evaluation considered the selection criteria presented in the preceding paragraph. The following paragraphs describe four gyro types and their unique characteristics. SDOF units will not be described because their use appears to be inappropriate in light of less complex, better performing units.

DYNAMICALLY TUNED (TWO DEGREE OF FREEDOM) GYRO--The dynamically tuned gyro (DTG) employs a spinning mass similar to the floated single degree of freedom (SDOF) unit, but is extremely simple by comparison. It uses far fewer parts, is less sensitive to contamination, is assembled dry, and is lower cost because it requires substantially less labor at a lower skill level. Typical floated gyro problems such as complex fluid fill equipment, fluid warm-up, bubbles and contamination, stratification, output axis suspension complexity and stiction, disturbance torque inducing flex leads, super-clean assembly areas, highly temperature sensitive dynamic characteristics, and gas bearing "hard start" have been eliminated. The 2DOF DTG has substantially better producibility and drift characteristics equivalent or superior to the a SDOF gyro. Because the DTG is simpler and senses rates about two axes, it is less expensive and more cost effective than a SDOF unit.

The DTG consists of a ball bearing spin motor, tuned gyro wheel and flexure suspension, two axis differential transformer pick off, and permanent magnet feedback torquer. The synchronous hysteresis spin motor has its rotor connected by a flexure with the spring rate of the flexure dynamically tuned to near zero so that the gyro rotor is free to pivot without substantial friction or spring torque.

Four large companies are currently producing DTGs. Two of these (Kearfott and Litton) are presently producing and delivering large quantities of two degree of freedom gyros and gyro systems for aircraft and space applications. Kearfott has been producing the Gyroflex 2DOF gyro on which the Space Shuttle IMU is based. They are also currently in production with the smaller CONEX unit for the main battle tank and the Mark-48 torpedo. Litton is in production with their G7 unit for the MK-48 torpedo as well as military aircraft.

Teledyne is building the SDG5 used in the DRIRU and DRIMS. The SDG5 has a low drift (.01 to 3°/hr) due to its large angular momentum and precise compensation. However, this large momentum limits torquing capability. Nortronics is in volume production with the GTB2 for tactical missile applications.

RING LASER GYRO (RLG)--The ring laser gyro sensor is unconventional in that it detects and measures angular rates by measuring the path length difference between counter-rotating laser beams. When the gyro is at rest the two laser beams will have identical frequencies. However, when the gyro is subjected to an angular turning rate around an axis perpendicular to the plane of the beams, the path length of the CW laser beam will be different from the CCW beam. Because of this path length difference, the two beams converge to create an interference pattern directly proportional to angular rate. This difference is measured by digital means and converted into electrical pulses, each pulse representing an increment of angular rotation.

Near a zero rotation rate the sensor has a discontinuity that produces a phase lock phenomena and severely limits null performance. In a practical device, the sensor block is given an electromechanical angular rotation dither that interrupts this phase lock, to allow the sensor to accurately measure low rates.

The basic laser block, made of quartz or a special plastic, has a square or triangular cutout that contains a gas mixture. Continuous lasing of two laser beams is induced in this cavity by the application of high voltage between the cathode and the anodes. The lasing action is manifested in CW and CCW beams which are reflected around the cavity by mirrors. The resonant frequency is a function of optical path length. Lasing intensity is sensed and a servo loop controls path length by adjusting mirror position to compensate for temperature and other changes that would be detrimental to lasing action.

Major laser advantages are instant reaction (no warm-up), wide dynamic range, and stability. Laser gyros are insensitive to acceleration and operate over a wide temperature range. Bias drift in the range of 0.03°/hr or better is achievable with little difficulty. Scale factor errors are small and can be readily compensated so that vehicle rotations can be accommodated without loss of accuracy. Laser gyros are generally larger and heavier than equivalent spinning mass (iron) gyros. However, as mirror and dither removal technology improve, they are expected to shrink substantially.

The Transfer Orbit Stage (TOS) is developing and integrating a Honeywell RLG to be available in the late 1980s. This will be the first space usage and provides the confidence for subsequent usage by OTV and other programs.

The Ring Laser Gyro (RLG) has been in development and test for nearly 20 years and in production for more than five years. Honeywell has a production rate of 100-200 units per month for the Boeing 757/767 commercial aircraft. Litton has developed and produced hundreds of RLGs for the commercial A300 and A310 Airbus. Singer Kearfott entered the RLG arena several years ago and will soon be in substantial production.

FIBER OPTIC GYRO (FOG)--The Fiber Optic Gyro (FOG) is a recent rate sensing development where the light is confined to a long optical fiber. Light from a laser source is inserted into each end of the fiber coil using a beam splitter. (Figure 2.1.2.6-1).

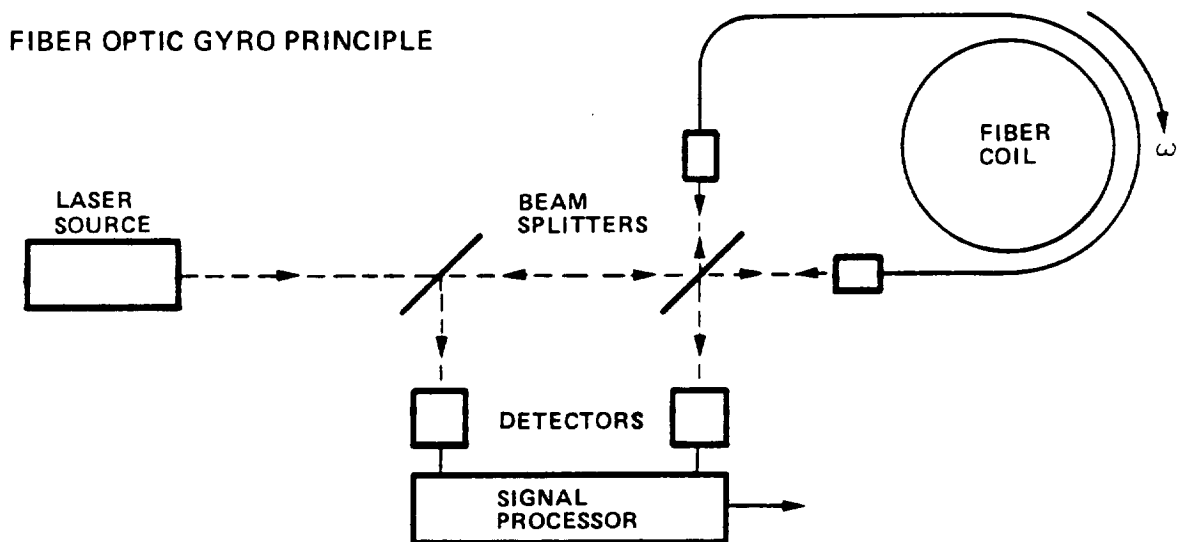


Figure 2.1.2.6-1 Fiber Optic Principle

The nonresonant Sagnac effect ring interferometer has the unique property that when it is rotated, light beams traveling in opposite directions experience a phase delay. Upon exciting the interferometer, the beams produce an interference pattern on photo detectors which shifts in proportion to the

angular rate. The sensitivity is increased (1000 to 10,000 times) over the RLG by multiple turns of a fiber optic path around a small path area - a capability not available in the ring laser gyro. Since the FOG light path is nonresonant, it does not have a frequency pulling and lock-in phenomena like the ring laser gyro and is linear at low input rates.

Because it has no moving parts, there is nothing to wear out. Other advantages are: all solid-state components, no gas laser seal integrity, or low voltages (as in the RLG). A thermal housing over the optics maintains the temperature and aids elevated temperature testing.

HEMISPHERICAL RESONATOR (SONIC) GYRO--The hemispherical resonator is a passive mechanical inertial rotation sensor that integrates rate regardless of its magnitude. Noise is introduced only from the electronics and external environment. The forces (and therefore power) required to sustain and control resonator vibration are extremely low. Figure 2.1.2.6-2 shows gyro construction. The Delco Electronics Division of GM is the only known developer at this time.

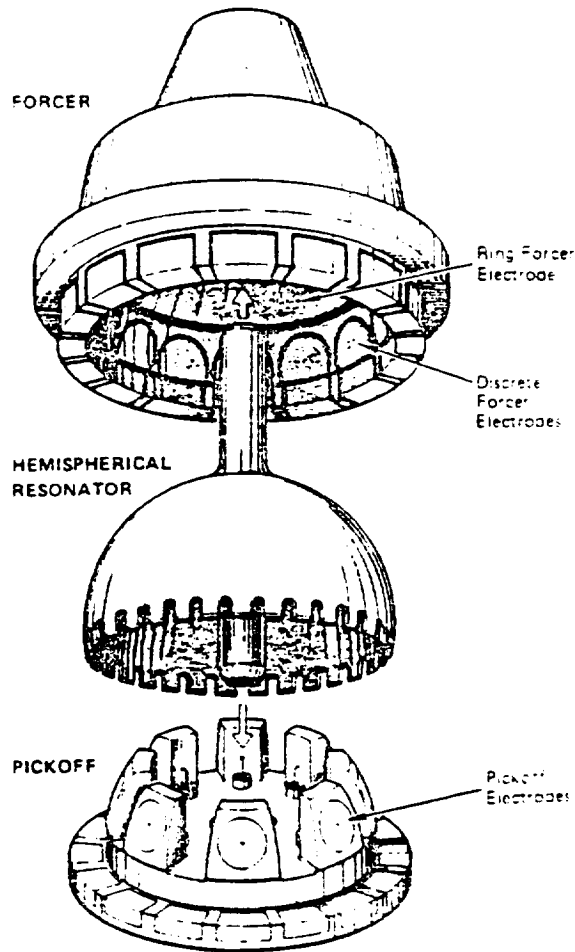


Figure 2.1.2.6-2 Principal Components of the HRG

The device is mechanically simple and consists of three fused quartz parts: 1) forcer, 2) resonator, and 3) pickoff, enclosed in a metal vacuum housing (Figure 2.1.2.6-2). The forcer sustains resonator vibration as well as suppresses quadrature. The resonator is tuned and vibrates in the audio frequency range (and hence the name sonic) like a fine wineglass.

Its vibratory pattern responds to an input by processing relative to the resonator through an angle exactly proportional to the input rotation. The pickoff includes the eight electrodes that sense shifts in the resonator's vibratory pattern. A significant advantage is that in the presence of a momentary power interruption or nuclear event the HRG does not lose attitude because of its ability to continue to integrate angular rate.

COARSE SCREENING--Because the fiber optic gyro (FOG) and hemispheric resonator gyro (HRG) are in development and/or in the laboratory, they will be discounted for this trade study. Until these designs emerge and become operational they have too much risk for serious consideration. However, the FOG should be reevaluated for progress in a year or two. The following will focus on implementations using the DTG and RLG.

EVALUATION AND CANDIDATE SELECTION--The trend for inertial grade gyros is shifting away from the high cost SDOF units to the lower cost DTGs.

The DTG (2DOF) unit has significant advantages over the rate integrating gyro the most obvious being two sensing axes and a simpler design. Although the lower friction gas bearing of an SDOF unit produces smaller drifts, it is susceptible to wear during start and stop because the rotor is suspended on a cushion of air. Ball bearings are more reliable and less expensive than the gas bearings of SDOF units, but introduce more errors. Thirdly, 2DOF gyros do not have flex leads that introduce unbalance torques. Table 2.1.2.6-1 summarizes DTG and RLG and Table 2.1.2.6-2 compares them with various evaluation criteria.

Overall performance heavily favors the RLG. It has fewer, more stable error sources that are readily compensated and has an inherent digital output.

The major RLG drawbacks are their large size, weight, and power. It is assumed that these will be reduced over the next few years to become more competitive with spinning mass units. In fact the weight of a DTG with equivalent accuracy is also high. For example, the DRIRU II that uses the SDG5 gyro weighs nearly 40 lbs.

Table 2.1.2.6-1 DTG vs RLG Gyro Comparison

Spinning Mass DTG	Ring Laser Gyro
Mature Design	In Production
Two-Axis Sensing	Single-Axis Sensing
Moving Parts	Mechanical Dither
Wide Dynamic Range	Wider Dynamic Range
Analog Output	Digital Output
G-Sensitive Errors	Few Dynamic Errors
Moderate Weight	Heavy
Slow Reaction	Fast Reaction Time
Bearing Life Limit	High Voltage Gas Laser/Optics Life
0.1°/hr drift	0.01°/hr drift
Temp Controlled	Temp Compensated

Table 2.1.2.5-2 Gyro Weighting and Rating

Factor	Weight	DTG	RLG
Overall Performance	5	(2) 10	(5) 25
Weight	4	(5) 20	(3) 12
Power	3	(5) 15	(4) 12
Cost	3	(4) 12	(4) 12
Reliability/Fault Tolerance	4	(5) 20	(4) 16
Development Status	5	(5) 25	(4) 20
Maintainability	5	(2) 10	(5) 25
Totals		112	122

Reliability and development status favor the DTG because it provides two output axes from a single instrument and has been space proven. The RLG will require much less maintenance because it has far fewer error sources that are more stable. This is a very important consideration for space basing.

The RLG is the choice for the ground-based cryogenic ACC OTV and all space-based versions. The ground-based storable perigee stage could possibly benefit from an existing DTG based IMU in order to minimize weight and risk.

GYRO COMPARISON--With the exception of the Third Generation Gyro (TGG) SDOF rate integrating gyro design, has essentially remained static for the last 5 yrs. The TGG is a very expensive unit being developed for MX which incorporates substantial complexity to achieve extremely high performance. However, the state of the 2DOF gyro art is progressing with more companies currently involved in their production.

Several significant differences in SDOF and 2DOF construction should be pointed out. The obvious difference is that two sensing axes are available in nearly the same package as the SDOF unit. Another difference is in the spin motor bearing area. SDOF units are being produced with either ball or gas bearings. The lower friction of gas bearings produce lower drifts and unbalance because the rotor is suspended on a cushion of air only a few thousandths thick. Although gas bearings have lower friction during run, they are susceptible to wear during start and stop. Ball bearings are more reliable and less expensive but introduce more errors. Because of their suspension method 2DOF units are only produced with ball bearings. Thirdly 2DOF gyros do not have flex leads that can introduce unbalance torques.

Three categories of SDOF gyros by performance and cost are as follows:

- In high performance SDOF gyros, with drift rates about or better than $.01^{\circ}/\text{hr}$, the candidates are the Nortronics ATG-G and the Bendix PM-64. Unit costs range from 75-175 K each.
- Medium performance ($.05-.1^{\circ}/\text{Hr}$) units include the Kearfott Alpha II, Nortronics K1K7G, Honeywell Mod. MIG and the Hamilton Standard 1010 costing between 40 and 50K.
- Lower performance ($1-5^{\circ}/\text{hr}$) and low cost (2-5K) units are the Nortronics G-6, Honeywell GG1111 and the Timex 1G10.

Most companies appear to be shifting away from the high cost SDOF gyros to low cost miniature 2DOF units. Using these gyros, the constant biases are trimmed out at the systems electronics level to achieve a system performance of $.01$ to $.1^{\circ}/\text{Hr}$.

Four companies have built 2DOF gyros (Litton, Kearfott, Teledyne and Nortronics). Two of these (Litton and Kearfott) have delivered miniature two axis gyros in production quantities. They are presently producing large quantities of two degree of freedom gyros, and gyro systems for aircraft systems. Both companies will supply not only the component gyro but the associated hybrid electronics containing the amplifier-demodulator, torquer power supply, and wheel supplies.

Kearfott has been producing the large Gyroflex 2DOF gyro for a number of years. The Space Shuttle IMU as well as numerous aircraft systems are based on the Gyroflex. They are also currently in production with the small CONEX unit for the main battle tank. Teledyne is building the SDG5, a large 2DOF tuned rotor gyro, and expects to begin production of a smaller unit the SDG7 in 1982. The larger 2DOF units have relatively low drifts ($.01$ to $3^{\circ}/\text{Hr}$) due to their large angular momentum and fine trimming at the component level. However because of this momentum they also have limited torquing capability.

Their cost is in the 15-40K range. Two other companies (Litton and Nortronics) are also involved in 2DOF units. Litton is in production with their G7 unit and Nortronics expects to be in production with their GTB2 in 1982. These smaller 2DOF units weigh 100/200 grams, exhibit a $.2 \cdot 10^0$ /Hr drift rate, and are expected to cost 5-10K each. The Litton units are in production for the MK-48 torpedo and pre-production for military aircraft.

The Ring Laser Gyro (RLG) has been in development and test for over 10 years without having gone into quantity production. However, Honeywell expects to have a production rate of 100-200 units per month by late 1982 or early 1983 for the Boeing 757/767 commercial aircraft. Raytheon is currently developing a multioscillator RLG for aerospace applications and Litton is developing a commercial unit for the A300 Airbus. Several other companies (Sperry, Hamilton Standard) are not actively pursuing their earlier RLG activities.

The Fiber Optics Rate Sensor (FORS) appears to be a promising new development. Several companies (Hamilton Standard, Nortronics and Martin-Orlando) have been investigating it and Martin has several study contracts. The major advantages of the FORS over the RLG are the absence of high voltage and the lack of a dither motor.

2.1.2.7 Electro-Optical Navigation Sensors

PURPOSE--Celestial, earth, and sun sensors are electro-optical devices used for on-orbit attitude determination. They allow on orbit alignment and initialization and updating of an existing attitude reference, such as an Inertial Measurement Unit (IMU), and/or maintain pointing with respect to some known reference (sun, stars). The objective of this study is evaluate recent advances that may be more attractive for OTV applications. For example the increased use of all solid state designs should result in reduced size, weight, and cost along with improved reliability and maintainability. This study will compare advanced electro-optical navigation sensors with OTV requirements to identify new designs for incorporation into the avionics design.

SUMMARY--A study was performed to evaluate and select the most attractive electro-optical navigation sensor for OTV attitude initialization and update. Earth horizon sensors and sun sensors were eliminated as the primary devices for accuracy reasons. Two star sensor implementations were considered and traded off: 1) star trackers, and 2) star scanners. Only solid state versions of these instruments were considered because of weight and power considerations.

Solid state star scanners have been space proven whereas star trackers are presently under development. For early OTV applications star scanners appear to be the most promising due to their inherent redundancy and low risk. Trackers have better accuracy and present fewer operational constraints. Due to their flexibility they are more attractive for space-based operations. A tracker being developed by BASD that combines existing Shuttle technology and a retro reflector field tracker detector is most attractive.

STATEMENT OF PROBLEM--A number of electro-optical sensors are used for initialization and autonomous update of onorbit attitude. Three different devices, earth, sun, and star sensors were considered. The emphasis was placed on star sensors because of their greater accuracy and flexibility.

CANDIDATE SENSING DEVICES--

Earth (or Horizon) Sensors--The earth sensor is an infrared sensing device that allows tracking of the earth's horizon by detecting the thermal gradient in the transition from earth to space and vice-versa. These transitions are used to determine the direction to the center of the earth. Earth sensors are characterized by moderate accuracy, medium weight and can be used over a wide altitude range. Accuracy is a fraction of orbital attitude. One or more optical heads provide pulses as a readout of the angle of declination of the horizon from a predetermined spacecraft reference. Electronic processing of these pulses supplies two-axis (pitch and roll) attitude information.

Sun Sensors--Sun sensors are simple, reliable, and relatively inexpensive devices that establish a direction to the sun for attitude determination. The simplest is the analog type that use a shadow mask and a photovoltaic (solar) cell detector. They are designed as a nulling type of sensor with a limited range. The linearity of their output degrades significantly off the sun line. The digital sun sensor is a more accurate, but not simple device. In this design a slit of sunlight falls across a light-sensitive detector covered by a binary coded mask to provide a digital representation of vehicle attitude.

The sun sensor, like the horizon sensor provides attitude data in only 2 axes. It is substantially less accurate than the earth sensor and substantially less expensive.

Star Sensor--Two basic star sensing devices that can be used to update vehicle attitude are: 1) star tracker, and 2) star scanner. In the first, star tracking, the vehicle is pointed to search for and acquire a star in its boresight. One or two stars are sensed in order to measure the offnull star position and compute a new vehicle attitude. This results in an accurate attitude fix either as part of the basic initialization or as an update that compensates for IMU instrument drift. Less maneuvering is required to determine attitude than with a star scanner because the unit has an internal search capability and is sensitive to a larger number of stars.

The second method, star scanning, involves sweeping through a segment of the celestial sphere. A star catalog (containing selected stars up to a certain magnitude) is stored in the computer. The stage is slewed at a fairly low rate (0.1-1.0°/s) to cross stars and monitor star pulses which are then correlated to the star map stored onboard. Star scanning requires more maneuvering and therefore RCS propellant.

One advantage of star trackers is that a large star catalog can be used and the software for deriving the update information is simpler. In addition, the stars that are selected can be isolated and bright, minimizing problems

with star discrimination, and tracker threshold. Star tracking requires some RCS propellant but has the advantage of inherent operational and hardware simplicity. The scanning method requires more computer storage for pointing and scanning maneuvers and star correlation.

NAVIGATION SENSOR TRADE--Of the types of sensors described, star sensors provide the most accurate attitude update. Early star sensors were heavy and complex whereas advanced stellar sensors can be small, light weight, low power and highly reliable. This is a result of replacing bulky electron tube detectors with all solid state charge transfer device (CTD) detectors. CTD based sensors do not require the high operating voltages nor need the calibration and environmental protection of an image dissector tube. CTD technology may also permit pointing accuracy and stability beyond that achievable by any image dissector or photomultiplier tube-based design.

SELECTION CRITERIA--The primary criteria for star sensor selection are low cost and risk, fault-tolerance, reliability and maintainability. Weight and power are also key selection factors. Accuracy must be better than 0.1 degree. Extreme accuracy is not required because updates are only necessary before engine burns, aeroentry or after long periods of attitude coast. Sensitivity to the brightness of stars (star magnitude) is another factor to be considered. Greater sensitivity minimizes the maneuvering required to find target stars. Development status, fault-tolerance and computational requirements are three more factors. Development risk is an important factor that impacts front end costs. Fault-tolerance influences mission success and maintainability and is a significant factor in life cycle cost. Operational flexibility relates to the ease of performing an update. G & N computer software is also a consideration. The selection factors and assigned weights are given in Table 2.1.2.7-1:

TABLE 2.1.2.7-1
Scanner/Tracker Factor Weights

<u>Factor</u>	<u>Weight</u>
Cost	4
Weight	3
Power	3
Accuracy	2
Sensitivity	4
Fault Tolerance	4
Operational Flexibility	4
Software	2
Risk	5

DESCRIPTION OF CANDIDATE STAR SENSORS--For purposes of attitude update, stars are essentially point sources fixed in inertial space. Since the stars are at a great distance from our solar system the subtend angles less than one second of arc when observed from any point in earth orbit. Star sensor accuracy is therefore limited by instrument errors and fundamentally independent of source dimensions.

Two star characteristics are most important in sensor design. These are: 1) stellar brightness (quantity of radiation) and 2) spectral characteristics (quality of radiation).

Star position or distribution about the celestial sphere is the third consideration.

The astronomical unit of brightness or intensity is stellar magnitude with the magnitude number being inverse to brightness. A star having a magnitude of 1 has been arbitrarily defined as being 100 times as bright as a star magnitude 6 so that each magnitude is 2.512 times as bright as the one below it. Stars are divided into classes depending upon their spectral radiation or colors. There are seven classes in order of decreasing effective temperature and increasing wavelength.

Two techniques have been used for attitude update. The sensor can be pointed in the general direction of the star based on an initial reference (star tracking) or the spacecraft can be rotated about a known reference line such that the sensor field of view intersects the desired target (star scanning). Acquisition in the first method is faster than the second since rotating about a reference line and scanning the celestial sphere is time consuming.

An accurate attitude reference is required with a star tracker to slew between target stars.

Initial tracker pointing and accuracy are critical to the final result. A trade off between telescope field of view (FOV) and star magnitude must be made. The smaller the search field of view the dimmer the star the higher the probability that neighboring stars will interfere with the desired image.

Upon acquisition the tracker develops error signals as a function of distance off the telescope centerline. A second star acquisition is required for a three-axis update. The final result is used to update the attitude vector within the guidance and navigation computer.

Star scanners use a much smaller catalog (IUS has about 30 stars) to correlate the occurrence of detected crossings and determine inertial attitude. Scanners tend to be less sensitive to star brightness or magnitude than star trackers. The entire space vehicle is rotated through an angle of about 90° to detect two independent stars. Maneuvering to accomplish this can be time consuming and a significant impact to time critical phases of flight.

Star trackers have seen more use on missiles, spacecraft and particularly on the Space Shuttle. Scanner use has been greatest on programs such as DMSP and IUS. Early devices were implemented with a photo-tube detector although recent scanners incorporate a solid state detector. Solid state trackers have been in development for about five years by at least three firms. The following paragraphs describe tracker and scanner operation in more detail.

STAR TRACKERS--Although existing star trackers are based on image dissector tubes (IDTs), solid state trackers are presently in development. In operation, a threshold star magnitude is commanded and the vehicle is maneuvered to bring a target star within the tracker's field of view (FOV). The tracker then begins searching the FOV until a star image brighter than the command threshold is encountered. Upon finding such a star IDT-based tracker shifts from the search to track mode. A solid state tracker can simultaneously detect all the star images throughout the field of view. Therefore a single view provides both location and magnitude data so that processing to identify target stars and initiate tracking can be almost instantaneous. By comparison, search intervals for IDT trackers often last 10-15 seconds. During tracking, X-Y coordinates of the star image in the tracker frame of reference (FOR) and a measured star magnitude are output. Tracking continues until the star leaves the FOV or a "break track" command is received. With the solid state tracker a special algorithm is required to find the centroid of the star image because it will illuminate several pixels of the CTD array. Using this mapping scheme and a large catalog of stars (several thousand) evenly distributed over the sky, a tracker can compare star masses within its FOV with the catalog in the navigation computer to establish a precise attitude; i.e., it can be used to "boot strap" a precise attitude with no need for previous coarse attitude information. Alternatively, it can be used to update a coarse attitude with as few as two stars in the catalog provided they are visible and maneuvers are not a constraint.

STAR SCANNERS--Star scanners are based on a solid state detector lying behind a precisely scribed slit in an opaque mask. The solid state detectors, either silicon or charge coupled devices (CCD's), are arranged in linear patterns under the slits. The BASD CS-203, the Honeywell C/S, and the Perkin-Elmer Star Mapper are of this type. In operation, the vehicle is maneuvered to bring the scanner FOV near a target star using coarse attitude information. A threshold magnitude is commanded to the scanner and the vehicle is rotated, typically in roll, to pass the star image over the scanner's slit(s). As the image crosses a slit, a pulse is generated for any star that exceeds the threshold. Internal electronics make estimates of the leading-edge, trailing-edge, or peak time of passage of the star image, and the time-tagged detection pulse and magnitude are output to the navigation computer. The process is repeated for at least one other star, and the navigation computer converts delta time between the detection pulses to star positions in the navigation frame. These positions are then used to update vehicle attitude.

COARSE SCREENING--Although IDT-based star trackers and scanners will be characterized below for information purposes, they have been eliminated from serious consideration because of their cost, complexity, reliability, and environmental constraints. As previously indicated there are no issues to be traded for either sun or earth sensors.

EVALUATION AND CANDIDATE SELECTION--Table 2.1.2.7-2 compares the characteristics of candidate star sensors from the primary suppliers. The first column tabulates an image dissector tube (IDT) based unit from the space shuttle for comparison only..

TABLE 2.1.2.7-2 Scanner / Tracker Comparison

CHARACTERISTIC	Data Only	SCANNER			TRACKER	
	BASD SST	BASD CS 203	HI Blk-5D	BASD SS/SST	PERKIN ELMER	HI ASTROS
Detector	IDT	Silicon Slit	Silicon Slit	CID	CID	CCD
FOV(degrees)	8x8	5x5	10x10	6x6	7x7	2x4
Sensitivity (Star Magnitude)	5.7	1.6	2	9	5.7	8.2
Accuracy (min)	0.5	1.0	1.0	0.5	0.3	.02
Acq. Time	11 sec	5 min	5 min	4 sec	.4 sec	20
Self Test	yes	yes	yes	yes	yes	yes
Power(watts)	20	7	10	16	33	53
Weight(lbs)	20	12	7	15	22	48
Cost(\$M)	H	M	M	M-H	H	VH
Remarks	Shuttle Use	IUS			In Lab	Fine Point

Table 2.1.2.7-3 rates the candidate star sensors and applies the weighting factors derived in Section 4.

CONCLUSION--In summary the difference between the two star scanners and the BASD star tracker is not significant. Scanners fare quite well because they are flight proven, light weight, inherently redundant and relatively lower cost. They suffer in the areas of operational flexibility and sensitivity. They are also less accurate although this does not appear to be especially critical for OTV. Solid state trackers do very well in operational flexibility because they have a larger star catalog, are more sensitive and can acquire stars from virtually any orientation. The added flexibility of a solid state tracker could benefit the ACC cryogenic OTV that must find its way into orbit.

Near term development of a solid state tracker for the NASA and the space shuttle by Ball Aerospace would make their unit a logical OTV choice. Ball would merge their Shuttle IDT-based tracker technology with the CID detector array from the recent successful Retroreflector Field Trackers (RFT) experiment. This would still satisfy the basic OTV requirement and may be a more logical choice for a ground based OTV. Selection is somewhat dependent upon OTV schedule and tracker progress.

In summary the BASD SS tracker is recommended for all OTV configurations except the storable ground based.

Table 2.1.2.7-3 Scanner/Tracker Evaluation

FACTOR	Weighting	RATING FACTOR				
		SCANNER		TRACKER		
		BASD CS 203	HI BIK5D	BASD SS/SST	PEPKIN ELMER	HI ASTROS
Weight	3	(4) 12	(5) 15	(4) 12	(3) 9	(1) 3
Power	3	(5) 15	(5) 15	(4) 12	(3) 9	(2) 6
Accuracy	2	(2) 4	(3) 6	(3) 6	(3) 6	(5) 10
Sensitivity	4	(2) 8	(2) 8	(5) 20	(4) 16	(5) 20
Fault Tolerance	4	(5) 20	(5) 20	(3) 12	(3) 12	(2) 8
Operational Flexibility	4	(2) 8	(2) 8	(5) 20	(5) 20	(5) 20
Software	2	(5) 10	(5) 10	(3) 6	(3) 6	(2) 4
Risk	5	(5) <u>25</u>	(4) <u>20</u>	(4) <u>20</u>	(2) <u>10</u>	(3) <u>15</u>
Cost	4	(5) <u>20</u>	(5) <u>20</u>	(4) <u>16</u>	(3) <u>12</u>	(2) <u>8</u>
Totals		122	122	124	100	93

2.2 AEROASSIST TRADE STUDIES AND ANALYSES

INTRODUCTION--An aeroassist maneuver uses the earth's atmosphere to reduce the vehicle's velocity, thereby reducing the rocket burn required to enter low earth orbit when returning from GEO or other higher orbits. This aeromaneuver is accomplished by grazing the upper atmosphere and converting the vehicle's kinetic energy to heat. To correct for density variations and navigational uncertainties during the aeropass, precise aerodynamic control is required. Two methods are available for accomplishing this: aeromaneuvering, which uses vehicle lift for control; and aerobraking, which varies vehicle drag to correct for density variations.

The purpose of these trade studies is to assess aeroassisted system concepts ranging from drag devices to mid L/D systems. Selection of the recommended concept is based on weight and performance trades, braking maneuver heat flux and loads, heatshield material and thicknesses, stability and control, payload retrieval, and growth.

With selection of the preferred aeroassist device, an analysis to develop the optimum design is presented. The design methodology, geometrical parameters, aerodynamics, thermal environment, TPS characteristics, and sizing curves for the aeroassist device are included. The emphasis is on providing useful information for a lightweight, reliable aerobraking system that will meet all mission requirements.

2.2.1 Aeroassist Concepts Evaluation and Selection

The aeroassist concept evaluation section can be divided into four major trades; all-propulsive versus aeroassist; low versus mid L/D; drag vs lift; and the amount of L/D required for control. Seven aeroassist concepts are used in the trade studies. To insure no concept is penalized or influenced by stage configuration or payload capability, all concepts are sized for a 14K manned mission and configuration optimized based on system design data from previous studies were applicable. Since the benefits of the aeroassist concepts will be compared based on their heat shielding requirements, weight and performance, a section on thermal protection is included. In this section, TPS requirements are identified and an evaluation of TPS designs and alternatives is made to ensure minimum-mass TPS concepts are employed on the candidate aeroassist heat shields.

2.2.1.1 All Propulsive Versus Aeroassist

Significant fuel savings can be made if atmospheric drag is used instead of retrothrust during the return from GEO to LEO, thus leading to the aeroassisted OTV, or AOTV. This aerobraking option is attractive because a large portion of the retropropulsion fuel weight savings can be translated into increased payload.

This leads to our first trade which is to provide data to substantiate the benefits of aeroassist over an all-propulsive return to LEO. In this analysis, a cryo reference configuration with a 460 Isp and two missions, a 20K delivery and a 14K round-trip were used. Performance analyses for each option were run and propellant saved by aeroassist vs the aeroassist weight as a percentage of the retrieved or returned weight was computed. The results are plotted in Figure 2.2.1.1-1. For comparison, the 7.5K manned mission of the Rev. 8 mission model has a peak propellant savings of 28%.

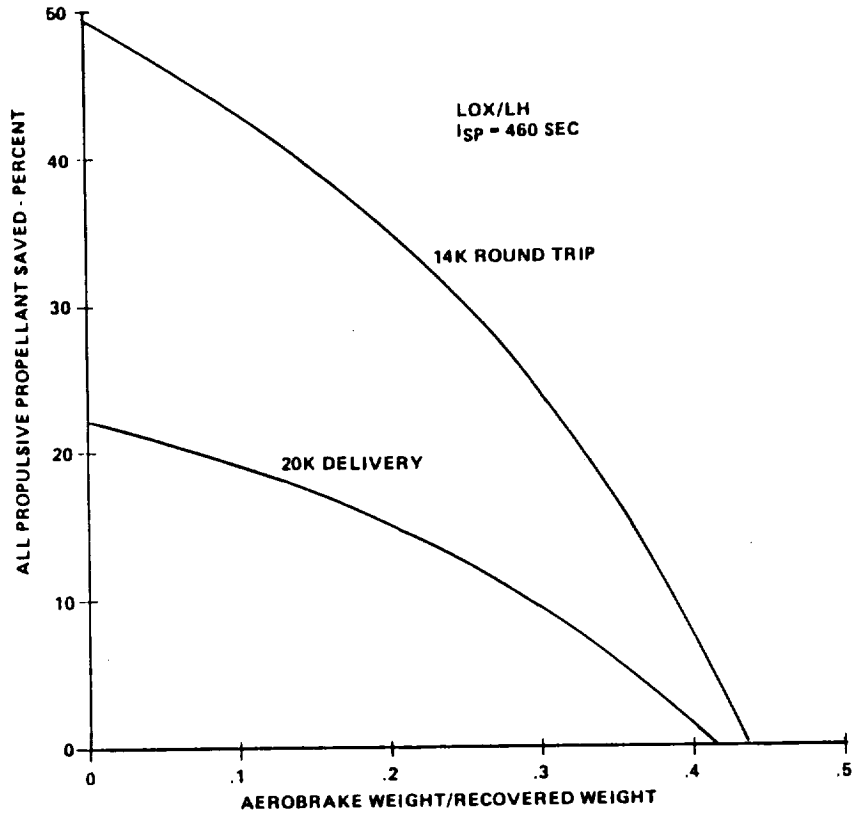


Figure 2.2.1.1-1 All Propulsive vs Aeroassist Analysis

For aeroassist to be a cost-effective device, we need to realize 10 to 20 percent propellant savings. This means the device must end up being 10 to 30 percent of the retrieved weight. Thus for aeroassist to be a viable concept, the weight of the aerobraking device must be light enough to accrue benefits as a propellant savings technique. It should be noted too that if the mission model changes to include heavier return payloads or to increase the number of missions, aeroassist will accrue more benefits increasing its advantage over all-propulsive concepts.

2.2.1.2 Candidate Aeroassist Techniques

For aeroassist to be beneficial, the aeroassist device must be light enough to take advantage of the aerobraking fuel savings. Therefore, a minimum weight aeroassist concept is needed. Candidate OTV aeroassist techniques include: the ballute, mechanical drag, and aerospike for drag modulation; the offset c.g. brake and aeroshaped body for lift modulation; and the mid-L/D hypersonic biconic sled for an aeromaneuvering vehicle. In the configuration versus weight trade study, the weight statements from these candidates along with their performance and system integration impacts will identify the preferred aeroassist approach. Since ground-based flights are a small percent of the mission model, two space-based missions were selected for this trade. They are the 20,000-lb delivery to GEO and 14,000-lb manned round trip. The candidates have been sized and auxiliary equipment identified for the OTV return from GEO and for return of the 7.5 foot radius by 23 feet long manned capsule. Propellant type, core configuration, and payload impingement were considered in sizing the candidates.

The selected candidate aeroassisted CTVs that will be used in the trade studies are in Fig. 2.2.1.2-1. The concepts span the range from drag modulation to mid L/D lift control. The size, airloads, and TPS requirements of the aeroassist devices were determined for a 14,000 lb manned capsule return

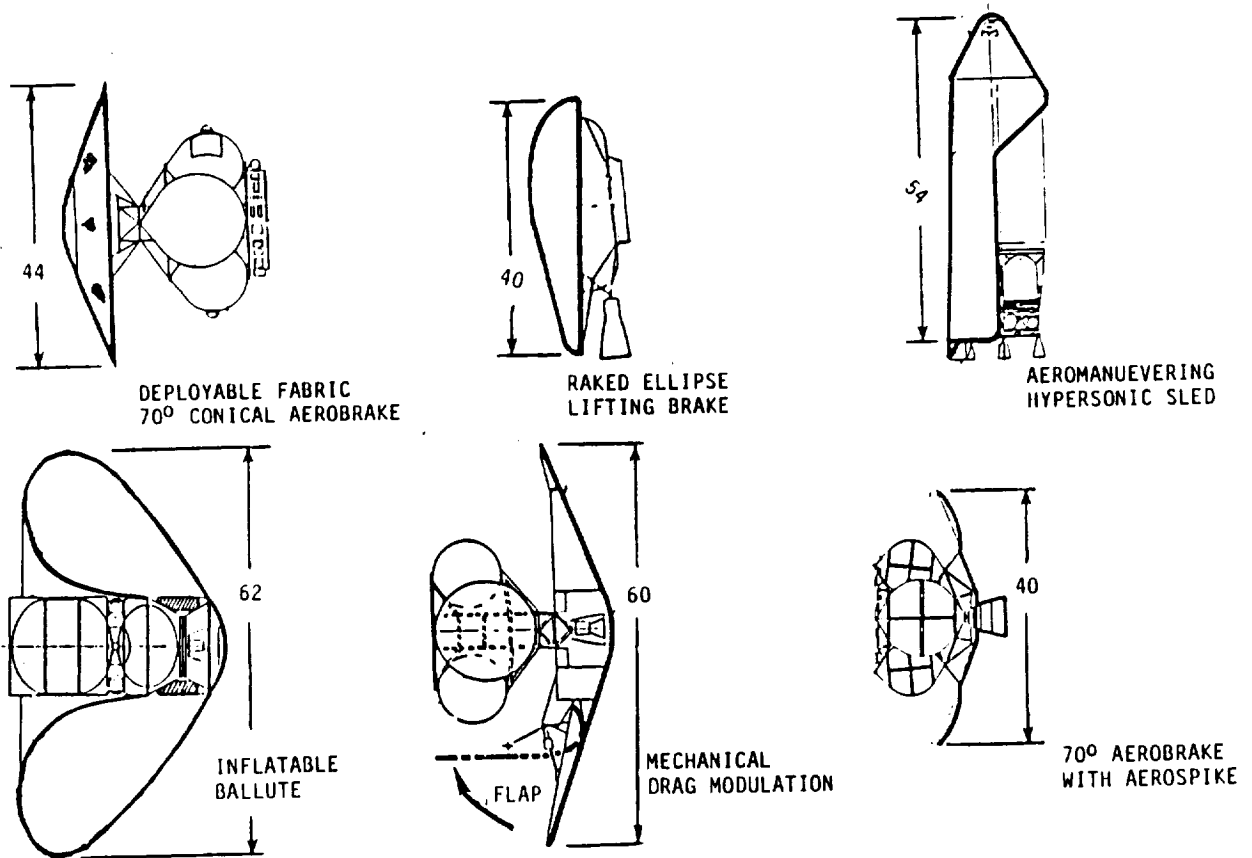


Figure 2.2.1.2-1 Aeroassist Configuration Options

payload (23 ft long). These data was used to generate mass property statements so aeroassist weight and performance trades could be made. The weight trade data is shown in Table 2.2.1.2-1.

Table 2.2.1.2-1 Aeroassist Characteristics - Configuration vs Weight

CONFIGURATION	L/D	W/C _D A	W _A	λ
DEPLOYABLE CONICAL FABRIC LIFTING BRAKE	0.12	10	1500	.07
BLUNT RAKED ELLIPSE LIFTING BRAKE	0.27	15	1800	.08
AEROMANEUVERING HYPERSONIC BICONIC SLED	1.00	70	6800	.27
INFLATABLE BALLUTE MECHANICAL DRAG MODULATION	0.0 0.0	6 8	3700 5640	.15 .22
** 70° AEROBRAKE WITH FLUID AERO-SPIKE	0.0	4	1520	.22

NOTE: W_A = WEIGHT OF AEROASSIST DEVICE
 λ = RATIO OF AEROASSIST DEVICE TO VEHICLE RETURN WEIGHT (14K)
 ** = DELIVERY ONLY

The ballistic coefficient ($B = W/C_D A$), weight of the aeroassist TPS (W_a), and its ratio to the return dry weight ($\lambda = W_a/W_{dry}$) are given for each concept. The four major aeroassist trade techniques are listed below. The first two options can be selected just on weight comparisons.

1. Mechanical vs Aerodynamic Modulation
2. Fluid Aerospike vs Inflatable Ballute C_D Variation
3. Drag vs Lift Aeroassist
4. Low vs Mid L/D

The mechanical drag brake was designed for an area variation of 2.5 which represents the bare minimum level that can maintain trajectory control. The large diameter of this aerobrake was required to achieve the desired turn down ratio and to provide payload protection. The use of flap actuators to drive the control surfaces required the flaps to be of rigid/stiff TPS. This resulted in its high aeroassist weight and an unattractive option compared to aerodynamic drag modulation.

Analysis of the fluid aerospike concept resulted in 420 lbs. of fuel to perform the aeropass with no payload return. This consumable, added to the fabric aerobrake's weight, gives a total assist weight of 1520 lbs. and does not include the extra fuel required to get the additional 428 lbs of propellant to GEO. The fluid aerospike concept provides large C_D variation, but its propellant use, limited corridor, and jet counterflow instabilities cause benefits to be offset by its feasibility. Due to the weight and feasibility issues of this concept, it was dropped in the study prior to evolving it to space-based manned missions. It should be noted that this was the only concept out of the six that was not sized for a 14K payload return.

It can be seen that the drag modulation concepts have the basic brake shape and or TAS as low L/D's. The additional complexity of their active area or fluid modulation system combined with associated uncertainties in analytical methods and dynamic modeling inhibit technical validation of the drag brakes. Thus assessment of their feasibility is moderate and it is assumed that feasibility can be demonstrated without major impact on design characteristics.

With four candidate aeroassist concepts and three assist techniques (ballute drag modulation, symmetric and raked conical low L/D aerobrakes, and a mid L/D aeromaneuvering vehicle, the following sections evaluates their thermal protection options and their aeroassist device size and weight data.

2.2.1.3 Aerothermal Protection For Space-Based Aeroassist Device

INTRODUCTION--The thermal protection system (TPS) developed for the OTV must match or exceed the derived requirements shown below. The TPS requirements result from detailed analyses of the thermal environment the vehicle will encounter. A heating rate of 15-36 BTU/ft² sec with a corresponding temperature range of 2200 - 3300°F capability of the TPS is required. Other factors include the optical and catalytic properties of the TPS material.

Additional requirements are addressed that could limit the performance of candidate TPS materials. They include durability, weight, reusability, raw material size, minimum bend radius, ease of manufacture, orbit assembly, and repair characteristics.

TPS REQUIREMENTS

1. Heating capability 15-36 Btu/ft² sec
2. Temperature capability 2200 - 3300°F
3. Durable and light weight
4. Optimum optical properties and noncatalytic
5. Minimum seams or joints (number of gores or tiles)
6. Reusable, orbit assembly and repair
7. Manufacturing

Several types of potential flexible and rigid insulation materials are available and their utilization on the OTV aerobrake will be dictated by the temperatures at those locations. In areas where temperatures do not exceed 750°F, a coated organic flexible felt, Felt Reusable Surface Insulation (FRSI), could be used. Continuing research and development of flexible TPS materials has resulted in a flexible inorganic ceramic blanket based on high purity silica components with a limiting temperature of 1500°F. This TPS material, called Advanced Flexible Reusable Surface Insulation (AFRSI), has been used successfully on STS. A modified AFRSI made of advanced ceramics, known as TABI, is under investigation.

Rigid Surface Insulation (RSI), in addition to flexible insulation, will play a role on OTV. These rigidized, silica fiber tiles will withstand temperatures of 2700°F. Unlike AFRSI, which is bonded directly to the outer skin with a silicone adhesive, RSI tiles must use an intermediate strain isolation pad (SIP) to mount to the structural skin. The tiles are bonded to the SIP which in turn is bonded to the skin with a silicon adhesive. The final rigid insulation is reinforced carbon-carbon (RCC). This insulation material is best suited for high temperature applications with a limiting temperature of 3000°F. The one obstacle in using RCC is that it weighs 10 to 15 times more than competitive materials which makes its use attractive only for aerobrake locations which experience extremely high temperatures.

Our assessment of 1990 material maximum surface temperature capabilities for both single and multiple reuse indicate major improvements in currently available materials (see Table 2.2.1.3-1).

Two types of current orbiter tile systems are shown in Figure 2.2.1.3-1. The rigid surface insulation (RSI) shown has the fused coating providing the hard over shell over the softer interior. These individual tiles are glued to a felt strain isolator pad which in turn is glued to the filler bar attached to the aluminum outer skin structure.

The advanced flexible reusable surface insulation has a silica glass fabric exterior and interior facing, with silicate glass thread used to sew the cover cloths and inside glass fabric together. The internal felted silica glass layer is 1 to 4 cm thick. Silicon adhesive bonds the sewed sandwich to the outer skin with no intermediate felt layer. Integrity of the silical glass threads is essential to prevent cloth flutter damage and edge distortion.

Table 2.2.1.3-1 Classes of Heat Shield Materials

Material	Density Lb/Ft ³	Current Single Flight Design Limit, °F	Current Temp Capability Multiple Reuse, °F	1990 Technology Material Temp Limit for Single Flight, °F	1990 Technology Material Capblty Multiple Reuse, °F
FRSI	6	750			
AFRSI	9	1500	1200 - 1500	1800 - 2600	1800 - 2500
RSI	12	2700	2700	3000	3000
RCC	99	3000	2800-3200	3800 - 4000	3800 - 4000

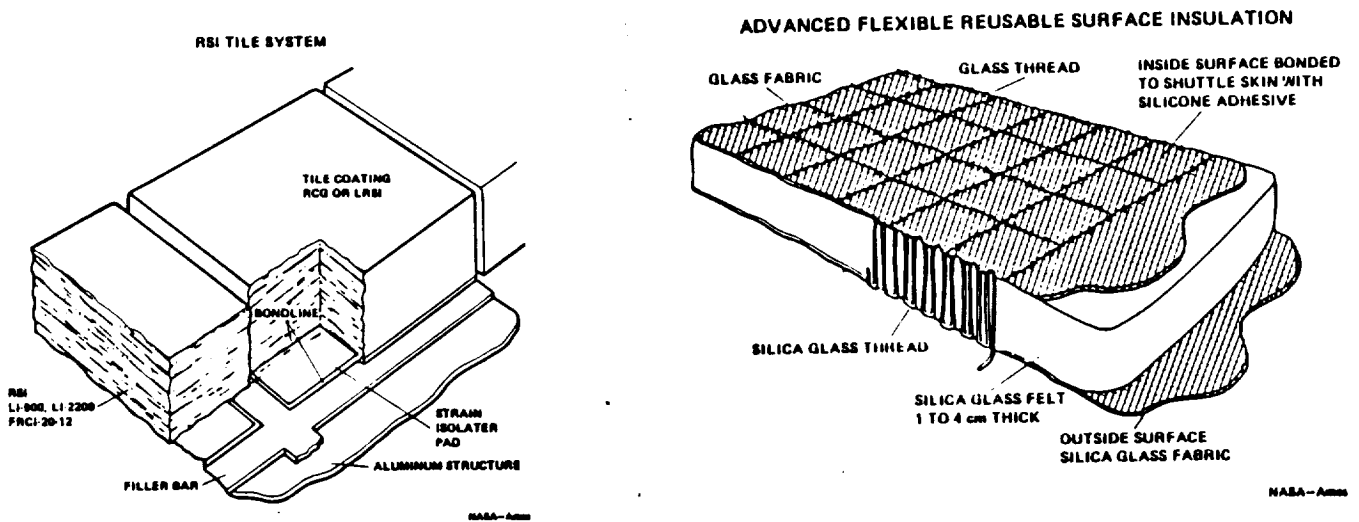


Figure 2.2.1.3-1 Developed Heat Shields

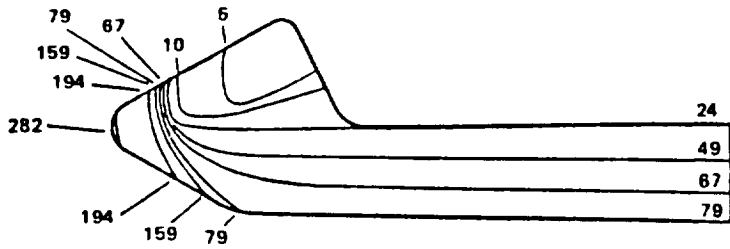
TPS OPTIONS AND SELECTION FOR CANDIDATE OTV CONCEPTS--Many flexible and rigid TPS materials have been considered as construction materials for the aeroshield on several of the OTV concepts. This section details the available materials and evaluates them for use in the aerobraking environment. The section is divided into two parts, TPS options for the Hypersonic Biconic Sled concept and fabric materials for the aerobrakes on several of the low L/D OTV concepts.

PART 1: TPS OPTIONS FOR THE HYPERSONIC BICONIC SLED CONCEPT--The Hypersonic Biconic Sled is one of the space-based OTV concepts and is expected to experience the environments shown in Figure 2.2.1.3-2. The TPS options which could be used to shield the vehicle from these environments are evaluated per the following criteria: (1) temperature capability, (2) reusability and (3) density. Following evaluation, candidate options were then determined.

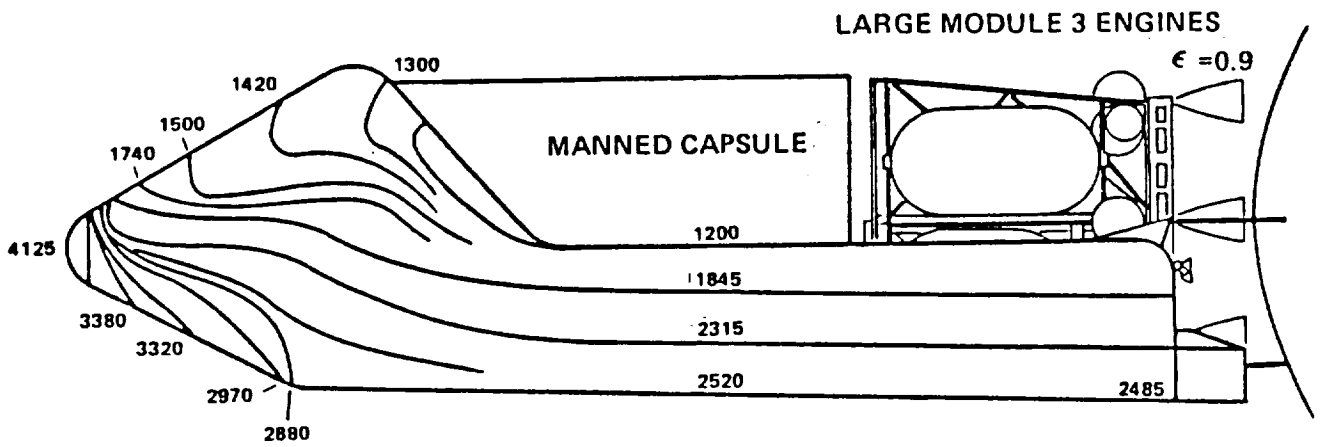
For the purposes of evaluation, the sled was divided into four regions according to expected environment as shown in Figure 2.2.1.3-3. The TPS options will be discussed separately for each section for both present and future technology. Recommendations are then made accordingly.

PRESENT TECHNOLOGY TPS

- A. Region 1 - Because the temperatures expected in the region are extreme, ablative, advanced carbon-carbon (ACC), and exotic metals were evaluated for use. Advanced carbon-carbon was eliminated due to the lack of a coating which would make it usable in this temperature range. Exotic metals were eliminated due to weight, cost, need for internal insulation, and possible deformation concerns. This resulted in only ablative materials remaining for consideration. The only disadvantage of these materials is their non-reusability or limited reusability aspect, therefore only minimum recession materials were considered to maximize possible reusability. Of these, the quartz-nitrile-phenolic (QNP) ablator exhibited the best possibilities and is the recommended option for this region based on present technology.
- B. Region 2 - The temperatures in this region range from 2520°F to 2970°F and ACC was the prime consideration (Option #1) for this area as shown in Figure 2.2.1.3-3. It is also possible that with refinements in FRCI or HPT ceramic tile technology that this region could fully utilize tiles as shown in Option #2 of Figure 2.2.1.3-3.
- C. Region 3 - The temperatures expected in this region range from 1845°F to 2520°F and ceramic (RSI) tiles were the prime consideration in this region. Presently, the FRCI-20-12 tiles are flight verified, however lower density versions (8 and 10 PCF) exist but have tensile strengths approximately 40-60 percent of FRCI-20-12's 123 PSI. From a thermal standpoint, all three have similar conductivities and specific heats, therefore the selection should be based on structural requirements and weight penalty considerations. Nevertheless, the FRCI tile is recommended for use in this region.



PRESSURE DISTRIBUTION AT $\alpha=30^\circ$, (PSF)



EQUILIBRIUM TEMPERATURE ISOTHERMS (°F)

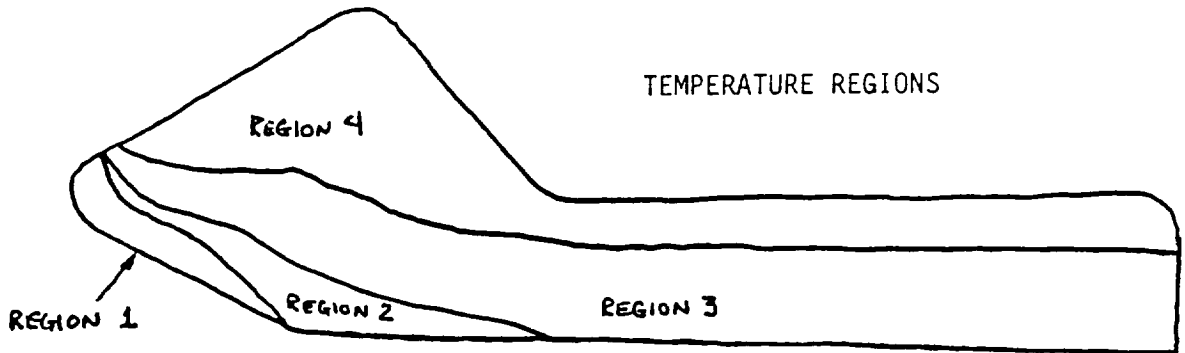


Figure 2.2.1.3-2 Pressure / Temperature Distributions - Raked Brake

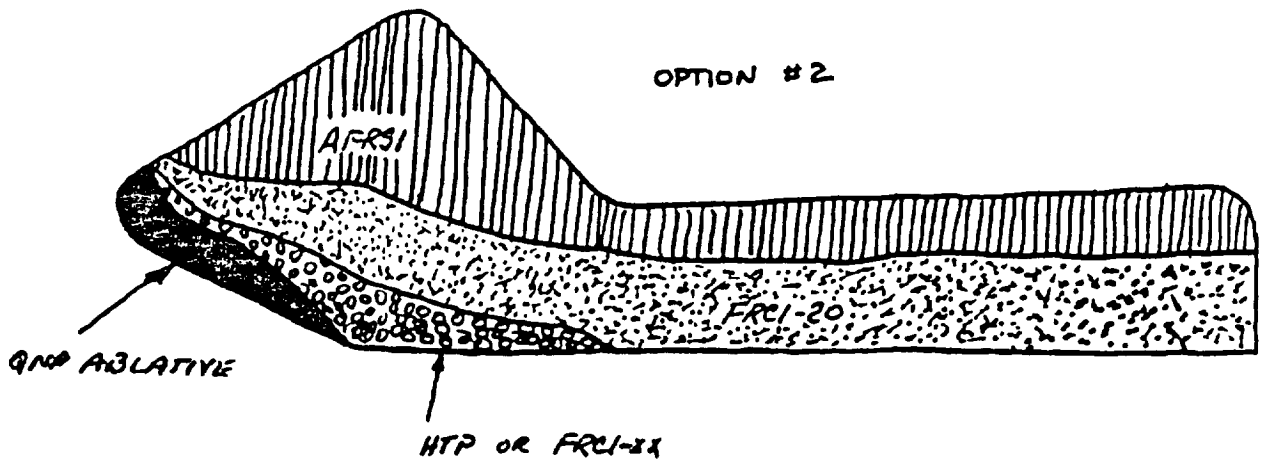
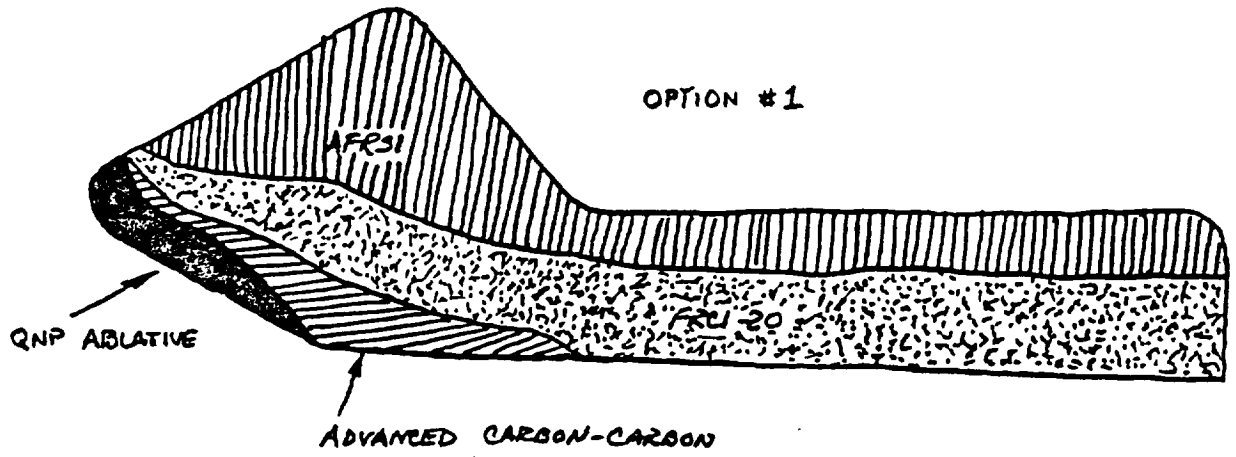


Figure 2.2.1.3-3 Present Technology Configurations

- D. Region 4 - Temperatures in this region are expected to be 1845°F and lower. Materials considered for use here included AFRSI and Nextel cloth. The Nextel cloth was eliminated due to reusability and airflow instability considerations. It is recommended that the easily attached, reusable, and more substantial AFRSI material be used in this region.
- E. Conclusion - Two possible TPS configurations based on present technology are depicted in Figure 2.2.1.3-3 and material properties of the materials are shown in Table 2.2.1.3-2. These represent the best configurations based on present technology.

Table 2.2.1.3-2 Material Properties

Material	Reusability	Temp. Capability	Density
ACC	100	3000°F	100 PCF
FRCI-20	100	2600°F	8-12 PCF
AFRSI	100	1500°F	6 PCF
QNP	Limited	3000°F+	97 PCF

FUTURE TECHNOLOGY TPS--It is expected that ten years from now the technology of the previously mentioned materials will have changed sufficiently to modify the TPS configuration of this vehicle. From the literature, it was determined that ten year technology advancements are expected to be as shown in Table 2.2.1.3-1. Assuming these advancements, the recommended TPS candidate configurations would change to those shown in Figure 2.2.1.3-4. As shown, the lower limit of future technology would extensively use the AFRSI and restrict the limited reusability ablative to the nose cone area only. If the upper limit of future technology capabilities were achieved, the configuration would consist of ACC and AFRSI only, eliminating the need for RSI and ablative materials. State-of-the-art RSI ceramic tile technology is discussed below.

There are three rigid tile candidates for use in future space transportation systems: FRCI, Ultrafiber, and HTP. The significant points within each of these areas are as follows:

1. FRCI Technology

- a. FRCI-20 gives best combination of properties-thermal and mechanical.

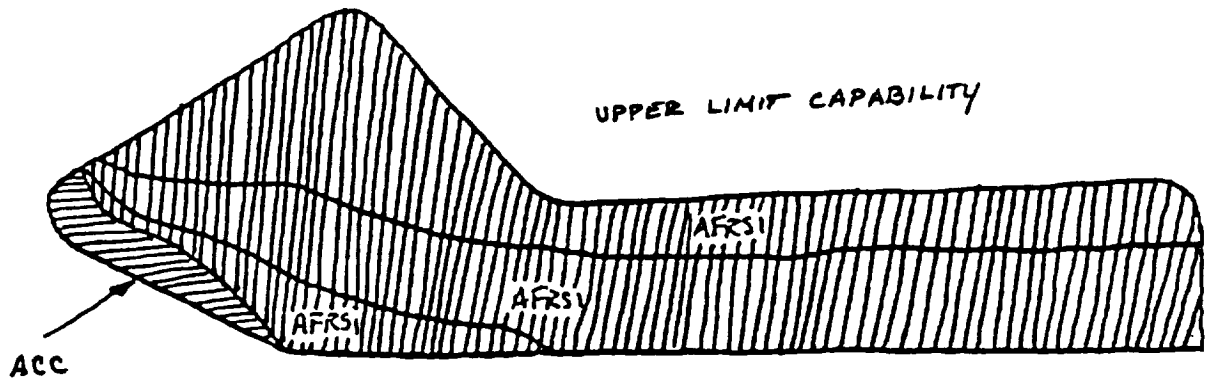
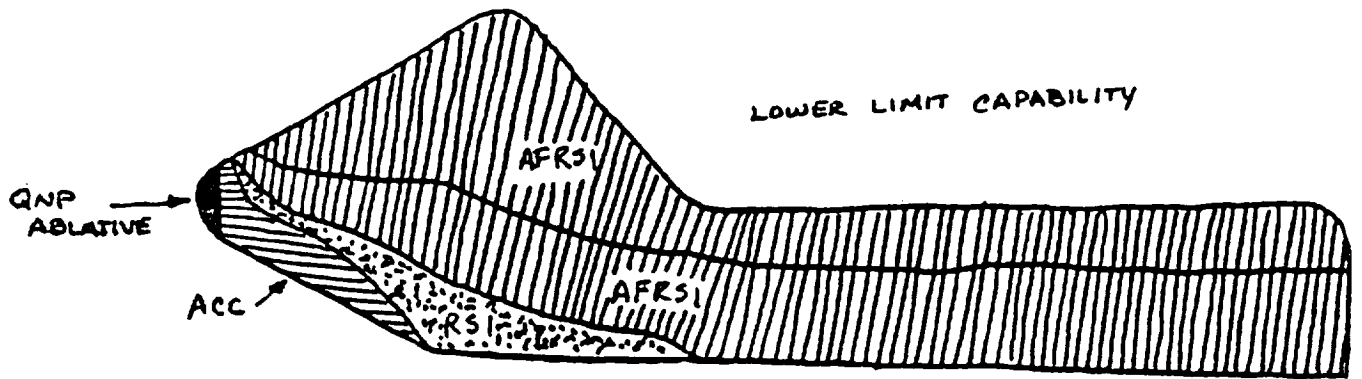


Figure 2.2.1.3-4 Future Technology Requirements

- b. FRCI-40 gives no thermal capability improvement and slight mechanical property improvement.
- c. FRCI-60 and FRCI-80 give slight improved temperature capability (100°F capability increase) but mechanical properties decline significantly (20-30% decrease for the FRCI-60).
- d. FRCI-20 can be made in 8 pcf, 10 pcf, 12 pcf, and higher densities. Mechanical properties will decrease with a decrease in density. For example, the FRCI-20-12 strength is 123 psi while that of the FRCI-20-8 is 46 psi.
- e. FRCI differs from the silica tiles presently used on the orbitor (LI-2200) in that the FRCI contains a proportion of Nextel fibers.

2. Ultrafiber Technology

- a. The ultrafiber is just a smaller diameter fiber than the Nextel used in FRCI. The ultrafiber is 2-4 pcf vs. 11 pcf for the Nextel used in FRCI.
- b. The smaller diameter fiber allows more Nextel to be used, giving improved properties over FRCI.
- c. Early results indicate that the addition of ultrafiber at a 10% level gives a 100% strength increase and a conductivity decrease over the FRCI-20 material.
- d. Ultrafiber still in development stages.

3. HTP Technology

- a. HTP tiles consist of silica fibers, aluminum oxide fibers, and boron nitride.
- b. Lockheed reports improvements in both thermal and mechanical properties over FRCI.
- c. NASA Ames is of the opinion that this claim is conflicting since there is a trade-off between thermal and mechanical properties in RSI technology.

CONCLUSIONS--The recommended TPS configuration of the sled concept based on present material technology are as shown in Figure 2.2.1.3-3. They would provide maximum reusability and minimum weight while protecting the sled structure from the expected environments. The disadvantages are the limited reusability of the ablative material and the required usage of 4 or 5 different materials. Significant improvement would be shown in ten years

should the expected future technology capabilities develop. The recommended configurations (Figure 2.2.1.3-4) would be composed mainly of AFRSI and ACC, providing much improved reusability, slight weight reduction, and utilize fewer materials.

PART 2: FABRIC SELECTION FOR CANDIDATE LOW L/D OTV CONCEPTS--Fabric materials have been considered as construction materials for the aerobrakes on several of the OTV concepts. This portion details the available fabrics and evaluates them for use in the aerobraking environments. In addition, the topics of low emissivity fibers to limit radiation of heat from the brake's backface onto the OTV structure and future fabric technology will be addressed.

FABRIC EVALUATION--A summary of the currently available fabrics and their pertinent properties are displayed in Table 2.2.1.3-3. The temperature capability for both single and multiple OTV flight reuse of candidate tailorable, flexible materials of silica, aluminoborosilicate, and silicon carbide fibers are shown, together with the manufacturers maximum continuous temperature recommendations, on Table 2.2.1.3-4. The maximum heat flux the fabric can be exposed to before it becomes irreversibly brittle is also shown and is based on experimental data reported in AIAA paper 84-1770. This maximum heat flux characteristic in conjunction with the limiting fabric temperature is essential to efficient, light weight, reusable aerobrake design and operation. The typical expected environment of the aerobrake is a temperature of 2500°F-3000°F, pressure of 14 to 50 psf, and a heat flux of 15-36 Btu/ft² sec. The only fabrics capable of performing in the OTV

Table 2.2.1.3-3 Fabric/Filament Data

Fabric	Comp.	Filament Density No. ft ³	Manufacture Temperature Capability*	Filament Modulus (MSI)	Filament Strength (KSI)
Glass	E-Glass	156.07	800°F	10.5	500
Leached Silica	SiO ₂	137.34	1800°F	-	-
Quartz	SiO ₂	137	1800°F	10	126-188
Carbon/ Graphite	Carbon	106-125	600-750°F	33-105	200-700
Nexel 312	Alumina boria-silica	169	2300°F	22	200-250
Nicalon	SiC	162	2300°F	27	390
Kevlar	Aramid	94	500°F	19	525

* At Sea Level Conditions

Table 2.2.1.3-4 Tailorable Advanced Ceramic Materials

Fabric Temperature Capability*	Single Flight	Multiple Flight	Manuf Cont Limit	Max Heat Flux**
Silica (Current AFRSI)	2000	1500	1800	4
Nextel 312 (Aluminoborosilicate)	2200	1800	2200	9
Nextel 440	?	?	2800	9
Silicon Carbide (Nicalon)	2600	2000	2300	34

* Temperatures in °F

** Heat Fluxes in BTU/FT²-sec (Heating limit when fabric condition becomes brittle)

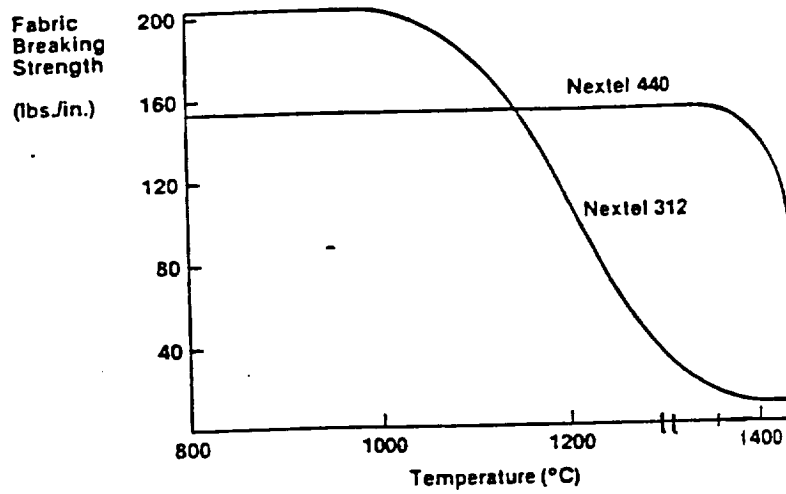
environment would be the Nicalon and Nextel materials. The Nextel 440 fabric has the best continuous temperature capabilities and suffers no major compositional breakdown at high temperatures as shown in Figure 2.2.1.3-5. The Nextel 312 and Nicalon fabrics show compositional changes at a lower temperature range (Figure 2.2.1.3-5). Therefore, the Nextel 440 would be preferred for its strength, but was not selected for the cover cloth because of its low heat capability and potential contamination from boria outgassing.

LOW EMISSIVITY TECHNOLOGY--No existing fiber will consistently exhibit low emissivity characteristics over the total wavelength spectrum. The Nextel filaments will, however, exhibit low emissivity (0.2-0.6) characteristics in the 0.4-2 wavelength range as shown in Figure 2.2.1.3-6. If this is the expected application conditions; Nextel could be used as a low emissivity material for the brakes backface, otherwise no total low emissivity fibers/fabrics exist and the use of coating would stiffen and/or fuse the fibers together.

FUTURE FABRIC TECHNOLOGY--In conversations with the various filament and fabric suppliers, an understanding was gained as to the future direction of technology. The major area of concentration will be other ceramics such as silicon nitride and silicon carbide-nitride materials. As the technology becomes available, other ceramics will also be investigated. The major improvement is expected to be the temperature capabilities of the materials.

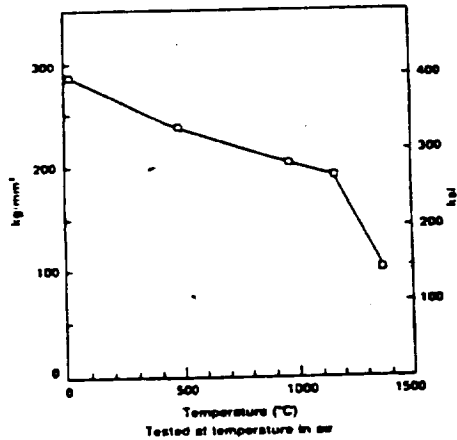
Nextel 312 vs. Nextel 440

Fabric Breaking Strength vs Heat Treatment Temperature*



Nicalon

GRAPH 2: TENSILE STRENGTH OF NICALON FIBER



GRAPH 3: TENSILE STRENGTH OF NICALON FIBER AFTER HEAT TREATMENT

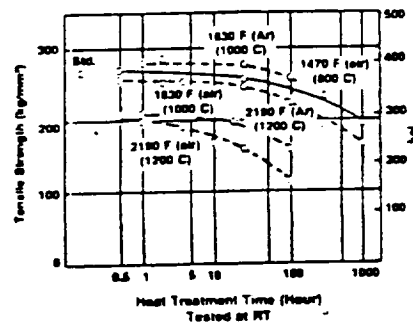


Figure 2.2.1.3-5 Compositional Heat Stability

Spectral Hemispherical Emittance
of White and Black Nextel Fabrics (w/sizing)

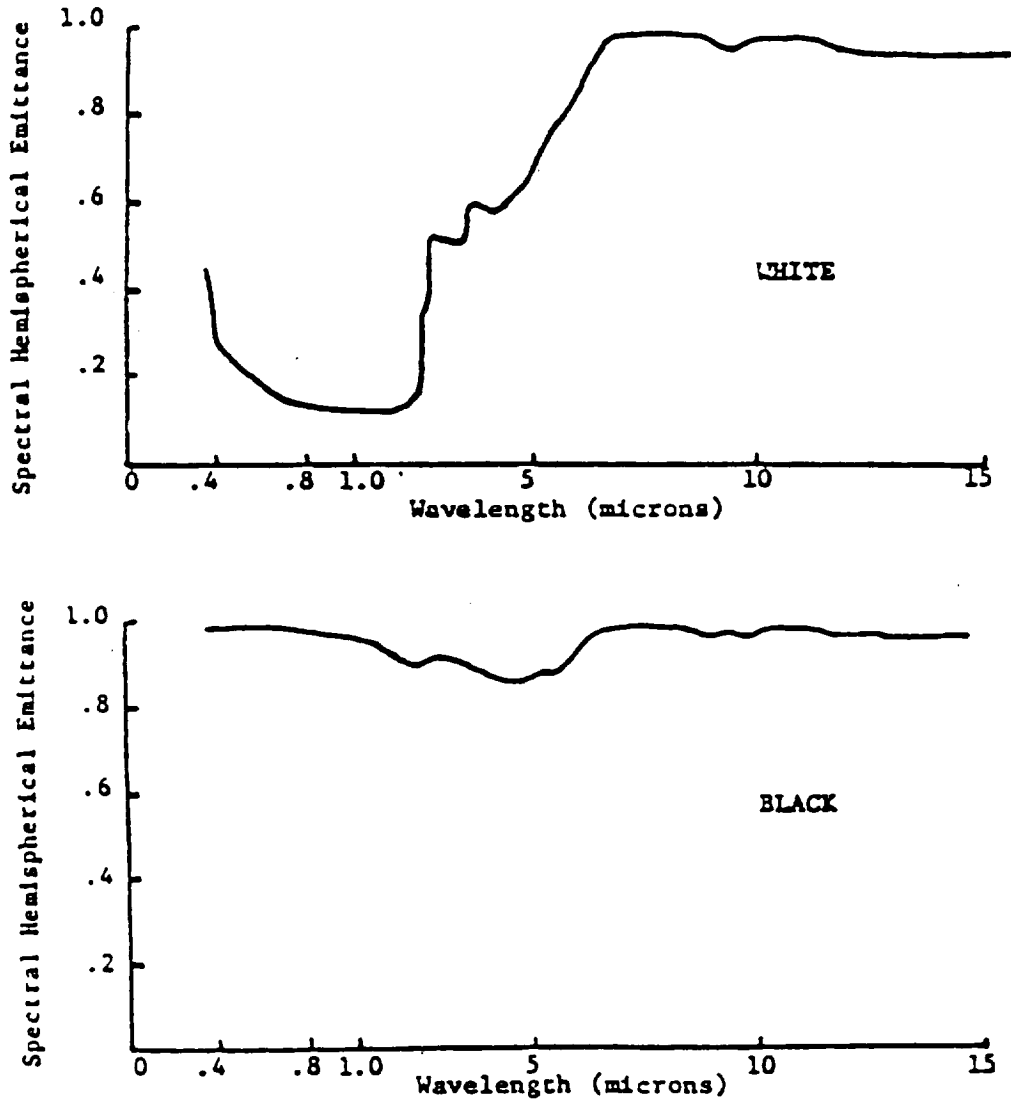


Figure 2.2.1.3-6 Nextel Emittance Data

Flexible ceramic insulation has proven to be a very attractive alternative to rigid tile systems and the Tailorable Advanced Blanket Insulation (TABI), seen in Figure 2.2.1.3-7, is the next step in flexible blanket technology. TABI's approach to blanket design is a three-dimensional woven structure filled with an insulation filler. The use of advanced ceramic yarns to weave these complex, integrally woven core structures for TPS applications is required. Possible core geometries being investigated are rectangular and triangular type construction of single or double layer design. Unlike previous blanket designs, which incorporate standard foam fillers, TABI will use flexible silica fillers or rigid ceramic fillers for increased mechanical and insulative performance. The pattern of a fluted woven core structure illustrates the interweaving of ceramic yarns.

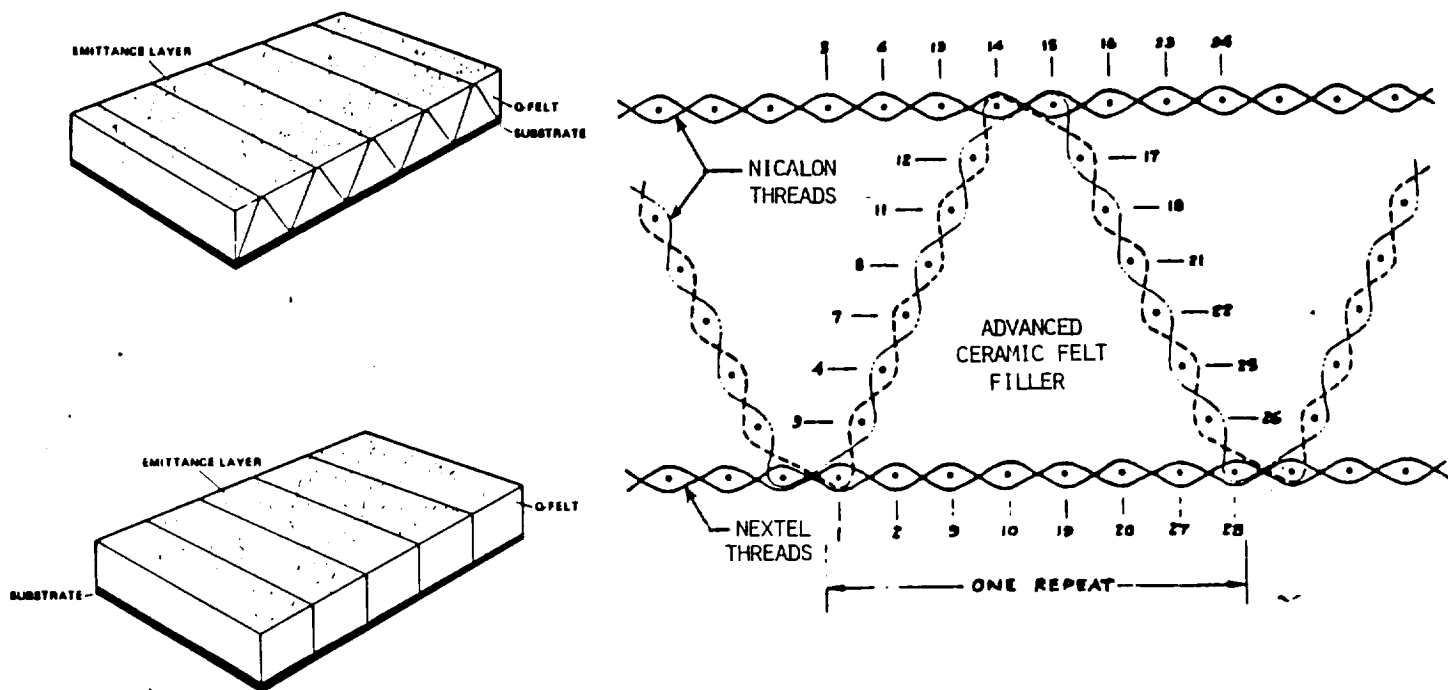


Figure 2.2.1.3-7 Tailorable Advanced Blanket Insulation (TABI)

Candidate materials for the TABI design are also shown in Figure 2.2.1.3-7. The thermal environment encountered by the OTV dictates materials selection and where these materials will be used in the TABI design. The high heating rates of 15 - 36 BTU/ft² sec suggest that Nicalon, silicon carbide, is best suited for the emittance layer or cover cloth. The core cloth would also be of Nicalon and act as a back-up cover cloth. The substrate layer or

back cloth would use Nextel (aluminoborosilicate), for its structural strength. Advanced ceramic felt is inserted between the cover cloths and a room temperature vulcanizing silicone rubber sealer is applied to the back cloth as a sealer.

Development of integral woven core structures using advanced ceramic yarns with ceramic insulation for the core is currently being pursued at NASA Ames Research Center. Their ongoing program has demonstrated the weaving capability of advanced ceramics into TABI. Continuing objectives include determination of surface properties and structural and thermal characteristics of the blankets. A technology development program is needed to evaluate reuse, repair and full scale manufacturing.

CONCLUSION--For the present application, the preferred material is the Nicalon. The only question which remains is with respect to its denier, warp, and reusability possibilities. No current data base exists to support the possible reusability aspects of the TABI. Characterization testing is needed to provide this data base.

In future applications, materials with improved temperature capabilities are expected to become available which may be used. These improved materials will be based on other ceramic materials as the technology becomes available.

The selection of TABI fabric for the flexible portion of the aeroshield face is based on the inherent safety from burn through in the internally woven three dimensional construction. Fabrication involves minimum threading and pierce points on the previously manufactured bulk material. The core size and shape may be varied to obtain the required thermal barrier properties. Density of the sandwich material and insulation characteristics may be tailored to meet local surface heating environments. The truss like interweaving inherently stiffens the material to reduce flutter and distortion over the AFRSI. A simpler installation, over a low cost composite ribbed frame, requires minimal substructure support while providing insulation efficiencies comparable to rigid surface insulations at a lower unit weight. A smoother surface finish and improved durability due to the minimized surface thread protrusions means improved durability and surface flow characteristics compared to AFRSI materials.

ADVANTAGES OF TAILORABLE ADVANCED BLANKET INSULATION FOR AEROBRAKE--

1. Integral construction
2. Minimum threads and pierce points
3. Vary core size and shape to obtain optimum design properties
4. Fail safe capability from 3D woven structure
5. Control density and insulative properties to local surface heating environments
6. Reduced Flutter and distortion over AFRSI
7. Simple installation, low cost, minimum substructure support
8. Comparable insulation effectiveness to RSI
9. Lower weight per unit area than RSI
10. Smoother surface and improved durability to AFRSI

2.2.1.4 Aeroassist Low Versus Medium L/D Selection

The selection criteria used in the low versus mid L/D trades is outlined below.

Lift control can be used to cover trajectory dispersions and for inclination steering. Use of lift to change inclination in the atmosphere reduces the plane change requirements at GEO. The velocity savings gained by going from an L/D of 0.25 to 1.00 vs 620 fps by using the additional inclination change capability equated to propellant savings at the end of the 14K round trip mission results in 1160 lb for storable or 840 lb for cryo. Therefore, to have a net performance benefit by increasing L/D, the increase in vehicle dry weight to produce this L/D must not exceed the propellant weight saved.

Between lifting brakes and lifting bodies, the best weight ratios are for the lower L/D's. The heat pulse and airloads associated with the low L/D lifting brakes are lower, improving their aeroassist benefits. In addition, they provide better adaptability to payload shape, size, and growth. Thus, low lift for an AOTV is desired, but the amount of L/D is a function of the control corridor required to handle atmospheric and trajectory dispersions, and the propellant savings from using excess lift for plane change.

Various L/D vehicles were chosen for the low vs mid L/D performance trade that are capable of performing manned missions. Their TPS and stage weight were calculated based on their thermal and structural requirements to perform these missions. The propellant savings of the higher L/D concepts were then traded against the reduced TPS weights of the lower L/D concepts. (This trade is illustrated in Figure 2.2.1.4-1).

Since storables provide a higher propellant weight savings with increased L/D, an apogee (2nd stage) storable mid L/D lifting body was selected for the trade. The small tank structure of the apogee stage also benefits the mid L/D because of the lighter core structural weight which lowers $W/C_D A$ and thus the TPS thicknesses.

A family of cryogenic vehicles were also evaluated to make a trade comparison based on propellant. The selected mid L/D concept for this trade is the single stage slant-nosed cylinder based on the work performed at NASA Langely Research Center, Reference AIAA-85-0966.

Table 2.2.1.4-1 summarizes the results from the low vs. mid L/D performance/weight trade. It shows that the propellant savings for the mid L/D vehicles is offset by its required TPS weight increase in all cases. Thus, there is no net performance benefit by increasing L/D for inclination steering and the vehicle should have only enough L/D as required for corridor control.

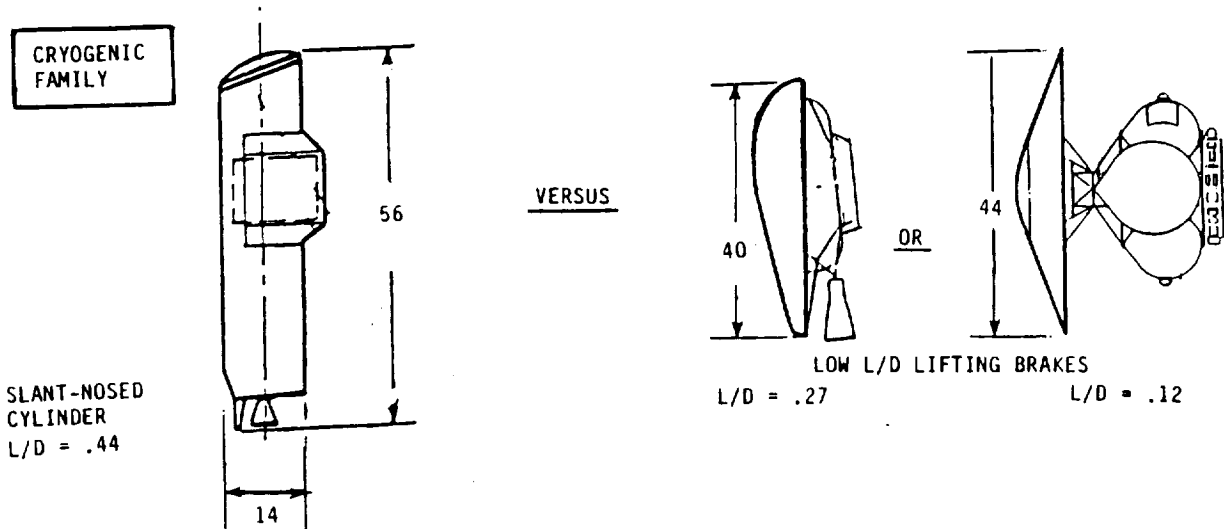


Figure 2.2.1.4-1 Low vs Mid L/D Performance Trade

CONFIGURATION	STORABLE TRADE		CRYOGENIC TRADE		
	HYPERSONIC BICONIC SLED	RIGID/ FLEXIBLE AEROBRAKE	SLANT NOSED CYLINDER	RAKED ELLIPTICAL LIFT BRAKE	RIGID/ FLEXIBLE AEROBRAKE
L/D	1.00	0.12	0.44	0.27	0.12
W/C _D A	70.0	10.8	65.0	15.1	9.9
W _{TPS}	3357	1343	3023	1855	1490
W _{DRY}	12.585	6553	11.574	9757	7640
FUEL SAVINGS BENEFIT	1410	+4662		-234 +1583	-415 +3519

- PROPELLANT SAVINGS FROM INCREASING L/D DOES NOT OFFSET VEHICLE WEIGHT INCREASE IN TPS.
- THE NET PERFORMANCE BENEFIT IS WITH LOW L/D AND NO INCLINATION STEERING.

Table 2.2.1.4-1 Low vs Mid L/D Aeroassist

2.2.1.5 Vehicle Lift Vs Drag Aeroassist Maneuvering

The remaining three primary aerobrake candidates are shown below in Figure 2.2.1.5-1 the inflatable ballute drag brake, the raked ellipse lifting brake and the symmetric Viking-shaped fabric lifting brake. The ballute and fabric brakes both utilize flexible thermal protection systems usually surrounding a rigid spherical nose cap with protective doors covering the main engines. The raked ellipse employs rigid thermal protection materials over the entire exposed area. The raked ellipse concept is based on the NASA Johnson Space Center design, Reference AIAA-85-0965.

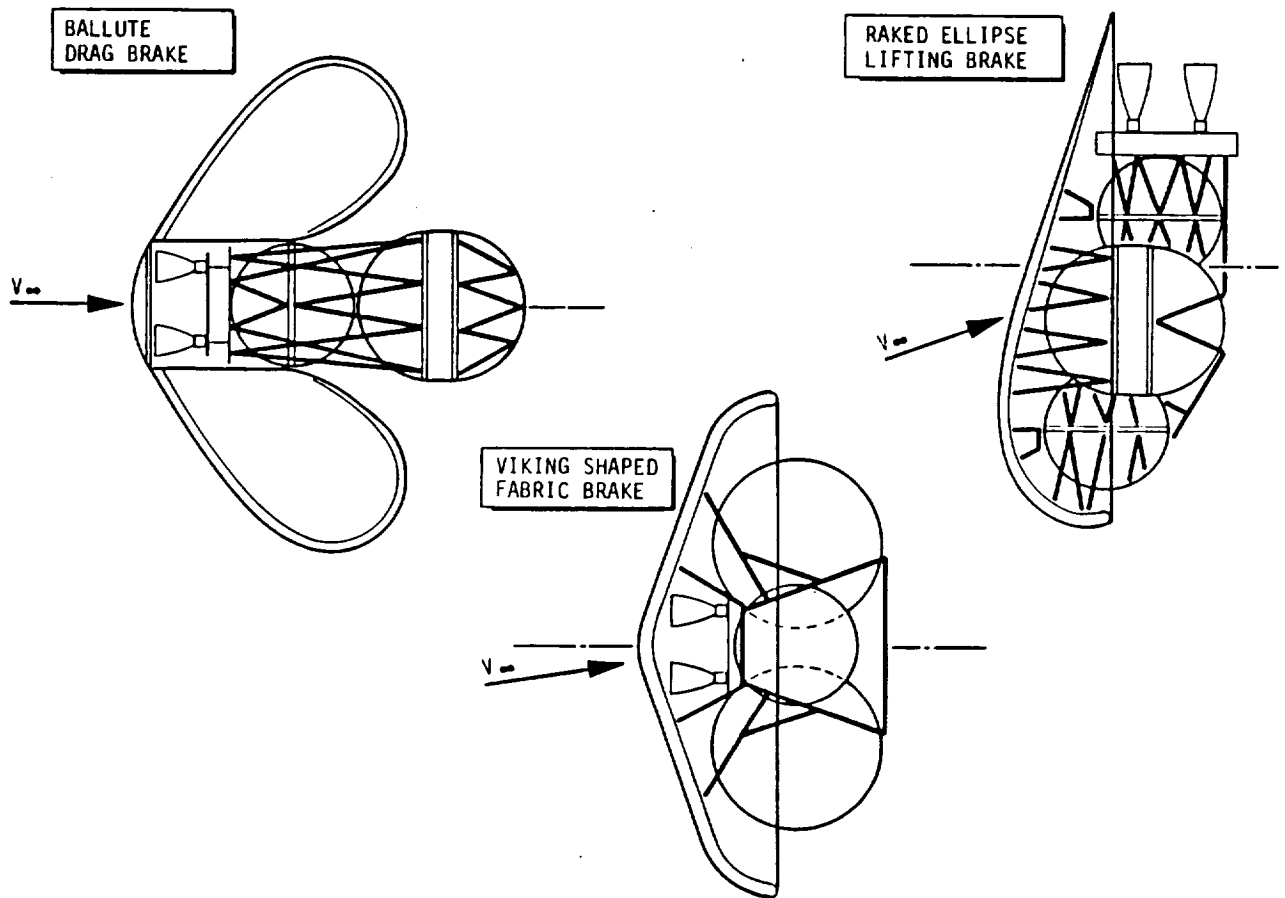


Figure 2.2.1.5-1 Low L/D Aero - Configuration Concepts

Table 2.2.1.5-1 provides comparisons of six areas for the three candidate aerobrake system designs: the ballute, the raked elliptical cone and the rigid/flexible TPS aerobrake. Design factors for both drag and lift devices; aerobrake/stage characteristics; operational impacts on launch to orbit; Space Station reuse and replacement, payload sizes, brake dimensions, weights and

Table 2.2.1.5-1 Aerobrake Concept Comparison

Factor	Inflatable Ballute	Raked Elliptical Cone	Rigid/Flexible Aerobrake
I. Design Summary			
o Data Source	BAC Studies	JSC Studies	MMC Studies
o L/D	Zero	0.3 or lower	0.12
o W/C _D A PSF	4.6/13/3	8.1/15.1	4.0/11.6
o Control Mode	Area Variation	Roll Control	Roll Control, Offset C.G.
II. Characteristics			
o Geometry	Blunt Conical Spherical Nose	Raked Cone Ellipsoidal Nose	Blunt Conic Spherical Nose
o Brake Base Dia	50 ft	40 ft	44 ft
o Stage Dimensions	14D x 34L	38D x 14L	38D x 25L
o Aeroshield TPS	Rigid/Flex	Rigid	Rigid/Flex
o Long. Stability (Stable CG Range Aft of Nose)	C.P. Varies With TDR (25 ft)	1 Radius Aft of Aerobrake Base (34 ft)	Wide C.G. Latitude (43 ft)
III. Operations			
o Shuttle Transport to Space Station	Ship Folded Fabric as Unit	Disassembled in Sections, Assembly Required	Ship Assembled As a unit with Fabric Folded
o Space Station - Reuse	Not Practical, Recharge Pressurant	Yes - Visual Check	Yes - Visual Check
- Replacement	Simple - Install Unit	Complex - Replace Tiles or Entire Brake	Simple-Install As A Single Assembled Unit
IV. Size-Controlled by			
	Long. Stability & Turn Down Angle	Flow Impingement	Wake Heating
20K P/L Delivery			
o Aerobrake Dia,Ft.	40	37	38
o Aerobrake Mass (Struct & TPS,LB)	1569	1587	1270
o Stage Dry Wt, LB	8070	9489	7140
o W brake/W return	.194	.167	.178
7.5 Man Geo Sortie			
o Aerobrake Dia,Ft	50	40	44
o Aerobrake Mass,lb	2452	1855	1407
o Stage Dry Wt, lb	8950	9757	7560
o W brake/W return	.149	.107	.093
15K Manned Lunar Sortie			
o Aerobrake Dia, Ft	62	40	44
o Aerobrake Mass,lb	3700	1923	1489
o Stage Dry Wt, lb	10250	9825	7640
o W brake/W return	.146	.077	.066

Table 2.2.1.5-1 Aerobrake Concept Comparison (Continued)

Factor	Inflatable Ballute	Raked Elliptical Cone	Rigid/Flexible Aerobrake
<u>V. OTV Design Impact</u>			
o ACC Use	Good with Storable Prop.	Over Sized for Many Missions	Good ACC Use, No Ascent Loads
o Configuration	Tandem Or Toroidal Tanks	Integrated Concept Optimized With Parallel Tanks	No Constraints 4 Ball Tanks Best
<u>VI. Concerns-Risks</u>			
TPS	-Single Resue -Assembly Joint -Local & Global -Lobe Radiation Trap -TPS Packaging Volume	-Assembly Joints -On Orbit Assembly -Payload Wake Heating	-Local delta P Flutter -Base Heating -Flex TPS Reuse -Asembly Joints
Control	-Preentry Spin-Up -Assymmetric Loading -Deflation -Brake/Stage Dynamics -Turn Down Ratio Limited	-Separate LH2 Descent Tank, C.G. Control - Payload Local On Return vs Delivery -Side Firing Engine	-C.G. Trim Error -Favorable Aerocharacteristics -ACS Location
Basic Feasibility	Moderate -Engine Doors -Shape Stability -Fabric Flutter	Low -OnOrbit Assembly and Maintenance	Moderate -Engine Doors -Fabric Maintenance
Weight Growth	Moderate -Limited In Return Payload Growth	High -Block Change To Increase Tankage Or Brake Size -Return Payload Shape and Size Variable -Payload C.G. And Mounting Orientation	Low -Moderate for Dia Increase -Compact Stage Has C.G. Margin For Return Payload Growth

efficiency ratios; OTV design impacts and risks for TPS, control, feasibility, and weight growth are shown. This assessment leads to our continuing recommendation of the combined rigid/flexible TPS for both our ground and space-based OTV configurations.

The aeroassist decision criteria used for selecting the desired aeroassist approach is tabulated in Table 2.2.1.5-2. The decision logic is based on a score of 1 to 10 and the preceding comparison tables. The major drivers in selection of the rigid/flexible aerobrake are weight, control, risk, growth/reuse, and the use of advanced technology.

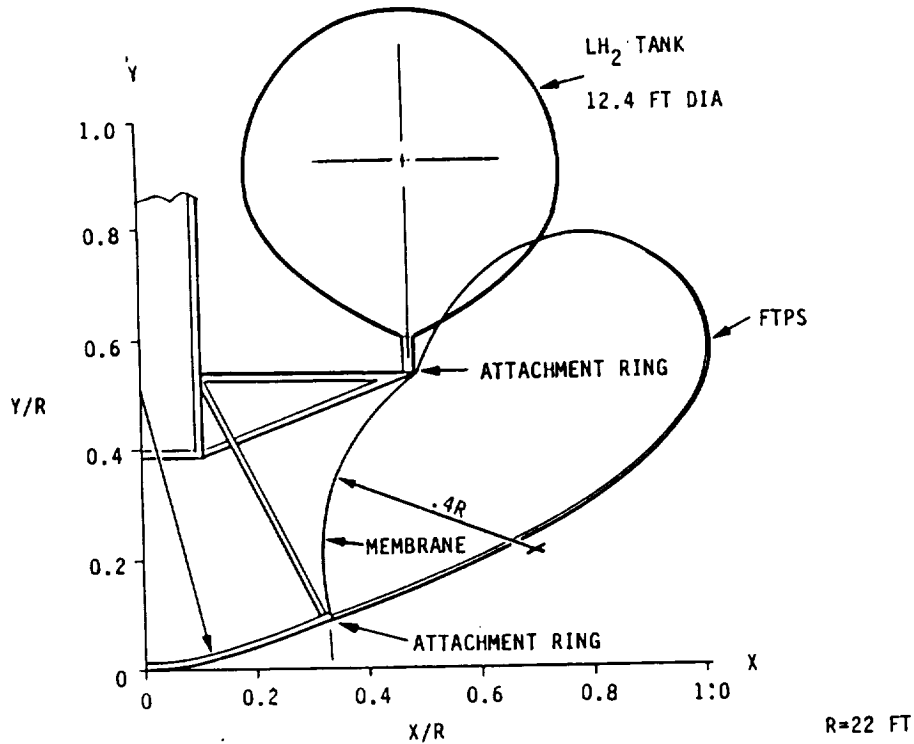
Table 2.2.1.5-2 Aeroassist Decision Logic and Selection

AEROASSIST DECISION CRITERIA	INFLATABLE	RAKED	RIGID/FLEXIBLE
	BALLUTE	ELLIPTICAL CONE	AEROBRAKE
- FEASIBILITY	5	10	7
- PERFORMANCE/WEIGHT	7	9	10
- DEVELOPMENT/COST	7	10	8
- RELIABILITY/CONTROL	5	10	8
- MAINTENANCE AND ACCESS	7	6	10
- GROWTH	6	7	10
- REUSE	3	10	8
TOTAL	40	62	61

- DRAG MODULATION INCREASES WEIGHT AND RISK WITH DECREASES IN CONTROL MARGIN AND GROWTH/REUSE
- LOW L/D WITH ADVANCED TECHNOLOGY IS THE SELECTED APPROACH

To ensure the drag concept was not penalized by its stage configuration (tandem tanks), adaption of a ballute aerobrake to our parallel tank stage approach was investigated. The purpose of this configuration trade is to see if the tandem tank stage penalized drag modulation and to create a common base for comparison.

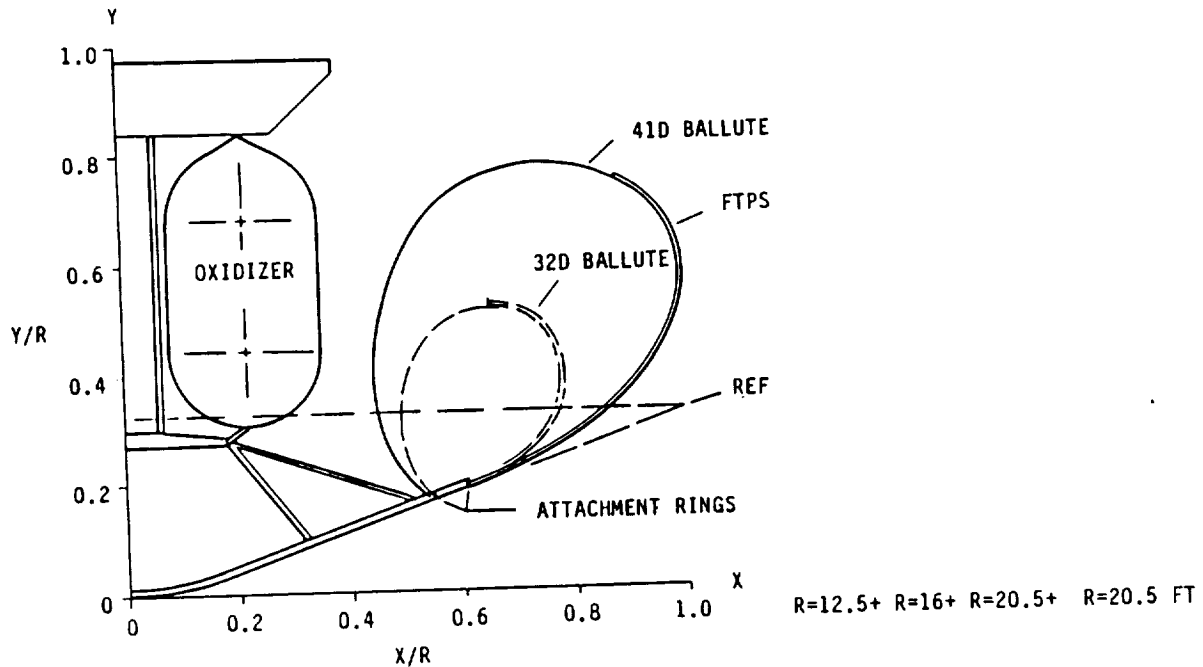
A concept for using a 44 foot diameter Ballute with the Space Based Cryogenic OTV 55K is presented in Figure 2.2.1.5-2. The forward attachment point is at $X/R = .33$. The Ballute shape shown is the isotenoid shape for a pressure ratio $P_i/P_s = 0.95$. The Ballute is closed by a membrane with an $X/R = .4$, that is $R = .4 \times 22 = 88.8$ feet. A middle attachment ring that supports the Ballute and membrane is indicated near the base of the structure that supports the LH2 tanks. The isotenoid Ballute shape for a pressure ratio of 0.95 indicates that there will be some interference with the tank. A slightly lower pressure ratio isotenoid shape or a nonisotenoid shape can be established to eliminate the local interferences. A preliminary weights analysis for the ballute fabric components results in 1,161 lbs. and a total aerobrake weight (nose region and ballute) of approximately 1650 lbs.



COURTESY OF GOODYEAR AEROSPACE COOPERATION

Figure 2.2.1.5-2 Space Based Cryogenic OTV - 55K Propellant - 44 Foot Ballute

An approach for using Ballutes with the 53K Space Based Storable OTV is shown in Figure 2.2.1.5-3. The 41D aerobrake is shown for reference. The desired 25D is illustrated as using a portion of the present MMC design. The 32D is obtained by adding a small toroidal Ballute with a P_i/P_s ratio of 0.90 to the 25D portion. The 41D is obtained by adding a Ballute with a P_i/P_s ratio of 0.95 to the 25D portion. Mounting rings at the forward and aft locations need to be added to the basic 25D structure. A single aft ring can be used for either the 32D or 41D Ballute. Ballute fabric weights for the 32 and 41 foot diameters are 426 and 780 lbs., respectively and are packagable around the tankage of a storable OTV.



COURTESY OF GOODYEAR AEROSPACE COOPERATION

Figure 2.2.1.5-3 53K Space Based Storable OTV - 32 and 41 Foot Ballutes

As a final comparison of a ballute concept versus a fixed, passive structure, wind tunnel data of these two approaches were compared, References NASA TN D-5840 and MMC TR-3709014. Similar conclusions were drawn from the aerocharacteristics of these two approaches as were made back in the early Viking-Mars Lander studies. The inflatable lifting brake is a lower performer. This can be seen both in C_L , C_D , and L/D of Figure 2.2.1.5-4. For the same L/D , the AID body must fly at almost twice the angle of attack. This higher angle of attack not only increases brake edge heating, but also restricts payload lengths due to flow impingement. Another important comparison is the stability or center of pressure for the two brakes. The Viking 70° conical brake c.p. lies 1.01 brake diameters aft while the AID brake was only 0.3 diameters aft.

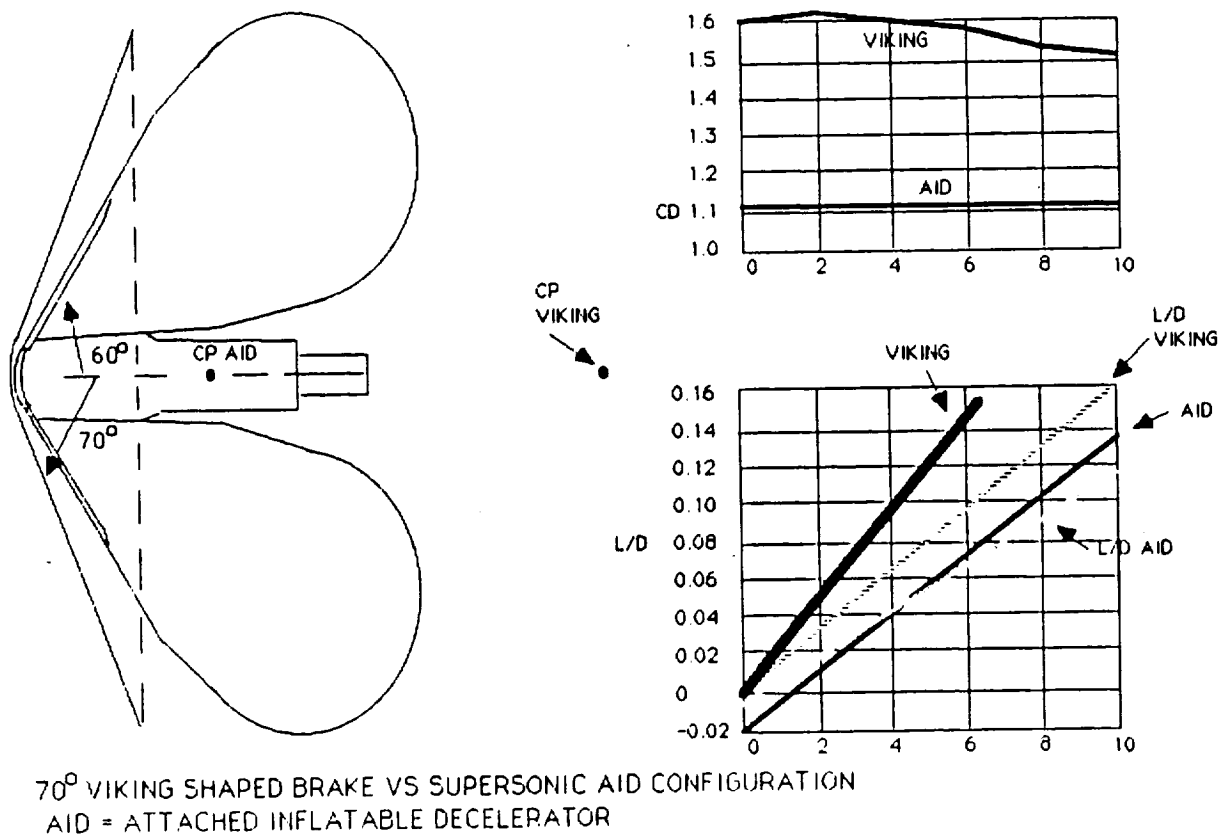


Figure 2.2.1.5-4 Fixed vs Inflatable Flex TPS Lifting Brake

2.2.1.6 Aeropass Environment and L/D Selection

The aerothermodynamic flight domain of an AOTV is shown in Figure 2.2.1.6-1. An STS trajectory is shown for comparison. The AOTV decelerates at a much higher altitude than STS and makes its aeropass in a very energetic environment of the upper atmosphere. STS peak heating occurs in a dissociated oxygen dominated convective heating environment. The AOTV's entry into the atmosphere is almost twice as energetic as STS. The environment associated with the passage of the OTV through this high altitude consists of radiation from chemically relaxing air (also known as nonequilibrium radiation) and convection from dissociated, ionized air. It has been shown (Reference AIAA Paper 83-0406) that a regime exists for blunt bodies where continuum theory applies although a slip condition may occur. The limit of applicability of continuum theory for a blunt body is called the quasi continuum limit and is illustrated in Figure 2.2.1.6-1.

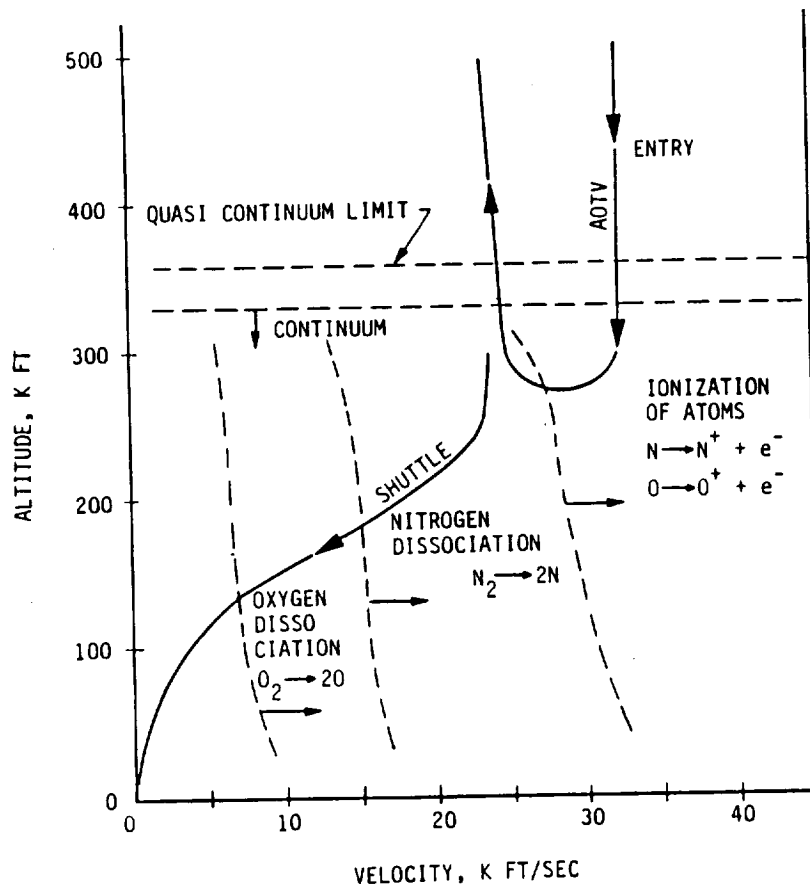


Figure 2.2.1.6-1 Aerothermodynamic Environment

Figure 2.2.1.6-2 illustrates the trajectory correction process performed in the aeropass. Safe flight through the atmosphere is restricted to a region which can be controlled by the OTV. The vehicle uses lift vector pointing to modulate its trajectory. The limits of this control are continuous lift vector up and continuous lift vector down. Trajectories run with these two conditions define lower and upper (respectively) boundaries for vehicle flight. Conditions which exceed these boundaries will result in either skip-out or reentry.

The aeromaneuver is accomplished by using the vehicles' lift to climb or descend, and thereby correcting for density variations and pointing uncertainties. The maneuver must be done in a precise manner to avoid losing too much velocity and reentering, or losing too little velocity and coasting

back out to a high altitude. These boundaries characterize the corridor or zone within which the OTV must fly for a successful aeropass. The size and depth of the corridor is a function of the vehicle's L/D and establishes the heating environment and TPS requirements of the aerobrake.

GEO DOWNLEG

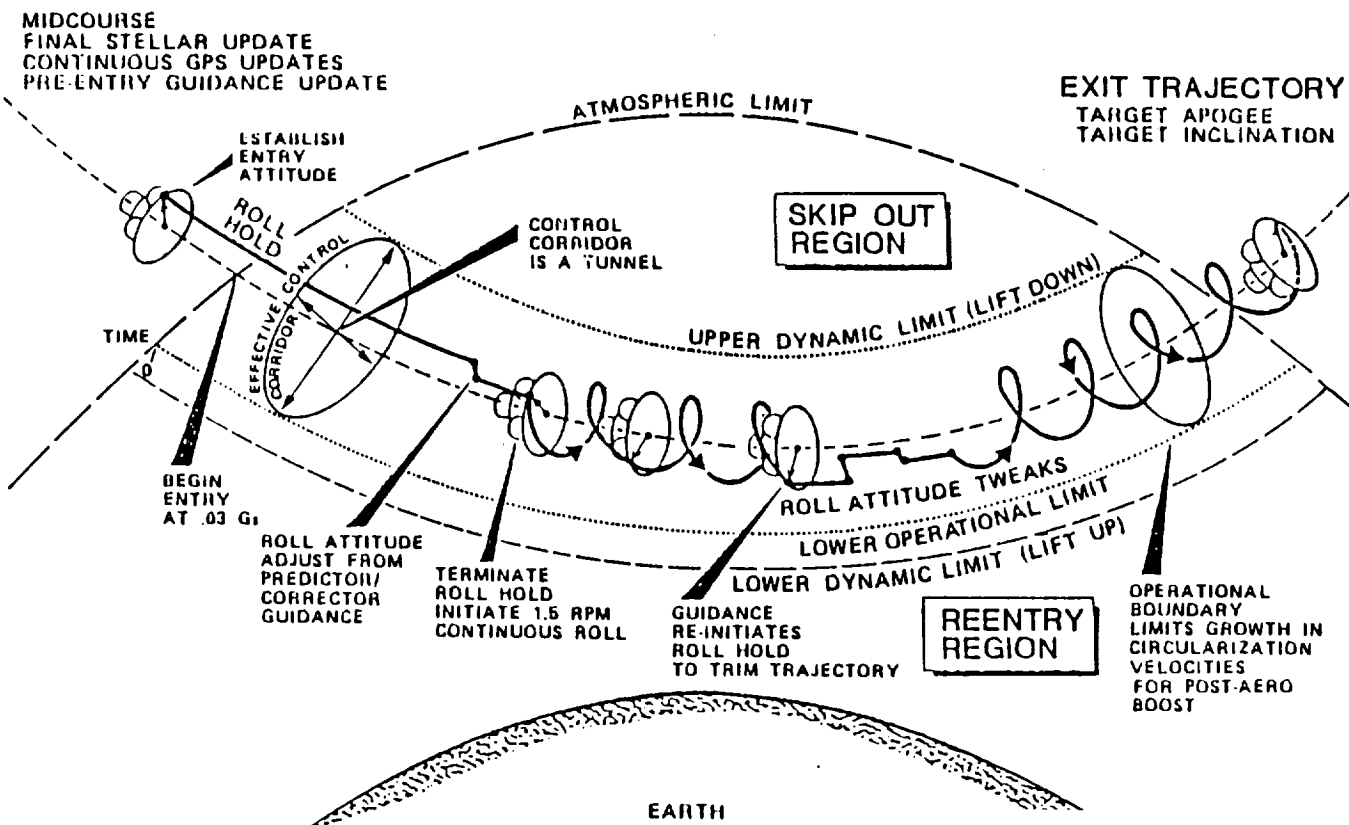


Figure 2.2.1.6-2 Aero-entry Overview

The effect of increased L/D on the vehicle heating corridor is presented in Figure 2.2.1.6-3. As L/D increases from 0.12 to 0.20, the corridor widens resulting in higher peak heat flux values for the same $W/C_D A$. Effects are shown for a 40 ft diameter brake at ballistic coefficients from approximately 2 through 12. This increase in heating, as a vehicle flies at higher L/Ds, is caused by the deeper penetration depth into the atmosphere the vehicle can fly and still perform a successful aeropass.

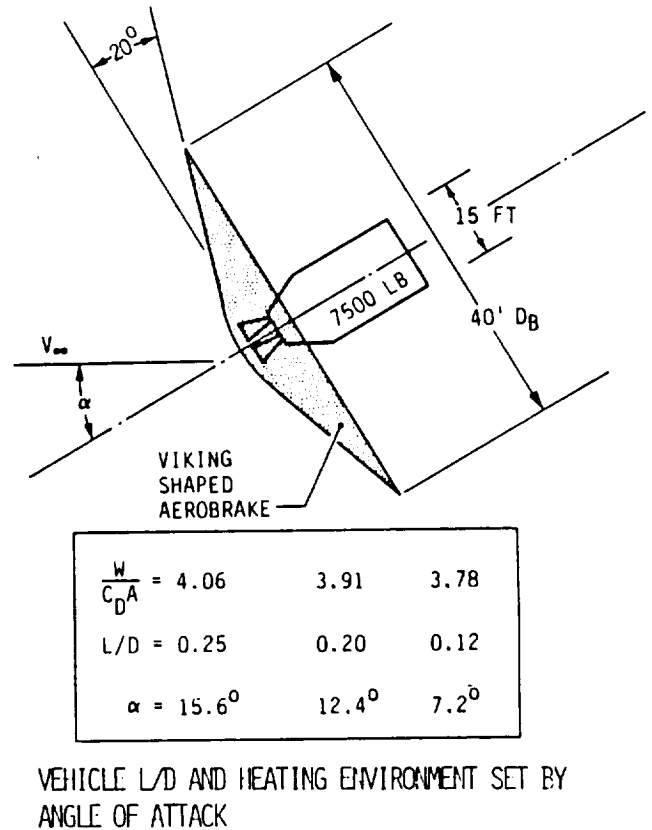
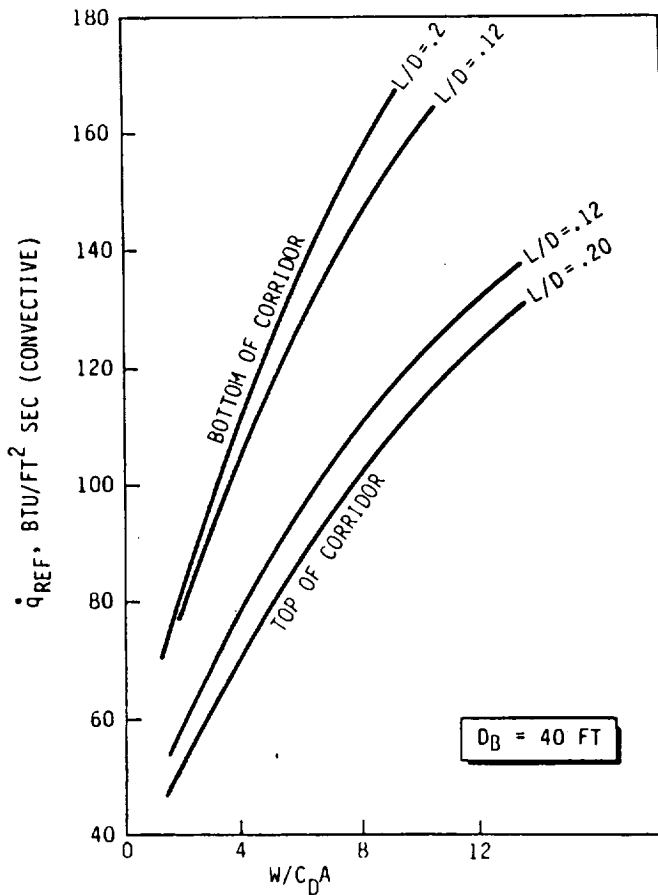


Figure 2.2.1.6-3 Heat Flux Correlation With Ballistics Coefficient and Lift to Drag Ratio

Typical control corridor effects from L/D and $W/C_D A$ based on trajectory simulations are shown in Figure 2.2.1.6-4 for $W/C_D A$ from 4.0 to 9.0. The effect of ballistic coefficient (or vehicle weight) on control corridor location is shown for a brake diameter of 40 ft. Also, the effect of L/D on flight corridor width is shown for both an L/D of 0.12 and 0.20 for a $W/C_D A$ of 4.0. With increased L/D, the corridor becomes wider and has a further penetration depth into the atmosphere. This results in a more severe heating environment and reduces the ballistic range of operation.

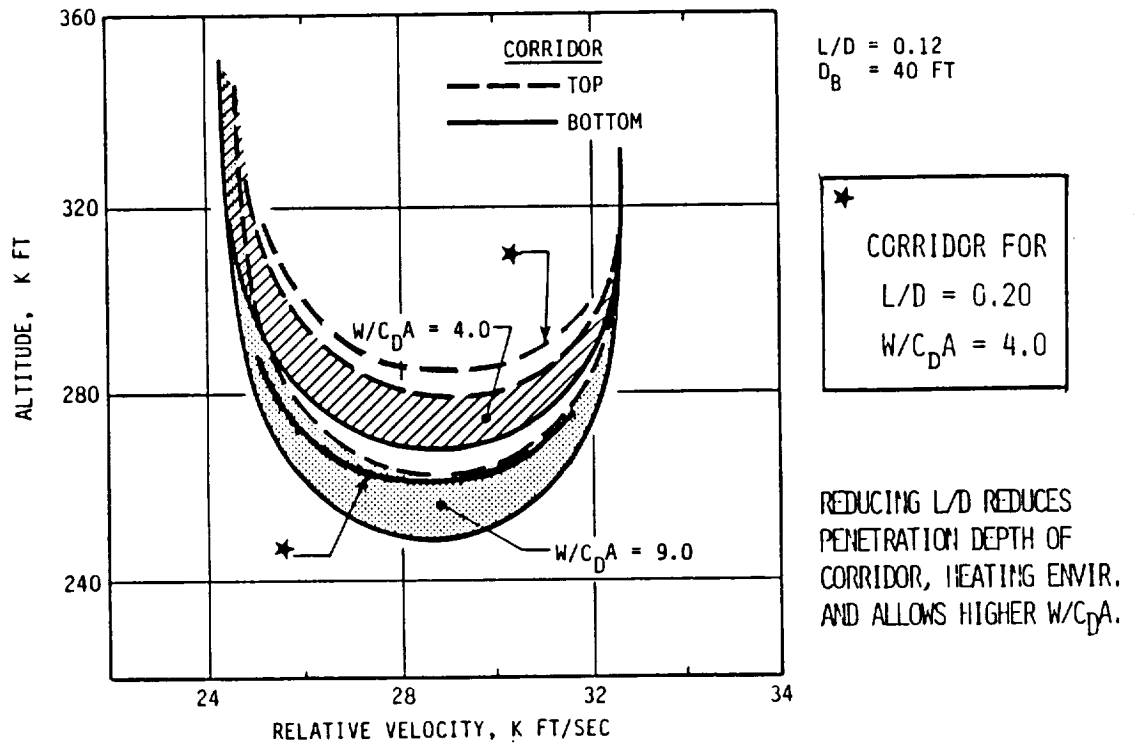
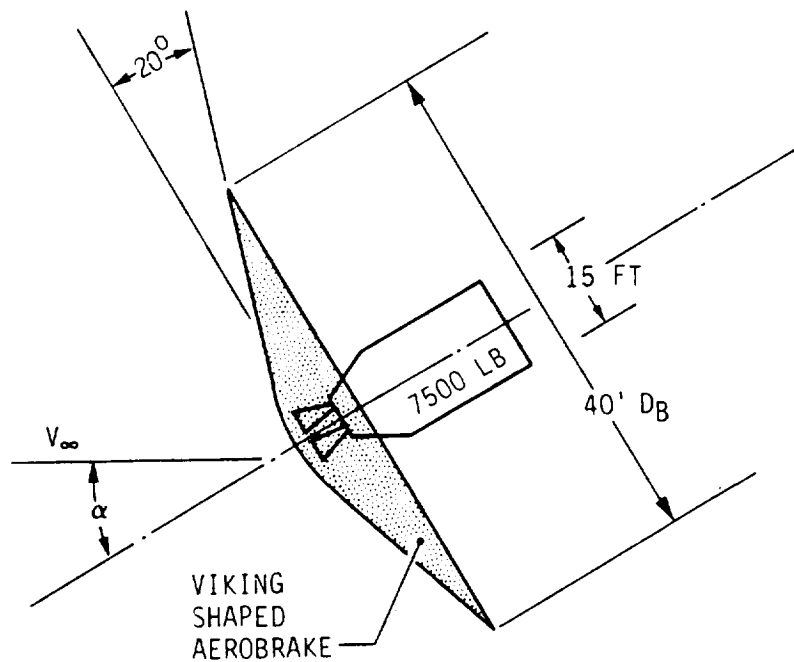


Figure 2.2.1.6-4 Typical AOTV Flight Trajectories

The desired vehicle trim angle is set by offsetting the vehicle's center of gravity. This trim angle establishes the vehicle's L/D and ballistic coefficient as seen in the illustration of Figure 2.2.1.6-5. Holding the vehicle configuration constant (i.e., weight and brake size), an increase in its trim angle results in higher values for L/D and $W/C_D A$.

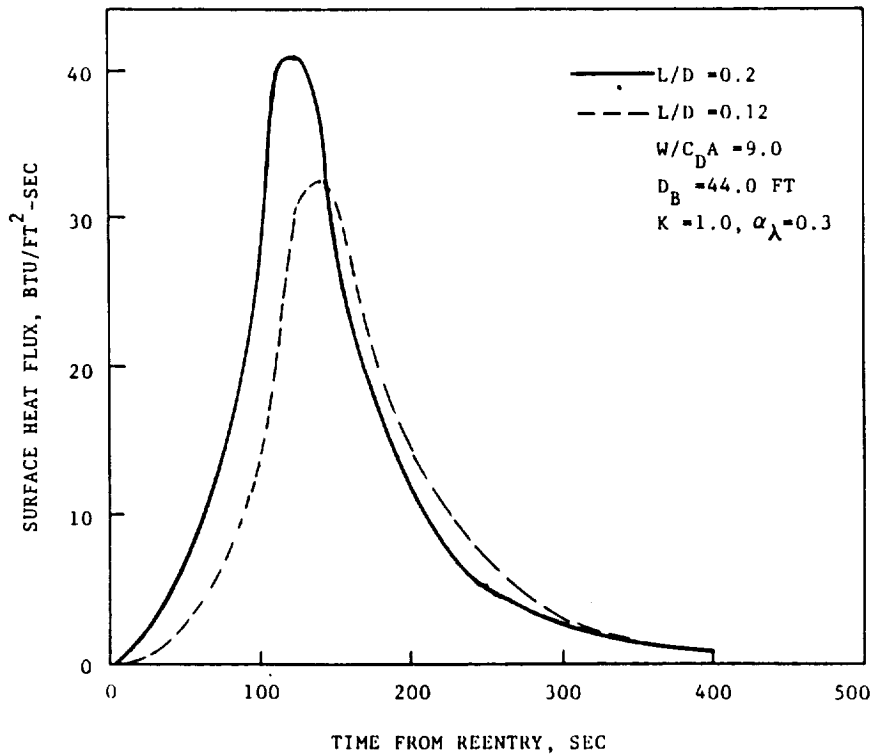
A comparison of the aerobrake surface heat flux histories versus L/D for a 44 foot diameter aerobrake is shown in Figure 2.2.1.6-6 for a L/D of 0.20 and 0.12. The heat fluxes are for a fully catalytic surface having a spectral absorption coefficient of 0.3. With an L/D of 2.0, a peak heat flux of 41 BTU/ft²-sec, is obtained using a finite catalytic reaction rate, a peak value of 31.



$\frac{W}{C_D A}$	= 4.06	3.91	3.78
L/D	= 0.25	0.20	0.12
α	= 15.6 ⁰	12.4 ⁰	7.2 ⁰

Figure 2.2.1.6-5 Vehicle L/D and Heating Environment Set By Angle of Attack

BTU/ft²-sec is achieved with surface temperatures above 2900°F. This heating environment requires aerobrake diameter growth for mission capture with a flexible TPS system or the use of RSI at both the center and perimeter of the brake. The brake weight penalties for either of these options are unacceptable. To reduce the vehicle's heating environment and brake diameter, the trim angle or L/D needs to be reduced. Lower angles of attack reduces edge heating and penetration depth of the corridor by narrowing its width via L/D. This reduced heating environment will allow higher ballistic coefficient vehicles and thus a better aeroassist system.



AEROBRAKE'S PEAK HEAT FLUX AND HEAT LOAD REDUCED WITH LOWER L/D

Figure 2.2.1.6-6 Heating Environment vs L/D

The impact of edge radius on the aerobrake's size, surface area, and weight stability margin is illustrated in Figure 2.2.1.6-7. For an optimum, low weight brake design, accurate knowledge of the forebody heating profile is required.

Our extensive experimental wind tunnel data base on the Viking shaped aeroshell and afterbody configuration enables accurate predictions of the aerobrake's front face and aft body heating distribution. The heat flux distribution on the brake and around its edge for two trim angles (or L/D) is shown in Figure 2.2.1.6-8. Note the higher aerobrake heat load and edge heating for the 12 degree angle of attack for an L/D = 0.20 compared to the 8 degree trim angle for the smaller L/D of 0.12 (Ref. MMC TP-3720318 & AEDC-TR-73-195). Similar increases in the base heating, can be seen as the angle of attack increases based on in-house VOIR tests. Thus, increased trim angle provides higher L/D at the cost of increased brake weight due to TPS requirements, which results from the increased forebody and edge heating.

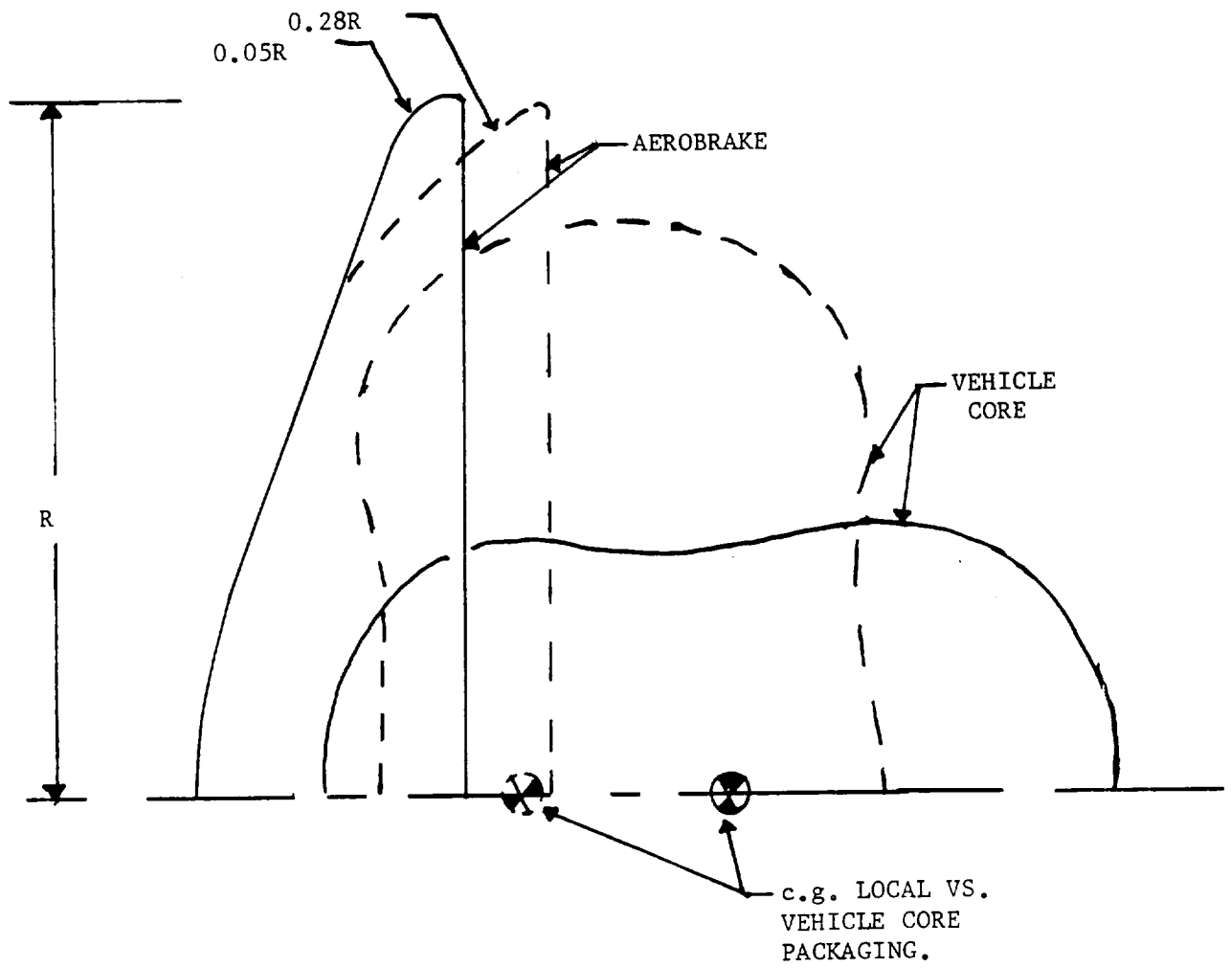


Figure 2.2.1.6-7 Impact of Edge Radius on Aerobrake Size, Surface Area, and Weight Stability Margin

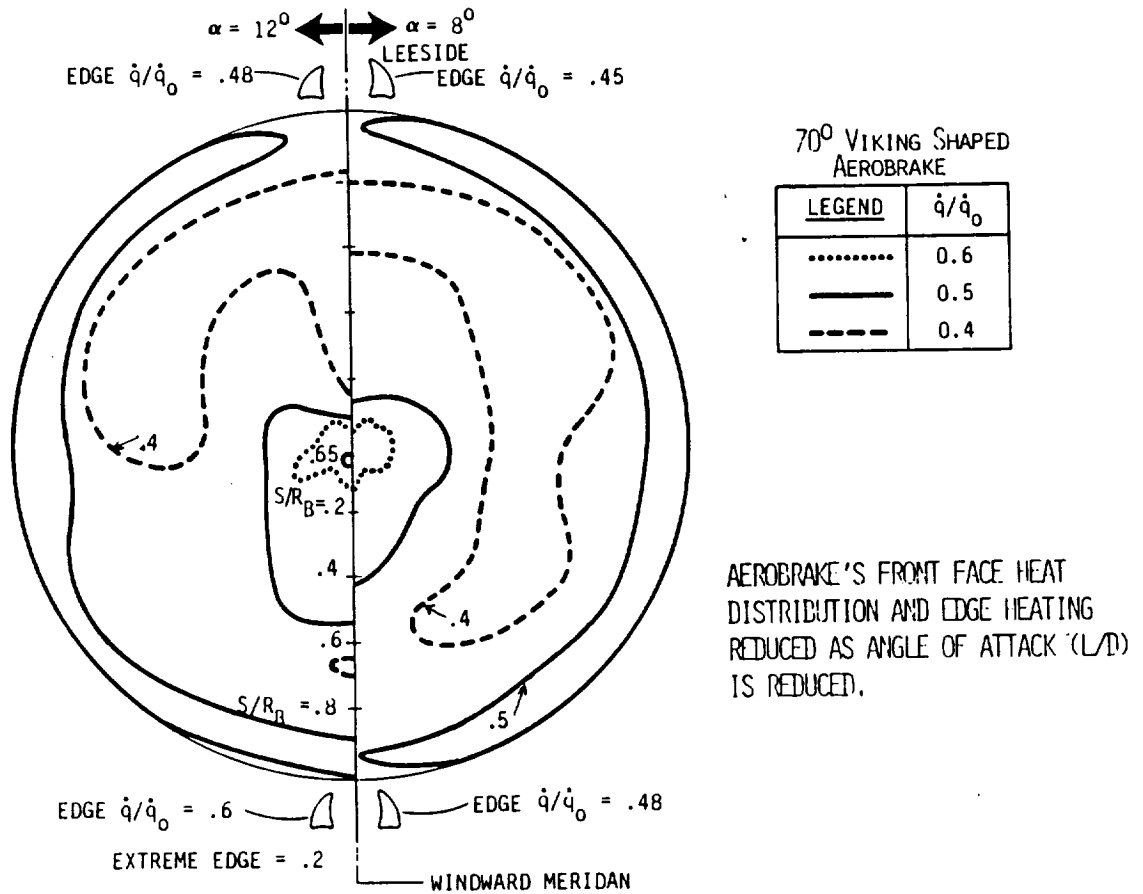
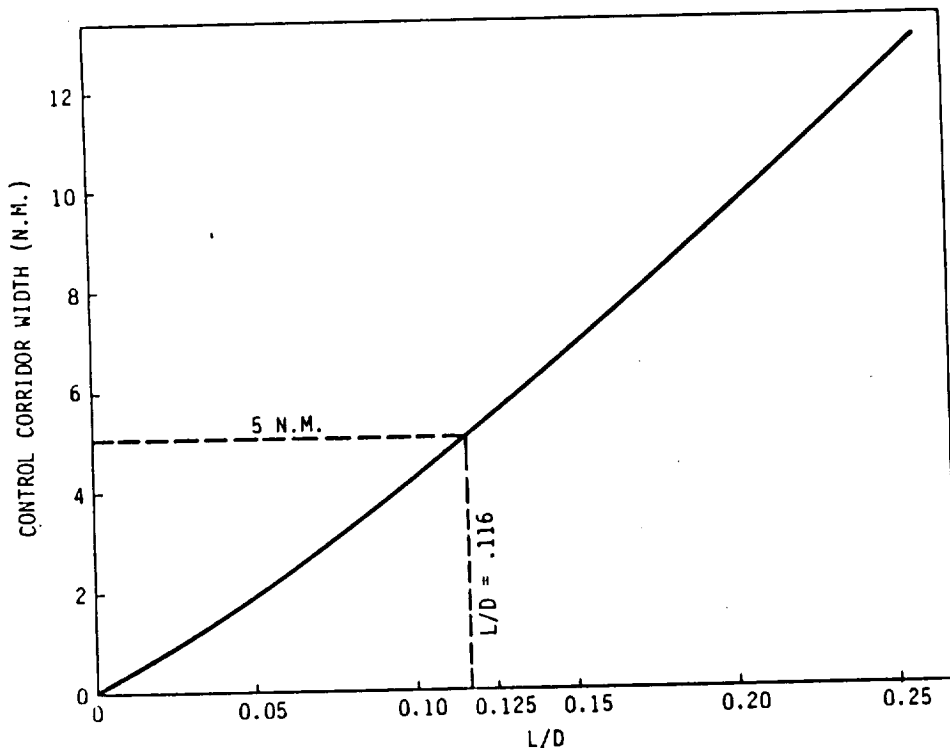


Figure 2.2.1.6-8 Heat Flux Distribution vs L/D

In order to reduce the aeropass heating environment, the corridor size is optimized based on a guidance and navigational error analysis. The output of this analysis was the selection of L/D that provides a design margin adequate to account for atmospheric effects. Results from our atmospheric and vehicle performance aero-entry dispersion analysis defines a 5 mile corridor width for control. This requires a vehicle trim L/D of 0.12. For our 70 degree conical aerobrake, a trim angle of 7.2 degrees provides the required L/D of 0.12 (see Fig. 2.2.1.6-9).



- 5 N.M. CONTROL CORRIDOR REQUIRES L/D OF 0.116
- USE OF VIKING CONTINUUM FLOW DATA RESULTS IN AN ANGLE OF ATTACK = 7.23° (REF: VIKING AERODYNAMIC DATA BOOK, NASA TR-3709014)
- FREE MOLECULAR FLOW ANALYSIS RESULTS IN NO SIGNIFICANT IMPACT TO ANGLE OF ATTACK

• OTV DESIGN ATTITUDE FOR ENTRY IS 7.23 DEG

AERO-ENTRY ERROR ANALYSIS INDICATE AN L/D OF 0.12 PROVIDES SUFFICIENT CONTROL MARGIN

Figure 2.2.1.6-9 L/D vs Control Corridor

2.2.1.7 Aerobrake Space-Basing Accommodations

After completing functional requirements and accommodation designs to facilitate OTV space-based operations, the aerobrake design was reviewed and optimized to reflect these functional requirements. These changes shall be reviewed in detail in the following write-up.

There is currently no way to launch a piece of hardware to orbit measuring 44 feet in diameter. Our design enables the aerobrake to be folded into a configuration that does not exceed 14' 6" diameter, and requires a minimum cargo bay length (under 10 feet). The structure consists of an interface ring approximately 13 feet in diameter around which are spaced 12 trusses. Each truss consists of a rib supported by two struts, which when folding, requires provision be made for the fold of exterior flexible material (see Figure 2.2.1.7-1).

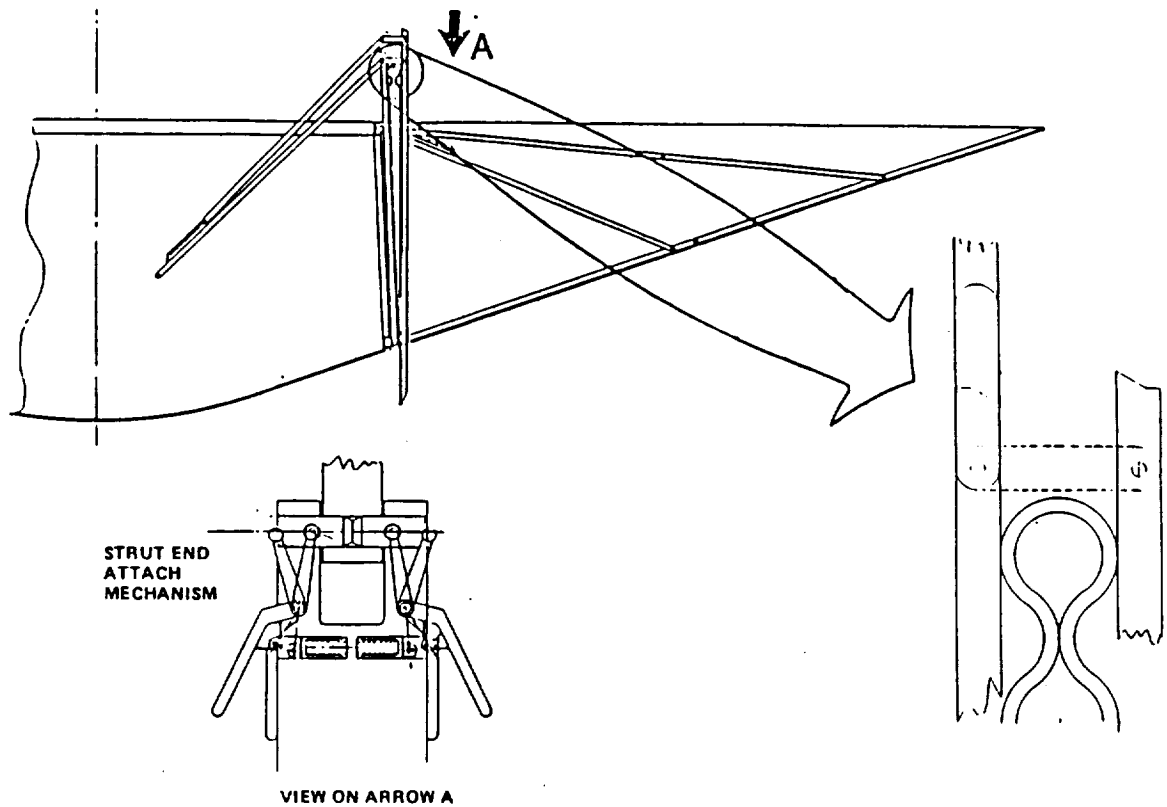


Figure 2.2.1.7-1 SBOTV Folding Aerobrake

Figure 2.2.1.7-2 shows initial delivery of the disassembled space-based OTV to Space Station. As indicated, all subsystems will fit into the Orbiter Payload Bay, and delivery, in essence, will require two equivalent Shuttle flights. In that the dry weight of the SBOTV is on the order of 8000 lbs, we do not advocate delivery in two flights; rather, SBOTV subsystem delivery should be manifested across a larger number of Shuttle flights to optimize weight and volume deliveries to Space Station.

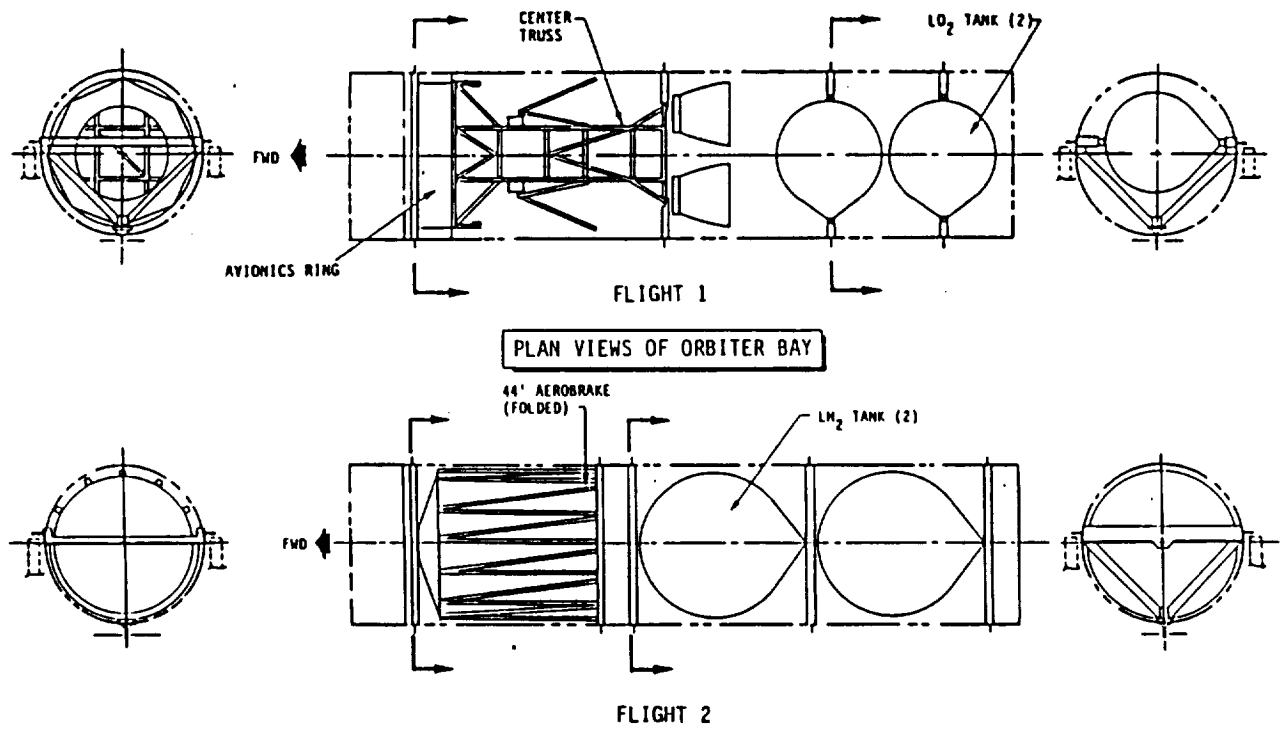


Figure 2.2.1.7-2 Initial Delivery of the Space-Based Foldable Aerobrake

The aerobrake is only refolded on orbit when its mission life is completed. Once flexible covering is exposed to the atmospheric reentry, it will rigidize, necessitating it to be cut away before the aerobrake can be refolded if the fabric is bonded to the ribs at strategic points.

The unwieldy size of the aerobrake makes EVA removal/replacement impractical. The use of robotics dictates that changeouts of major components of the vehicle be made as simple as possible (no nuts and bolts). This aerobrake interface mechanism would require the robotic arm to produce a clamp-type motion at a single point to the aerobrake interface ring. This motion would effectively actuate all 12 latches simultaneously, leaving the aerobrake free to be pulled from the core structure. This latch release mechanism is illustrated in Figure 2.2.1.7-3. Thus, use of a single robotic arm equipped with a clamp fixture, and an aerobrake configured with a cable actuated latch release mechanism, removal and replacement of the SBOTV aerobrake becomes a routine maintenance task.

In the scenario developed, once the SBOTV has been installed in the cradle carriage and checked out, the payload is moved from its storage area by the MRMS, which in turn hands the payload off to the space crane or a robotic arm. The crane (or arm) places the payload in the payload cradle carriage, and very slowly and carefully, under positive control, the carriage is moved toward the SBOTV until mating is accomplished. After mating, checkout of the payload and the SBOTV is again performed to verify connections and that no damage has occurred.

Once checkout has been completed, the OMV is moved from its storage area by the MRMS, which in turn hands off the OMV to a robotic arm. The arm places the OMV at the aft of the aerobrake allowing mating to occur. An OMV umbilical is mated with the OMV, and the entire vehicle stack is checked out.

A three-fingered configuration for the docking mechanism was selected due to its versatility in mating with the most popular payload interface configurations. It will mate with the MMS three pin design, and adapt to most sizes of circular payload interface rings. Its adjustment and clamp action is driven by three acme threaded shafts powered from a single bevel gear, producing the action of the jaws of a chuck. For docking OTV/OMV or OTV/MMS, the end of the fingers would have conical recesses, whereas for circular interface rings, a straight V recess across could be employed. Either configuration produces a semi-soft dock. The deployable/retractable docking pin design is shown in Figure 2.2.1.7-4.

Three of these deployable/retractable docking pins, mounted within the rigidized portion of the aerobrake, would be evenly spaced producing an MMS configuration. The end of the pin would be the interface of OTV/OTV, while the OMV interface would be made by retracting the pin halfway down its length.

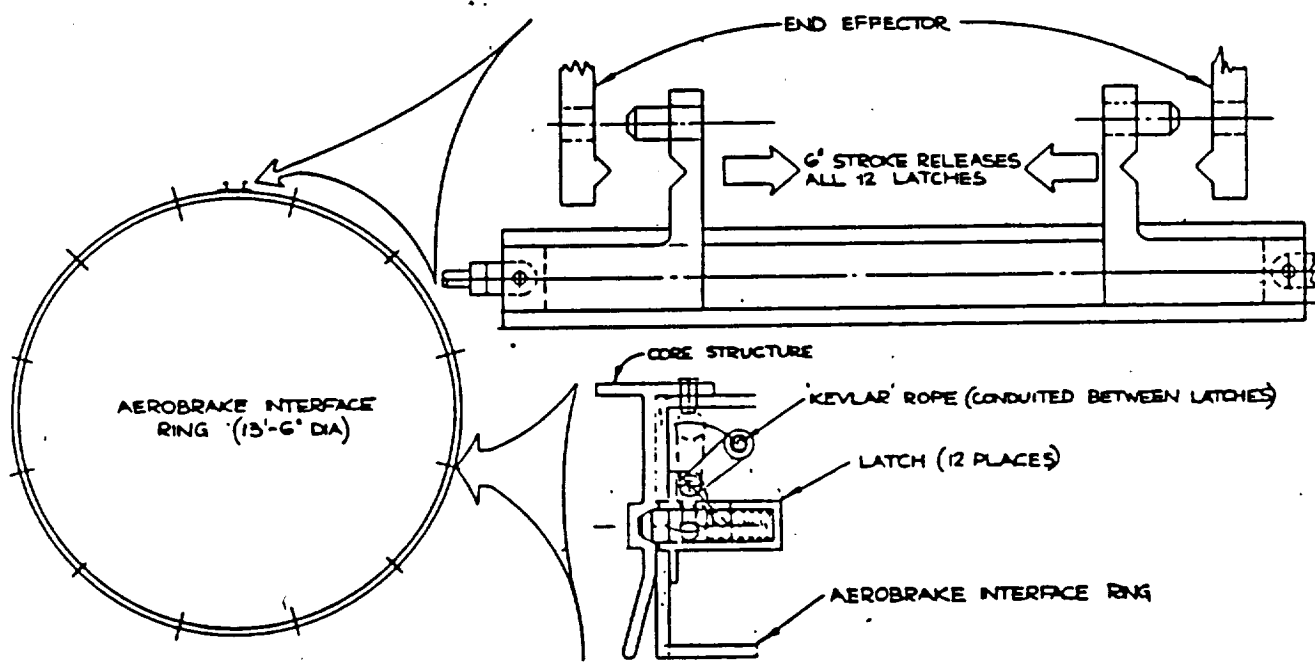


Figure 2.2.1.7-3 Aerobrake Ring Interface Mechanism for On-Orbit Changeout

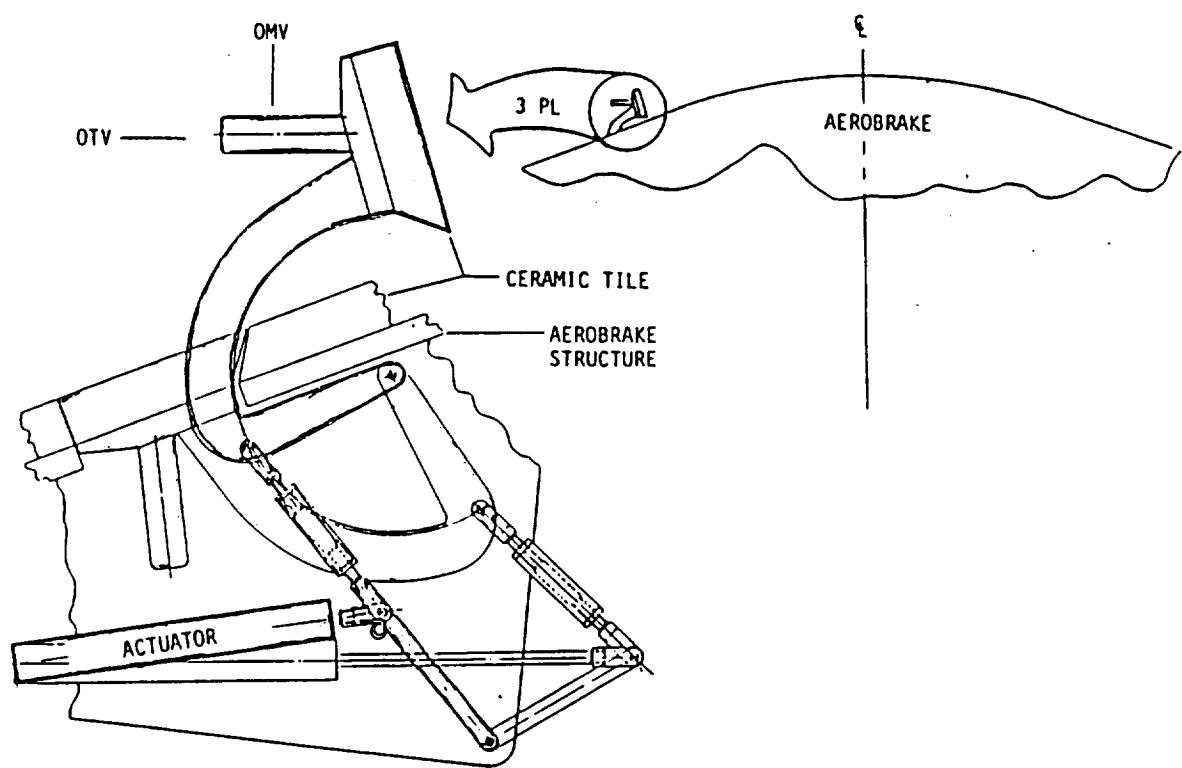


Figure 2.2.1.7-4 SBOTV Aerobrake Deployment/Retractable Interface Mechanism

2.2.2 Definition of Selected Aeroassist Concept

With the selection of an 0.12 L/D aerobrake for the OTV aeroassist device the following section describes the design approach, aerodynamic and thermodynamic environments, TPS selection, and sizing of the rigid/flexible TPS low L/D aerobrake.

2.2.2.1 Design Philosophy and Concept Overview

Table 2.2.2.1-1 outlines the philosophy used to establish a feasible aerobrake design. The major points incorporate inherently flight proven approaches. We have tried to make maximum use of our ground and flight test experience so predictable airloads and heat fluxes can be made. This allows optimization of TPS and structural weights and facilitates vehicle design. An inherently stable aeroshell with minimum moving parts is desired to minimize control authority requirements. Use of an aerodynamically stable brake in conjunction with a compact stage provides margin for a variety of payloads. In addition, a single, standardized brake is desired that has built-in growth and flexibility to minimize DDTE and block changes. Finally, the aerobrake must not only be compatible with the ACC for ground-based operations, but also provide heritage for the space-based manned OTV. Space-basing design considerations include delivery, installation on orbit as a single, fully assembled unit, and OMV interfacing with the minimal EVA requirements.

Table 2.2.2.1-1 Aerobrake Design Philosophy

1. INHERENTLY CONSERVATIVE DESIGN
 - o MAXIMIZE OUR GROUND AND FLIGHT TEST EXPERIENCE
 - o USE PROVEN TECHNOLOGY (STS, APOLLO, GEMINI, VIKING) FOR DOORS, RCS, ETC.
 - o STANDARDIZATION-PROVIDE GROWTH, FLEXIBILITY WITH ONE BRAKE
 - o MINIMIZE MOVING PARTS
 - o ASSURE DERATING OF MATERIALS

2. MINIMIZE AEROHEATING ENVIRONMENT
 - o DEPLOYABLE PORTION OF AEROBRAKE MUST BE ABLE TO WITHSTAND PREDICTED HEAT LOAD
 - o KEEP INSULATION WEIGHT TO A MINIMUM

3. HAVE PREDICTABLE AIRLOADS FOR STRUCTURAL WEIGHT OPTIMIZATION AND TO FACILITATE STRUCTURAL DESIGN
 - o LARGE DATA BASE FROM VIKING FOR 70° AEROSHELL
 - o RECENT EXPERIMENTAL DATA AVAILABLE ON OTHER SHAPES (VOIR)

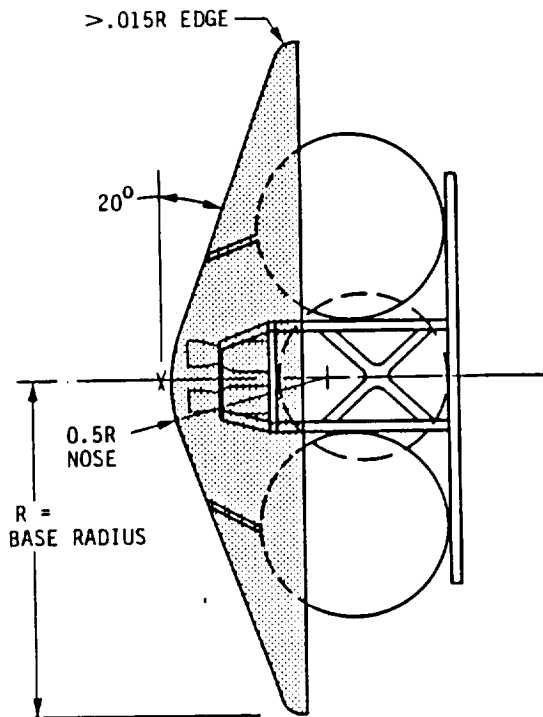
4. AERODYNAMICALLY STABLE
 - o MINIMIZE CONTROL AUTHORITY REQUIREMENTS
 - o MINIMIZE DEPTH OF BRAKE TO KEEP VEHICLE COMPACT
 - o PROVIDE MARGIN FOR VARIETY OF PAYLOADS

Table 2.2.2.1-1 Aerobrake Design Philosophy (cont.)

5. ACC STORAGE
 - o 70° AEROSHELL CONCEPT IS COMPATIBLE WITH ACC GEOMETRY
 - o LAUNCH LOADS CARRIED BY ACC SUPPORT INSTEAD OF OTV
 - o USE MINIMUM FOLDS, NO SHARP EDGES FOR FLEXIBLE TPS
 - o ADAPTABLE TO PAYLOAD BAY CONCEPTS
6. MINIMIZE AEROHEATING EFFECTS ON OTV COMPONENTS
 - o LARGE DATA BASE FROM VOIR STUDY
 - o PROVIDE PROTECTION FOR MAJOR COMPONENTS
 - o COMPONENT HEATING ANALYSIS MUST CONSIDER RADIATION HEATING FROM AEROBRAKING, AS WELL AS BASE CONVECTIVE HEATING
7. ADAPTABLE TO SPACE-BASING
 - o SUBSYSTEM DELIVERY IN ORBITER PAYLOAD BAY
 - o UNITIZED ASSEMBLY
 - o REMOVAL AND REPLACEMENT OF AEROBRAKE
 - o COMPATIBLE WITH CHECKOUT AND MAINTENANCE TASKS OF OTV SPACE-BASED OPERATIONS
 - o MINIMIZE USE OF EVA
8. MISSION NOT LOST IF OUTER PORTION OF AEROBRAKE FAILS
 - o MULTIPLE PASS RETURN REQUIRED TO STAY WITHIN LOAD LIMITS USING HARD AEROBRAKE ONLY

Our selected aerobrake for OTV is a 70 degree conical lifting brake, which is a constant drag concept with small lift capability that provides the maneuverability to compensate for atmospheric dispersions. The configuration, shown in Figure 2.2.2.1-1, is based on the Viking aeroshell shape and has a nose radius equal to half its base radius, and an edge radius greater than 0.015 the base radius.

Major features of this aeroshell concept include inherent stability compared to other forecone angles and simple design and passive structure. Its geometry incorporates asymmetry which overcomes the rolling instability found in symmetric shapes; lateral distribution of fuel tanks provides improved base heating protection and additional payload length capability.



RECENT PROGRAMS, STUDIES AND TEST DATA INDICATE:

- THE 70° AEROBRAKE ANGLE APPEARS TO BE THE OPTIMUM FORE CONE ANGLE FOR THIS TYPE OF AEROBRAKING VEHICLE.
- 70° FOREBODY GIVES GOOD INHERENT STABILITY CHARACTERISTICS
- AEROBRAKE ALLOWS LATERAL DISTRIBUTION OF FUEL TANKS, PROVIDING PROTECTION TO BASE COMPONENTS (PAYLOADS) FROM THE AERODYNAMIC HEATING
- BRAKE CONFIGURATION'S CENTER OF PRESSURE LIES ONE BRAKE DIAMETER AFT, GIVING LONGITUDINAL STABILITY TO PAYLOADS OVER 24 FT LONG (BASED ON MID C.G. LOCALS)
- PASSIVE AEROBRAKE STRUCTURE INCREASES MISSION SUCCESS

Figure 2.2.2.1-1 Aerobrake Configuration and Characteristics

Figure 2.2.2.1-2 outlines the primary design features of the space-based OTV aerobrake concept. The nominally 70 degree cone is designed to alleviate high edge-heating effects by the proper selection of edge radius and flight trim angle. The brake is sized to prevent hot-gas impingement on the payload. The heatshield support structure is made of ribs and support struts to the interface ring, which allows mating to the body using a simple attach ring. The heatshield is made in two sections. For the outer section, flexible ceramic blankets are used. For the inner nose region, rigid, low-density ceramic tiles are used. The aerobrake fabric and composite supporting structure frame folds compactly for transfer to orbit fully assembled and is erected and checked at the Space Station prior to OTV launch. The aerobrake system is passive throughout the flight, reusable for five or more flights and is never folded after the STS flight to LEO. The central rigid aerobrake section includes fold-away doors to allow engine nozzle extension through the aerobrake for ascent. The nozzles retract forward and the doors are closed prior to the aerodynamic reentry maneuvers. Ground-based cryogenic vehicles utilize a similar aerobrake design.

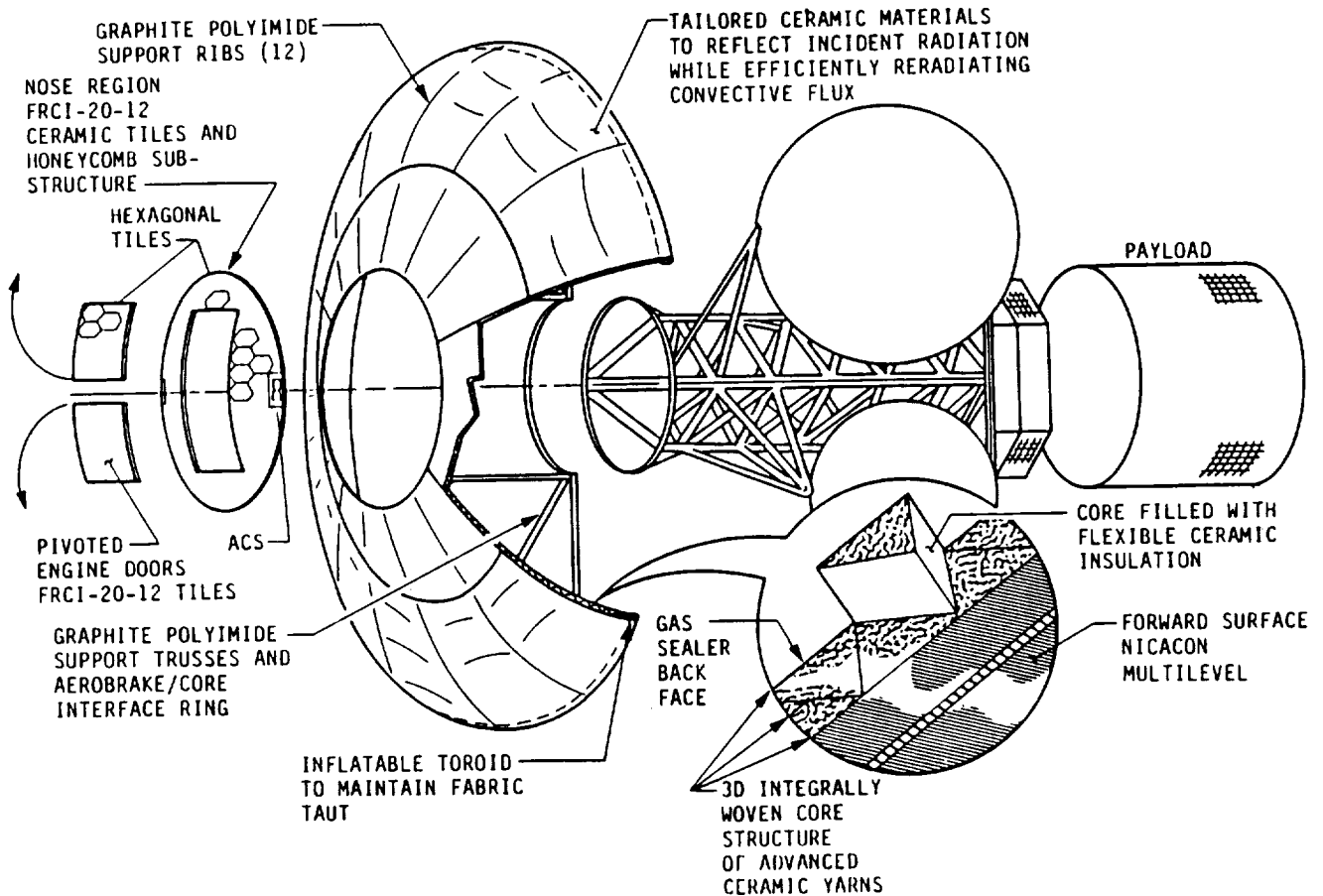


Figure 2.2.2.1-2 OTV Rigid / Flex TPS Aerobrake

Shown in Figure 2.2.2.1-3 is the flexible ceramic insulation known as Tailorable Advanced Blanket Insulation (TABI), that is used for the outer portion of the aeroshield. The TABI design uses a 0.026 inch thick Nicalon (a silicon carbide fiber cloth) for the aeroshell forward surface and was selected for its high heat flux capability. The same material, but thinner gauge (0.14 inch), forms the interior woven cell structure. The back side of the blanket utilizes Nextel cloth, 0.014 inch thick for its structural strength. A RTV silicone coating (0.010 inch) acts as a sealer and prevents hot gas flow through the composite fabric structure. The interior cell structure is filled with an advanced ceramic felt creating an internally woven insulation blanket. The blanket is attached directly to the support ribs making the blanket an integral part of the aerobrake's structural strength (which is based on the inherent structural integrity of umbrella designs). The substructure is composed of graphite polyimide support ribs shaped to provide the necessary strength and rigidity to minimize deflection during the braking pulse. The thickness of the TABI blanket is sized for the peak heat load it will experience (which is at the rigid/flex interface) and has a uniform thickness radially and circumferentially.

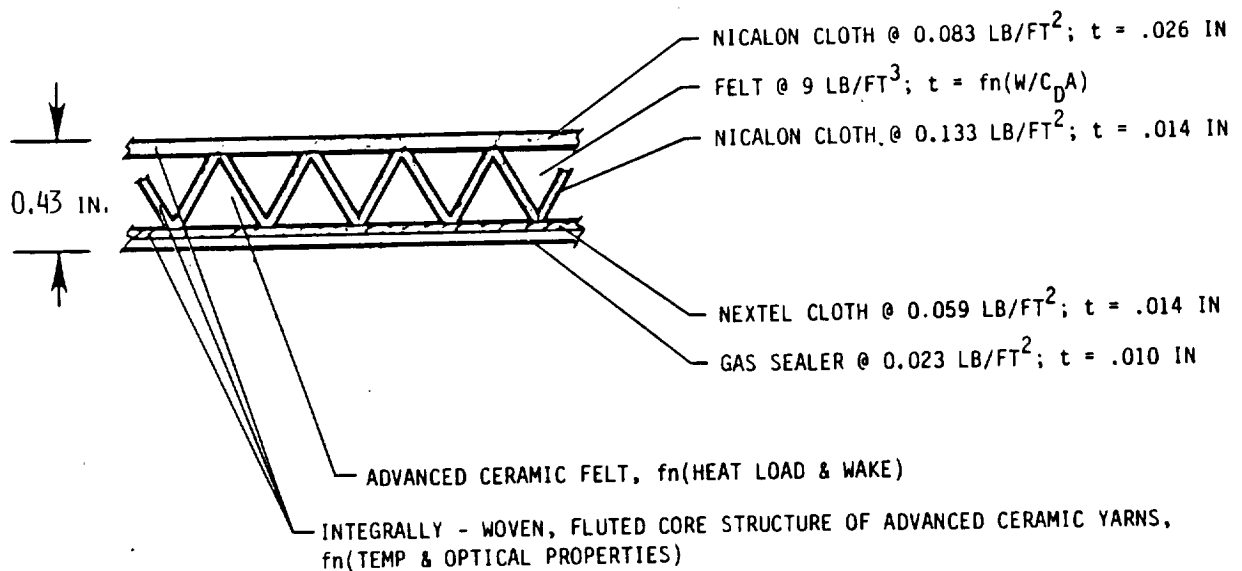


Figure 2.2.2.1-3 Flexible TPS Selection and Construction - Tailorable Advanced Blanket Insulation (TABI)

The nose region and retractable engine cover doors utilize a rigid surface tile. A surface coating with appropriate optical properties, such as HRSI, 0.01 inch thick, is applied over the FRCI-20-12 tiles which are approximately 0.5 inches thick and hexagonal in shape. The hexagonal tile arrangement has several advantages over predecessors by utilizing a universal, and interchangeable tile component. From a thermal analysis standpoint, polygonal tiles will minimize the gap running length, decreasing potential thermal enhancement associated with gap heating. RTV silicone adhesive bonds the ceramic tiles to the center aeroshell honeycomb substrate. Two 0.01 inch graphite polyimide skins are adhesively bonded to the 0.25 inch high temperature hexagonal celled honeycomb to complete the shell structure (See Figure 2.2.2.1-4).

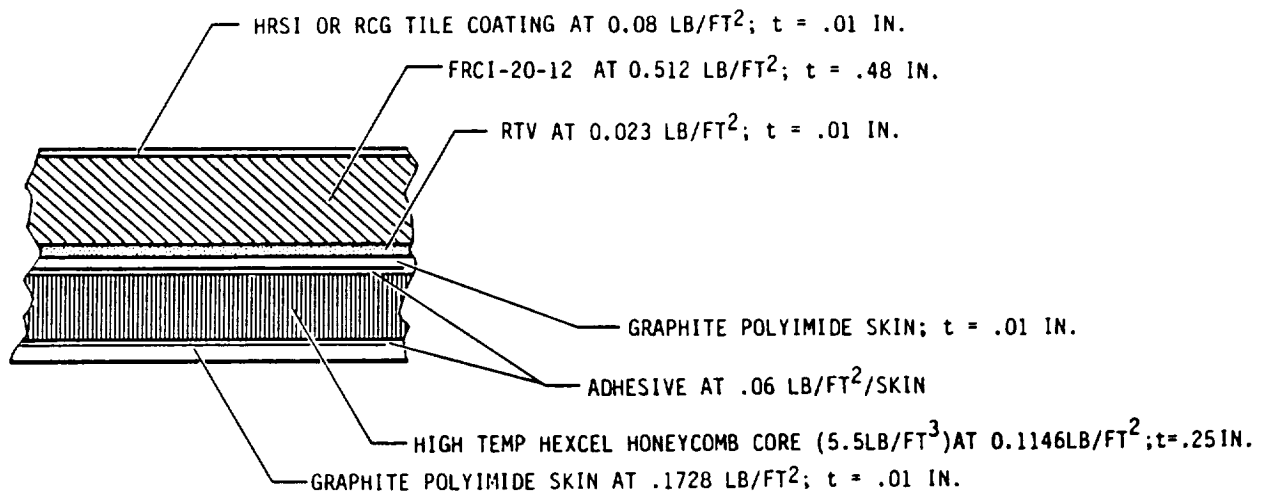


Figure 2.2.2.1-4 Nose Region and Engine Doors TPS Detail

The OTV aerobrake design calls for a movable engine cover to facilitate engine nozzle retraction after the descent. To accomplish this movement, a rigid engine cover, as opposed to a flexible skin, was designed to allow engine nozzle extension and gimbaling during ascent and thermal protection during descent. The engine cover is lifted forward and rotated 180° from the reentry position and retained during the main engine powered flight phase. The single mechanism for each door provides reusable lifting, rotating and retention for this critical flight design element. The engine cover maintains a leakproof aerobrake by use of door seals and a positioning mechanism as seen in Figure 2.2.2.1-5.

The aeroassist concept is composed of two similar brakes, one for ground-based OTV which provides heritage and evolution to the space-based OTV. Both brakes use the same design approach, the only major differences being: their diameters; and that one is stowed in the ACC attached to the vehicle and the other is transported in the payload bay and mated to the vehicle on orbit. There is currently no way to launch a piece of hardware to orbit measuring 44 feet in diameter. Our design, shown in Figure 2.2.2.1-6, enables the aerobrake to be folded into a configuration that does not exceed 14' 6" diameter, and requires a minimum cargo bay length (under 10 feet). The structure consists of an interface ring approximately 13 feet in diameter around which are spaced 12 trusses. Each truss consists of a rib supported by two struts, which when folding, requires provision be made for the fold of exterior flexible material. A fold radius equal to four times the TPS thickness was used as a design requirement. The trusses are unfolded and connected to the interface ring at the Space Station, where then the assembled unit is mated to the attach ring of the core structure.

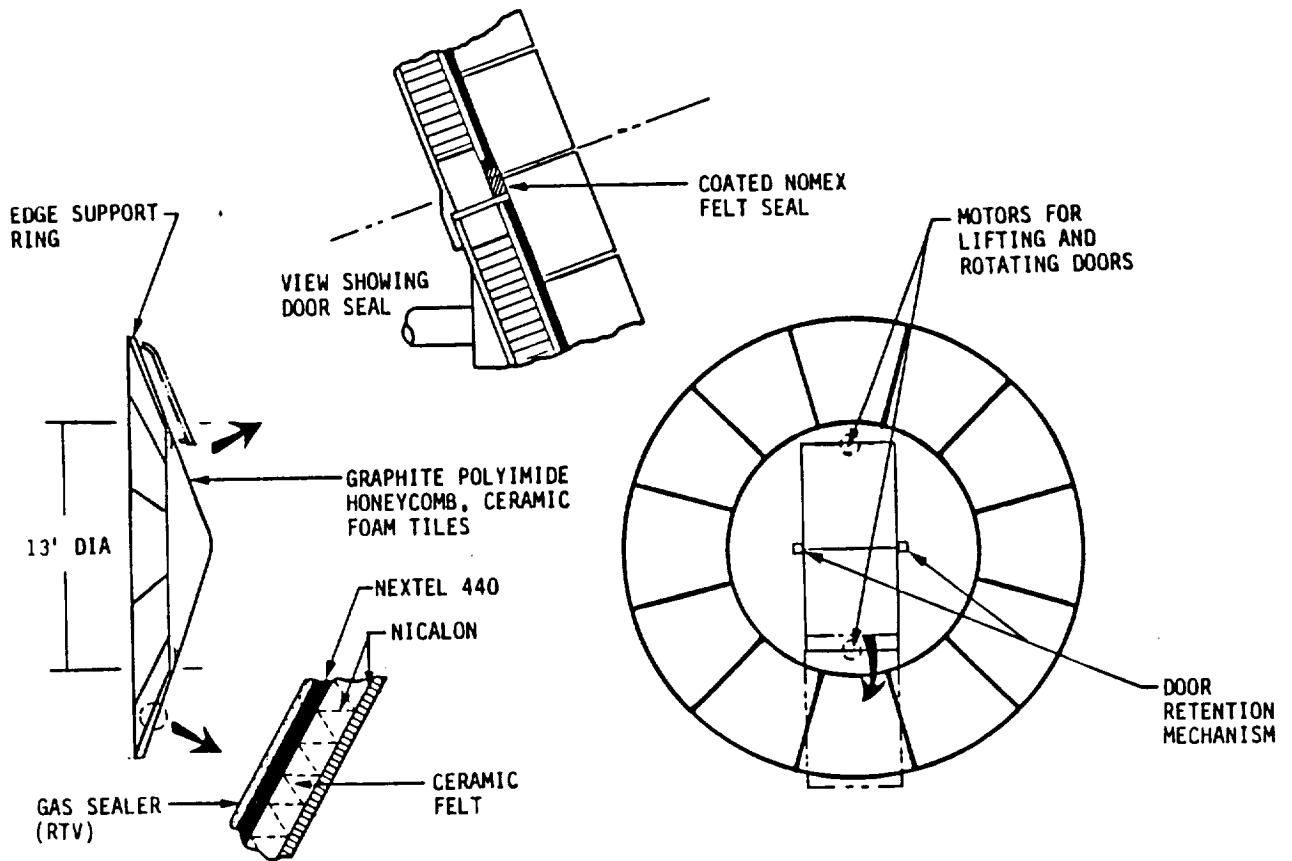


Figure 2.2.2.1-5 Aerobrake TPS and Engine Cover Mechanism

Figure 2.2.2.1-7 illustrates the interface and sealing design concepts of the ground-based vehicle for ACC launch stowage of the fabric aerobrake. Diameter limitations in both the orbiter bay and the aft cargo carrier require the flexible outer sections to be folded and stowed umbrella-like during the orbiter launch to low earth orbit. During brake deployment, the rigid and flexible surface interface to obtain a continuous TPS aerobrake outer surface as shown. The fabric brake can be stowed without forming creases or small radius folds in the TABI. This concept prevents stretching of the TABI cover cloth when the brake is folded up or fully deployed. The TABI is attached to the ribs using a silicon adhesive.

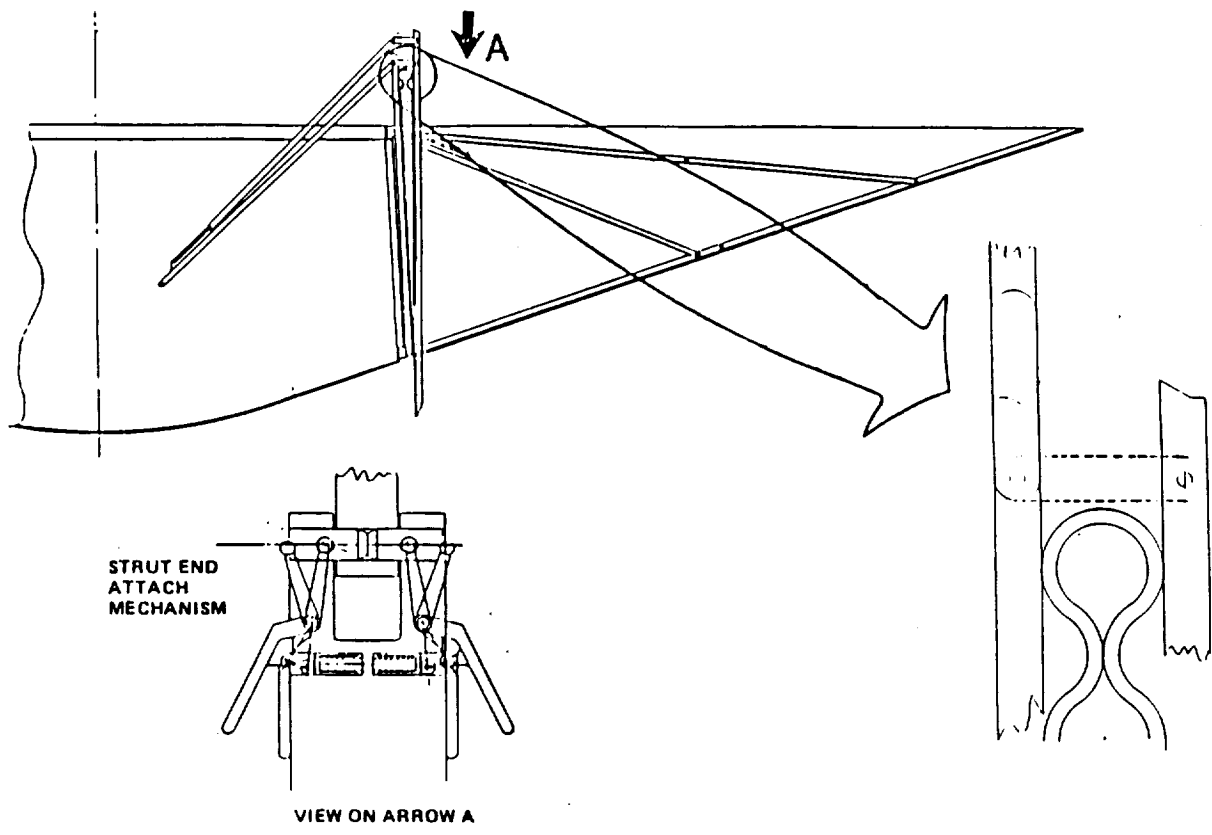


Figure 2.2.2.1-6 Space Based Folding Aerobrace

Our final vehicle aerobrace baseline design is shown in Figure 2.2.2.1-8. A detailed weight breakdown for this aerobrace system and our ground-based brake is presented in Table 2.2.2.1-2.

1990 technology estimates of the maximum operating heating rate of flexible advanced ceramic blankets is 30 BTU/ft.²-sec. Figure 2.2.2.1-9 illustrates the growth margin built into current space-based 44 foot diameter aerobrace. With the 7,500 lb. manned capsule, the return vehicle has a ballistic coefficient of 6.0 which corresponds to a peak heat flux to the flexible surface insulation (FSI) of 21.4 BTU/ft.²-sec. or a heat flux margin of 29%.

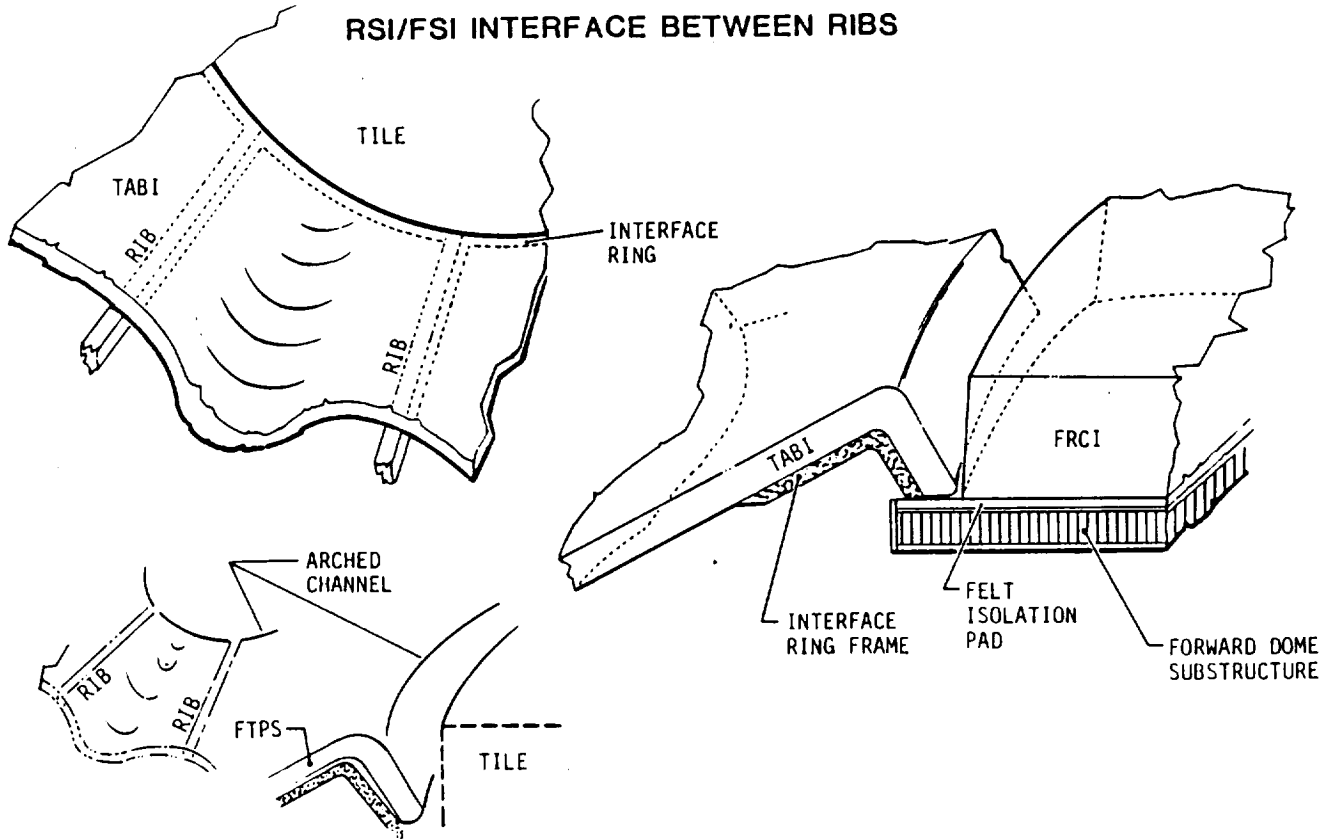


Figure 2.2.2.1-7 Ground Based Aerobrake Deployment

$W/C_D A = 6.0$
 $D_B = 44 \text{ FT}$
 $R_N = 11 \text{ FT}$
 $L/D = 0.12$
 $\alpha = 7.5^\circ$

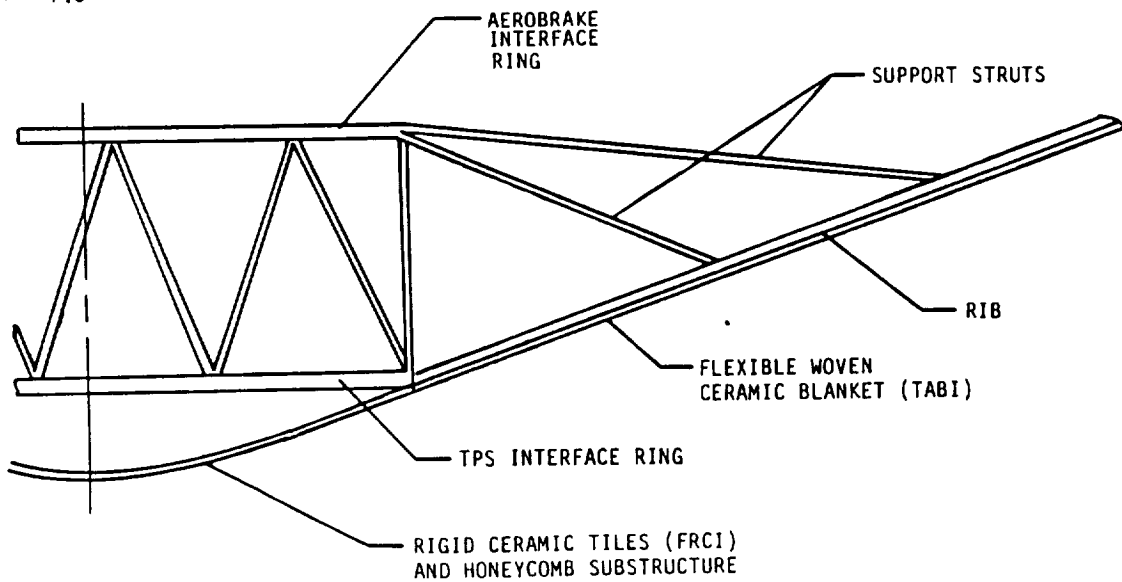


Figure 2.2.2.1-8 Aerobrake Design Detail
166

GROUND-BASED

SPACE-BASED

FLEXIBLE TPS	568	FLEXIBLE TPS	767
RIGID CENTER TPS	177	RIGID TPS & HONEYCOMB STRUC.	174
DOOR & MECHANISM	101	DOOR & MECHANISM	97
RIBS & STRUTS	<u>302</u>	SUBSTRUCTURE	
GBOTV AEROBRAKE ASSEMBLY	1148	INTERFACE RING	217
		RADIAL BEAMS	120
		STRUTS & SUPPORTS	220
		MISC. ATTACH HDW.	<u>72</u>
		SBOTV AEROBRAKE ASSEMBLY	1667

Table 2.2.2.1-2 Aerobrake Weights

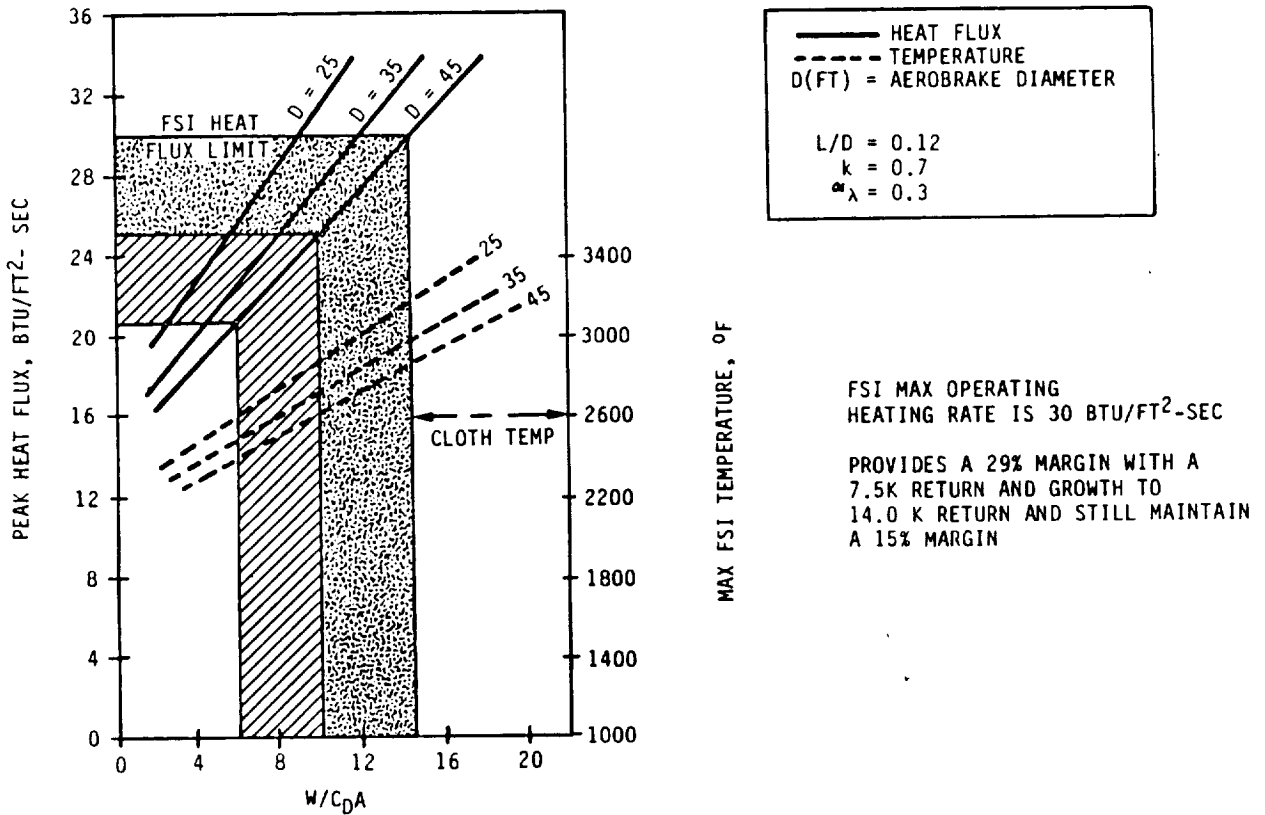


Figure 2.2.2.1-9 Aerobrake Heating Design Margin

Growth to the 14,000 lb. manned round trip mission raises the ballistic coefficient to 9.9. This results in a peak FSI heat flux of 25.6 BTU/ft.²-sec. which provides a heat flux (or future growth) margin of 15%. The net result from these heating margins should increase the FSI reuse life.

A NASTRAN analysis shown in Figure 2.2.2.1-10 indicates the aerobrake has a rib deflection of 4.1 inches when returning a 7.5K payload.

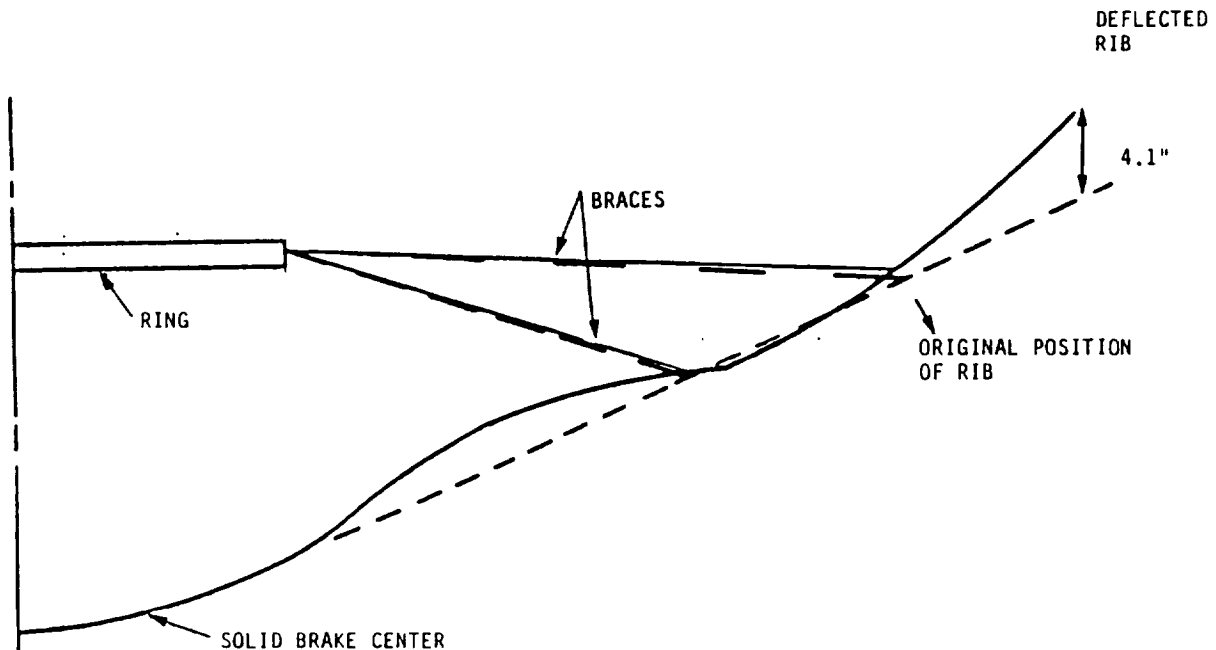


Figure 2.2.2.1-10 Space Based Aerobrake Rib Refection

2.2.2.2 Aerodynamic Characteristics

Aerodynamic flight of the OTV will take place near the edge of the atmosphere at high hypersonic velocities. Due to the rarefaction of the air at high altitudes, and the effects of heat and viscosity with chemically relaxed molecules, the flow field around the vehicle and the forces acting on the vehicle vary significantly from those encountered in continuum fluid flow. The continuum regime includes the lower three-fourths or so of the atmosphere or altitudes below 356,000 feet.

For the free molecular flow regime (altitudes above 600,000 feet), it is necessary to consider the air molecules impacting the forward vehicle surface without affecting each other, and the reemission of the molecules from the surface. Transition to this regime begins with viscous effects dominating, (slip flow) then a disappearance of the boundary layer and a thickening of the shock wave. Pressure modification by chemical nonequilibrium viscous effects

in the slip regime results in a degradation in L/D, and has an associated effect on C_M . This, and the C_p shift with flow regimes, affect the vehicle's attitude control system and must be considered in analyzing stability and control requirements.

Aerocoefficients from free molecular to continuum flow are required for accurate trajectory simulations and design of the guidance and control system. These flow regimes are outlined below.

The aerodynamic behavior of the Viking shaped entry vehicle is the result of its forebody with a blunt-nosed 70 degree half angle cone and a ratio of nose radius to base radius of 0.5. An extensive data base of experimental, analytical, and flight data exists which enhances the reliability of the aerodynamic predictions for AOTV configurations based on Viking Lander entry aeroshell shapes.

The aerodynamic characteristics (lift, drag, static and dynamic stability, and trim angle of attack) in the continuum flow regime are outlined in Figure 2.2.2.2-1. Numerous Viking and Venus aerobraking studies (both vehicles utilize a 70 deg - blunt conical aeroshell) enable the aerodynamic performance and degradation in the transitional and free-molecular regimes to be evaluated. In addition, comparison of flight determined drag coefficients with wind tunnel data allows estimates in C_p changes due to nonequilibrium slip flow to be made, reducing trim error predictions to approximately a half of a degree.

- DATA FROM WIND TUNNEL TESTS AND VIKING ENTRY FLIGHT DATA

- TRIM CONDITIONS

$$\alpha = -7.48^\circ$$

$$C_L = 0.1893$$

$$C_D = 1.5781$$

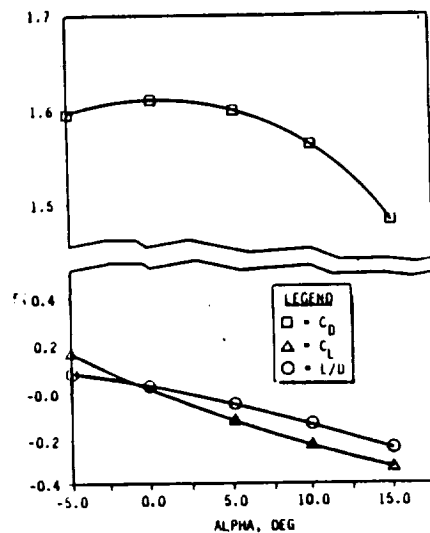
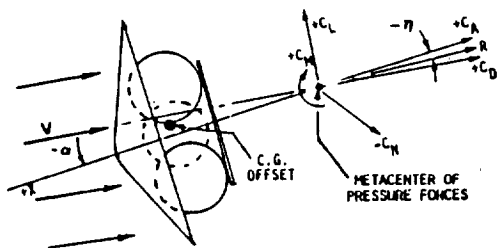
$$L/D = -0.120$$

- STATIC STABILITY CRITERIA

$$C_p = -1.035 D_B$$

$$R = \text{C.G. OFFSET TRIM LINE}$$

$$\eta = \alpha + \tan^{-1} C_L/C_D$$



- GROUND AND FLIGHT DATA PROVIDE ACCURATE CONTINUUM FLOW AEROCHARACTERISTICS
- NOTE HOW FAR AFT THE C.P. IS FOR THE VIKING SHAPED BRAKE

Figure 2.2.2.2-1 Aerocharacteristics vs Angle of Attack

Stable trim is maintained by an offset center-of-gravity location. The offset is selected to provide the desired trim L/D, and thus sets the vehicle's angle of attack. Our earlier studies and programs indicate that this conic configuration exhibited the most reasonable degree of inherent aerodynamic stability and required a minimum amount of attitude control system fuel. In addition, its center of pressure location provides a large longitudinal stability range for payload return.

Free molecule flow calculations were performed to predict the performance of the AOTV at extremely high altitudes. Results of these calculations are presented in Figure 2.2.2.2-2. Past flight data shows that diffuse reflection dominates for space vehicles in this regime, and are the coefficients used in our trajectory simulations.

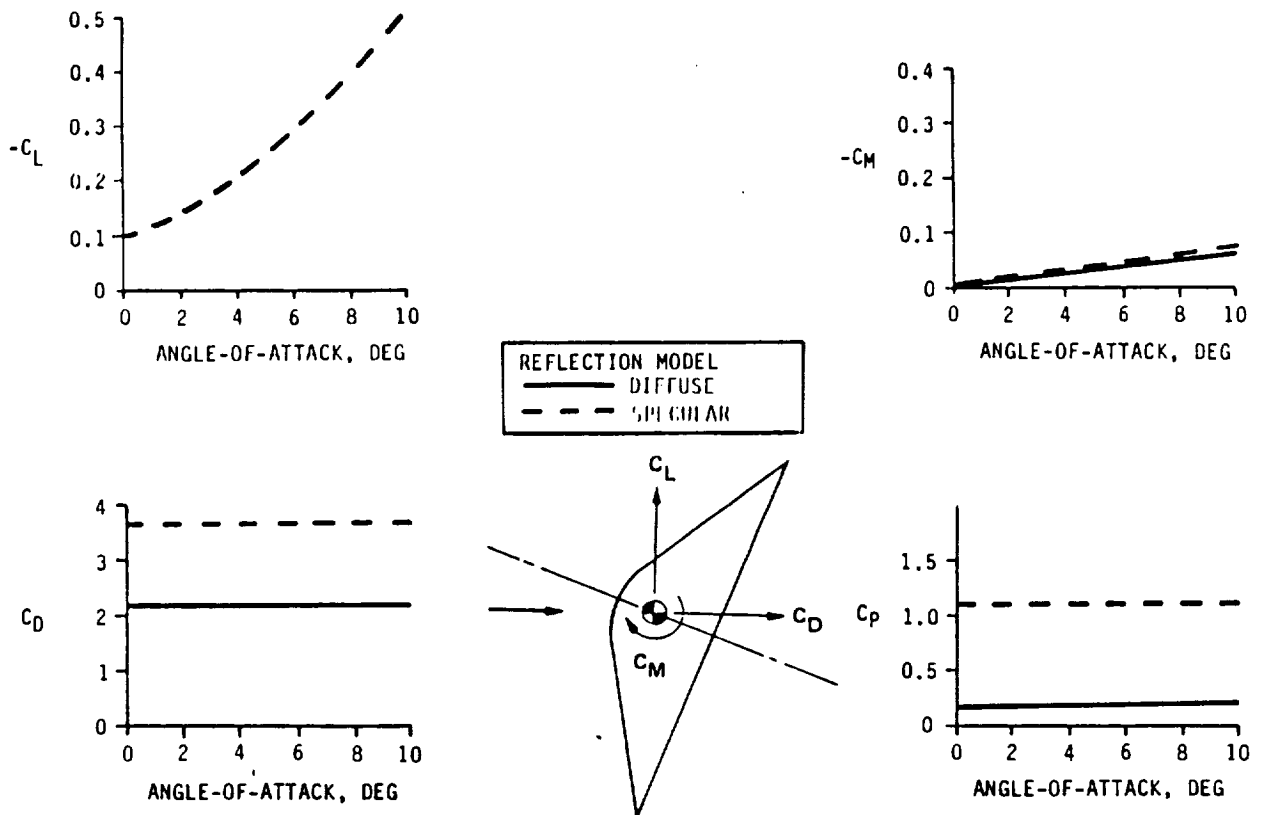
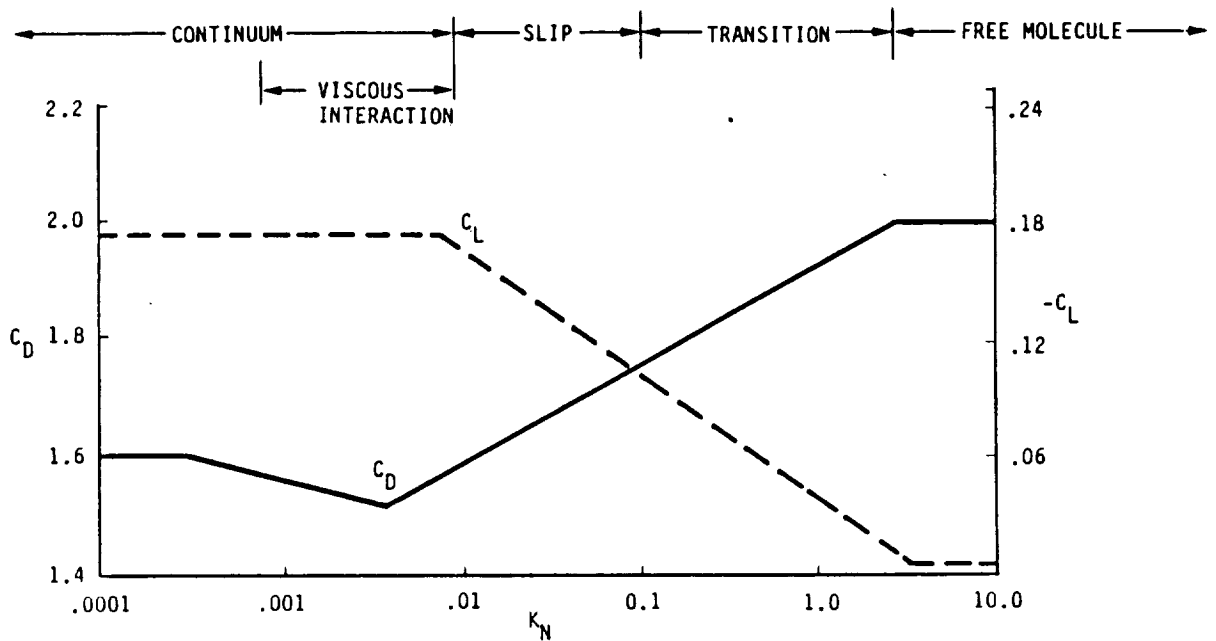


Figure 2.2.2.2-2 Force and Moment Coefficients for Free Molecular Flow

Over the high Reynolds number flight regime, the drag coefficient (C_D) is nearly constant at a value of 1.6. Just below a Reynolds number of 10^5 , a decrease in C_D has been observed, References 2.2.2.2-3. This is due to a transition from equilibrium to nonequilibrium flow in the shock layer. Based on Viking flight data, C_D is reduced to approximately 1.55 at $Re = 10^4$ (wind-tunnel data indicates a decrease in C_D to 1.48). Then as the Reynolds number becomes lower, an increase in C_D occurs as transitional and then free-molecule flow are obtained. A simplified bridging technique for use in trajectory simulations is shown in Figure 2.2.2.2-3.



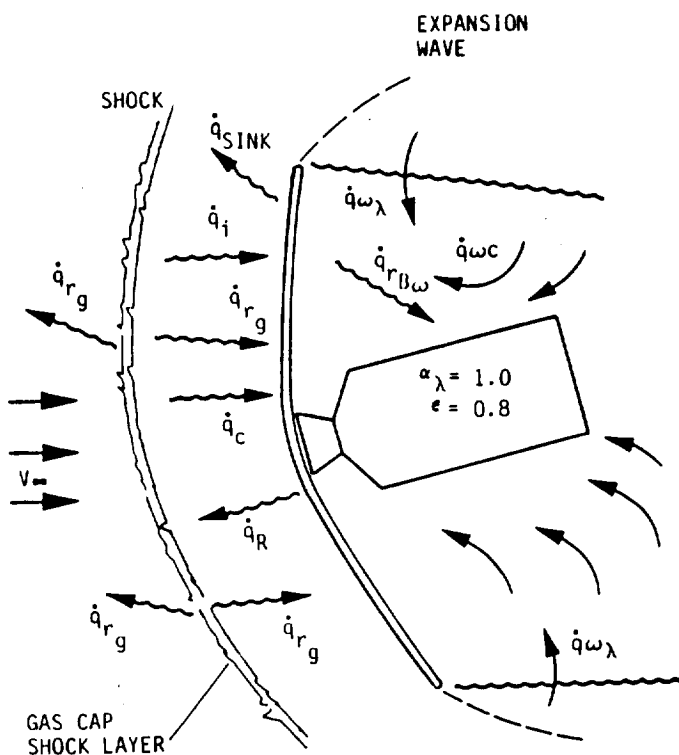
GROUND TEST AND FLIGHT DATA DEFINE THE VISCIOUS-INTERACTION REGION AND L/D DEGRADATION OF THE TRANSITIONAL TO FREE-MOLECULE FLOW REGIMES.

Figure 2.2.2.2-3 Flow Regime Transition Criteria Based on Viking Flight and Wind Tunnel Data

2.2.2.3 Aerothermodynamic Heating and Thermal Protection

The primary emphasis in the following analysis is on aerobraking heat flux calculations, the thermal response of the AOTV to these heat fluxes, and the resulting thickness of the thermal protection system.

A schematic of the thermal analysis model used for definition of the aerobrake heating environment is illustrated in Figure 2.2.2.3-1. The principal contributors to the surface heat flux are identified. The main components of the front face incident surface flux are nonequilibrium radiation and convection.



α_λ = SPECTRAL ABSORPTION COEFFICIENT (0.3)

K = CATALYTICITY FACTOR (0.7)

\dot{q}_{r_g} = NONEQUILIBRIUM RADIATION EMISSION

\dot{q}_c = CONVECTIVE HEAT FLUX

\dot{q}_{ij} = INCIDENT SURFACE ENERGY
($j = F = \text{FACE}$, $j = B = \text{BACK}$)

\dot{q}_R = REFLECTED INCIDENT RADIATION

\dot{q}_{r_B} = AEROBRAKE BACKWALL RADIATION

\dot{q}_{w_λ} = WAKE RADIATIVE EMISSION = $0.06 \dot{q}_{r_g}$

\dot{q}_{w_c} = RECIRCULATIVE CONVECTIVE BASE HEATING

$$\dot{q}_{i_{\max}} = \dot{q}_c + \dot{q}_{r_g}$$

$$\dot{q}_{i_F} = K\dot{q}_c + \alpha_\lambda \dot{q}_{r_g}$$

$$\dot{q}_R = (1 - \alpha_\lambda) \dot{q}_{r_g}$$

$$\dot{q}_{r_B} = \sigma \epsilon F (T_B^4 - T_{\text{OTV}}^4) + \sigma \epsilon (T_B^4 - T_W^4)$$

$$T_W = (\alpha_g \dot{q}_{w_\lambda} / \epsilon_B \sigma)^{.25}$$

$$\dot{q}_{i_B} = \dot{q}_{w_\lambda} + \dot{q}_{w_c}$$

Figure 2.2.2.3-1 Aerobrake Analytical Heating Model

Much of this incident heat flux is reflected or reemitted due to the properties of the selected advance ceramic cover cloth. The analysis uses an aero-surface spectral absorption coefficient and a finite rate surface catalytic factor of 0.3 and 0.7, respectively.

The back surface of the brake and vehicle core are subjected to radiation emission from the wake flow gasses and convective base heating. Wake radiation intensities are based on References 2.2.2.3-5 and -6. Wake recirculation heat fluxes are based on the work presented in Reference 2.2.2.3-7

In the analysis, the brake back surface was also allowed to radiate to the vehicle core and the recirculating base flow. A radiation equilibrium temperature for the recirculating gas is based on the assumption that for a sufficiently thick aerobrake, the gas will follow the wake flux (w) and its radiation absorption ability ($g = 0.2$). In addition, the local gas temperature will be altered somewhat by the presence of the brake structure (A). This approach of back wall radiation to the base flow gas is conservative compared to radiating to deep space.

Computer code printouts of the several heat transfer models used in the analysis are shown in Figure 2.2.2.3-2. The Q-felt and FRCI aerobrake thickness values were varied in order to perform the flexible and rigid TPS sizing analysis. All other values were held constant. TPS thickness requirements were based on maintaining the back wall RTV sealer below 600°F.

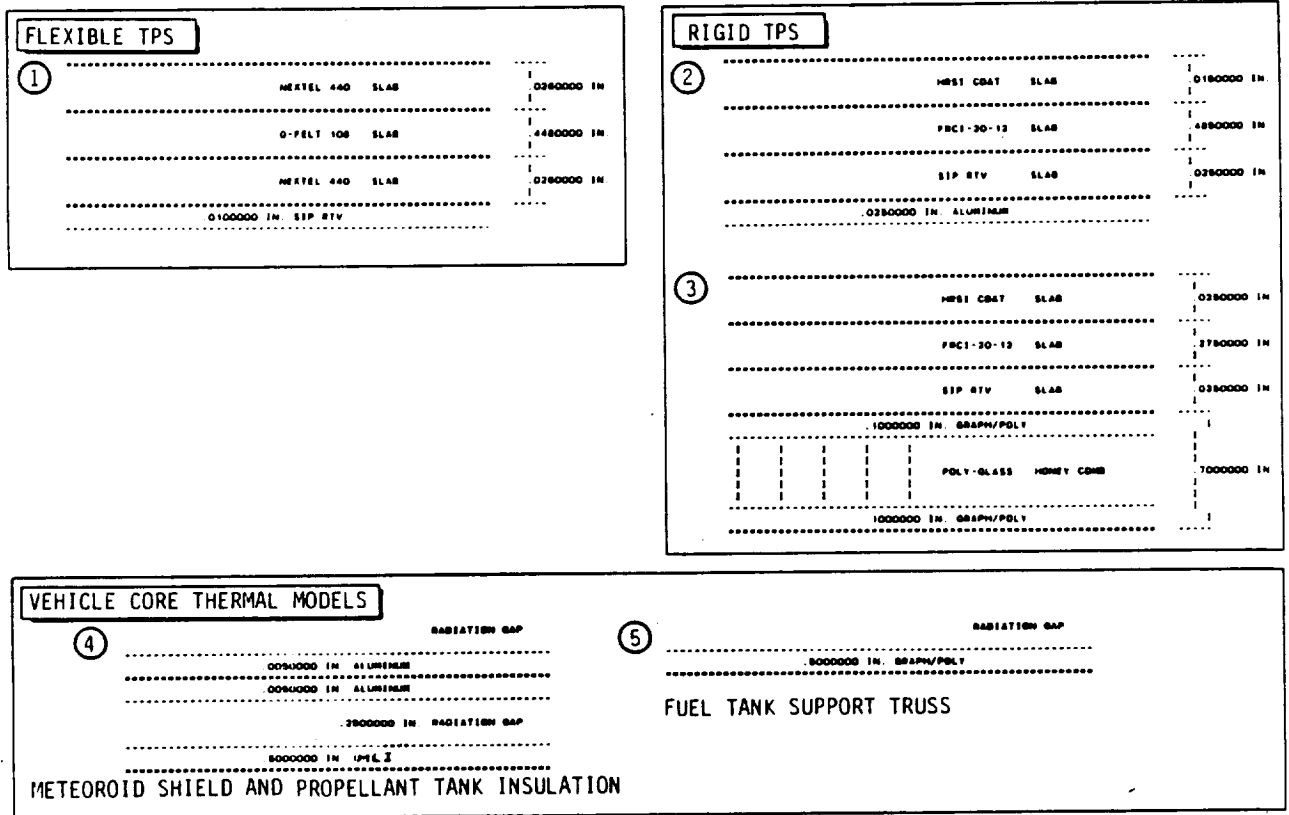


Figure 2.2.2.3-2 Aerobrake TPS Heat Transfer Models

ORIGINAL PAGE IS
OF POOR QUALITY

The vehicle core thermal models were used to determine meteoroid shield and propellant tank insulation candidate materials, thicknesses and standoff distances. Similar models were utilized in the analysis to confirm the design of graphite composite truss members. Thermophysical properties of the aerobrake TPS materials are listed in Tables 2.2.1.3-1 through 2.2.1.3-4.

Experimental laminar boundary-layer heat-transfer-rate data are presented in Figure 2.2.2.3-3 for the Viking Mars Entry vehicle. The heating distribution of the aeroshell is shown from two different wind tunnel tests for comparison. The open circle testing data was conducted at AEDC-VKF Tunnel F at a Mach number of 16 and Reynolds number of 0.5×10^6 , based on a 19.3 inch model diameter, Reference 8. The solid circle data is from tests at the NASA LaRC Mach-8 Variably Density Hypersonic Tunnel with a Reynolds number of 1.7×10^6 , based on a model diameter of 4 inches, Reference 2.2-9. Using the stagnation heat-transfer rate for a hemisphere of the same nose radius as the aerobrake as a reference value, the stagnation point heat-transfer rates on the aerobrake front face are found.

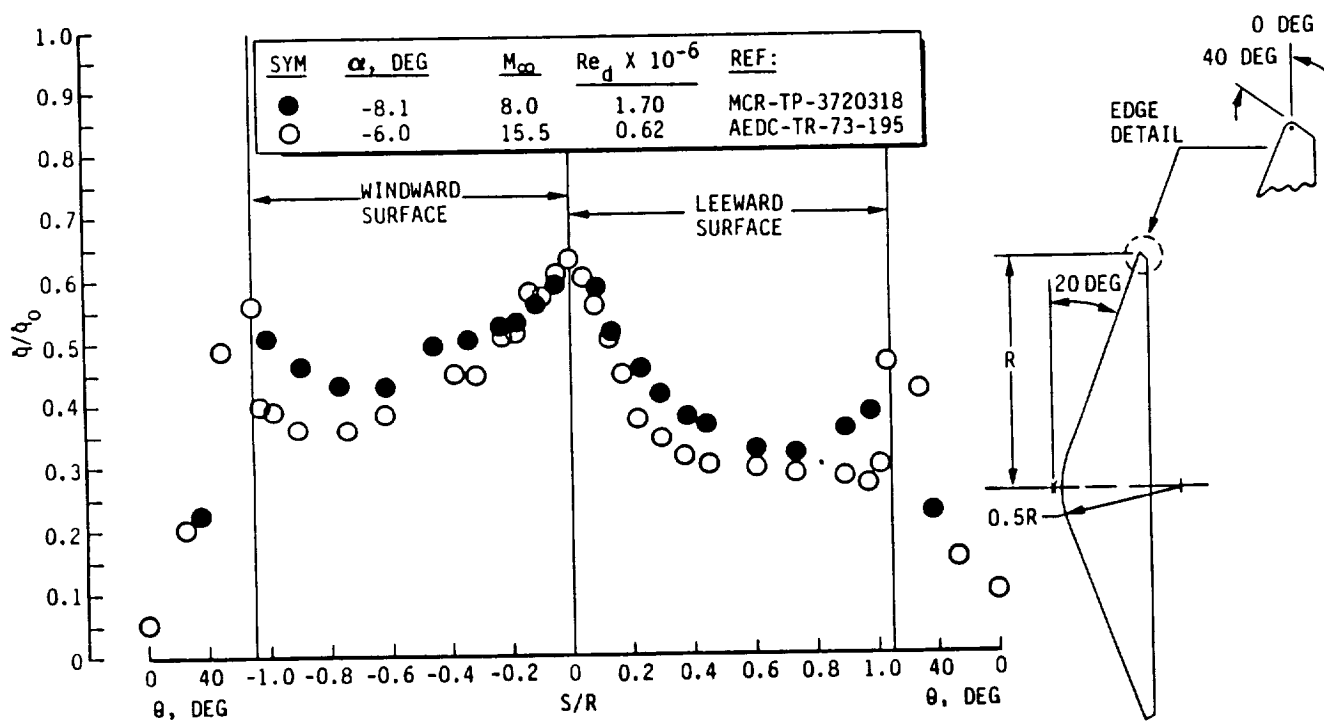


Figure 2.2.2.3-3 Heating Rate Distribution on Models of the NASA-MMC Viking Mars Entry Aeroshell

Incident convective heating rates are calculated based on the boundary layer method of Fay and Riddell for equilibrium - continuum flow and a Lewis Number of 1.4. A modified boundary layer flow method is used to calculate subsonic flow heating by a modification of the velocity gradient. The calculation is made for a hemisphere equal to the aerobrake nose radius with the appropriate heat amplification factors, q/q_0 and h_{rib} , applied.

For the thermal analysis of the rigid tiles, the stagnation point heat flux ($S/R=0$) and heat factor, q/q_0 , of 065 (from Figure 2.2.2.3-3) was used. The calculation for the convective heat flux to the flexible blanket is based on the nose radius heat flux multiplied by the 7.5° entry angle heat distribution factor at the rigid/flex interface point. Using Figure 2.2.2.3-3 and the TPS interface S/R value of 0.3, q/q_0 equals 0.5. An additional heat amplification factor, $h_{rib} = 1.15$, is applied to the flux to account for potential rib protrusion effects. The boundary layer thinning on the ribs and boundary layer growth on the sagging part of the skin makes it difficult to predict the detailed nature of the heat transfer variation. The experimental data of Reference 2.2-10, which predicts the effects of the deviation of the flow from that over a spherical segment, is used to predict heat transfer increases resulting from the protruding rib contours. The net incident heat flux to the TPS is the resultant sum of the above convective fluxes and the nonequilibrium radiative heat flux value.

The magnitude of the convective heat flux depends on brake size, reentry weight, and the flight path through the aeropass corridor. Flight through the bottom of the corridor produces maximum heat rates and surface temperature, but has a shorter flight duration in the atmosphere. A top of the corridor trajectory results in the highest total heat load and actually sizes the TPS because the higher atmospheric pass must be of longer duration to achieve the deceleration for the orbital change maneuver. Shock-layer radiation from chemically relaxing air is the dominant radiation source. Current analytical calculations of the dissociating and ionizing nonequilibrium flow behind the shock predict a peak nonequilibrium radiative heat flux of 20 BTU/ft² sec (References 2.2-11, -12, and -13) and a transient heat flux history that follows the convective flux histories. The nonequilibrium radiation heat flux is applied to the entire aerobrake surface. This is a conservative assumption since the radiation component diminishes radially due to shock curvature.

It should be noted that the above heat flux values are maximums and do not take into account surface thermal/optical characteristics. Applying more realistic surface catalytic ($K=0.7$) and optical coefficients ($\epsilon = 0.3$) to the convective and radiative components, respectively, defines the net heating environment for the aerobrake. Figure 2.2.2.3-4 shows the resulting design environment for a 44 foot aerobrake with an L/D of 0.12 at two different ballistic coefficients, $W/C_D A = 3.3$ and 9.0.

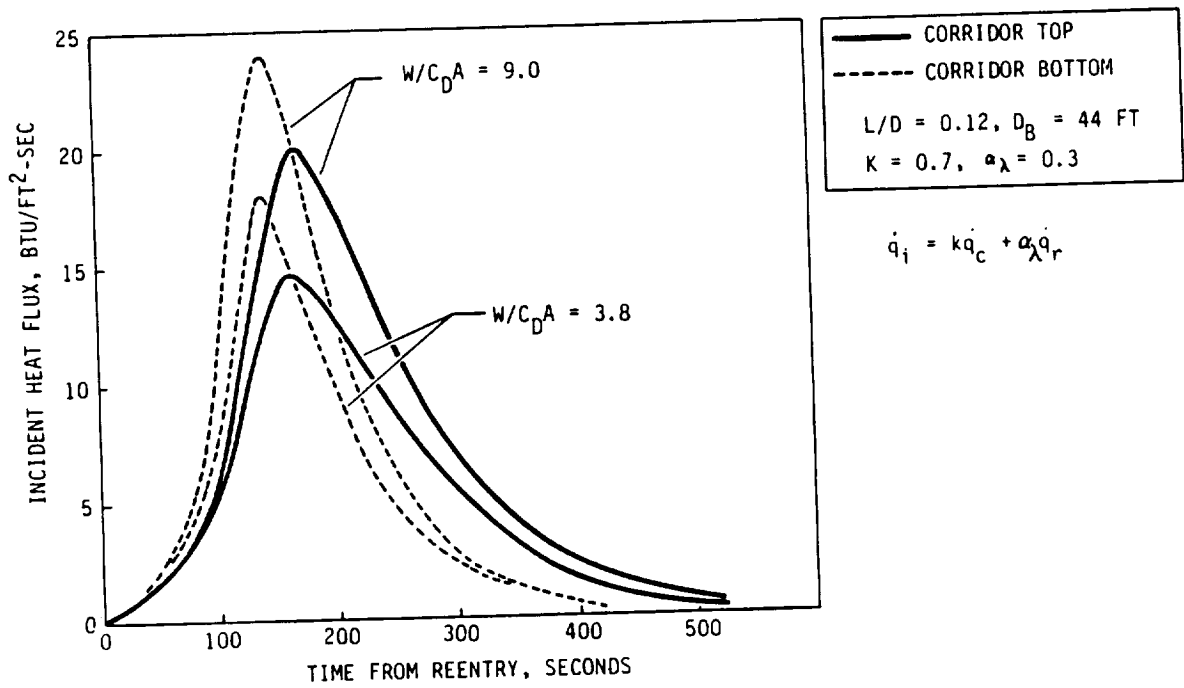


Figure 2.2.2.3-4 Typical AOTV Heating Environments

Typical peak heat flux profiles for the 44 foot diameter baseline aerobrake with a ballistic coefficient of 9.9 is shown in Figure 2.2.2.3-5. Also shown is the rigid/flex TPS interface point. Because of the large door area required for gimbal clearance of the two extended engine nozzles and a desire for the highest ballistic coefficient thermally achievable, the engine cover/nose area of the aerobrake is constructed of rigid surface insulation (RSI). This 13 foot diameter RSI engine door sets the range of S/R and associated heat flux histories to be used for the flexible surface insulation (FSI) thermal design criteria.

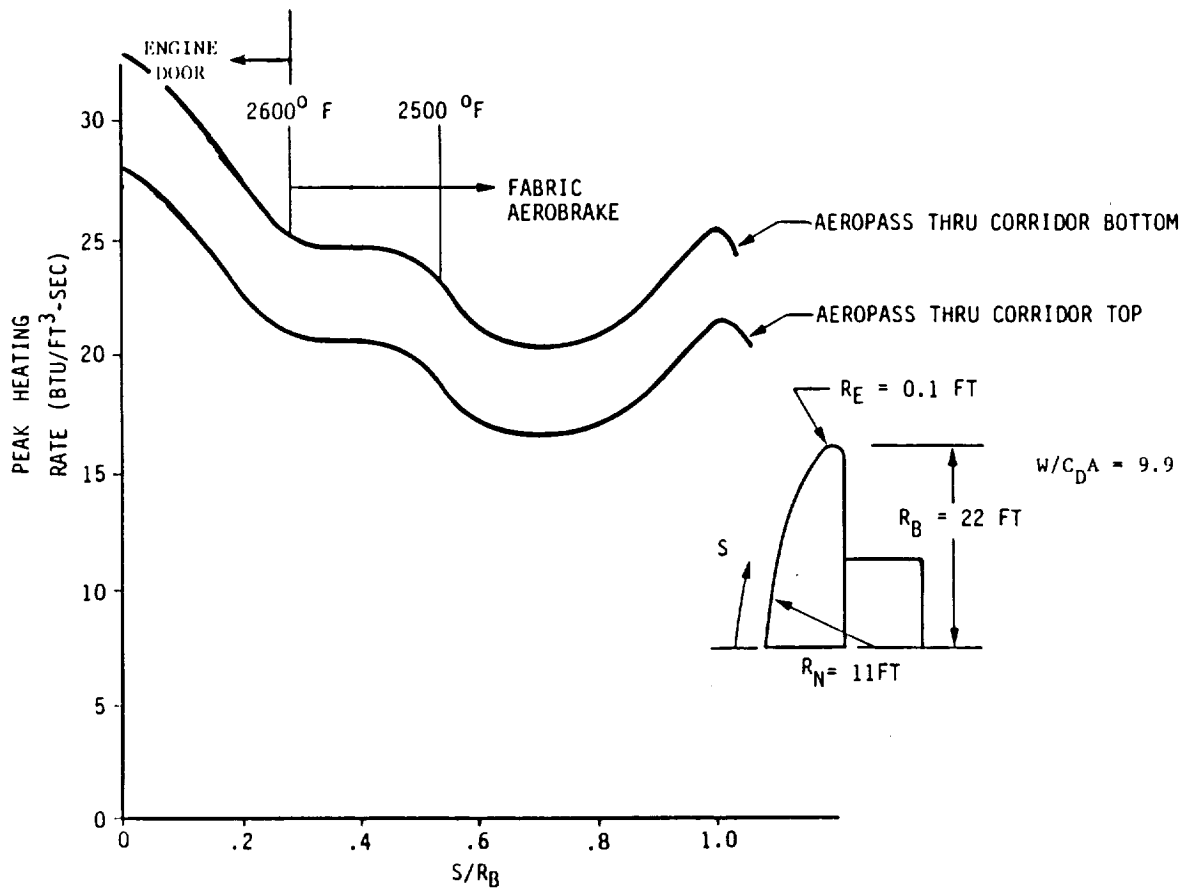


Figure 2.2.2.3-5 Aerobrake Heat Transfer Distribution

Figure 2.2.2.3-6 presents the surface temperature profile for the windward meridian of the 44 foot aerobrake at a $W/C_D A$ of 9.9 psf. The lower rigid TPS temperatures at the center of the brake is due to the high emissivity (0.9) of the RSI coating. The flexible TPS surface emission coefficient drops to 0.5 at temperatures of 2500°F creating increased thermal temperatures on the blanket.

The correlation of brake diameter and ballistic coefficient to the peak incident heat flux and surface temperature is shown in Figure 2.2.2.3-7 for the flexible TPS of the aerobrake. Using thermal limits of 30 BTU/ft² sec and 2600°F for the cover cloth, the maximum ballistic coefficient for a given brake diameter can be determined. This parametric chart was developed to provide temperature and heat flux constraints using trajectory simulations through the bottom of the flight corridor.

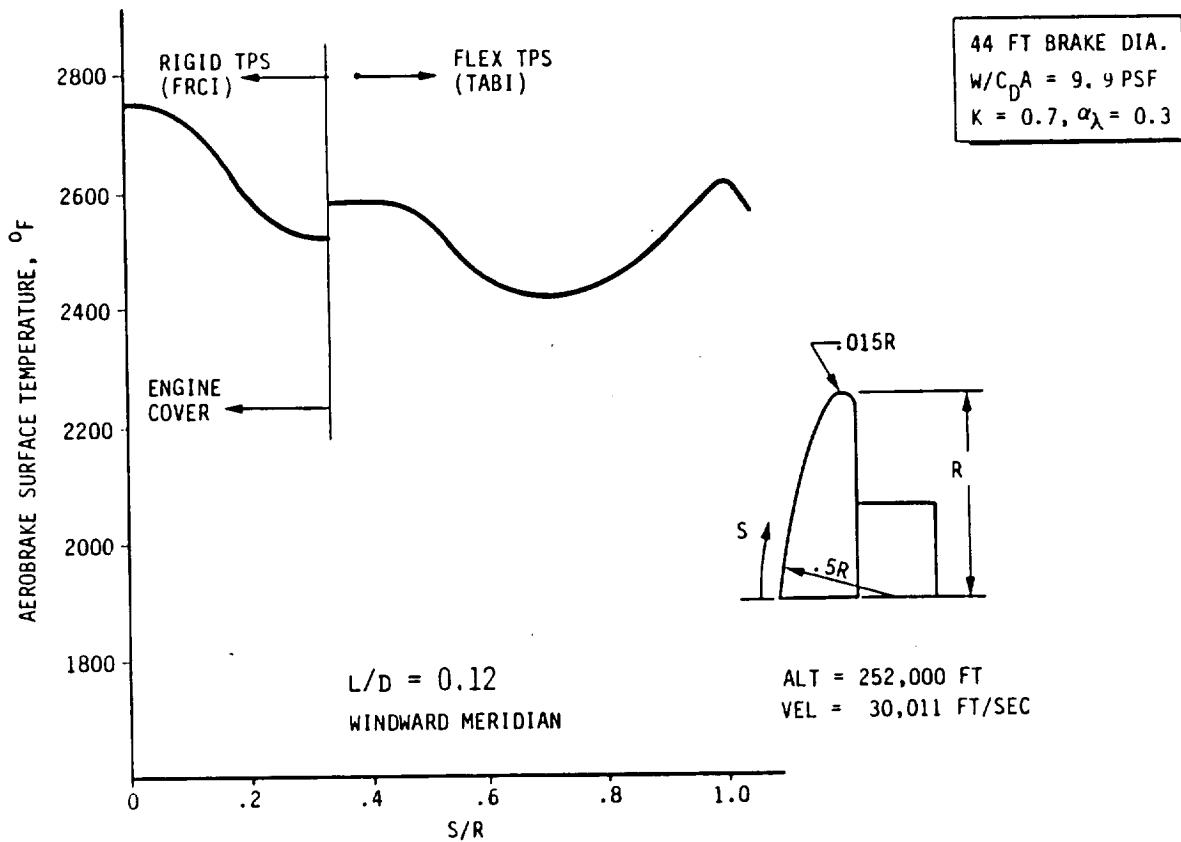


Figure 2.2.2.3-6 Aerobrake Peak Temperature Profile

This chart is based on an L/D of 0.12 and is entered by selecting the peak heat flux for the candidate nicalon material (30 BTU/ft² sec). Moving laterally to the selected aerobrake diameter (45 ft.), the maximum W/C_pA (14.6) can be found on the lower horizontal line. The resulting surface temperature of the flexible blanket at the W/C_pA limit of 14.6 is 2870°F and is determined using the dashed lines. The predicted maximum allowable temperature for the surface material is 2600°F, and using the dashed aerobrake diameter temperature of 45 ft, the allowable W/C_pA based on temporal limits is 10.0.

Although heat transfer rates are used as a measure of thermal capability instead of temperature to avoid the need for assuming material or coating optical properties, the lower W/C_pA value associated with the temperature limit was selected for determining our maximum return weight on the 44 foot baseline aerobrake. Selection of the lower W/C_pA also provides margin and conservatism to the design.

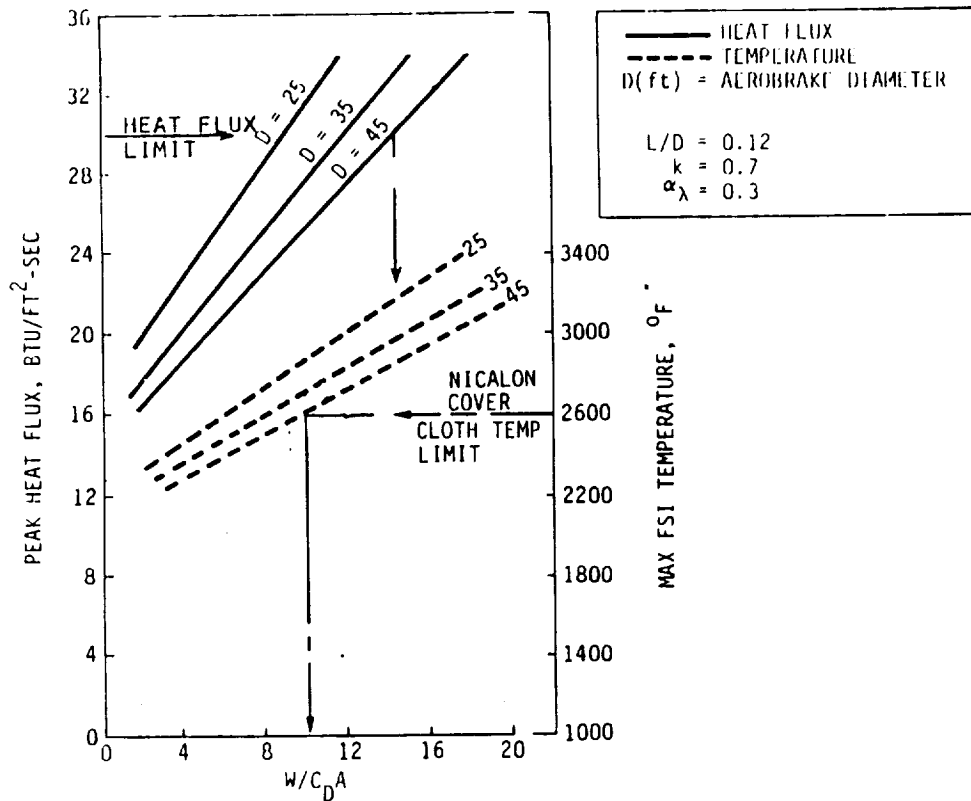
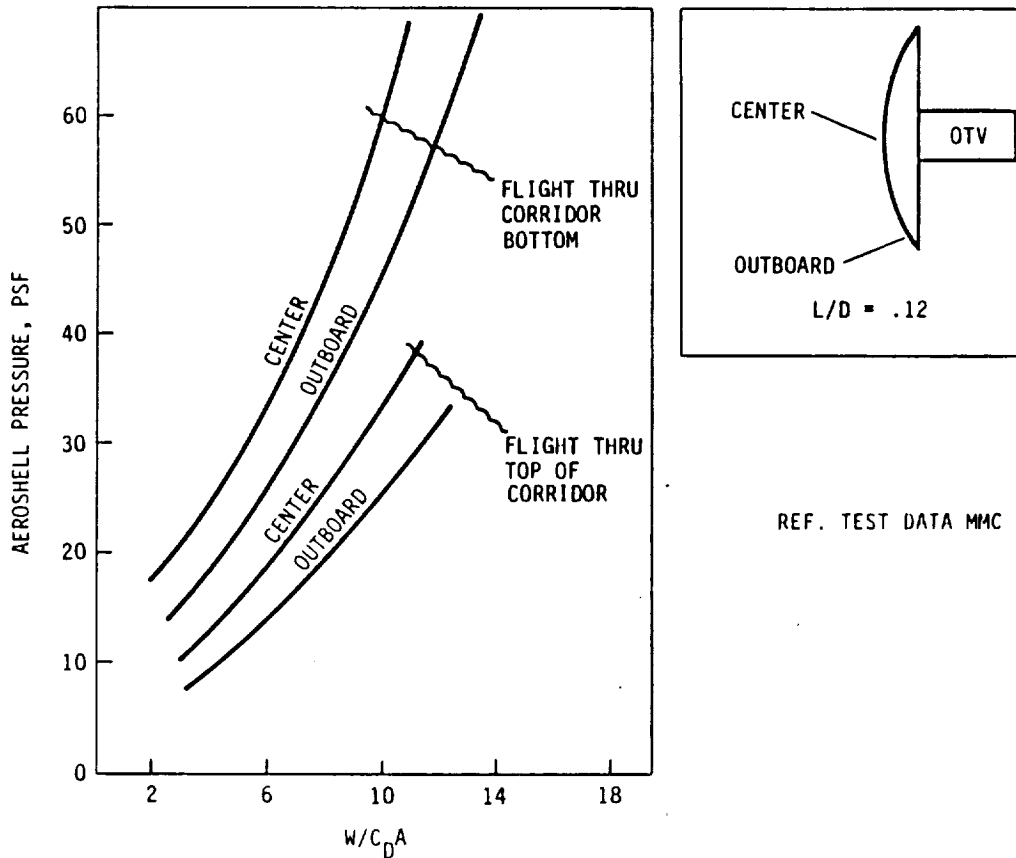


Figure 2.2.2.3-7 Correlation of Peak Heat Flux and Temperature With Ballistic Coefficient and Brake Diameter

The variation in aeroshell face pressures from the center to outboard edge of the conical aerobrake is shown for both top and bottom of the flight corridor for a $W/C_D A$ range from 2 to 12 in Figure 2.2.2.3-8. These pressure distributions are based on wind-tunnel data from Reference 2.2-9 and are used in defining the substructure structural loading requirements. Center pressures are consistently higher than the outboard edge and the bottom corridor flight imposes nearly twice the face pressures of the longer duration top corridor. Therefore, the bottom corridor curves were used in the design criteria along with a 3g load requirement.



REF. TEST DATA MMC TP-3720318

Figure 2.2.2.3-8 Correlation of Aerobrake Face Pressure Distribution with Ballistic Coefficient for $L/D=0.12$

2.2.2.4 OTV Aerobrake Sizing

The size of the aerobrake diameter is determined based on the thermal constraints of the surface material and on avoiding direct flow impingement of air molecules to the vehicle core or payload. Using a $30 \text{ BTU/ft}^2 \text{ sec}$ heat flux constraint for the Nicalon cover cloth and the parametric data of Figure 2.2.2.3-7, a relation between OTV return weight and aerobrake diameter can be computed. The results are plotted in Figure 2.2.2.4-1. The other constraint shown in this figure is based on wake flow impingement.

C-3

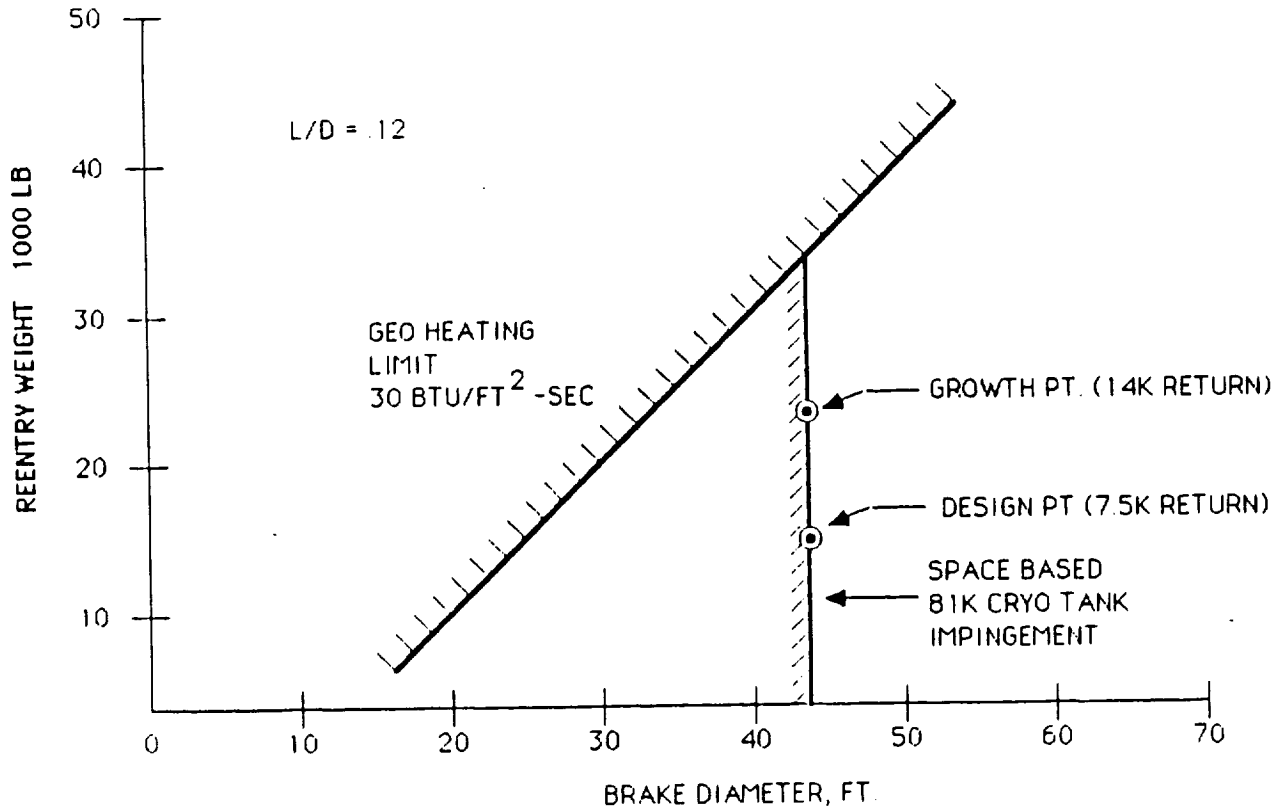


Figure 2.2.2.4-1 Aerobrake Sizing Criteria

To evaluate the boundary between the recirculating base flow and the direct flow impingement region to the spacecraft, it is necessary to determine the angle of the flow as it turns the aerobrake corner. The flow impingement region is computed by combining the maximum flow turn angle of 8.0° (based on the pressure in the aerobrake/spacecraft base region being zero), a 7.5° angle of attack during entry, and a 2° maximum vehicle attitude coning motion (see Figure 2.2.2.4-2). This flow impingement angle is used to determine the minimum aerobrake size required to avoid flow impingement to the vehicle or payload, and in defining the dividing streamline location for use in base heating calculations.

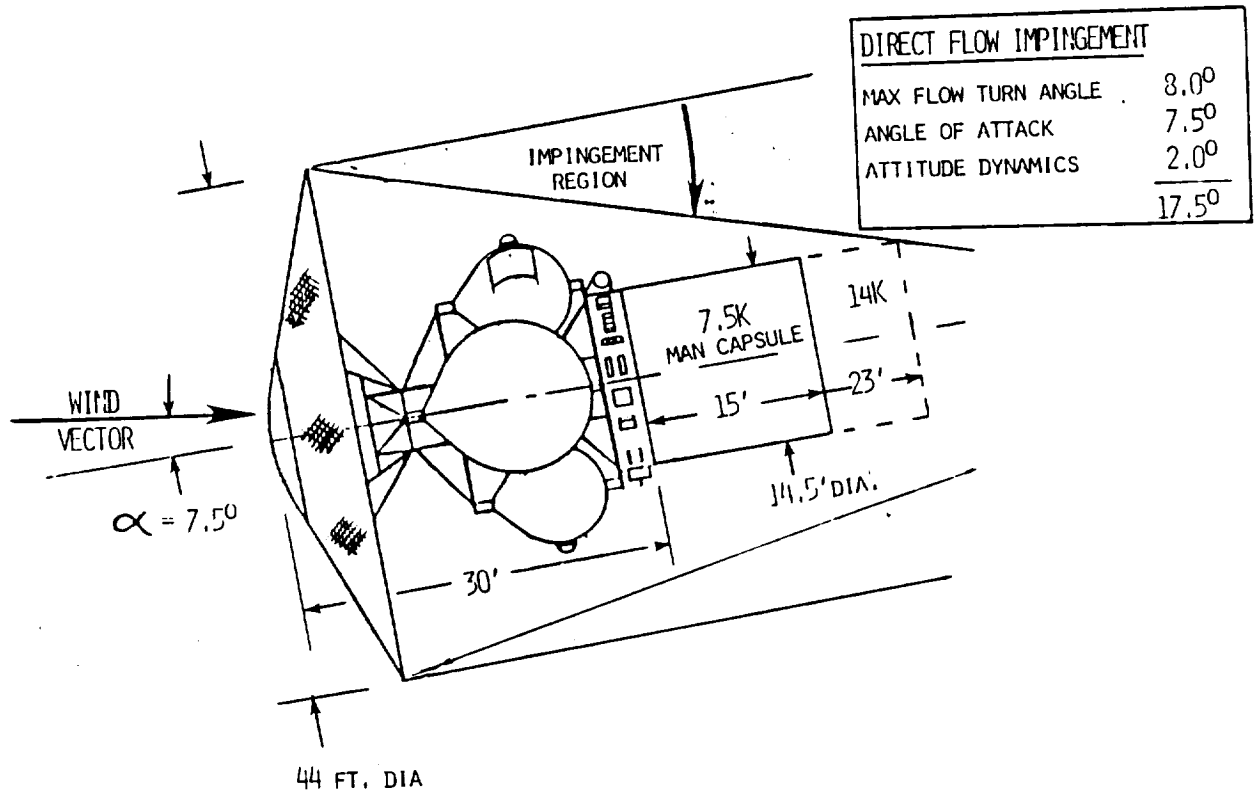


Figure 2.2.2.4-2 OTV Impingement Heating

This theoretical calculation of the impingement angle agrees very well with experimental data. The OTV payload impingement summary shown in Figure 2.2.2.4-3 is from Reference 2.2-14 and is based on the wind-tunnel data of Reference 2.2-15. For a 7.5° angle of attack, the experimental data indicates the wake impingement angle will be 19.2° compared to the theoretical value of 17.5° .

Aerobrake sizes for all candidate OTV designs are driven by impingement rather than the heating constraint. For the 55K cryogenic space-based OTV design, a 42 foot minimum diameter brake is required to prevent impingement on the vehicle's LH₂ tanks. Vehicle growth to 81K propellant tanks to handle the manned lunar mission with a 15,000 lb payload return to LEO is again sized by the flow impingement on the LH₂ tank and requires a brake diameter greater than 43 feet. Use of a 44 foot brake on this vehicle allows impingement clearance for the tanks, and for payload lengths up to 24 ft. In order to have growth potential, single DDT&E occurrence and to minimize logistics, a single 44 foot aerobrake was selected for all space-based OTV operations. Thus, one aerobrake size will service both delivery and payload return requirements that has growth above the current 7,500 manned capsule design point. A similar philosophy was used for the ground-based ACC cryogenic vehicle. A minimum 38 foot brake is required due to impingement, however, to provide a margin of safety and to add conservatism to the design analysis, a 40 foot aerobrake was baselined.

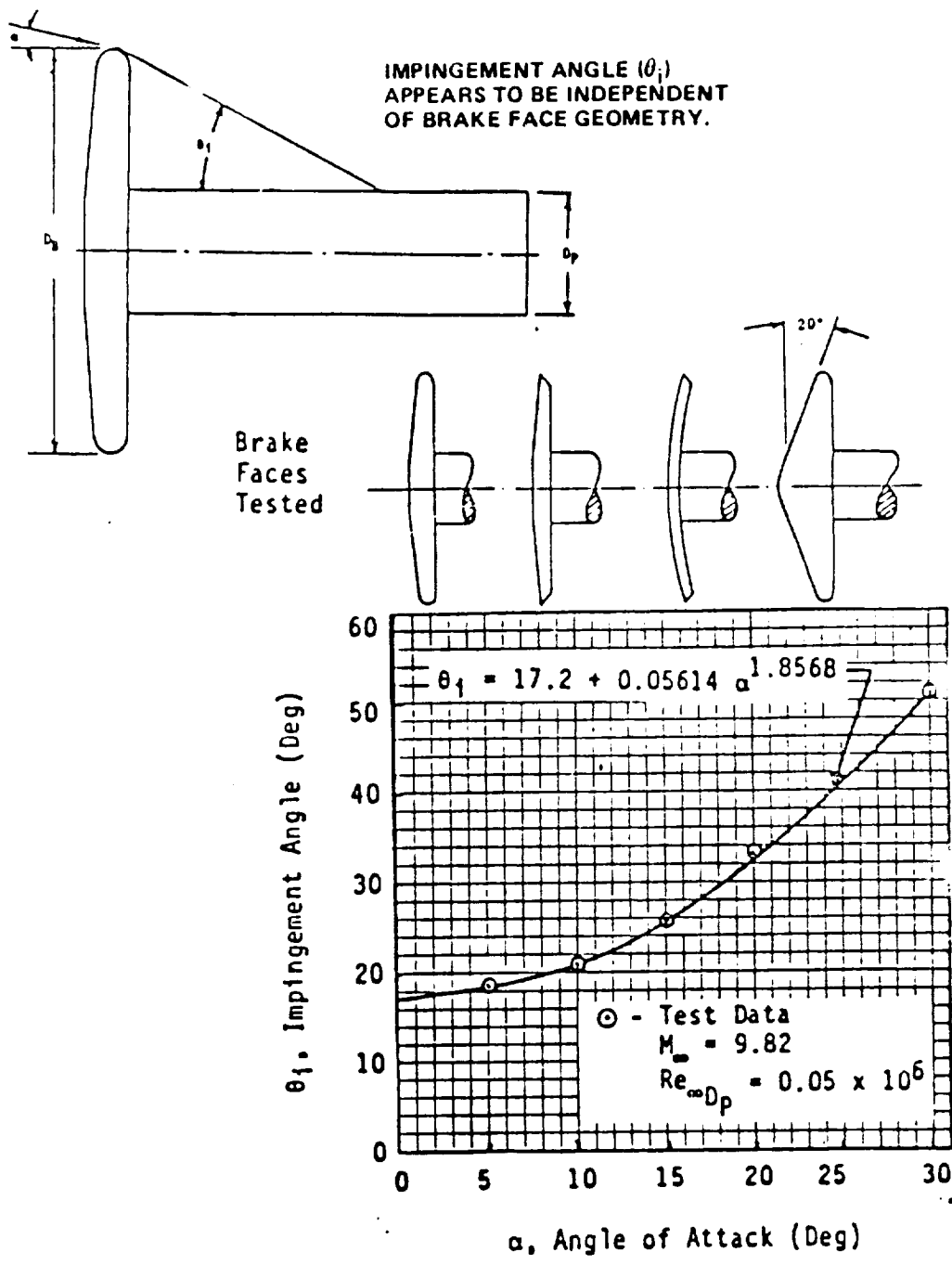


Figure 2.2.2.4-3 Aeroassist Flight Experiment OTV Payload Impingement Summary

For TPS sizing, the thickness of the aerobrake's flexible surface insulation (FSI) is based on maintaining the aerobrake's back face gas sealer (RTV) temperature below 600°F. Heat transfer run times of 600 seconds were used in the analysis to ensure heat soak into the FSI and peak heat shield back face temperatures had occurred. The higher integrated heat loads associated with the corridor top flight trajectories were used in sizing the TPS.

Results from the TPS sizing heat transfer runs are shown in Figure 2.2.2.4-4. This figure relates aerobrake diameter and ballistic coefficient to the integrated heat load of the aeropass and the required FSI thickness to keep back face temperatures below 600°F. Use of the chart is shown by two examples, which are representative of a typical delivery to GEO mission and a 15,000 lb return mission payload using the same sized aerobrake.

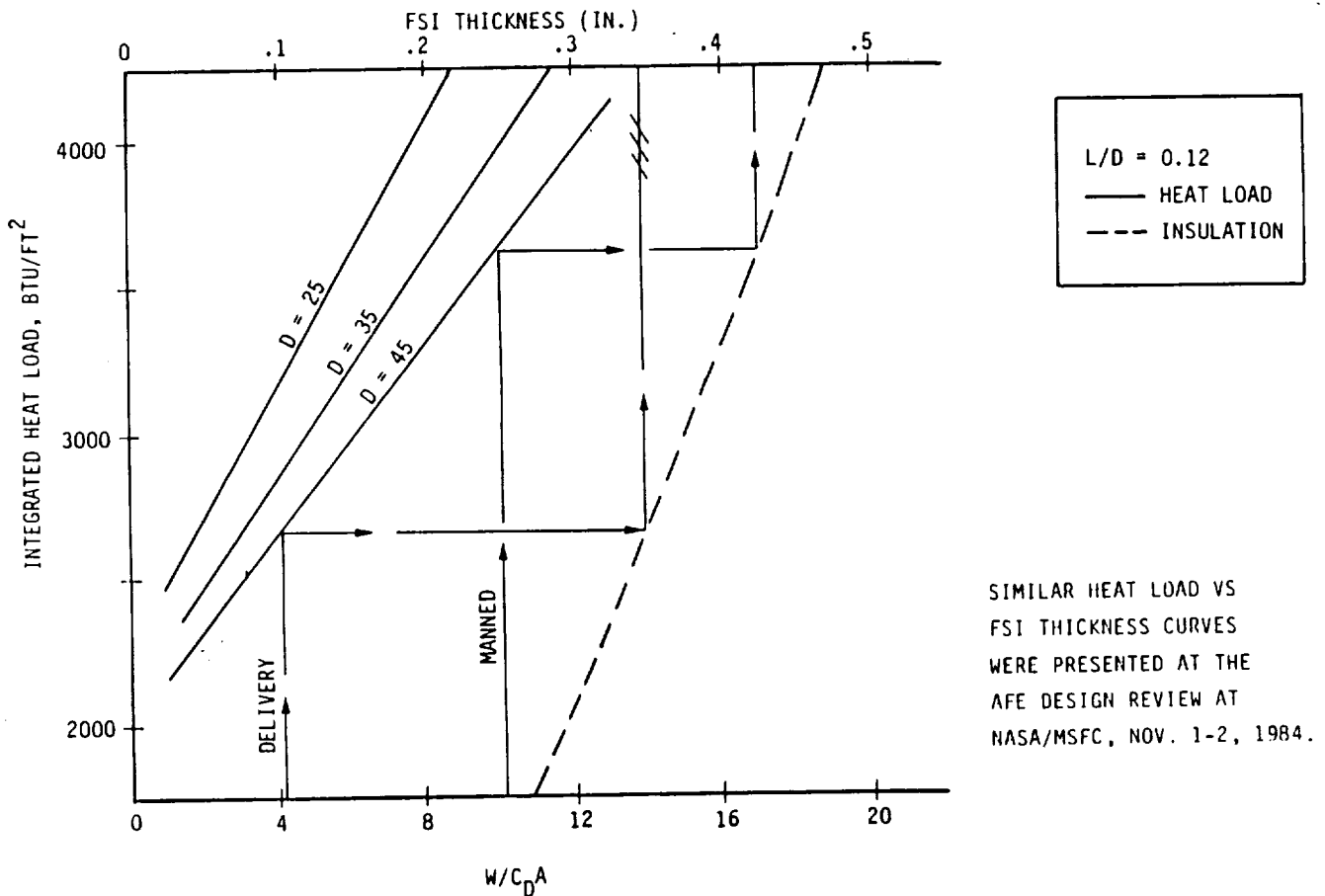


Figure 2.2.2.4-4 Integrated Heat Load Correlation with Ballistic Coefficient and Insulation Thickness

A summary of the aerobrake design requirements for the cryogenic propelled OTVs are listed in Table 2.2.2.4-1. The peak surface heating environment, thermal and structural design loads, and TPS thicknesses for both the rigid and flexible portions of the aerobrake are defined.

Table 2.2.2.4-1 Aerobrake Design Requirements (Cryogenic OTV)

CRYOGENIC VEHICLES L/D = 0.12, GEO TO LEO

CONFIGURATION	W/C D ^A	BRAKE DIAMETER (FT)	TPS	q ^{MAX} (BTU/FT ² SEC)	q ^{MAX} (BTU/FT ²)	T ^{MAX} (°F)	TPS THICKNESS (IN.)	W _{BRAKE} / W _{RETURN}	DESIGN LOAD (PSF)	
									CENTER	OUTBOARD
** GROUND BASED	3.7	40	FSI RSI	17.9 21.5	2650 3180	2230 1970	0.34 0.39	0.19	23	17
SPACE BASED										
DELIVERY	4.1	44	FSI RSI	18.4 21.6	2660 3190	2280 2200	0.38 0.43	0.14	35	27
P/L CARRIER RETURN	5.1	44	FSI RSI	19.6 23.0	2890 3470	2340 2240	0.38 0.43	0.12	35	27
UNMANNED SERVICE	5.9	44	FSI RSI	20.5 24.0	3050 3660	2380 2280	0.38 0.43	0.10	35	27
** MANNED CAPSULE	9.9	44	FSI RSI	25.6 33.3	3680 4420	2600 2520	0.43 0.48	0.06	63	27

MAN CAPSULE - 14,000 lbs, 14 1/2' W x 23' L

** AEROBRAKE BASELINE

2.2.2.6 REFERENCES--

- 2.2-1 Monti, P.S., "OTV Fuel Cell and Avionics Cooling System Design", TM C.2.4.5.0-01, Martin Marietta Corporation, Denver, Colorado, 7 January 1985.
- 2.2-2 Monti, P.S., "OTV Fuel Cell System Weight Assessment", TM C.2.4.5.0-02, Martin Marietta Corporation, Denver, Colorado, 7 January 1985.
- 2.2-3 "Viking 75 Project Aerodynamics Data Book," TR-3709014, Rev. E, Martin Marietta Corporation, Denver, Colorado, December 1974.
- 2.2-4 "Viking Aerophysics Data Book," TR-3720003, Rev. G, MMC, Denver, Colorado, June 1975.
- 2.2-5 "Entry Data Analysis for Viking Landers 1 and 2", TN-3770218, MMC, Denver, Colorado, November, 1976.
- 2.2-6 Seiff, A., Kirk, D. B., Intrieri, P. F., "Aerodynamic Behavior of the Viking Entry Vehicle: Ground Test and Flight Results," J. Spacecraft, Vol. 15, No. 4, July 1977.
- 2.2-7 Pitts, W. C., Murbach, M. S., "Thermal Response of an Aeroassisted Orbital Transfer Vehicle with a Conical Drag Brake," AIAA Paper, 84-1712, July, 1984
- 2.2-8 Park, C. "Problems of Radiative Base Heating," AIAA Paper 79-0919, May, 1979
- 2.2-9 Schmidt, D. A., "Base Heating on an Aerobrake Orbital Transfer Vehicle," AIAA Paper 83-0408, January, 1983.
- 2.2-10 Little, R. L. and Boudreau, A. H., "Heat Transfer on a 14-Percent Scale Model of the NASA-MMC Viking Mars Entry Vehicle at Mach Number 16," AEDC-TR-73-195, December, 1973.
- 2.2-11 "Experimental Pressure Distributions of the Viking Entry Vehicle at Supersonic and Hypersonic Speeds", Martin Marietta Corporation, TR-3720318, November, 1972.
- 2.2-12 Goldberg, A., and Snakevics, J. O. A, "Hypersonic Heat Transfer to a Class of Scalloped Three-Dimensional Bodies, ARS Journal, pages 278-280, February, 1962.
- 2.2-13 Park, C., "Problems of Rate Chemistry in the Flight Regimes of Aeroassisted Orbital Transfer Vehicles," AIAA Paper 84-1730, June, 1984.

- 2.2-14 Menees, G. P., "Aerothermodynamic Heating Analysis of Aerobraking and Aeromaneuvering Orbital Transfer Vehicles," AIAA Paper 84-1711, June, 1984.
- 2.2-15 AFE Steering Committee, "Aeroassist Flight Experiment, Definition Review," April 22-24, 1985.
- 2.2-16 Hair, L. M., Engle, C. D., Sulyma, P. R., "Low L/D Aerobrake Test at Mach 10," AIAA Paper 83-1509.

2.3 PROPULSION TRADE STUDIES AND ANALYSES

2.3.1 Man-Rating and Mission Reliability

The OTV program man-rating requirement was:

- o No single credible failure shall preclude the safe return of the crew.

This criterion means that the crew will be able to return safely to the Orbiter or the Space Station from any point in the mission profile before mission objectives are complete. Rescue by OMV from failures in LEO will be considered in survivability calculations, but rescues in high orbits will be disallowed as an additional conservatism. This is to be interpreted as minimum criteria. Selected redundancy to enhance the probability of mission completion may be added on a cost-effective basis. The application of this criterion shall in no way obviate the requirements associated with launch, handling, and operation in the vicinity of Space Station or the Space Shuttle.

This requirement dictates at least one on-board back-up propulsion system to protect against loss of an engine. In order to assess the impacts of various options to meet this requirement, two factors were considered: the mission reliability cost and propellant cost. Single engine, multiple engines and various back-up concepts were evaluated. Table 2.3-1 summarizes the back-up concepts evaluated, including using a second engine for manned missions only and improving performance with a single engine during unmanned missions.

Engine reliability as a function of non-independent failure rate () for several fail safe (F/S) and fail operational (F/O) concepts is shown in Figure 2.3.1. The single engine shows the advantage of multiple engines or back-up schemes with the same engine single burn reliability. The non-independent failure rate is the probability that the failure or manufacturing defect of one engine will effect a failure in other engines in a multiple engine system. Essentially, it is the measure of how well multiple engines behave as independent systems. For example, the STS Space Lab - 2 flight experienced an engine-out because of a faulty temperature sensor. Temperature sensors almost shut down a second engine, but was overridden. Both sensors were of the same design. A catastrophic failure of a turbo pump would be another example where a single engine failure results in loss of the system. After discussions with Pratt & Whitney and Rocketdyne, we found that 5 to 10% was their estimate of this failure rate based on their experience in engine testing. The data shows that if coupling is greater than 3.5%, an independent RCS back-up has a better reliability than 2 engines. The general trend was that more engines reduced the main propulsion reliability as () increased and for an one-engine out case, more than 2 engines reduced the reliability.

Table 2.3-1 Evaluation of Backup Concepts

OPTION	COST (OPTION COST) (REF COST)	DRY MASS (LBM) PENALTY	ΔI_{sp} (SEC) (AT OPT C)	MAINTENANCE SERVICING	MAN-RATING & RELIABILITY	REMARKS
1 1 ENGINE 15000 LBF	REF	REF	REF	SIMPLEST	NOT FAIL- SAFE	o SIMPLE VEHICLE DESIGN AND AEROBRAKE INTERFACE
2 1 ENGINE 15000 LBF BACK-UP TPA	<u>DDT&E</u> 1.05-1.1 <u>UNIT</u> 1.5	240	REF	COMPLICATED BY TPA	FAIL SAFE EXCEPT FOR THRUST CHAMBER AND NOZZLE	o ENGINE DEVELOPMENT TESTING CONCERNS o SIMPLE VEHICLE INTERFACES o ATTRACTIVE APPROACH
3 1 ENGINE 15000 LBF RCS BACK-UP 1000 LBF	<u>DDT&E</u> 1.1-1.2 <u>UNIT</u> 1.0	1200 EFFECTIVE (PROP MARGIN)	RCS 440 SEC	COMPLICATED RCS CONDITIONING SYSTEM	FAIL SAFE FOR MANNED MISSIONS	o LOW THRUST GEO DRODIT o THRUSTER LIFE CONCERNS
4 ONE ENGINE UNMANNED 15000 LBF TWO ENGINES MANNED 15000 LBF/EA	<u>DDT&E</u> 1 <u>UNIT</u> 1-2	900	REF	ONORBIT RECONFIGURATION	FAIL-SAFE FOR MANNED MISSIONS	o COMPLICATES DESIGN/DEVELOPMENT o DEVEL. 1 & 2 ENGINES FEED SYSTEM
5 2 ENGINES 7500 LBF EACH	<u>DDT&E</u> .95 <u>UNIT</u> 1.5	450	-2 TO +2 SEC	2 ENGINES TO MAINTAIN (SMALLER VOL. PER ENGINE)	FAIL-SAFE ALL MISSIONS	o COMPLEX CONTROLS LARGE GIMBAL ANGLE o LARGE AEROBRAKE DOORS
6 3 ENGINES 5000 LBF EACH	<u>DDT&E</u> .90 <u>UNIT</u> 2.2	750	-2.5 TO +2.7 SEC	3 ENGINES TO MAINTAIN (SMALLEST VOL. PER ENGINE)	FAIL-SAFE AT LOWER RELIABILITY THAN 5 OR FAIL OP/FAIL SAFE	o MORE COMPLEX CONTROLS o GIMBAL ANGLE SMALLER THAN 2 ENGINES

ASSUMPTIONS:
FAIL SAFE - ONE ENGINE OUT MINIMUM
REQUIREMENTS FOR MAN-RATING

The performance of multiple engines was determined for a single perigee burn and GEO delivery mission to assess the cost of propellant as a function of redundancy. A single stage was used for both cryogenic and storable OTV's in this analysis. The data used in the parametric analysis is shown in Figure 2.3-2 for the advanced expander cycle LH₂/LO₂ engine and in Figure 2.3-3 for the advanced gas generator MMH/N₂O₄ engine. These were generated from manufacturer's data for the coarse screening. Thrust, area ratio, and length were optimized later as the engines and vehicles were better defined (see Section 2.3.2). The results for a cryogenic stage and the 20K delivery mission are shown in Figure 2.3-4. Pratt & Whitney and Rocketdyne data were used because they bounded the range of engine performance. The optimum total thrust for a given number of engines was about 15000 lbf; however, the P&W data showed a slight advantage to 30000 lbf with 2 engines. The amount of propellant increased with number of engines.

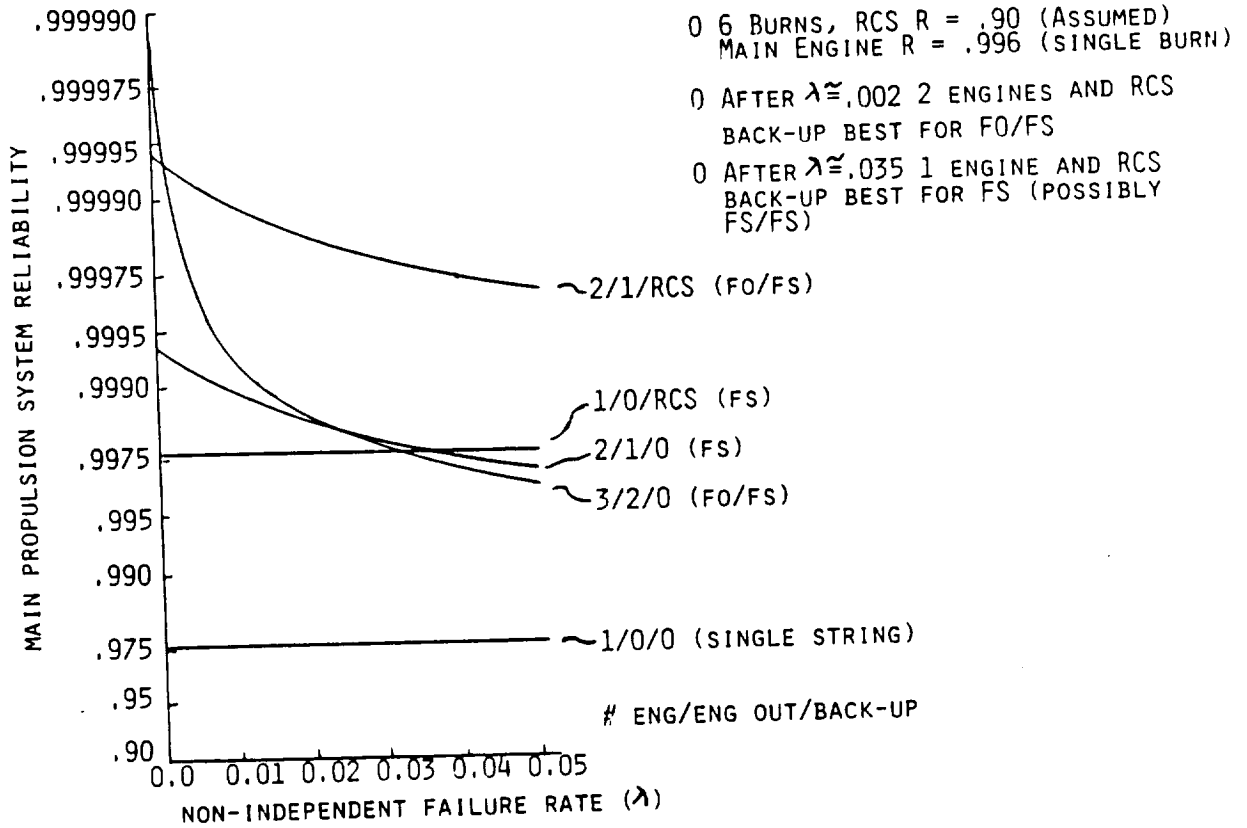


Figure 2.3-1 Propulsion System Reliability

CRYOGENIC ENGINES

	PRATT WHITNEY				AEROJET				ROCKETDYNE			
	Isp	IWT	LENGTH	DIA	Isp	IWT	LENGTH	DIA	Isp	IWT	LENGTH	DIA
THRUST $\times 10^{-3}$ LBS	SEC	LBST	IN.	IN.	SEC	LBST	IN.	IN.	SEC	LBST	IN.	IN.
15.0	478.6	376	120	57	484.4	384	170	70	491.5	395	150	74
7.5	476.3	331	102	47	483.5	272	118	50	490.0	240	130	58
5.0	475.8	243	91	40	482.8	160	100	41	489.5	200	120	51
3.75	473.1	210	83	36	482.5	130	90	34	488.7	170	110	46
EXPANSION RATIO	640:1				1000:1				1200:1			

Figure 2.3-2 MPS Parametric Data for Trade Studies

STORABLE ENGINES

XLR-132				
THRUST $\times 10^{-3}$ LBS	I_{sp} (SEC)	WEIGHT (LB)	LENGTH (IN.)	EXIT DIAMETER (IN.)
3.75	342.4	114	52 ✓	26 ✓
5.0	343.1	146	60	30 ✓
7.5	344.1	213	74	37 ✓
15.0	345.7	426	104	52
20.0	346.1	578	119	59
25.0	346.6	738	133	66
30.0	346.9	905	145	72
€ 400:1				

DATA OBTAINED DIRECTLY FROM ENGINE CONTRACTOR (ROCKETDYNE)

Figure 2.3-3 MPS Parametric Data for Trade Studies

The results for the storable stage are shown in Figure 2.3-5 for the 20K delivery and 14K round trip. This more clearly illustrates increasing propellant with increasing number of engines. The total thrust was about 15000 lbf for the 20K delivery and about 25000 to 30000 lbf for the 14K mission with a single stage.

The reliability and performance analyses indicated that the minimum number of engines to meet the man-rating requirement should be used. A single engine was used as a reference since it had the highest performance. Because of the high performance of a single engine, a single thrust chamber with redundant turbopumps was evaluated. The pump would be in a stand-by mode preventing degraded performance and reliability. Figure 2.3-6 shows a RL10-IIB schematic with redundant TPA. Based on the above parametric studies, the concepts selected for further study were 2 engines, RCS back-up and back-up TPA.

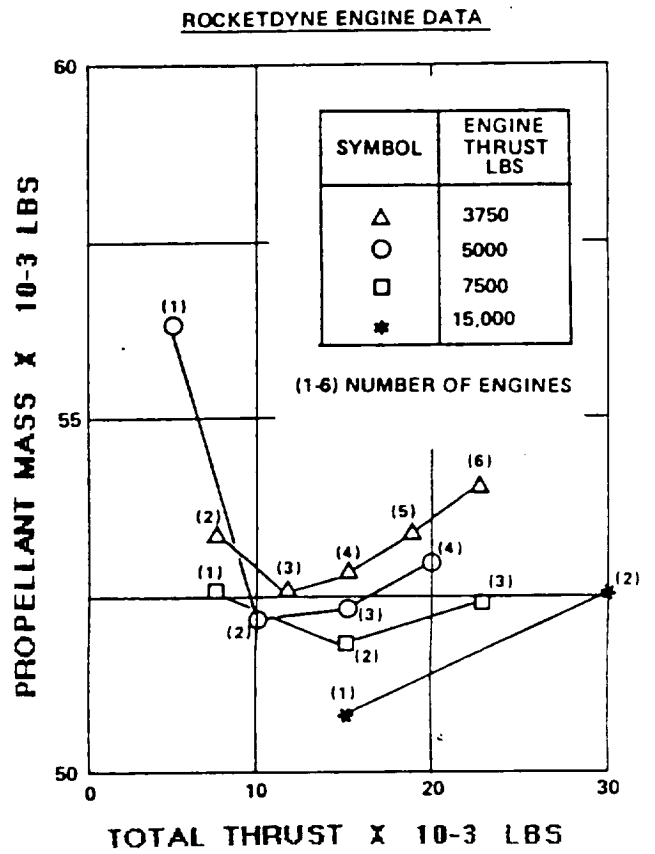
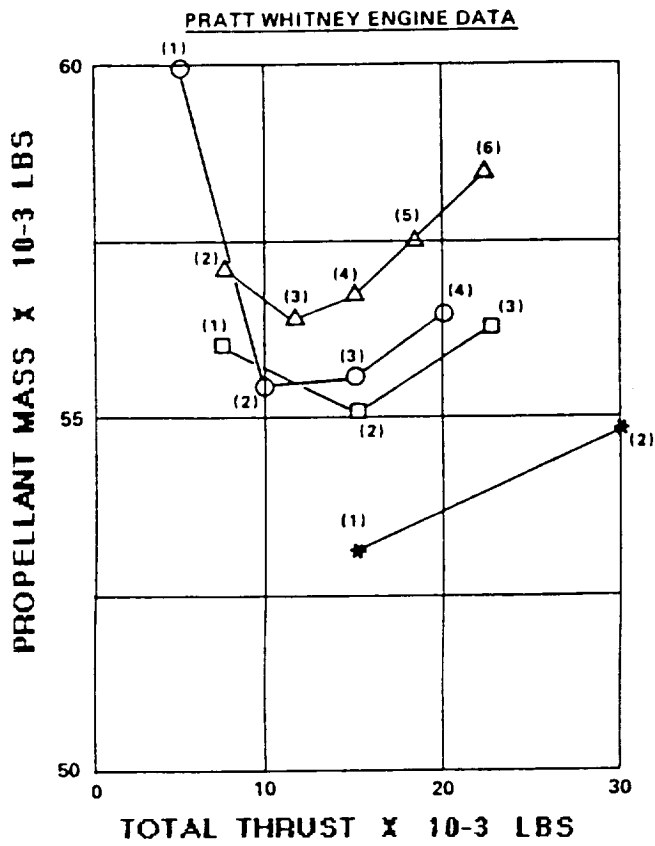


Figure 2.3-4 Thrust vs Propellant Weight for Cryo 20K Delivery Mission

ENGINE THRUST LBS	SYMBOL
3750	(1)
5000	(2)
7500	(3)
15000	(4)
20000	(5)

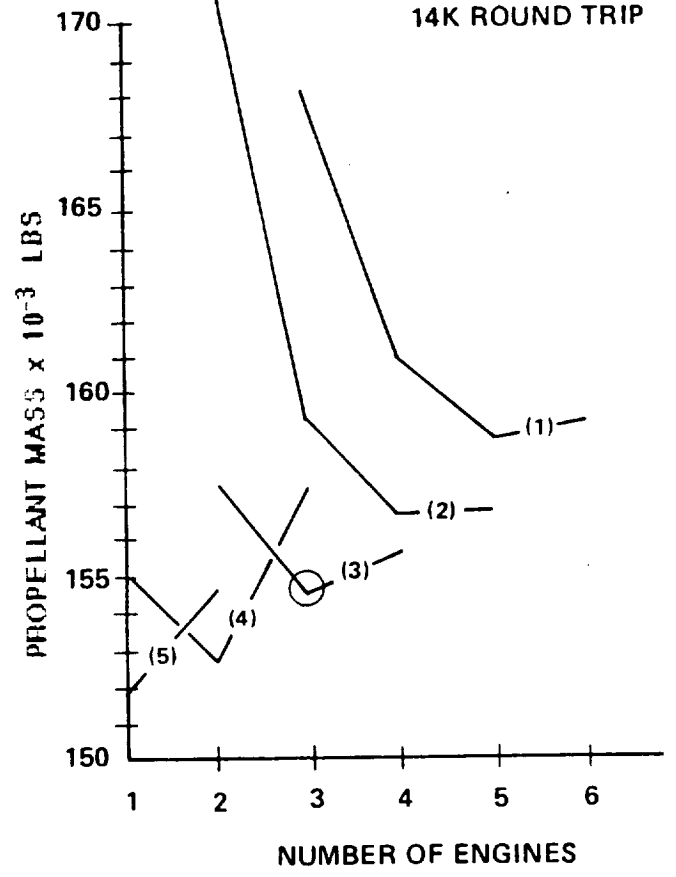
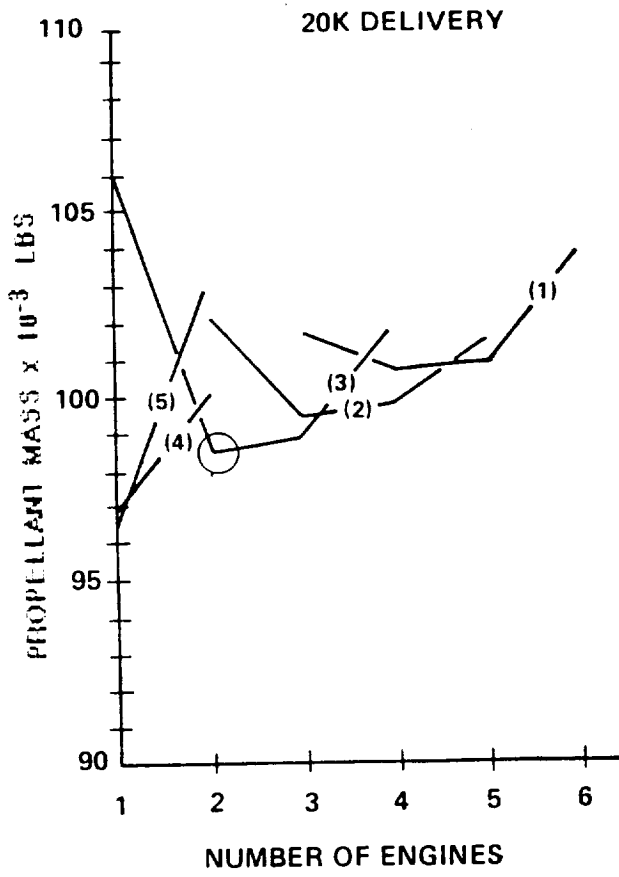


Figure 2.3-5 Preliminary Storable Engine/Stage Data

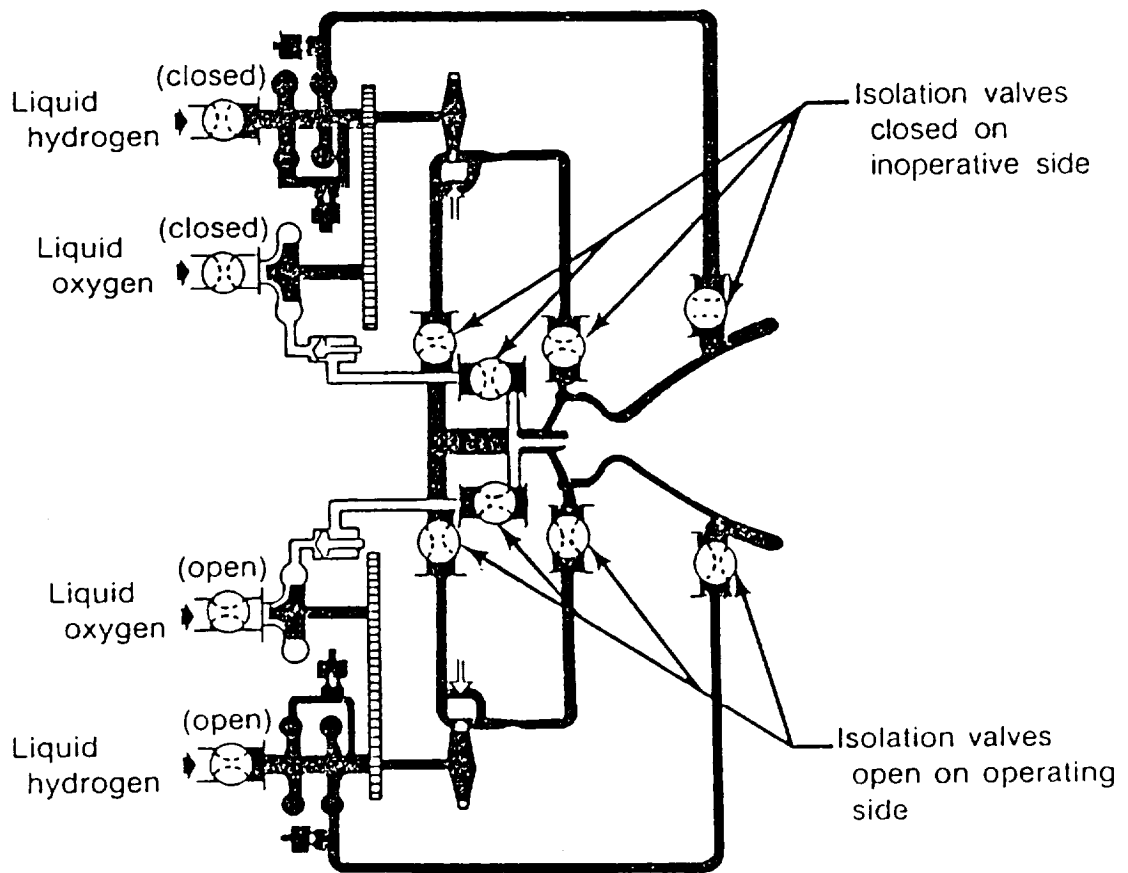


Figure 2.3-6 RL-10 With Redundant Turbopumps

Figure 2.3-7 compares the performance and reliability cost of PCS backup, redundant turbopump, and two engines for the Rev 7 mission model. The cost of engine redundancy was the sum of propellant costs at \$1500/lbm, and mission lost costs of \$184M. A single engine reference case had a six burn reliability of .9819 which gives a total mission lost cost of \$1.37B, assuming 412 missions. The RCS backup cost assumed that the RCS propellant mass penalty of 5400 lb_m would be carried on the 43 manned missions and the remaining 369 had a mission loss relative to the single engine reliability. Based on an RCS back-up reliability of .9982, this option had a redundancy cost of over \$1.6B. The back-up turbopump option required 510 lb_m more propellant/mission due to delta dry mass and had an estimated reliability of .9982; this resulted in a net redundancy cost of \$0.44B. The 2 engine option required additional propellant/mission of 551 lb_m (for delta dry mass) and 825 lb_m for I_{sp} losses and had a reliability of 0.9996, resulting in a total redundancy cost of \$0.88B. A 0% was assumed for the two engine case. Increasing to 5% would increase the mission lost cost for both engine and back-up TPA. Decreasing propellant cost reduces the difference between the two lowest options. The I_{sp} loss for the two engine case was

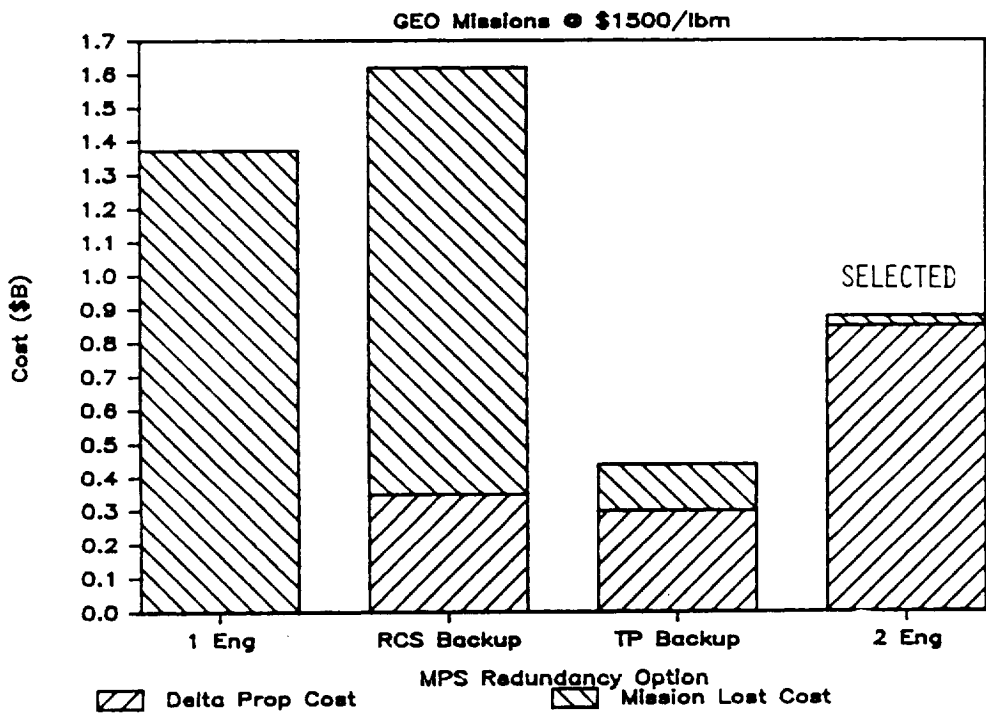


Figure 2.3-7 MPS Redundancy Cost Trade

reduced with further optimization as indicated in Table 2.3-1 (see Table 2.3-5). The Rev 8 mission model reduced the savings more because only 145 missions are flown in the low model. The relative value remained the same, but the absolute value changed from \$440M to \$26M LCC (undiscounted). The redundant TPA technology increases the development risk and is not completely redundant, i.e., single string valves, single thrust chamber and nozzle. Additionally, there are several failure modes not addressed by redundant TPA (i.e., failure to ignite, loss of coolant, failure of extendable nozzle). Therefore, the two engine configuration was chosen as the preferred man-rating redundancy option.

2.3.2 Main Engine Analysis

Analyses were performed to determine optimum LH₂/LO₂ and MMH/N₂O₄ Main Propulsion System (MPS) engines for the ground and space-based OTV's. This included thrust level, technology level, number of perigee burns, aerobrake interface, and engine geometry.

Ground Rules and Assumptions - The selection criteria used in the OTV study engine selection analysis were:

CRITERIA	RATIONALE	METHOD
<u>Ground-Based</u>		
Mass	Single-Shuttle Lift Capability	Analysis
Technology 1987	Consistent with IOC	Judgment
Low DDT&E Cost	Reduce OTV Front-End Cost	CER, Analysis
<u>Space-Based</u>		
Mass	Reduce Propellant (LCC)	Analysis
Simplify Maintenance	Reduce Turnaround EVA Cost	Judgment/Analysis
Evolution to Manrating	Capture Mission Model	Judgment

The ground rules used in the analysis were:

- 1) Rev 7 mission model
- 2) Performance as quoted by engine contractors
- 3) 2% delta v margin, 1% residuals on MMH/N₂O₄, 1.5% residuals on LH₂/LO₂
- 4) Velocity losses determined by trajectory analysis, and
- 5) Two engines for fail safe return of crew for man-rating.

The Revision 7 mission model's 20K delivery mission was used to optimize engine geometry and thrust; therefore, the results will apply to the Revision 8 model which contains this mission. Velocity losses used in the analysis are shown in Figure 2.3-8. Additions or modifications to these ground rules are stated as required.

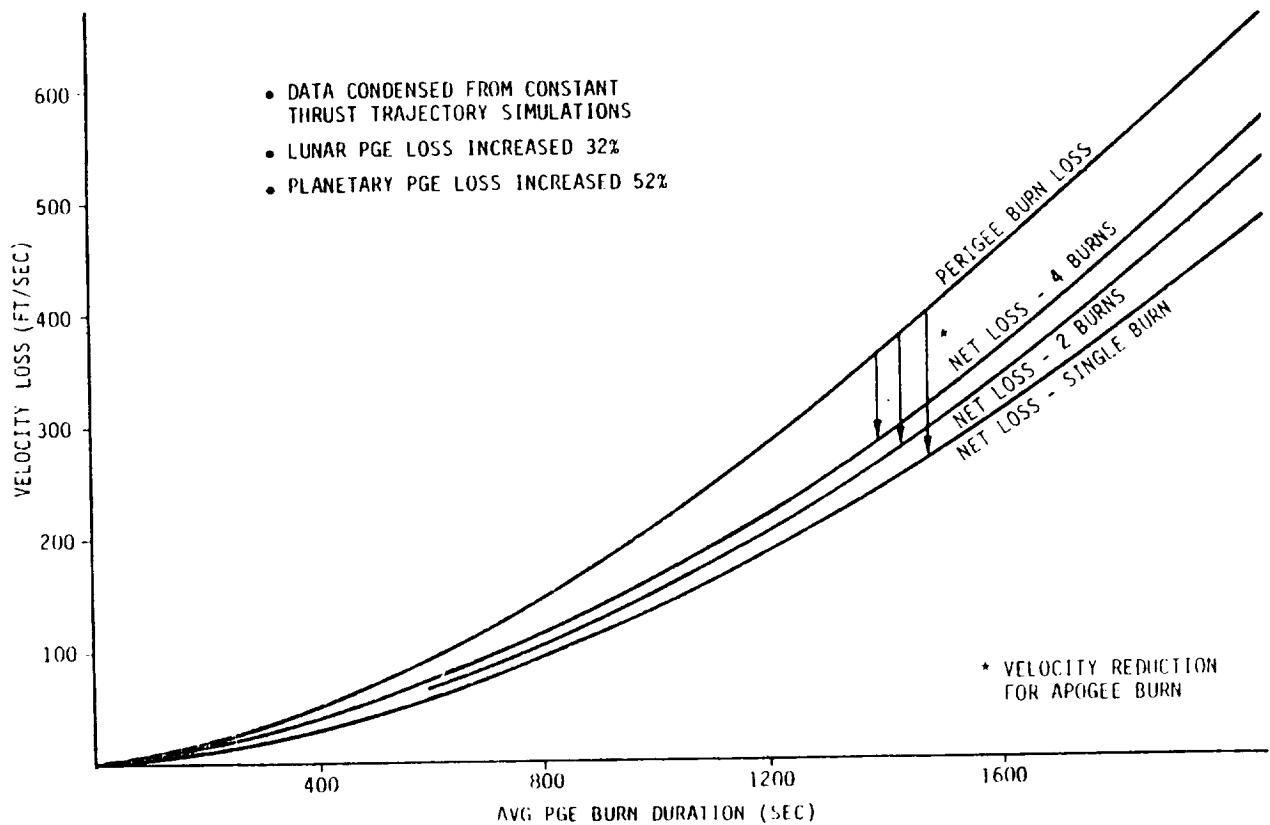
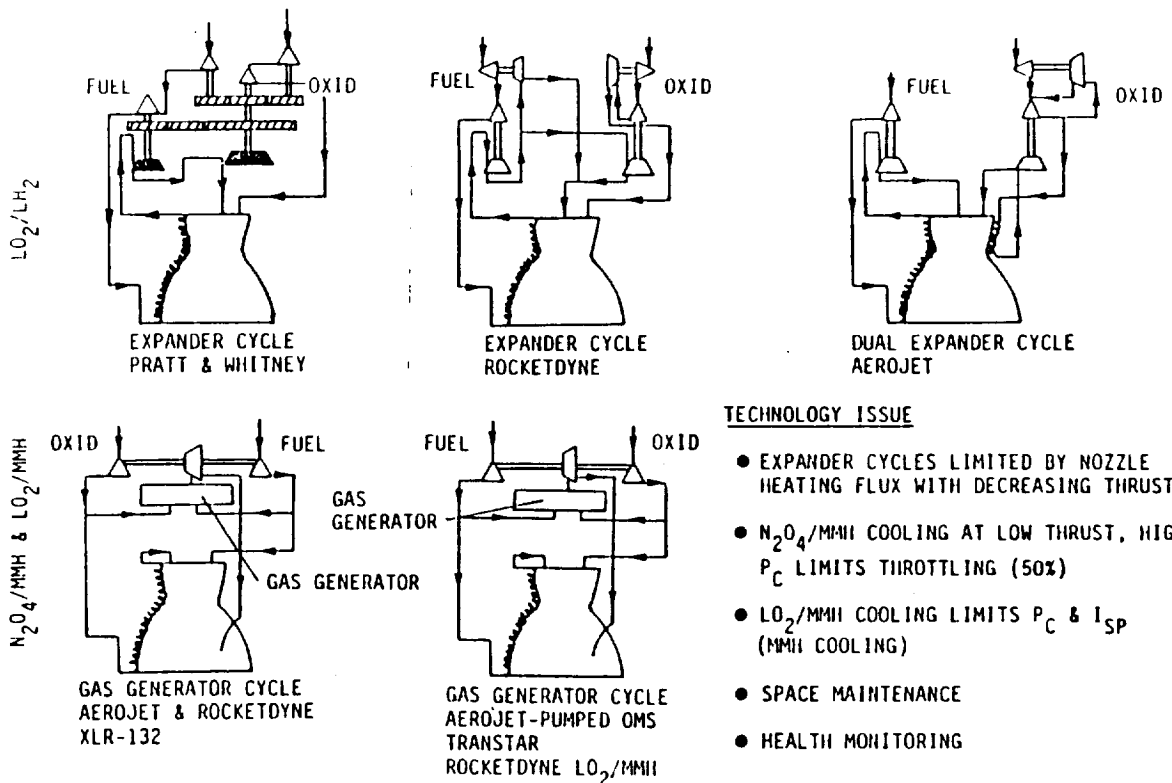


Figure 2.3-8 GEO Mission Finite Burn Velocity Losses

MPS ENGINE CYCLES--The engines considered in the analysis are shown in Table 2.3-2. MPS engine cycles are shown in Figure 2.3-9 for the candidate engines. The Pratt & Whitney advanced expander cycle uses fuel as the coolant. The fuel is then expanded through turbines to drive both fuel and oxidizer pumps. Lower pressure pumps are gear driven. The engine runs on a simple open loop minimizing active controls. Current and derivative RL-10s use gear driven LO₂ pumps. The Rocketdyne advanced expander cycle has fuel driven turbines for both turbopumps and the fuel boost pump. The Aerojet dual expander cycle uses both fuel and oxidizer as coolants which are then expanded through the respective turbines. Rocketdyne and Aerojet use closed-loop control.

Table 2.3-2 MPS Candidate Engines

ENGINE	I _{sp} MR	THRUST 10 ⁴ Lb	LIFE, HR NO. STARTS	DEV STATUS	CYCLE	MASS DRY (10 ³ Lb)	P _c (PSIA)	ε	NPSH/MPSE		
									FUEL	OXID	
LO ₂ /LH ₂	RL10A-3-3A	446 5.0	16.5	125 20	OPERATIONAL	305	405	61.3	28.6 PSIA	43 PSIA	
	RL10A-3-3B	440 6.0	15	125 20	QUAL	305	415	61.3	28.6 PSIA	43 PSIA	
	RL10-11B	460 6.0	15	5 190	PRODUCT DEVELOPMENT CONTRACT	392	400	205.3	14 FT	7.5 FT	
	RL10-11C	455 6.0	15	125 20		374	400	205.3	20.6 PSIA	43 PSIA	
	RL10-111	470 6.1	7.5	5 190	PROD IMPROVEMENT	400	400	100.3	14 FT	7.5 FT	
	RL100	475 6.0	15	10 300	COMP TECH DEV CONT	427	1500	640.3	15 FT	2 FT	
	RL100	474 6.1	7.5	10 300	STUDY	300	1200	600.3	15 FT	2 FT	
	RS44 CORE	463 6.0	15	10 300	COMPONENT TECHNOLOGY DEVELOPMENT CONTRACT	342	1540	275.3	15 FT	2 FT	
	RS44 INCR CAP	481 6.0	15	10 300		461	1540	625.3	15 FT	2 FT	
	RS44 FULL CAP	492 6.1	15	20 500		407	2052	1175.3	15 FT	2 FT	
	AJ23-154	483 6.0	3	20 500		30	2000	1000	0 FT	0 FT	
	N ₂ O ₄ /MMH	XLR-132	342 2.0	3.75	10 (CURRENT) 10		114	1500	100.3	17 PSIA AT 70 DEG F	37 PSIA AT 70 DEG F
		AJ23-153 TRANSTAR	328 1.8	3.75	NA 15	DEVELOPMENT	128	350	136.3	26 PSIA AT 90 DEG F	57 PSIA AT 90 DEG F
		AJ23-151 PUMP FEED OMS	334 1.53	6.0	15 NA	TEST CONTRACT	322	350	154.3	30 PSIA AT 90 DEG F	60 PSIA AT 90 DEG F
AJ23-156 TRANSTAR III		343 2.1	3.75	NA 15	TECHNOLOGY DEVELOPMENT	104	1430	100.3	28 PSIA AT 90 DEG F	67 PSIA AT 90 DEG F	
ROCKETDYNE DESIGN		367 1.4	6.0				1000	100.3	37 PSIA	67 PSIA	
LC MMH											



TECHNOLOGY ISSUE

- EXPANDER CYCLES LIMITED BY NOZZLE HEATING FLUX WITH DECREASING THRUST
- N₂O₄/MMH COOLING AT LOW THRUST, HIGH P_c LIMITS THROTTLING (50%)
- LO₂/MMH COOLING LIMITS P_c & I_{sp} (MMH COOLING)
- SPACE MAINTENANCE
- HEALTH MONITORING

Figure 2.3-9 MPS Engine Cycles

Gas generator cycles are used for all the storable and LO₂/MMH engines with either oxidizer or fuel used as the coolants.

The LH₂/LO₂ expander cycle's chamber pressure is limited by the amount of energy available to drive the pumps with gasified propellants. Aerojet's dual expander cycle shows higher chamber pressures at the lower thrust levels. The N₂O₄/MMH engines use MMH cooling at chamber pressures below about 800 psia depending on thrust and MR, changing to N₂O₄ cooling at pressures above about 1500 psia. This leads to some throttling difficulties with 2 phase N₂O₄ in the cooling jackets. LO₂/MMH engines have cooling problems which limits the chamber pressure to about 1000 psia with MMH cooling and therefore limits performance and possibly life.

MMH/N₂O₄--The initial storable screening evaluated near term or advanced technology engines, as summarized in Table 2.3-3. The AFRPL/Rocketdyne XLR-132 was considered advanced engine technology. The level of technology required, for the initial ground based OTV, was evaluated by considering a perigee (GEO transfer orbit) stage, propelled by either 2 AJ-23-151 (pump fed OMS-E) engines or 2 XLR-132 based engines designed to run at 7.5K thrust, and calculating the required propellants to deliver a range of payloads to GEO. Figure 2.3-10 shows that both engine configurations can capture the 12,200 lb_m delivery mission while remaining within the STS lift limit. The AJ-23-151 engines, however, require at least 1780 lbm more propellant than the XLR-132 "Type" engines to perform a given mission. This is due to a combination of thrust, Isp, and stage mass differences. Based on the potential propellant savings and growth, compared to the relatively low DDT&E costs for the XLR-132 engines (estimated at \$130M by MSFC for a reusable 3750 lbf), the AJ-23-151 engines were dropped from further consideration for either ground or space-based storable OTV's. A single MPS engine developed for both scenarios was found to be more cost effective than developing separate engines.

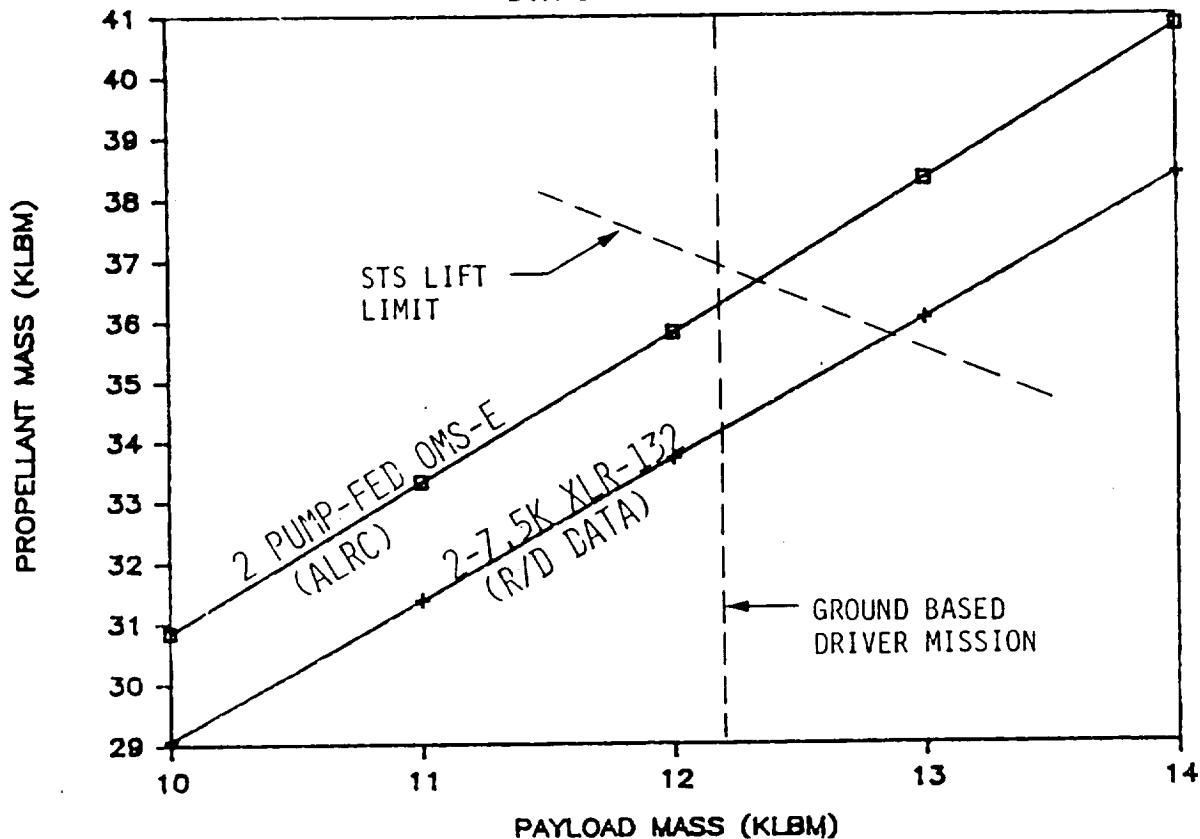
Table 2.3-3 N₂O₄/MMH Engine Technology Assessment.

TECHNOLOGY LEVEL	FLIGHT ENGINE AVAILABILITY	ENGINE CANDIDATE			
		ENGINE	Pc(PSIA)	ε	Isp(SEC)
1985	1987	AJ 23-151 PUMP	350	154:1	334
	TO	FED OMS (ALRC)			
	1988	AJ23-153 TRAN-STAR (ALRC)	350	136:1	328
1986	1989	XLR-132 EXPENDABLE (AFRPL)*	1500	400:1	342
		XLR-132 REUSABLE (AFRPL)*	1500	400:1	342

* ROCKETDYNE DATA. ALRC DATA SIMILAR

ALRC AND R/D DATA

51K STAGE OFFLOADED



7500 LBF XLR-132s HAVE HIGH PERFORMANCE AND CAN MEET IOC

Figure 2.3-10 Ground-Based MMH/N₂O₄ Engine Selection.

The storable engine was optimized for the space-based missions. Optimal engine geometry (eg., length, area ratio) was determined for several thrust levels and numbers of engines by optimizing the propellant to perform the 20000 lbm GEO delivery mission. Changes in Isp, aerobrake diameter, and stage dry mass were considered. The results showed that the optimum area ratio was 600:1 for a two engine configuration as shown in Figure 2.3-11 for a single perigee burn, corrected for delta velocity losses.

PERIGEE STAGE N204/MMH

2 ENGINES 20 K DELIVERY

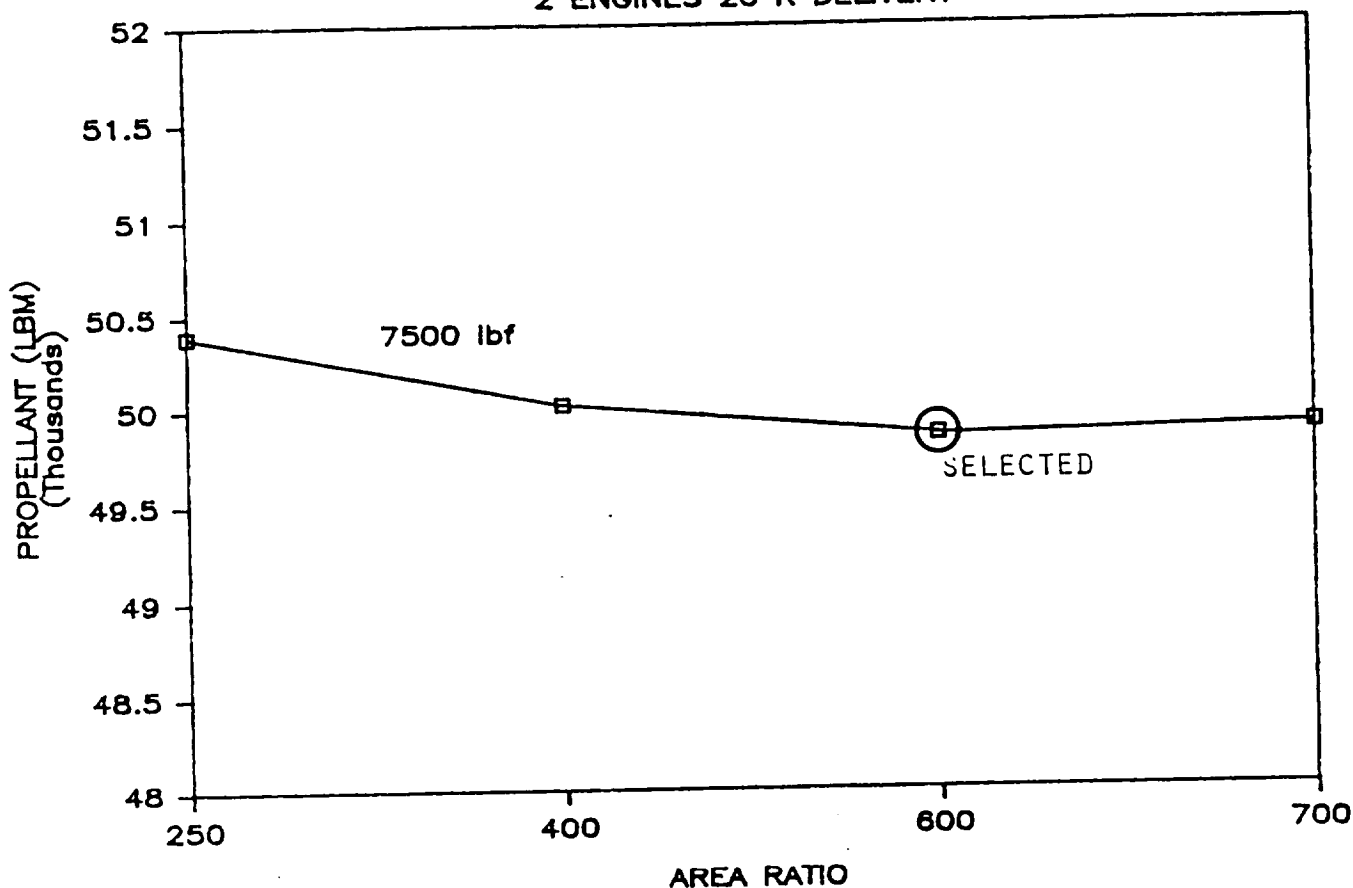


Figure 2.3-11 Optimum Expansion Ratio-Storable

The optimum thrust was determined for multiple perigee burns. Figure 2.3-12 shows the results of multiple perigee burns for optimum expansion ratio engines and up to 4 perigee burns. The reference design was 7500 lbf with the optimum thrust/engine 10000 lbf. To allow for flexibility, multiple perigee burns were not used to size the vehicle thrust. Figure 2.3-13 shows the same analysis for a single engine OTV. The RCS propellant was stored in the main tanks and would have a small impact on multiple burns since the high pressure storage bottles would be a fixed size. There were no midcourse corrections assumed during the coast periods between perigee burns.

PERIGEE STAGE (ROCKETDYNE)

2 ENGINE 20 K DELIVERY

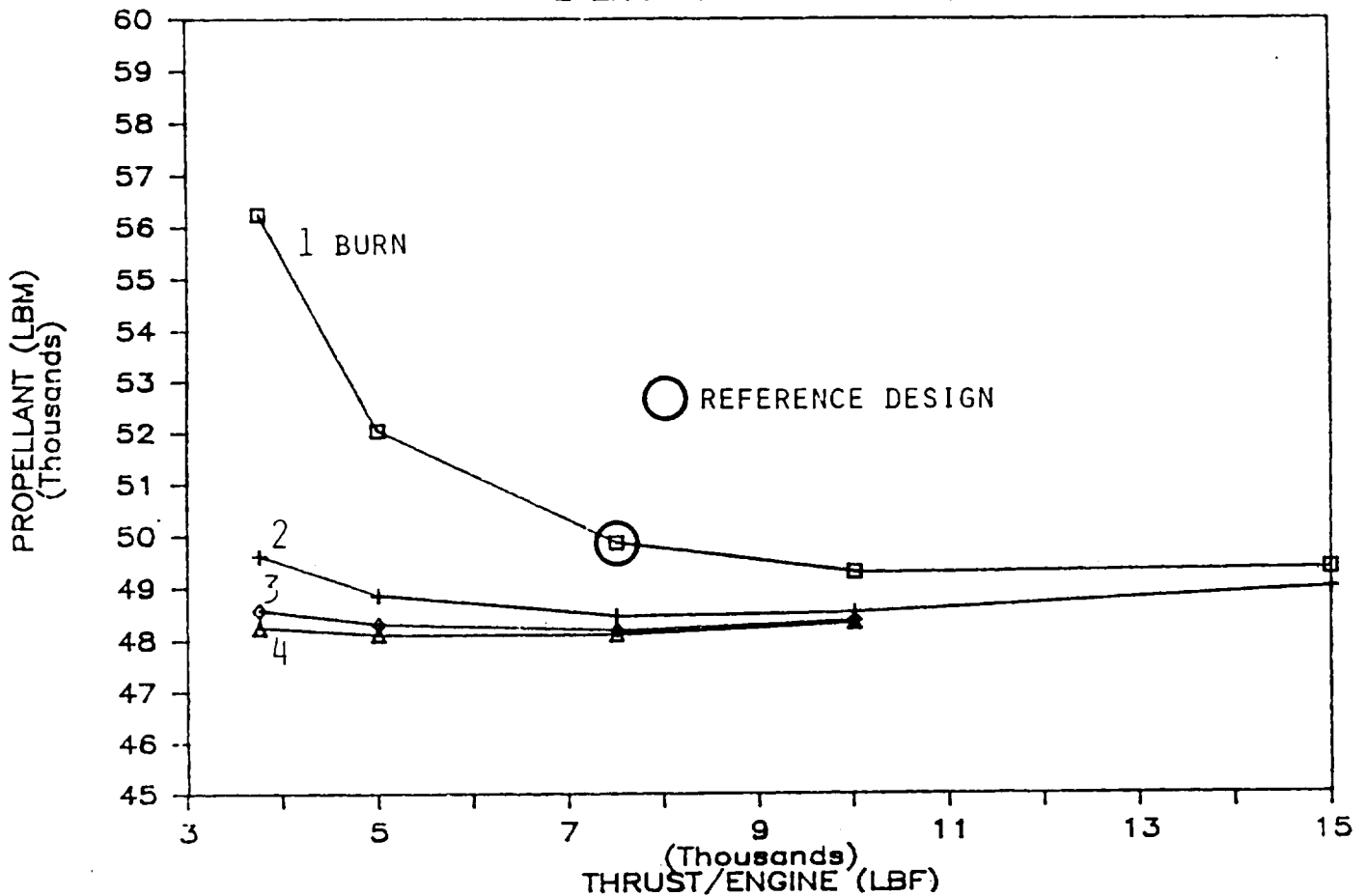


Figure 2.3-12 AOTV Thrust Level MMH/N₂O₄

The OTV low thrust missions require a maximum g-level 0.1. One option to provide low thrust was to use 7500 lbf engines for nominal missions and shut down and/or throttle the engines for the low thrust missions. Throttling storable engines, however, is inefficient with significant decreases in engine Isp as shown in Figure 2.3-14. Figures 2.3-15 and -16 illustrate some of the concepts and conditions in throttling a storable engine. This option was dropped in favor of mounting lower thrust engines for low-g missions. This solution is attractive under the assumption that the 3750 lbf XLR-132 engine under study at AFRPL will be developed to meet Air Force needs and will be available at no DDT&E cost impact. Development cost for the 7500 lbf engine was assumed to be paid by the OTV program. A mounting kit would be used to minimize OTV scar. The option would allow for both low and high thrust missions while minimizing the performance penalty on each mode of operation.

PERIGEE STAGE (ROCKETDYNE)

1 ENGINE 20 K DELIVERY

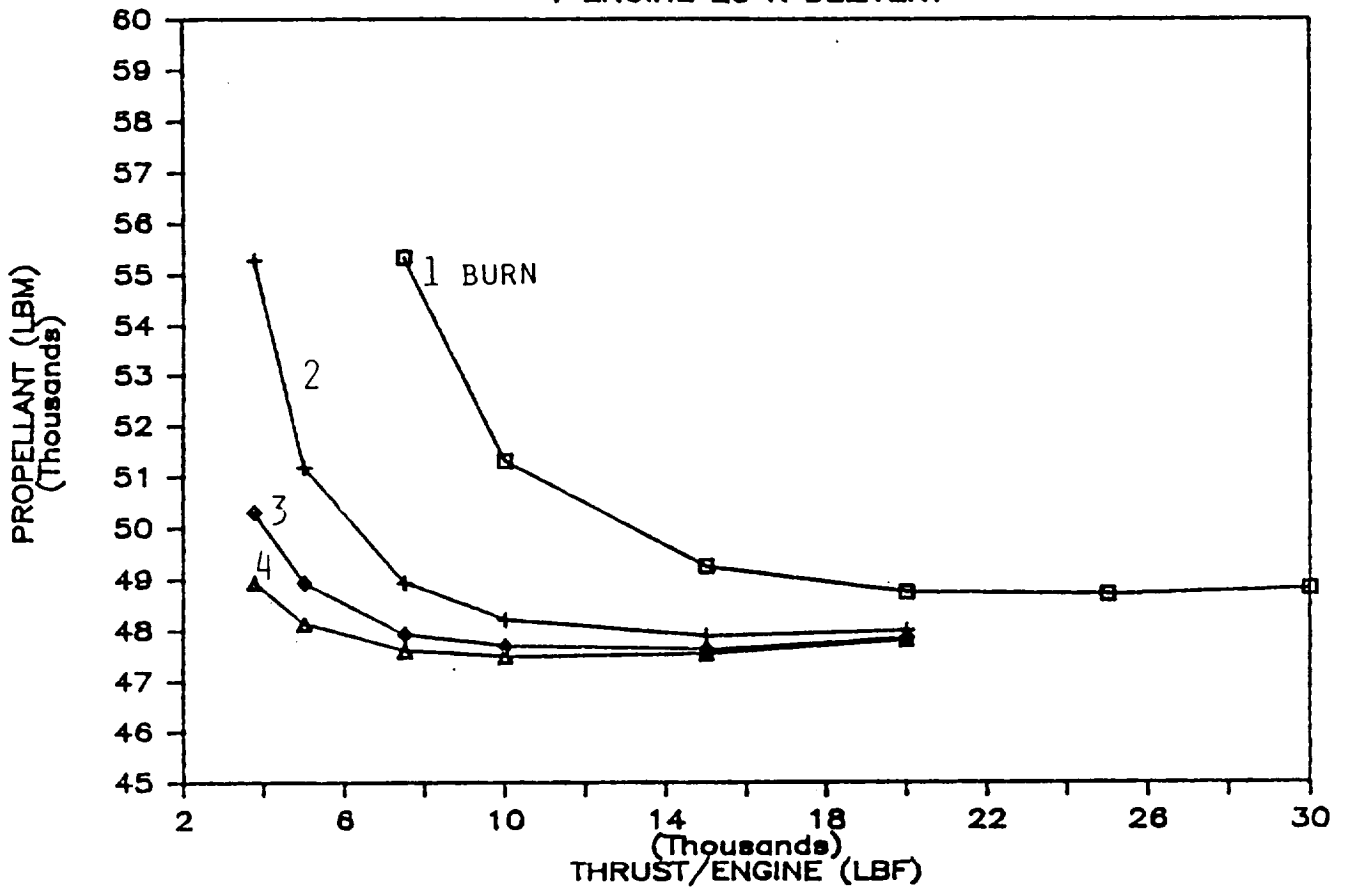
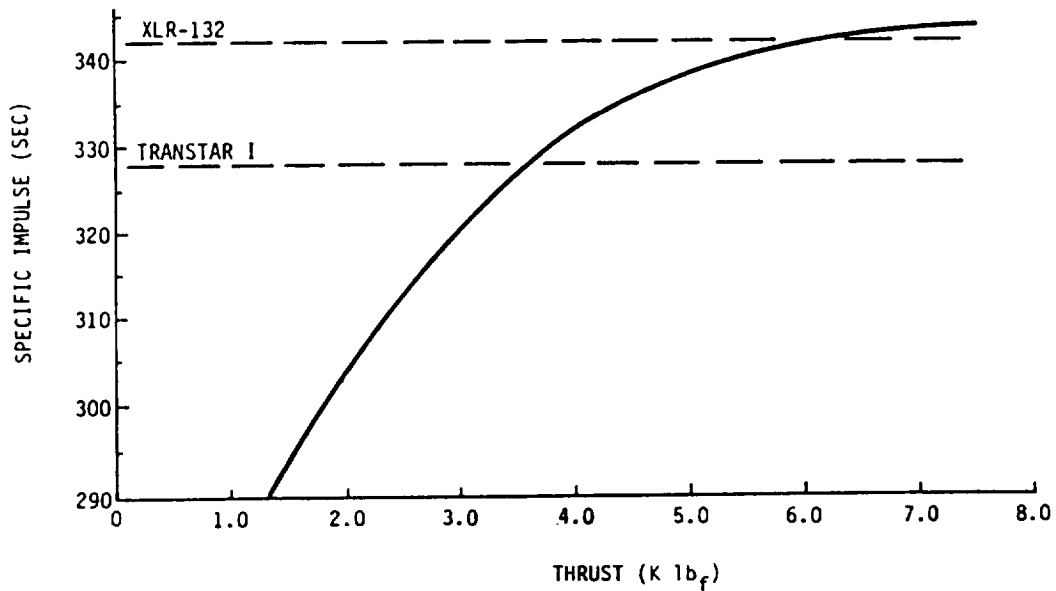


Figure 2.3-13 ACTV Thrust Level MMH/N₂O₄



SELECTED TWO 3750 LB_F XLR-132 FOR 0.1g MISSION

Figure 2.3-14 MMH/N₂O₄ Throttling Performance

- | <u>METHOD</u> | <u>CONCERNS</u> |
|---|---|
| <ul style="list-style-type: none"> • CHAMBER PRESSURE | <ul style="list-style-type: none"> • TWO-PHASE FLOW IN COOLANT JACKET • LOW PUMP FLOW COEFFICIENT • SYSTEM-COUPLED STABILITY |
| <ul style="list-style-type: none"> • CHAMBER FLOWRATE (PUMP RECIRCULATION) | <ul style="list-style-type: none"> • DURATION OF THROTTLED MODE • HEATING OF PROPELLANT • PUMP NPSH |

Figure 2.3-15 Engine Throttling (Rocketdyne)

ENGINE PARAMETERS	THRUST LEVEL, PERCENT (1)		
	100(2)	15	10
THRUST (LB PER ENGINE)	3750.	2280.	1550.
CHAMBER PRESSURE (PSIA)	1500.	910.	620.
MIXTURE RATIO	2.9	2.0	2.1
DELIVERED SPECIFIC IMPULSE (SEC)	341.	340.6	338.
PUMP SPEED (RPM)	64700.	46400.	36420.
NTO PUMP FLOW RATE (LB/SEC)	7.3	4.5	3.1
NTO PUMP DISCHARGE PRESSURE (PSIA)	2570.	1390.	887.
MMH PUMP FLOW RATE (LB/SEC)	3.8	2.2	1.5
MMH PUMP DISCHARGE PRESSURE (PSIA)	2070.	1080.	720.
NTO STATE AT COOLING JACKET DIS	LIQUID	LIQUID	2-PHASE
NTO COOLING JACKET DIS TEMP (°R)	750.	752	725.
NTO COOLING JACKET DIS PRESSURE (PSIA)	1950.	1090.	710.

(1) PERCENTAGE OF TOTAL CLUSTER THRUST

(2) DESIGN POINT

Figure 2.3-16 XLR-132 Throttling Conditions (Rocketdyne)

LH₂/LO₂--The initial LH₂/LO₂ screening included current, derivative, and advanced technology engines. The technology assessment is summarized in Table 2.3-4. Current and derivative engines were the Pratt & Whitney engines, whereas the advanced engines included the Pratt & Whitney, Rocketdyne and Aerojet designs. The level of technology required for an ACC OTV was evaluated by considering a single shuttle launch, single stage GEO delivery and calculating the propellants required to deliver a range of payloads to GEO and return a 1500 lb multiple payload adapter. The results for single derivative engine configurations, a two (7.5 K-lbf) engine RL-100 (Pratt & Whitney Advanced Engine), and a single (15 K-lbf) engine RL-100 configuration are shown in Figure 16. The RL10 IIB/IIIB engines were limited by packaging in the ACC to a single thrust chamber.

Table 2.3-4 LO₂/LH₂ Engine Technology Assessment

TECHNOLOGY LEVEL	FLIGHT ENGINE AVAILABILITY	ENGINE CANDIDATE POINT DESIGNS			
		ENGINE	Pc(PSIA)	ε	Isp(SEC)
1985	1990-	RL10-III (P&W)	400	400:1	470
	1991	RL10-IIB (P&W)	400	205:1	460
		RS44 (R/D)	1540	225:1	463
1990	1995	RL-100 (P&W)	1500	640:1	479
		RS44 ADVANCE	1540	625:1	481
		CORE (R/D)			
		RS44 - FULL	2000	1175:1	492
		CAPABILITY R/D			
		AJ23-154 (ALRC)	2000	1000:1	483

NOTE: NEW TECHNOLOGY ENGINE DATES BASED ON NORMAL GROWTH
ACCELERATED GROWTH COULD MOVE DATES BACK BY TWO YEARS

An OTV with a RL10A-3-3B or RL10-IIC cannot capture the 12.2 K-lbm driver mission without exceeding the STS lift limit. STS lift capability was based on 72,000 lbm to LEO including ASE and ACC. The net lift capability for OTV, payload, and propellant was 67,190 lbm. The derivative engines, RL10-IIB and RL10-IIIB, nearly capture the drive mission within the STS limit. Either engine could be used with an optimized vehicle. The advanced RL-100 easily captured the ground based mission. If STS performance does not reach 72K, the advanced engines would be required for the ground based cryogenic OTV.

Space-based cryogenic engine optimum geometry was determined for the advanced expander cycle engines as a function of thrust level and numbers of engines. Propellant impacts included those due to changes in Isp, aerobrake diameter, and stage dry mass. Pratt & Whitney and Rocketdyne data were used. Resulting optimum expansion ratio for a two-engine configuration is shown in Table 2.3-5. The primary reason for the difference between the two manufacturer's data is in performance at high area ratios. Pratt & Whitney does not predict an improvement in Isp at higher area ratios as compared to Rocketdyne's data. We have used the data as provided by the manufacturers.

Table 2.3-5 Engine Data Summary

Rocketdyne Data						Pratt and Whitney Data				
Thrust (LBF)	Length (in)	ε	ISP (SEC)	DIA (IN)	WT (LB)	Length (LBF)	ISP (SEC)	DIA (IN)	WT (LB)	
3.0K	111	1200:1	488.8	42.9	155	80	600:1	473	34.3	200
5.0K	111	1000:1	488.5	46.3	184	88	600:1	476	40	245
7.5K	111	900:1	487.8	51.9	240	112	600:1	476.2	48	300
10.0K	111	800:1	487.1	52.9	255	116	600:1	476.5	50	320
15.0K	111	600:1	485.8	52.7	318	120	600:1	478.5	54.3	375

Using the optimum expansion ratio engines, the optimum thrust level was determined for up to 4 perigee burns including finite burn losses. One and two engine configurations using Pratt & Whitney and Rocketdyne data were considered. The impact of multiple perigee burns on performance is presented in Figures 2.3-17 thru -21. A cost trade on multiple perigee burns was performed to determine the system impacts in selecting the desired number of burns. The trade considered propellant delivery cost, operation costs, mission loss cost, and cost impact of more frequent engine changeouts. Propellant cost was \$1500/lbm for STS Tanker delivery and \$500/lbm for scavenged. Operation costs were \$109K/hr based on a 5 man shift. Mission loss cost in this analysis was \$388M/loss. The total cost assumed for engine changeout, transportation and unit cost was \$9M per engine set. Thrust levels used were 1 perigee burn at 10K, 2 perigee burns at 6K, and 3 and 4 perigee burns at 4K. Figure 2.3-22 presents the results relative to the single burn mode. The net savings were maximized with two perigee burns. More than two perigee drive up operation, mission loss, and engine costs faster than propellant savings. The net cost savings for 2 perigee burns was less than \$1M/flt at a propellant delivery cost of \$1500/lbm and 10 hr engine life. The

- LEGEND
- RL10-II B
 - + RL10A-3-3B
 - ◇ RL10-IIIB
 - △ RL-100
 - × RL-100 (2 ENG)
 - ▽ RL10-II C

PRATT & WHITNEY DATA

57K STAGE OFFLOADED, 1500 LBM P/L DOWN

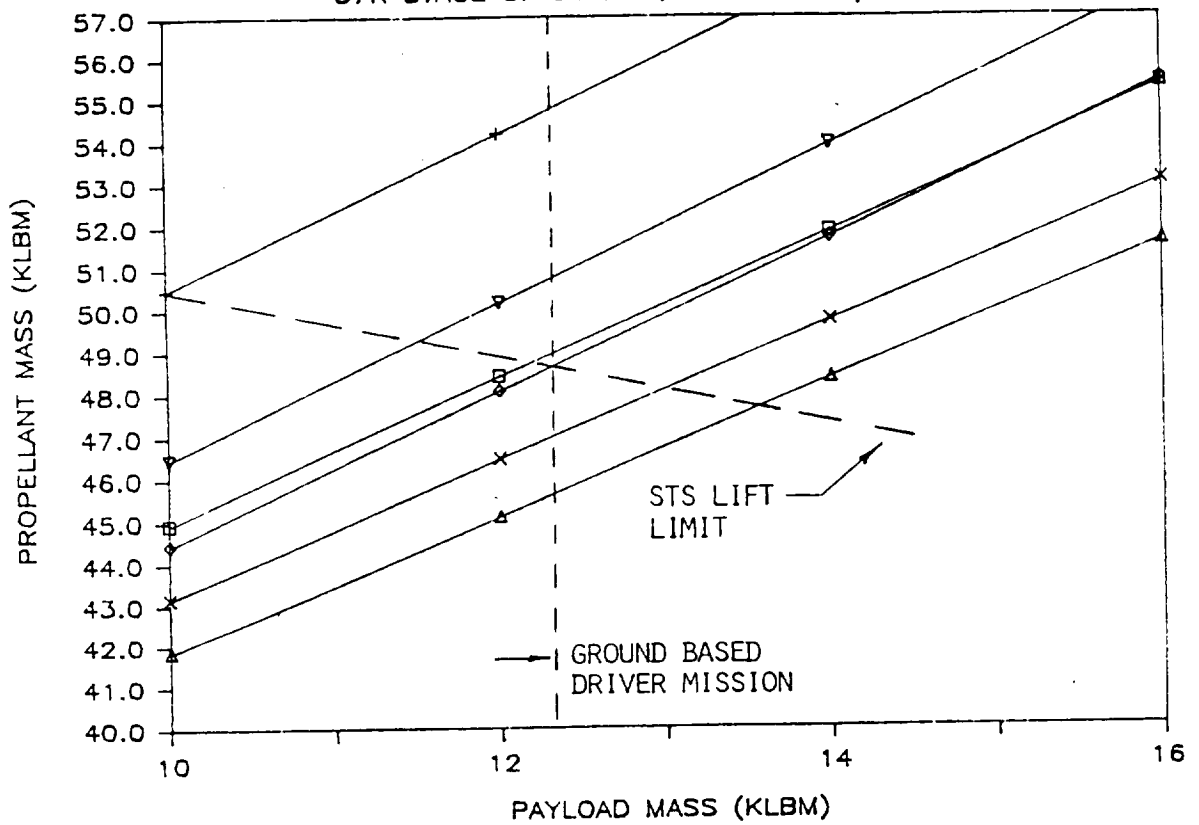


Figure 2.3-17 Ground-Based LH₂/O₂ Engine Selection

MULTIPLE PERIGEE BURNS— PRATT & WHITNEY

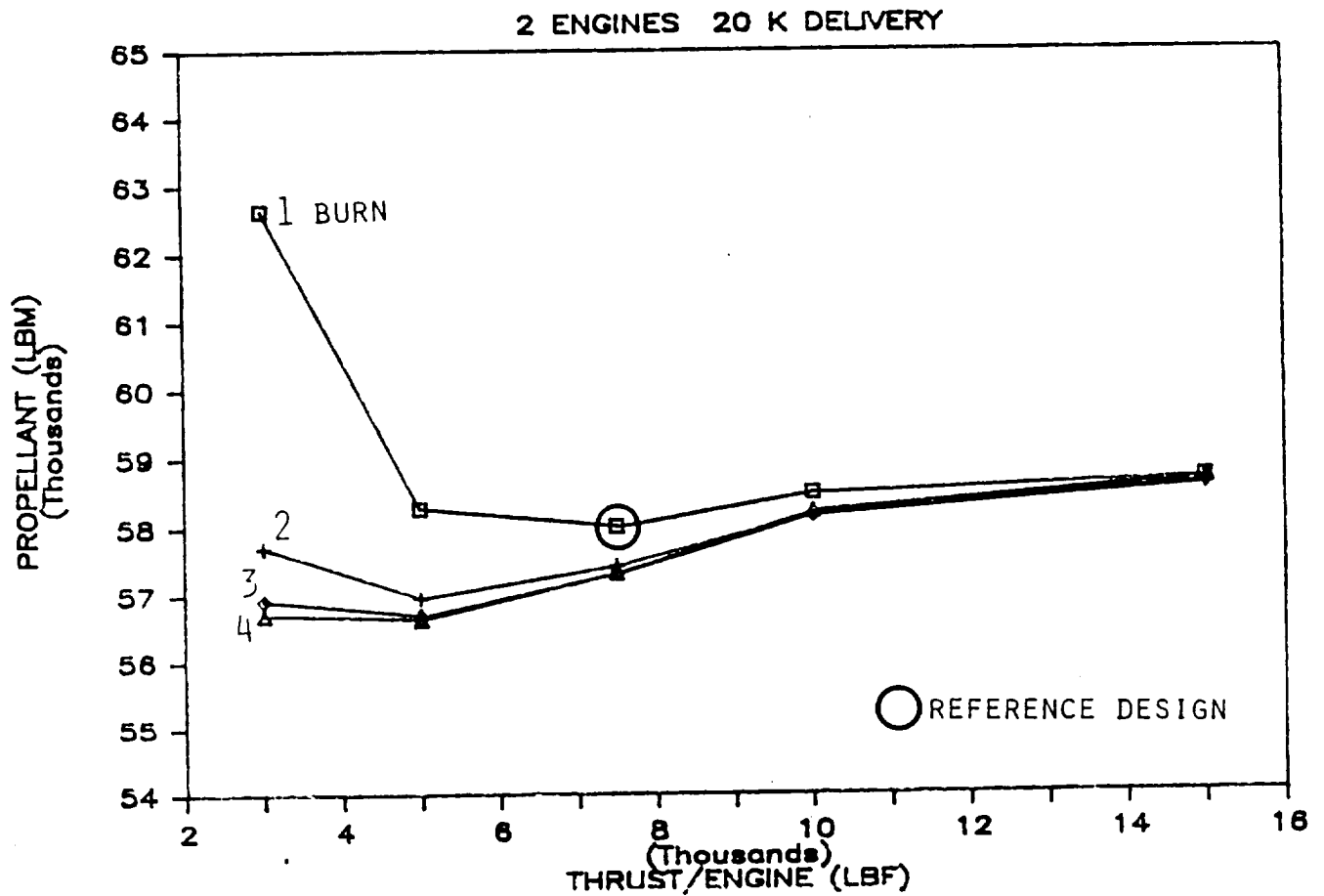


Figure 2.3-18 AOTV Thrust Level LH₂/LO₂

ROCKETDYNE MULTIPLE PERIGEE BURNS—

2 Engine 20 K DELIVERY

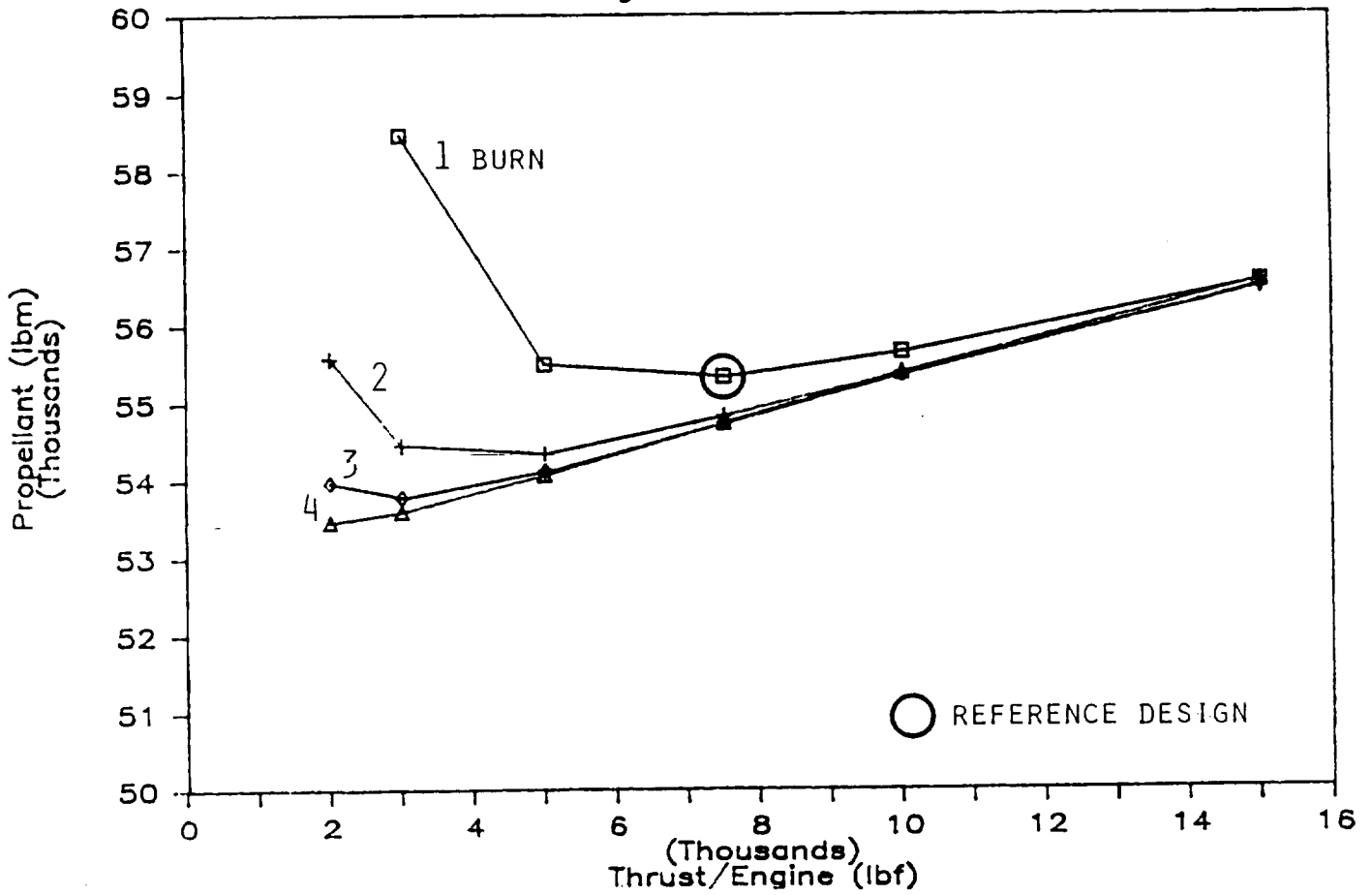


Figure 2.3-19 AOTV Thrust Level 1 LH₂/LO₂

MULTIPLE PERIGEE BURNS— PRATT & WHITNEY

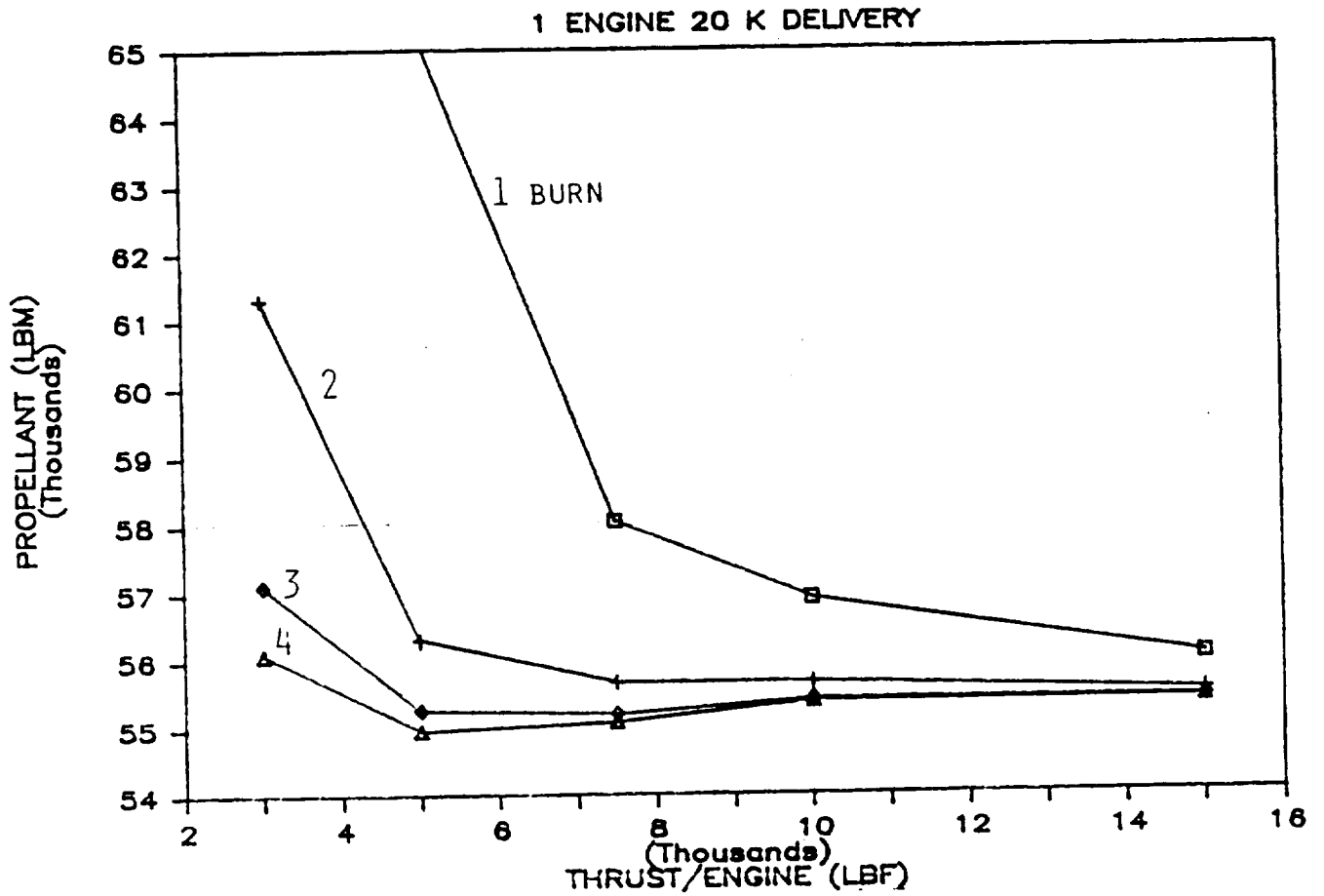


Figure 2.3-20 AOTV Thrust Level LH₂/LO₂

MULTIPLE PERIGEE BURNS— ROCKETDYNE

1 Engine 20 K DELIVERY

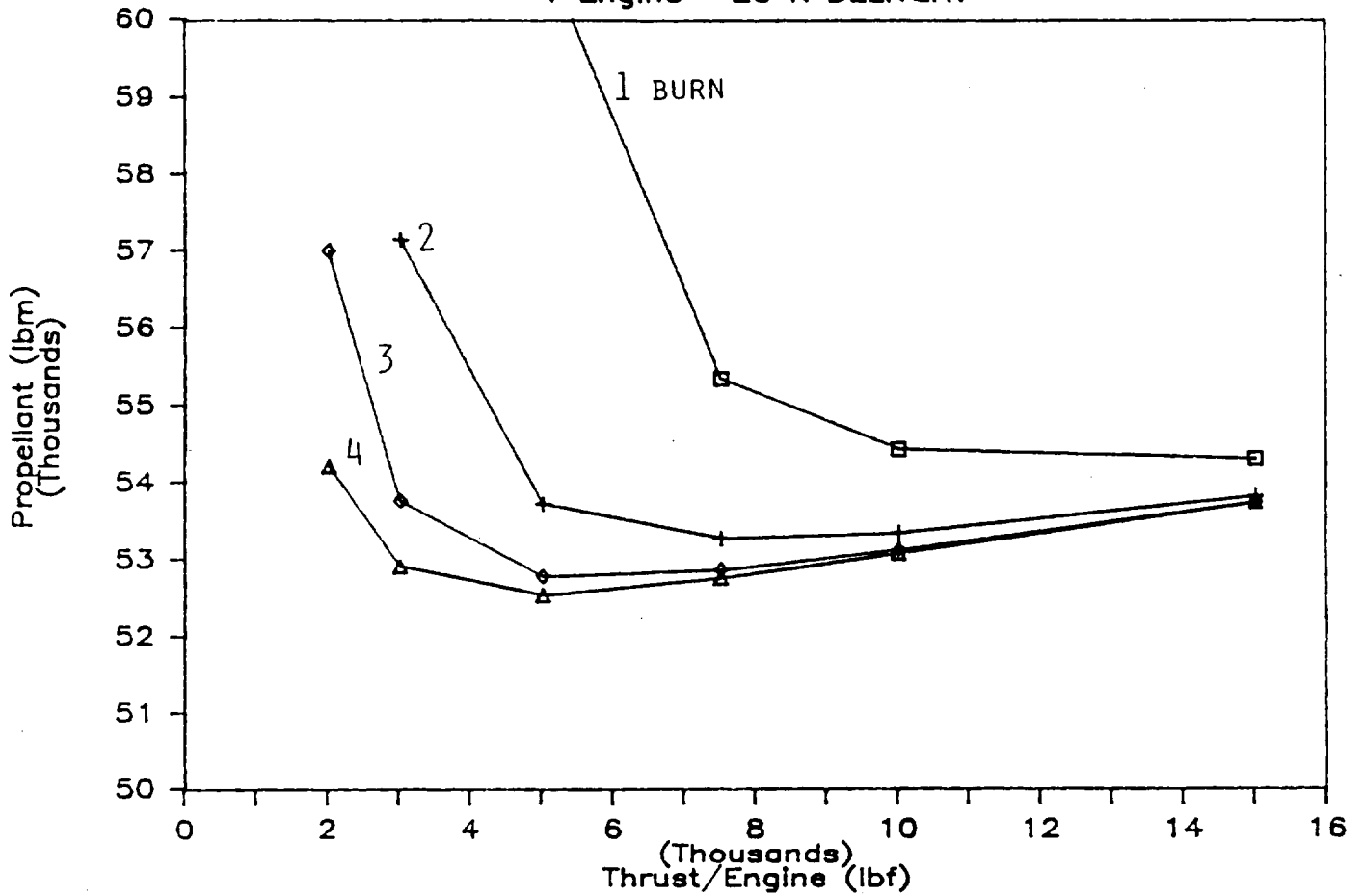
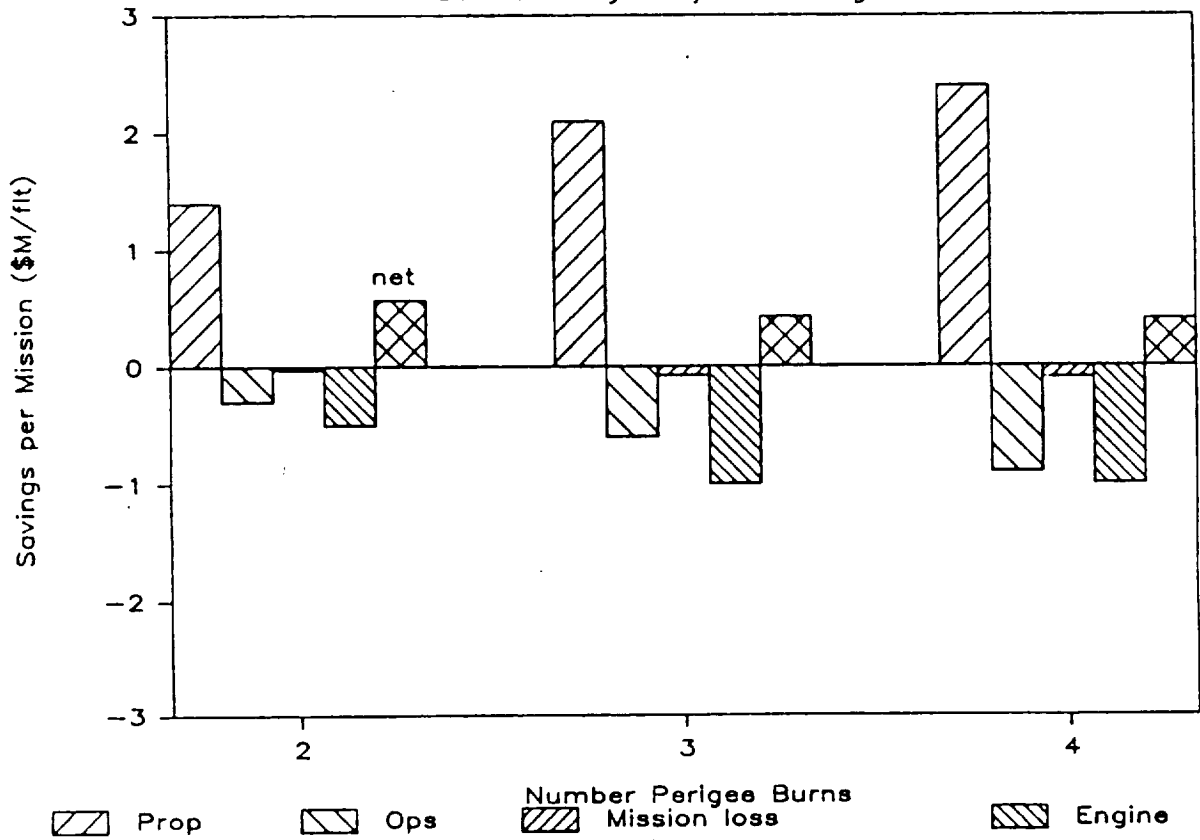


Figure 2.3-21 AOTV Thrust Level LH₂/LO₂

Multiple Burn vs Single Perigee Burn

20 k Delivery LH₂/LO₂ 2 Engines



RECOMMEND SIZING FOR 1 PERIGEE BURN

Figure 2.3-22 Multiple Burn Cost Trade

engine life was assumed to be constant with thrust. The cost was reevaluated after midterm with 15K, 10K, 6K, and 4K thrust levels for 1 through 4 burns, respectively, \$500/lbm propellant delivery cost, and 5 hr life. Figure 2.3-23 shows the cost savings were eliminated. Two 7500 lbf engines and one perigee burn were selected for sizing the space-based LH₂/LO₂ OTV. The 7.5K engines also allow for growth and are better for planetary missions. Figure 2.3-24 illustrates the effect of thrust on a high energy planetary mission. Multiple perigee burns are difficult to perform with planetary missions because of the large perigee delta V. Lunar missions, however, were found to be reasonably performed with 2 perigee burns.

MULTIPLE PERIGEE BURN COST TRADE

SAVINGS OVER SINGLE BURN, 2 ENGINES

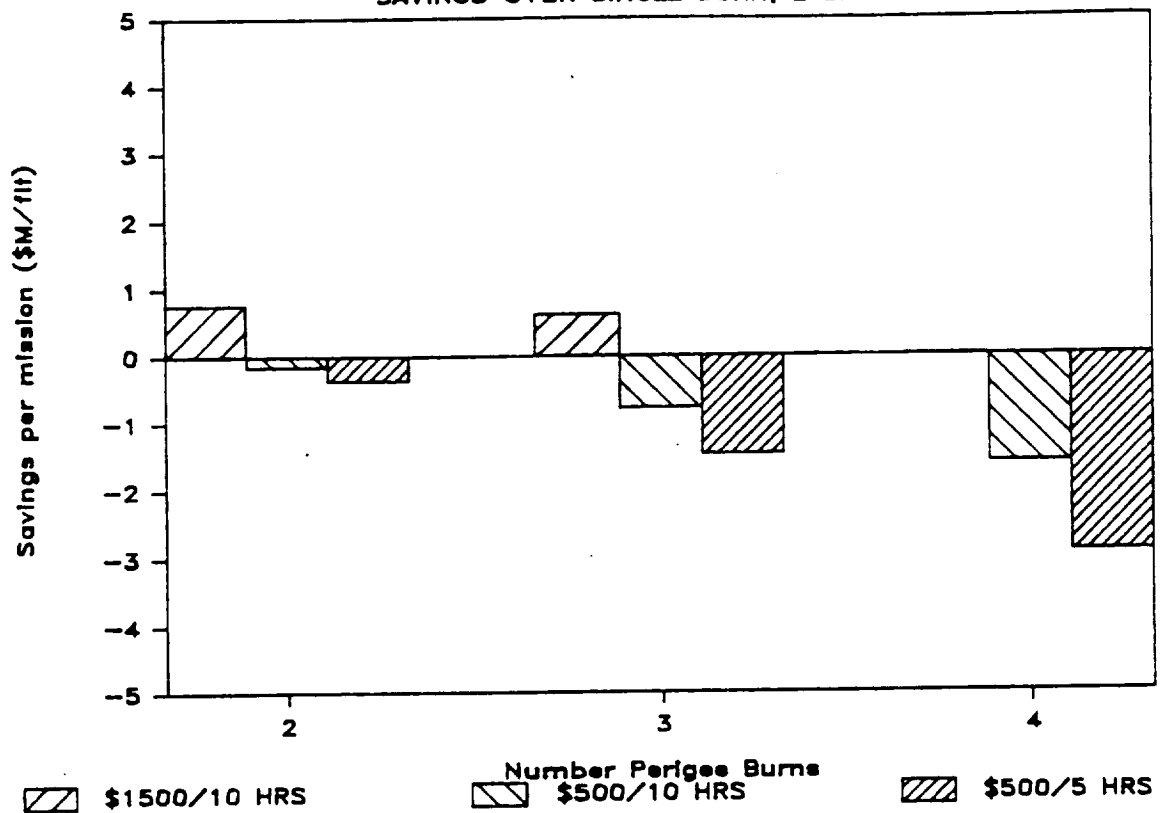


Figure 2.3-23 Multiple Perigee Burn Cost Trade

The low thrust (0.1g) mission and its impact on the engine were evaluated. Step throttling vs continuous thrust was considered. For step throttling the thrust was lowered to 3.2K for the entire mission. Velocity losses would be controlled with multiple perigee burns. Continuous throttling had the advantage of throttling the engine to the maximum thrust allowable with decreasing stage mass which minimizes the Isp losses and velocity losses. However, since this was found to require a significant burn time multiple perigee burns would also be used. Isp losses could also be contained by "kitting" the injector for the lower thrust.

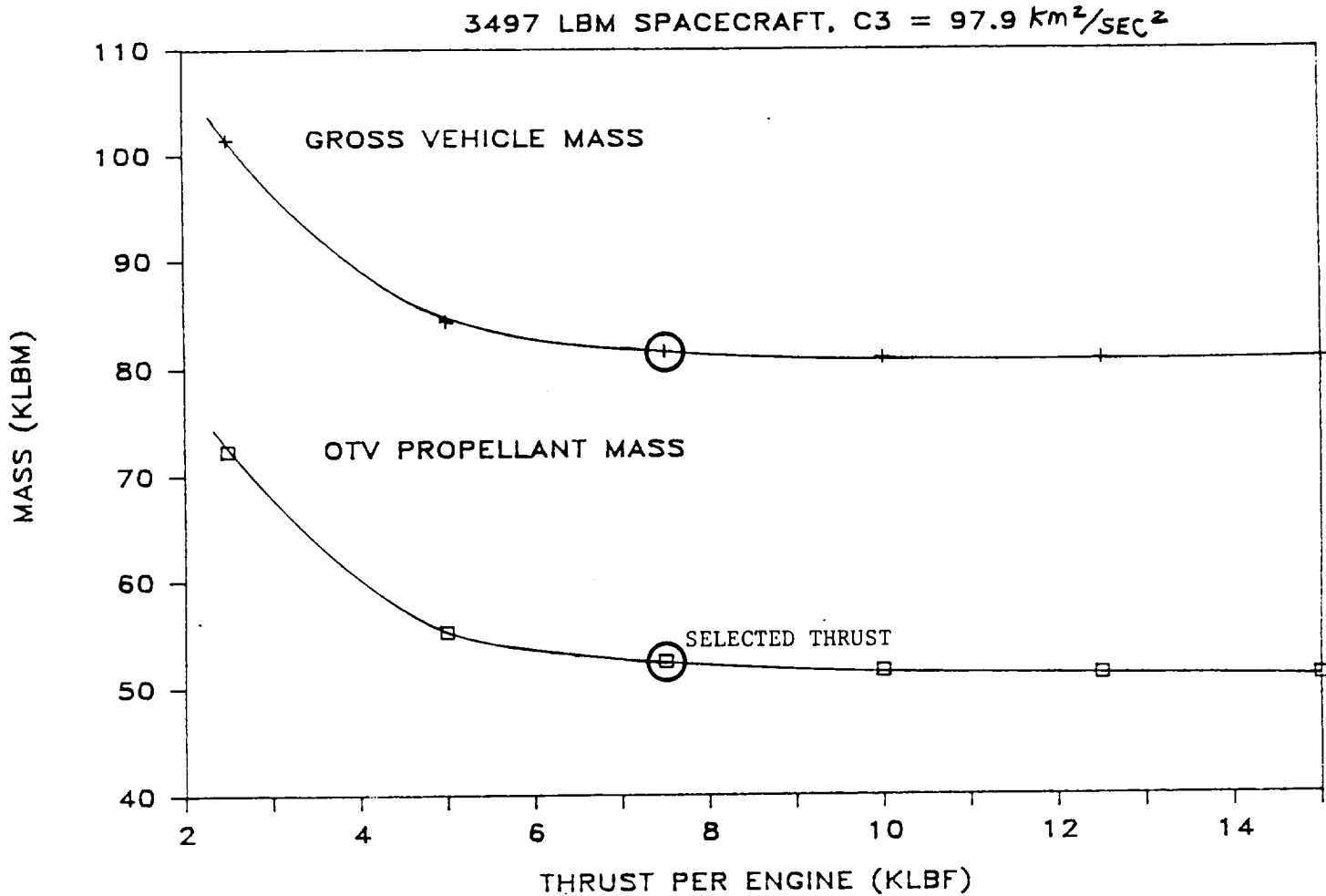


Figure 2.3-24 OTV Planetary Mission Thrust

The analysis shown in Figure 2.3-25 compared the propellant required for an ideal impulsive burn (no velocity losses and constant I_{sp}) to step throttling with a 10 sec (2%) I_{sp} loss. This provided an order-of-magnitude assessment of the penalty for step throttling to determine the cost-benefit of improving low thrust capability. The multiple burn case in this analysis used a 20 fps RCS mid-course correction between each burn as an additional penalty. The larger dry mass was due to larger tanks. The net effect was about 4000 lbm of propellant over the idealized case. The benefit of approaching the ideal, impulsive burn was determined by the cost of the propellant for both the low and nominal Rev 8 mission model. The results show that the present value of the saving is not sufficient to justify the additional engine development for the small number of low-g missions. In constant \$85 the LCC cost savings, approximately balances the DDT&E cost.

DRIVER: MAXIMUM THRUST WITH 20 KLbm PAYLOAD <0.1g

STAGE MASS (LBM)	ISP (SEC)	RESIDUALS (LBM)	BOIL-OFF (LBM)	USABLE PROP RCS, MPS & FUELLCELL (LBM)	20FPS PERIGEE CORRECT (LBM)	TOTAL PROP (LBM)
IMPULSIVE BURN (IDEAL CASE) 7271	475 @ 6:1	850	275	55033	75	56233
4 PERIGEE BURNS 1-7.5K STEP THROTTLED TO 3.2K 7315	465 @ 6:1	850	325	58824	390	60389
DELTA PROPELLANT						4156

DELTA LIFE-CYCLE COST @ \$1500/LBM

	PRESENT VALUE \$85	CONSTANT \$85
LOW MODEL 6 MISSIONS	\$5.2M	\$37M
NOMINAL MODEL 7 MISSIONS	\$8.6M	\$43M

CONTINUOUS THROTTLING DDT&E COST VARY FROM ~ \$20M (CONTROLLER) TO ~ \$50M (CONTROLLER AND INJECTOR MODIFICATIONS)

STEP THROTTLING TO ~3.2K RECOMMENDED FOR 7.5K ENGINE

Figure 2.3-25 LH₂/LO₂ Engine Step Throttling

TWO POSITION NOZZLES--The use of two position nozzles for the MPS engines on the OTV provides two benefits. First, the radiation cooled portion of the engine can be extended outside the aerobrake, thus reducing the insulation requirements that would be imposed if the engine were installed submerged in the OTV structure. Secondly, the two position nozzle provides a stage weight reduction because the stage length and diameter and the aerobrake can be reduced and still provide similar wake heating protection to the stage.

The two position nozzle MPS engine is shown in Figure 2.3-26 with the radiation cooled section in the stowed or retracted position. The nozzle is split at the expansion ratio where the engine changes from regenerative cooling to radiation cooling. The retraction/extension mechanism will consist of three equally spaced electro-mechanical screw jacks that can be commanded to translate the radiation cooled skirt. This system design would require fail operational capability for retraction and fail safe to deploy.

ORIGINAL PAGE IS
OF POOR QUALITY

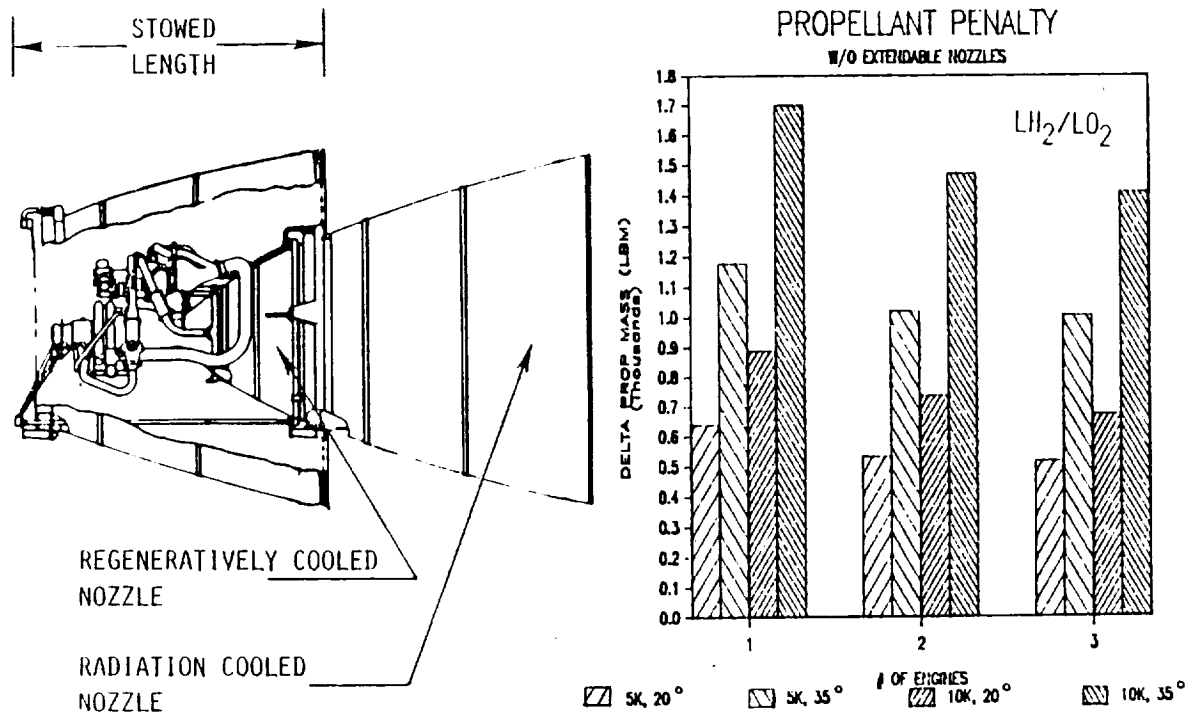


Figure 2.3-26 Extendable Nozzle Trade

The two position nozzle extends the radiation cooled skirt outside of the aerobrake when the MPS engines are firing. This minimizes the exhaust plume impingement. Also, the nozzle can radiate its heat directly to space, rather than to the interior of the vehicle as in the submerged nozzle case.

The two position nozzle also allows positioning the aerobrake at the start of the radiation cooled section of the MPS engines. This weight impact on the stage, considering the aerobrake diameter, aerobrake door weight, and the weight of the nozzle extension hardware is shown in Figure 2.3-26 for 1, 2, and 3 MPS engines for 5K and 10K engines. The average saving is 400 lbs of dry weight. The propellant weight savings is 1260 lbs/flight.

SUMMARY--The MMH/N₂O₄ engine thrust for a perigee stage was 7500 lbf with an area ratio of 600:1. An engine based on the XLR-132 design was selected. The stage was sized with a single perigee burn for the nominal mission, and 4 perigee burns for the 0.1g low thrust transfer mission using a single XLR-132 engine of 3750 lbf. The low thrust is based on the assumption that the XLR-132 @ 3750 lbf will be available as an off-the-shelf item in 1996.

The LH₂/LO₂ MPS engine thrust appears to be independent of engine manufacture. The area ratio is not independent of engine design. The LH₂/LO₂ stage should be sized for a single perigee burn and 2, 7500 lbf engines. The program recommendation at the mid-term was the advanced expander engine based on life cycle cost. The ground based OTV engine selection criteria is low DDT&E and 1987 technology, but to improve evolution and life cycle cost of the space-based OTV, an advanced engine was selected for both. Accelerated development of the LH₂/LO₂ advanced expander cycle engines would improve their availability so that they could be used for the ground-based OTV. A more detailed cost assessment of LH₂/LO₂ engines was conducted after midterm and is discussed in the next section.

2.3.3 LH₂/LO₂ Engine Selection

COST--Engine Cost data are shown in Table 2.3-5A. An initial operating capability (IOC) engine cost was derived from discussions with engine contractors and MSFC in order to identify a lower cost OTV program. The approach taken was, how much should the OTV program invest in an engine; as opposed to what do the two extremes cost. The RL10 derivatives and advanced engine costs were ground ruled by MSFC. We visited Aerojet, Pratt & Whitney, and Rocketdyne during the latter half of the program to understand the cost and performance issues of derivative and advanced engines. Our conclusion was that the advanced engine performance and cost could be reduced to obtain an IOC engine option. This cost assessment was not with the total agreement of

Table 2.3-5A Martin Marietta Cost Estimates

	ISP, SEC	** DDT&E \$M	Unit \$/ENG	Refurb. \$/ENG	OPS \$/YR	Life* (HRS)
RL 10-IIB 15K-LBF	460	98.2	1.99	0.6	11	5 Hrs
RL 10-III 7.5K-LBF	470	104.4	2.0	0.6	11	5 Hrs
IOC Engine 7.5K-LBF	475	175	2.85	1.0	11	5 Hrs
Advanced Engine 7.5K-LBF	483	350	3.0	1.0	11	10 hrs

* MTBO - Assume One Overhaul

** Includes Testing and Integration Excluding Fee, Propellant, and Testing at Government Facility

all the engine contractors. The 7500 lb+ IOC engine can meet the Rev 8 Mission Model and should be designed to evolve to a more advanced engine if future missions dictate, and funding constraints allow. However, it was found at this point in the study that a single engine used throughout the OTV program was preferred. Figure 2.3-27 shows the payback options referenced to the RL 10A-3-3B.

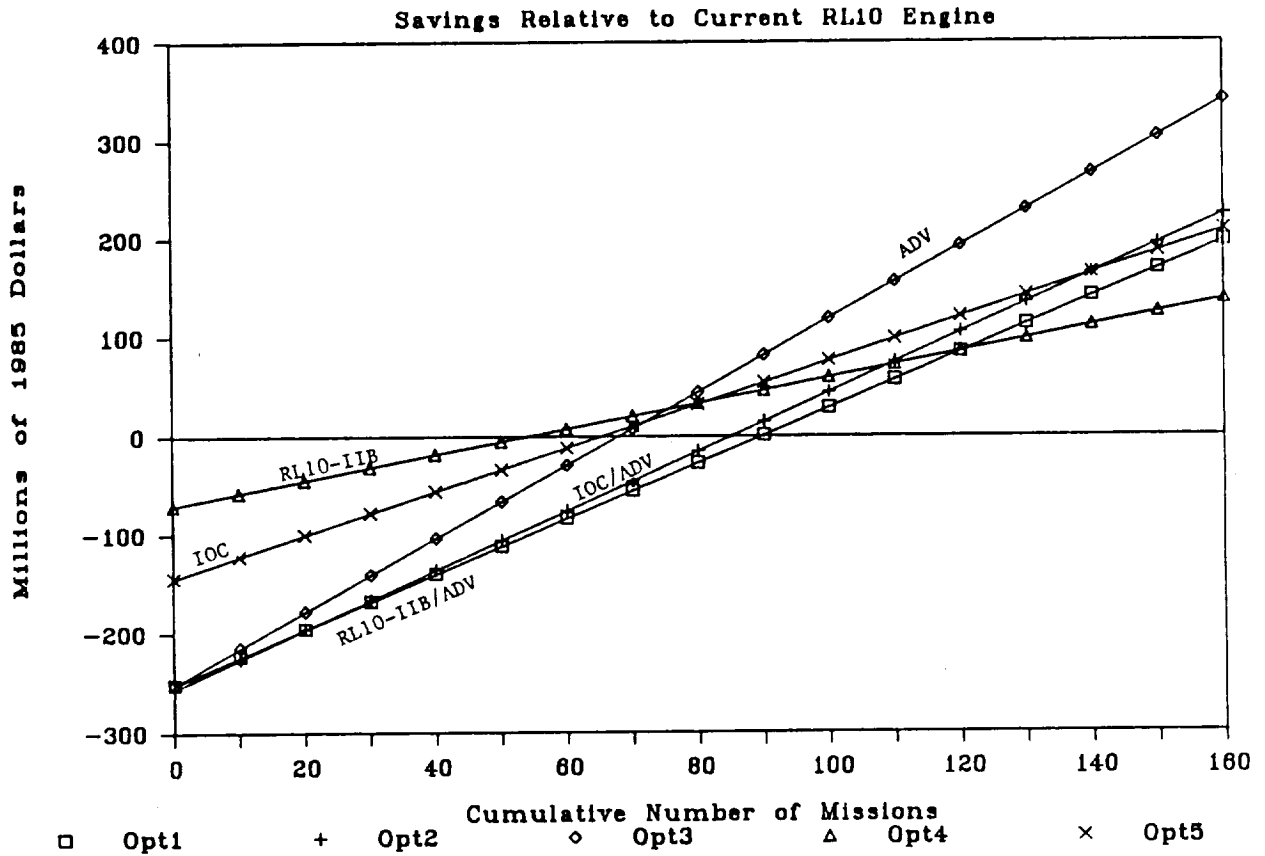


Figure 2.3-27 Engine Payback for Various OTV Engines

Other economic factors considered were Life Cycle Cost (LCC), Return On Investment (ROI), DDT&E, and Cost Per Flight (CPF). More detail is contained in Volume III OTV Systems and Program Trades, Sec 3.1.5.

Another advantage to a single engine development program and developing a new engine as soon as possible is illustrated in Figure 2.3-28.

Rev 8 Mission Model (Start 1994)
Milestones

Nominal		1997	1998	2002	2006
Engine History	Hours (accum)	20	34	92	153
	Starts (accum)	252	420	1140	1896
Low		1999	2004	2008	2015
Engine History	Hours (accum)	20	61	98	120
	Starts (accum)	252	756	1212	1488
First Launch OTV (1994)	Driver Mission: 12000/0, 1 7500 LBF Engine, Unmanned.				
Growth Space Station (1997)	Driver Mission: 20000/0, 2 7500 LBF Engines, Engine-out ORU (Orbital Replacement Unit)				
Operational GEO Platform (1998)	Driver Mission: 20000/0, Step Throttling				
Manned GEO Sortie (2002)	Driver Mission: 7500/7500, MAN Rating Required				
Manned Lunar Sortie (2006)	Driver Mission: 80000/15000				
Reliability With Flight Program:	Space Based:	.9995			
	Manned Mission	.9997			

Figure 2.3-28 Time Phased Engine Requirements

The key Rev 8 mission model milestones are related to the OTV engine requirements. The initial ground-based missions can be done with a single 7500 lbf engine with little performance penalty. Prior to the manned mission, the OTV engine will have accumulated up to 1140 starts which results in a 6 burn, 2 engine mission reliability of .9997 (non-independent failure factor = .05). This assumes 700 accountable tests during the development program and all flight successful. Total accumulated run time of the OTV engine in space will be 330,600 sec.

The OTV engine at the beginning of space-basing will have accumulated 73080 sec of mission burn time. The reliability for a 2 engine OTV at this time can be as high as .9995 with the same assumption noted above and 252 starts.

ENGINE REQUIREMENTS--The recommended requirements for the initial operational capability liquid hydrogen/liquid oxygen OTV engine are given in Table 2.3-6. They were derived from the analysis presented in this section (2.3). The dimensions were based on the engine optimization done for both the Pratt & Whitney RL-100 and the Rocketdyne engine. The engine exit diameter affected the spacing between engines and gimbal requirements with the attendant impacts on stage length, aerobrake diameter, and engine doors. Engine stowed length had a direct effect on both the stage length and aerobrake diameter. A two position nozzle was used.

Table 2.3-6 Recommended IOC Engine Requirements

	REQUIREMENT	RATIONALE
PERFORMANCE	> 475 SEC @ 6:1 MR	COST TRADE BETWEEN EXISTING AND ADVANCE TECHNOLOGIES. MINIMUM ISP.
THRUST	7500 Lbf	PERFORMANCE ANALYSIS- SINGLE PERIGEE BURN AND 2 ENGINES
MASS	280-300 LBm	PERFORMANCE ANALYSIS OF 2 ENGINE VEHICLE
DIMENSIONS DIAMETER	< 50"	VEHICLE OPTIMIZATION WITH FIXED AERBRAKE AND 2 ENGINES GIMBALLED THRU C.G. WITH 20 DEG MAX GIMBAL.
LENGTH	< 60" STOWED < 120" EXTENDED	
PRESSURIZATION AND CHILLDOWN	GO2/GH2 PRESSURIZATION THI START @ 15 PSIA NPSH 15' H2, 2' O2	NON-CONDENSIBLE PRESSURANT COMPLICATES ON-ORBIT REFILL, ELIMINATES GHE PRESSURIZATION.
THROTTLING	STEP THROTTLING 50% @ >465 SEC	REV 8 MODEL CONTAINS 6-7 LOW THRUST MISSIONS. CONTINUOUS THROTTLING COMPLICATES ENGINE DEVELOPMENT.
AERBRAKE IMPACTS	LAST FIRING 1 HR BEFORE AERO-MANEUVER FIRING 10 MIN AFTER EXIT ATMOSPHERE	THI USED FOR MID-COURSE, COULD BE USED FOR RAISING PERIGEE AFTER AEROPASS
DEVELOPMENT COST	\$175M, 60 MOS	5 HR LIFE, MINIMIZE TECHNOLOGY RISK, ENTIRE ENGINE IS ORU

Aerobrake impacts illustrate the time available to retract nozzles and close protective doors. The requirements were selected to minimize development cost. The low DDT&E reflects reduced engine life testing, as well as reduced performance requirements. Advanced engine technology programs should also be focused to reduce DDT&E program risk.

RECOMMENDATION--The LH₂/LO₂ engine selection is summarized in Figure 2.3-29. The IOC engine was not the optimum, but was a compromise between the low DDT&E of the RL10 derivatives and the long term benefits of the advanced engines. The recommendation is that a lower capability advanced engine be developed for the entire OTV program. Further study should be directed towards the cost sensitivity of OTV engine performance and attributes.

	<u>PRO</u>	<u>CON</u>
RL-10 DERIVATIVES	o HIGHEST ROI o LOWEST DDT&E o PROVEN FLIGHT RELIABILITY o 54 MISSION PAYBACK	o HIGH LCC o GROWTH LIMITED & MASSIVE o LOWEST BENEFITS
ADVANCED ENGINES	o LOWEST LCC o GREATEST BENEFITS o LOWEST CPF o MODERATE PAYBACK AND ROI	o HIGHEST DDT&E o SCHEDULE RISK
IOC ENGINE	o GROWTH CAPABILITY o GOOD PAYBACK PERIOD, ROI o LOW DDT&E	o HIGH CPF o LOW BENEFITS

ALTERNATIVES BETWEEN ADVANCED ENGINE AND EXISTING TECHNOLOGY EXIST

RECOMMENDATION: IOC OTV ENGINE
475 SEC \$175 DDT&E

Figure 2.3-29 Main Engine Recommendation

2.3.4 Space Maintenance of Propulsion Systems

A trade study was performed to determine the advantage of modular main engines. Modular main engines refers to orbital replacement (organizational level maintenance) of engine components such as turbopumps, nozzles, etc. The turbopumps were found to be the critical component for engine life, and the largest cost was found to be transporting the long engines. Therefore, orbital replacement of pumps was compared to replacing the entire engine which would be transported to the ground for overhaul (depot level maintenance). The trade is summarized in Table 2.3-7.

The first two columns of Table 2.3-7 list the modular Turbopump Assembly (TPA) options. One engine overhaul was assumed and would consist of replacing the TPA only. The TPA would therefore contain the additional valves and components that have a high failure rate. The module was estimate at 40 lbm each or 80 lbm for the fuel and oxidizer modules for an engine. The IVA time for TPA replacement was estimated from our Space Station accommodation studies and data supplied by Rocketdyne. IVA cost was estimated at \$16,000/hr. The engine recurring cost was representative of Pratt & Whitney and Rocketdyne data and the refurbishment was estimated at 1/3 of the initial engine cost. The total engine servicing cost for the modular TPA options was the sum of

Table 2.3-7 Modular Turbopump for New Engine

	FUEL AND OXIDIZER TURBOPUMP REPLACEMENT		ENGINE REPLACEMENT
	ON OTV	OFF OTV	
MASS	40 LB/EACH	40 LB/EACH	290 LB EACH(20% ASE)
LENGTH	--	--	6 FT (APPROX)
DIAMETER	--	--	5 FT (APPROX)
VOLUME	1.2 FT ³ /EACH	1.2 FT ³ /EACH	118 (CYLINDER)
TRANSPORTATION COST*			
MASS	\$240K	\$240K	\$870K
CARGO BAY CHARGE	\$31K (VOL)	\$31K (VOL)	\$6.85M (LENGTH)
IVA TIME	9.5 HRS	14.5 HRS	5.0 HRS
IVA COST	\$152K	\$232K	\$80K
TOTAL SERVICING COST	\$392K	\$472K	\$6.93 M
REFURBISHMENT COST+	\$2 M	\$2 M	\$2 M
ENGINE COST*	\$6 M	\$6 M	\$6 M
TOTAL ENG. REPLACE- MENT COST**	\$15.322 M	\$15.402 M	\$21.86 M
COST SAVINGS	\$6.538 M	\$6.458 M	REF

* 2 ENGINE SET

+ ESTIMATE AT 1/3 ENGINE COST

** ONE REFURBISHMENT

initial transportation of the entire engine, transportation of the TPAs, unit and refurbishment cost, and onorbit maintenance time. The cost is shown for replacement of the TPA with the engine on the stage or the engine removed and the TPA removed in a fixture in the Space Station hangar. The major difference was access problems and IVA time.

Similar cost breakout is shown for replacing the engine onorbit and transporting the engine to the ground for overhaul. It was found that the major cost for this option is the transportation of the entire engine because it pays by length, not mass. The length was determined by placing two engines side by side to reduce the length in the payload bay and retracting the nozzles. Since the cost is by length, it does not matter if the retracted nozzle extension is transported. The total servicing cost was the sum of transporting the engine to orbit twice, unit and refurbishment cost, and onorbit maintenance. Return-to-earth cost was considered negligible.

The LCC savings are shown in Figure 2.3-30. The nominal model was used. Both present value and constant dollar are shown. The LCC cost savings are the difference between replacing the turbopumps onorbit and replacing the engine and transporting it to ground for refurbishment. There is an economic advantage to modular TPA, provided the development cost incurred for engine and Space Station accommodations is less than \$20M to \$30M in 1985 dollars, depending on Mean Time Between Overhaul (MTBO). This neglects a reasonable payback period for the initial investment which will make the option less attractive.

ORIGINAL PAGE IS
OF POOR QUALITY

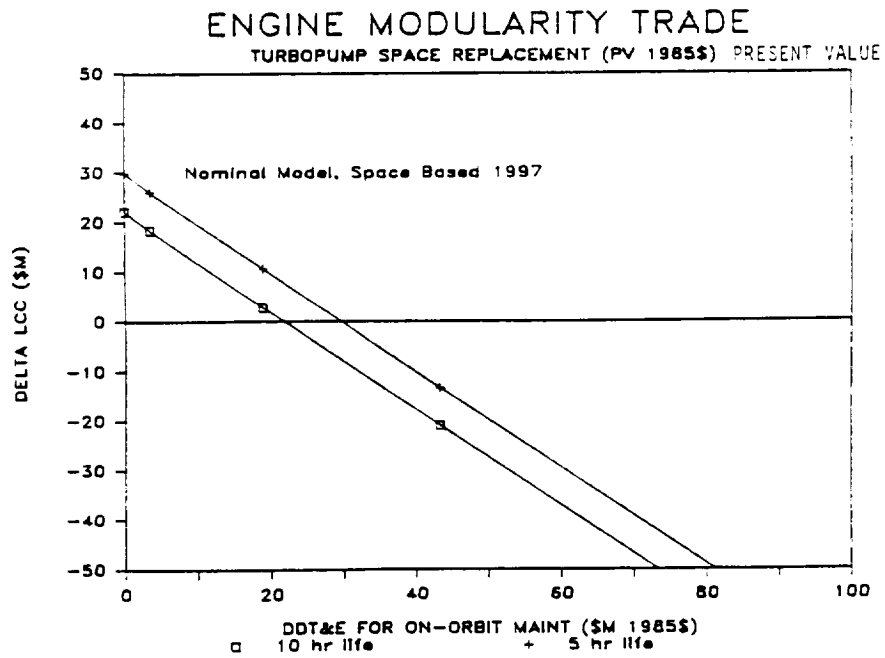
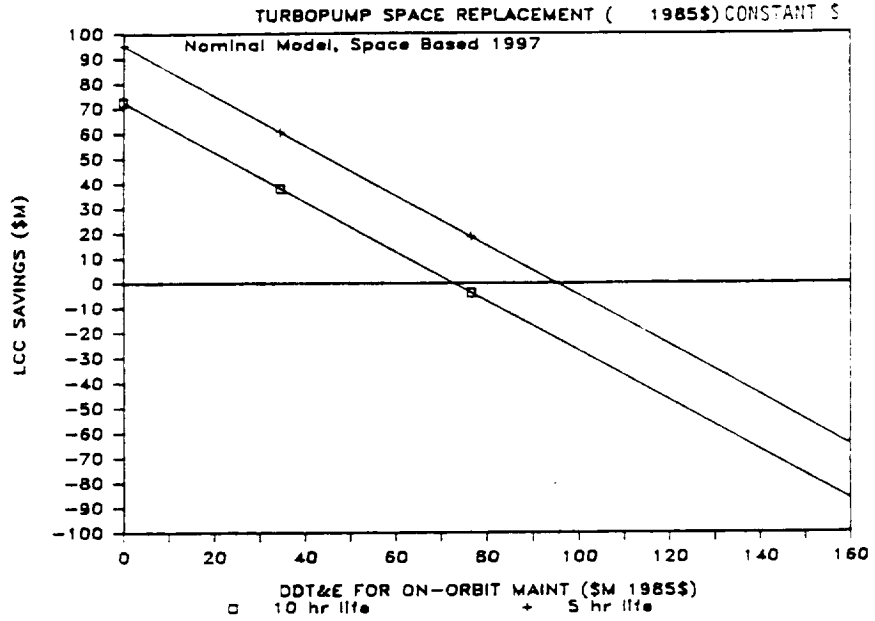


Figure 2.3-30 Engine Modularity Trade

The optimum engine life was determined based on the cost of maintenance and engine life development and testing cost (assumed at \$3M/hr to assess sensitivity). Engine replacement for depot level maintenance was assumed in this analysis with one overhaul during the engine's useful life. The Revision 8 mission model was used except the LCC reflects onorbit engine replacements beginning in 1995 at an average cost of \$10.93M. The results, shown in Figure 2.3-31 indicate an optimum MTBO of 7.5 hrs (low) and 10 hrs (nominal) with a small savings after 5 hrs. Engine replacements beginning in 1997 should reduce the optimum life because there are fewer missions. The effect of number of units on engine recurring cost was not considered. Decreasing the delta DDT&E cost per hour of life to \$1M/hr shifted the optimum MTBO to 15 hours.

2.3.5 Pressurization System

REQUIREMENTS AND GROUND RULES--The requirements of the candidate OTV engines are shown in Table 2.3-8. The primary differences between the operational LH2/L02 expander cycle, derivative RL10's and advanced expander cycles relative to the stage pressurization requirements are: start NPSH, steady state NPSH and GOX pressurant. The RL10A-3-3A/B require subcooled propellants at 29.5 psia for LH2 and 48 psia for L02 at start while the derivative RL10-II/IIIB and advanced engines allow superheated or two phase conditions during THI start. The RL10A-3-3A/B does not presently have GOX available, but the other engines do because of the GOX heat exchanger used for THI or dual expander cycle. The MMH/N2O4 gas generator engines require a positive NPSH for engine start.

The selection of the pressurization systems was based on engine requirements, mass, complexity, technology level risk, and evolution to space maintenance.

CRYOGENIC OPTIONS--The engine selection was the major factor in selecting the LH2/L02 pressurization system. An autogenous system was selected because of the advantages of Tank Head Idle (THI). Propellants flow to the engine inlet under tank conditions for chilldown and settling, and eliminate the requirement for an external pressurant source. Two phase flow (usually less than 40% vapor) is allowed before the pumps accelerate to full speed. Before the engine selection was made, however, the RL10A-3-3B was considered, and to meet the start and chilldown requirements, a helium pressurization system was selected for propellant tank start and oxygen tank steady state requirements. Helium pressurant was bubbled up through the L02 in order to subcool the liquid and reduce the pressurant requirement. GH2 was used for steady state pressurization of the hydrogen tank. The mass penalty over the autogenous system with RL10-IIB was 400 lbm. The helium was stored at ambient conditions because of maintenance concerns regarding embedding the tanks in the propellant tanks or maintaining the helium at cryogenic temperatures over long missions.



Table 2.3-8 MPS Candidate Engines Interfaces

PROPELLANT	ENGINE	I_{SP}		THRUST 10^3 LB	DEV STATUS	CYCLE	P_c (PSIA)	ϵ	NPSH/HPSP	
		MR							FUEL	OXID
L ₂ / L ₂	RL10A-3-3A	116 6.0		16.5	OPERATIONAL	SINGLE EXPANDER	465	61:1	28.6 PSIA	43 PSIA
	RL10A-3-3B	140 6.0		15	QUAL		415	61:1	28.6 PSIA	43 PSIA
	RL10-11B	160 6.0		15	PRODUCT DEVELOPMENT CONTRACT		400	205:1	14 FT	7.5 FT
	RL10-11C	159 6.0		15			400	205:1	28.6 PSIA	43 PSIA
	RL10-111	170 6:1		7.5	PROD IMPROVEMENT		400	400:1	14 FT	7.5 FT
	RL100	479 6.0		15	COMP TECH DEV CONT		1500	640:1	15 FT	2 FT
	RL100	474 6:1		7.5	STUDY		1200	600:1	15 FT	2 FT
	RS44 CORE	163 6.0		15	COMPONENT TECHNOLOGY DEVELOPMENT CONTRACT		1540	225:1	15 FT	2 FT
	RS44 INCR CAP	481 6.0		15			1540	625:1	15 FT	2 FT
	RS44 FULL CAP	492 6:1		15			2052	1175:1	15 FT	2 FT
	AJ23-154	483 6.0		3		DUAL EXPANDER	2000	1000	0 FT	0 FT
N ₂ / MMH	XLR-132	342 2.0		3.75		OAS GENERATOR	1500	400:1	17 PSIA AT 70 DEG F	37 PSIA AT 70 DEG F
	AJ23-153 TRANSTAR	328 1.8		3.75	DEVELOPMENT		350	136:1	26 PSIA AT 80 DEG F	57 PSIA AT 80 DEG F
	AJ23-151 PUMP FED OMS	334 1.93		6.0	TEST CONTRACT		350	154:1	30 PSIA AT 90 DEG F	60 PSIA AT 90 DEG F
	AJ23-156 TRANSTAR III	343 2.1		3.75	TECHNOLOGY DEVELOPMENT		1430	400:1	28 PSIA AT 80 DEG F	63 PSIA AT 80 DEG F
	ROCKETDYNE DESIGN	367 1.4		6.0	—		1000	400:1	37 PSIA	16.3 PSIA

The helium systems were also found to be a disadvantage for on-orbit resupply. In addition to adding another fluid to resupply on the OTV, the non-condensable He in the tanks complicates fill. The expander cycle does not use combustion products to run the turbopumps. Vaporized propellants are used in both the dual expander cycle (GH₂ & GO₂) or single (GH₂) expander cycle with the latter utilizing a heat exchanger to provide gaseous oxygen for tank pressurization. Therefore, the autogenous system would not contaminate the propellant tanks with combustion products but introduces pure propellant vapors. Autogenous pressurization does impact the boiloff because of the heat of condensation. This is more of a concern with multiple perigee burns.

PRECEDING PAGE BLANK NOT FILMED

One of the advantages of space-basing is the reduced loads the propellant tanks experience. Tank gauge can then be reduced depending on manufacturing limits and operating pressures. The LH₂/LO₂ OTV tank pressure is partially a function of the propellant vapor pressure. However, reducing the vapor pressure below atmospheric requires active cooling on the space station or launching the propellant in the low vapor pressure state. Figure 2.3-32 shows the advantages and disadvantages of reduced tank pressures. The 1.02 psia triple point of hydrogen presents a problem in the throttle valve of the OTV and Space Station TVS. The current concepts reduce the LH₂ from the 1 atmosphere tank conditions to 5 psia in the TVS to obtain a delta temperature of 5.7 deg R. Reducing the saturation pressure of the OTV to 5 psia would complicate the passive, coupled TVS used on the space station storage tanks. Scavenged propellant would also require active cooling. Engine THI becomes difficult because the low interface pressure during start could reduce the chamber pressure below the 1 psia required to insure ignition. Tank boost pumps could be used, but redundant pumps are required and increase maintenance. Based on these system considerations, the OTV tank pressure assumed propellants saturated at 1 atm. This corresponded to normal operating pressures of 17-18 psia for LH₂ and 19-20 psia, for LO₂ for MPSH of 15 ft and 2 ft, respectively.

REDUCE HYDROGEN SATURATED STATE FROM 1 ATM TO 5 PSIA

	ADVANTAGES	DISADVANTAGES
ENGINE	NONE	- NPSH INCREASES WITH DECREASING TEMPERATURE - BOOST PUMPS REQUIRED FOR CHILLDOWN, THI, AND LINE LOSSES (+ 165 LB \$17M)
THERMAL CONTROL	1.7% HIGHER HEAT VAPORIZATION H ₂ 5% HIGHER DENSITY H ₂	- THROTTLING IN TVS CONCERNS WITH LOW TRIPLE POINT (1.02 PSIA) - PROPELLANT CONDITIONING AND LOW VAPOR PRESSURE LOGISTICS - REFRIGERATION REQUIRED FOR LONG TERM STORAGE
TANK MASS	MASS REDUCED - 23 LB/PSI (4 TANKS) VAPOR RESIDUALS REDUCED-14 LB/PSI (BOTH PROPELLANTS)	- TANK MANUFACTURING, TESTING, AND HANDLING CONCERNS AT .005" WALL THICKNESS - REDUNDANT BOOST PUMPS COMPLICATE MAINTENANCE & DECREASE RELIABILITY

CONCLUSION: o LOW VAPOR PRESSURE PROPELLANT INCREASE OTV OPERATIONAL COMPLEXITY
o HIGHER STRENGTH LOWER DENSITY 2019 LI-AL AT 1 ATM PROVIDES SAVINGS COMPETITIVE TO 2219 AL AT 5 PSIA

Figure 2.3-32 Tank Pressure Trade

ORIGINAL PAGE IS
OF POOR QUALITY

STORABLE OPTIONS--Storable pressurization options are shown in Table 2.3-9. The trade used the results of the Storable Space Tug studies (Reference 1) and the Advanced Spacecraft Deployment Systems Study (Reference 2) The Storable Space Tug trade studies were done for 57,000 lbm of MMH/N₂O₄ propellant at a MR = 2.0 which compared to our 51,000 lbm space-based configuration at a MR - 2.0, therefore, the mass trade results were applied directly. The Tug study tank pressures were 17.5 psia (MMH) and 35 psia (N₂O₄) which compare to those of the MMH/N₂O₄ OTV design. Reducing the tank pressures improves the regulated helium option compared to the more complicated options. The qualitative results were reviewed to reflect our requirements.

Table 2.3-9 System Comparison of MMH/N₂O₄ Pressurization Candidates

SYSTEM COMPARISON OF MMH/N₂O₄ PRESSURIZATION CANDIDATES

PRESS SYSTEM TYPE	RELATIVE MASS (LBM)*	PRESSURIZATION CANDIDATES											REMARKS
		MAINTENANCE AND REUSE**	*EFFECTIVE RATIO**	RESTART CAPABILITY**	PROPPELLANT DUMP CAPABILITY	RELATIVE COST**	RELIABILITY/COMPLEXITY**	STATE OF DEVELOPMENT**	MISSION CAPABILITY SENSITIVITY**	PREVIOUS USAGE	SELECTED		
HELIUM BLOWDOWN	+336	6	5	6	YES	5 (EXCL. TANKS)	6	6	6	6	TITAN II SATELLITE SYSTEMS	NO	LARGE MASSIVE PROPELLANT TANKS GOOD CANDIDATE FOR RCS AND SMALL SYSTEMS
REG. HELIUM (AMBIENT STORAGE)	0 (REF)	6	5	5	YES	4	4	6	6	6	APOLLO TRANSO DELTA CENTAUR OMS	O.B. & S.B. MMH N2O4 ACC & C.B.	GOOD FOR EARTH STORABLES BECAUSE OF RESTART (NO THI)
REG. HELIUM (SUPERCRITICAL STORAGE)	-39	3	4	5	LIMITED	3	3	3	1	1	APOLLO-LEM SIVB	NO	DUTY CYCLE DEPENDENT FOR MMH/N2O4 RESUPPLY AT SPACE STATION COMPLICATED
REG. HELIUM (CASCADE)	-10	3	4	6	LIMITED	2	2	2	1	1	DEVL TESTED	NO	DUTY CYCLE DEPENDENT LIMITED MISSION DURATION COMPLEX/EXPENSIVE SYSTEM
ALTERNATIVES	+7	1	6	1	NO	6	4	6	2	2	TITAN CENTAUR SATURN	NO	LIMITED RESTART CAPABILITY AND DETERMINATION PRIORITIES (RE MMH/N2O4)
DEDICATED GAS GENERATION (AMB STORAGE)	-17	2	4	4	YES	3	3	3	6	6	LANCE (SOLID OO)	NO	CONTAMINATION PROBLEMS GOOD MISSION FLEXIBILITY
TANK BOOST PUMPS (N2O4)	-50	3	3	5	YES ELECTRIC PUMPS	3	2	4	4	4	CENTAUR	NO (REDUCE N2O4 NP5H)	MAINTENANCE PROBLEMS WITH EMBEDDED PUMPS REDUCE TANK MASS REDUNDANT PUMPS FOR MANNED MISSIONS

* BASED ON MMH/N₂O₄ SPACE TUG STUDIES - MASS FROM REG. HELIUM WITH COMPOSITE SPHERE
 ** RELATIVE RATINGS 1 THROUGH 6 WHERE 1 REPRESENTS WORST AND 6 BEST (NO ABSOLUTE SCALE) BASED ON MMH/N₂O₄
 ACC = AFT CARRIER CARRIER CB = CARRIER BAY - (R) = (R) BASED - (S) = SPACE BASED THI = TANK HEAD IDLE RESTART

The helium blowdown was too massive for use in the OTV but represents a simple and reliable system. Regulated ambient stored helium was the baseline and was selected for all the storable configurations. The system was not the lightest, but was simple and provided the engine start NPSH and did not contaminate the tanks with combustion products. The system does complicate onorbit resupply because the helium must be removed before the tanks with a total acquisition device can be filled. The supercritical storage and cascade systems reduced the storage system mass with cryogenic temperatures and heating the gas residuals, respectively. Savings were small compared to the resupply concerns and complications. Autogenous systems contaminated the fuel tanks while still requiring pre-pressurization and was therefore not selected. A dedicated monopropellant gas generator such as N_2H_4 would introduce ammonia into the fuel tank which must be removed onorbit for refill. The N_2O_4 could be heated with the gas generator but requires excess hydrazine. An alternate method is to use engine heat exchangers to heat the N_2O_4 vapor or use helium for the oxidizer tank. The gas generator system could eliminate or reduce the helium requirements but requires management of ammonia at the space station. The separation of helium from vapor was considered less difficult. Tank boost pumps would reduce the helium system mass but redundant pumps are required. The preferred approach would be to reduce the engine oxidizer NPSH. A 15 ft (10 psi) N_2O_4 reduction from the current 35 ft (22 psi) is the goal of the AFPRL XLR-132 program and was assumed to be achieved for the space-based stage.

The oxidizer tank can experience a pressure rise during coast. Flight data from the Titan Transtage has shown about a 15 psi rise in the N_2O_4 tank pressure. Analysis from the Tug studies showed that the increase is mainly attributed to ullage heating and thermodynamic equilibrium of N_2O_4 vapor in the ullage. The largest rise is after the longest engine burn where the transient helium pressurization displaces the liquid volume faster than propellant mass transfer can establish equilibrium vapor pressure. This increase in pressure can be reduced by two possible methods. The first, investigated by the Tug Studies, is to heat the incoming helium so that the rise due to mass transfer is cancelled by the ullage cooling during coast. The tank pressure increase was 9 psi with this concept. The helium could be heated in the engine and the engine interface could be combined with the turbine start system. The second method is to promote mass transfer during the pressurization process by bubbling the helium gas through the liquid. This concept is used in the Centaur liquid oxygen tank and also in the ET oxygen tank to suppress geysering. The pure helium bubble would present an interface to the N_2O_4 liquid which would then establish its vapor pressure inside. The bubble would rise under the thrust of the main engine, and the rise time would determine the degree of equilibrium. The result would be N_2O_4 vapor in equilibrium with the ullage at engine cut-off. The helium should also be in thermal equilibrium with the liquid. The low solubility of helium in N_2O_4 at low pressures should not degrade engine performance or cavitation performance. This reduces the pressure rise during coast due to evaporation of the N_2O_4 , but ullage heating and heat soak back from the engines could still introduce some pressure rise.

The cargo bay storable OTV requires pressurization for propellant dump to meet the orbiter landing C.G. Figure 2.3-33 shows the results of a trade study we conducted for a similar stage under an Air Force contract (Reference 3). The tank pressure in the orbiter bay during dump is 45 psia for both tanks. Away from the shuttle, low factors of safety apply. The system weight included helium system, tank, dump, and feed systems.

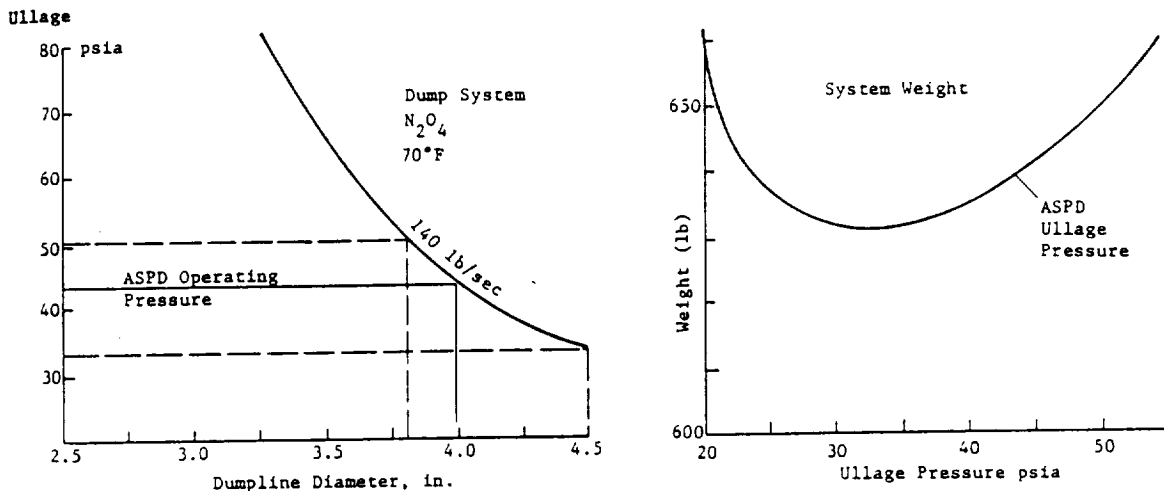


Figure 2.3-33 Pressurization and Propellant Dump System Trade

2.3.6 MPS Retrieval Considerations

For the ground-base ACC cryogenic OTV it is necessary to separate the LH₂ tanks from the OTV in order to store the OTV and tanks in the orbiter cargo bay. At the conclusion of the OTV mission as much as two percent of the propellants will still remain in the tanks, assuming a 1% flight performance reserve and 1% propulsion residuals. The storable OTV, since it is a smaller stage, can be returned intact. Thus each concept will require its own retrieval scenario.

GROUND-BASED STORABLE ACC OTV--The ground-based storable OTV will be returned intact in the orbiter cargo bay after the Main Propulsion System (MPS) and Reaction Control System (RCS) systems have been safed. MPS safing will be accomplished by providing dual fault tolerance in the propellant feed system and venting the ullage pressure from the flight pressure of 45 psia to 20 psia. Additionally, all propellants between the propellant tank isolation valves and the engines will be dumped during a short RCS burn. It may also be

necessary to extend this RCS dump/burn to ensure the OTV residuals are within the Shuttle landing weight center of gravity constraints, or auto pilot band width for sloshing if the propellant quantities are large because of an aborted mission. At the completion of MPS safing the RCS system will be shut down and safed with the required three independent containments to prevent a catastrophic thruster firing or propellant leakage.

After OTV safing has been completed, the orbiter will rendezvous with the OTV using its RCS system. The Shuttle RMS will then be used to grapple the OTV and move it to the cargo bay attachment fittings in the OTV ASE. No provisions have been included to provide a propellant dump capability through the orbiter propellant dump system. During reentry only a small increase in tank pressure would occur as temperatures gradually increase in the cargo bay.

GROUND-BASED CRYOGENIC ACC OTV--The ground-based cryogenic OTV's LH₂ tanks must be disassembled for return to the ground in the orbiter cargo bay. The residual propellants (up to 2%) will be burned and dumped in a nonoptimum burn during the maneuvers that raises the perigee after the aeropass. The maneuver will use the MPS engine to consume some portion of the residuals and finish with an RCS vernier burn during which the remaining propellant, approximately 250 lbs, will be dumped through 2.5" dump valves in the MPS feed system.

This complex propulsive dumping maneuver was required because if the tanks were dumped nonpropulsively, about 70% of the residuals could freeze, as shown in Figure 2.3-34, when the triple point pressure for hydrogen of 1.02 psia was reached. LO₂ is not as prone to freezing because it has a triple point pressure of 0.022 psia. Before we selected the propulsive dump, several alternatives were considered as shown in Figure 2.3-34.

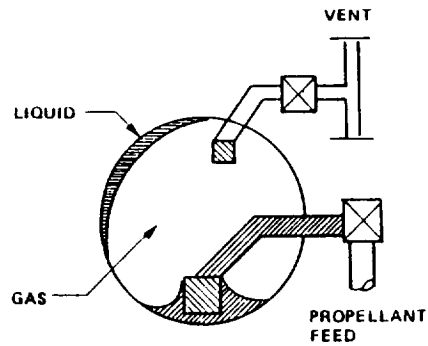
Some of the options considered were: 1) not recovering the tanks during the same STS mission, and, 2) providing a separate deorbit system. Neither of these alternatives were attractive. The first would still require rendezvous on a future mission while keeping track of the tanks inbetween missions. The latter would increase the system cost because of the deorbit system and the complexity of operational support .

The Multilayer Insulation (MLI) could be removed, increasing the heat leak significantly to sublime propellants, but required securing the insulation before the tanks were removed. Heaters were also considered, but were discarded because a separate power source would be required which would have to be connected during an EVA. Both techniques extended the retrieval time, thus increasing the cost.

Stowing the LH₂ tanks with residual solid hydrogen in the cargo bay was ruled out because of the safety issues associated with venting.

The last option was to oversize the propellant acquisition system so that the OTV could dump in low gravity. This device could contain 105 lbs internally when the screen broke down. The weight of this device would add 180 lbs/tank. This option was dropped because of mass and it still did not eliminate all propellants.

- o PROBLEM
 - VENTING LH₂ IN LOW GRAVITY CAN RESULT IN 70% OF RESIDUAL LIQUID FREEZING
 - WHAT IS BEST SOLUTION FOR SAFING TANKS FOR RETRIEVAL AND RETURN TO GROUND IN STS PAYLOAD BAY
- o OPTIONS
 - DO NOT RETRIEVE TANKS IN STS
 - ADD ENERGY TO VAPORIZE SOLIDS
 - BOTTOMING PROPELLANTS*
 - STOW TANKS WITH RESIDUALS IN PAYLOAD BAY
 - OVERSIZE START TRAP TO CONTAIN ALL RESIDUALS



*SELECTED RETRIEVAL APPROACH

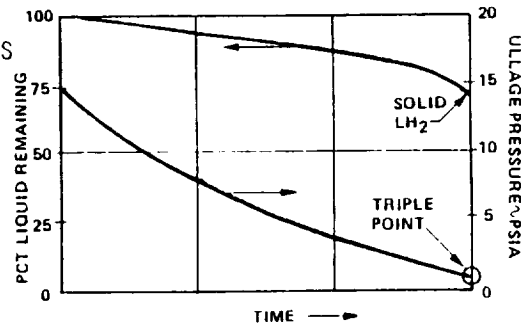


Figure 2.3-34 Ground Based Cryo - LH₂ Tank Retrieval

In the concept selected, all liquid residuals are dumped, and then both the LOX and LH₂ tanks are vented to vacuum to complete the inerting process. We expect that 30 minutes of exposure will be sufficient to eliminate all residuals based on the experience gained in STS inerting of the MPS plumbing on the orbiter. The OTV and the hydrogen tanks are stowed separately in the orbiter cargo bay and connected to a helium system in the ASE. The required Helium to repressurize the tanks to 20 psia for reentry was 46 lb with 395 lb of composite bottles and valves.

Figure 2.3-35 shows the removable cryogenic tank concept for ground-based OTV. It is similar to the space-based tank design.

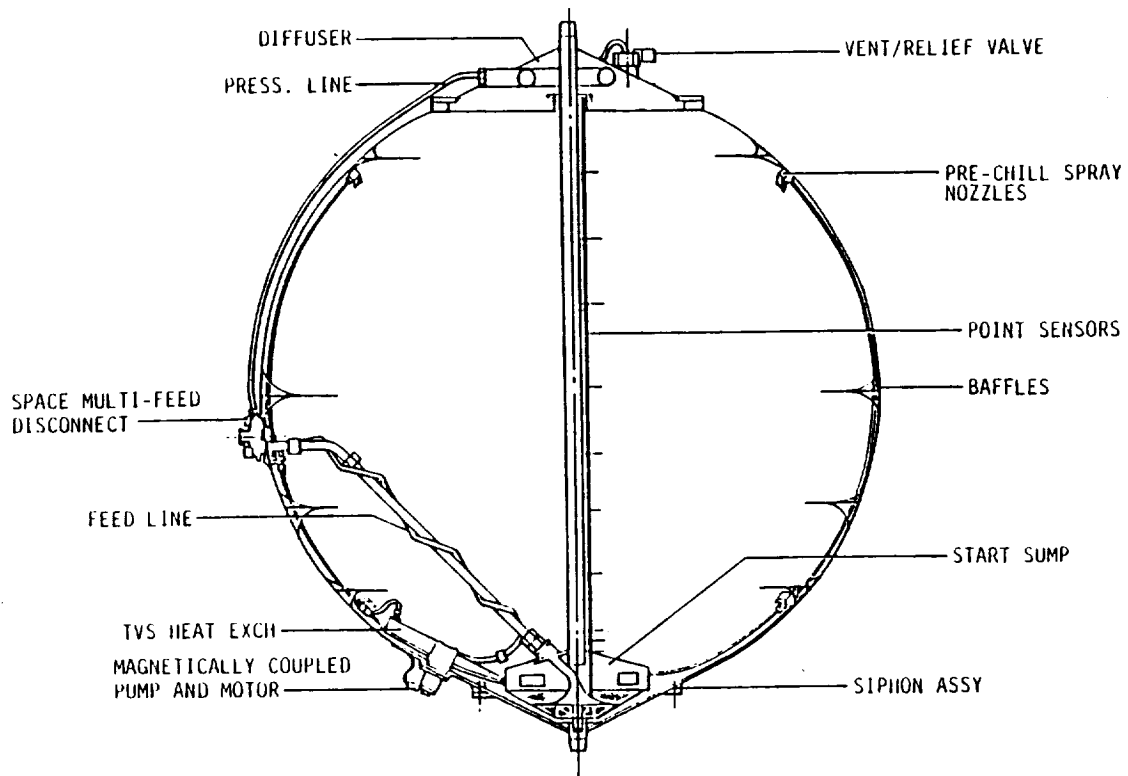


Figure 2.3-35 Removable Cryo Tank Concept

2.3.7 Reaction Control System (RCS)

An RCS concept for the various OTV designs was selected. These included ground-based LO_2/LH_2 and N_2O_4/MMH , and space-based LO_2/LH_2 and N_2O_4/MMH OTVs. Table 2.3-10 shows the option and the corresponding ground rules and assumptions used in the trade study.

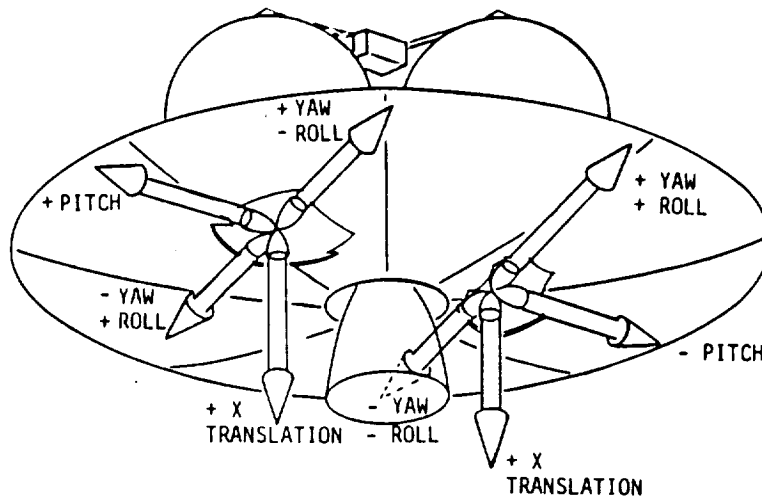
The resulting configuration for both ground-based OTVs was a low cost simple hydrazine (N_2H_4) RCS. The space-based OTVs used flexible common propellant RCS with common storage.

Table 2.3-10 RCS Ground Rules and Assumptions.

Option	Thruster Description	I _{sp} (sec)	MR	Feed System	Fixed* Mass lb
N ₂ H ₄	24 IUS at 25-30 lbf	230	-	Bladder Tank 400 psia 3.5:1	120
MMH/N ₂ O ₄	24 R-1E at 25-30 lbf	280	1.65	Surface Tension Device, 400 psia 3.5:1	190
MMH/N ₂ /O ₄	24 R-1E at 25-30 lbf	285	1.65	Surface Tension Device, Regulated Helium 400 psia	200
GH ₂ /GO ₂	24 at 25-30 lbf	400	4.0	Composite tanks Sized for 1/2 Total Impulse Charged from MPS w/TPA Backup 2000 psia 500°R	210
GH ₂ /GO ₂	24 at 25-30 lbf	378+	3.6	Composite Tanks Sized for 1/10 Total Impulse Dedicated TPA 1000 psia 200-300°R	210
LH ₂ /LO ₂	24 at 25-30 lbf	400	4.0	Aluminum Tanks Supercritical in Pressure, Liquid Storage with TPA Backup 300 psia (LH ₂) 1000 psia (LO ₂)	310

*Thrusters, Valves, and Feed System Mass except TPA
+400 sec I_{sp} Thruster Degraded for G.G. Flow

The RCS tradeoff for the reference OTVs was based on mass, complexity, and maintenance. Thrust was initially set at 25 to 30 lbf but 100 lbf is required on the space-based OTV's. Figure 2.3-36 illustrates the final placement of thrusters. Twenty-four thrusters were used in the initial trade although fourteen were required on the final designs. STS safety of three containments to prevent a catastrophic failure was observed for the feed systems for both ground and space-based OTVs.



ALL JETS ARE ON OTV SIDE OF AEROBRAKE
 JET EXIT PLANES ARE COPLANAR WITH
 AEROBRAKE (SCARFED)

- NO 6-DOF TRANSLATION REQUIREMENTS
- ALL VEHICLES HAVE SAME RCS CONFIGURATION
- 2 RCS JET CLUSTERS SCARFED INTO AERO-BRAKE. AFT LOCATION MINIMIZES C.G. TRAVEL IMPACT
- ATTITUDE:
 6 JET DIRECTIONS
 (PAIRED FOR FAULT TOLERANCE)
 = 12 ATTITUDE JETS
- TRANSLATION
 2 SOLO JETS
 (REDUNDANCY FROM ATTITUDE JETS)
 VERNIER BURNS & FUEL DUMPS
- 14 JETS TOTAL
- THRUSTERS SIZED BY AERO-MANEUVER:
 GROUND BASED = 30 LB THRUST
 SPACE BASED = 100 LB THRUST (14K P/L)

Figure 2.3-36 RCS Configuration - All Vehicles

The results of the mass trade is shown in Figure 2.3-37. The N_2H_4 RCS had the lightest dry mass, up to about 100,000 lbf-sec total impulse (Curve 3). The bipropellant concepts had better performance but were slightly higher in dry mass below about 100,000 lbf-sec (curves 4 and 5). For the ground-based OTVs the common RCS was not selected because of cost and higher wet mass at the lower impulse requirements. However, both space-based OTV's used the common propellant RCS. The storable OTV was resupplied from the main engine pump. This required filling the RCS tanks twice, because half the total impulse required on a manned mission was used after GEO circularization.

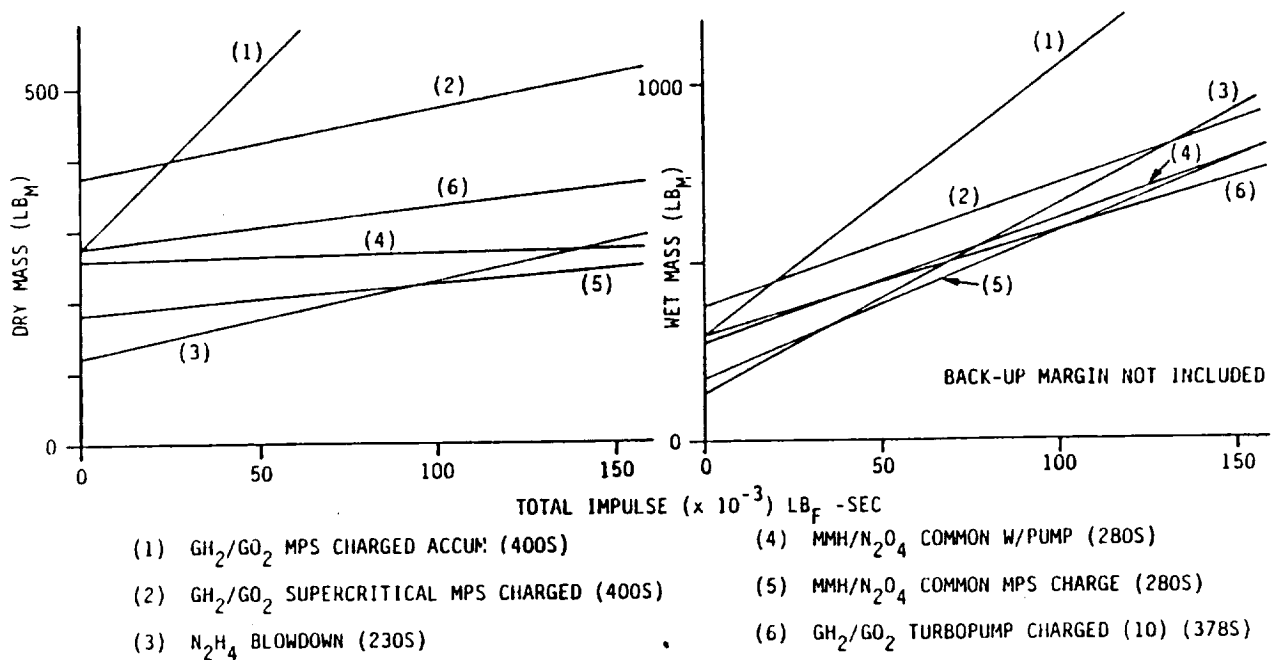


Figure 2.3-37 OTV RCS Parameterics

The mass of the common system is shown in Figure 2.3-37, curve 5. Based on Martin Marietta TUG studies (Reference 1), redundant RCS pumps and a controller would add about 70 lb. (Curve 4). The electrically driven pump required 150 to 200 watts to charge the tanks in 10 minutes with the power decreasing with charge time. Independent pumps avoid coordination resupply with engine firings but were not selected because of mass.

In contrast, the LO₂/LH₂ RCS is resupplied from a separate conditioning system (curve 6). It was found to be less massive.

The other approaches to a common GO₂/GH₂ RCS were found to be too massive and less flexible than the turbopump conditioning system. Using the autogenous GH₂ and GO₂ capability requires storing the gas at 500°R and about 2000 psia. Storage bottles become too massive (curve 1). Resupply time had to be coordinated with the engine firings and, therefore, were sized for 1/2 total required impulse. The H₂ and O₂ could also be stored in the liquid state, taken from the MPS engine and stored at supercritical pressure. A tank similar to the PRSA for the orbiter could be used. The additional complexity and power was not offset by any mass savings (curve 2). The system required a power source to condition propellants to thruster inlet requirements. Also considered was a concept which placed saturated liquid in an accumulator and heated the fluid to condition it for the gas thrusters. To obtain 100°R hydrogen gas a 4000 psi pressure vessel was required as shown in Figure 2.3-38. Figure 2.3-39 shows the conditioning energy per lbm required for the liquid feed.

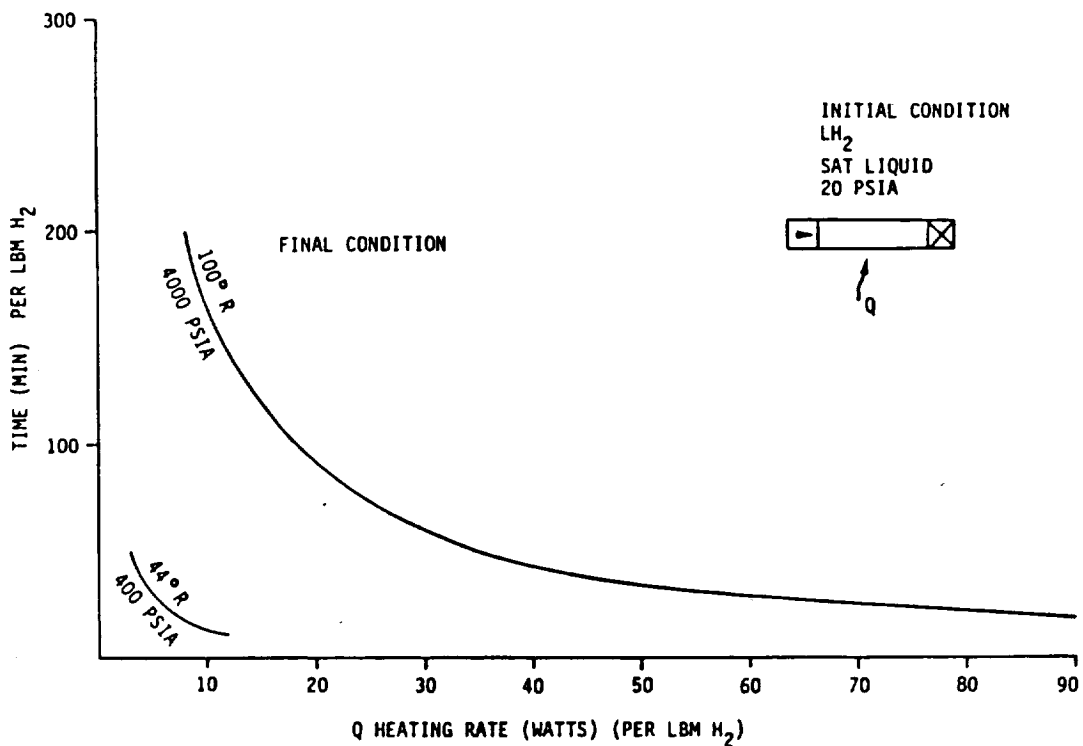


Figure 2.3-38 Heating Rate Required for H_2 Conditioning at Constant Volume

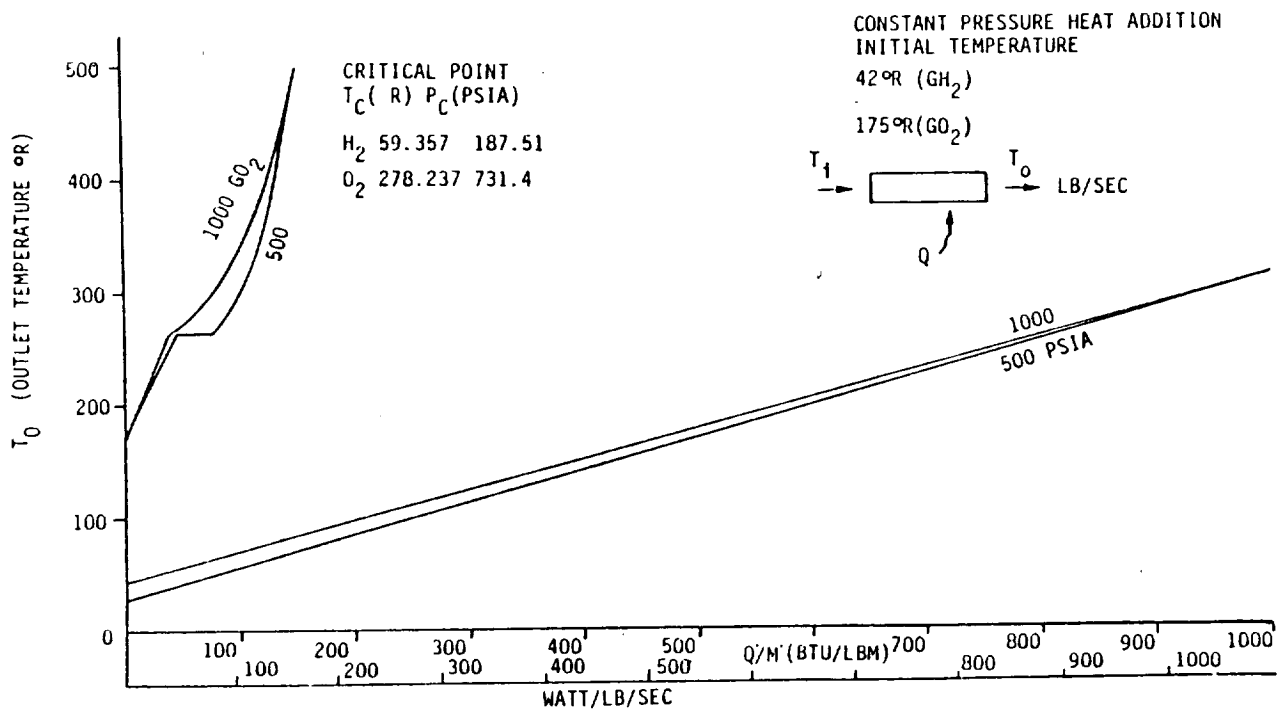


Figure 2.3-39 Conditioning Energy for GH_2/GO_2 RCS

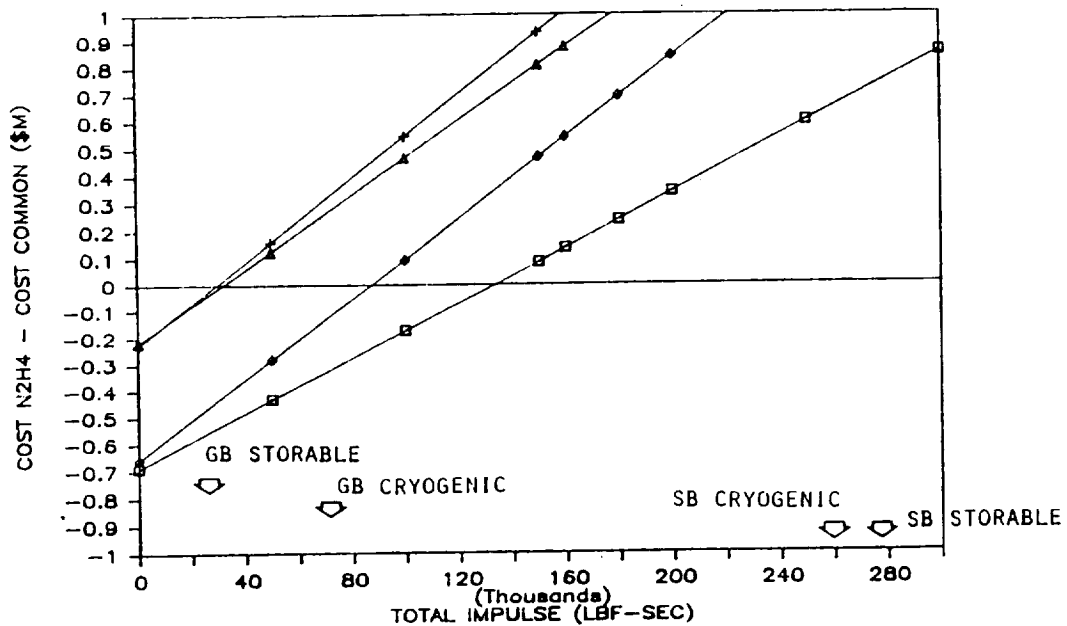
A positive displacement pump could be used to charge the GH₂/GO₂ RCS bottles, replacing the turbopump. Without an RCS backup requirement, the power requirement was reduced as a function of charging time. A gas generator would be used for the conditioning power and could therefore run the pump reducing fuel cell requirements.

RCS DDT&E cost estimates in FY84 dollars are:

N ₂ H ₄	\$ 18M
MMH/N ₂ O ₄	\$ 30M
GH ₂ /GO ₂	\$ 54M

The N₂H₄ and MMH/N₂O₄ costs were taken from Reference 1. The GH₂/GO₂ cost was taken from Reference 4, but had to be modified because the referenced CER included an additional cryogenic storage and feed system. Using the CER directly gave a cost of \$166M or greater. Additional sources agreed with the \$54M estimate although they were slightly lower. Reference 5 showed \$44M and Reference 3 gave \$30M (1984 dollars).

The common RCS for the space-based OTV showed an advantage in resupply over a N₂H₄ system. Resupply costs were estimated by the cost of delivering propellants and are shown in Figure 2.3-40. This analysis considered the higher dry mass between hydrazine and common RCS, but did not consider any complexity or cost incurred because of resupplying an additional fluid (N₂H₄).



GH₂/GO₂ □ \$1500/LB + \$500/LB
 MMH/N₂O₄ ◇ \$1500/LB △ \$500/LB
 N₂H₄ CONSTANT AT \$1500/LB

Figure 2.3-40 RCS Resupply Trade

The projected RCS requirements for space-based OTVs was in the range of 120,000 lb-sec, and both storable and LH₂/LO₂ are expected to be available at \$500/lb. Resupplying the common RCS was less costly for space-based OTV's.

A common RCS simplifies onorbit resupply of an OTV but is more complicated. Technology to develop more efficient and less complex methods should be studied.

Using boil-off for fuel cells and RCS was also investigated. The power required to compress the H₂ TVS output from 5 psia to 1000 psia was 330 watts per lbm/hr. Most of the GH₂ was used for RCS since the fuel cell requires an 8:1 mixture ratio. The GO₂ only required 59 watts per lbm/hr. However, 50% of the GO₂ is used in the fuel cell on long missions. The heat of compression raises the temperature of the vapor such that the high pressure storage tanks become large. This was more of a penalty for hydrogen than oxygen. The oxygen was cooled to 550°R with a small amount of cooling from the fuel cell coolant loop, or passive heat pipes could be used. Hydrogen temperature was too low (380°R) to take advantage of cooling methods available. The results showed no advantage to using hydrogen boil off, but there was some advantage to using oxygen. On a manned mission, 600 lb of boil off could be scavenged. On a delivery mission, 54 lb was scavenged. The net mass penalty was 22 lb for tanks and 17 lb for a compressor and valves. Because boil off occurs over the mission and dry mass is always carried, the net propellant required is about the same for delivery missions, but 1300 lb is saved on a manned mission.

RCS GH₂/GO₂ thruster performance is shown in Figure 2.3-41 and -42. Regeneratively cooled thrusters could be a problem with the REM's scarfed into the aerobrake. Materials that can withstand the thermal environment without coolant are required. Technology work at JPL has shown some advantages to using Rhenium; however, more development work is needed. Figure 2.3-43 illustrates the life and performance as a function of temperature.

MPS vs RCS - the MPS engine for small Vs was compared to RCS engine usage to reduce propellant consumption. The trade was for both monopropellant (N₂H₄) and common (GH₂/GO₂) for the cryogenic OTVs.

The storable engine was considered, but since it does not have tank head idle capability it was judged inappropriate for the small V burns anticipated. The XLR-132 requires helium for turbine spin-up and N₂H₄ would be required to control the stage during transients. The start/stop transients are about 3 sec, about 1/2 the burn time for 10,000 lb-sec. The starts also degrade engine life.

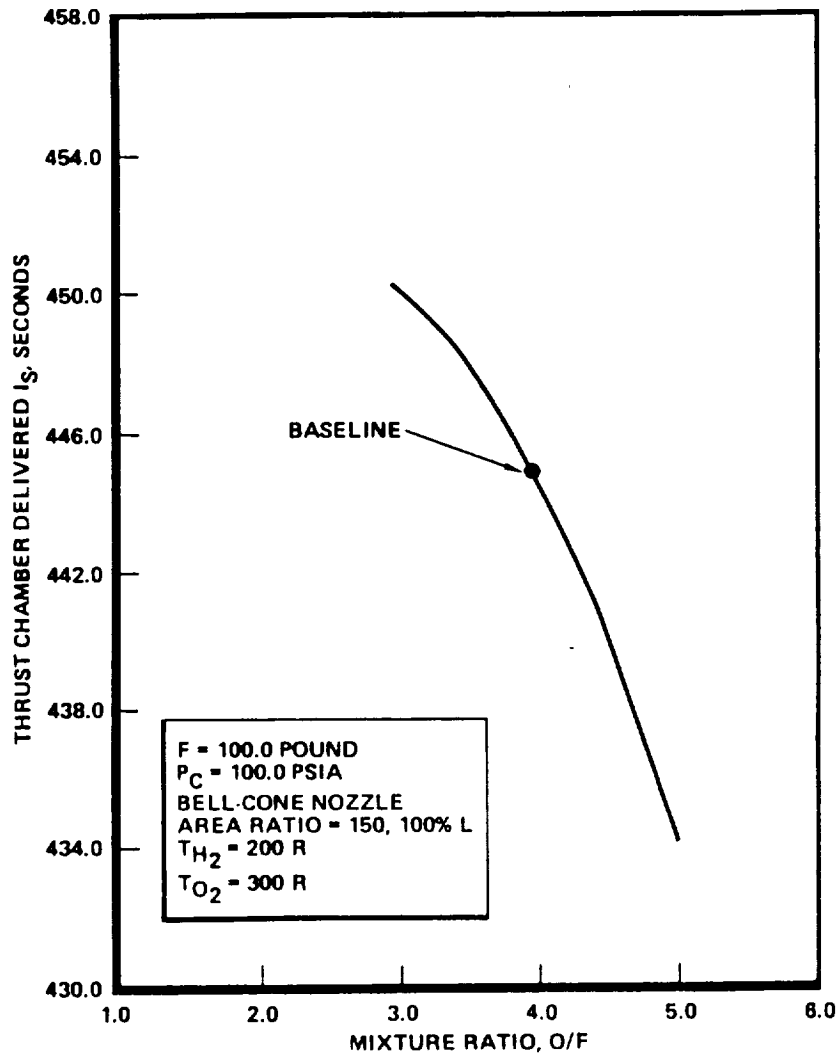


Figure 2.3-41 Film cooling Sensitivity (Rocketdyne)

The cryogenic main engine has varying start and shutdown losses depending on the mode of operation. Tank Head Idle (THI) mode can use superheated propellant provided the start pressure is above 16 psia and steady state is above 10 psia. The turbo-machinery is not rotating. Pump head idle (PHI) mode accepts some 2-phase propellants because the pumps are rotating at a low speed. Full thrust requires subcooled propellants. The main engine has a higher specific impulse and could save propellant provided the losses do not cancel the savings.

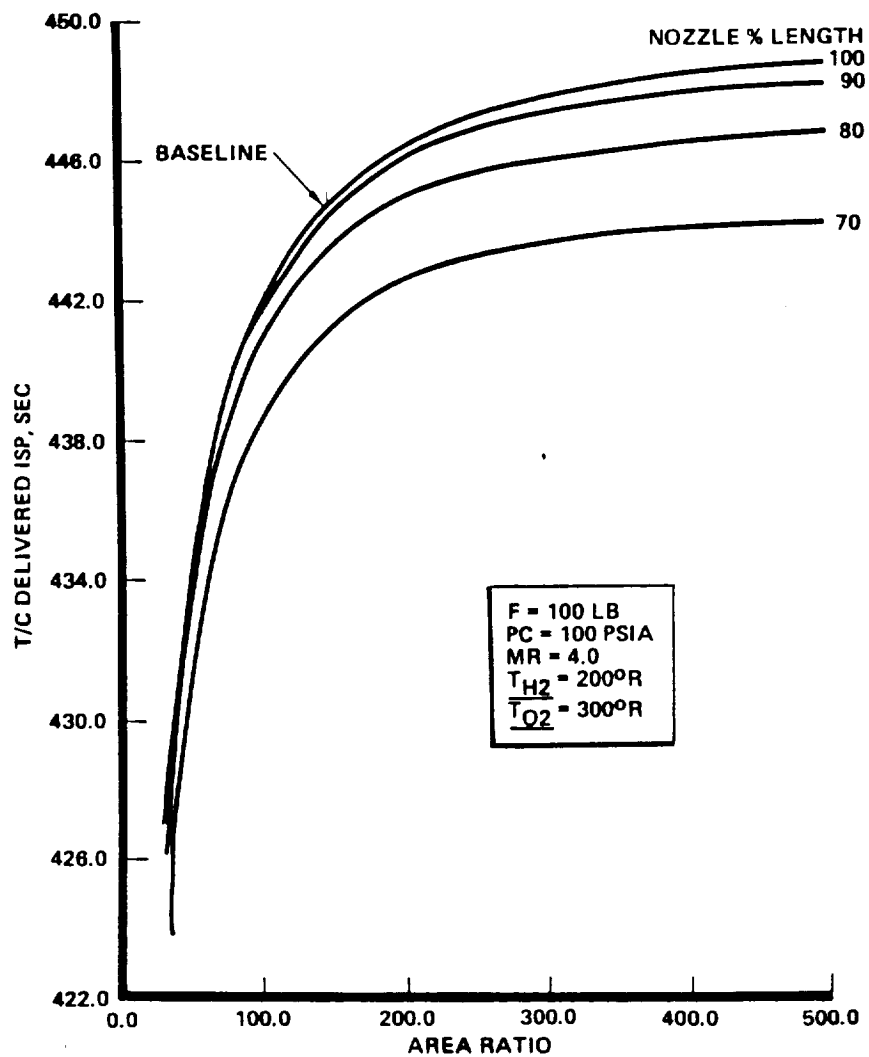


Figure 2.3-42 T/C Performance Regen-Radiation Cooled Concept (Rocketdyne)

ORIGINAL PAGE IS
OF POOR QUALITY

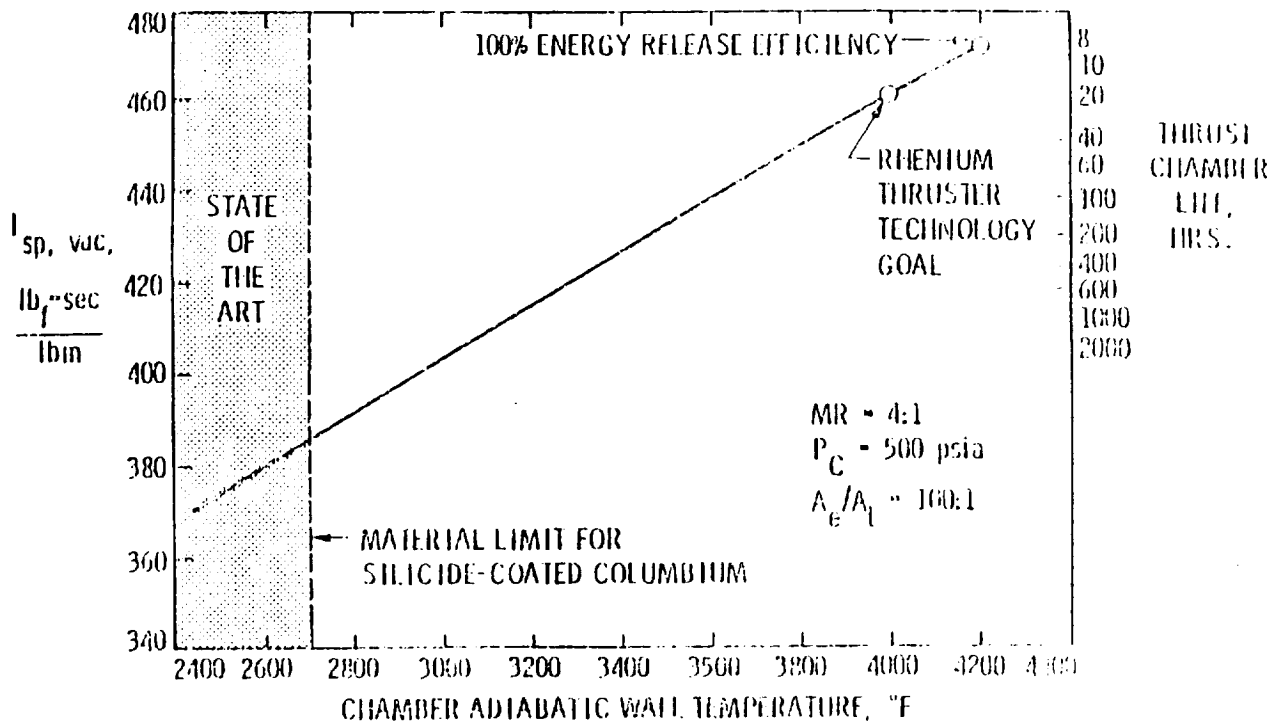


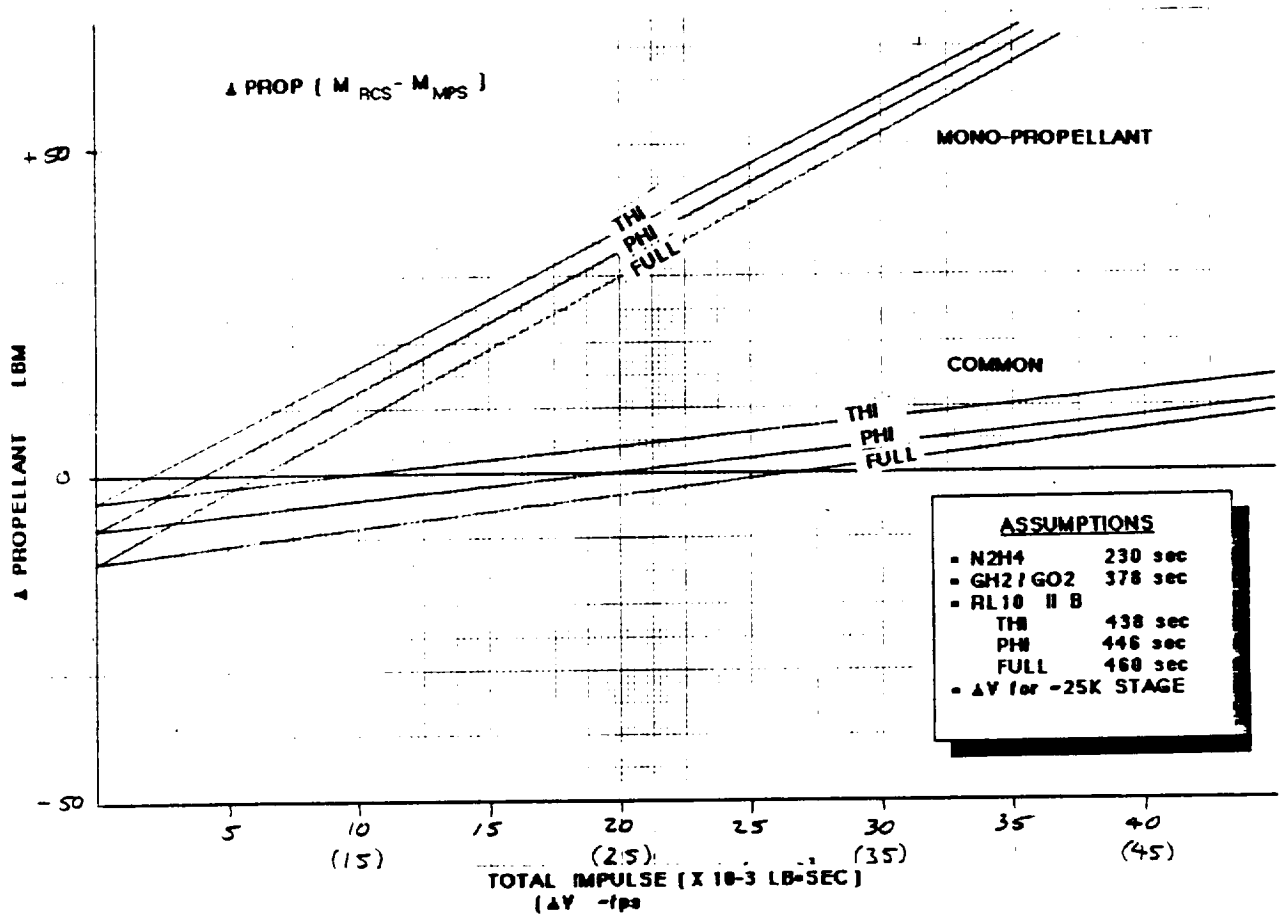
Figure 2.3-43 Predicted Performance High Temperature GO_2/GH_2 Rhenium Thruster (JPL Data)

The assumptions used in the MPS-vs-RCS trade were:

	N_2H_4	GH_2/GO_2	MPS
o I_{sp} (sec)	230s	378s	THI 438s
			PHI 446s
			FULL 460s
o Stage mass	25,000 lb _m		

The results, shown in Figure 2.3-44, are to use the THI mode of the RL-10 IIB or advance cryogenic engine compared to a common RCS for total impulse greater than 10000 lb-sec. For a monopropellant or storable bipropellant RCS used with the LO_2/LH_2 stage, the MPS should be used for total impulse greater than about 2500 lb-sec.

ORIGINAL PAGE IS
OF POOR QUALITY



THI has a negligible impact on the engine's life and reliability. This was confirmed with Pratt & Whitney.

The shutdown transients with THI and the power required both indicate little or no penalty compared to N₂H₄ RCS. Figure 2.3-45 shows the transients with liquid at the engine interface. Transients could be difficult to predict and may not be repeatable because of the nature of boiling heat transfer. If pumped head idle (PHI) is used these same conditions will occur since the engine always starts in THI.

ORIGINAL PAGE IS
OF POOR QUALITY

--- COOLDOWN MODE ---
PWA - OTV ADVANCED EXPANDER CYCLE ENGINE

COOLDOWN WITH PUMPS AT 500 DEG-R

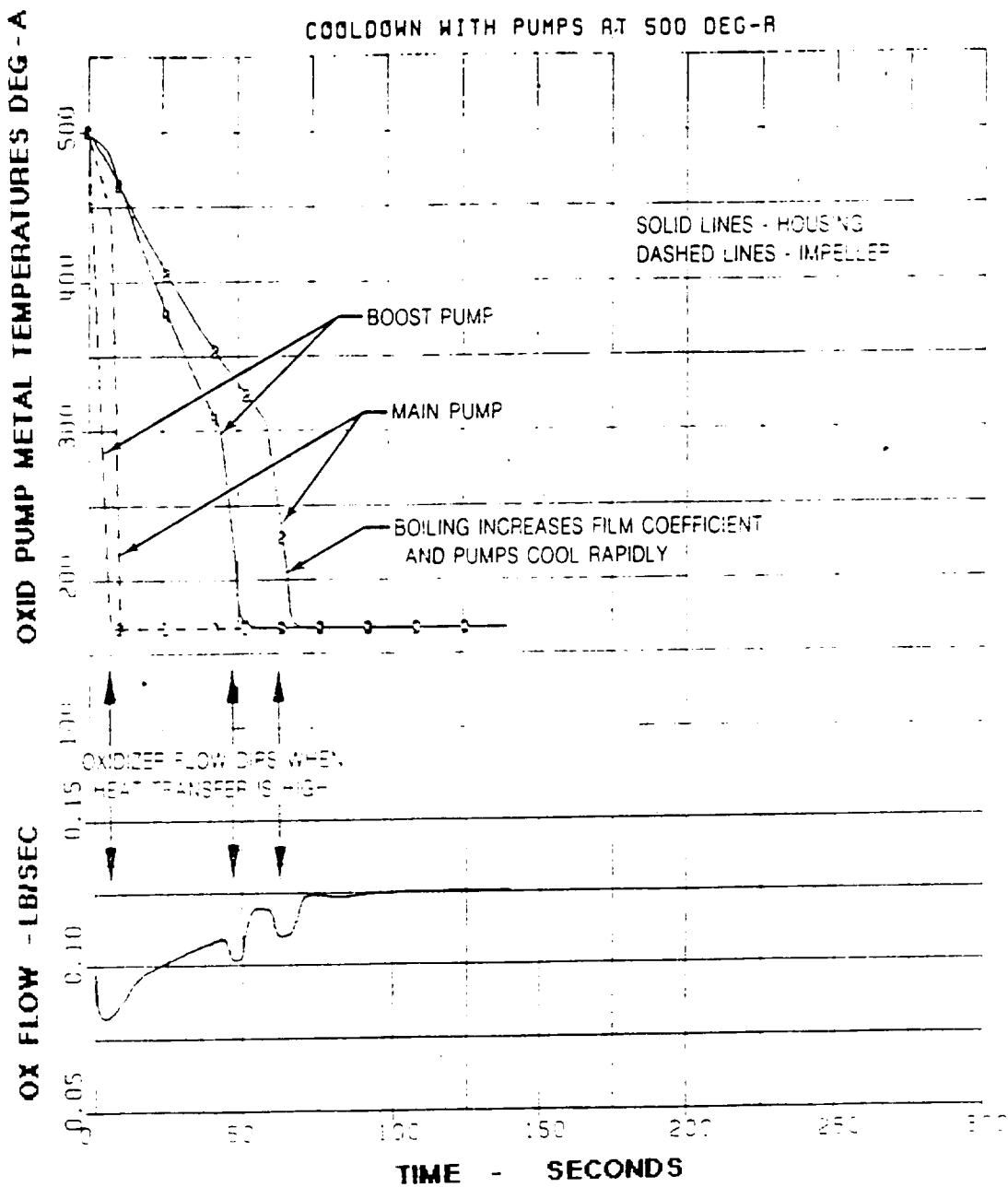


Figure 2.3-45 Boiling Increases Heat Transfer Causing Oxidizer (Pratt and Whitney)

2.3.8 REFERENCES

1. Space Tug Studies (Storable) Vol. 5 Sec II, MCR-73-235, Sept 1973
2. Advanced Spacecraft Deployment System Study, Vol. II, Technical MCR-80-551, July 1980.
3. Advanced Spacecraft Propulsion Design, AFPRL TR-82-048, April 1983
4. Space Station Propulsion Technology Study, NASA-JPL, JPL D-972, December 1983.
5. Advanced Orbit Transfer Vehicle Propulsion System Study, Martin Marietta, NASA CR-174843, February 1985.
6. Liquid Oxygen/Liquid Hydrogen Auxiliary Propulsion Systems for Space Tug - Final Report, Rockwell International, NASA CR-134790, June 1975.

2.4 STRUCTURE TRADE STUDIES AND ANALYSES

2.4.1 OTV/ACC Weight vs ACC Beam Stiffness

PURPOSE--The purpose of this study is to maximize the delta payload weight to geosynchronous orbit by optimization of the ACC beam stiffness.

SUMMARY--The trade study shows that weight savings can be accomplished on both the OTV and the ACC by increasing the beam depth within the confines imposed by facilities and the necessary required LH₂ aft dome clearance. Similarly, by going to a parallel beam there is also a net weight saving on both the OTV and ACC. The recommendation is a maximum depth parallel beam of 25.5 inches which requires the ACC/OTV interface to be moved further aft to Sta 2194. This beam has a potential weight saving of 18 lbs on the OTV and 110 lbs net on the ACC (excluding attachment hardware) from the baseline ACC/OTV configuration originally proposed by L. Edwards (Ref. 1). Any further stiffness increase in the ACC beams will incur a weight penalty with only an additional 3 lbs maximum potential weight saving in the OTV rack structure.

STATEMENT OF PROBLEM--The loads induced by flight accelerations produce out of plane deflections of the OTV to ACC attachment points. This out of plane deflection induces loads into the OTV structure resulting in a higher OTV rack weight. By increasing the stiffness of the ACC beams, this out of plane deflection can be reduced, thus reducing the OTV rack weight. The stiffness of the ACC beams can either be increased by increasing the beam cap areas and consequently the ACC beam weight, or by increasing the beam depth and varying the taper. The payload weight partial to geosynchronous orbit of the OTV versus ACC is 4.5. Consequently, the OTV and ACC weight can be traded to achieve an optimum ACC beam configuration.

DISCUSSION OF RESULTS--For this study, the OTV and ACC beams will be addressed separately and at a later date the selected configuration combined and evaluated.

The trade on the OTV was conducted on the Reference 1 ACC/OTV baseline configuration with the 9 degree of freedom attachment to the ACC beams. The OTV NASTRAN model was used to obtain internal loads for the flight accelerations and for unit out-of-plane deflections of the ACC attachment interface. These loads were then combined for the design case with the loads for various deflections (1.5, 1.0, 0.5 and 0.0 inches). The FORTRAN sizing program was then used to size and weigh the basic rack structure (excluding attachment hardware). The variation in the out of plane deflections have a negligible impact on the propellant tanks and the aerobrake, hence no weight saving will be considered in those areas. Figure 2.4-1 shows the results of this study with a maximum potential weight saving of 21 lbs going from a 1.5 inch to 0.0 inch out of plane deflection.

The trade on the ACC beams was approached in a different manner. The accelerations in the X direction only were considered for the calculation of the X deflections of the ACC beams, as the Y and Z accelerations tend to rotate the OTV to ACC attachment plane as opposed to distorting it. This and the symmetry of the ACC beams and the OTV assembly simplifies the loading.

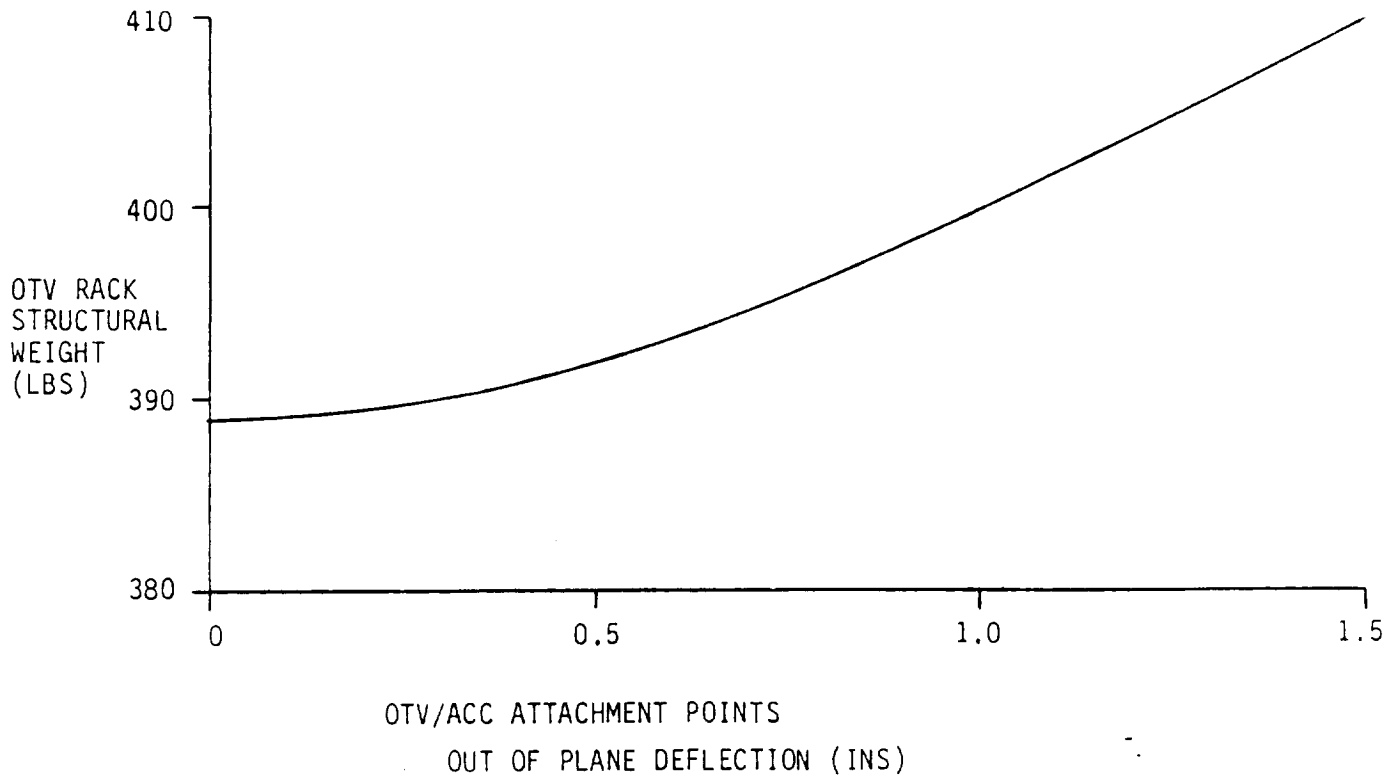


Figure 2.4-1 OTV Rack Weight vs Interface Out-of-Plane Deflection

The ACC beam attachment to the ACC skirt is assumed to be simply supported as the rotational restraint of the skirt is small compared to the beam stiffness. This assumption will give a conservative maximum bending moment in the beam. Figure 2.4-2 shows the ACC beam and the resultant simplified loading condition. Figure 2.4-2 also shows the two dimensions h , beam height at L_{O_2} attachment, and $\tan \theta$, slope of the top cap, that were varied in this study. For each geometrical configuration, a required cap area, weight and deflections at the L_{O_2} and L_{H_2} attachment points were calculated.

Figure 2.4-3 shows the results of the deflections of the L_{H_2} and L_{O_2} tank attachment points versus the beam slope ($\tan \theta$) for various beam heights, h .

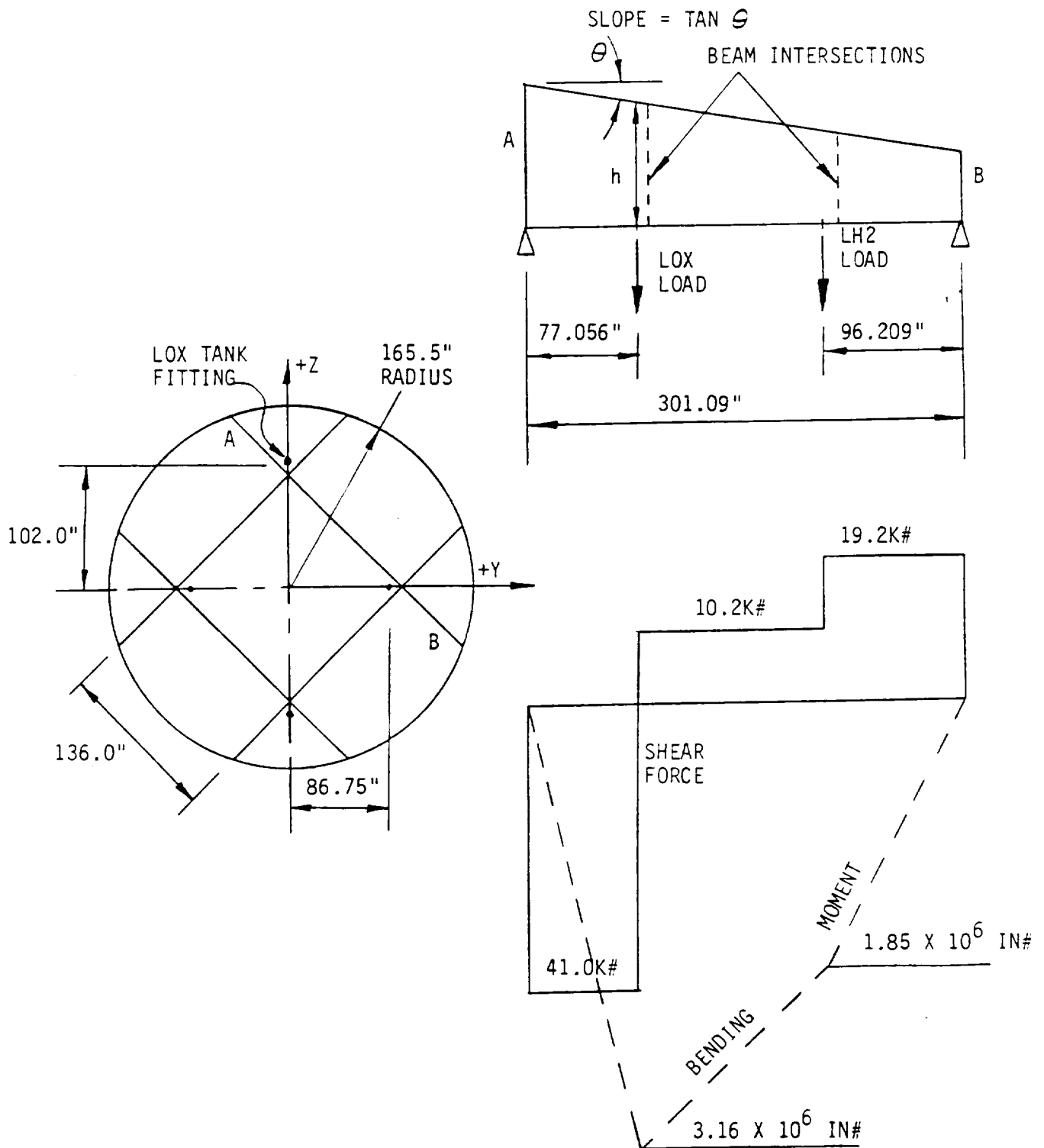


Figure 2.4-2 Basic ACC Beam Geometry and Simplified Loading

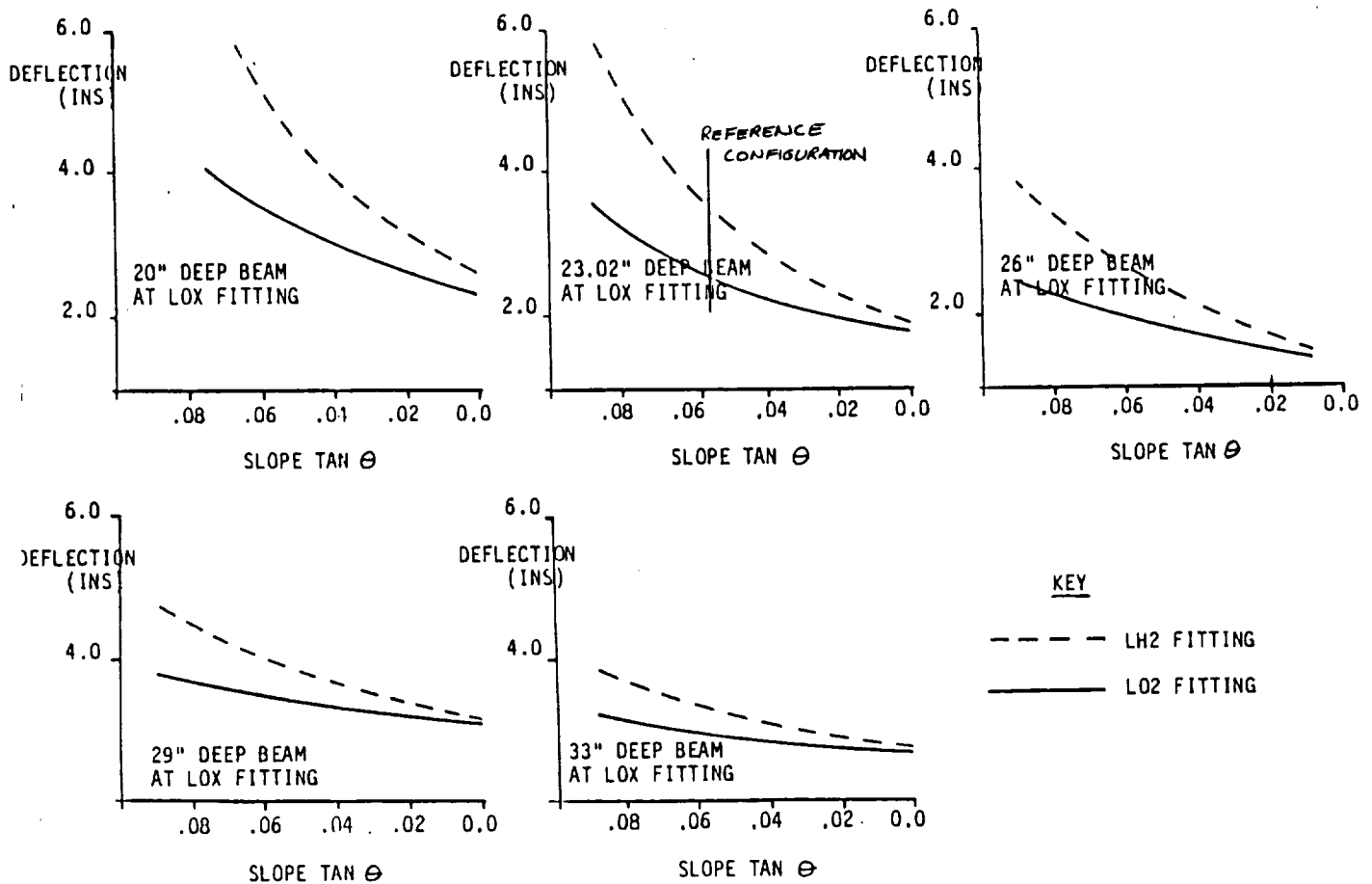


Figure 2.4-3 Beam Deflections vs Slope of Top Cap for Various Beam Depths

It can be seen from these graphs that to minimize the out of plane deflection of the ACC/OTV interface attachment points, the beam should be parallel and deep as possible. Figure 2.4-4 shows the beam weight versus the beam depth for various slopes (tan theta) of the top cap. This graph also indicates that the lightest weight beam is a parallel beam of maximum depth. A more detailed explanation of the ACC beam analysis is given in Reference 2.4-2.

The forward station of the ACC beams (Sta 2168.5) was determined from a deflection analysis of the ACC beams, ACC skirt and the LH₂ aft dome during launch with the requirement of no interference between the LH₂ aft dome and the ACC beams. Reference 3 shows a deflection study that was paralleled for the dedicated ACC beams.

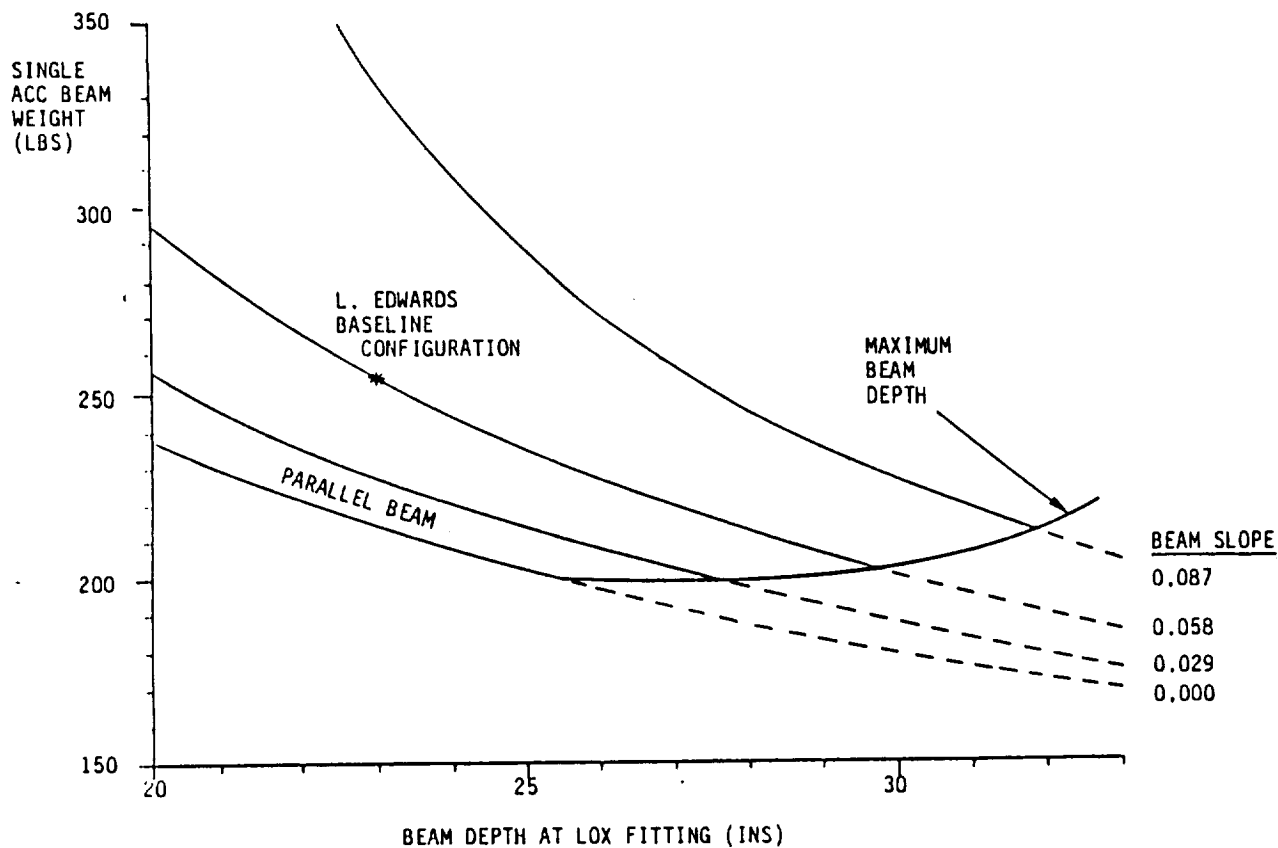


Figure 2.4-4 ACC Beam Weight vs Beam Depth (For Various Tapering Beams)

Facilities determined the furthest aft station of 2194.0 inches of the ACC beams, as any further aft would require major structural changes to the current facility. This gave a maximum depth of ACC beam of 25.5 inches at the interference point.

Simple NASTRAN models of the ACC beams of both the L. Edwards initial configuration (27" to 10" deep tapering beams) and the current recommended configuration (25.5" deep parallel beam) were made and the flight loads from the OTV applied. The internal loads of the recommended configuration were then used to size the caps and webs.

RECOMMENDATIONS--The study shows that no trade is necessary as there is a weight saving in both the OTV rack structure and the ACC. The recommendation is then to move the interface of the OTV and the ACC off to Sta 2194, thus allowing the maximum depth parallel beam.

2.4-2 - OTV Dedicated ACC Payload Beam Depth and Taper Study, MMC 3016-85-001.

2.4-3 - Payload support beam and shroud honeycomb base optimization for general purpose ACC - MMC 3016-83-156.

2.4.2 9 DOF vs 10 DOF OTV to ACC Attachment Weight Impact

PURPOSE--This study was conducted to assess the possible weight reduction in going from a 9 degree of freedom OTV attachment to the ACC beams to a 10 degree-of-freedom attachment (Figure 2.4-5).

	<u>9 DOF Y Displacement (Inches)</u>	<u>10 DOF Y Displacement (Inches)</u>
-Y Attachment	2.228	0.206
+Y Attachment	2.180	0.000

Base of Liquid Oxygen Tanks

	<u>9 DOF Y Displacement (Inches)</u>	<u>10 DOF Y Displacement (Inches)</u>
<u>+Z</u> Side	6.716	3.937

Base of Liquid Hydrogen Tanks

	<u>9 DOF Y Displacement (Inches)</u>	<u>10 DOF Y Displacement (Inches)</u>
+Y Side	6.500	3.708
-Y Side	6.749	4.011

Figure 2.4-5 Interface Between OTV and ACC at X = 2185

SUMMARY--The study shows that there is approximately 75 lbs weight saved in the ground based baseline configuration rack structure by going to the 10 degree of freedom OTV to ACC attachment. There is also another beneficial effect of the additional degree-of-freedom restraint. It reduces the deflection of the top of the LH₂ tanks by 2.0 inches (Figure 2.4-5) in the Y direction during liftoff.

TASK DESCRIPTION--The trade was conducted on the Reference 1 ACC/OTV baseline configuration rack structure and addressed the attachment of the OTV structure to the ACC beams. The attachment interface consists of four attachment points, each of which is above either a liquid oxygen or liquid hydrogen tank on the OTV. Figure 2.4-6 shows the degrees of freedom restrained by each of the attachments. In the 9 degree of freedom attachment, the Y direction acceleration loads of the LH₂ tanks are transmitted via the OTV structure to the Y reaction points above the LO₂ tanks. In the 10 degree of freedom attachment, this load is transmitted directly to the ACC beams.

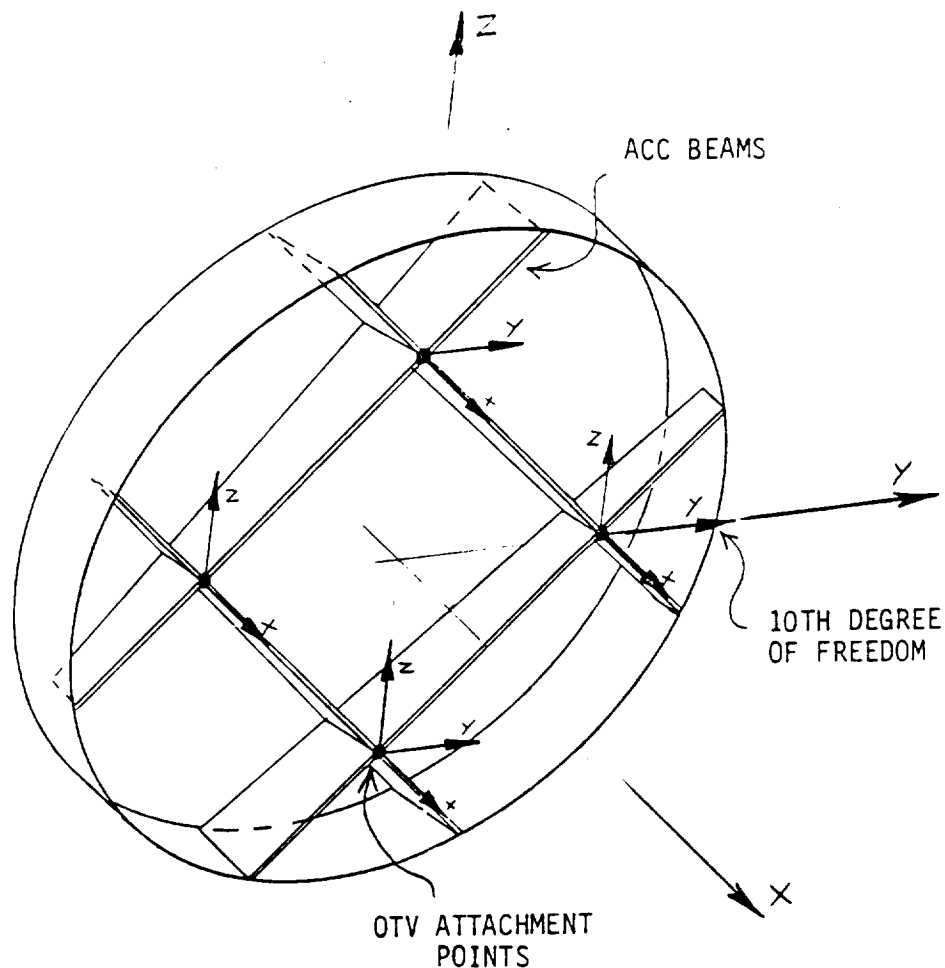


Figure 2.4-6 Degree-of-Freedom Attachment Restraints

A NASTRAN finite element model was constructed of the OTV for the two attachment configurations. These models reflected the OTV sizes as defined by the initial study completed in October 1983. The critical load cases and unit deflections were applied to the NASTRAN models and the internal loads obtained.

The NASTRAN model shows that OTV deflections in the Y direction are high and would interfere with the ACC shroud. The Y direction acceleration is the dominant contributor to these deflections (Figure 2.4-5), and in the design liftoff case, the maximum Y direction acceleration has gone from +0.21 g to +0.71 g, resulting in the large deflections.

The current proposal makes the OTV rack structure out of graphite composite. This composite would have a Youngs modulus on the order of 2 to 3 times higher than aluminum, thus reducing the deflections by that same order. However, the deflections are not addressed in this study.

A FORTRAN program was used to size the OTV rack structure for the critical loads obtained from the NASTRAN model. The unit deflection case was used to impart loads into the OTV due to the relative X displacement (Figure 2.4-6) between the interface attachments encountered during flight. This relative displacement was taken as 1.5 (1.45) inches as defined in Reference 2.4-4. The program reads in the beam heights and calculates the required cap areas and geometry, also the required web thickness for each end of the beam members that make up the rack structure. Consideration was taken for Euler column stability, crippling and bending strength in the sizing of the caps. The cap dimensions are then assumed to taper linearly from one end of the beam to the other in the calculation of the basic rack weight, excluding attaching hardware. The structural weight was based on the practical sizing of the structure.

Figure 2.4-7 and Figure 2.4-8 show the OTV structure and the associated beam cap loads and structure weight.

REFERENCE--

2.4.4 OTV/dedicated ACC interfaces ICD 80900000025, September 30, 1983, 3rd Preliminary Draft, Rev. 9-30-83.

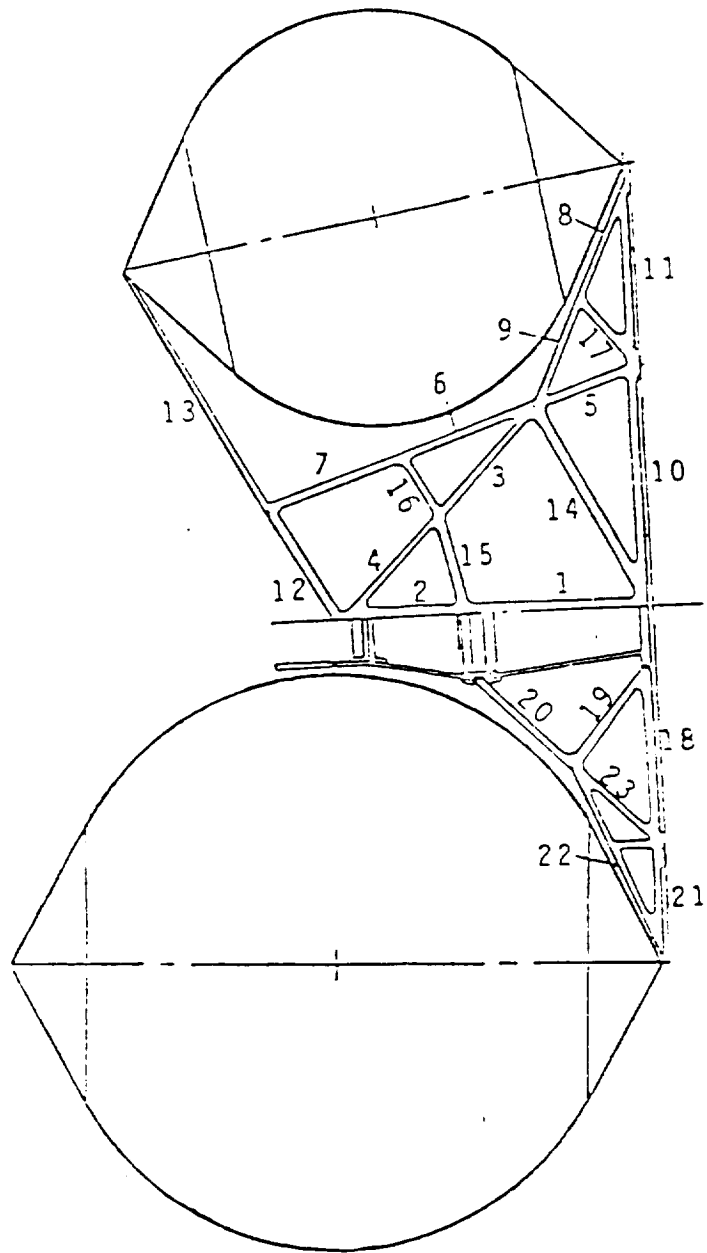


Figure 2.4-7 OTV Structural Members

MEMBER CAP LOADS (KIPS)
FOR 9 AND 10 DOF ATTACHMENT

MEMBER NO.	9 DOF		10 DOF	
	LIMIT	ULT	LIMIT	ULT
1	-58.6	-82.1	-43.4	-60.8
2	43.8	61.4	56.9	79.6
3	46.5	65.1	26.3	36.8
4	43.2	60.4	57.1	80.0
5	7.3	10.2	5.5	7.7
6	-12.9	-18.1	- 8.8	-12.3
7	- 7.5	-10.4	- 7.7	-10.8
8	50.6	70.9	39.4	55.2
9	50.8	71.1	39.6	55.4
10	-85.7	-119.9	-44.3	-62.0
11	-58.4	-81.8	-42.8	-60.0
12	71.7	100.4	56.7	79.3
13	63.9	89.4	49.5	69.3
14	21.9	30.7	14.1	19.8
15	3.8	5.3	4.2	5.8
16	1.7	2.4	- 3.4	- 4.8
17	- 5.3	- 7.4	- 1.7	- 2.4
18	28.8	40.4	13.3	18.7
19	- 1.7	- 2.4	- 1.6	- 2.2
20	-31.2	-43.7	-29.0	-40.6
21	28.5	39.9	13.9	19.5
22	-31.0	-43.4	-33.7	-47.2
23	- 0.7	- 0.9	- 0.6	- 0.8
TOTAL				
RACK				
WEIGHT				
	410 LBS		335 LBS	

Figure 2.4-8 Member Cap Loads (KIPS) for 9 and 10 DOF Attachment

2.4.3 Trade Study of Umbilical Locations for Ground-Based Cryo OTV

PURPOSE--The purpose of the study is to establish the best location for the LH₂/LO₂ and electrical disconnect panels for the ground based cryogenic OTV when mounted to the Strawman II configuration of the External Tank Aft Cargo Carrier. Figure 2.4-9 shows the area under consideration.

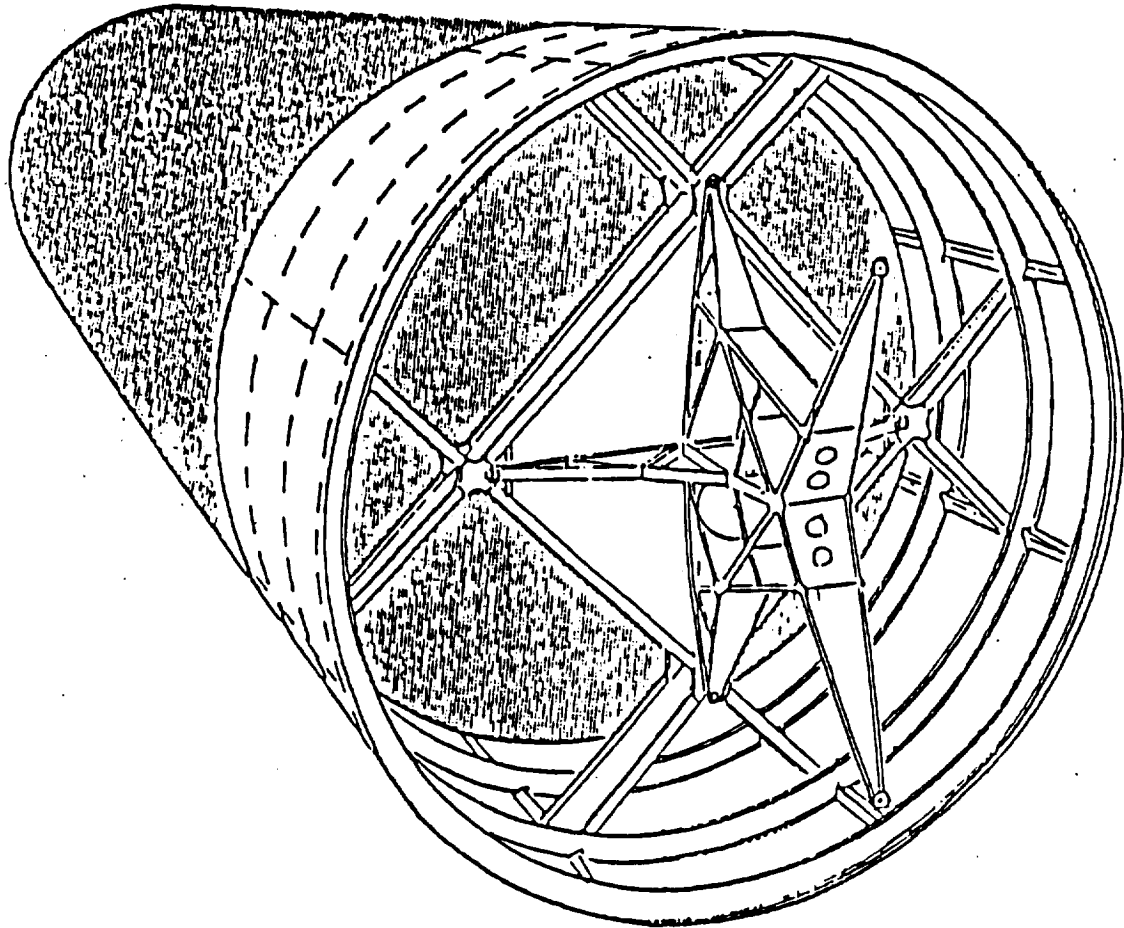


Figure 2.4-9 View Looking Forward with Tanks Removed Showing Area Under Consideration for Umbilical Locations

SUMMARY--Of five alternative locations investigated the recommended design represents the closest points to the intersection of the ACC and OTV beams that still enable a physical fit for disconnect size.

Support bracketry takes the form of two simple beams, one for the ACC and one for the OTV, and eliminates the need for cantilevering the umbilical plates. The location also allows adequate room for plumbing.

ORIGINAL PAGE IS
OF POOR QUALITY

STATEMENT OF PROBLEM--The present ACC location for the umbilical (Figure 2.4-9) requires cutting away a large portion of the flange in the OTV oxygen tank support structure to accommodate the umbilical plates.

For the purpose of the study, the following conditions and criteria were assumed.

- 1) The use of an ET type umbilical with explosive separation bolts for mechanical attachment per Reference 2.4-4 (Figures 2.4-10 and -11).

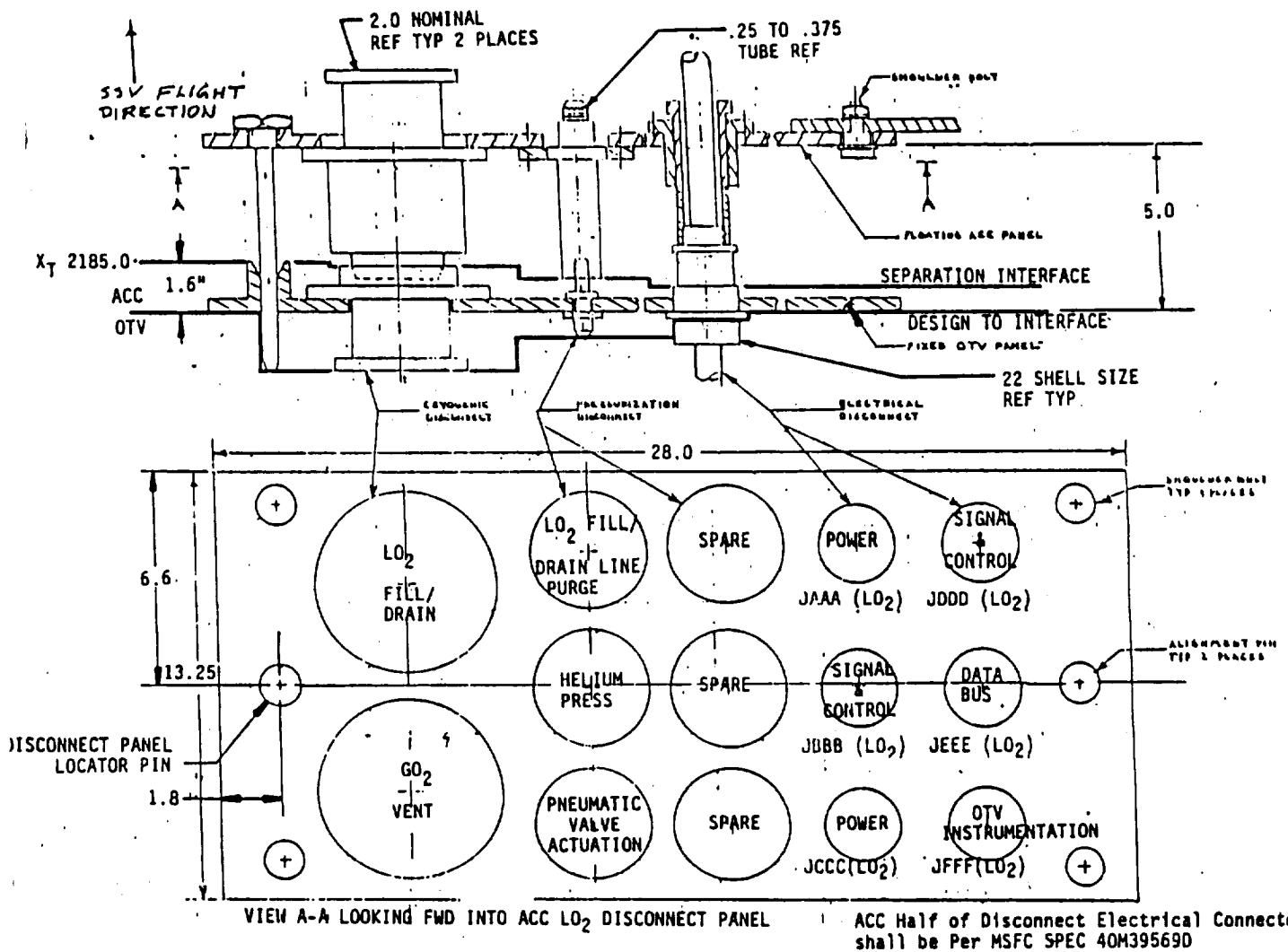


Figure 2.4-10 ACC/OTV LO₂ Disconnect Panel

ORIGINAL PAGE IS
OF POOR QUALITY

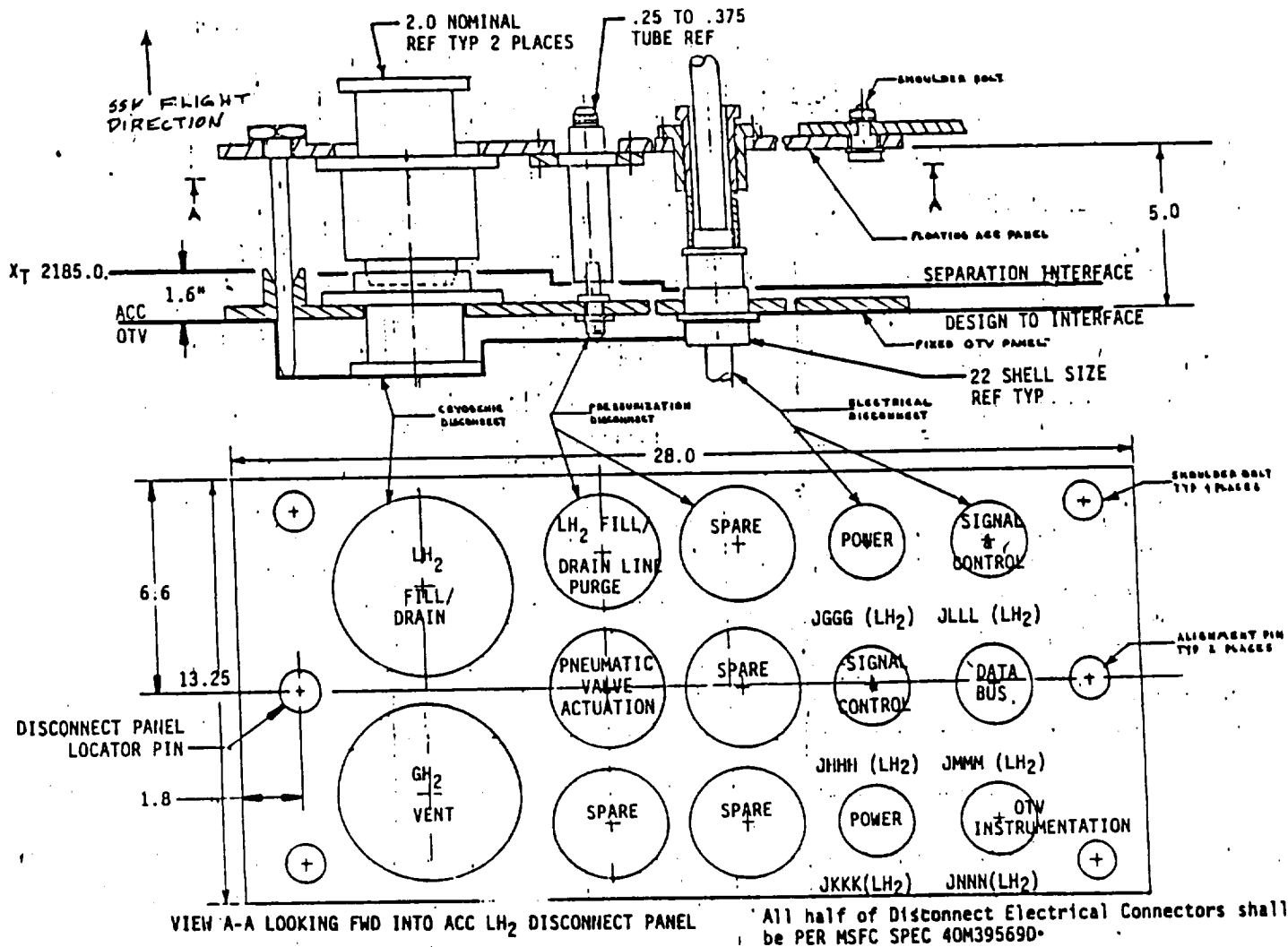


Figure 2.4-11 ACC/OTV LH₂ Disconnect Panel

- 2) The ACC Strawman II crossbeam configuration illustrated in Figure 2.4-9 is to be used in conjunction with the baseline ground based cryo ACC/OTV configuration (Reference 1).
- 3) There would be no requirements for inspection and maintenance access to the umbilical plates after the mated vehicles are on the pad without major disassembly. This is a condition in line with present KSC ground operations planning for future vehicles and is an important factor in deciding the optimum umbilical location.
- 4) Other factors considered were weight/cost trades, disconnect reliability, access for plumbing, and structural integrity.



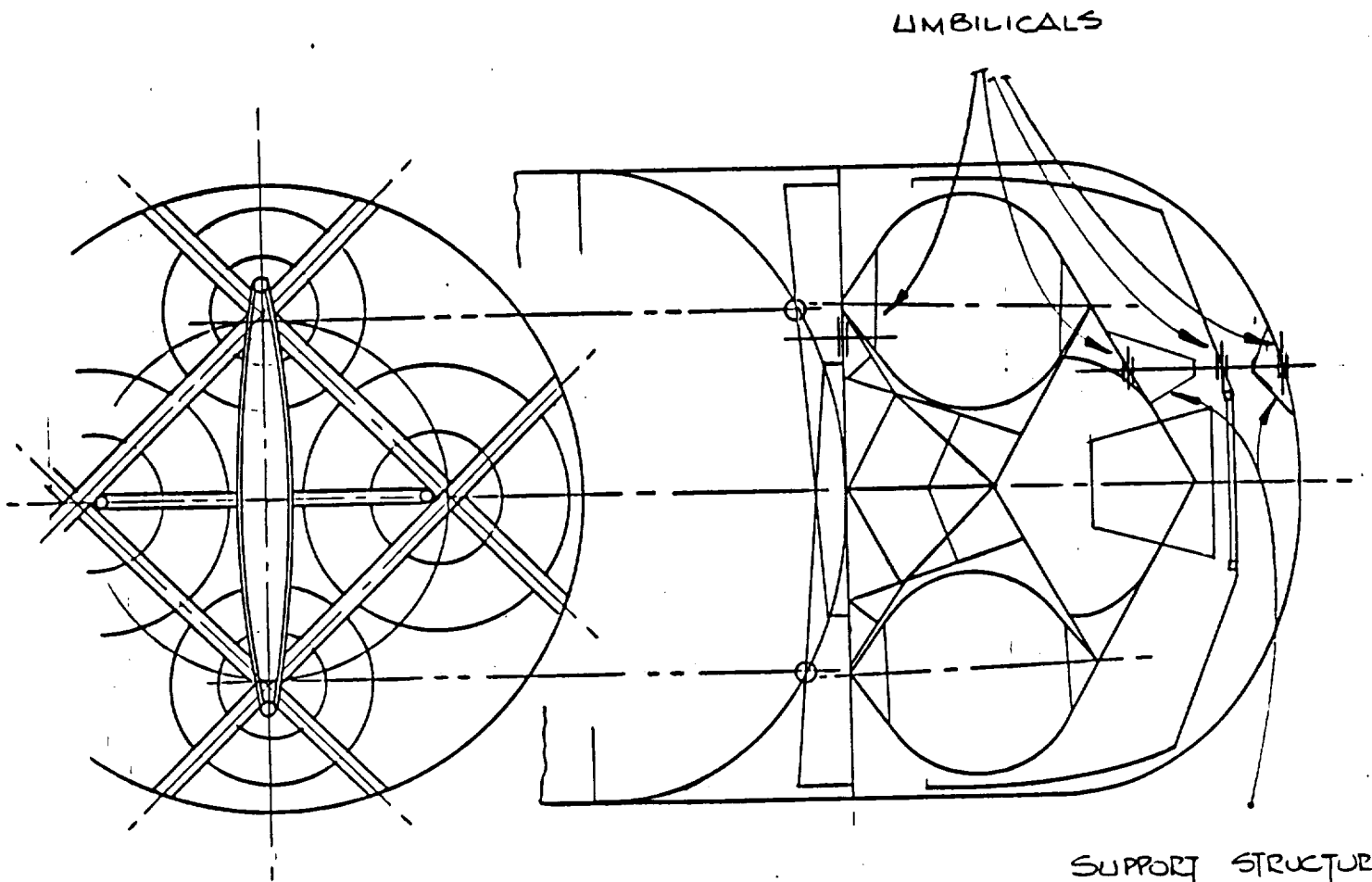


Figure 2.4-12 Tail Service Mast Concept

- 6) An OTV main beam umbilical at $X_t 2185.0$ would still be required for some systems, therefore, a total of four separation planes are required with possible duplication of systems.
- 7) Possible problems of flame impingement upon fuel and electrical disconnects.
- 8) The aft end of the vehicle gives poor locations for fuel outlets and disconnects with reference to heat from the adjacent engine location.

It was felt that the above obstacles were of such magnitude as to render the design unfeasible and the study concentrated upon the remaining concept.

Since datum $X_t 2185.0$ gives a common interface with both vehicles, it is the obvious choice of location in the X_t plane.

The four options studied were therefore simple variations of location in the Y-Z plane since the basic problem resolved into finding an area sufficiently large, yet equally adjacent, to bolt ACC beams and the OTV beam.

The location shown in Figure 2.4-13 is taken from the Interface Control Document (ICD) (Reference 4) and shows the intended positions of both umbilicals on the +Z axis. The fact that the umbilical plate is much larger

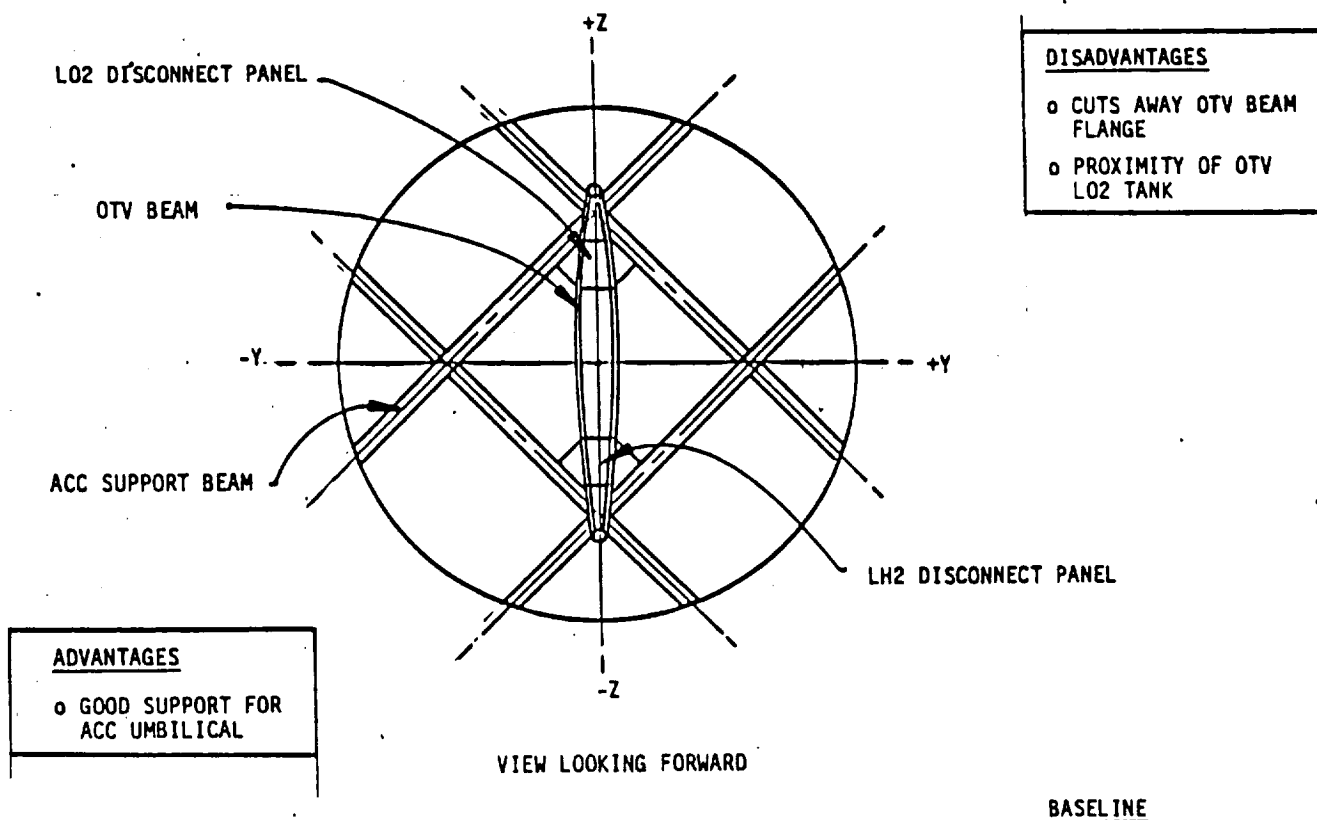


Figure 2.4-13 ACC/OTV Disconnect Panels, Forward View, Baseline

than the OTV beam in the interfacing area suggests the umbilical plate should interface at a wider area of the beam. Figure 2.4-14 shows such a location which requires the umbilical on the ACC to be cantilevered from the ACC beams which is not desirable from the standpoint of weight required to minimize umbilical deflection. Also, much of the OTV beam flange would be cut away, even then necessitating costly reinforcement of the flange.

Further problems concern the necessary plumbing on the External Tank or forward side of the ACC beams which in this concept would be virtually impossible due to the proximity of the LH₂ tank dome. Plumbing below or aft of the beams would need to be routed from inboard to outboard of the OTV frame requiring further cut outs and reinforcing with subsequent weight penalties.

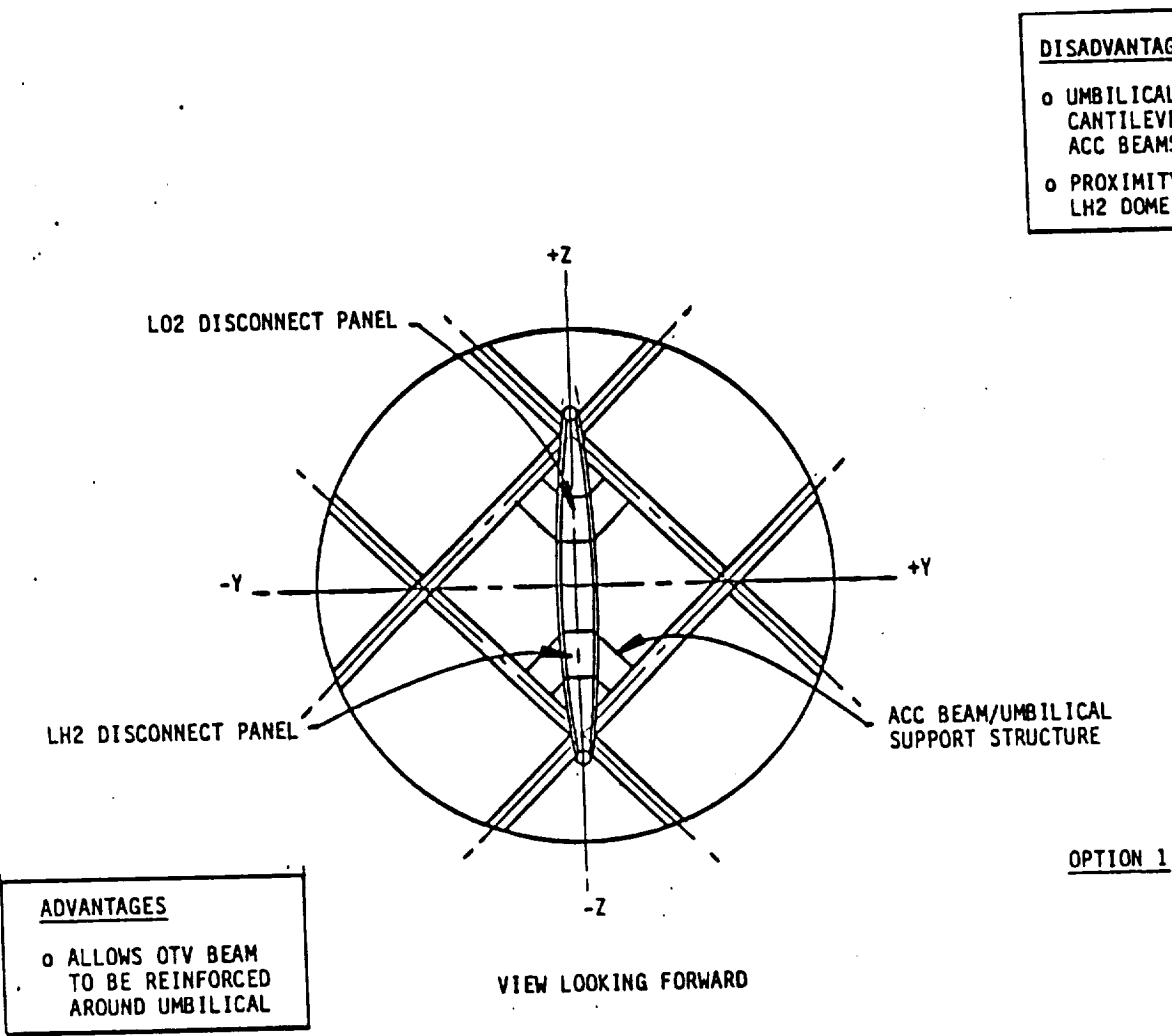


Figure 2.4-14 ACC/OTV Disconnect Panel, Forward View, Option 1

This location gives no access for on pad inspection or maintenance. Access can only be achieved by separation of the ACC-OTV or removal of the LO₂ tank.

Figure 2.4-15 shows an alternative umbilical arrangement which, due to the proximity of the LO₂ tank and the need for functional plumbing aft of the OTV beam, requires the separation plates to be a considerable distance from the OTV beam in the +Y plane.

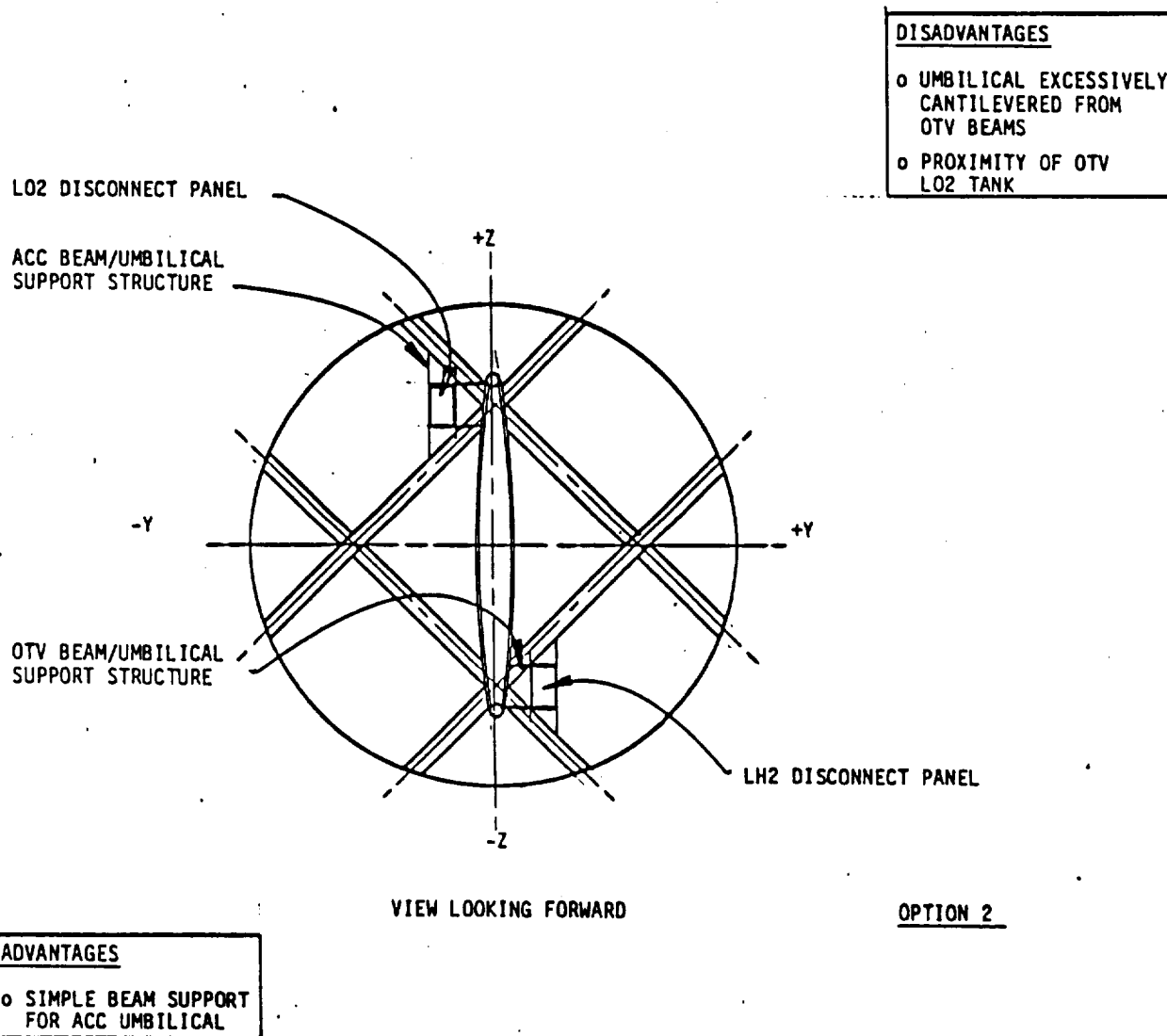


Figure 2.4-15 ACC/OTV Disconnect Panel, Forward View, Option 2

The umbilical supports from the ACC beams would be of a single simple beam construction, but the OTV umbilical support structure would be excessively cantilevered from the OTV beam.

This concept was deemed unsuitable for the above reason (being cantilevered), yet study shows that should the umbilicals require on pad inspection or maintenance without component breakdown, this location would be the best solution.

This would probably require some form of modification to the top of the LO₂ tanks for plumbing clearances. The proximity of the ACC/OTV attachment points would lend stability to the disconnect process but would require redesign.

Similar conditions prevail for the concept of Figure 2.4-16 here as were mentioned previously on the Figure 2.4-15 concept.

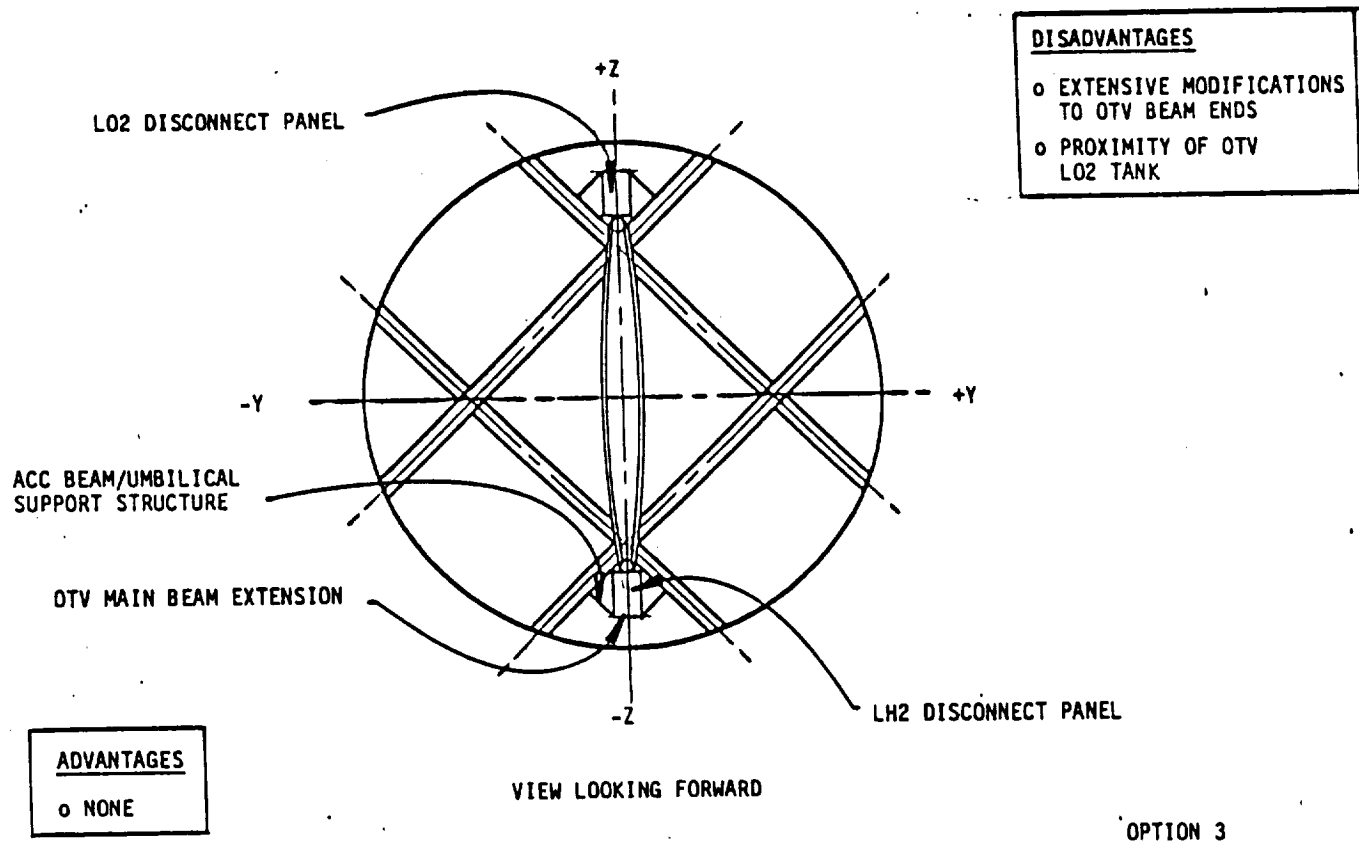


Figure 2.4-16 ACC/OTV Disconnect Panel, Forward View, Option 3

A simple beam could be utilized for the ACC disconnect plate, but for the OTV plate extensive modifications would need to be done to the OTV top beam in the form of extensions at the $\pm Z$ ends.

These extensions would need to be of sufficient length to give a plate location sufficiently outboard to show the required L_{O_2} tank plumbing clearance. Failing this, the only solution would be modifications to the L_{O_2} tank top. In fact, any suggestion of mounting in this area would entail modification to the L_{O_2} tank.

The combination of L_{O_2} tank modification together with the proximity of both the tank attachment points and extensions to the main beam length would suggest major design alterations.

This location is the only one which would give totally unimpeded access to the umbilicals should they need to be inspected "on pad". Provision of access doors would be necessary, ideally in both the skirt and shroud of the ACC - forward and aft of the ACC crossbeams.

CONCLUSION--Reference to Figures 2.4-17, 2.4-18, and also to the final Dwg No. GH1A-01T-02 shows the resultant chosen location for the disconnect plates.

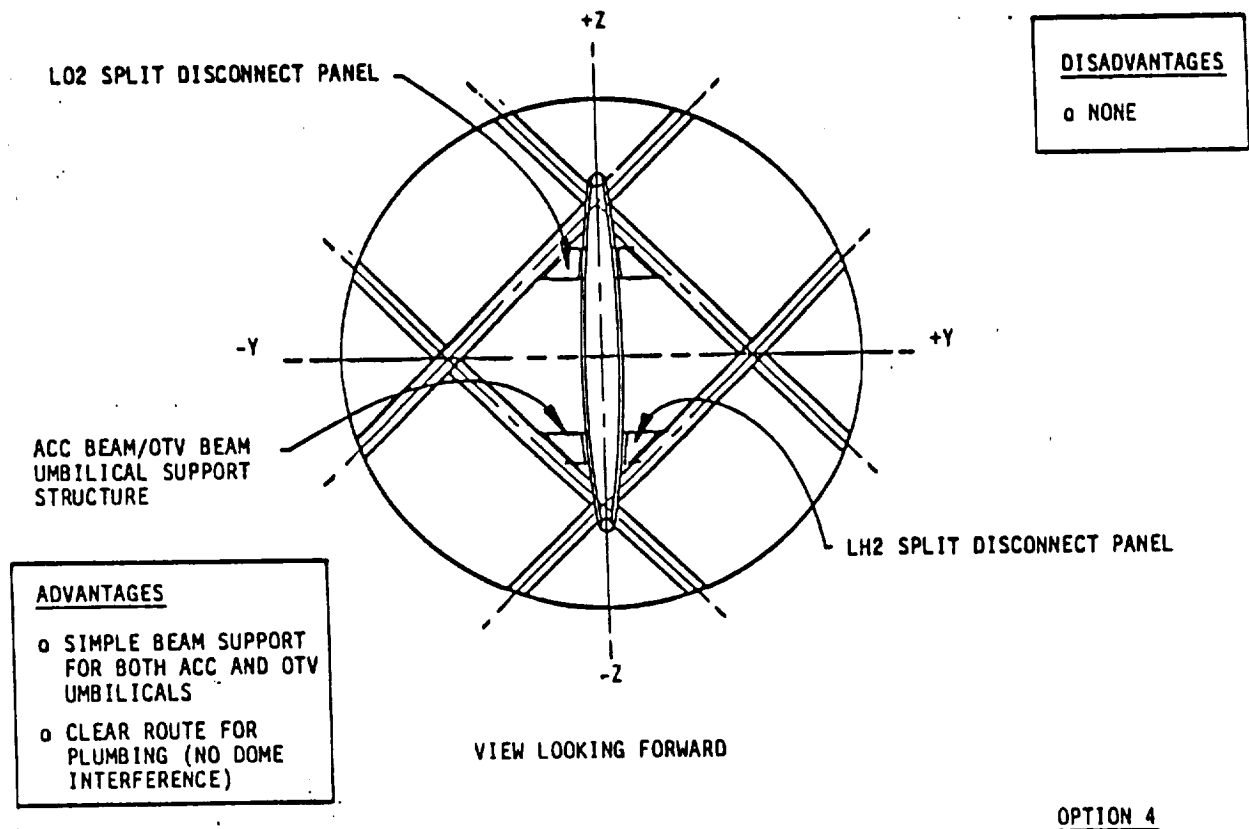


Figure 2.4-17 ACC/OTV Disconnect Panel, Forward View, Option 4

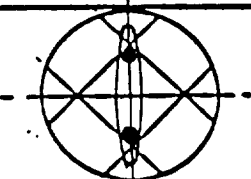
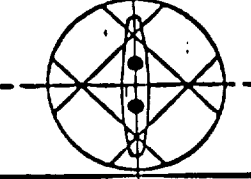
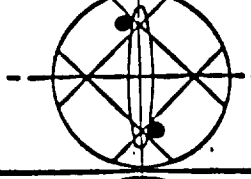
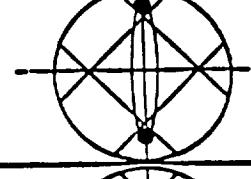
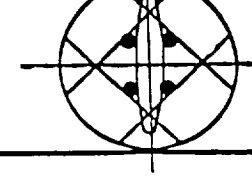
CONFIGURATION	ADVANTAGES	DISADVANTAGES
BASELINE 	<ul style="list-style-type: none"> GOOD SUPPORT FOR ACC UMBILICAL 	<ul style="list-style-type: none"> CUTS AWAY OTV BEAM FLANGE PROXIMITY OF OTV L02 TANK
OPTION 1 	<ul style="list-style-type: none"> ALLOWS OTV BEAM TO BE REINFORCED AROUND UMBILICAL 	<ul style="list-style-type: none"> UMBILICAL EXCESSIVELY CANTILEVERED FROM ACC BEAMS PROXIMITY TO ET LH2 DOME
OPTION 2 	<ul style="list-style-type: none"> SIMPLE BEAM SUPPORT FOR ACC UMBILICAL 	<ul style="list-style-type: none"> UMBILICAL EXCESSIVELY CANTILEVERED FROM OTV BEAMS PROXIMITY OF OTV L02 TANK
OPTION 3 	<ul style="list-style-type: none"> NONE 	<ul style="list-style-type: none"> EXTENSIVE MODIFICATIONS TO OTV BEAM ENDS PROXIMITY OF OTV L02 TANK
OPTION 4 	<ul style="list-style-type: none"> SIMPLE BEAM SUPPORT FOR BOTH ACC AND OTV UMBILICAL CLEAR ROUTE FOR PLUMBING (NO DOME INTERFERENCE) 	<ul style="list-style-type: none"> NONE

Figure 2.4-18 Ground-Based Cryo OTV Umbilical - Conclusions

It represents the closest points to the intersection of the ACC and OTV beams that would still enable a physical fit for the disconnect plate size.

The location also provides optimum clearance both forward and aft of Sta X_t 2185.00 that would give free plumbing routes without undue interference of the External Tank LH₂ tank dome and the OTV LH₂ tank tops.

To comply with the above requirements and to obtain sound structural mounting points that would give trouble free disconnection, it was necessary to split the umbilicals into two plates, one for fluids and the other for electrical - an arrangement which in itself could be advantageous.

The resulting support bracketry in the form of two simple beams, one for ACC and one for OTV, obviates the need for cantilevering from either beam with the resultant possible disconnect problems that bending and vibration might generate.

The required plumbing routes for the final concept would use fuel and vents at the new location alongside the OTV beam.

2.4.4 Composite Material Trade Study

The material concerns for the OTV are dependent upon the OTV environment. The environment concerns for both the ground based and space based OTV are similar in several ways. Both alternative OTVs would operate in both low earth orbit (LEO) and geostationary orbit (GEO); therefore, material effects caused by atomic oxygen, vacuum, etc.. are important. Specific concerns are identified in Figures 2.4-19 and -20. Estimated maximum temperatures in space for the truss and aerobrake structures are 250°F and 600°F, respectively. Approximately 30 missions ranging from 3-25 days are projected for both OTV options.

Truss Structure Material Concerns

- Atomic Oxygen Effects
- Coefficient of Thermal Expansion
- Cost
- Cryogenic Performance
- Density
- Ease of Modification
- Flame Retardation
- Impact Resistance
- Manufacturability
- Repairability
- Specific Strength
- Specific Modulus
- State of the Art
- Stiffness
- Strength
- Thermal Vacuum Stability (Outgassing)
- Toxicity
- Wearability

Figure 2.4-19 Major Material Concerns for Truss Structure

There are several environmental concerns which are not common to both OTV options. The ground based OTV experiences higher acoustical environments because it is carried to LEO in the Aft Cargo Carrier. The space based OTV is stored (probably under vacuum) in a hangar in the Space Station; whereas, the ground based OTV is retrieved by the Space Shuttle and brought to Earth between missions.

Property values and assessments of several material concerns for 11 generic composite systems are reported in Tables 2.4-1 and -2. Four material concerns stated in Figures 2.4-19 and -20 that are not represented by Tables 2.4-1 and -2 are a) attachability, b) repairability, c) ease of modification and d) atomic oxygen effect. Due to the nature of the data concerning these four items, it was deemed more appropriate to discuss the data of these items in the body of this report rather than include that data in tabular form.

Aerobrake Structure Material Concerns

- * Atomic Oxygen Effects'
- * Attachability
- Coefficient of Thermal Expansion
- Cost
- Cryogenic Performance
- Density
- Ease of Modification
- Flame Retardation
- * High Temperature Performance
- Impact Resistance
- Manufacturability
- Repairability Specific Strength
- Specific Modulus
- State of the Art
- Stiffness
- Strength
- Thermal Vacuum Stability (Outgassing)
- Toxicity
- Wearability

*This parameter is not included in Figure 2.4-19

Figure 2.4-20 Major Material Concerns for Aerobrake Structure

- A) The attachability of the composites of Tables 2.4-1 and -2 are basically the same. The use of special fasteners and/or adhesives for composite is warranted for all of the composite materials considered.
- B) The repairability of all of the composites considered, except for the two graphite/glass systems, are essentially equal. The repair techniques for these systems include 1) bonding, 2) bolting, and 3) patching. For the two graphite/glass systems, the repair techniques are 1) "melting-into-place" repair by heating to 3000°F, and 2) adhesive bonding because of the thermoplastic nature of the material.

ORIGINAL PAGE IS
OF POOR QUALITY

Table 2.4-1 Composite Material Properties

COMPOSITE MATERIAL* Fiber	Matrix	RT	Specific Strength (10 ⁶ in)						RT	Specific Modulus (10 ⁸ in)						Ultimate Tensile Strength @RT (ksi)	Modulus of Elasticity @RT (Msi)	Density (lb/in ³)
			-65	-250	250	450	600	1000		-65	-250	250	450	600	1000			
Graphite _{HS}	Epoxy	5.5	5.3	4.5	5.5	NR	NR	NR	3.6	3.6	3.4	3.7	NR	NR	NR	300	21	0.057
Graphite _{UHM}	Epoxy	1.3	ND	0.8	1.6	NR	NR	NR	6.8	ND	7.8	7.7	NR	NR	NR	81.5	41.6	0.061
Graphite _{Pitch}	Epoxy	2.0	ND	1.96	ND	NR	NR	NR	8.3	ND	2.3	ND	NR	NR	NR	120	48.7	0.059
Graphite _{HS}	Polyi- side	3.7	3.7	3.7	3.7	3.7	3.5	NR	3.4	3.4	3.4	3.4	3.4	3.4	NR	210	19	0.056
Graphite _{HS}	BMI	3.9	3.9	3.7	3.7	3.6	NR	NR	3.5	3.5	3.4	3.8	3.3	NR	NR	220	20	0.057
Boron	Epoxy	2.6	2.7	3.0	2.5	NR	NR	NR	4.2	4.3	4.4	4.0	NR	NR	NR	209	30	0.072
Kevlar	Epoxy	3.7	3.6	2.9	2.4	NR	NR	NR	2.3	2.3	2.3	ND	NR	NR	NR	185	11.50	0.050
Graphite _{HS}	Glass	1.2	ND	ND	1.2	1.2	1.2	1.2	3.4	ND	ND	3.4	3.4	3.4	3.4	84.3	24.4	0.072
Graphite _{KM}	Glass	0.7	ND	ND	0.7	0.7	0.7	0.7	4.3	ND	ND	4.3	4.3	4.3	4.3	51.2	31.2	0.072
Graphite	Phenolic	0.25	ND	ND	0.19	0.15	0.14	0.09	0.51	ND	ND	0.32	0.30	0.28	0.19	13	2.7	0.053
Graphite _{UHM}	Polyi- side	1.5	ND	ND	1.7	1.8	1.8	NR	6.7	ND	ND	6.7	6.7	6.3	NR	85	38.0	0.057

NR = Not recommended for use at specified temperature.

ND = No data

*Kevlar/Epoxy and Graphite/Phenolic systems are woven fabric. All other materials listed are unidirectional tape.

Both Graphite/Glass systems demonstrate good properties at temperatures up to 1800°F.

Subscripts: HS=high strength, KM=high modulus, UHM=ultrahigh modulus, Pitch=Pitch based ultrahigh strength fibers.

Specific Strength=FTU/Density

Specific Modulus=Modulus/Density

Table 2.4-2 Composite Material Properties

Composite Material* Fiber	Matrix	Thermal Conduct ivity ***	Coef. of Thermal Expansion ***		Flame Retar- dance	Toxi- city	Thermal Vacuum Stabil- ity	State of the Art	Wear ability	Manu- factur- ability	Ease of Repair	Notched Impact Strength ft lb in ²	Decompo- sition Temper- ature (°F)	Glass Transi- tion Temper- ature (°F)	Cost per Pound
			0°	90°											
Graphite _{HS}	Epoxy	ND	0.5	11.0	A	A	A	A	ND	1	2	15	670	507	65
Graphite _{UHM}	Epoxy	28-35	0.5	11.0	A	A	A	A	ND	1	2	15	670	507	1000
Graphite _{Pitch}	Epoxy	ND	0.5	11.0	A	A	A	A	ND	ND	2	15	670	507	65
Graphite _{HS}	Polyi- side	152	0.5	11.0	A	C	A	A	ND	2-3	3	ND	1060	818	65
Graphite _{HS}	BMI	ND	0.5	11.0	A	C	A	B	ND	2	3	ND	ND	560	65
Boron	Epoxy	17-31	2.5	13.1	B	A	A	A	ND	2	2	22.8	670	507	281
Kevlar	Epoxy	1-4	-2.2	32	B	A	A	A	ND	2	2	87	670	507	40
Graphite _{HS}	Glass	107	-0.05	2.6	ND	ND	ND	C	Low coef of fric- tion equals GR/E	1	1	15	3000°F	2000°F	600**
Graphite _{KM}	Glass	107	-0.3	3.6	ND	ND	ND	C	3x to 10x GR/E	1	1	15	3000°F	2000°F	ND
Graphite	Phenolic	3.5-4.4	ND	ND	A	A	B	A	ND	1	2	ND	ND	ND	ND
Graphite _{UHM}	Polyi- side	ND	ND	ND	A	C	A	B	ND	2-3	3	ND	ND	ND	1000

* See remark under Table 3.

See Notes for State of the Art, Manufacturability, Flame Retardance, Toxicity, Thermal Vacuum Stability and Ease of Repair

** Potentially cheaper than GR/E

Subscripts: HS=high strength, KM=high modulus, UHM=ultrahigh modulus, Pitch=Pitch based ultrahigh strength fibers.

*** Thermal Conductivity = Bru-in/hr ft²-°F. Coef. of Thermal Expansion = 10⁶ in/in/°F

- C) The ease of modification for a structure made of the given composite systems would be essentially equal. While drilling holes in fibrous composites gives rise to high stress concentrations, modification of a composite structure by drilling a hole into it to place a fastener in the structure can be successfully accomplished without seriously affecting the structural integrity of the part if proper precautions are taken.
- D) During STS-8 a myriad of material systems were exposed to space environment at LEO. Analysis of the environmental effects of LEO on those material systems was relayed to Martin Marietta Aerospace, Michoud Division by Johnson Space Flight Center. Based on the results for a minimal number of graphite/organic matrix composites, the total expected recession for an 11 year solar cycle is 360 microns (14 mils). This was reported in the data after noting the similarity of the reactivities of the graphite/organic matrix composites and organic films. Candidate protective concepts recommended by the atomic oxygen effect report of STS-8 included 1) vapor deposited or sputtered metal or Teflon base coatings applied to the outside wall of the truss for the Space Station, 2) applied metal foils such as aluminum, and 3) applied perfluorinated films such as Teflon. The selected protective coating should be durable since surface defects (due to handling, deployment, etc.) would allow atomic oxygen attack and subsequent part damage.

Several conclusion and/or recommendations can be drawn from Tables 2.4-1 and -2. For strength critical composite structures not exceeding 250°F, high strength or ultrahigh strength graphite fiber/epoxy resin composite is recommended. Operating under the same temperature constraints for modulus critical composite structure, ultrahigh modulus graphite fiber/epoxy resin is recommended. In composite applications where maximum operating temperatures do not exceed 600°F, high strength graphite fiber/polyimide resin is recommended for strength critical components and ultrahigh modulus graphite fiber/polyimide resin is recommended for modulus critical components. All graphite/organic matrix composites should be coated to prevent the effects of atomic oxygen.

NOTES

STATE OF THE ART--

- A = Production article in use
- B = Test articles only
- C = No specific applications

MANUFACTURABILITY--

- 1 = Readily available equipment
- 2 = Modifications required
- 3 = Very hard to make
- ? = No applications

FLAMMABILITY--Materials tested per NHB 8060.1A in Spacelab Cabin Air (23.8%O₂/N₂ at 14.5 psia) are rated as follows:

- A = The materials are noncombustible or self-extinguishing, within 6 inches from the bottom, in upward propagation test. See NHB 8060.1A, Test 1 for test procedures and criteria.
- B = The materials have downward propagation rates less than 0.3 inch/second and flash and fire points greater than 450°F per NHB 8060.1A, Tests 2 and 3.
- C = The materials have downward propagation rates greater than 0.3 inch/second and have flash and fire points greater than 450°F as defined in NHB 8060.1A, Tests 2 and 3.

TOXICITY--Materials tested per NHB 8060.1A are rated as follows:

- A = The level of total organics, excluding water, in the tested configuration does not exceed 100 micrograms/gram of sample tested, the level of carbon monoxide does not exceed 25 micrograms per gram of sample tested, and the odor rating is no greater than 2.5 (average of 10 tests).
- B = The material fails one or more of the "A" rated requirements, but will meet the "A" rating requirements when provided with a specific control, such as one having a leak rate no greater than 10⁻⁴ standard cc/sec, with a pressure differential on 14.7 psia when back filled with an inert gas.
- C = Materials with this rating are not acceptable for use in the indicated application category until their acceptability has been established. A "C" rated material must be shown, by test or analysis, to meet all of the requirements of an "A" rating for each specific design application.

THERMAL VACCUUM STABILITY--Materials tested per SP-R-0022A are rated as follows:

- A = The total weight loss is no greater than 1.0% and the volatile condensable products are no greater than 0.1% with cure processes/treatments specified in JSC 08962. CAUTION: The cure process/treatment can alter the thermal vacuum stability of materials. Additional tests must be conducted for other processes/treatments.
- B = The total weight loss is no greater than 3.0% and the volatile condensable products are no greater than 1.0%. These materials shall be limited to an exposed area of two square inches for each part or component and shall be approved on an individuals basis.

C = Materials with this rating are not acceptable for use in the indicated application category until their acceptability has been established. A "C" rated material must be shown, by test or analysis, to meet all the requirements of an "A" rating for reach specific design application.

EASE OF REPAIR--

- 1) Available methods include bolting, hot patches, adhesive which require solvent evaporation, and melting.
- 2) Everything in above section "1" except melting.
- 3) Adhesive bonding and hot patches only.

2.4.5 Metal Selection for Metal Tanks and Air Frame

INTRODUCTION--The overall objective of this report is to investigate the metal requirements of preliminary OTV concepts. References 2.4-5 through 2.4-12 provide the metals properties resource used to prepare this section. The four current concepts under consideration are cryogenic ground based, cryogenic space based, storable ground based and storable space based tanks. The major differences associated with these different OTV concepts are that both of the ground based OTV concepts will experience higher loading being carried to low earth orbit (LEO) in the proposed Aft Cargo Carrier (ACC) of the External Tank (ET) or in the cargo bay of the Shuttle. Any ground based concepts using the ACC method for deployment will likely experience a much higher acoustical environment over Shuttle cargo bay deployment. Additionally, ground based OTVs will be retrieved by a Shuttle and returned to Earth between missions, thereby lowering its exposure to radiation, meteoroids and other detrimental environmental effects. Space based OTV concepts will in all likelihood be stored in a hanger at Space Station between missions to minimize environment effects.

The basic OTV metal usage picture may be divided into two parts. The first is the propellant tanks and the second is the different structural members. The metal requirements for the cryogenic propellant concepts and storable propellant concepts are considered similar. These requirements are based on the recommended performance needs of several different hypothetical OTV missions. Detail requirements of the different concepts have not been defined and no effort to develop exact requirements will be attempted.

It should be noted that the different systems material lists are intended as starting guides to aid in the beginning design phases of OTV. The following lists do not constitute a final acceptable or rejectable materials list, but only the preferred or predicted metal of choice.

It is expected that with the rapid development of new alloys and improved processes these different lists will likely increase. New alloys like titanium-aluminides or aluminum-lithium (alithalite) alloys and new innovative

processes like rapid solidification rate (RSR) will improve alloy performance with potential cost savings over conventional methods and in some cases can be accompanied with weight savings.

Many of these new alloys and processes will be in production in the next 3 to 15 years. These new alloys are all in various developmental stages and little production-type data currently exist. But, based on current RSR development, a 200°F to 450°F improvement in operating temperature is anticipated for the respective alloy system. All of these new alloys do offer significant possibilities for future applications.

Property improvement is accrued primarily through microstructural refinement or extended solid solubility ranges. These improved mechanical properties will in all likelihood be compromised on any high subsequent heating. For this reason, severe restrictions concerning welding or any other high temperature treatment will likely be imposed. The aluminum lithium alloys are a new class of metal with a high modulus of elasticity.

The short term goals of researchers involved in AL-Li alloy development are: To develop alloys that match properties of the existing 2000 and 7000 series AL alloys, with a decrease in density of 10% and an increase in stiffness of 10%. Significant quantities of AL-Li alloys will be available from pilot scale facilities in late 1986 or early 1987. Full-scale commercial ingot production facilities can start up approximately 24 months after sufficient demand has been established to justify them. This full-scale commercial availability could occur as early as 1988.

Guide to the Materials Selection List Items

- | | |
|-----------------------|---|
| 1) Material | Metals by industrial material designation |
| 2) Density | lb/in ³ |
| Usable min. temp. | The recommended minimum operating temperature for the particular materials. The temperature at which a significant reduction in strength or toughness occurs. Based on MSFC-HDBK-527 "Materials Selection Guide for MSFC Spacelab Payloads. |
| 3) Specific Strength | <u>Tank Material</u> - Yield strength at temperature divided by room temperature density.

<u>Structural</u> - Ultimate strength at temperature divided by room temperature density. |
| 4) Specific Stiffness | Modulus of elasticity at temperature divided by room temperature density. |

- 5) K_{Ic} The fracture toughness of a material is a measure of resistance to fracture. It can also be considered a measure of the material tolerance to flaws.
- 6) K_{Ic} at Temp
 $\frac{K_{Ic} \text{ at Temp}}{K_{Ic} \text{ at RT}}$ This is a relative indication of what happens to the fracture toughness at temperature. If the ratio is greater than one at a cryogenic temperature, the fracture toughness has increased.
- 7) Machinability Material rating code is based on current acceptable industrial technique (most favorable - readily machinable).
- 8) Weldability This material rating code is based on anyone of the current acceptable welding processes (most favorable - readily weldable).
- 9) Repairability Anticipated ease of repair welding with current technique.
- 10) Material rating codes Rating the various metals under different conditions are defined as (see table for details):
 - A) Acceptable for use without reservation in the indicated category
 - B) Acceptable with specific controls of acceptability for use in the indicated category provided additional specific controls are imposed.
 - C) Acceptability must be demonstrated; not acceptable for use in the indicated category without demonstration.

METAL SELECTION CRITERIA--Table 2.4-3 shows a list of candidate metals that meet or are expected to meet most or all of the baseline requirements for OTV tank applications. This table was compiled from several sources, which are listed in References 2.4-5 through -12. Where available, the data about the particular material property of the metal was included. It must be noted that this table is not complete in many areas and requires further investigation.

Baseline requirements for both cryogenic and storable propellant OTV tanks are:

- a) The propellant tank would have adequate strength in all imposed environmental conditions.
- b) Weldable materials are required for tankage usage.
- c) Adequate low and high cycle fatigue life (vibration and thermal)
- d) Resist creep and reduction of allowable strength due to sustained pressure loads.
- e) Resistance to propagation of crack or crack-like indications.

ORIGINAL PAGE IS
OF POOR QUALITY

Table 2.4-3 Preliminary Tank Metal Selection

MATERIAL	DENSITY () LB/CU IN.	SPECIFIC STRENGTH AT TEMP				PTU/DENSITY	SPECIFIC STIFFNESS X 10 ⁶ MODULUS OF ELASTICITY/DENSITY		USABLE MINIMUM TEMP F	KIC @ RT KSI IN	KIC AT -423 F KIC @ RT
		-423 F	-300 F	RT	+250 F		-423 DEG	STIFFNESS @RT			
AL ALLOY 2219-T87	0.102	675	585	500	461	115	103	-423	26	1.27	
AL ALLOY 5456-H343	0.096	594	531	427	ND	130	106	-423	35+	1.02 ^a	
AL ALLOY 6061	0.098	507	418	367	431	116	103	-423	31	1.24 ^b	
CRES301 (FULL HARD)	0.290	862	724	620	545	103	86	-300	ND	1.08 ^c	
Ti-6Al-4V STA	0.160	1675	1394	906	750	113	102	-300	42	0.95	
Ti-15V-3Cr-3Al-3Sn	0.172	ND	ND	930	843	ND	ND	ND	ND	ND	
NEW AL-Li ALLOYS* (2090)	0.092	997**	864**	739***	ND	ND	ND	ND	30 (TYP FOR 1" PLATE)	ND	

*NEW AL-Li ALLOYS WITH HIGH DAMAGE TOLERANCE
5456 SPECIFIC STIFFNESS BY COMPARISON

a = NOTCH TENSILE RATIO $K_T = 7.2$ IN 0.050 IN. SHEET
b = NOTCH TENSILE RATIO $K_T = 21$ IN 0.125 IN. SHEET
c = NOTCH TENSILE RATIO $K_T = 21$ IN 0.073 IN. SHEET

**ESTIMATED BASED ON FACT 2090 IS A MODIFIED 2219 ALLOY.

***ESTIMATED - A VALUE BASED ON 68 ksi

MATERIAL	CORR RTG	SCC RTG	N204 RTG	HDZE RTG	MACHINABIL- ITY RTG	WELDABIL- ITY RTG	INITIA- TION	PROPAG- TION	REPAIRABILITY RTG
AL ALLOY 2219	B	A	A	A	B	A	C	C	A
AL ALLOY 5456	B	A	A	A	B-C	A	A-C	A	A
AL ALLOY 6061	B	A	A	A	B-C	A	A-B	A	A
CRES 301 (FULL HARD)	A	A	A	A	B	A	ND	ND	A
Ti-6Al-4V	A	A	A	A	C	B	ND	ND	B
Ti-15V-3Cr-3Al-3Sn	A	A	A	A	C	B	ND	ND	A
NEW AL-Li ALLOY SYSTEM	ND	ND	ND	ND	B	A	ND	ND	A

KEY:

NR = NOT RECOMMENDED
ND = NOT DETERMINED

ATM CORR RATE: A = MEETS REQUIREMENTS OF MSFC-SPEC-250A CLASS II
B = MEETS MSFC-SPEC-250A, IF COATED
C = REQUIRES DEMONSTRATION

MACHINABILITY RTG
WELDABILITY RTG
A = MOST FAVORABLE
B = FAVORABLE
C = MECHANABILITY OR WELDABILITY
LW = LIMITED WELDABLE (SPECIAL HANDLING)

SCC RTG

A = HIGH RESISTANCE TO STRESS CORROSION CRACKING
B = MATERIAL SHALL BE FURTHER ANALYZED
C = ACCEPTABILITY MUST BE DEMONSTRATED

HDZE & N204 RTG

A = ACCEPTABLE
B = ACCEPTABLE WITH SPECIFIC CONTROLS
C = ACCEPTABILITY MUST BE DEMONSTRATED

Specific cryogenic tank material requirements:

- a) LO₂ compatibility
- b) LH₂ compatibility
- c) -423°F to +250°F

Specific storable tank material requirements:

- a) Compatibility (N₂O₄)
- b) Compatibility (HDZE)
- c) -250°F to +250°F

CRYOGENIC TANKAGE MATERIALS--The cryogenic propellant tanks can be fabricated from a wide choice of metals. It is most probable all of the materials and components for cryogenic tankage usage will need to be current or near future (next five years) state-of-the-art in fabrication technique. All of the commercial available aluminum alloys shown in Table 2.4-3 show excellent mechanical properties at cryogenic temperatures because of their face center cubic crystal structure. The aluminum lithium alloys are also expected to find applications as cryogenic tankage materials.

With a highly developed data base and a wealth of past experience, the preferred current choice state-of-the-art alloy would be 2219 aluminum. Although its raw material costs may be among the highest, the weld tooling and process parameter development would be minimal. It is one of the most easily welded and formed of the heat treatable aluminum alloys. This material would be a relatively low risk extension of current technology and would provide tanks within presumably the shortest time frame with a minimal developmental cost.

A first generation Al-Li alloy under development which look like a functional replacement for 2219 is 2090. It is expected to have properties very similar to 2219 but with slightly better strength and lower density. Preliminary welding tests indicated it welds like 2219. Further work is needed to determine the optimal welding parameters, best filler metal and characterize joint properties. Because of it's promise, and assuming a sufficient developmental effort, MMC has planned to develop some of the necessary supporting data. We believe 2090 could be used on the OTV cryogenic tanks with 2219 being the back up material if problems develop with 2090 alloy.

The lack of weldability and availability are the major reasons why the 2014 wasn't selected. It has been reported the production of 2014 was discontinued by the major suppliers and for this reason was removed from the tankage metal selection table. This alloy also experiences stress corrosion cracking and exfoliation problems.

The aluminum alloy 5456 is highly weldable and corrosion resistant, but lacks the strength of 2219.

Although 6061 isn't as strong as any of the other alloys in the table, it possess good formability and better corrosion resistance than 2000 series alloy.

STORABLE TANK MATERIALS--For storable propellant tanks, it is recommended that Ti-6Al-4V, Ti-15V-3Cr-3Al-3Sn (Ti-15-3) or stainless steel 301 (CRES 301) be selected. For near term storable tanks, the preferred material would be Ti-6Al-4V with its current state-of-the-art fabrication techniques and minimum development cost. Also the physical and mechanical properties are developed. Development of Ti-15-3 appears to be a viable low cost, formable sheet titanium alloy alternative to Ti-6Al-4V. It has a high strength to density ratio and was developed to be a highly formable sheet alloy. This emerging alloy has shown potential cost savings over conventional Ti-6Al-4V parts. This material is recommended for future usage because of high specific strength and formability.

For future use the new titanium alloy Ti-15V-3Cr-3Al-3Sn looks very promising. Initial results for fracture toughness and critical flaw growth data are high encouraging but a considerable amount of additional information on mechanical properties are required before optimized storable propellant tanks can be made.

A decision to use a particular material for storable OTV tanks can only be made tentatively with the recommendations made here serving only as a guide. It must be noted that there is no strong discriminator between any of the above mentioned materials, but the storable tankage metals do not look promising for cryogenic applications.

Not considered in the table but a possible alternate propellant tank would be a prestressed composite propellant tank. This propellant tank would combine a Kevlar 49 overwrap with a metal liner of welded CRES 301 or 304 which could result in an efficient high strength, lightweight composite tank. This is a low risk extension of current technology that would provide tanks within a short time frame at a minimum developmental cost.

STRUCTURAL MATERIAL SELECTION CRITERIA--This section will identify and characterize materials for structural application. Baseline requirements for structural applications are:

- a) The structural members would have adequate strength
- b) High specific stiffness
- c) Resist creep and reduction of allowable strength
- d) Resistance to propagation of crack or crack-like indications
- e) Must not be susceptible to stress corrosion cracking
- f) The lowest density materials where requirements are met is favored.

Typical mechanical and physical properties of selected structural metals are compared in Table 2.4-4. The structural applications are separated into two areas, main support members and aerobrake back up structure.

MAIN STRUCTURAL SUPPORT MEMBERS--The main structural support members of the OTV vehicle are the main truss and crossbeam which can be fabricated from a wide selection of material. Currently, composites like graphite epoxy are the preferred material to minimize weight of the main structural support members. But if a metal were to be used, a weldable material to take advantage

Table 2.4-4 Preliminary OTV Structural Metal Selection

MATERIAL	DENSITY (LB/CU IN)	USABLE MINIMUM TEMP F	SPECIFIC STRENGTH				SPECIFIC STIFFNESS X 10 ⁶				KIC @ RT KSI /IN.	KIC @-250 KIC @ RT
			AT TEMP		FTU/DENSITY		AT TEMP		E/DENSITY			
			-250 F	RT	+250 F	600 F	-250 F	RT	+250 F	600 F		
2219-T87	0.102	-423	710	617	556	NR	107	103	100	NR	26	1.27 (-423 po)
AL ALLOY 2024-T6	0.100	-320	737	670	603	NR	116	106	101	NR	22	1.09
AL ALLOY 5456-H343	0.096	-423	517	427		NR	114	106	ND	NR	+45	1.02 (-423 po)
AL ALLOY 6061-T6	0.098	-423	476	429	377	NR	110	102	ND	NR	31	1.24 (-423 po)
AL ALLOY 7050 T74	0.102	-250°	ND	706	598	NR	110	101	ND	NR	30	ND
AL ALLOY 7090-T6E192	0.103	ND	ND	912	708	NR	ND	117	ND	NR	32	ND
NEW AL-Li ALLOYS	0.092	ND	ND	904	ND	ND	ND	123	ND	ND	ND	ND
BERYLLIUM	0.066	-423	ND	606	545	460	ND	636	630	612	ND	ND
CROSS-ROLLED BERYLLIUM	0.067	-423	ND	970	873	728	ND	634	628	603	ND	ND
INCONEL 718	0.297	-423	771	623	602	586	ND	100	99	925	226	1.13*
Ti-6Al-6V-2Sn	0.164	ND	ND	1067	997	736	ND	110	ND	ND	31	ND
Ti-15V-3Cr-3Al-3Sn	0.172	ND	ND	1000	ND	ND	ND	96	ND	ND	ND	ND

KEY:

- NR = NOT RECOMMENDED
- ND = NOT DETERMINED
- * SHOULD NOT BE USED OVER 650°F IN REPEATED APPLICATIONS
- ** NEW AL-Li ALLOY SYSTEM WITH HIGH STRENGTH
- a = Notch tensile ratio $K_T = 7.2$ in .050" sheet
- ATM CORR RATE: A = MEETS REQUIREMENTS OF MSFC-SPEC-250A CLASS II
- B = MEETS MSFC-SPEC-250A, IF COATED
- C = REQUIRES DEMONSTRATION

- MACHINABILITY & WELDABILITY RT6
- A) = MOST FAVORABLE
 - B) = FAVORABLE
 - C) = LESS FAVORABLE

SLL RTG

- A = HIGH RESISTANCE TO STRESS CORROSION CRACKING
- B = MATERIAL SHALL BE FURTHER ANALYZED
- C = ACCEPTABILITY MUST BE DEMONSTRATED

HDSE & N204 RTG

- A = ACCEPTABLE
- B = ACCEPTABLE WITH SPECIFIC CONTROLS
- C = ACCEPTABILITY MUST BE DEMONSTRATED

MATERIAL	CORR RTG	SCC RTG	N204 RTG	HDZE RTG	MACHINABILITY RTG	WELDABILITY RTG	REPAIRABILITY RTG
AL ALLOY 2024-T6	B	A	A	A	B	B	A
AL ALLOY 2219-T87	B	A	A	A	B	B	A
AL ALLOY 5456-H343	B	A	A	A	B-C	A	A
AL ALLOY 6061-T6	B	A	A	A	B	A	A
AL ALLOY 7050-T74	B	A	A	A	B	NR	NR
AL ALLOY 7090-T6E192	ND	ND	ND	ND	B	ND	NR
NEW AL-Li SYSTEM	B	A	ND	ND	B	ND	ND
BERYLLIUM	A	A	A	U	C	NR	NR
CROSS-ROLLED BERYLLIUM	A	A	A	U	C	NR	NR
INCONEL 718	A	A	A	A	C	B	A
Ti-6Al-6V-2Sn	A	A	A	A	C	B-C	B
Ti-15V-3Cr-3Al-3Sn	A	A	A	A	C	B-C	A

of welding fabrication would be preferred. Aluminum alloys 2024 or 2219 would offer the best potential of minimizing weight at reasonable cost. It is clear that titanium alloys like Ti-6Al-6V-2Sn have higher strength and stiffness but would be a higher cost over aluminum alloys 2024 or 2219. For nonwelded applications, 7050-T6 or -T76 offers high strength and good exfoliation corrosion resistance. In addition, 7050-T6 or T76 has good fracture toughness.

AEROBRAKE STRUCTURAL SUPPORT METAL CRITERIA--The aerobrake system of the OTV is a flexible deployable thermal shield which is being proposed to provide the OTV with a braking function at a lower weight than a propulsive braking system would provide on return to low earth orbit. The two main structural problems associated with aerobrake using the Earth's atmosphere are high temperatures and large decelerations.

Design analysis of the aerobrake system predicted temperatures of 2600°F and pressures of 15 psf. The aerobrake must also prevent back thermal radiation onto the OTV main structural and tankage members and provide insulation to limit the temperature of the main aerobrake support members to a maximum temperature of 600°F.

Elevated specific strength and stiffness are primary factors in the design of the aerobrake support structures. Beryllium, with its light weight coupled with its high stiffness and strength, classifies as an ideal material for this application in which minimum weight is a primary concern. Beryllium and its alloys have the highest specific stiffness of the known metals. Beryllium has the highest specific heat capacity of all metals with its specific heat capacity at room temperature being 0.46 BTU/lb. For any given temperature change, beryllium has the ability to absorb more heat than other metals. The unique combination of a high modulus of elasticity and low density (high specific stiffness) shows beryllium to be 6 times greater in specific stiffness than the structural aluminum alloys.

The cost of this metal is not a physical or mechanical property but it may be an overriding factor in the final selection of an aerobrake support member. Based on economic consideration, beryllium may not be the choice metal for this particular case.

2.4.6 Transportability and Assembly of the Space-Based Cryogenic OTV

PURPOSE--The purpose of this study is to delineate the methods by which the space-based cryogenic orbital transfer vehicle (OTV) is transported by the Space Shuttle system from ground to near earth orbit and assembled in space.

SUMMARY--The study shows that by efficiently arranging the major assemblies of the OTV in a sequential order in the shuttle orbiter bay, a minimum of two flights will be required to transport the OTV to near earth orbit. The arrangement of the OTV major assemblies and the order of flight is such that the OTV will be assembled in space with a minimum of EVA activity.

STATEMENT OF PROBLEM--The transportation of OTV assemblies requires that each major assembly be firmly secured in the orbiter bay using appropriate airborne support equipment (ASE); that upon arrival in space each assembly be easily removed in a manner that provides for the orderly assembly in space; that overall dimensions of the assemblies stowed in the orbiter bay must fall within a cylindrical envelope 14.5 ft in diameter and 5.5 ft in length; and that the ASE be designed to interface with the orbiter longeron and keel fittings and provide interfaces for the OTV.

DISCUSSION OF RESULTS--For this study the 81K space based cryogenic OTV configuration is selected as the vehicle to be transported and assembled.

ORBITER 1 (Figure 2.4-21) accommodates the following. The center truss and folded tank support structures with two main engines and accompanying propulsion systems and avionics ring installed in place on the center truss. ASE cradles at each end of the center truss provide the required support in the Orbiter bay. Two LO₂ tanks supported at their forward and aft end by cradles complete the payload.

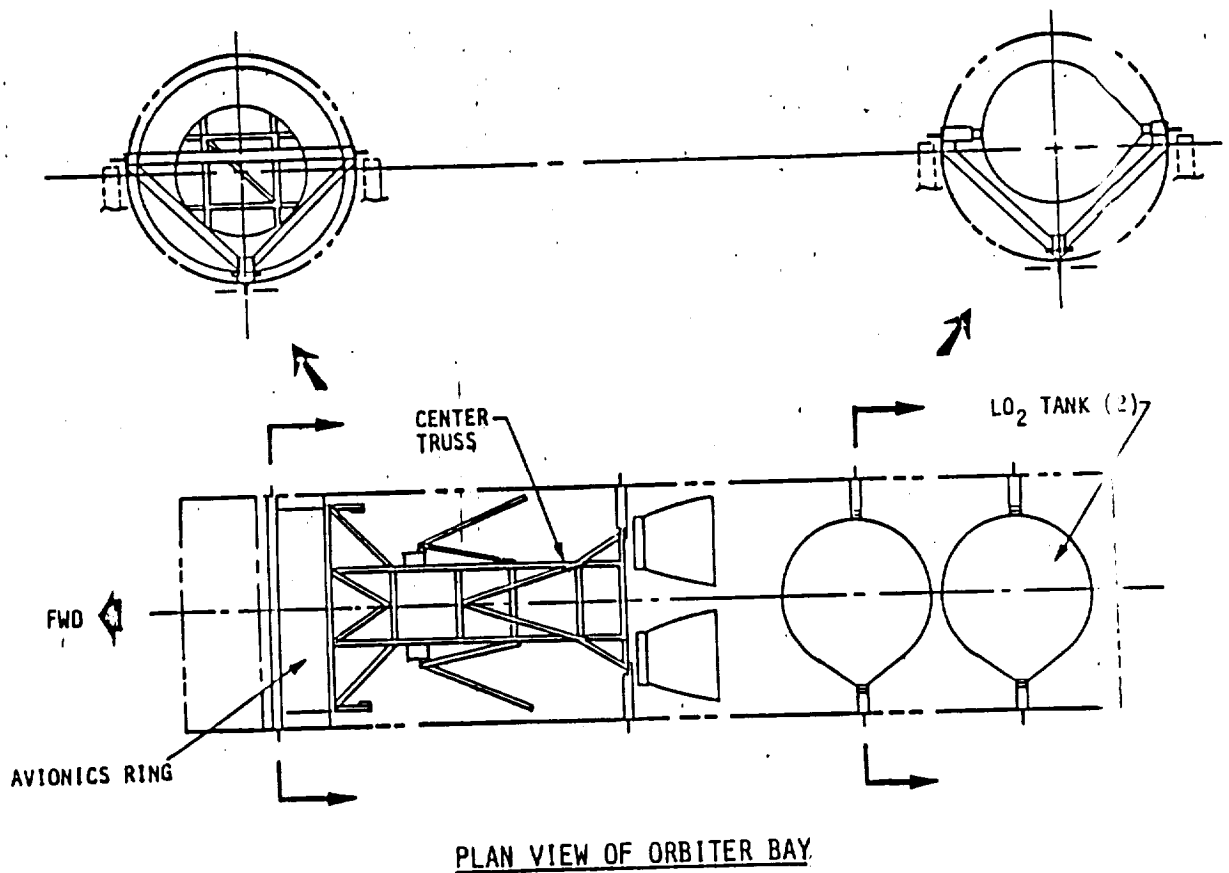


Figure 2.4-21 Space-Based Cryo OTV Transportation - Orbiter 1

ORBITER 2 (Figure 2.4-23) transports the folded 44-foot diameter aerobrake. Two LH₂ tanks supported at their forward and aft end by three cradles complete the payload.

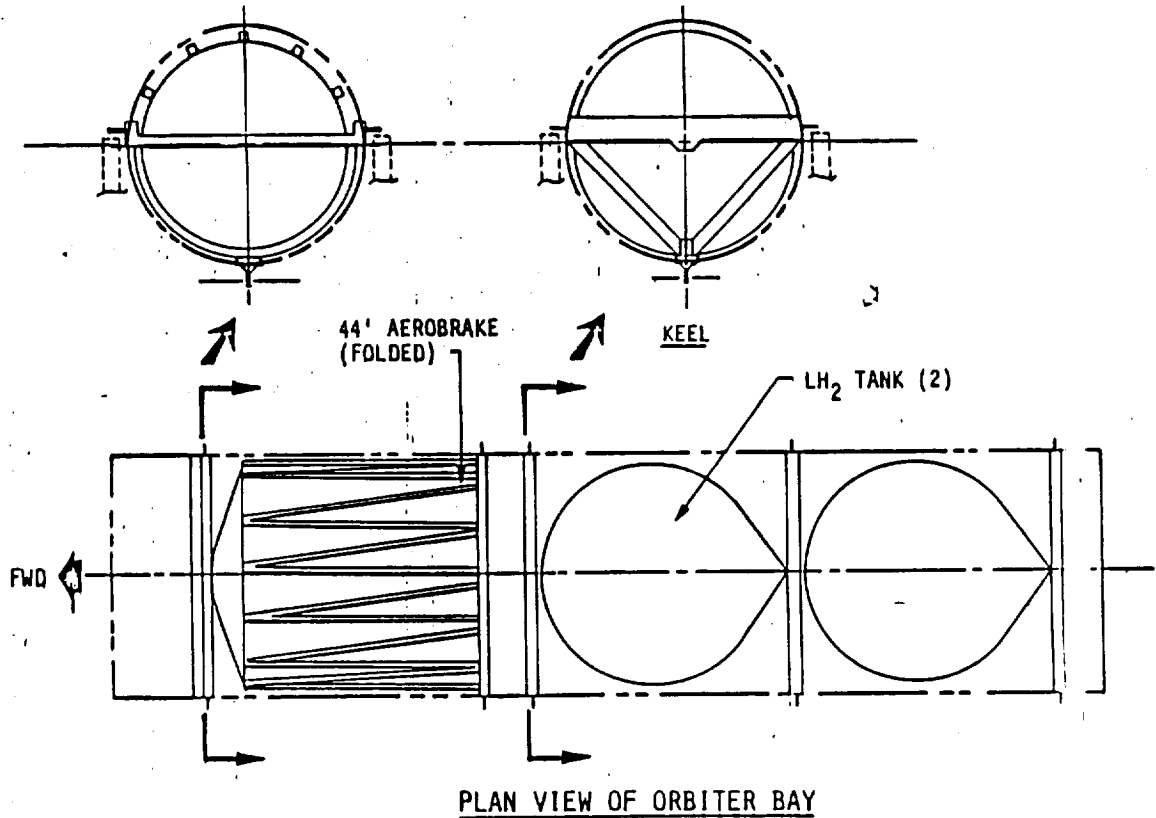


Figure 2.4-22 Space-Based Cryo Transportation - Orbiter 2

ASSEMBLY SEQUENCE-OPERATION 1--The center truss with attached engines and installed propulsion systems are removed from Orbiter 1. LO₂ and LH₂ tank support structures are unfolded and secured. The two LO₂ tanks are then installed.

OPERATION 2--The two LH₂ tanks are installed after removal from Orbiter 2.

OPERATION 3- The aerobrake is removed from Orbiter 2, deployed and installed on the vehicle.

2.4.7 Growth of Ground-Based 55K cryo OTV to 94K Space-Based OTV

PURPOSE--The purpose of the study was to determine if a logical growth was possible in going from a ground-based 55K OTV to a space based 94K OTV.

SUMMARY--The first part of the trade which looked at the geometry of having two RL10-IIB engines on the 55K ground-based OTV concluded that the combination would not fit in the ACC. Final tank size selected would not effect the results but the selection of a smaller engine is expected to effect the conclusion.

The second part of the trade which looked at the common parts in growing a 55K ground-based cryo with one engine to a 94K space based cryo OTV with two engines. It was found that only the original center support truss and structural part of the avionics ring could be called truly common. Here a smaller engine selection and slightly different size tanks would not effect this conclusion.

STATEMENT OF PROBLEM--For there to be a logical growth from a ground based 55K OTV to a space-based 94K OTV, both should have two engines to eliminate two engine feed system developments even though the man-rated two engine system is not required until later in space basing. So we must determine if geometry will allow a two engine 55K vehicle to fit within the ACC envelope.

The second part of the problem is to count up the systems that are common to the 55K ground based and the 94K space based to determine the degree of commonality possible with such a growth pattern.

DISCUSSION OF RESULTS--Figure 2.4-23 shows the ground rules that were used for the study. Figure 2.4-24 shows a layout of a two engine 55K ground-based OTV with RL10-IIB engines that falls outside the envelope of the longest possible OTV. The requirement to locate the engines so that with one engine out the remaining engine can still be gimballed through the worst case CG set the engine location. The conclusion would be relatively unaffected by minor changes in propellant load, but it would be sensitive to the selection of a smaller engine than the RL10-IIB.

The second part of the trade looked at what parts were common if we grew a one engine 55K ground based OTV to a two engine 94K space-based OTV. Assumptions for this study included using an avionics ring on both vehicles to maximize commonality. It was assumed the avionics for the 55K and 94K OTVs could be mounted on the same structural ring. Figure 2.4-25 shows that only the original center support truss and the structural parts of the avionics ring could be counted on as truly common. Plumbing attached to the original truss could also be designed to be common. The lower truss and its split plumbing, the larger tanks, larger aerobrake and aerobrake supports are all new. A smaller engine selection and slightly different size tanks would not effect this conclusion.

- o ENGINES RL10 - IIBs
- o ACC
 - 7.0 INCHES LONGER THAN GENERAL PURPOSE
 - USED SPECIAL PURPOSE ACC DESIGN (I.E., SPHERICAL DOME)
- o ENGINE NULL = 10° OUTBOARD
- o ENGINE GIMBAL ANGLES
 - OUTBOARD = 16° FROM NULL
 - INBOARD = 13° FROM NULL
- o CLEARANCE BETWEEN NOZZLES = 6 INCHES
- o WORST CG CASE - 15% FUEL LOAD

Figure 2.4-23 2-Engine, 55K, GB, Cryo OTV Ground Rules

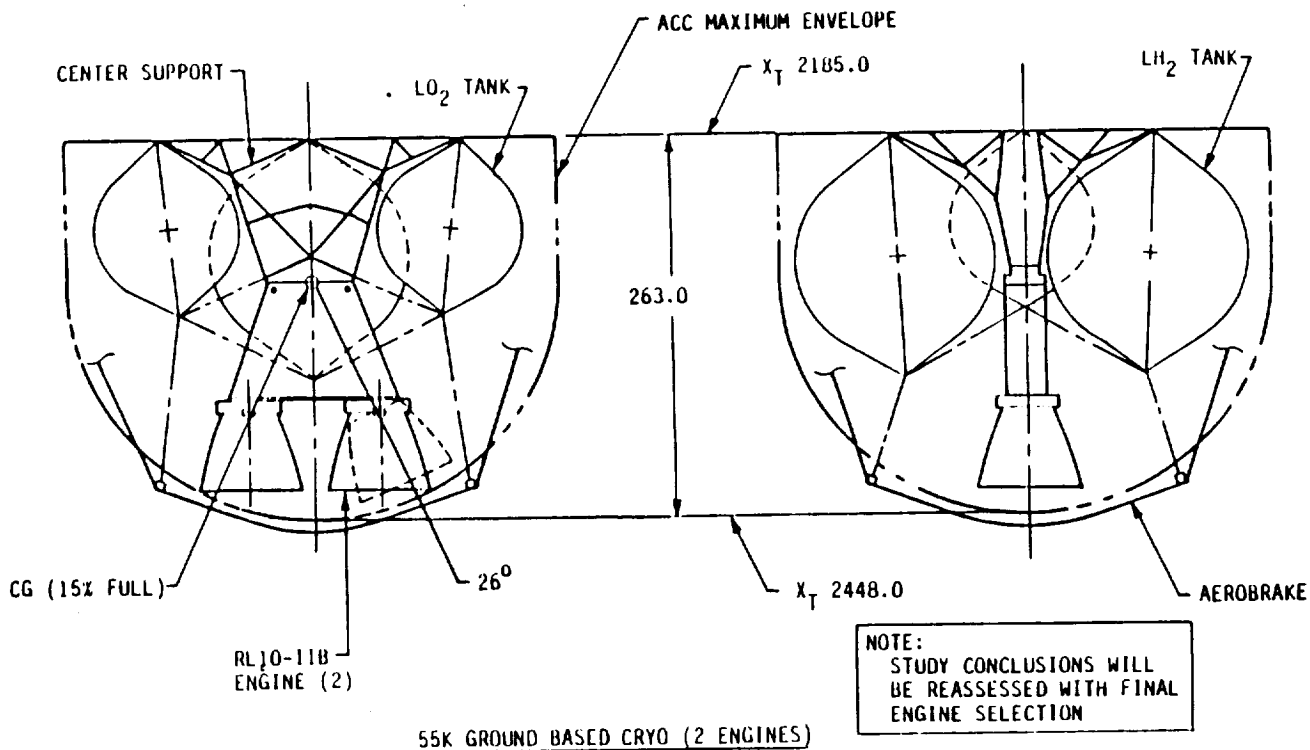


Figure 2.4-24 2-Engine, 55K, G/B, Cryo OTV Configuration

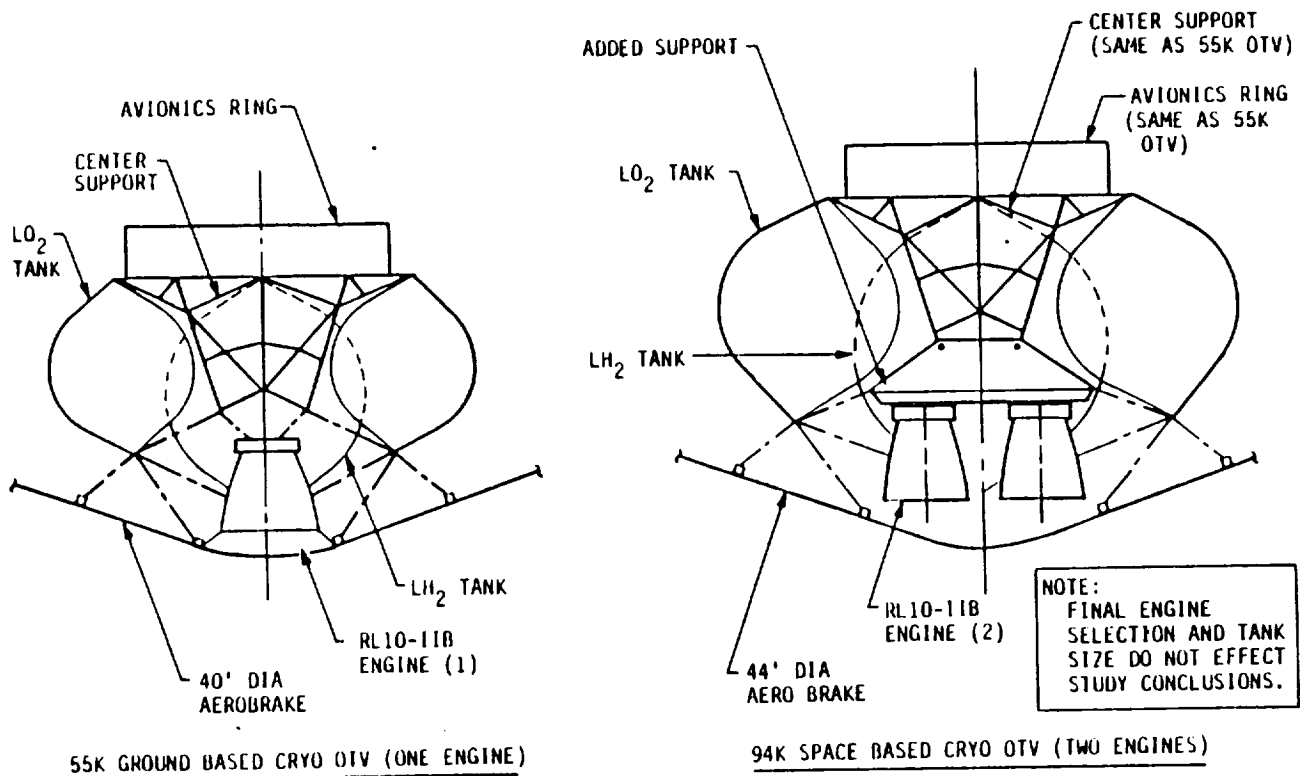


Figure 2.4-25 GB to SB Cryo OTV Configuration

2.4.8 Space-Based Cryogenic Drop Tank Configurations

PURPOSE--To make a weight comparison of two droptank versions of a space-based cryogenic OTV with the baseline (ref.) design 84K space based cryo OTV.

SUMMARY--It was established that the baseline 84K space-based cryo OTV with cluster tanks (4 tanks) laterally spread uses less propellant than the two droptank vehicles considered.

STATEMENT OF THE PROBLEM--This study was initiated to further explore the weights of candidate droptank vehicles. The configurations investigated are shown in Figure 2.4-26.

The droptank vehicle with cylindrical drop tanks has a cluster of four spherical main tanks that hold half the propellant while the outboard cylindrical droptanks contain the remaining half of propellant.

The droptank vehicle with tandem spherical drop tanks also has propellants split 50-50 between main tanks and drop tanks.

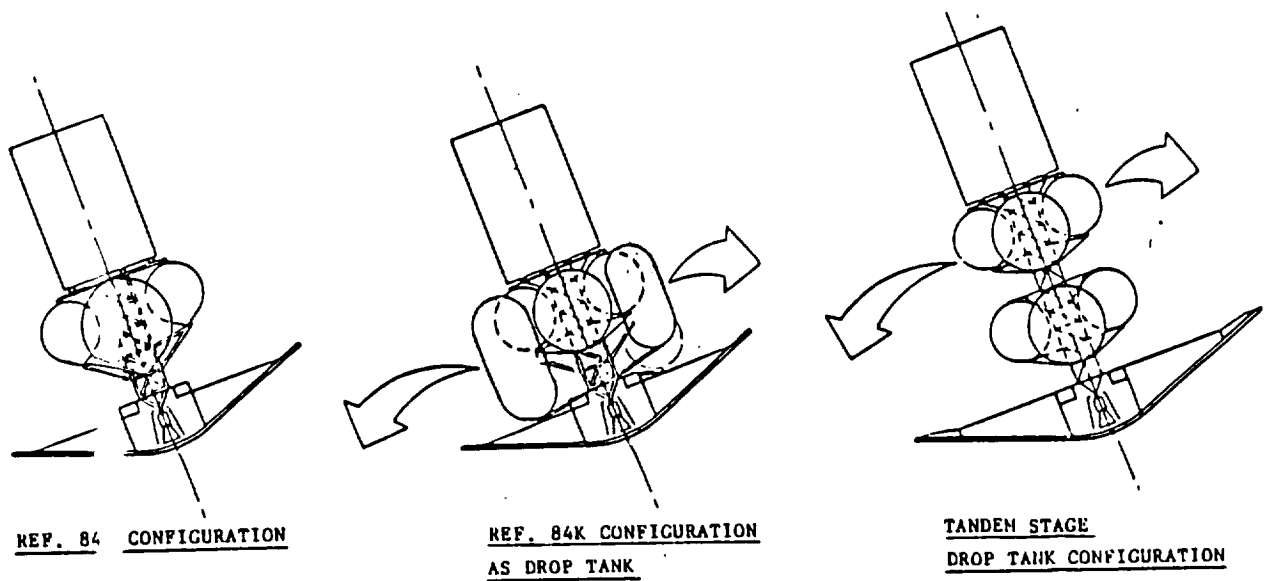


Figure 2.4-26 Cyro Droptank OTV Weight Trade

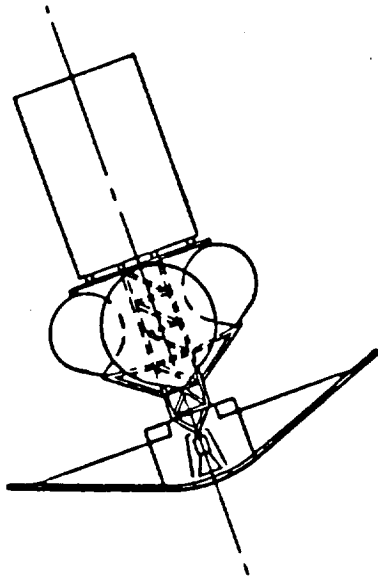
The two droptank vehicles and the reference vehicle were considered to have the following common properties:

- 1) Aerobrake material 0.961 lb/ft²
- 2) Tank material of 2219 aluminum with a covering of 1.0 inch MLI (1) and 0.025 minimum gage
- 3) A 20° cone angle of payload or tank protection to be given by the aerobrake under reentry conditions
- 4) Same total tank volume.

For the purpose of the study only tank delta weight, drop tank support structure weight, droptank eject system weight, drop tank feed system weight and aerobrake delta weight were considered since other items are considered common to all concepts.

(1) MAIN TANKS ONLY

SELECTION CRITERIA--Figure 2.4-27 shows the calculation of the weights of the tanks for the 84K reference vehicle. Figure 2.4-28 shows the calculations for the weights of the droptank vehicle with cylindrical drop tanks. Because of the weight of the support structure, the eject system for the droptanks and the delta weight for the droptank feed system, 1838.4 lbs of additional propellant is required for the up burn for the droptank OTV. Some 1104.91 lbs less propellant is required for the deorbit burn for the droptank OTV. This results in a net increase of 733 lbs of propellant for the cylindrical droptank vehicle.

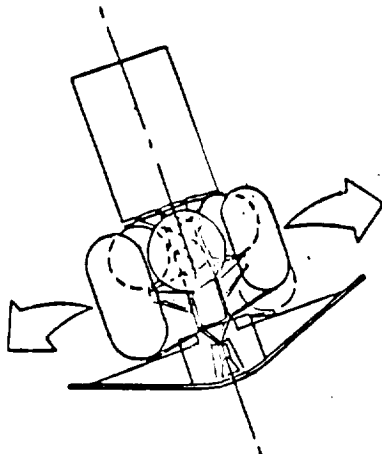


- (2) LO₂ TANKS AT 36K EA W/MLI $W_T = 560.9 \text{ lbm}$
- (2) LH₂ TANKS AT 6K EA W/MLI $W_T = \underline{1198.94 \text{ lbm}}$

1759.84 lbm

REF. 84K CONFIGURATION

Figure 2.4-27 Cryo Droptank OTV - Reference Configuration Baseline



REF. 84K CONFIGURATION WITH DROP TANK

- (2) LO₂ TANKS (SPHERE) @ 18K EA W/MLI $W_T = 324.24 \text{ lbm}$
- (2) LO₂ TANKS (CYLINDER) AT 18K EA $W_T = 305.2 \text{ lbm}$
- (2) LH₂ TANKS (SPHERE) AT 3K W/MLI $W_T = 627.3 \text{ lbm}$
- (2) LH₂ TANKS (CYLINDER) $W_T = 675.98 \text{ lbm}$
- 1932.72 lbm
- LESS BASELINE TANK $W_T = \underline{(1759.84 \text{ lbm})}$
- TANK DELTA $W_T = 172.88 \text{ lbm}$
- ADDED STRUCT. + EJECT DELTA $W_T = 400.00 \text{ lbm}$
- ADDED PROP FEED SYS DELTA $W_T = \underline{40.00 \text{ lbm}}$
- DELTA W_T UP = 612.88 lbm
- DROP (2) LO₂ TANKS = (305.24 lbm)
- DROP (2) LH₂ TANKS = (675.98 lbm)
- DELTA W_T DOWN = (368.3 lbm)

@ 3.0 lb/1.0 lb DRY WEIGHT;

DELTA W_T PROP UP = 1838.64 lbm

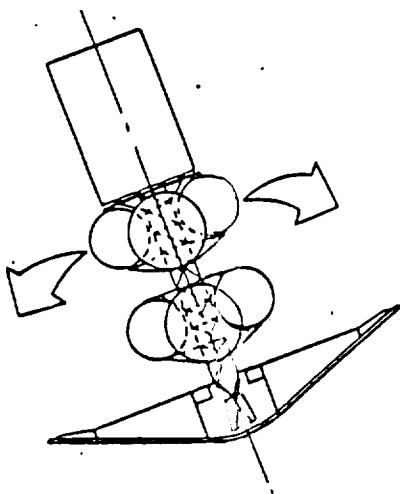
DELTA W_T PROP DOWN = (1104.91) lbm

DELTA W_T PROP = 733.74 lbm

Figure 2.4-28 Cryo Droptank OTV - Reference Configuration

Figure 2.4-29 shows the calculations for the weights of the cryo drop tank - tandem stage. The story is similar to the OTV with cylindrical droptanks but worse because a larger and heavier aerobrake is needed to protect the payload on the longer tandem vehicle. Results are summarized in Figure 2.4-30.

RECOMMENDATION--The study showed that the baseline vehicle uses less propellant than the two droptank vehicles and therefore it is recommended that the baseline vehicle be retained as the main line space based cryo OTV.



TANDEM DROP TANK STAGE CONFIGURATION

(4) LO2 TANKS AT 18K EA	$W_T = 602.24$ lbm
W/MLI	
(4) LH2 TANKS AT 3K EA	$W_T = \underline{1254.68}$ lbm
W/MLI	
	1856.92 lbm
LESS BASELINE TANK W_T	(1759.84 lbm)
	97.08 lbm
2ND STAGE STRUCTURE + EJECT W_T	= 400.00 lbm
2ND STAGE PROPULSION FEED SUBSYSTEM W_T	= 40.00 lbm
AEROBREAK $\Delta A = 4758f^2 - 2900f^2 - 1858f^2 \times 0.961b/f^2$	= <u>1783.68</u> lbm
	ΔW_T UP = 2320.76 lbm
	DROP (2) LO2 TANKS = (301.12 lbm)
	DROP (2) LH2 TANKS = (<u>627.34</u>) lbm)
	ΔW_T DOWN = 1392.30 lbm

AT 3.0 lbm/1.0 lbm DRY WEIGHT;
 ΔW_T PROP UP = 6962.28 lbm
 ΔW_T PROP DOWN = 4176.9 lbm
 PROP $\Delta W_T = 11139.18$ lbm

Figure 2.4-29 Cryo Droptank OTV - Tandem Stage

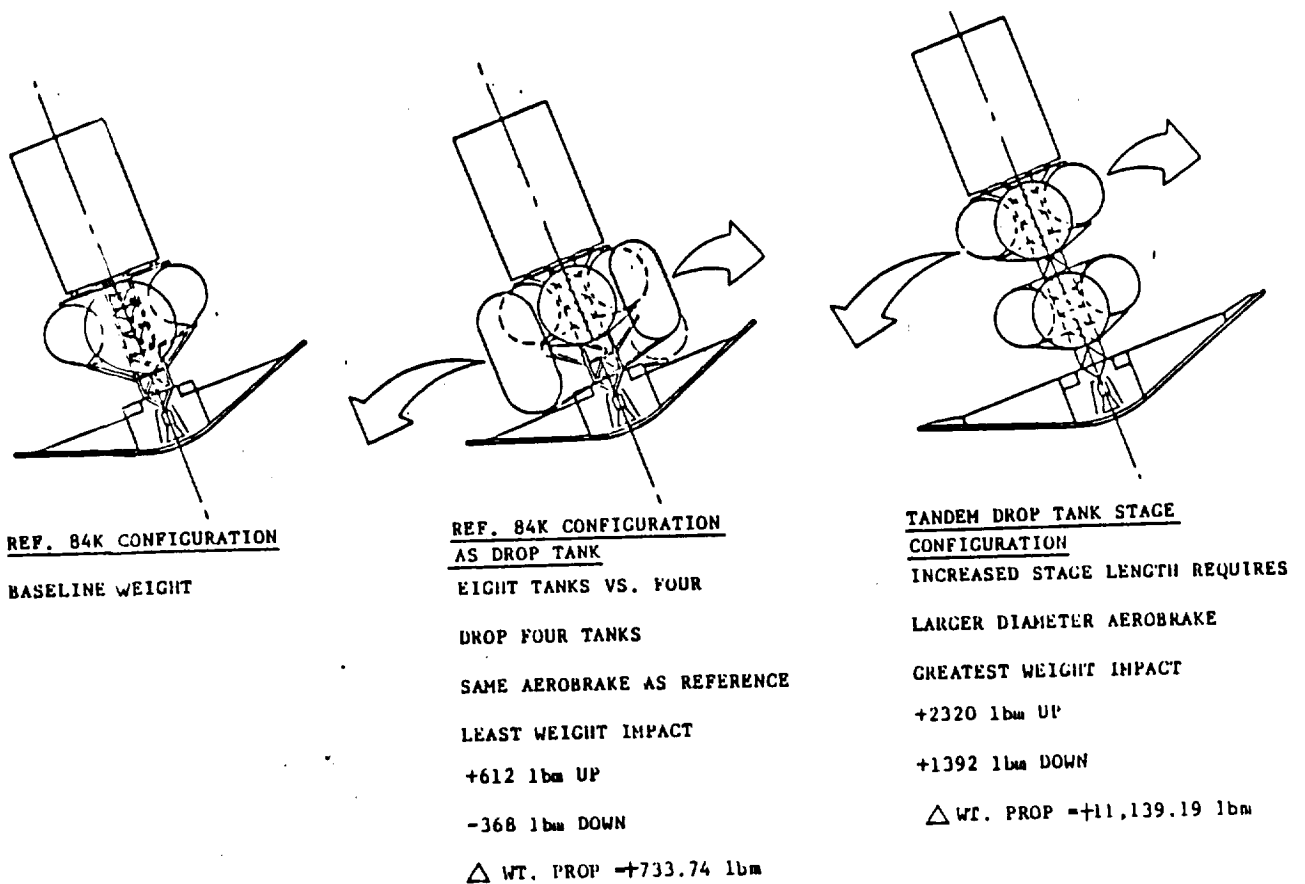


Figure 2.4-30 Cryo Droptank OTV Summary

2.4.9 Meteoroid Protection System

PURPOSE--The purpose of the study was to determine what meteoroid protection system is needed on the space-based 94K cryogenic configuration. The goal was a practical minimum weight protection system.

SUMMARY--The lightest weight system consists of an 0.006" aluminum bumper, a 2.82" gap and 1.03 inches of multilayer insulation (MLI) to capture particles of meteoroid and bumper. Variations which eliminate the gap or bumper proved to have unacceptable weight penalties over the baseline system.

STATEMENT OF PROBLEM--During the time that the space-based OTV is exposed to space environment (i.e., not hangered), there is the danger of meteoroid impact on the OTV. The greatest danger would be an impact to the pressurized

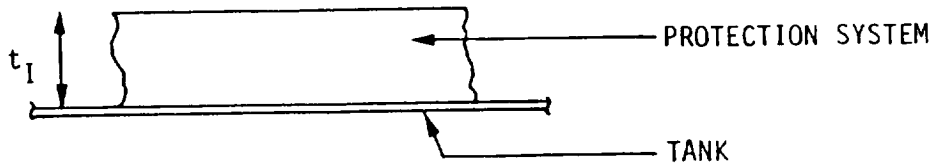
propellant tanks. Such an impact could result in an explosion. The assumptions used to design tank meteoroid shielding were:

- o No damage to propellant tank wall
- o Twenty percent intercomponent shielding
- o Man-made debris not addressed
- o Six inches maximum practical standoff

DISCUSSION OF RESULTS--The meteoroid environment used for this work is given in Figure 2.4-31 and is obtained from NASA SP 8013 meteoroid environment model 1969. The method used to calculate MLI thickness for a solid barrier is shown in Figure 2.4-32. The method for determining thicknesses for a bumper gap and backing layer system are given in Figure 2.4-33.

- o OBTAINED FROM NASA SP 8013 METEOROID ENVIRONMENT MODEL 1969
- o DESIGN METEOROID IS ASSUMED TO HAVE:
 - VELOCITY = 20 KM/SEC
 - DENSITY = 0.5 GM/CM³
- o RELIABILITY (PROBABILITY) $R = e^{-NAT}$
 - T = EXPOSURE DURATION
 - A = EXPOSED AREA
 - N = FLUX DENSITY OF METEORIDS OF MASS M OR GREATER
- o SPACE METEOROID ENVIRONMENT MODEL
 - $\log_{10} N = -14.57 - 1.213 \log_{10} M$ (INCLUDING EARTH SHIELDING & DEFOCUSING FACTOR)
 - M = METEOROID MASS

Figure 2.4-31 Meteoroid Environment



$$t_A = \text{THRESHOLD PENETRATION THICKNESS OF ALUMINUM PLATE}$$

$$= 0.224(M)^{0.352} (\rho_m)^{1/6} (V)^{0.875}$$

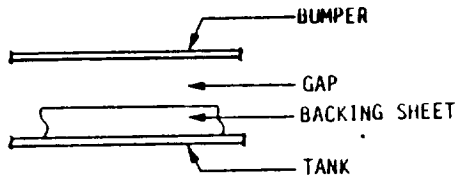
M = METEOROID MASS

ρ_m = METEOROID DENSITY 0.5 GM/CM³

V = METEOROID VELOCITY 20 KM/SEC

$$t_I \text{ REQUIRED INSULATION THICKNESS} = t_A \text{ DESIGN METEOROID} \times \frac{t_{ID} \text{ (DEMONSTRATED THICKNESS ON TEST)}}{t_{AD} \text{ (REQUIRED ALUMINUM THICKNESS FOR TEST PROJECTILE)}}$$

Figure 2.4-32 Meteoroid Protection - Method 1 (Solid Barrier)



$$\text{BUMPER: } \frac{\text{BUMPER THICKNESS}}{\text{METEOROID DIAMETER}} = 0.04$$

(FOR V = 20 KM/SEC)
DIRECTLY RELATED TO BUMPER DENSITY

$$t_{BA} \text{ THICKNESS OF BACKING ALUMINUM SHEET} = \frac{0.55 (\rho_m \cdot \rho_t)^{1/6} M^{1/3} V}{s^{1/2}}$$

ρ_m = METEOROID DENSITY
 ρ_t = BACKING MATERIAL DENSITY
S = GAP DISTANCE

FOR SPACING GREATER THAN 30 X METEOROID DIAMETER,
THE ABOVE EQUATION BECOMES INDEPENDENT OF S

FOR MAXIMUM BUMPER "EFFICIENCY" GAP = 30 X METEOROID DIAMETER

t_{BA} TRANSLATED TO REQUIRED INSULATION THICKNESS VIA
EQUATION IN METHOD 1

* FROM AIAA PAPER #69-372, HYPERVELOCITY IMPACT CONFERENCE

Figure 2.4-33 Meteoroid Protection - Method 2 (Bumper/Gap/Backing)

Figure 2.4-34 shows the meteoroid protection system weight vs. the reliability of no meteoroid penetration for a duration of 600 days. The meteoroid protection system weight includes an allowance for posts to stand the bumper away from the tank. A maximum practical standoff limit of 6 inches is shown for handling and installation. The weight penalty increases rapidly for reliability numbers above approximately 0.985. The 600 day design point and reliability of 0.982 equates to a 24 day single mission of 0.9993 reliability. At this design point, the meteoroid system weighs 340 lb and consists of a 0.006" aluminum bumper, 2.82 inch gap, and 1.03 inches of MLI.

- SPACE BASED CRYOGENIC OTV (SHIV-2) 84K PROPELLANTS
- 1881 SQ FT TANK SURFACE AREA
- 600 DAYS EXPOSURE DURATION
- NO RESULTANT DAMAGE TO TANK WALL
- METEOROID ENVIRONMENT FROM NASA SP 8013
- MINIMUM BUMPER GAGE = 0.006 IN.
- RELIABILITY FOR MANNED MISSION = .9993

SHIELD CONSTRUCTION

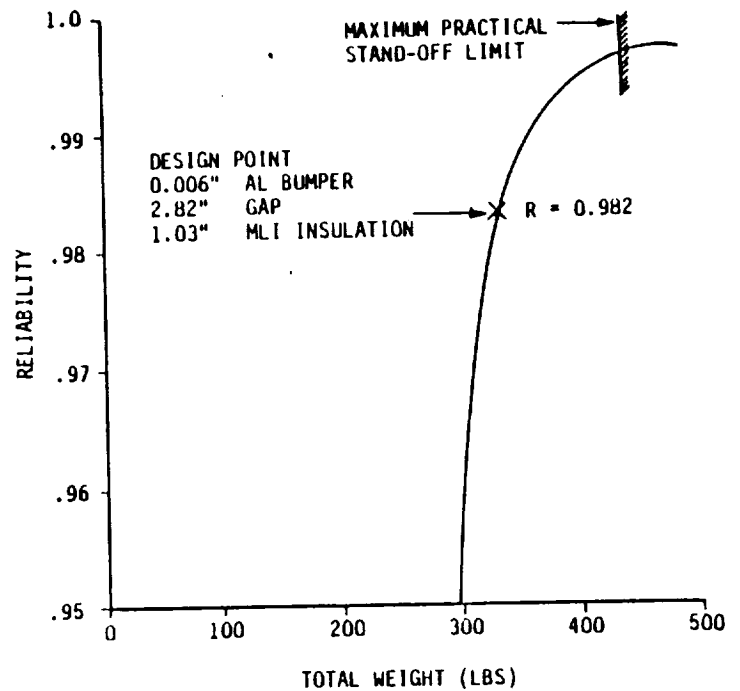
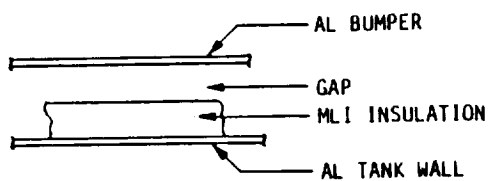


Figure 2.4-34 Baseline Protection System - Method 2

Figure 2.4-35 shows the reliability vs. weight for a solid MLI meteoroid protection system. For the same reliability as the baseline protection system, the weight for this method is 687 lb which produces a 347 lb penalty. This system requires a large standoff of 5.56 inches but has better handling than a system with a thin bumper of aluminum.

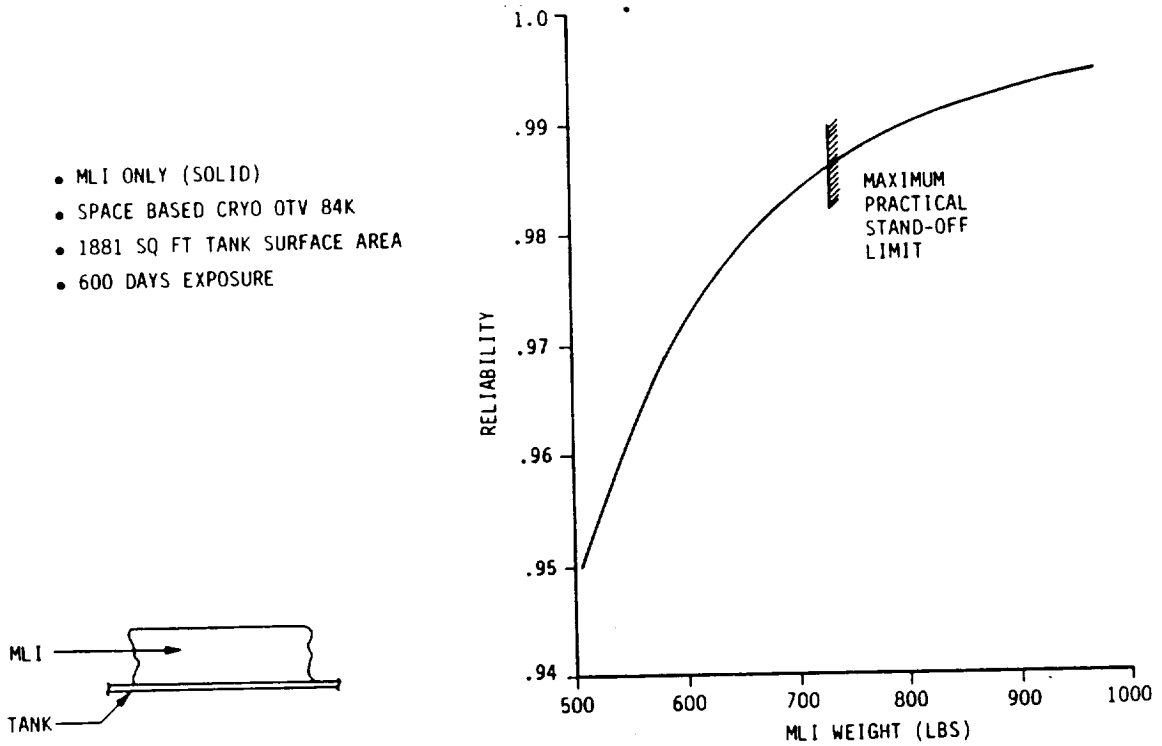


Figure 2.4-35 Penalty of No Bumper

The total thickness of the meteoroid protection system can be reduced by applying an aluminum sheet on top of the MLI. However, as Figure 2.4-36 shows, this addition has a high weight penalty. The two reliability design

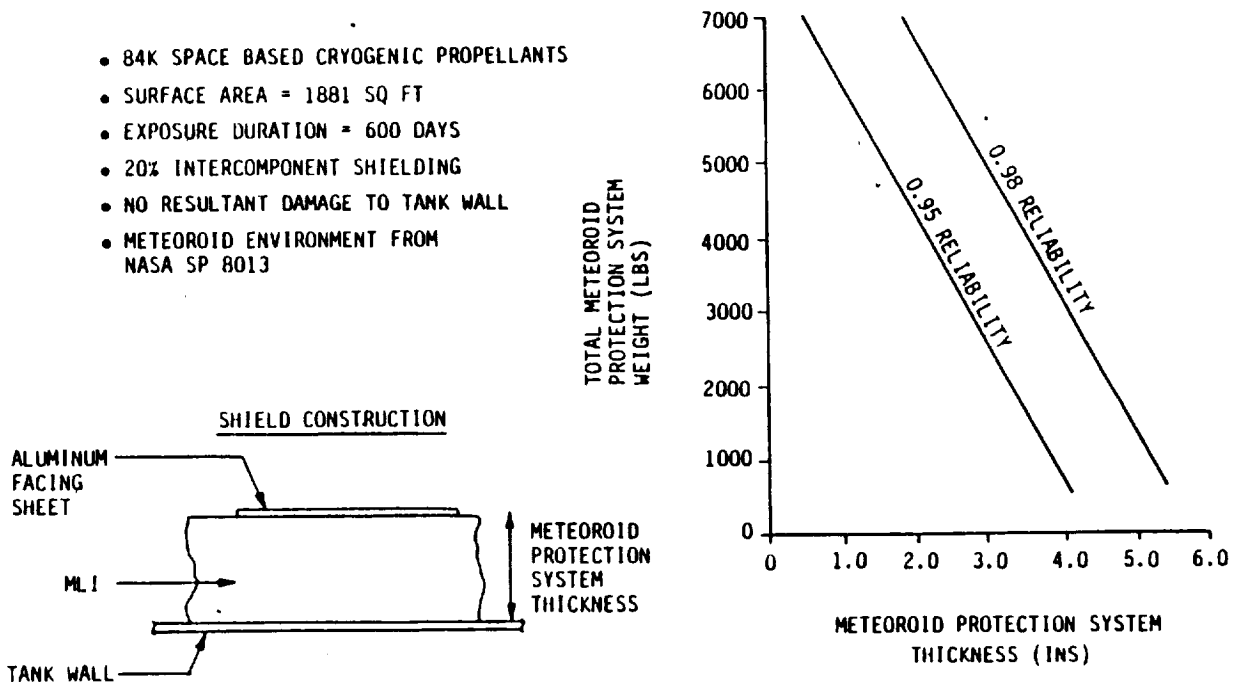


Figure 2.4-36 Penalty of No Gap

points start at the minimum weight where the thickness is all MLI. It eventually ends when the thickness is all aluminum. This system has improved ground handling and a small standoff but unacceptable weight penalty.

2.4.10 References

- 2.4.5-1) "Metallic Materials and Elements for Aerospace Vehicle Structures", Volume 2, MIL-HDBK-5D, DOD, Washington, DC
- 2.4.5-2) Materials Selection Guide for MSFC Spacelab Payloads MSFC-HDBK-527 Rev. B, by George C. Marshall Space Flight Center, Materials and Processes Laboratory.
- 2.4.5-3) "Application of Beryllium on the Space Shuttle Orbiter" by L. B. Norwood, SAMPE Journal, May/June 1984.
- 2.4.5-4) "Low Cost Titanium Propellant Tankage" by A. E. Leach and R. J. Szpakowski, AFRPL-TR-82-014 of Bell Aerospace Textron.
- 2.4.5-5) Cryogenic Materials Data Handbook, Vol. 1, Sections A, B, C, AFML-TDR-64-280, Air Force Materials Lab, AFSC, Wright-Patterson Air Force Base, OH, July 1970.
- 2.4.5-6) Titanium Alloys Handbook, MCIC-HB-02, R. A. Wood and R. J. Favor, Air Force Materials Lab Wright-Patterson Air Force Base, OH, December 1972.
- 2.4.5-7) Damage Tolerant Design Handbook, Vol. 1, 2, 3, MCIC-HB-01R, prepared by University of Dayton Research Institute, Dayton, OH, sponsored by Air Force Wright Aeronautical Laboratories, Materials Laboratory, Wright-Patterson Air Force Base, OH, December 1983.
- 2.4.5-8) Aerospace Structural Metals Handbook (formerly AFML-TR-68-115), Mechanical Properties Data Center Battelle's Columbus Laboratories, Columbus, OH, 1982.

2.5 Thermal Control Trade Studies and Analyses

2.5.1 Prelaunch Considerations and STS Ascent Environment

INTRODUCTION--The objective of the following analyses is to predict the prelaunch and ascent environments for the cryogenic and storable OTVs in the Aft Cargo Carrier (ACC) including the environment after shroud staging. These analyses were performed in three parts; pre-OTV pressurization, pressurization and ascent, and post shroud separation. OTV insulation requirements for prelaunch and launch are established by considering no SOFI and an early helium purge in the ACC versus SOFI with a late purge. In addition, the pressure/thermal environment on the OTV during prelaunch and launch and the radiative and convective heating after shroud separation are determined.

2.5.1.1 Thermal Analysis to Determine ACC/OTV (Ground-Based Cryo) Purge System Requirements--The purpose of these analyses is to predict the purge requirements for the Aft Cargo Carrier (ACC) with the 55K ground-based cryogenic Orbital Transfer Vehicle (OTV) as payload. The configuration of the ACC/OTV is depicted in Figure 2.5-1 and is defined in more detail in Volume II, Book 2 of this final report.

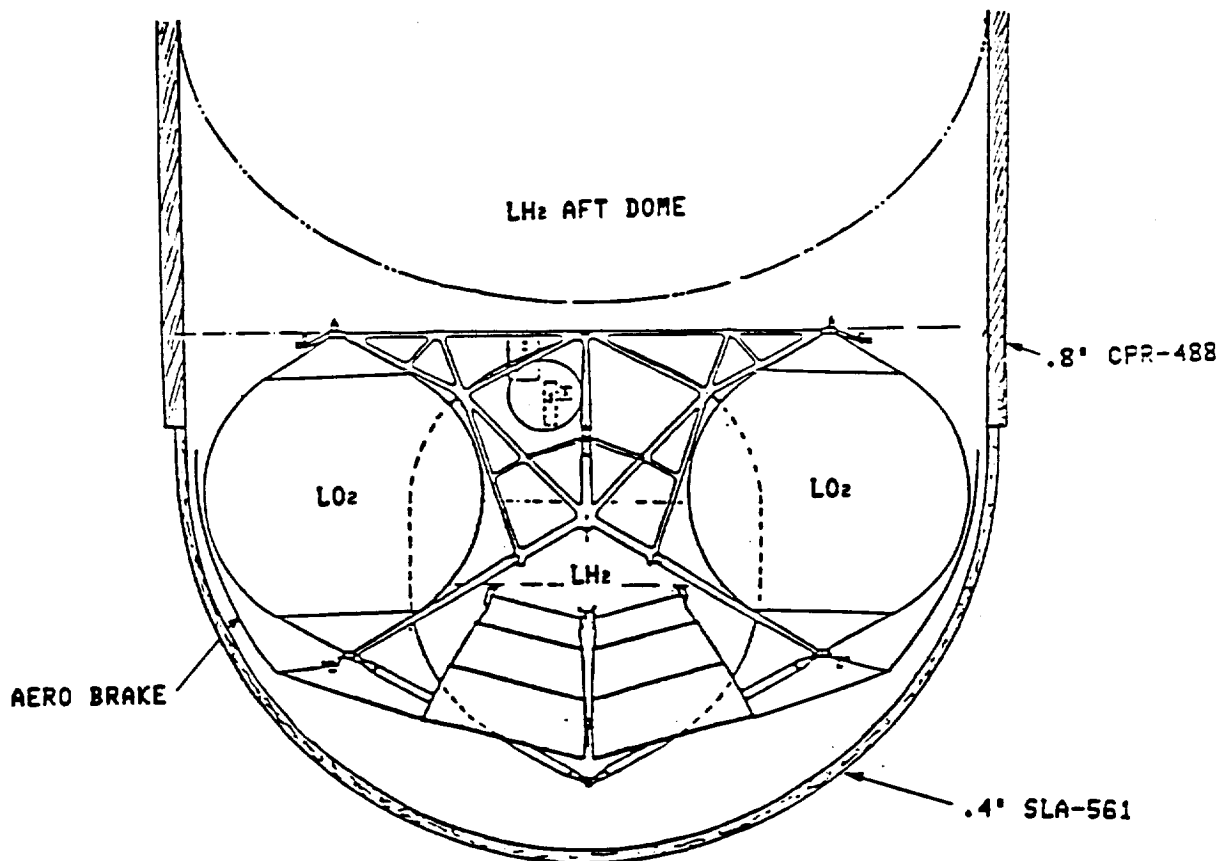


Figure 2.5-1 ACC/OTV Cryo Configuration

SELECTION OF PURGE GAS--Purge requirements for the ACC/OTV are based on maintaining a pressurized thermally controlled, inert atmosphere within the ACC during prelaunch operations. Two likely candidates for the purge gas are gaseous helium (GHe) and gaseous nitrogen (GN₂). Based on their acoustic characteristics, GHe is the preferred gas at liftoff because of its significant sound pressure level reduction (Reference 2.5-1). The relative merits of using GHe or GN₂ as the purge gas during OTV servicing is another facet of the purge assessment. During this period, the primary function of the purge flow is to maintain a nonexplosive mixture for a limited range of leakage and aid in the detection of a leak during prelaunch operations. A cost comparison was made between GN₂ and GHe assuming relative costs of \$7/1000 ft³ for GN₂ and \$67/1000 ft³ for GHe. For the case of a GN₂ purge, a 0.2" SOFI layer on the LH₂ tanks was assumed to prevent GN₂ condensate. This SOFI layer weight was calculated to be 38.71bm, assuming a GHe mass flow of 30 lbm/min (Reference 2.5-2) and equivalent GN₂ mass flow of 110 lbm/min based on maintaining the same volumetric flow rate, the use of GN₂ saved approximately \$15,500 over the use of GHe during the two hour OTV servicing period with cryogenic (LH₂) loaded. However, with a cost of \$8300/lbm of payload to GEO orbit, the SOFI weight penalty was equivalent to \$322,000 per flight. Thus, with an indicated net saving per flight of \$306,500, the use of a GHe purge during OTV loading was selected. It should be noted that this cost analyses ignores two minor opposing factors: The higher LH₂ boiloff incurred with GHe purge; and the manufacturing and production cost of spraying 0.2" foam on the OTV LH₂ tank prior to MLI installations to prevent condensation and freezing of the GN₂ when it is used as the purge gas.

ASSUMPTIONS AND CONSTRAINTS--Parametric analyses for the ACC/OTV GHe purge assumed 0.8" CPR-488 on the ACC skirt and barrel and an average of 0.4" SLA-561 on the ACC shroud (Figure 2.5-1). This insulation is to maintain the structural temperature of the ACC below 350°F during ascent and protect against ice/frost formation at the ET/ACC splice. Assumptions pertaining to the analysis included a wind of 5 to 7 knots and ambient temperatures between 30°F and 100°F.

The LH₂ aft dome was assumed to be insulated with an average of 1.25" of foam insulation (NCFI) and heat transfer to the dome was assumed equal to 1.3 times natural convection due to the purge. Insulation for the OTV was assumed to be 1.0" multilayer insulation (MLI) having an effective conductivity equal to that of GHe; OTV cryogenic surface areas (465 ft² of LO₂ and 896 ft² of LH₂) were derived from information presented in Volume II, Book 2 of this report. It was also assumed that the OTV payload is isolated from the compartment structure with no conduction between cryogenic tanks and other components. The assumed purge scenario based on References 2.5-2 and 2.5-3 is presented in Table 2.5-1.

Table 2.5-1 ACC Purge Scenario

Time Relative To Liftoff	Constraints	Purge	Comments
T-6:20 TO T-2:09 Hours	Inert Atmosphere Temperature Control	GN ₂ at 110 LBM/Min	Similar to ET Intertank
T-2:09 TO T-0:02 Hours	Inert Atmosphere Temperature Control	GHe at 30 LBM/Min	Change to GHe for GN ₂ Condensation Control Required for Loading
T-0:02 Hours to Lift-Off	Inert Atmosphere Temperature Control Acoustics Control ACC Pressurized to 0.9 ± 0.1 psig	GHe at 79 LBM/Min	Reduce ACC Vent Area and Increase GHe Purge Flow to Obtain Overpressure Needed to Enhance Structural Integrity of ACC

ANALYSES--GN₂ and GHe purge requirements for the Cryo ACC/OTV for the above mentioned constraints are presented in Figures 2.5-2 and 2.5-3 respectively. These results are shown for the compartment temperature extremes of 45°F (minimum) and 100°F (maximum). Purge requirements are defined in terms of flow rate and expanded purge inlet temperature downstream of the diffuser (manifold) orifice for the extremes in ambient temperature. These expanded purge inlet temperatures, together with temperature drop due to expansion through the orifice plus heat loss between GSE heater and orifice, are needed to identify facility heater requirements necessary to maintain acceptable ACC compartment temperatures. An active feedback and control loop similar to the ET intertank system could be used to regulate the compartment temperature prior to and during the ET and OTV cryogenic loading to accommodate the associated transient thermal load. However, the results presented herein suggest the possibility that an active feedback and control loop may not be required and that regulation of the GSE heater outlet temperature may be sufficient for maintaining ACC thermal control.

CONCLUSIONS AND RECOMMENDATIONS--The results of these analysis should be used in conjunction with other design analyses in achieving a more detailed ground-based cryo OTV design. For the previously defined purge flow conditions the results defined herein show a desired expanded GN₂ purge temperature of 120°F at 110 lbm/min and a desired GHe purge temperature of 230°F at 30 lbm/min. Allowing for expansion and a nominal facility loss similar to that of the ET intertank purge system, the minimum facility heater requirement for the ACC purge would be approximately 160 kw; current ET intertank GSE heater capability is approximately 180 kw.

ORIGINAL PAGE IS
OF POOR QUALITY

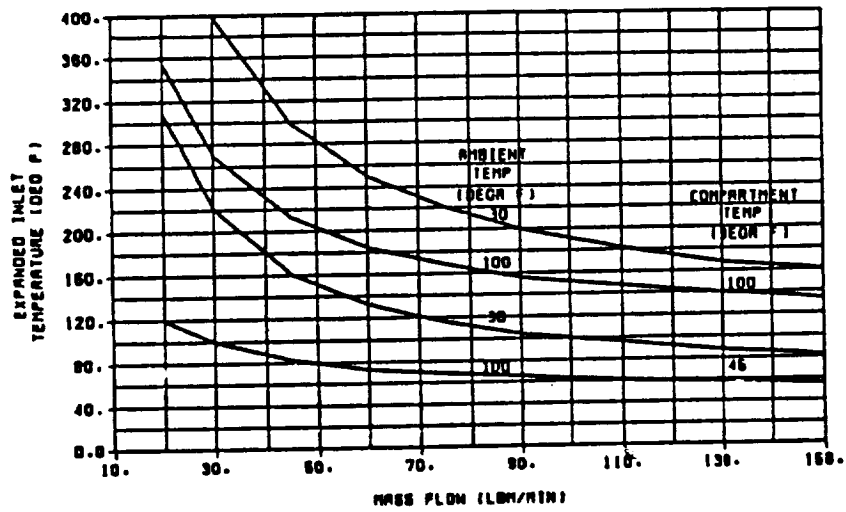


Figure 2.5-2 GN₂ Purge Requirement for ACC/OTV Compartment Temperature Control Prior to CRYO Loading

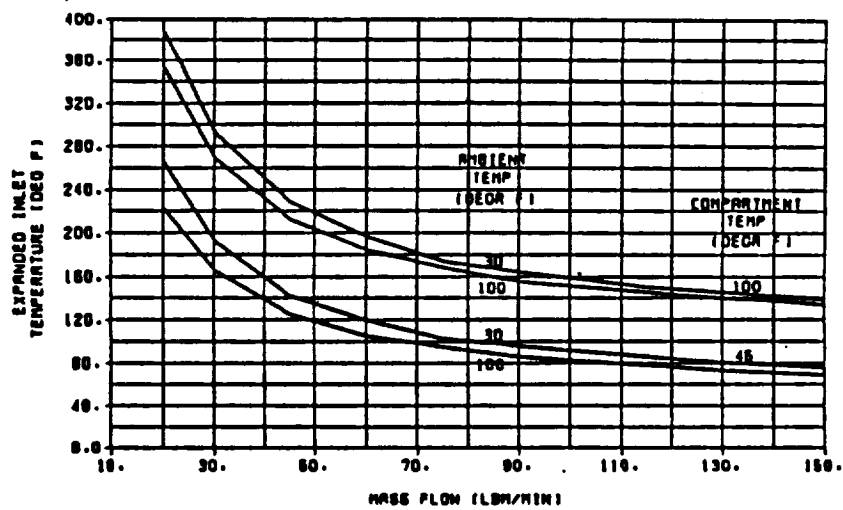


Figure 2.5-3 GHe Purge Requirement for ACC/Cryo OTV Compartment Temperature Control

2.5.1.2 Thermal Analysis to Determine ACC/OTV (Ground-Based Storable) Purge System Requirements--The purpose of these analyses is to predict the purge requirements for the AFT Cargo Carrier (ACC) with the 51K ground-based storable Orbital Transfer Vehicle (OTV) as payload. The configuration of the ACC/OTV is depicted in Figure 2.5-4 and is defined in more detail in Volume II, Book 2 of this report.

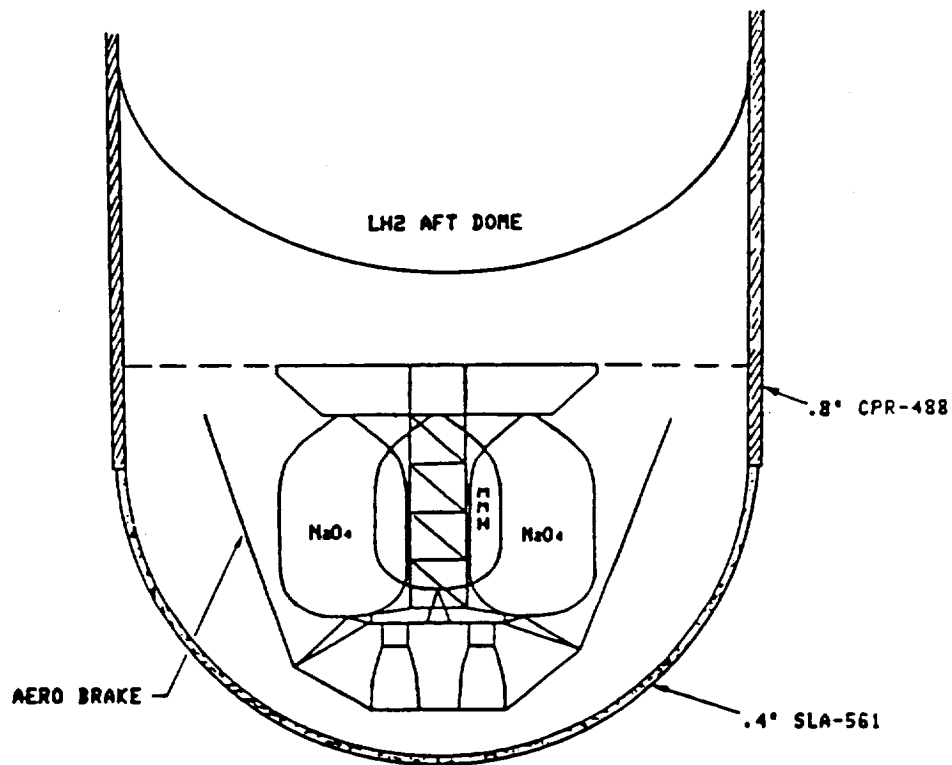


Figure 2.5-4 ACC/Storable OTV Configuration

SELECTION OF PURGE GAS--Purge requirements for the ACC/OTV are based on maintaining a pressurized, thermally controlled, inert atmosphere within the ACC during prelaunch operations. Two likely candidates for the purge gas are gaseous helium (GHe) and gaseous nitrogen (GN₂). Based on their acoustic characteristics, GHe is the preferred gas at liftoff. The relative merits of

using GHe or GN₂ as the purge gas during OTV servicing is another facet of the purge assessment. During this period, the primary function of the purge flow is to maintain a nonexplosive mixture for a limited range of leakage and aid in the detection of a leak using onboard sensors. Because of its cost, (\$7/1000 ft³ for GN₂ vs \$67/1000 ft³ for GHe) and ease of handling, GN₂ was selected as the purge gas for use during OTV servicing and loading.

ASSUMPTIONS AND CONSTRAINTS--Parametric analyses for the ACC/OTV purge assumed 0.8" CPR-488 on the ACC skirt and barrel and an average of 0.4" SLA-561 on the ACC shroud (Figure 2.5-4). This insulation is required to maintain the structural temperature of ACC below 350°F during ascent and protects prelaunch ice/frost formation at the ET/ACC splice. Assumptions pertaining to the analysis included a wind of 5 to 7 knots and ambient temperatures between 30°F and 100°F maximum.

The LH₂ aft dome was assumed to be insulated with an average of 1.25" of foam insulation (NCFI) and heat transfer to the dome was assumed equal to 1.3 times natural convection due to the purge. Insulation for the OTV was assumed to be 1.0" multilayer insulation (MLI) having an effective conductivity equal to that of purge medium; OTV storable surface areas (340 ft² of N204 and 291 ft² of MMH) were derived from information presented in Volume II, Book 2 of this report. The assumed purge scenario based on Reference 2.5-2 and 2.5-3 is presented in Table 2.5-1.

ANALYSES--GN₂ and GHe purge requirements for the ACC/OTV for the above mentioned constraints are presented in Figures 2.5-5 and 2.5-6 respectively. These results are shown for compartment temperature extremes of 45°F (minimum) and 100°F (maximum). Purge requirements are defined in terms of mass flow rate and expanded inlet temperature downstream of the diffuser (manifold) orifice for the extremes in ambient temperature. These expanded purge inlet temperatures, together with temperature drop due to expansion through the orifice plus heat loss between GSE heater and orifice are needed to identify facility heater requirements necessary to maintain accepted ACC compartment temperatures. ACC active feedback and control loop similar to the ET intertank system could be used to regulate the compartment temperature prior to and during the ET and OTV loading to accommodate the associated transient thermal load. However, the results presented herein suggest the possibility that an active ACC feedback and control loop may not be required and that regulation of the GSE heater outlet temperature may be sufficient for maintaining ACC thermal control.

CONCLUSIONS AND RECOMMENDATIONS--The results of these analyses should be used in conjunction with other design analyses in achieving a more detailed ground-based storable OTV design. For the previously defined purge flow conditions the results defined herein show a desired expanded GN₂ purge temperature of 120°F at 110 lbm/min and a corresponding 110°F for GHe at 30 lbm/min. Allowing for expansion and a nominal facility loss similar to that of ET intertank purge system, the minimum facility heater requirement for the ACC purge would be approximately 90 kw.

ORIGINAL PAGE IS
OF POOR QUALITY

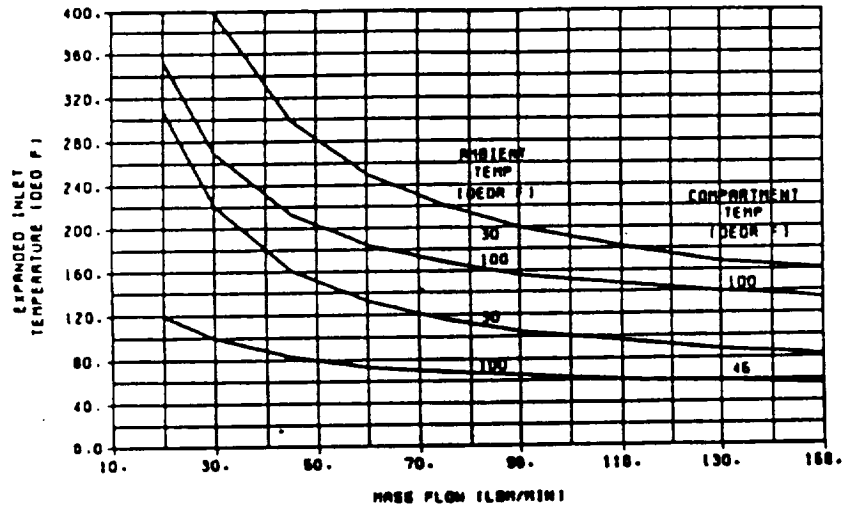


Figure 2.5-5 GN₂ Purge Requirement for ACC/Storable OTV Compartment Temperature Control

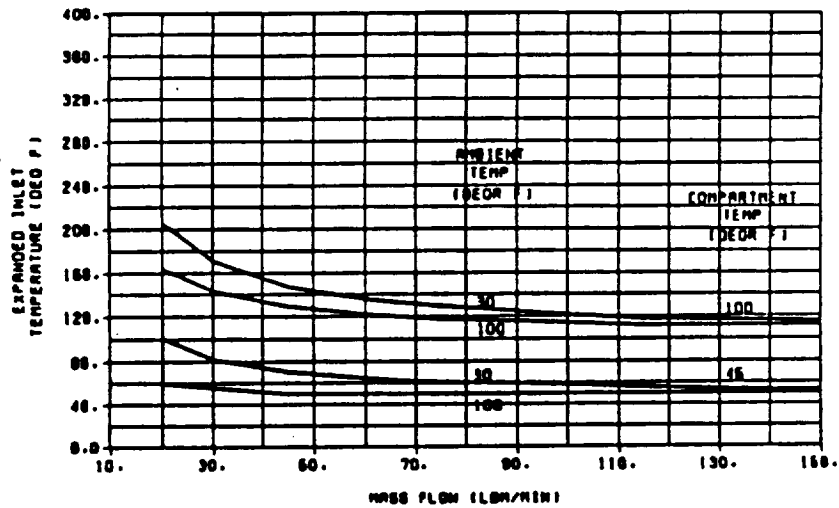


Figure 2.5-6 GHe Purge Requirement for ACC/Storable OTV Compartment Temperature Control

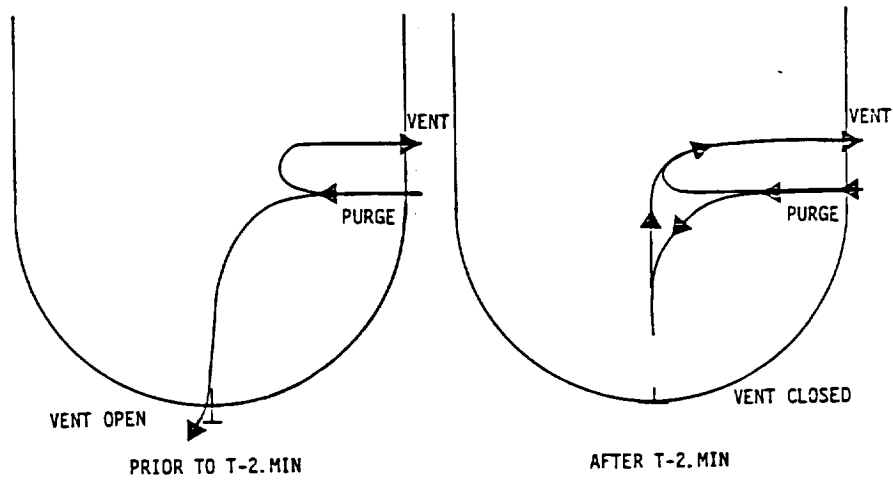
2.5.1.3 Compartment Temperature of ACC/OTV (Ground-Based) During Prelaunch and Ascent--The purpose of this analysis is to predict the dedicated Aft Cargo Carrier (ACC) transient compartment gas temperature from the time of ACC pressurization (T-2 min) until shroud separation (T+2:36 min). The general configurations of the ACC and the two OTV payloads (cryogenic and storable) are depicted in Figures 2.5-1 and 2.5-4 and are defined in more detail in Volume II, Book 2 of this report.

Thermal analyses were performed using a GHe purge prior to T-0 to maintain the compartment temperature within the limits of 45°F minimum and 100°F maximum. The purge scenario assumed herein is the same as that in Table 2.5-1, i.e., 30 lbm/min prior to T-2 and 79 lbm/min between T-2 and lift-off, with a pressure buildup to 0.9 psig. The ambient temperature was assumed to be 30°F for minimum and 99°F for maximum case conditions. Additionally, the OTV was assumed to be insulated with 1.0" multilayer insulation (MLI). The transient mass flow and compartment pressures from Reference 2.5-3 are shown in Figure 2.5-7 for prelaunch purge/vent and for inflight venting. Also used in the inflight portion of the analyses were the compartment skin temperatures resulting from ascent heating and TPS, as sized in Reference 2.5-6.

During prelaunch, the purge flow is altered at T-2 minutes when the vent area at the aft end is closed. This allows the ACC compartment pressure to increase to 0.9 psig with all the purge gas vented from the vent area on the skirt. During this period prior to liftoff, the purge flow through the lower portion of the ACC compartment (where the OTV is located) will be reduced. However, for this analysis, full circulation in the ACC is assumed with no stratification and uniform temperature. This assumption was conceived as having minimal impact on the results because of the thermal capacitance of the OTV and the ACC shroud, and due to the short time period (2 minutes) for which the assumption applies. During ascent, the gas will be vented through the skirt vent from all areas of the ACC compartment.

For cryo OTV, the resultant compartment temperature profiles for the minimum and maximum case are presented in Figure 2.5-8. The associated boiloff for the minimum and maximum cases is shown in Figure 2.5-9. Similar results for the storable OTV are presented in Figures 2.5-10 and 2.5-11.

It should be noted that, in Figures 2.5-8 and 2.5-10, the compartment gas temperature calculation has been terminated 80 sec. into flight because the gas concentration is negligible by this time. Therefore, in the heat transfer and boiloff calculations, the convective component decreases after liftoff. After 80 seconds, radiant heat transfer to the ACC skirt and shroud is the sole contributor.



TIME SEC	MIN, ACC LBM/MIN	MOUT, CRYO LBM/MIN	MOUT, STOR LBM/MIN	Pc, CRYO PSIA	Pc, STOR PSIA
PRIOR T0-120	30	30	30	14.84	14.84
-119	79	37	34.14	14.9	14.85
-110	79	53	49.32	15.0	14.99
-100	79	60	57.56	15.2	15.14
-90	79	63	61.22	15.3	15.29
-80	79	65	63.3	15.6	15.6
-60	79	79	79	15.6	15.6
-0	79	79	79	15.6	15.6
LIFT OFF	0	82.3	102.97	15.6	15.6
10	0	12.7	16.03	14.29	14.26
20	0	32	40.76	12.96	12.93
30	0	47.9	60.47	10.89	10.88
40	0	54.3	68.58	8.43	8.38
50	0	55.2	69.74	6.14	6.174
60	0	51.97	65.49	4.21	4.11
90	0	26.66	33.61	1.04	1.03
100	0	19.12	24.15	0.66	.66
120	0	10.04	12.75	0.28	.279
130	0	7.53	9.46	0.20	.19
150	0	4.4	5.6	0.10	.103
160	0	3.48	4.25	0.074	.0735

Figure 2.5-7 ACC/OTV Compartment Transient Pressure and Mass Flow

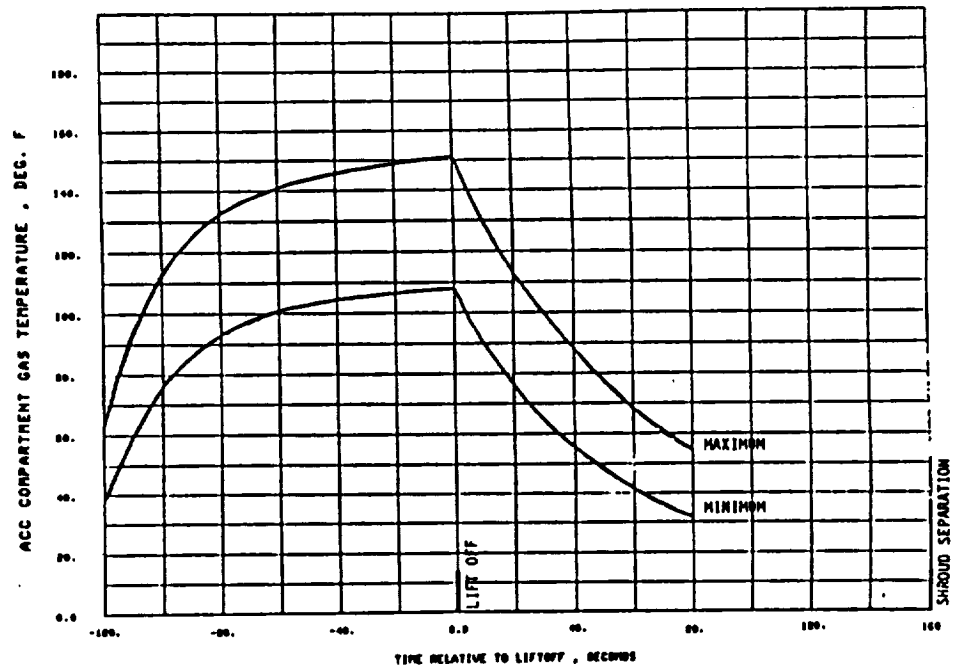


Figure 2.5-8 ACC/Cryo OTV Transient Compartment Gas Temperature

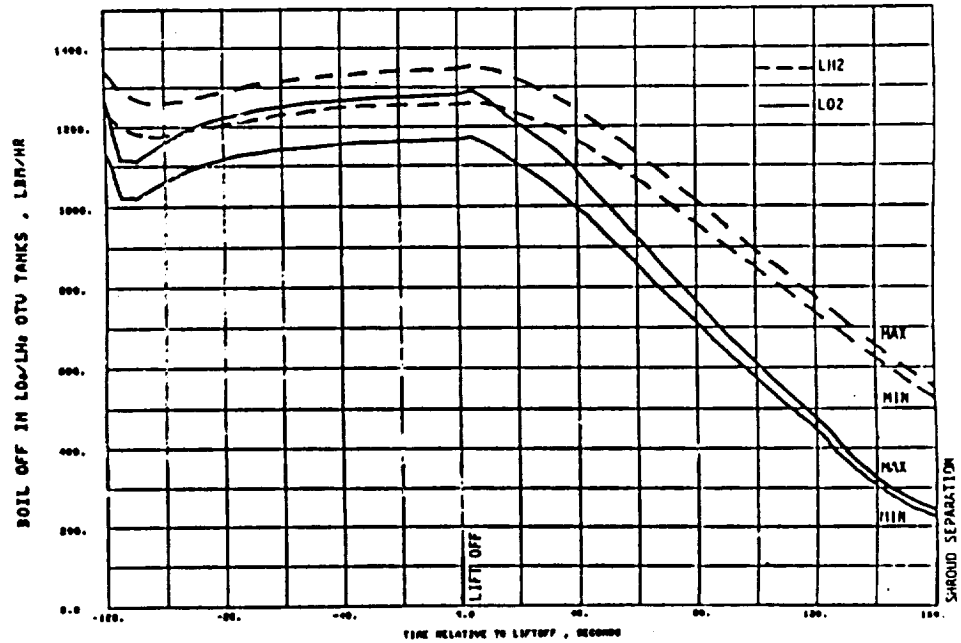


Figure 2.5-9 Transient Boiloff in Cryo Tanks of ACC/OTV

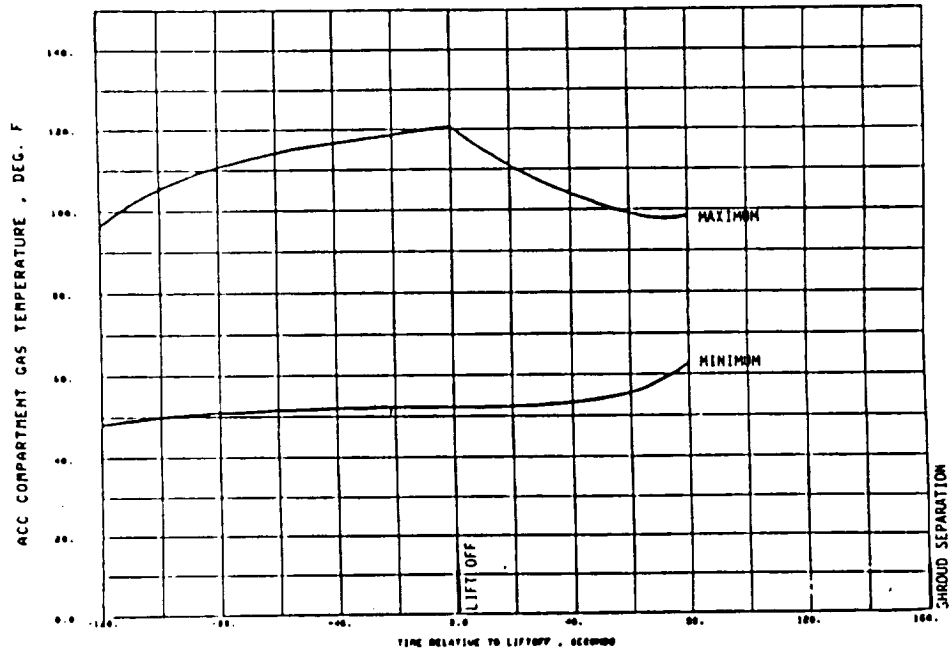


Figure 2.5-10 ACC/Storable OTV Transient compartment Gas Temperature

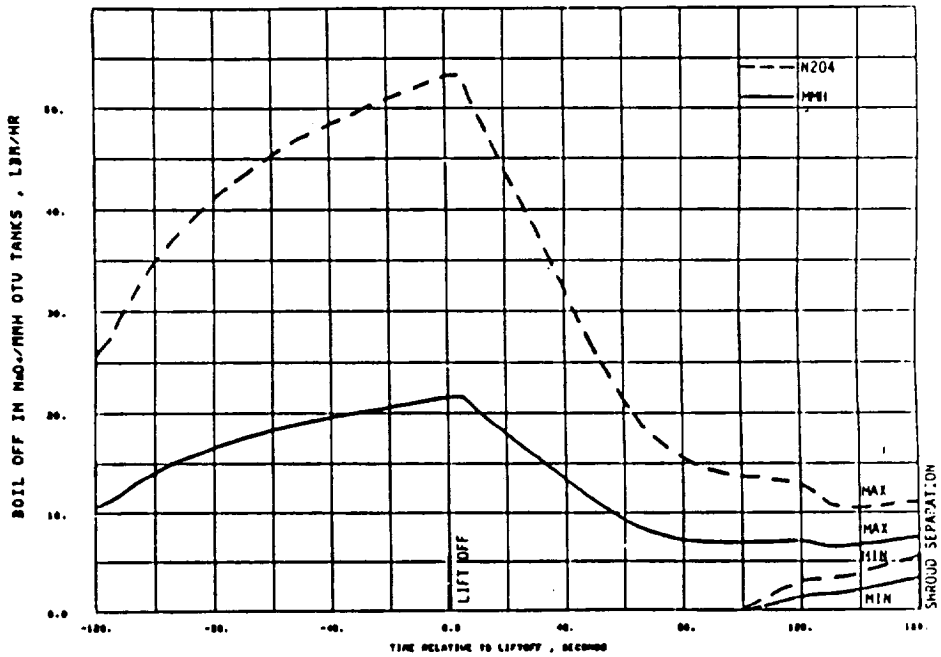


Figure 2.5-11 ACC/Storable OTV Transient Boiloff in Propellant Tanks

The results of these analyses should be used in conjunction with other design analyses to achieve a more detailed ACC/OTV design. An analysis of the transient ACC/OTV temperature and environment for T+2:36 min (shroud separation) to T+8:35 min (OTV separation) is documented in the next Section.

2.5.1.4 Post-Shroud Separation Thermal Analysis of Ground-Based OTV--The purpose of these analyses is to predict the environment and transient temperature of the Orbital Transfer Vehicles (OTV) from the time of Aft Cargo Carrier (ACC) shroud separation (T+2:36 min) until OTV separation (T+8:35 min).

Figure 2.5-12 depicts the thermal math model used for these analyses showing the composition of the aerobrake, insulation on the OTV tanks, and the heat transfer paths. It was assumed that the OTV tanks are shielded completely by the aerobrake from external heat loads. The plume environments used herein were impacted on the aerobrake and are the highest of those predicted by Remtech, Inc. in Reference 2.5-5 for the ACC envelope at the aerobrake location, i.e., 0.25 and 0.20 BTU/FT²-sec for the radiative and convective components, respectively. In addition to the plume induced heating, the aerobrake is exposed to solar (444 BTI/FT²-hr), radiates to space (-460F) and has a partial view of the orbiter. (See Figures 2.5-13 thru 2.5-16).

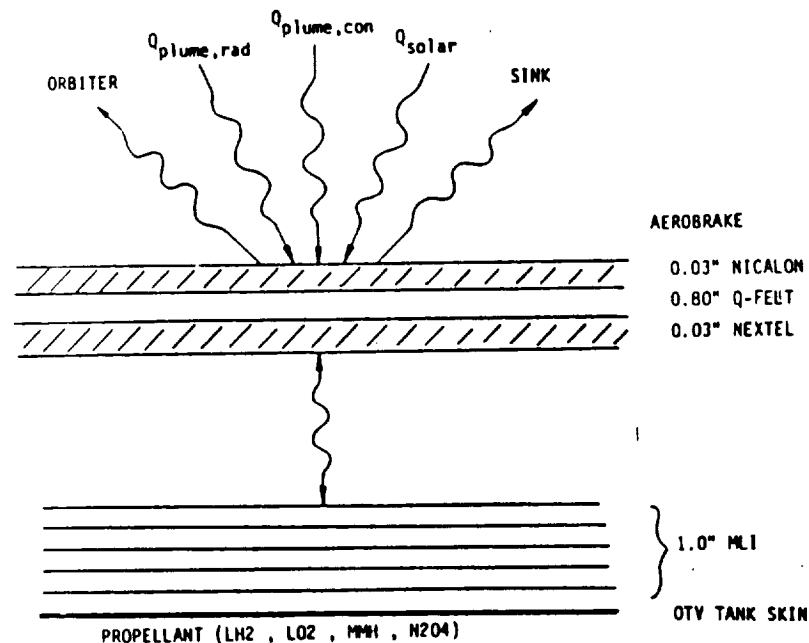


Figure 2.5-12 Thermal Math Model for ACC/OTV after Shroud Separation

ORIGINAL PAGE IS
OF POOR QUALITY

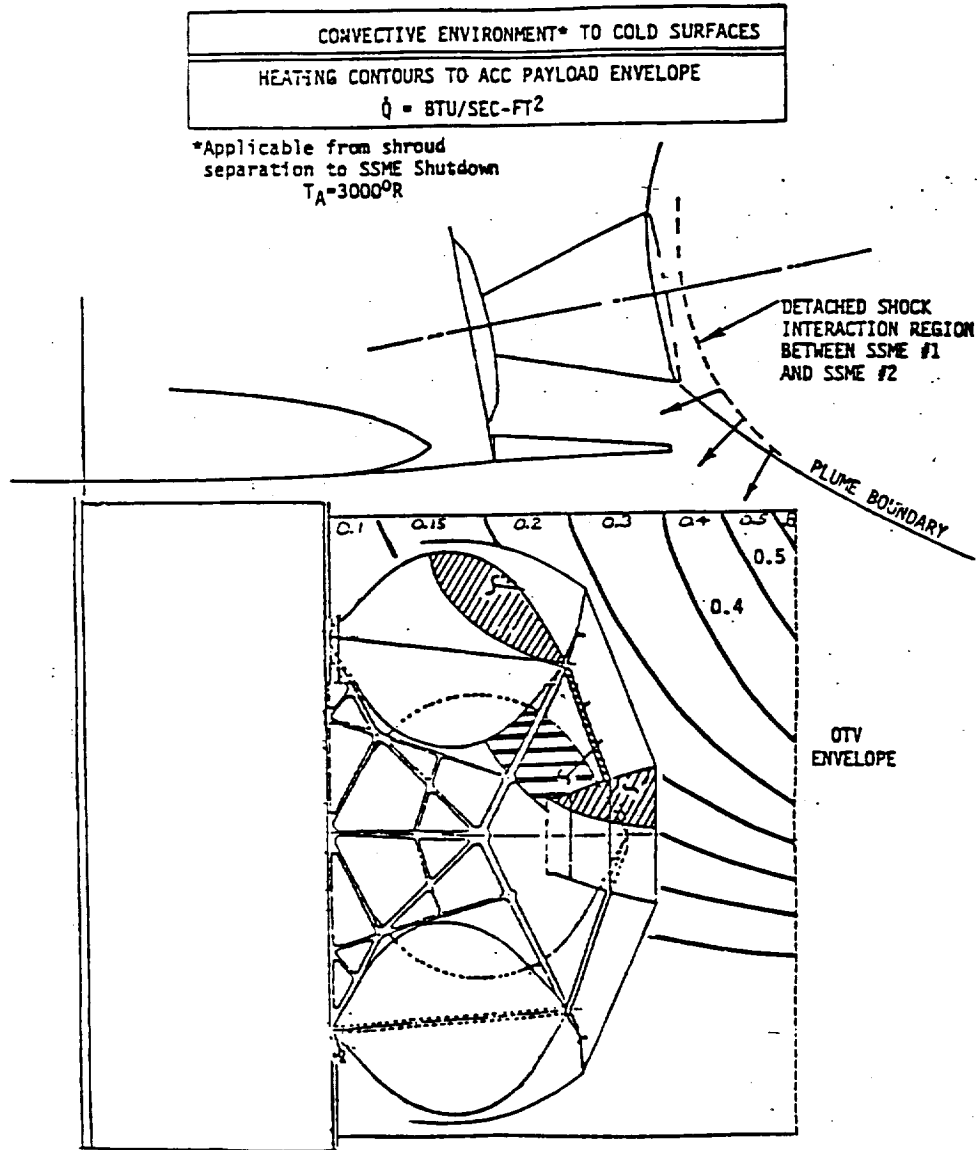


Figure 2.5-13 Convective Environment to Cold Surfaces

The methodology used in calculating the heat leak through the multilayer insulation (MLI) on the OTV tanks is detailed in Reference 2.5-6. This methodology considers the three components of heat transfer with pressure dependent coefficients for the convective component. For the analyses, a 1.00" blanket of perforated double aluminized kapton MLI with a density of 48

layer/inch and a sheet emissivity of 0.05 was assumed. It was also assumed that the MLI was purged prior to liftoff with gaseous helium and that the pressure within the MLI is equivalent to the local ambient pressure (i.e., no time lag).

Resultant temperature based on these environments and assumptions are shown in Figure 2.5-17. Heat leak to the various tanks is shown in Figure 2.5-18 and the corresponding boiloff is presented in Figure 2.5-19.

Results of these analyses should be used in conjunction with other design analyses in achieving a more detailed ACC/OTV design. These results should be considered as preliminary pending finalization of the MLI design and installation. The actual heat leak and boiloff data could deviate from these analytical data due to uncertainty of the MLI perforation pattern and the resulting vent of trapped gasses. Also, due to unknown structural design of MLI installation, heat leak resulting from struts, seams, penetration, etc. has not been considered in these analyses; Reference 2.5-6 suggests doubling the calculated heat leak to account for these leaks.

2.5.2 AOTV Flight Phase Thermal Control Analysis

Three principal areas of concern in the OTV flight phase thermal control subsystem studies are: use of passive thermal control techniques for avionics, propellant tanks and support struts TPS requirements, and the selection of the radiator and fuel cell based on vehicle power requirements. A summary of the OTV thermal control designs for both cryogenic and storable, ground-based and space-based vehicles are presented in the concept definition section of Volume II, Book 2 of this report. The fuel cell radiator design and its sizing is discussed below.

The radiator size is driven largely by the allowable operating temperature of the radiator, which is related to the allowable operating temperatures of the fuel cell and/or the avionics. For a fuel cell heating load only, the radiator was sized to allow its average temperature to range between 90° and 180°F recognizing that the fuel cell information available indicates that reasonable operating temperatures for the fuel cell and/or the radiator may be as high as 250°F. This could allow for radiator size reductions as the design develops, provided power requirements, as currently defined, do not increase substantially. When cooling the avionics is considered, the estimated maximum allowable operating temperature of the radiator is greatly reduced. The sizing analysis assumes 100° F for that maximum. This impacts the radiator size dramatically as summarized and illustrated in Figure 2.5-20. A brief trade study for utilizing a separate radiator system for the avionics was made with the results tabulated in Table 2.5-2. While the size and weight of that system is an improvement over a fuel cell/avionics combined cooling system, the low allowable operating temperature of the radiator system for avionics, alone, is still a driver in the radiator size and the complexity of an additional cooling system is not attractive. Passive thermal control of the avionics appears to be a better alternative for the avionics. A more detailed evaluation of the OTV fuel cell and avionics cooling system design is presented in Reference 2.5-7.

ORIGINAL PAGE IS
OF POOR QUALITY

CRYO

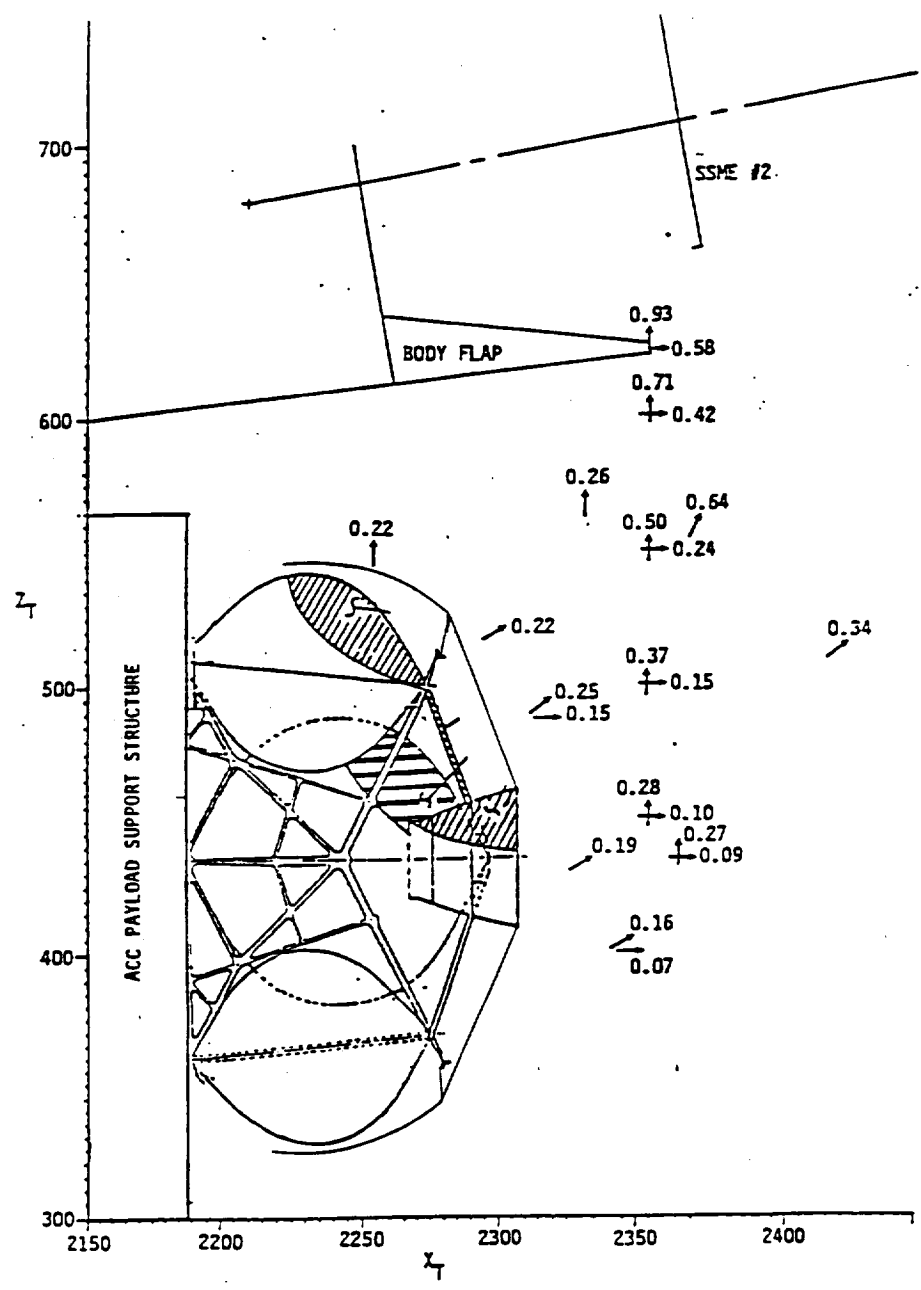


Figure 2.5-14 Incident SSME Plume Radiation Rates for Altitudes Above 150,000 Feet (Directions Shown Are Surface Normals)

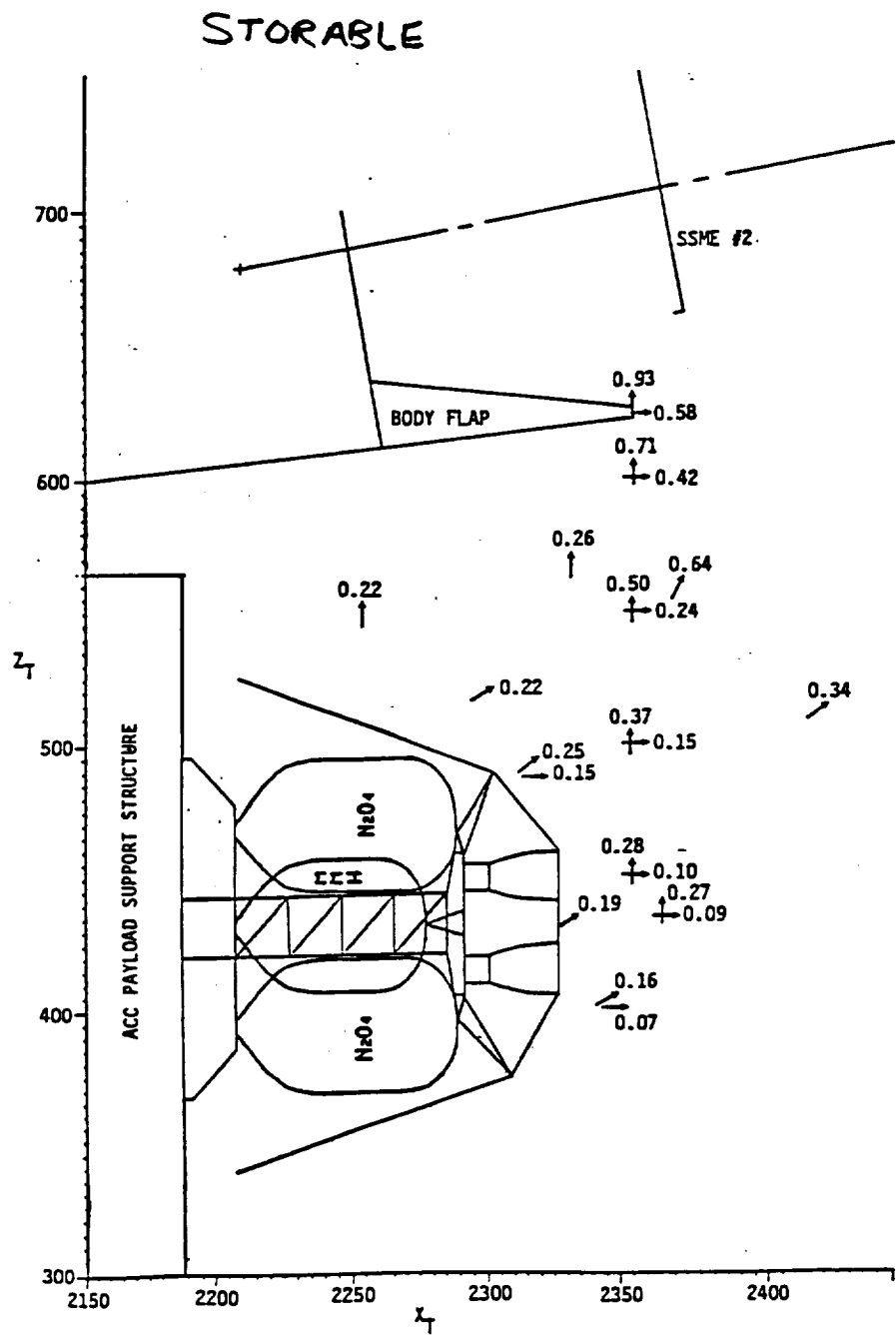


Figure 2.5-15 Incident SSME Plume Radiation Rates for Altitudes Above 150,000 Feet (Directions Shown Are Surface Normals)

ORIGINAL PAGE IS
OF POOR QUALITY

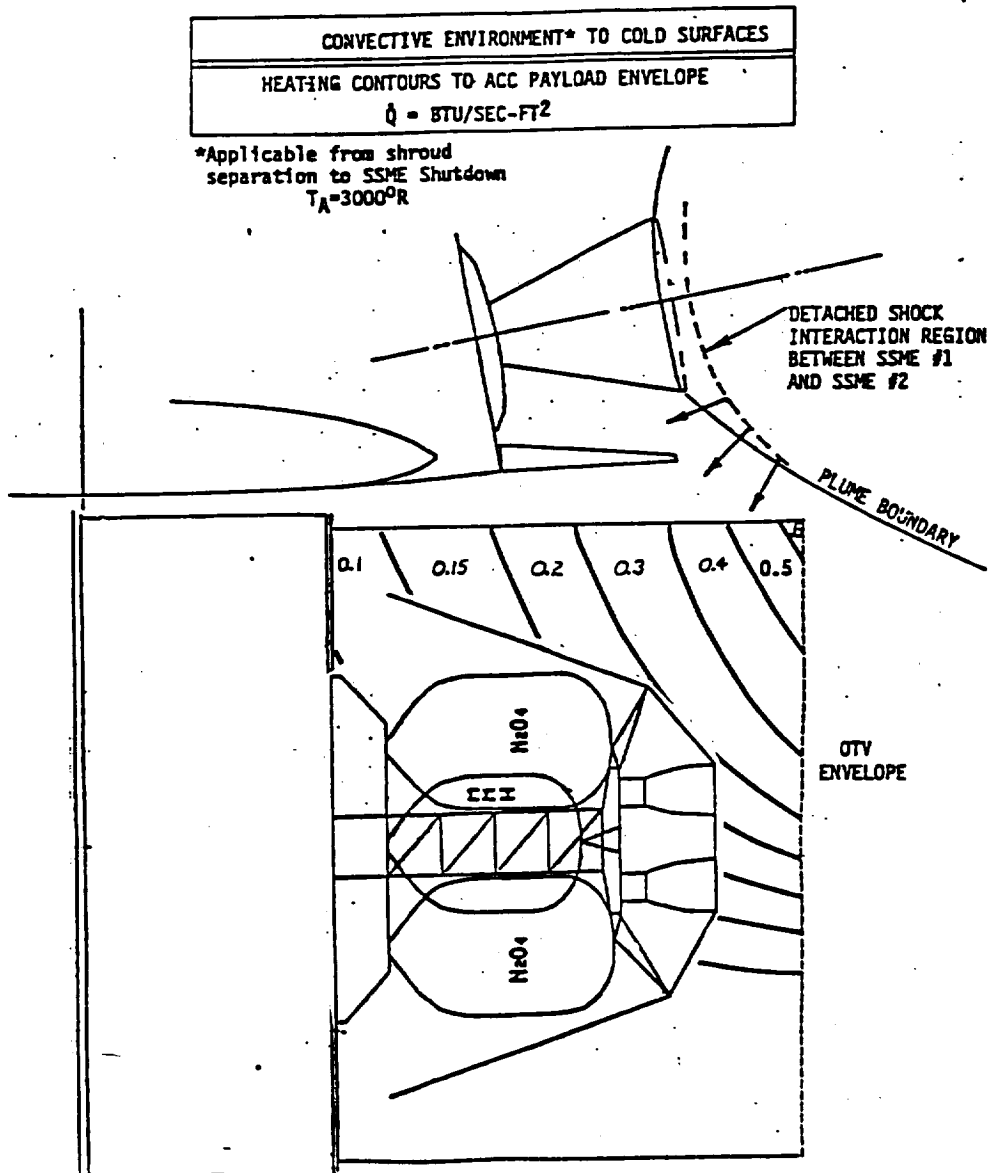


Figure 2.5-16 Convective Environment to Cold Surfaces

ORIGINAL PAGE IS
OF POOR QUALITY

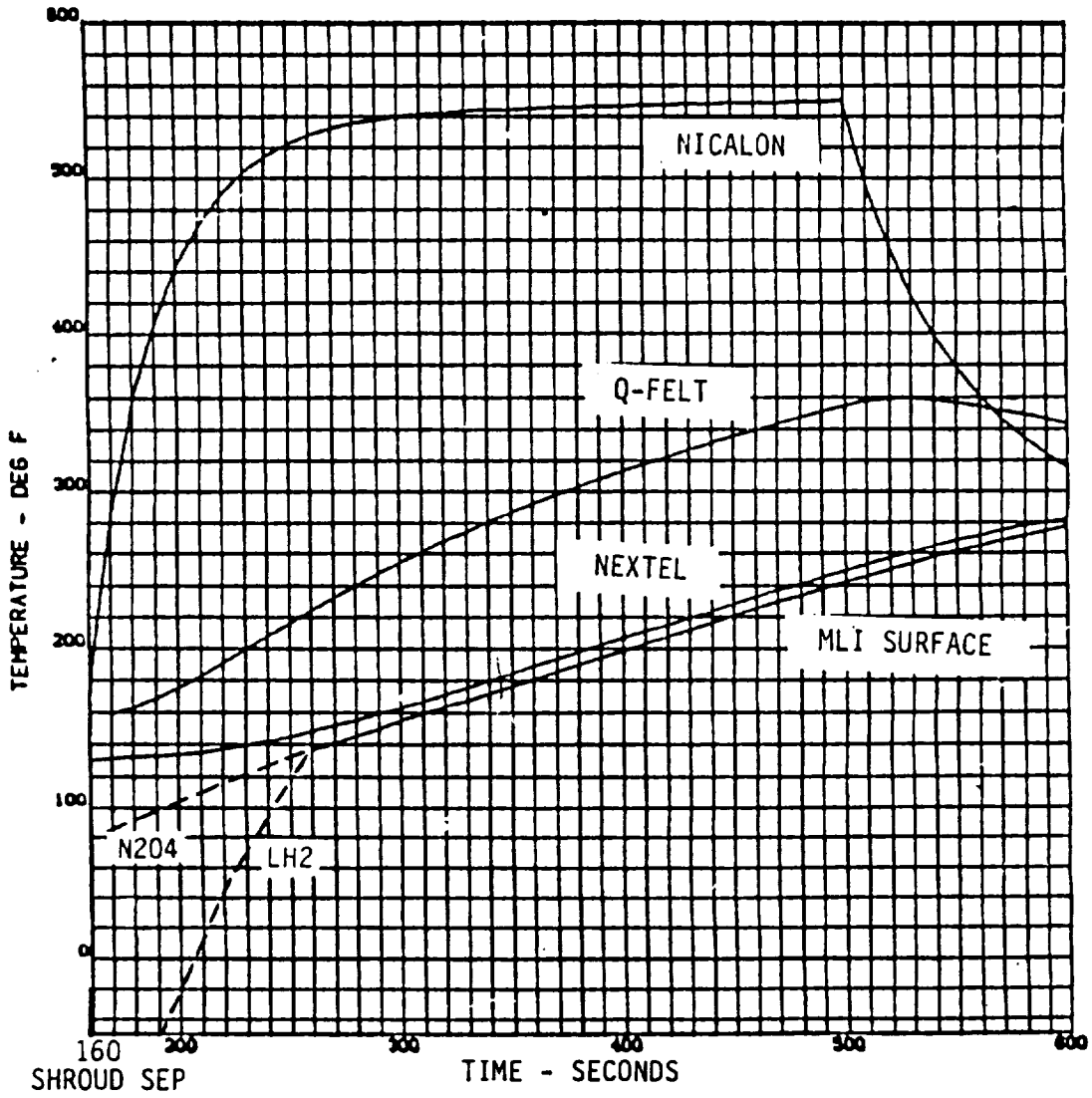


Figure 2.5-17 ACC/OTV Insulation Temperature During Ascent

ORIGINAL PAGE IS
OF POOR QUALITY.

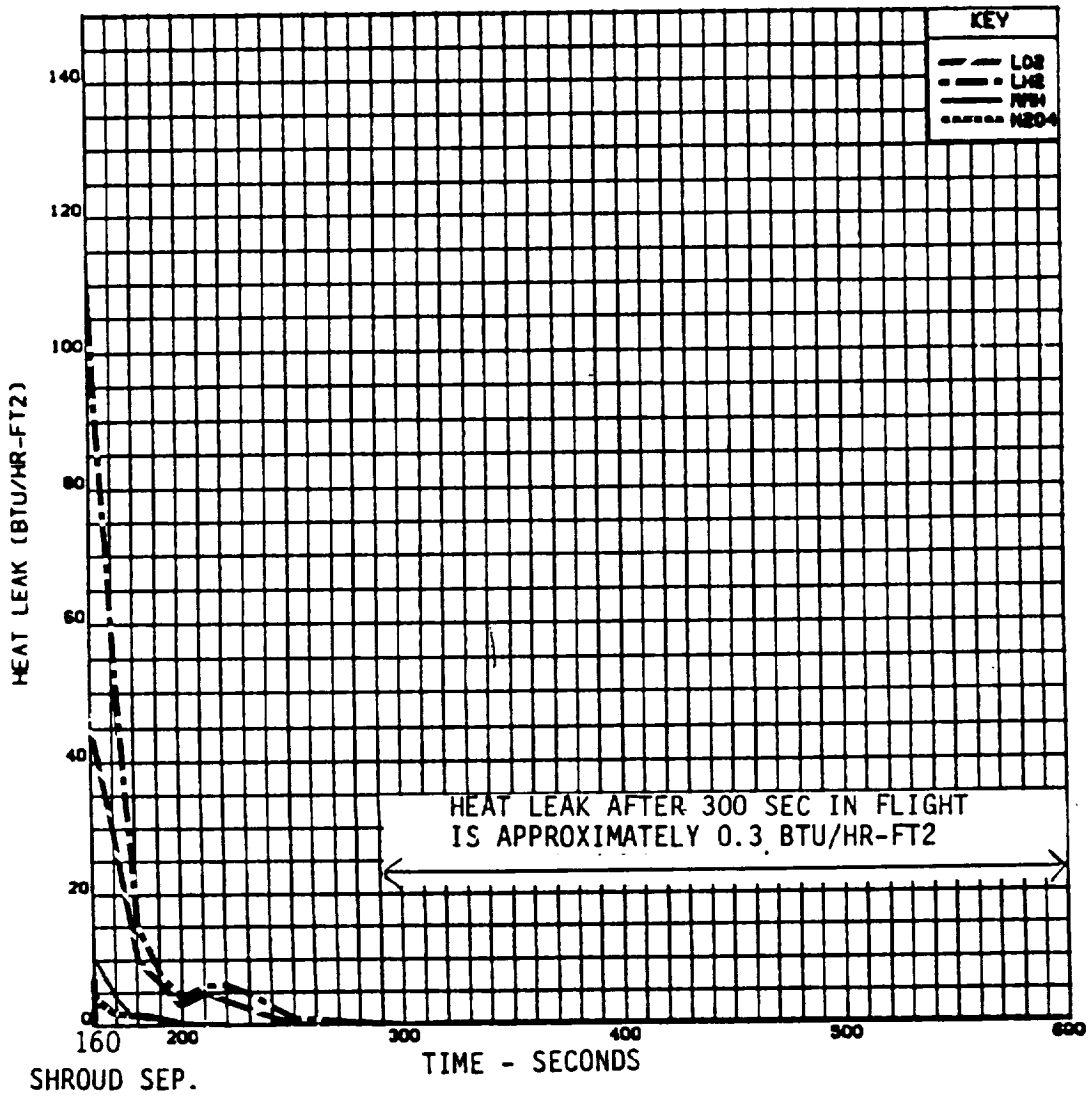


Figure 2.5-18 Heat Leak to ACC/OTV Tanks After Shroud Separation

ORIGINAL PAGE IS
OF POOR QUALITY

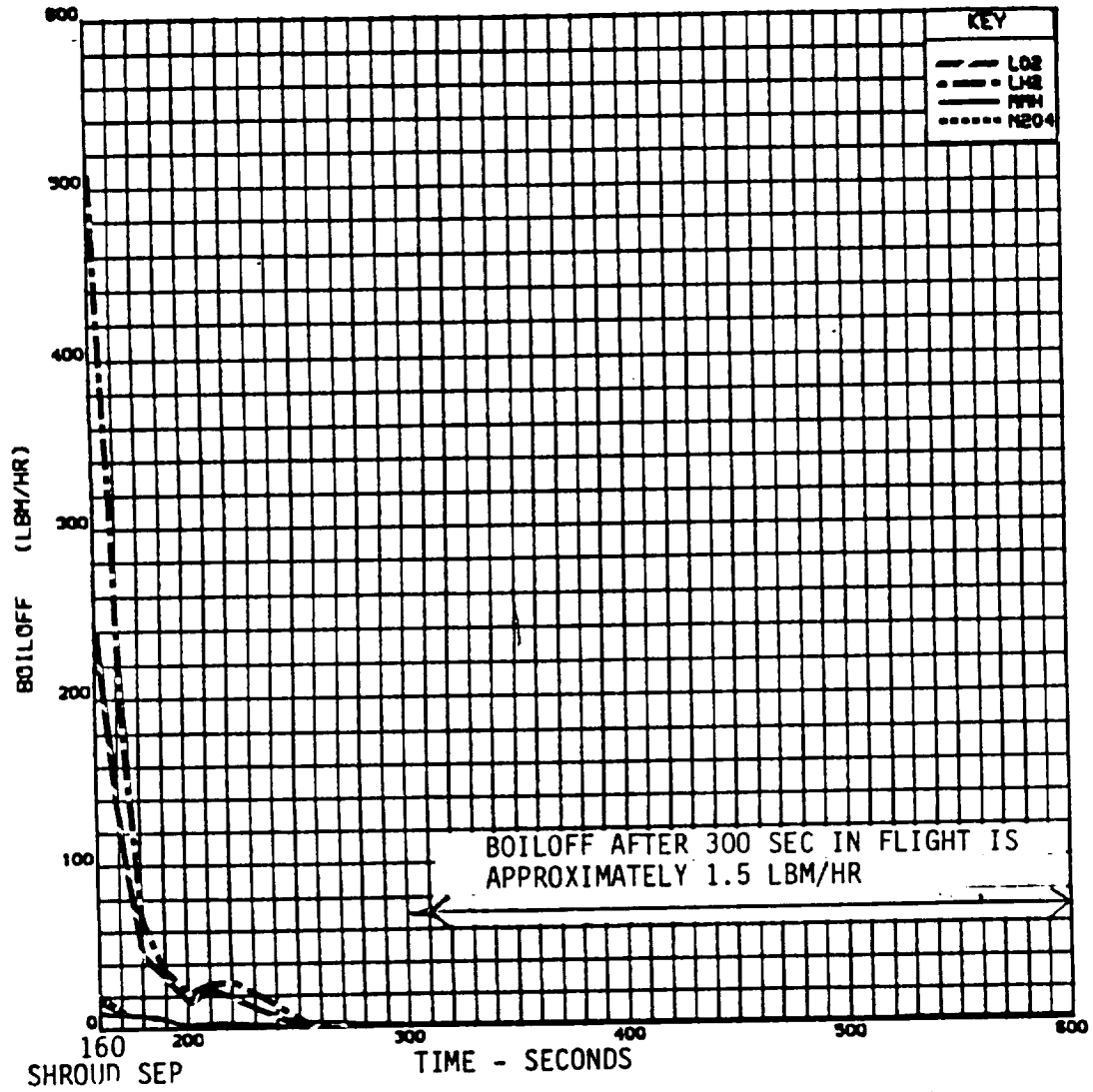


Figure 2.5-19 Boiloff in ACC/OTV Tanks After Shroud Separation

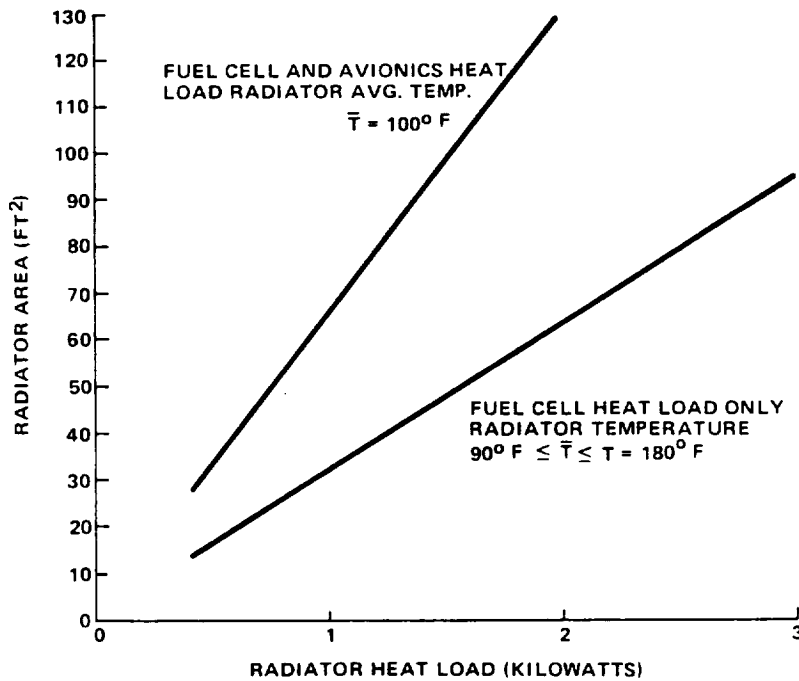


Figure 2.5-20 Radiator Sizing of Fuel Cells and Avionics (Hot Case)

A system weight for an OTV fuel cell power system has been established as shown in Figure 2.5-21. The radiator(s) weight, based on 1 lb/ft² was derived from radiator sizing analysis. A weight summary for the fuel cell system components (provided by G.E. Direct Energy Conversion Programs) was studied to determine fixed and variable component weights as a function of system power requirements. The range of power output levels considered was 0.5KW to 2.5KW, where the system weight was considered reasonably linear. A one fuel cell system weight was doubled to account for required redundancy in the system with results shown. Weights for plumbing from the fuel cell to the radiator(s), valves on those lines, and coolant in the lines and radiator(s), were estimated and are also shown in the Figure. The total system weight, excluding propellant, is the summation of the above and is shown in the Figure.

Table 2.5-2 Separate Radiator Trade

RADIATOR DUTY HEAT LOAD	MANEUVER	RADIATOR AREA
FUEL CELL ONLY 1.5KW	HOT CASE ROTISSERIE COLD CASE	47.9 38.7 32.0
FUEL CELL & AVIONICS 1.5KW + 1.125KW	HOT CASE ROTISSERIE COLD CASE	340.7 173.6 78.6
SEPARATE RADIATOR SYSTEM FOR AVIONICS 1.125 KW (1.5 KW F.C.)	HOT CASE	75.0 (47.9 F.C.)

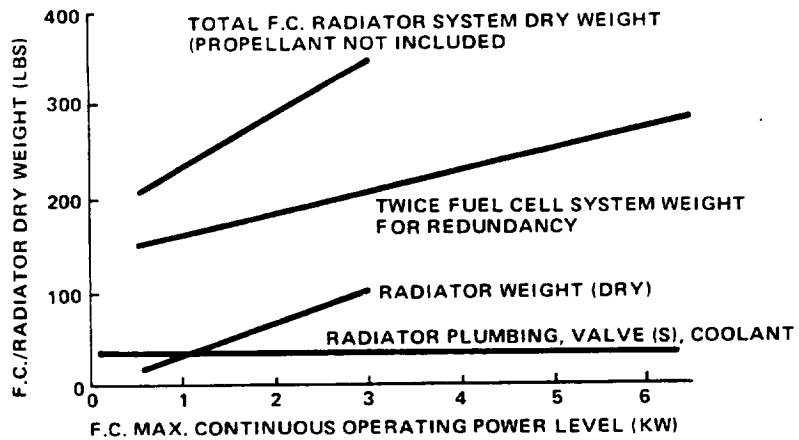


Figure 2.5-21 Fuel Cell/Radiator System Weight Breakdown

The fuel requirements for various estimated nominal mission durations were then superimposed on the above total fuel cell system weight and are shown in Figure 2.5-22. Further details on the OTV fuel cell weight assessment can be found in Reference 2.5-8

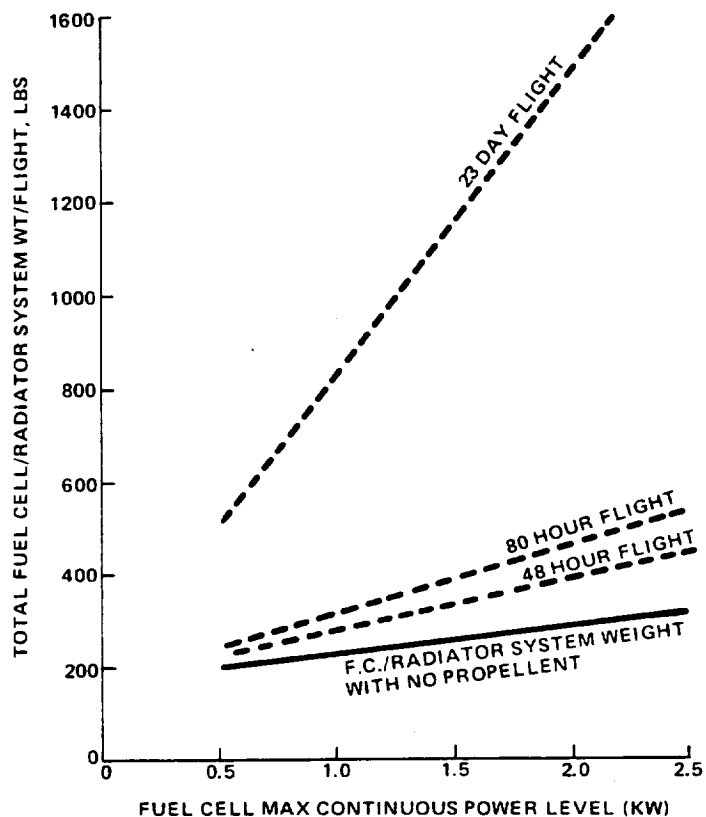


Figure 2.5-22 F.C./Radiator System Weight With Propellant Requirements for Various Mission Times

REFERENCES--

- 2.5-1) BB&N, Inc. Report No. 5065 "Acoustic Protection Study of Proposed Space Shuttle ACC", dated January, 1983.
- 2.5-2) MMC-3525-83-0018, "Updated Purge Requirements for ACC Compartments", by J. Monirian, dated April 8, 1983.

- 2.5-3) MMC-3533/A-84-169, "Preliminary Ground Purge and Ascent Venting Analysis for the OTV Dedicated Aft Cargo Carrier", P. Gandhi, November 15, 1984.
- 2.5-4) MMC-3525-83-0015, "Updated TPS Design for ACC".
- 2.5-5) MMC-3525-83-0077, "Thermal Environments for Aft Cargo Carrier", by J. Monirian, dated Dec. 9, 1983.
- 2.5-6) NASA CR-134477, "Thermal Performance of Multilayer Insulations (LMSC-D349866, Lockheed Missiles and Space Co., NAS3-14337) by C.W. Keller, G.R. Cunningham and A.P. Glostord, 1974.
- 2.5-7) Monti, P.S., "OTV Fuel Cell and Avionics Cooling System Design," TM C.2.4.5.0-01, Martin Marietta Corporation, Denver, Colorado, 7 January 1985.
- 2.5-8) Monti, P.S., "OTV Fuel Cell System Weight Assessment," TM C.2.4.5.0-02, Martin Marietta Corporation, Denver, Colorado, 7 January 1985.



APPENDICES

TRAJECTORY PROFILES--These appendices contain selected trajectory profiles for our closed loop aeropass simulation. Information from this simulation was used to size aerobrakes (structure & TPS), RCS fuel usage, postero burns as well as evaluating overall guidance performance. Each section includes the following ten profiles:

- 1) Roll angle & deceleration time history. The roll angle represents the clock angle position of the OTV lift vector (0° = up, angle measured positive clockwise if looking forward along the velocity vector).
- 2) Altitude time history.
- 3) Velocity time history. Velocity is measured with respect to a rotating atmosphere.
- 4) Inclination time history. Instantaneous orbital inclination is measured with respect to inertial space. The target condition is 28.5° with a tolerance of $\pm .02^{\circ}$ in all cases.
- 5) Flight path angle time history. This quantity is measured inertially with respect to local horizontal.
- 6) Dynamic pressure time history. The quantity $.5 * (\text{density}) * (\text{vel}_{\text{rel}})^2$ is displayed and represents the free-stream pressure.
- 7) Heat flux time history. The heating rate per unit area is derived from Chapman's equation for a 1.0 ft. sphere. This quantity does not include non-equilibrium or real-gas effects.
- 8) Roll dynamics time history. Three quantities are displayed:
 - a) Roll rate vs. time.
 - b) Roll thruster activity vs. time.
 - c) RCS fuel usage vs. time.NOTE: The RCS fuel usage is derived from roll jet activity only. Pitch & yaw activity, required for stability, is not modeled in this simulation.
- 9) Lift & drag time. History, the coefficients of lift and drag (C_L & C_D) are shown as they are affected by free molecular flow effects and angle of attack dispersions (the latter are implemented at entry interface)
- 10) Free molecular transition factor vs. time. This is a multiplicative factor which interpolates between free molecular and continuum flow data. A value of 1.0 indicates pure continuum flow and a value of 0.0 indicates pure free molecular flow. The negative regions for the C_D factor correspond to the drag coefficient decay region which occurs around a knudsen number of .005 (see "flow regime transition criteria based on Viking flight" chart).

The following simulation runs are included:

- Appendix A - 1962 std. atmos., angle of attack error = +1.5°
- Appendix B - STS 2 atmosphere
- Appendix C - STS 4 atmosphere
- Appendix D - STS 6 atmosphere
- Appendix E - STS 6 atmos., angle of attack error = + 1°
- Appendix F - STS 6 atmos., perigee aimpoint error = + .2 nm
- Appendix G - STS 6 atmos, bulk density shift (equivalently ballistic coefficient shift) = + 22%
- Appendix H - STS 6 atmos, navigation error: 2000 ft. position and 14 fps. velocity
- Appendix I - STS 6 atmosphere, space based OTV

APPENDIX A

OTV AEROPASS SIMULATION

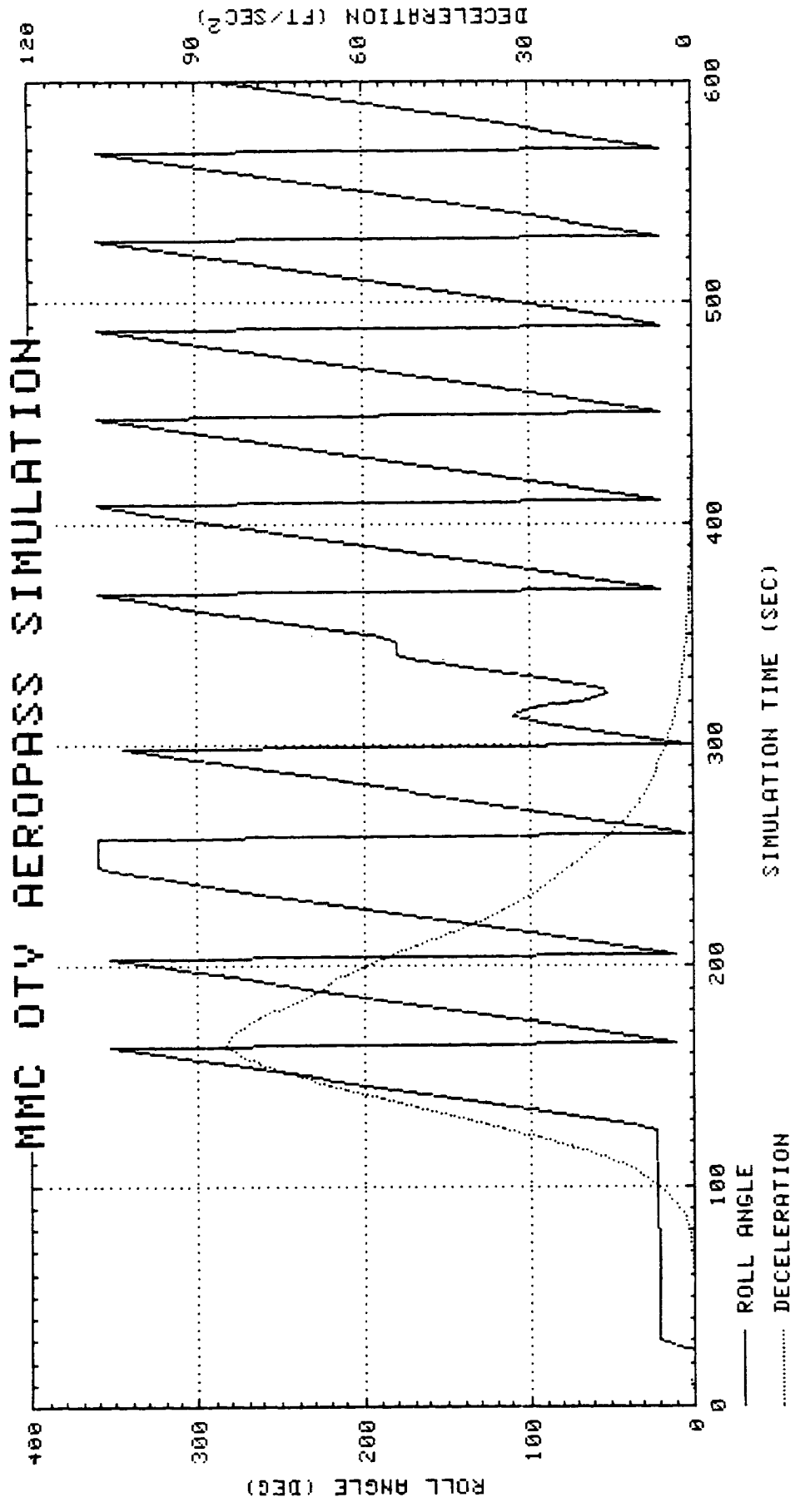
1962 STANDARD ATMOSPHERE

ANGLE OF ATTACK ERROR = 1.5°

EXIT APOGEE ERROR = .02 NM

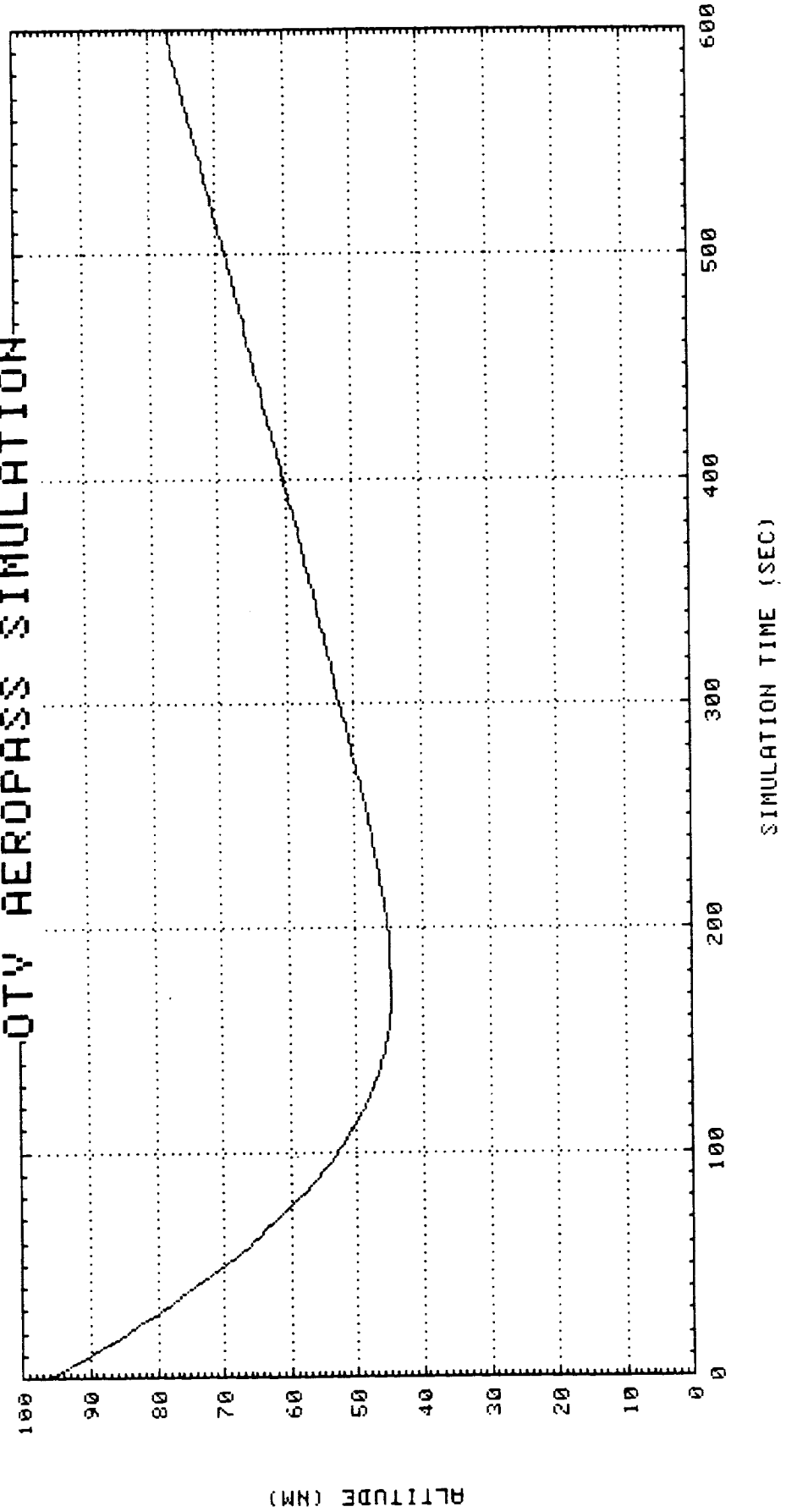
EXIT INCLINATION ERROR = .0043°

THIS PAGE INTENTIONALLY LEFT BLANK

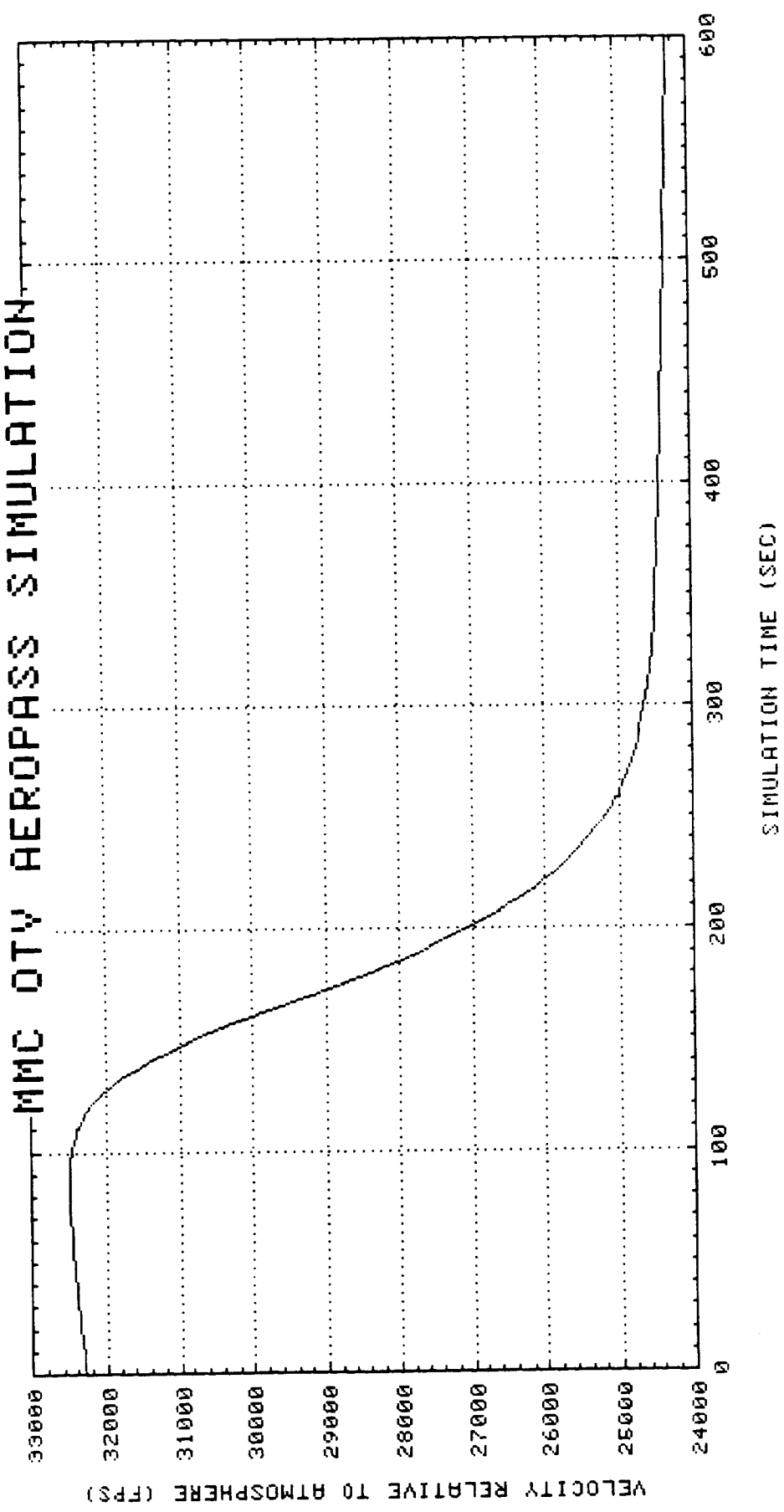


PRECEDING PAGE BLANK NOT FILMED

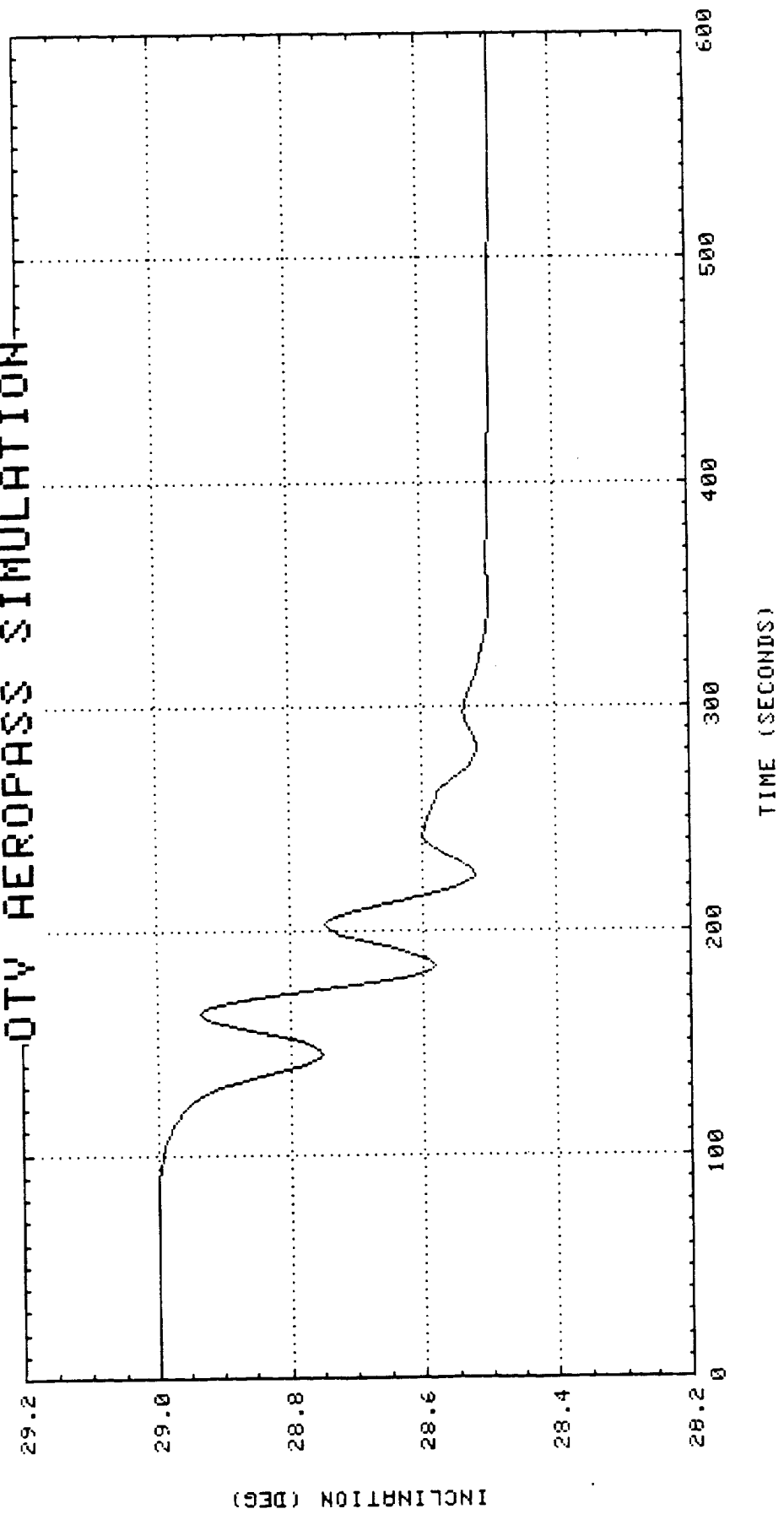
QTY AEROPASS SIMULATION



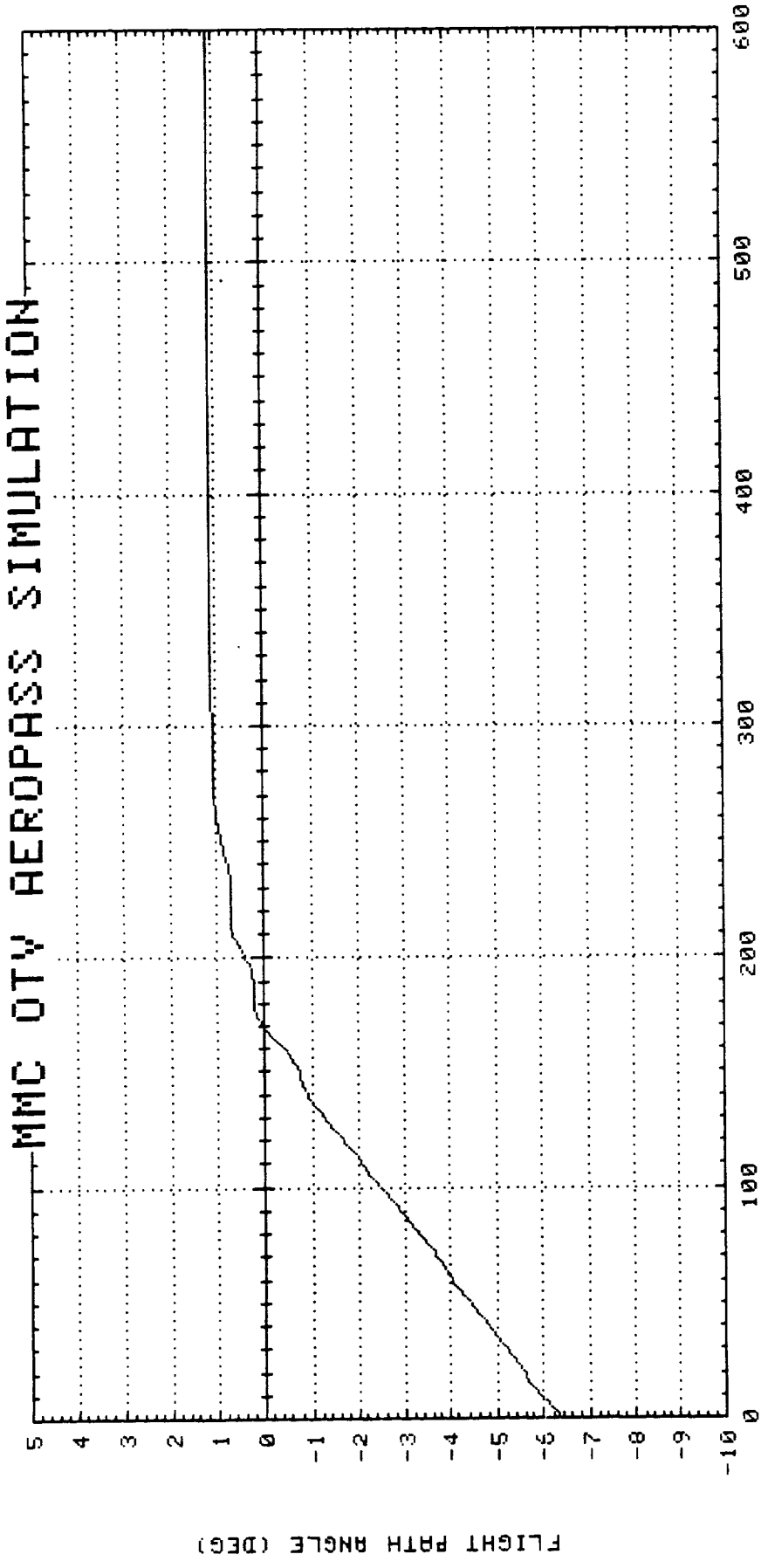
MMC DTY AEROPASS SIMULATION



QTY AEROPASS SIMULATION

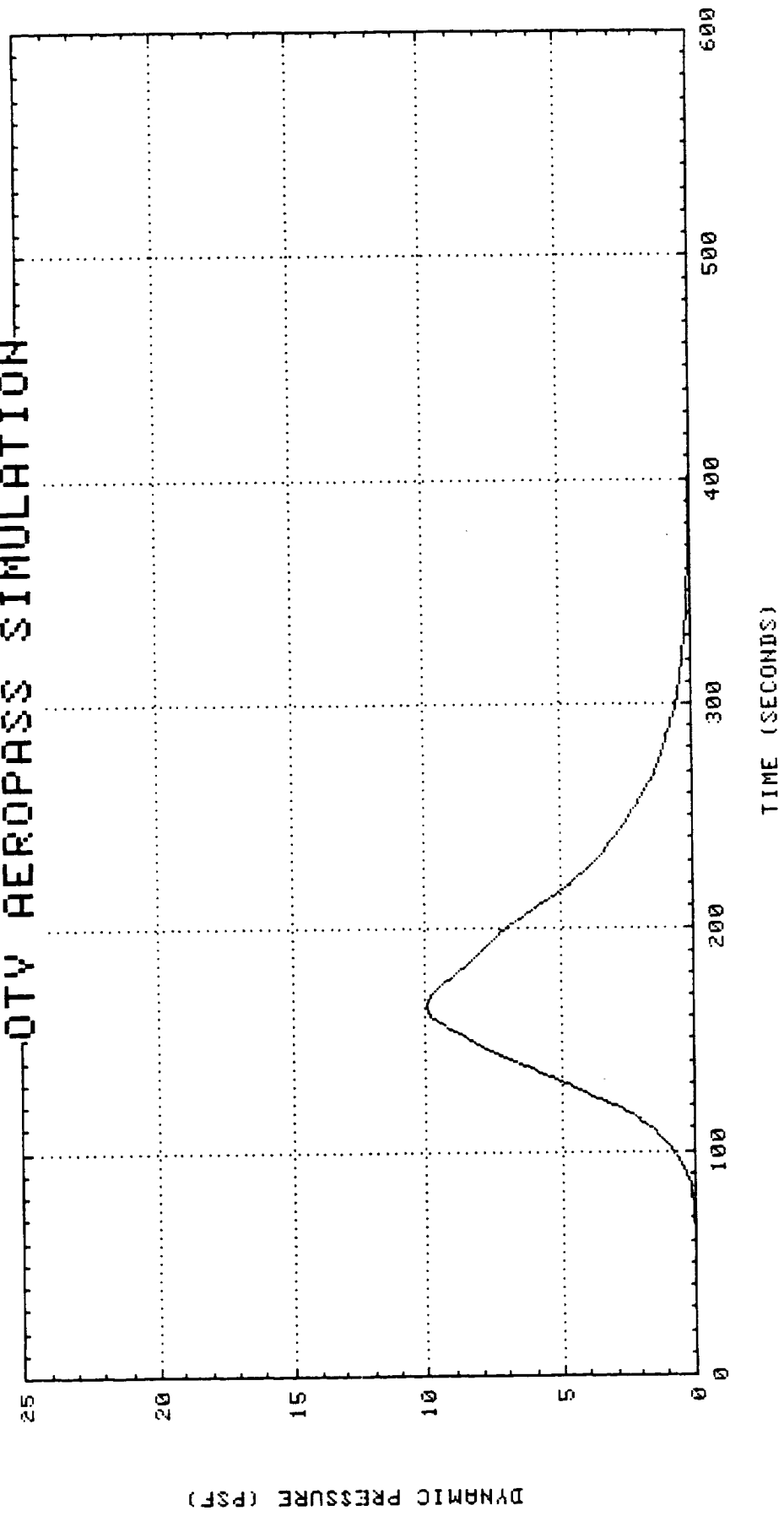


MMC OTY AEROPASS SIMULATION



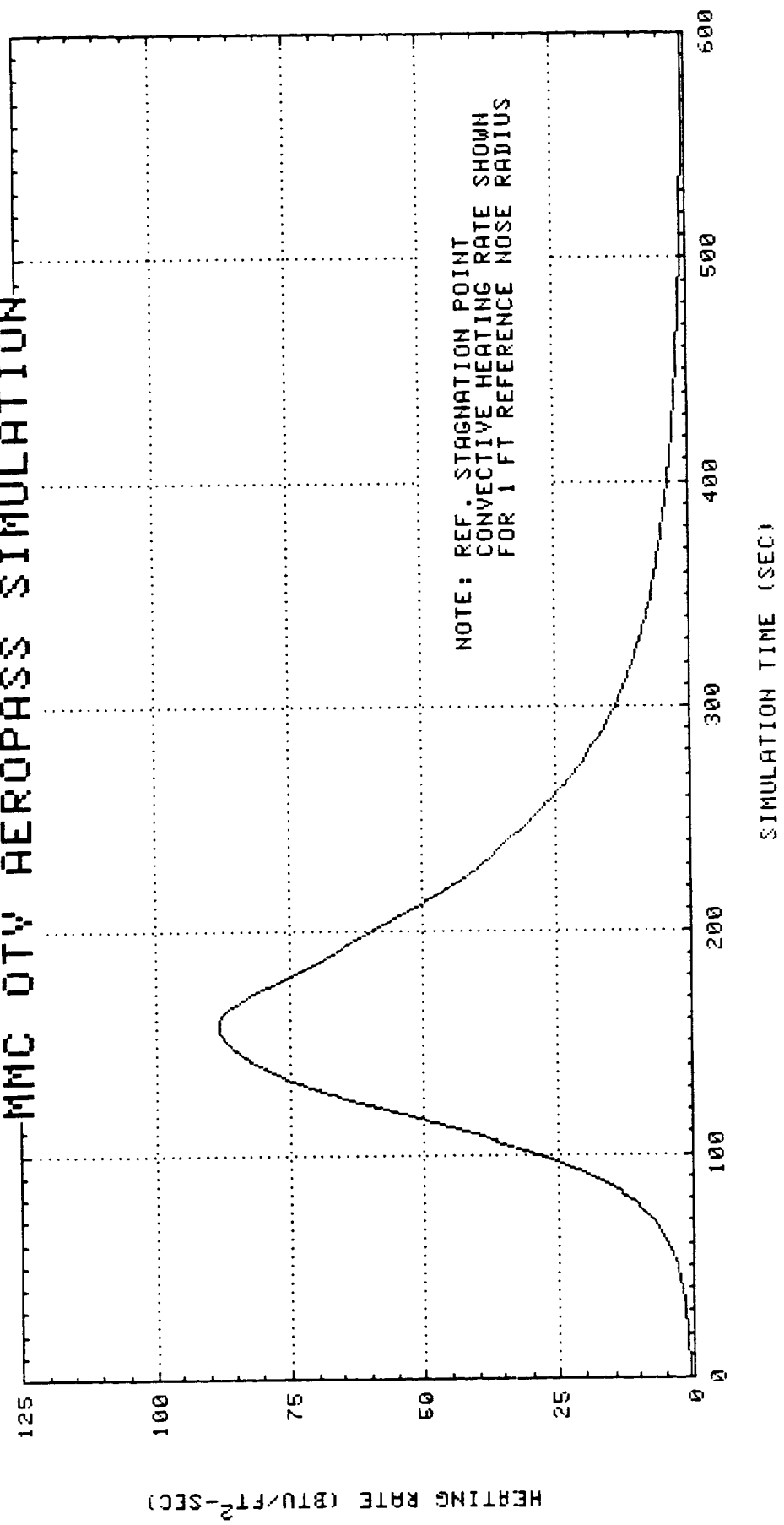
SIMULATION TIME (SEC)

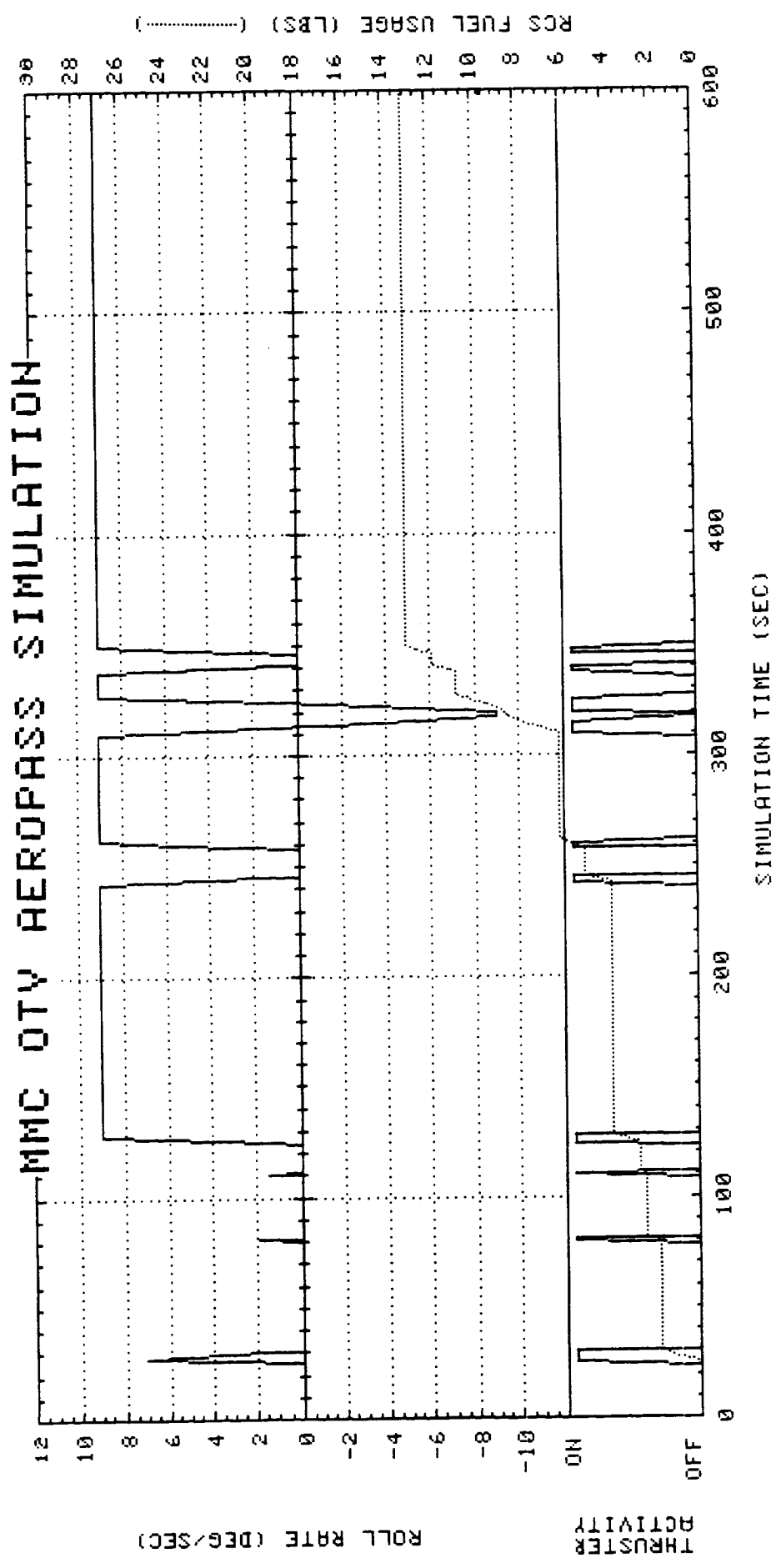
QTY AEROPASS SIMULATION



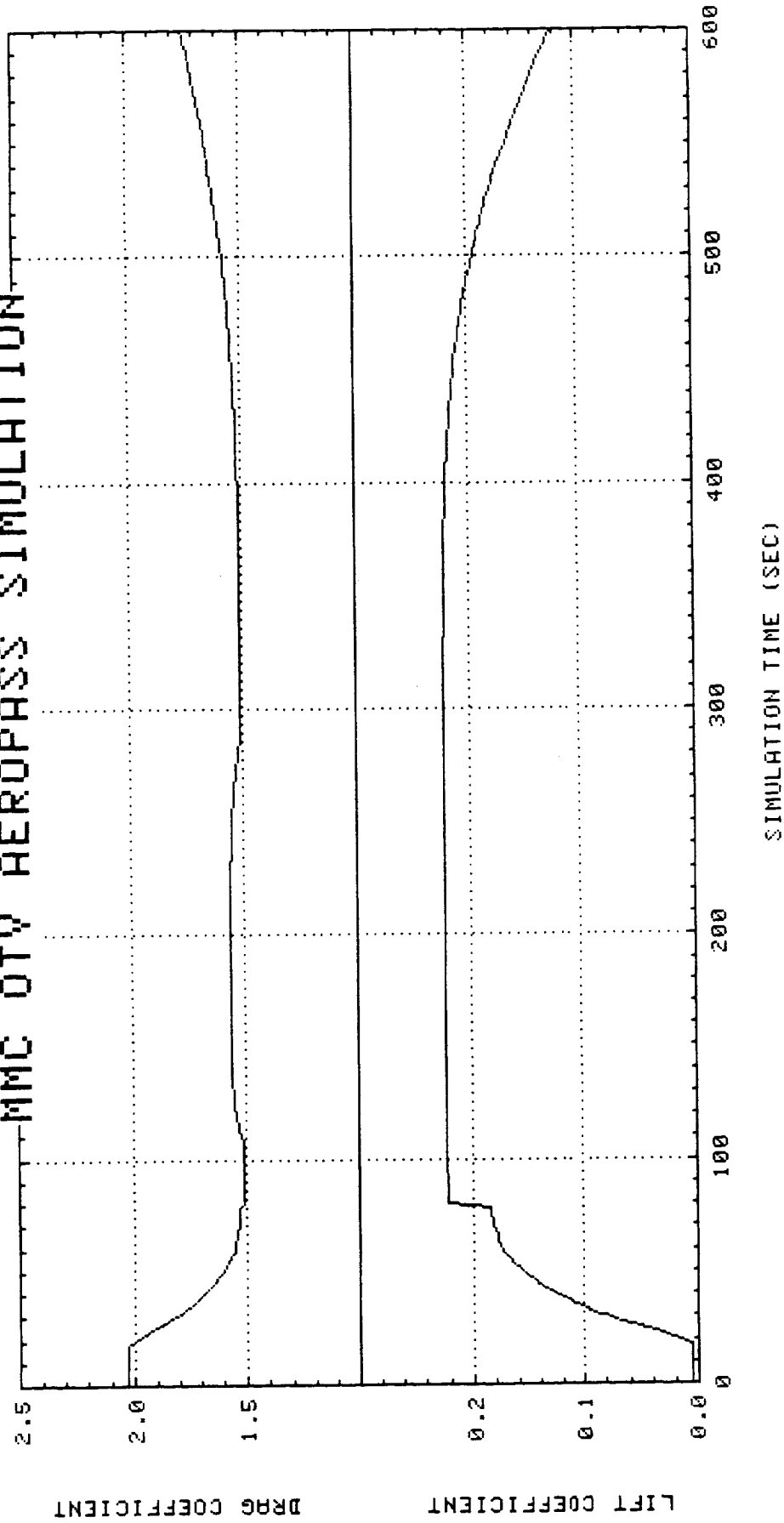
NOTE: DYNAMIC PRESSURE IS
FREE-STREAM VALUE

MMC OTV AEROPASS SIMULATION



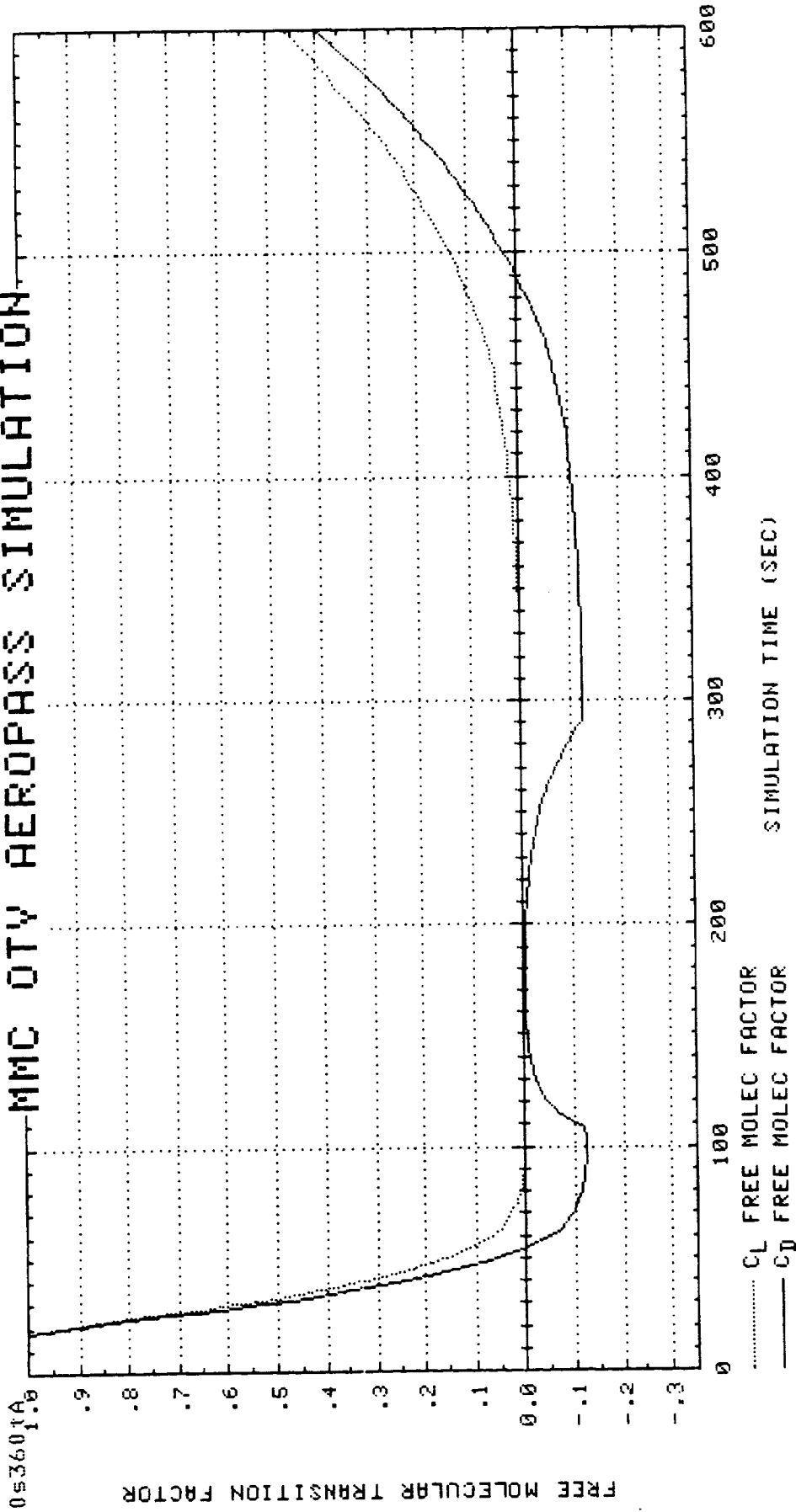


MMC DTW AEROPASS SIMULATION



MMC QTY AEROPASS SIMULATION

72053601A9



APPENDIX B

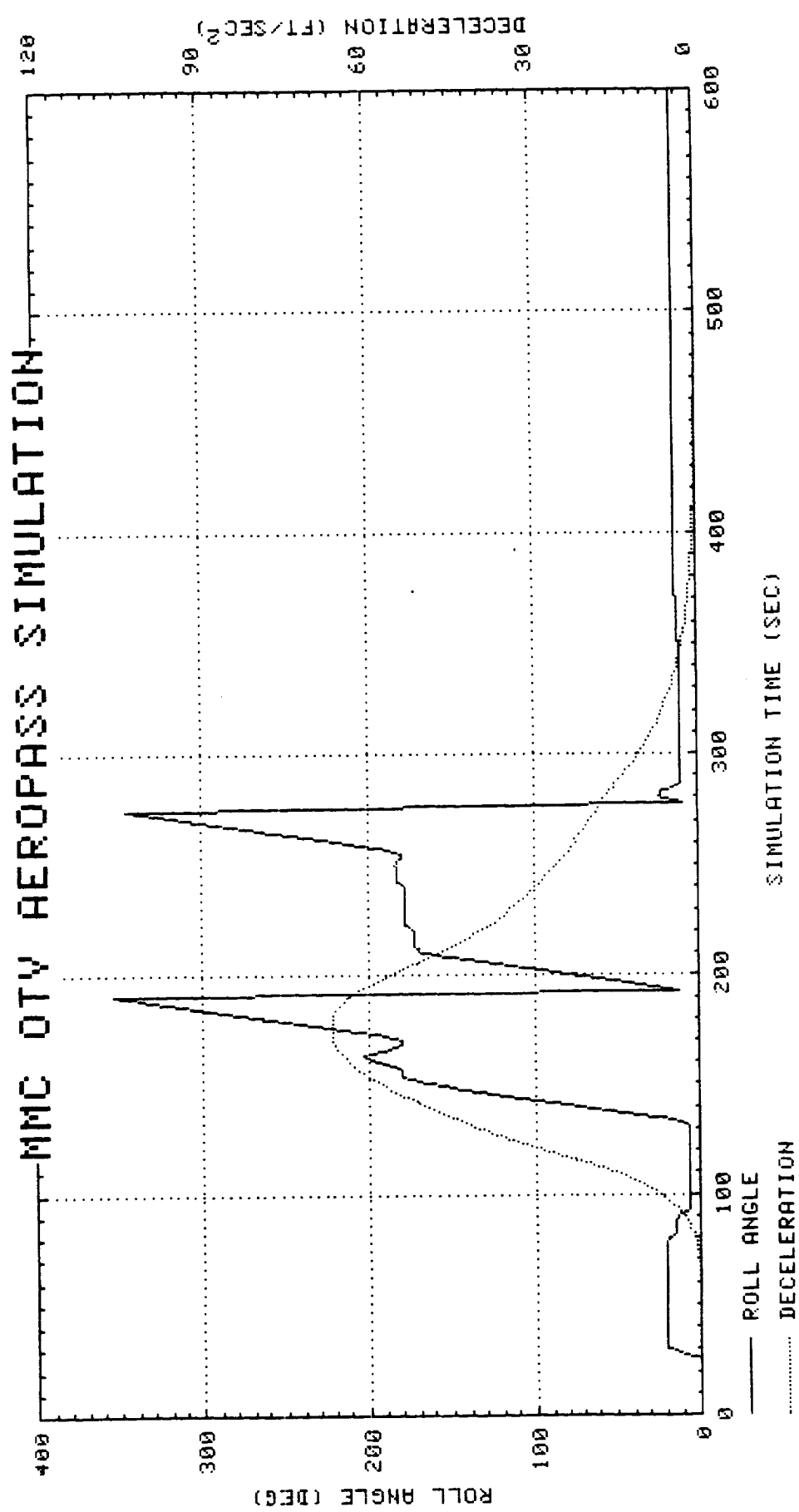
OTV AEROPASS SIMULATION

STS-2 ATMOSPHERE

EXIT APOGEE ERROR = 2.06 NM

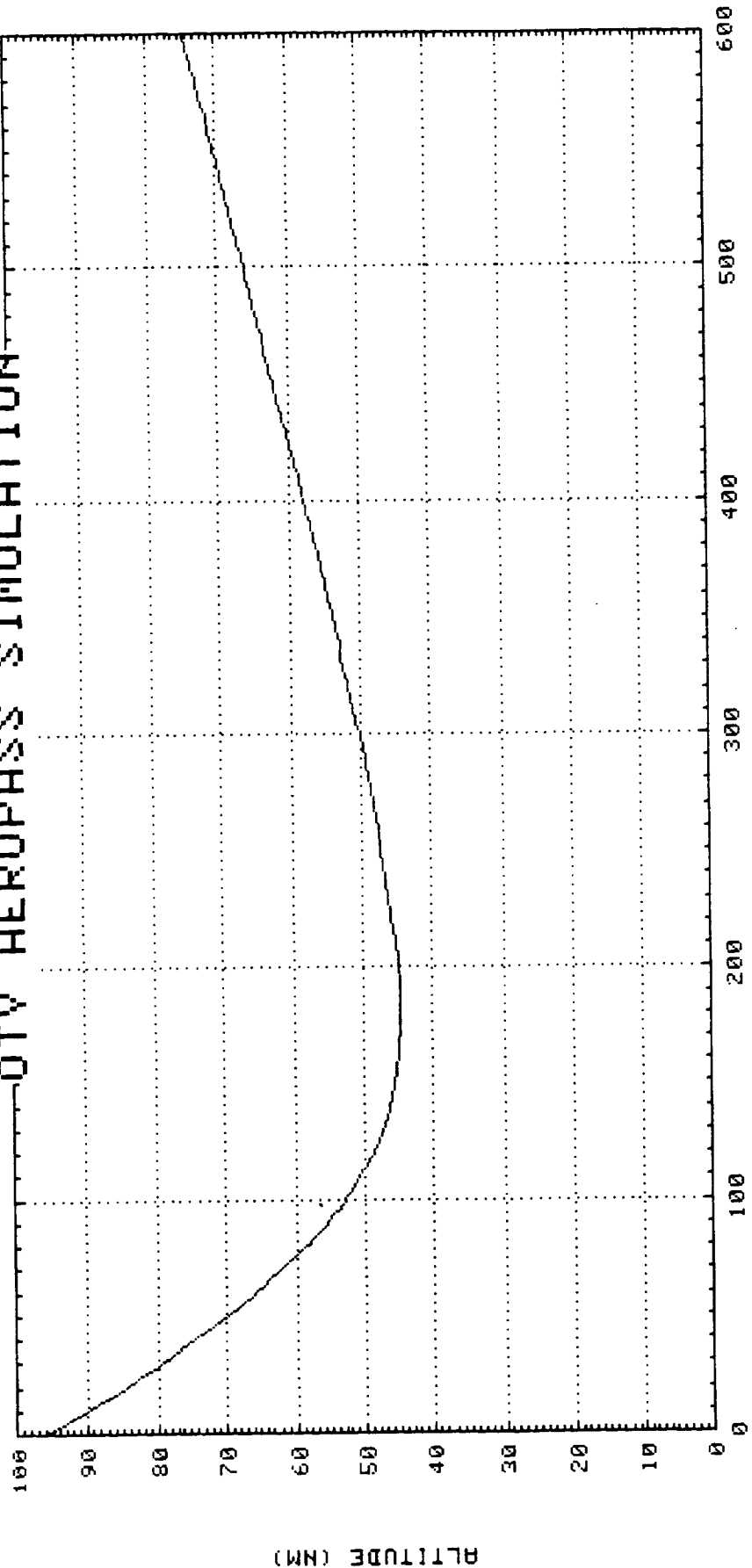
EXIT INCLINATION ERROR = .0036°

THIS PAGE INTENTIONALLY LEFT BLANK

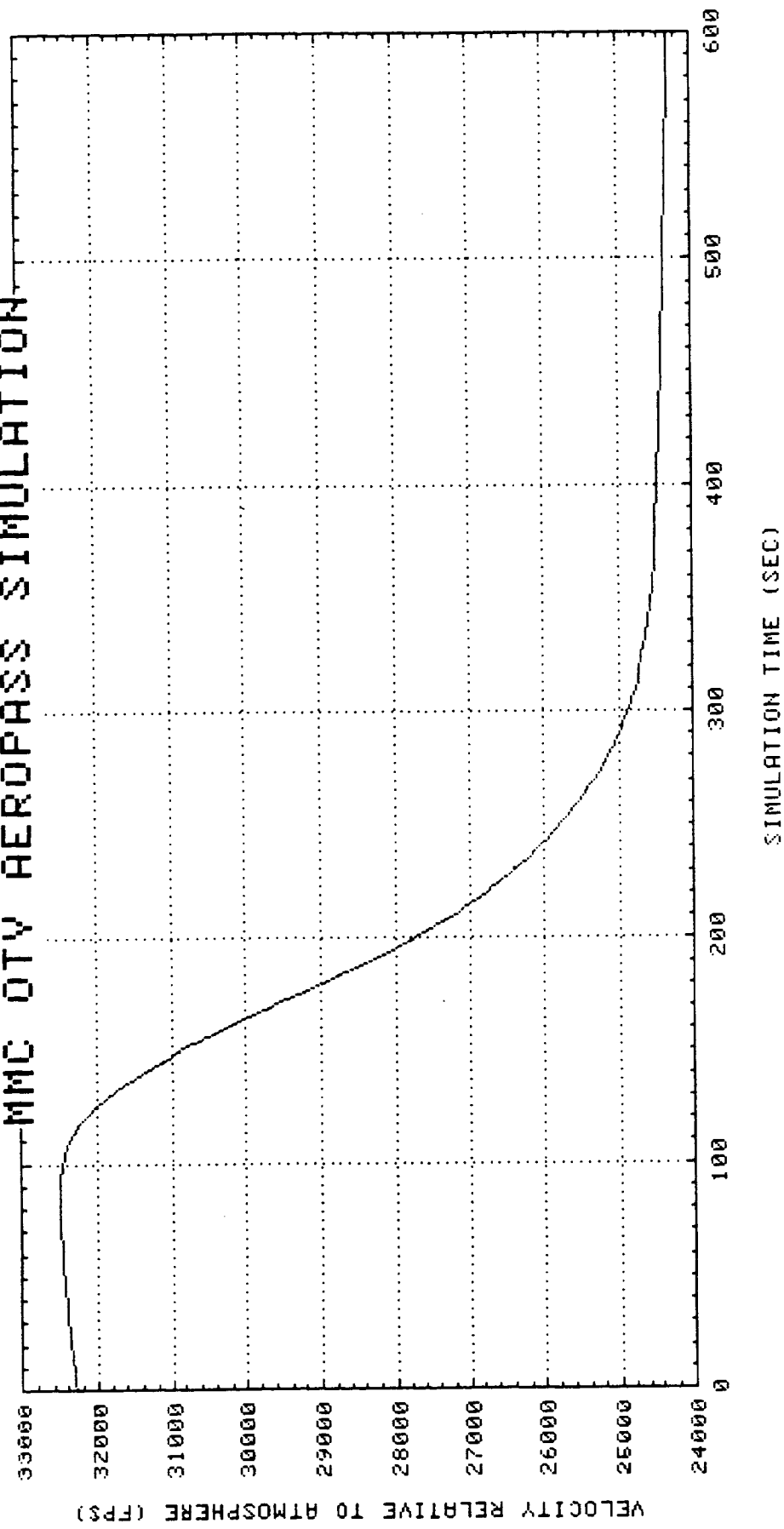


PRECEDING PAGE BLANK NOT FILMED

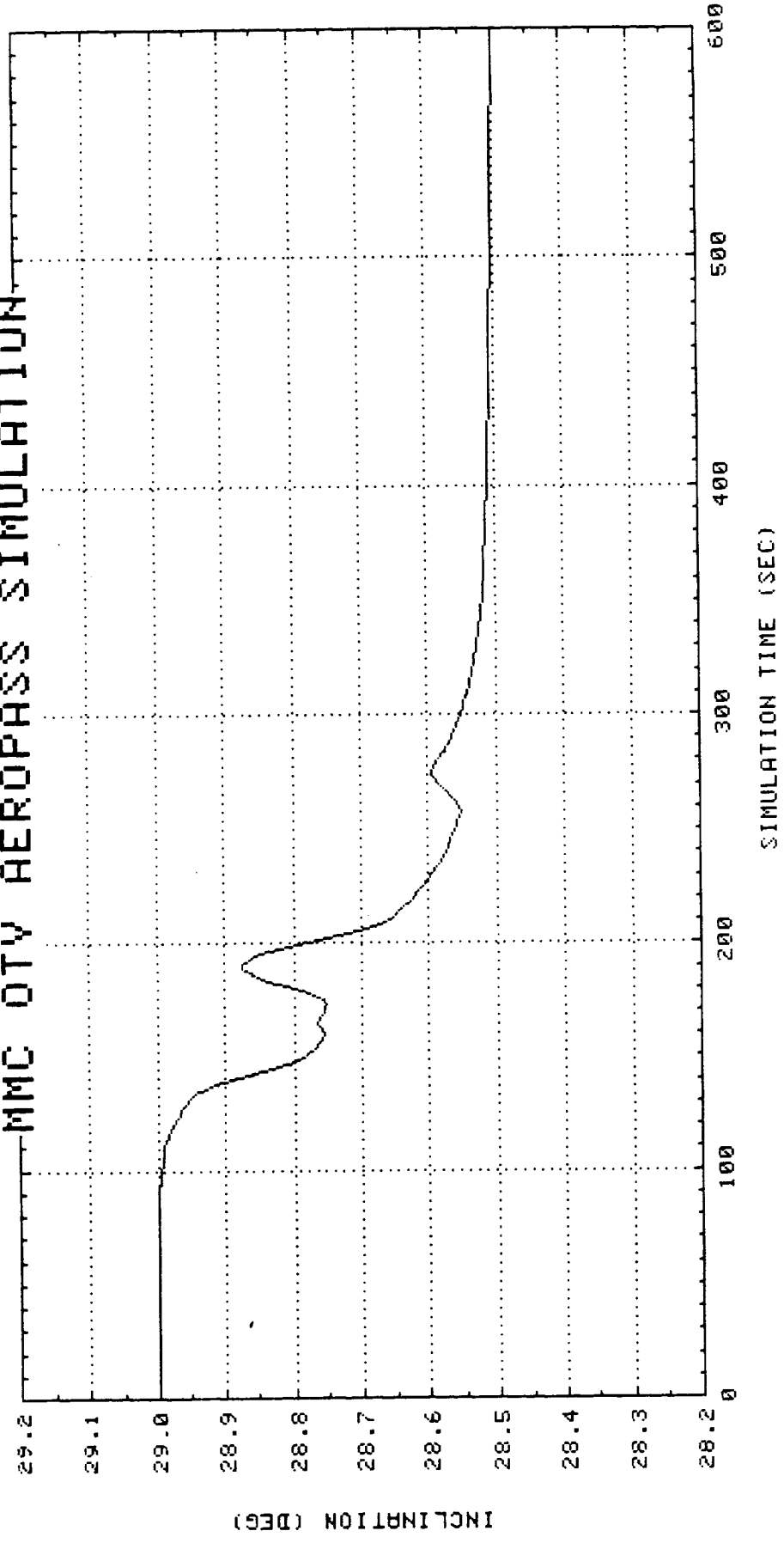
QTV AEROPASS SIMULATION



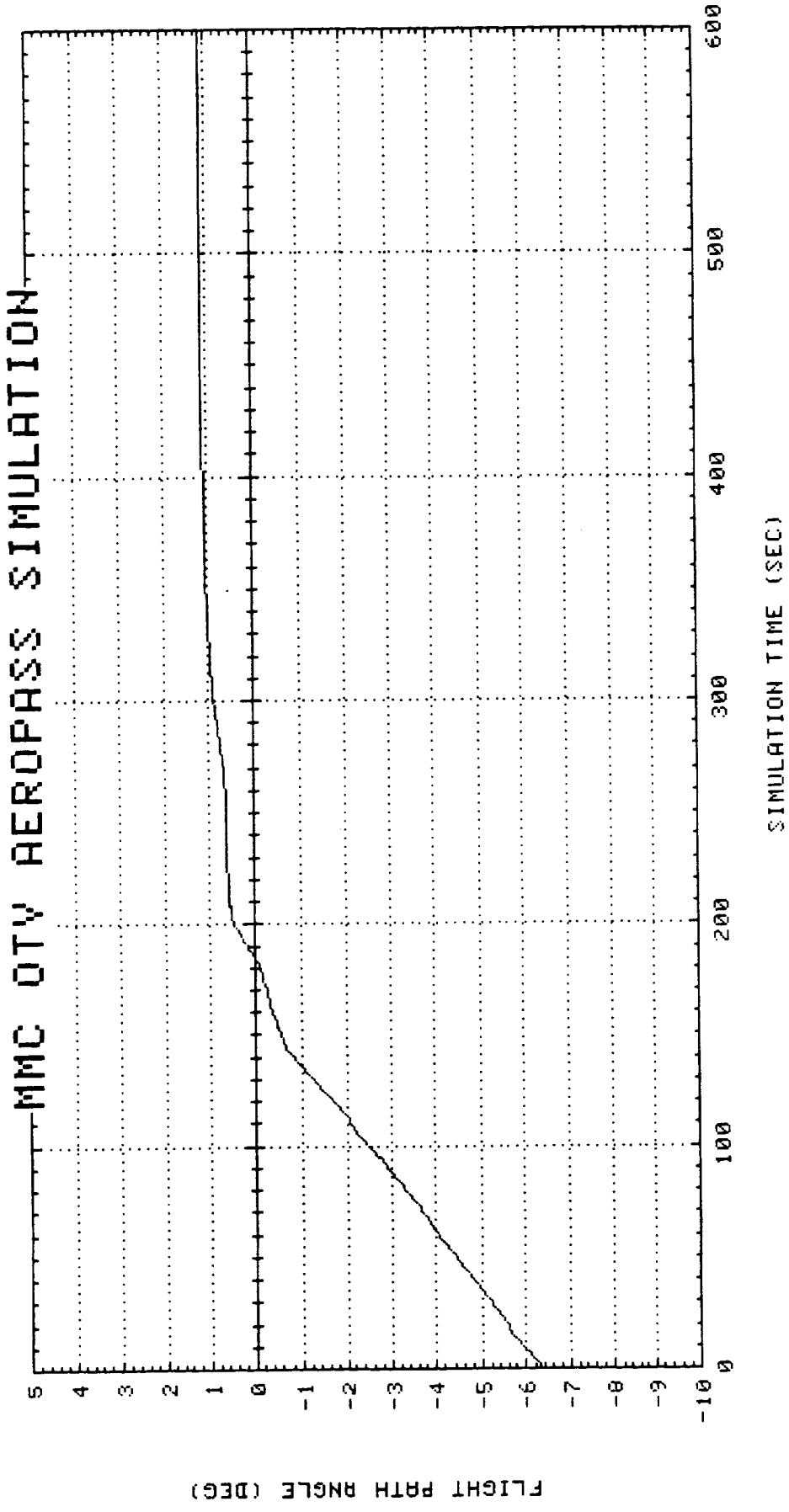
MMC DTV AEROPASS SIMULATION



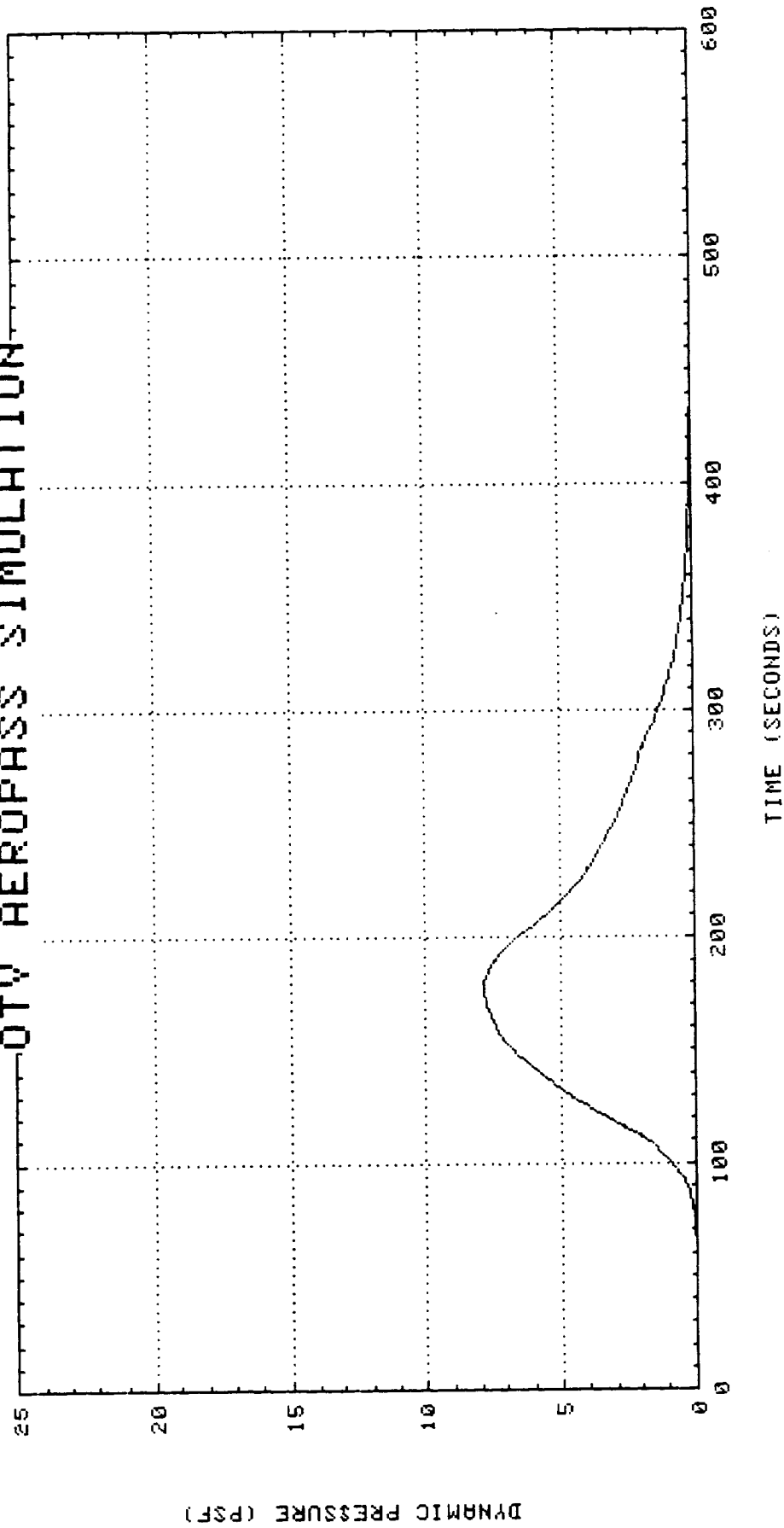
MMC OTV AEROPASS SIMULATION



MMC OTW AEROPASS SIMULATION

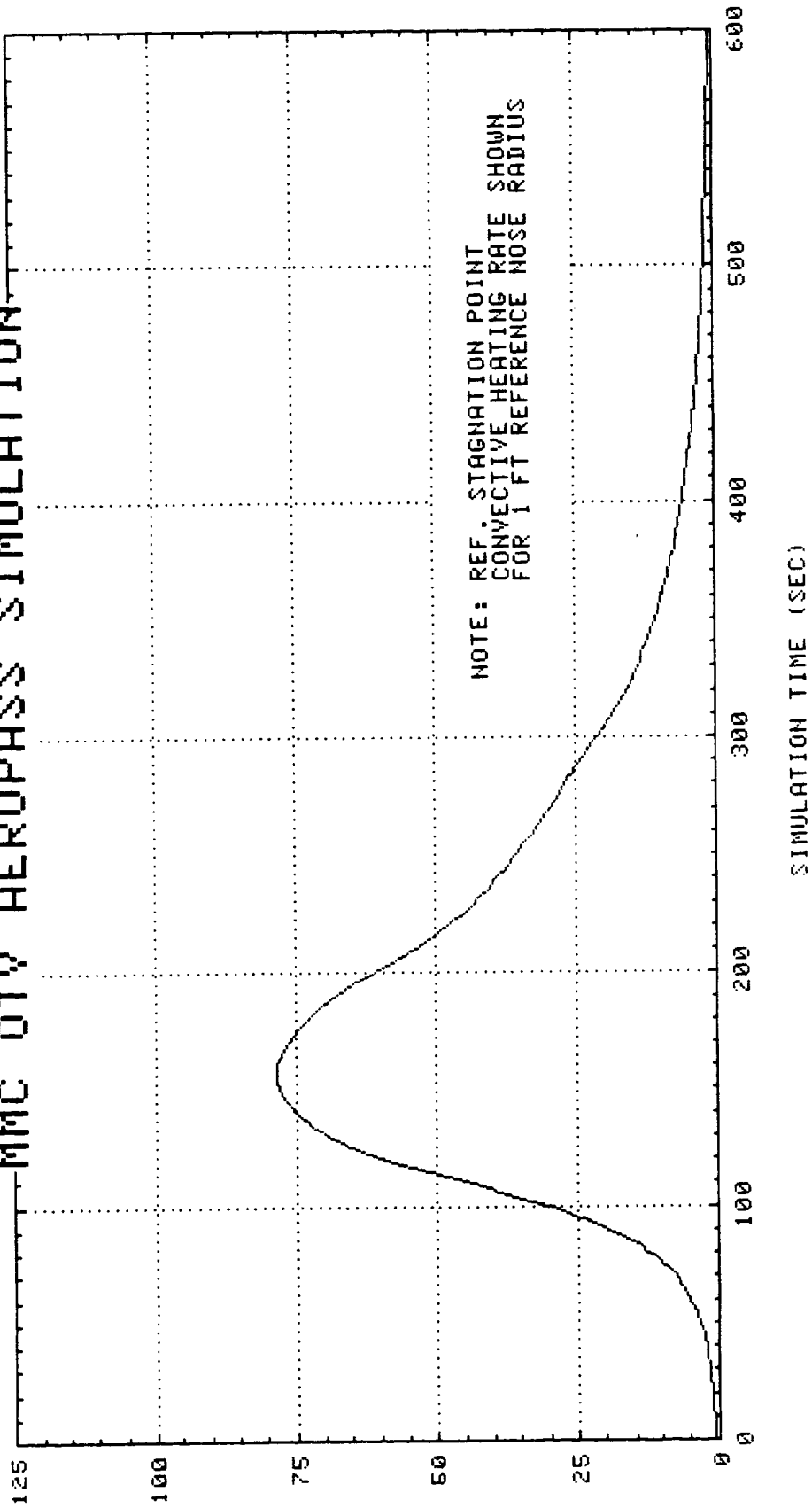


QTV AEROPASS SIMULATION

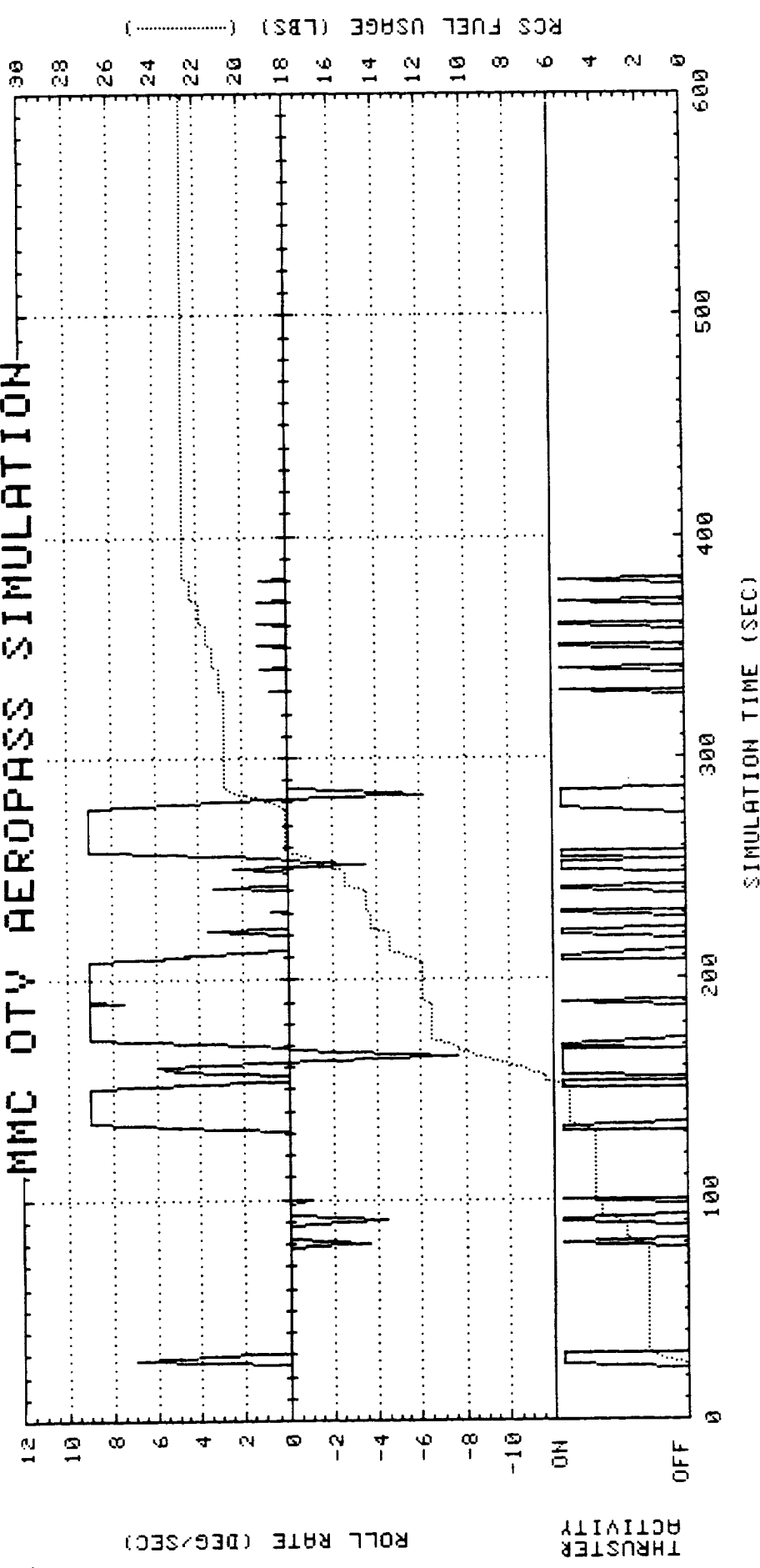


NOTE: DYNAMIC PRESSURE IS
FREE-STREAM VALUE

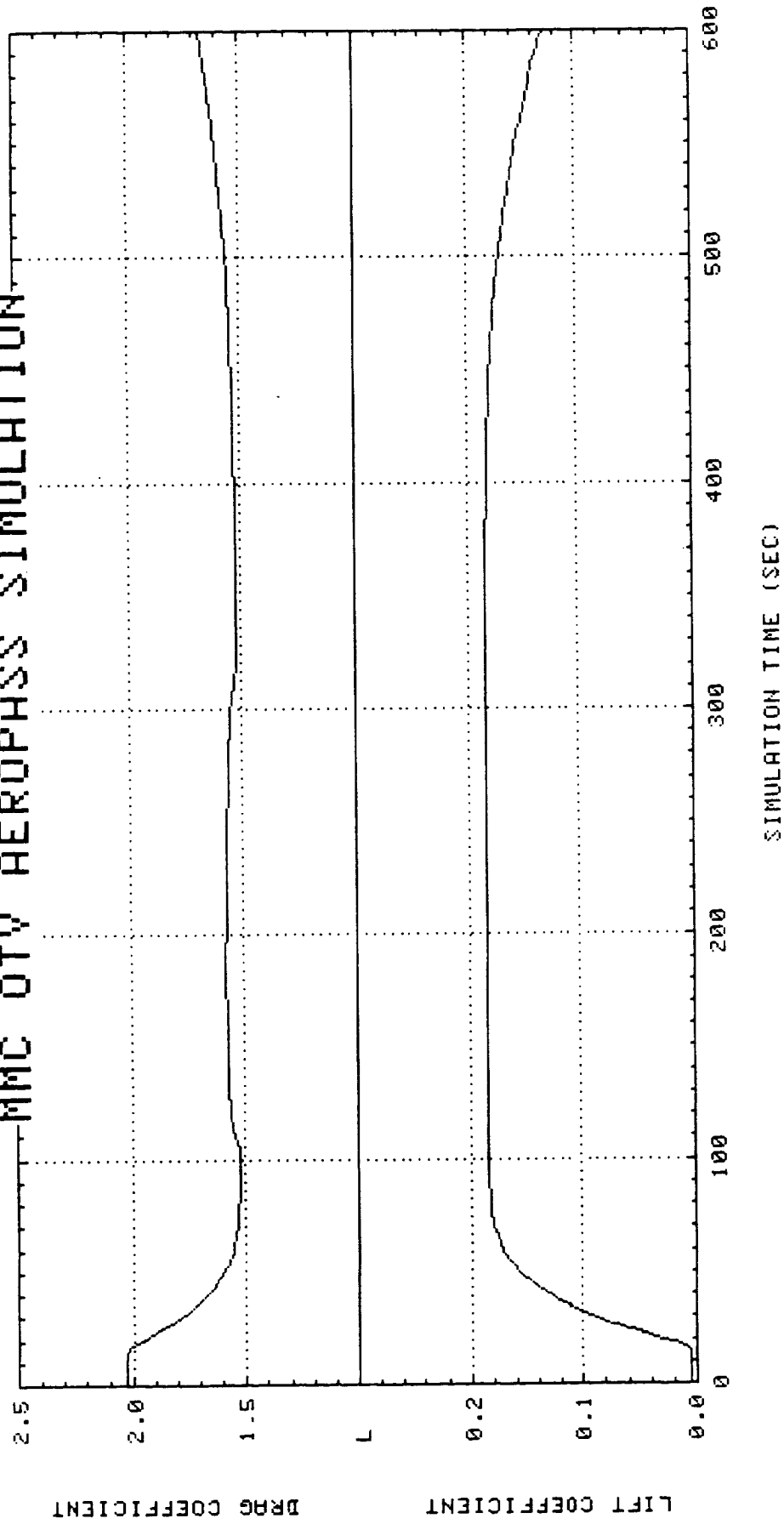
MMC OTW AEROPASS SIMULATION



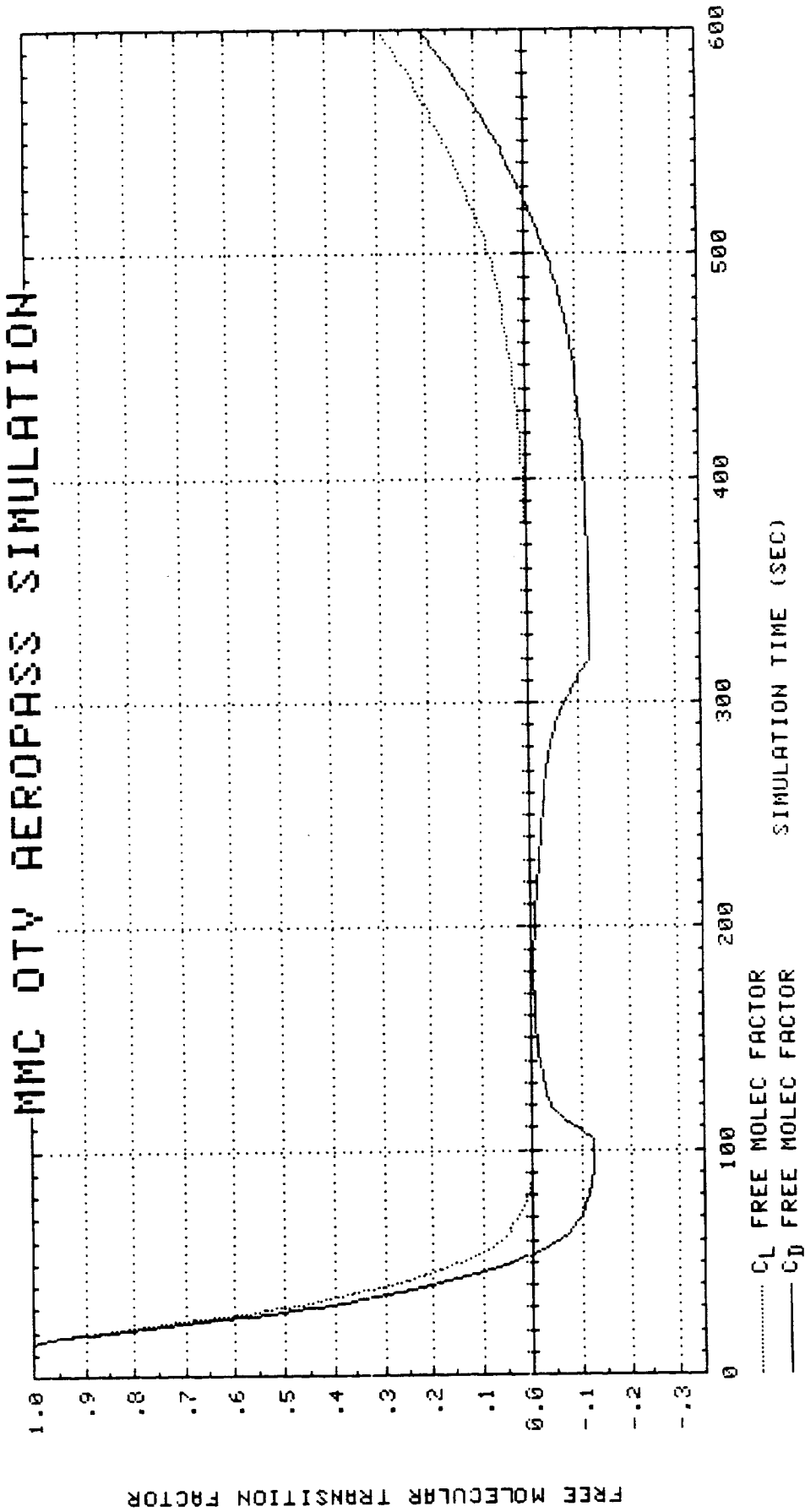
MMC OTV AEROPASS SIMULATION



MMC OTW AEROPASS SIMULATION



MMC QTY AEROPASS SIMULATION



APPENDIX C

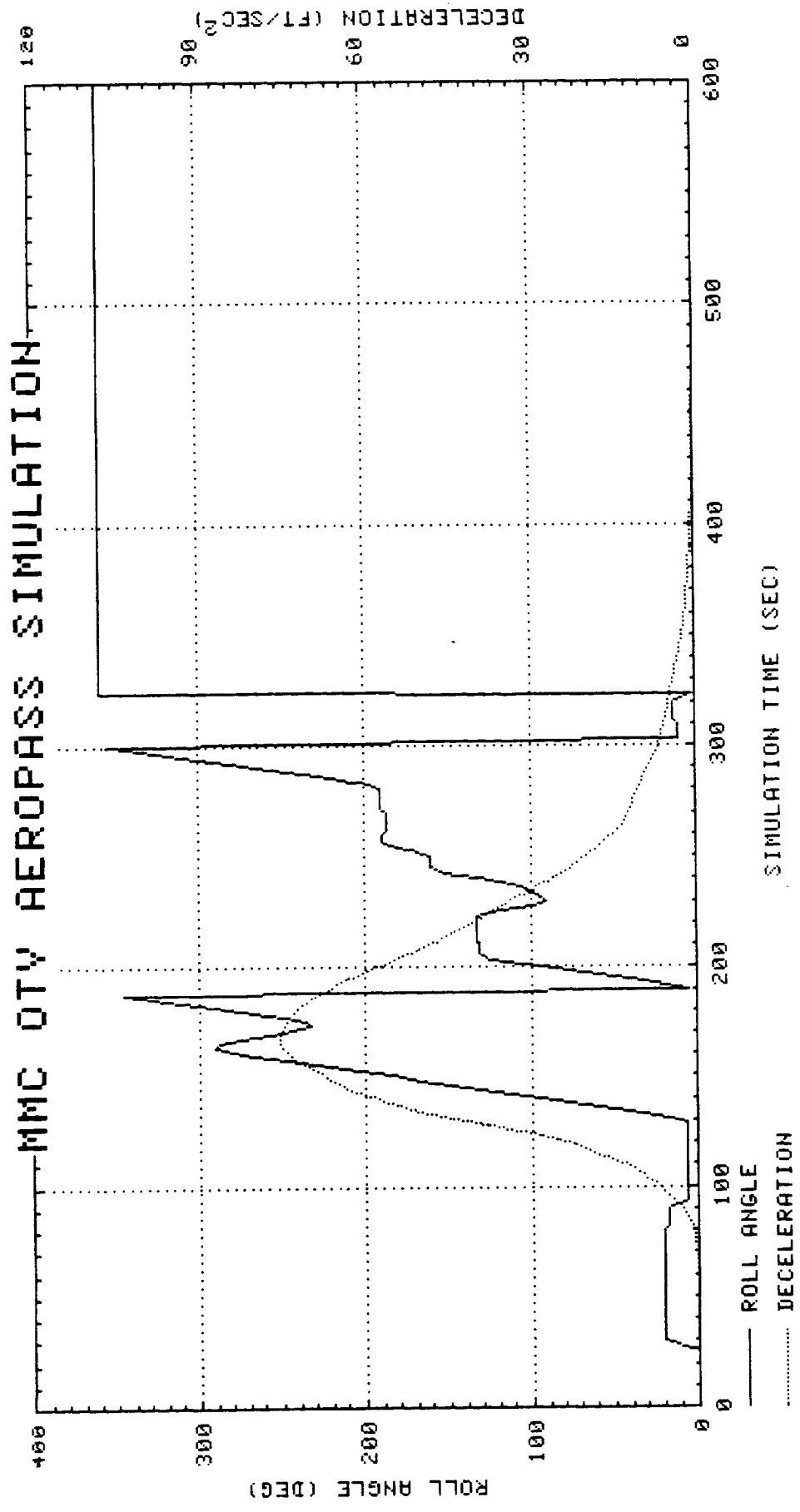
OTV AEROPASS SIMULATION

STS-4 ATMOSPHERE

EXIT APOGEE ERROR = 2.57 NM

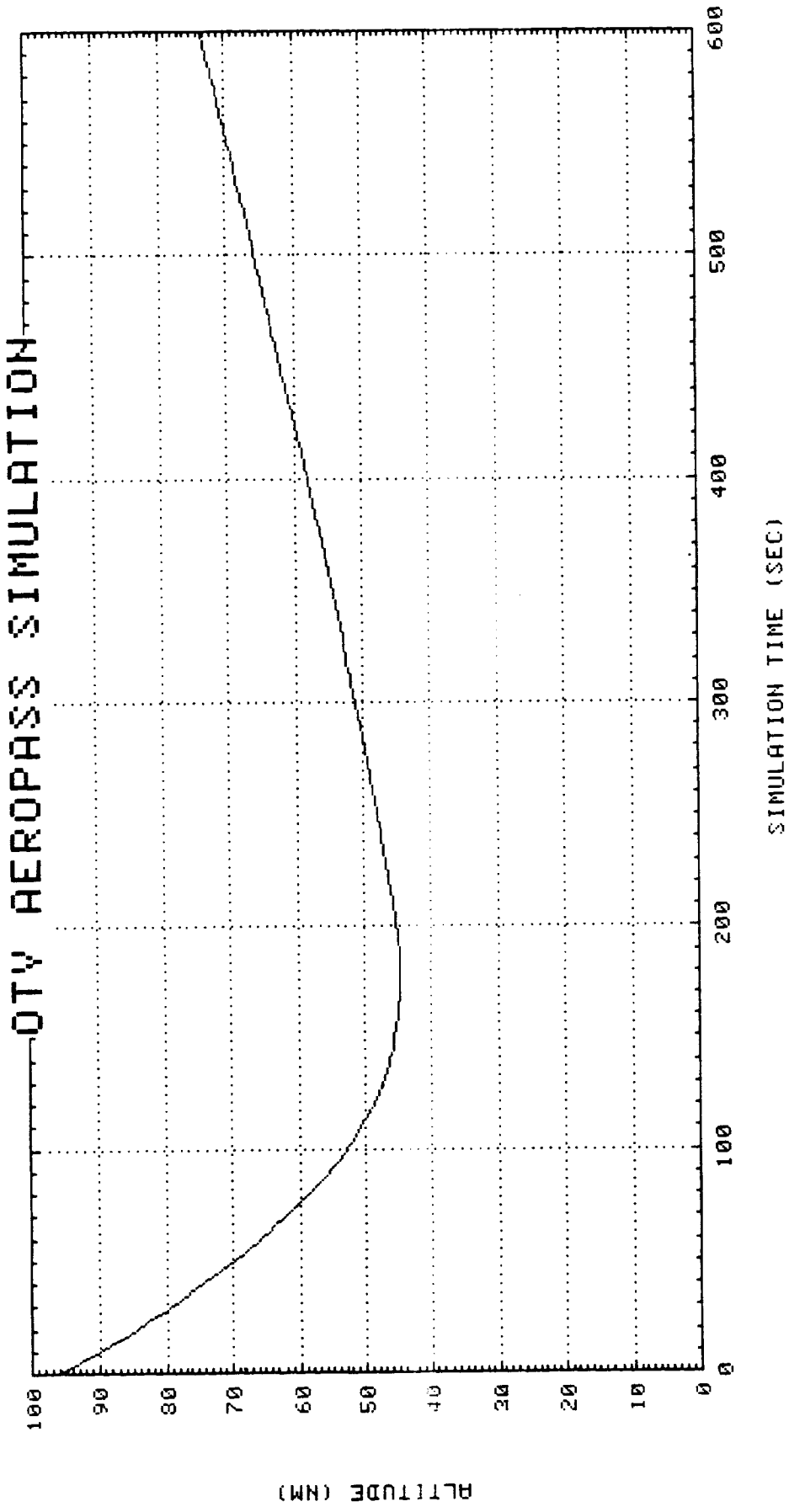
EXIT INCLINATION ERROR = .0024°

THIS PAGE INTENTIONALLY LEFT BLANK

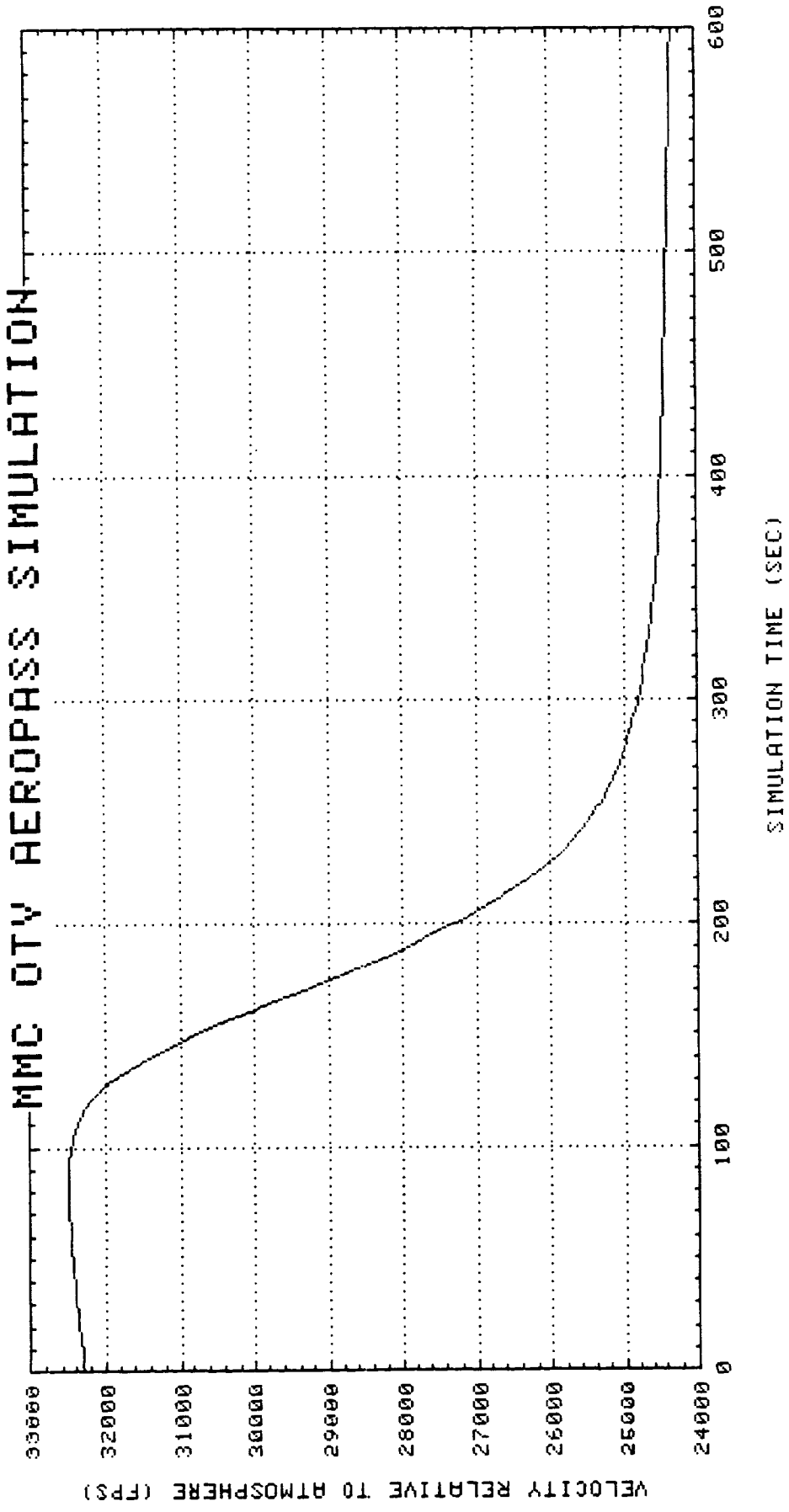


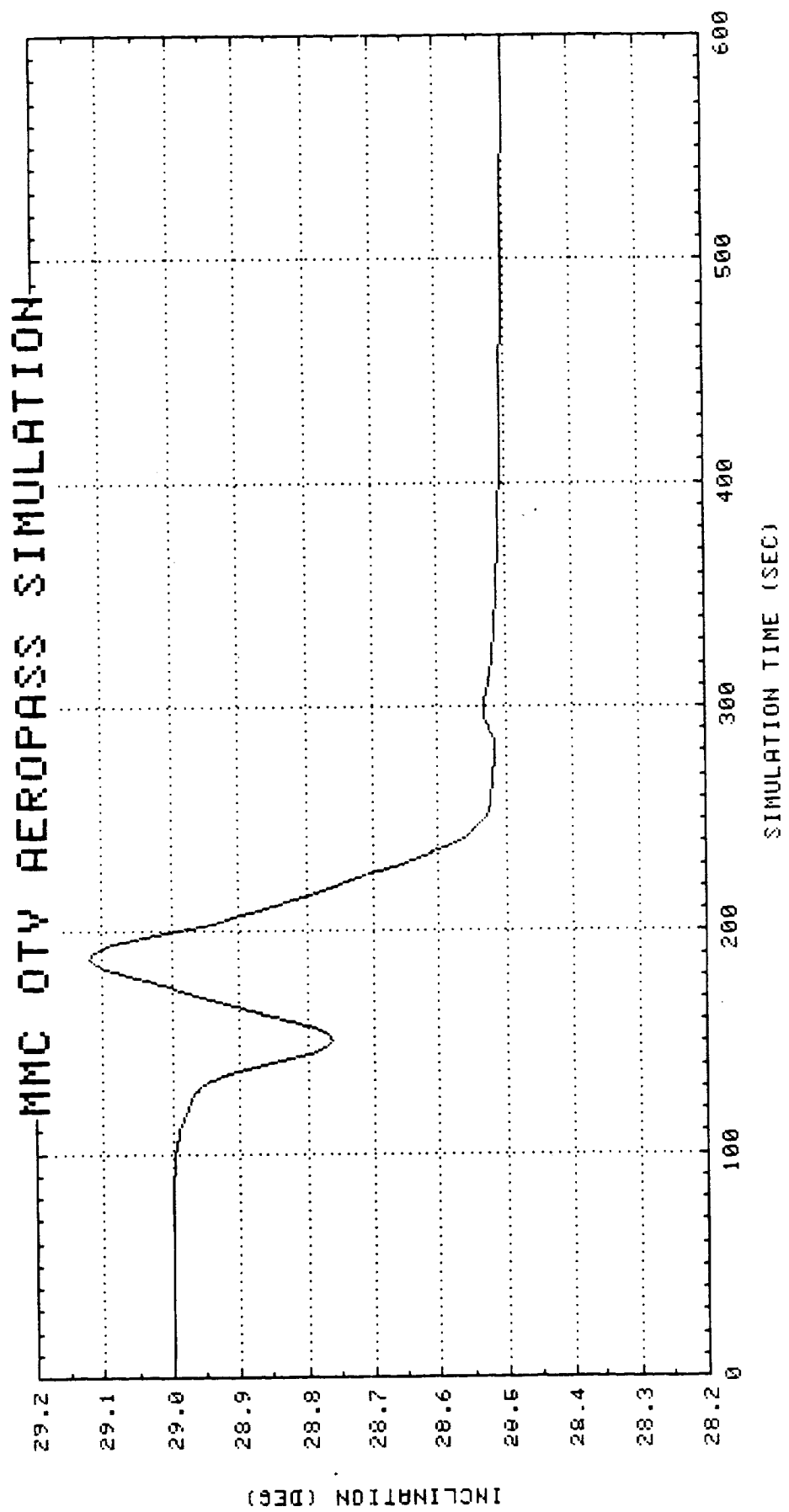
PRECEDING PAGE BLANK NOT FILMED

QTY AEROPASS SIMULATION

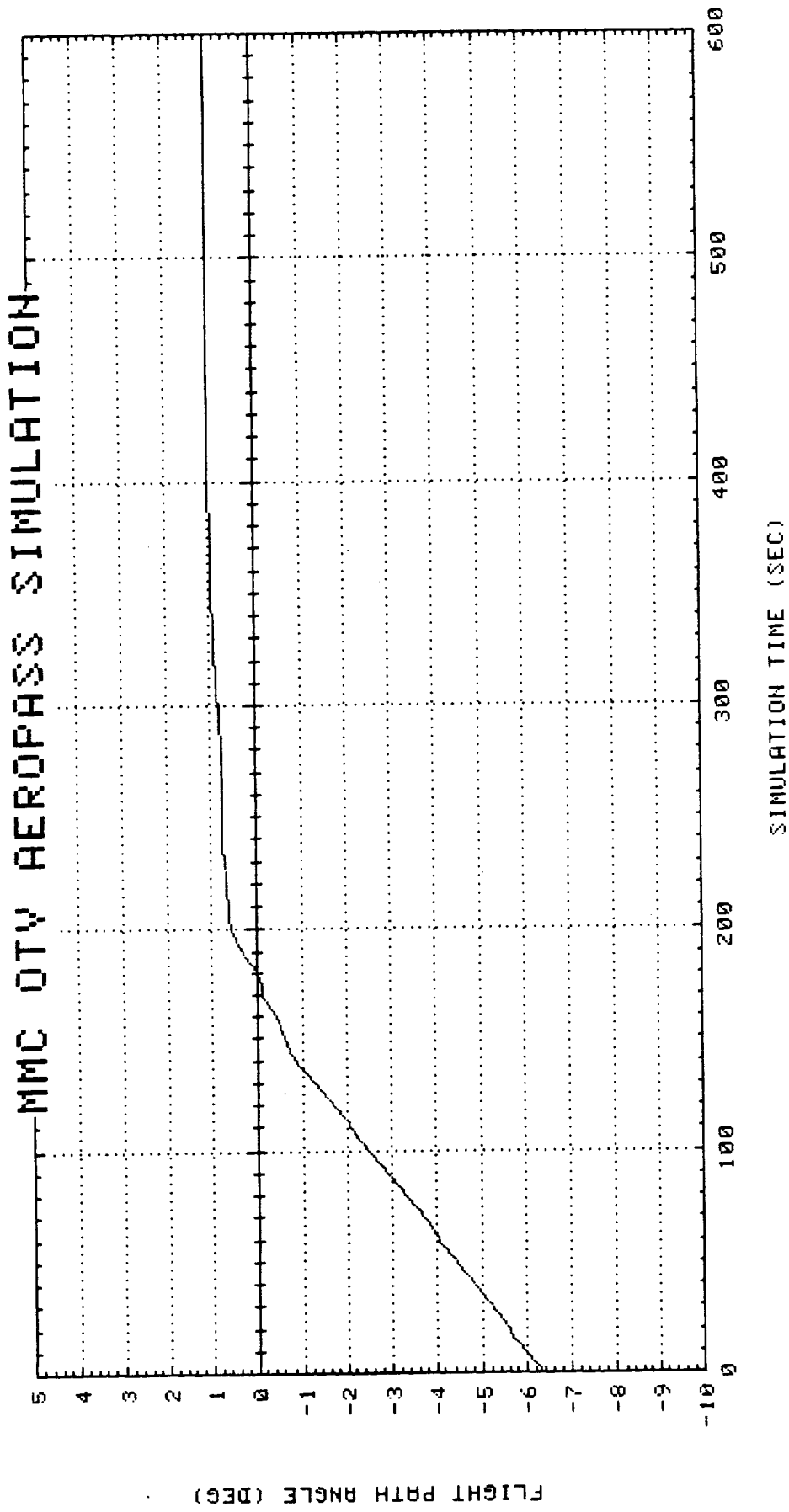


MMC OTY AEROPASS SIMULATION

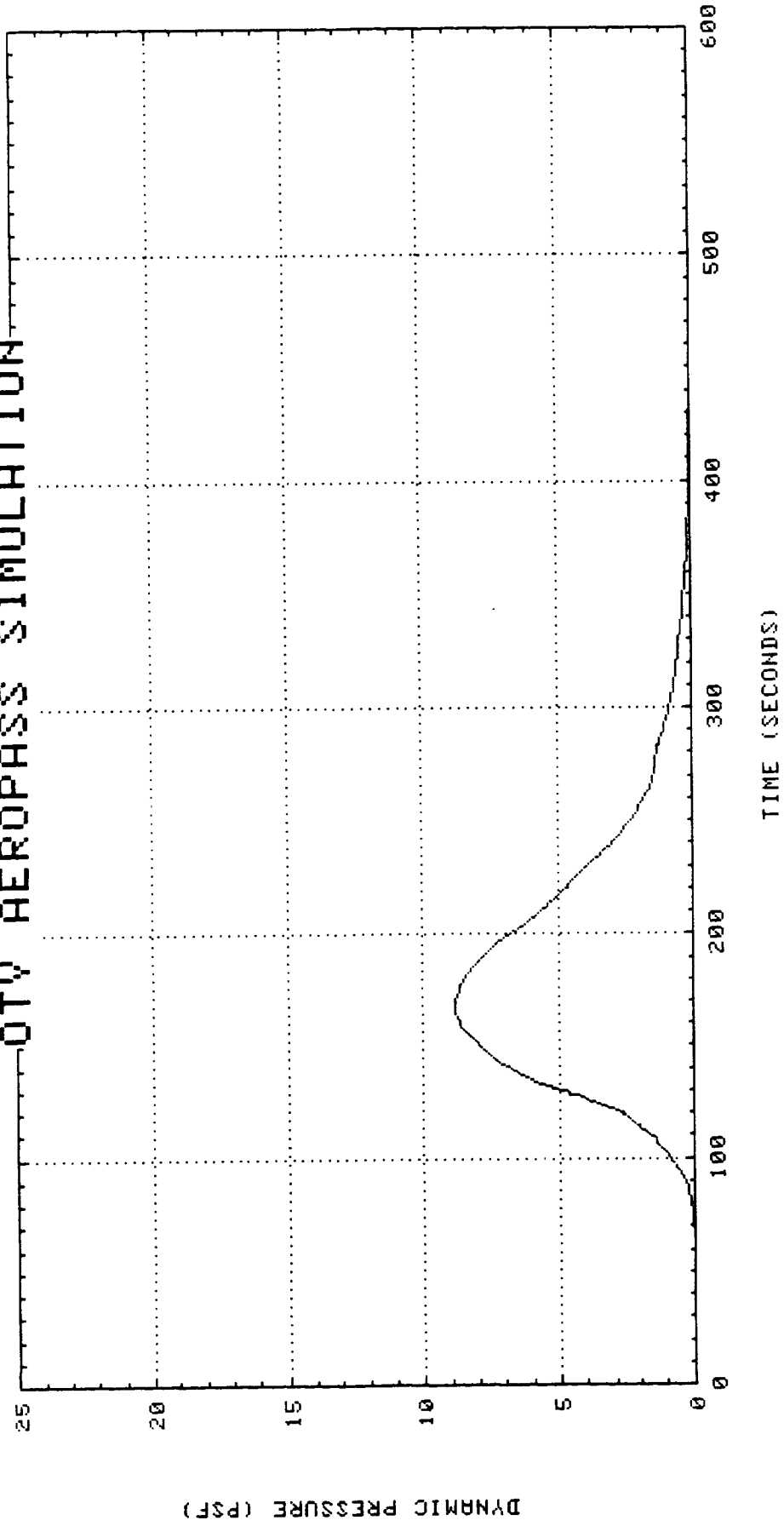




MMC OTV AEROPASS SIMULATION

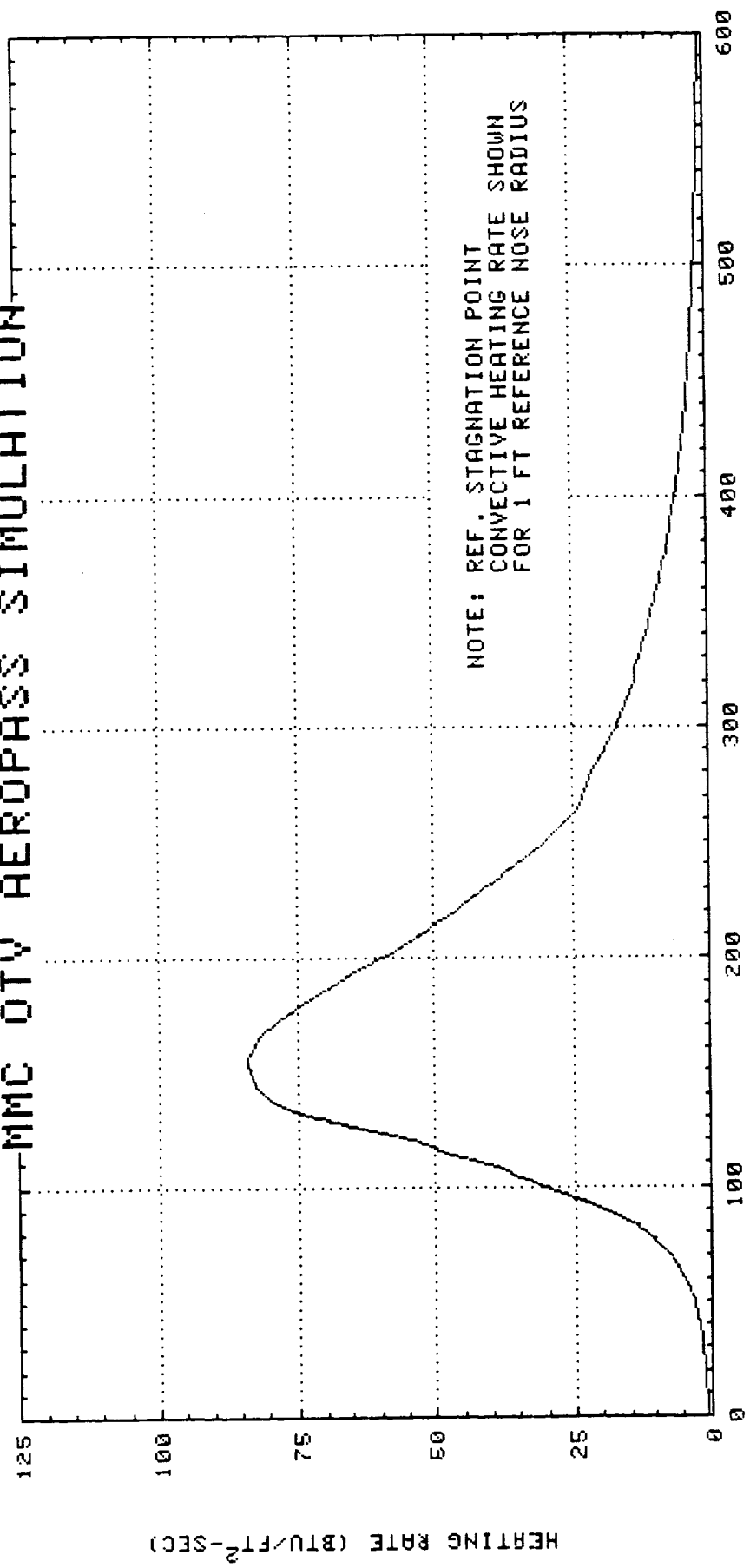


DTY AEROPASS SIMULATION



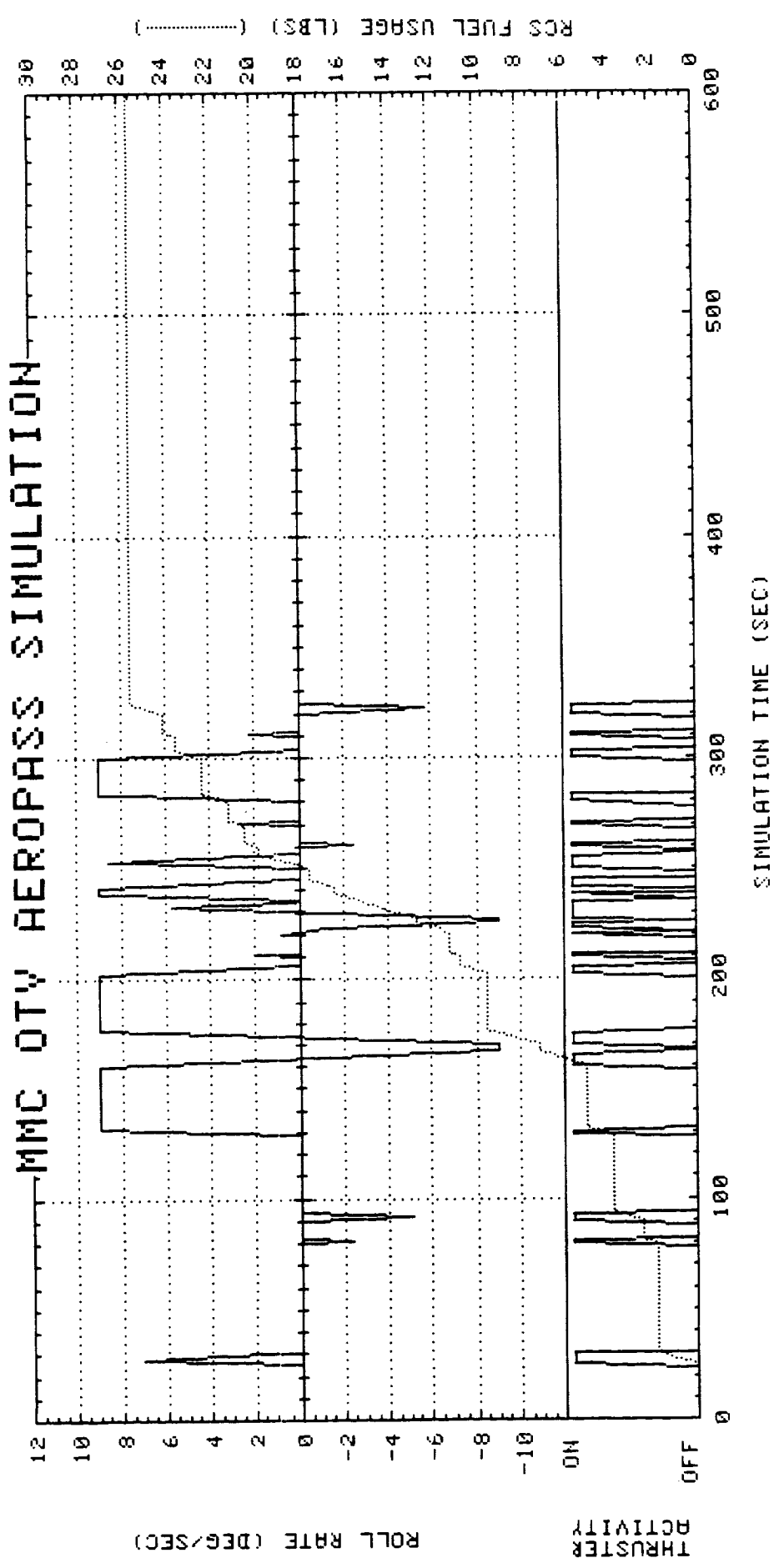
NOTE: DYNAMIC PRESSURE IS
FREE-STREAM VALUE

MMC OTV AEROPASS SIMULATION

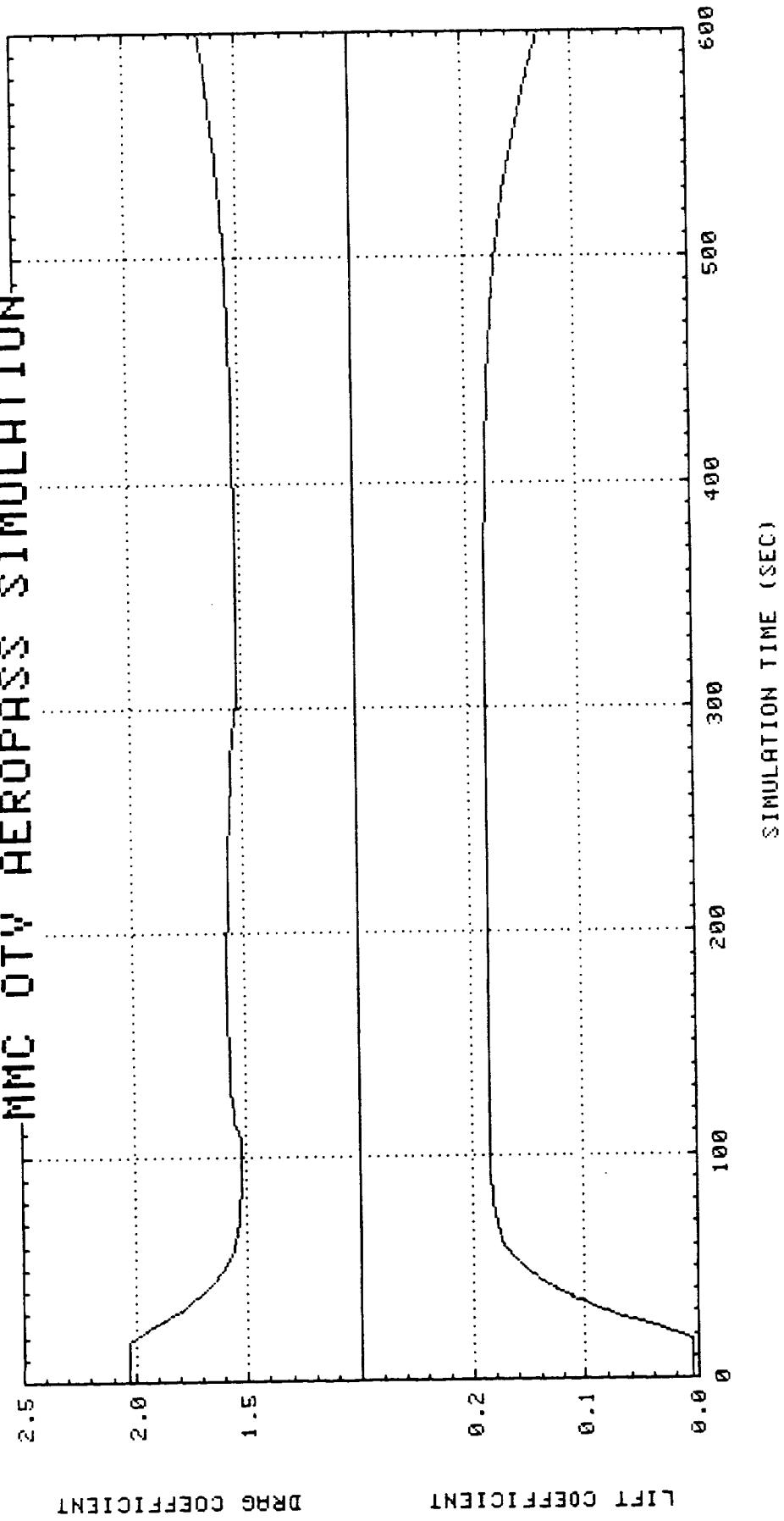


NOTE: REF. STAGNATION POINT
CONVECTIVE HEATING RATE SHOWN
FOR 1 FT REFERENCE NOSE RADIUS

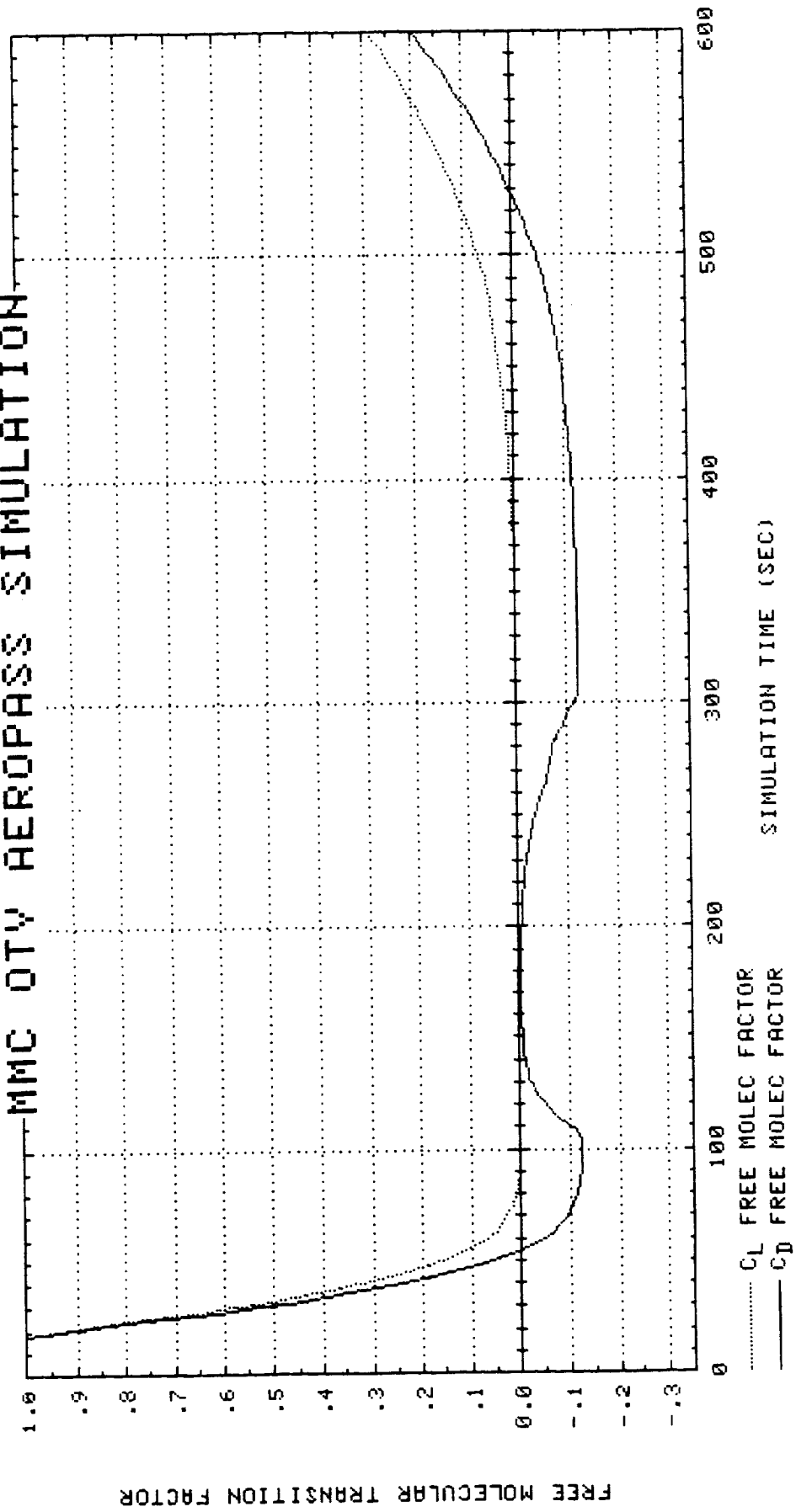
MMC DTW AEROPASS SIMULATION



MMC OTW AEROPASS SIMULATION



MMC OTY AEROPASS SIMULATION



APPENDIX D

OTV AEROPASS SIMULATION

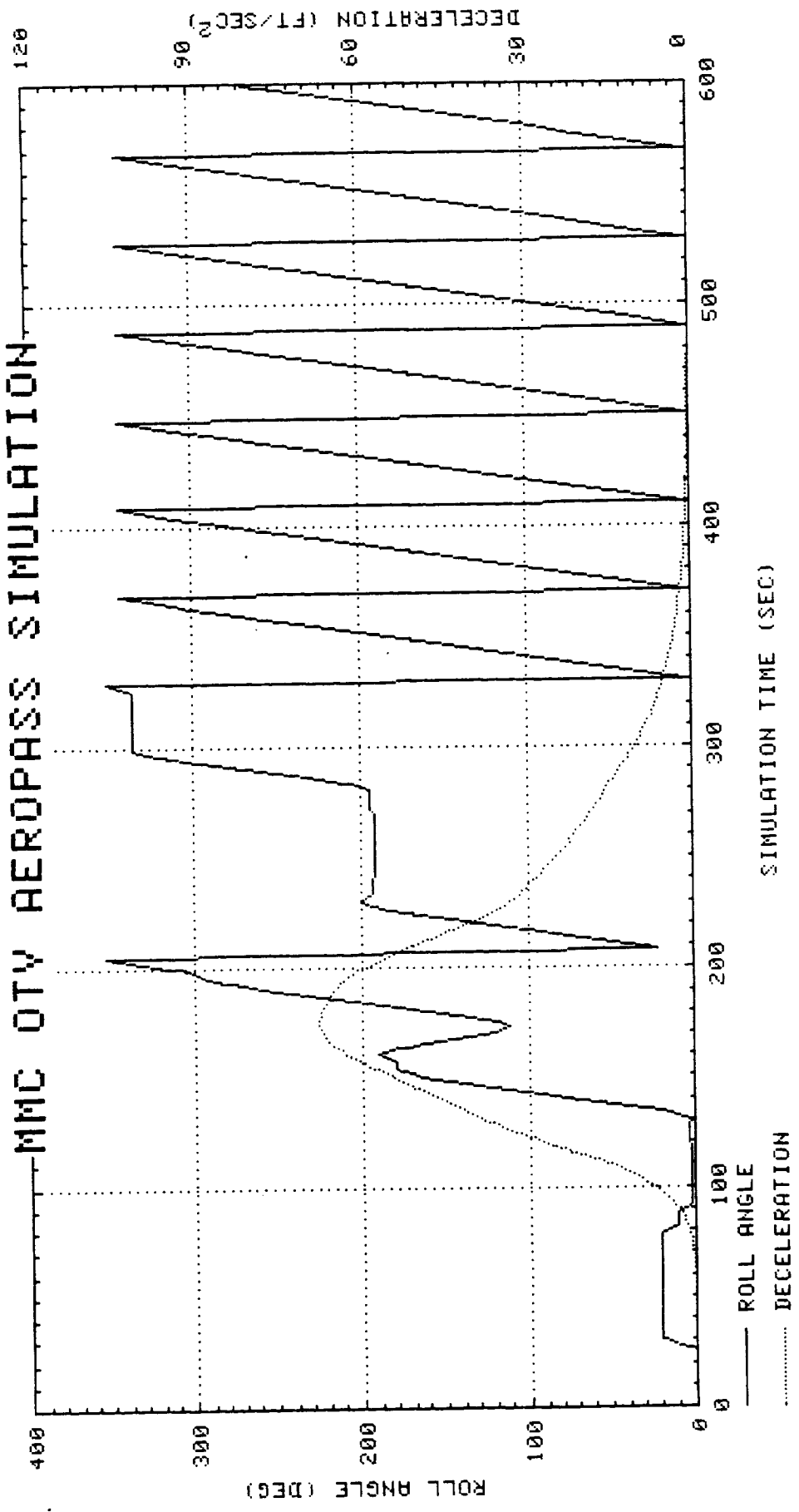
STS-6 ATMOSPHERE

EXIT APOGEE ERROR = 0.01 NM

EXIT INCLINATION ERROR = .0181°

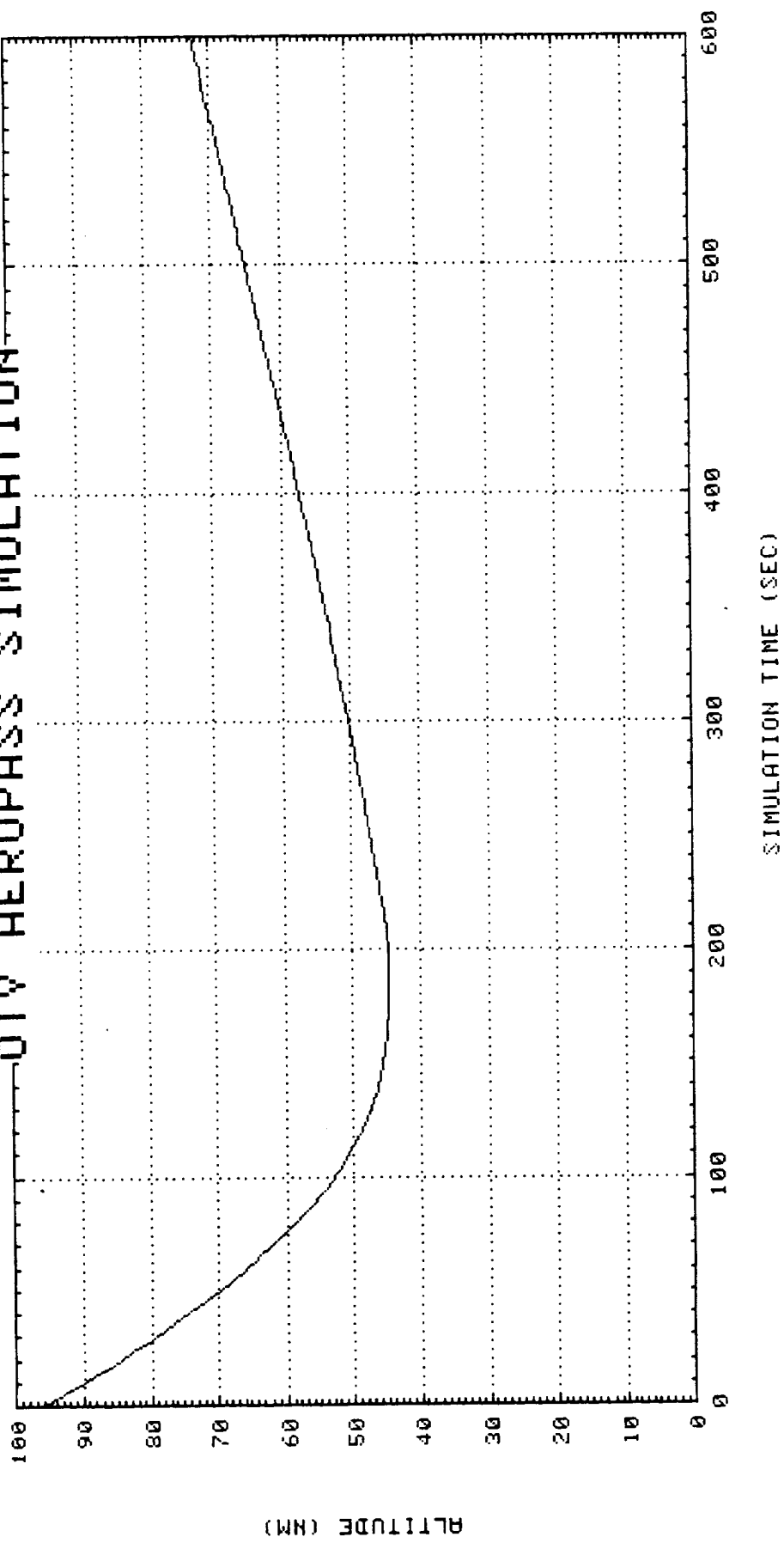
THIS PAGE INTENTIONALLY LEFT BLANK

MMC OTV AEROPASS SIMULATION

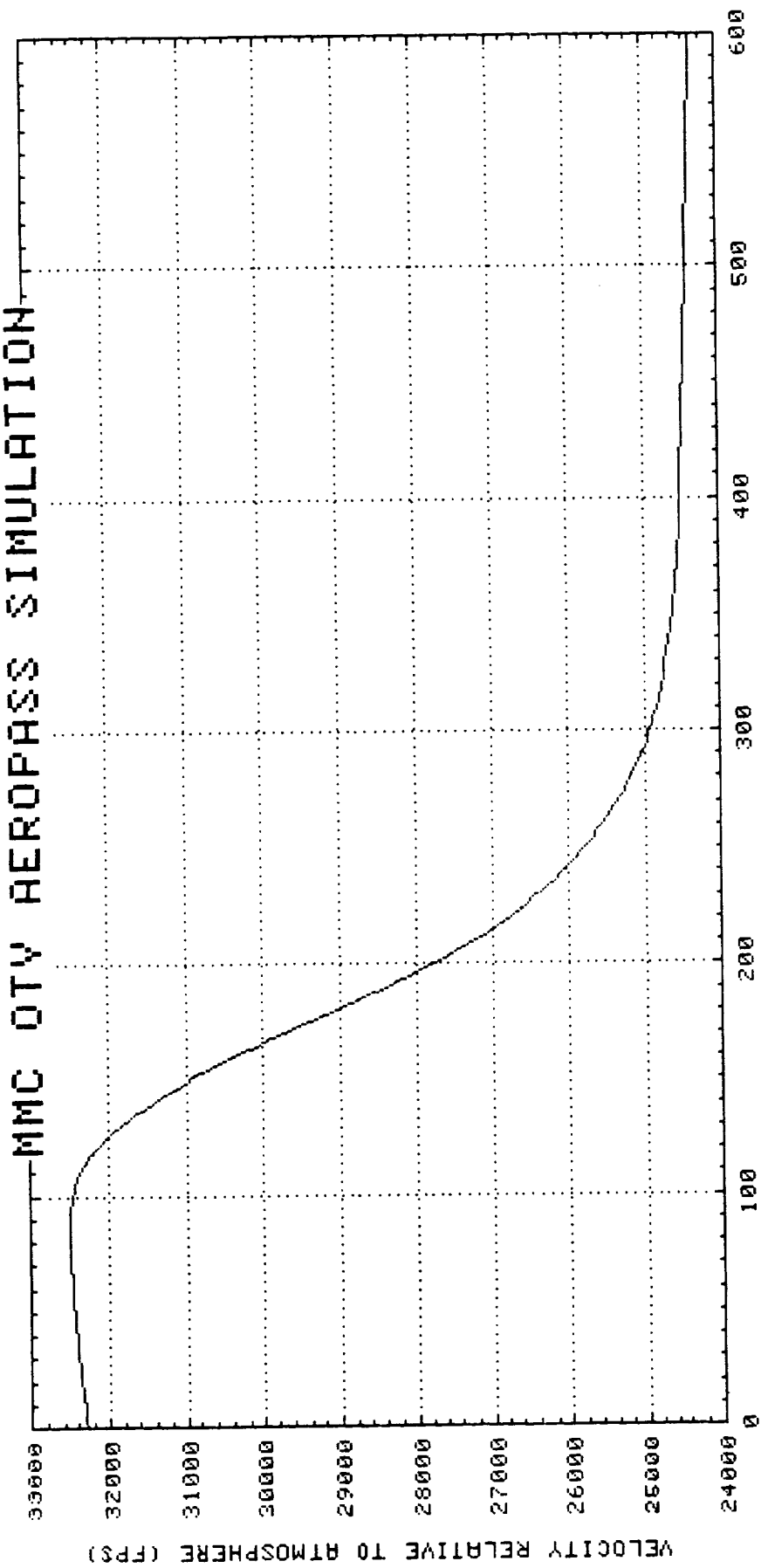


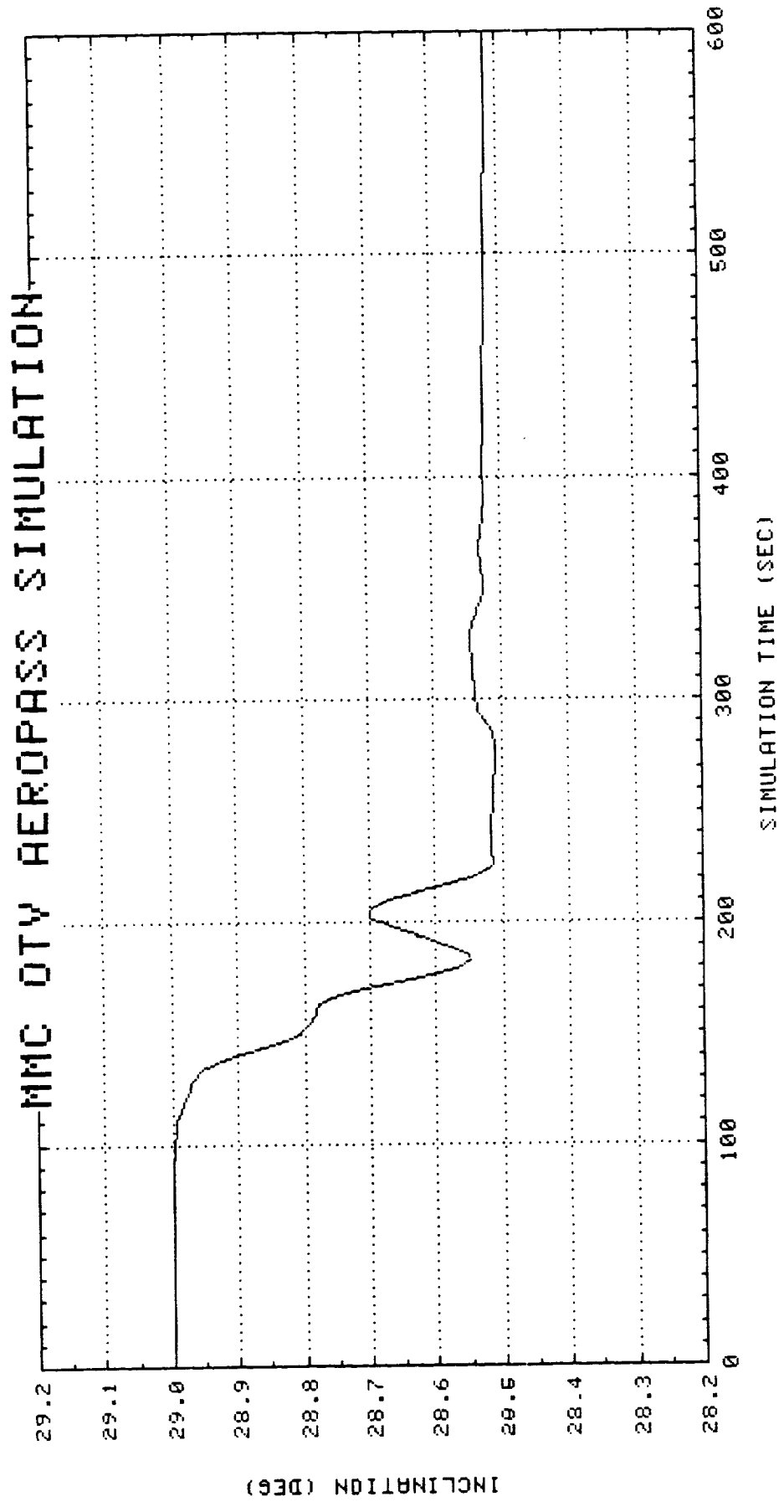
PRECEDING PAGE BLANK NOT FILMED

DTV AEROPASS SIMULATION

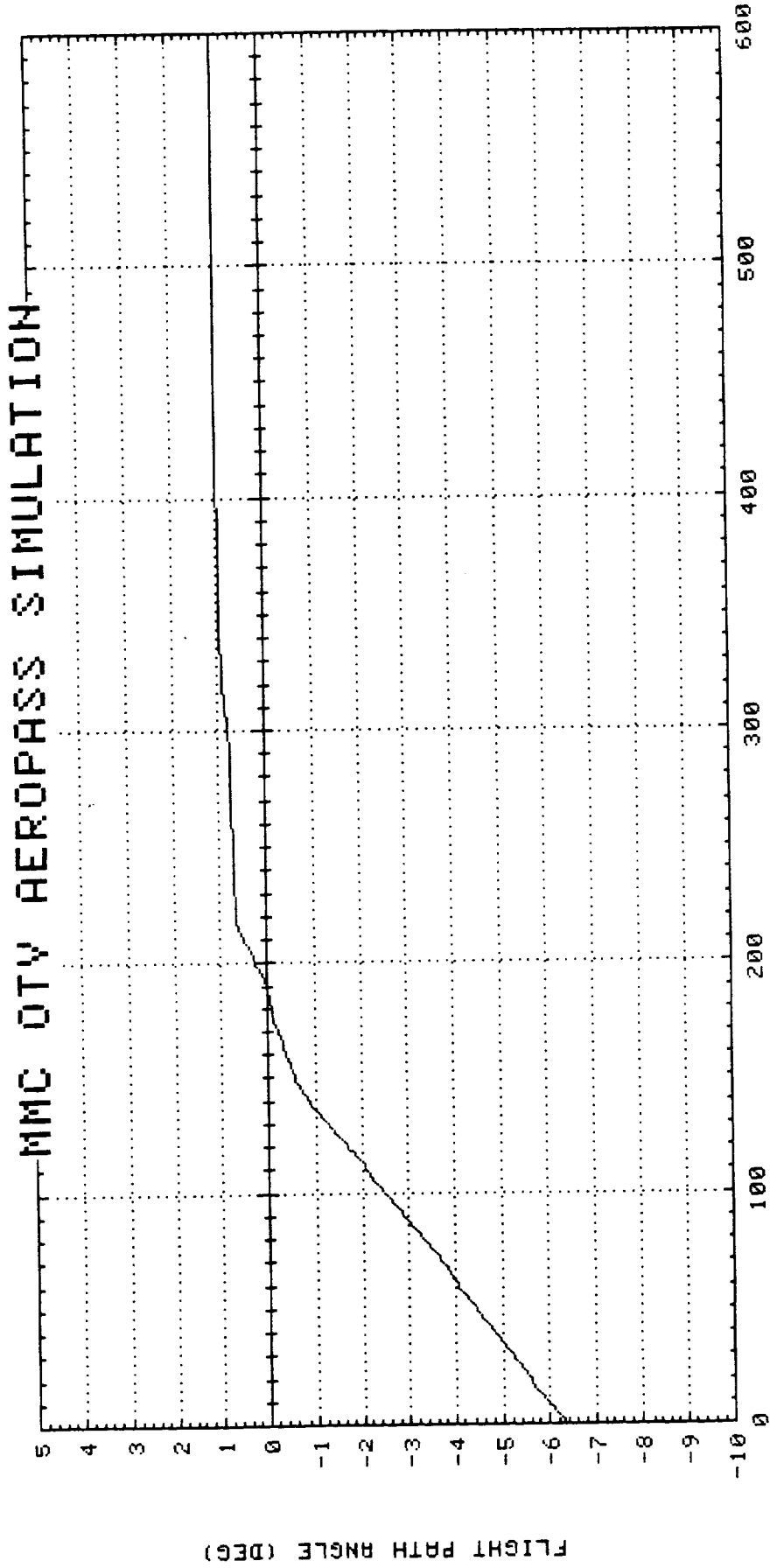


MMC OTV AEROPASS SIMULATION

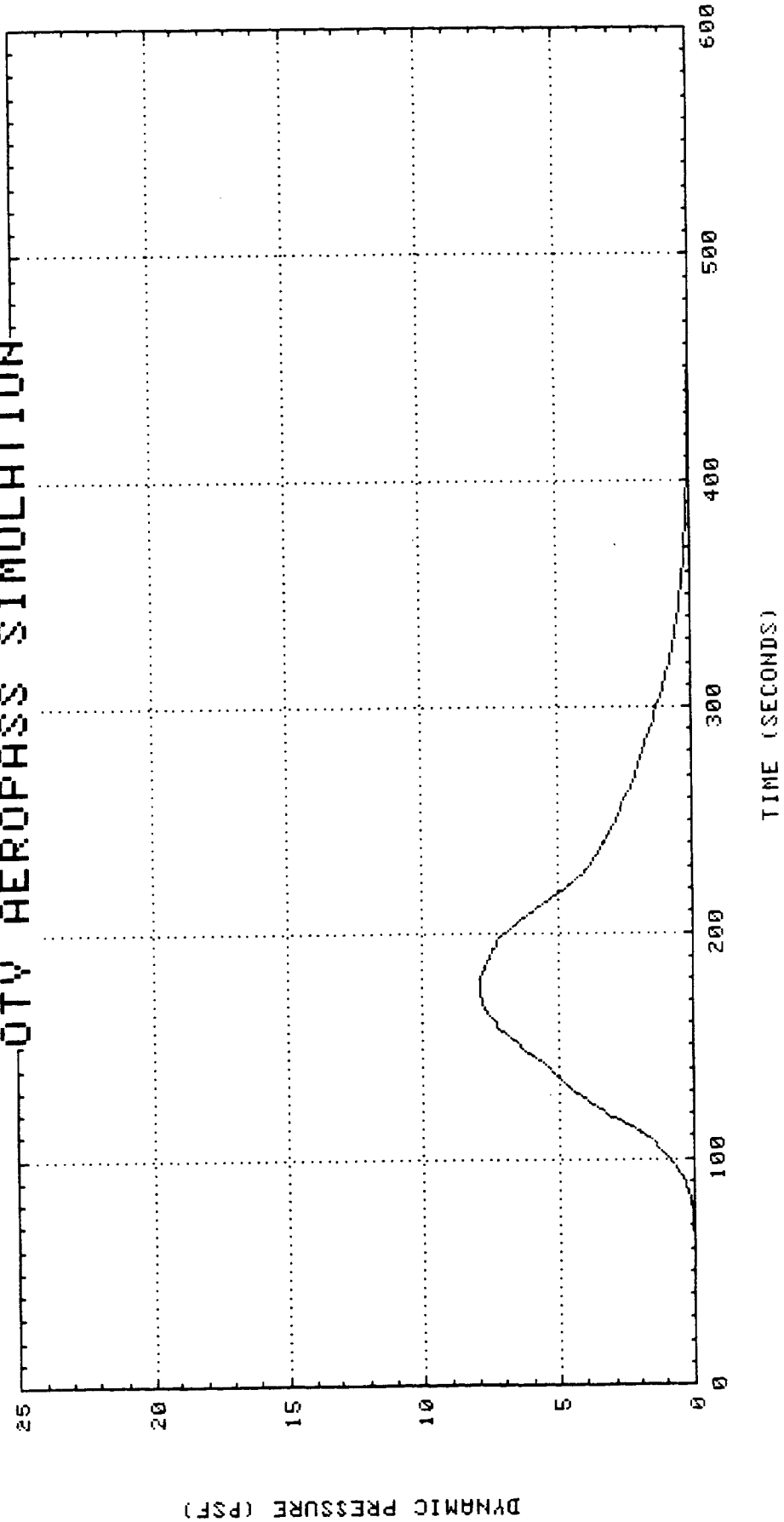




MMC DTW AEROPASS SIMULATION

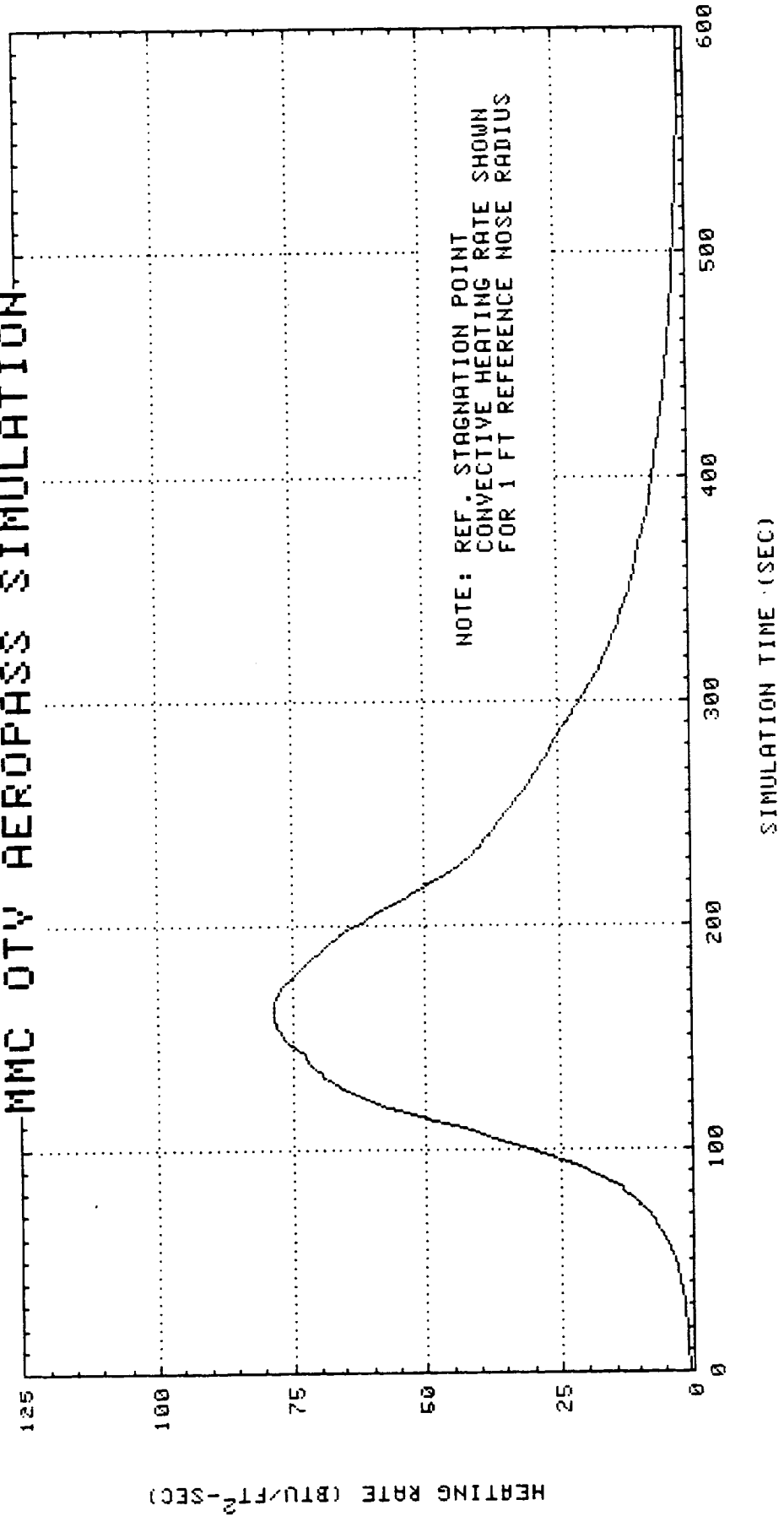


QTY AEROPASS SIMULATION

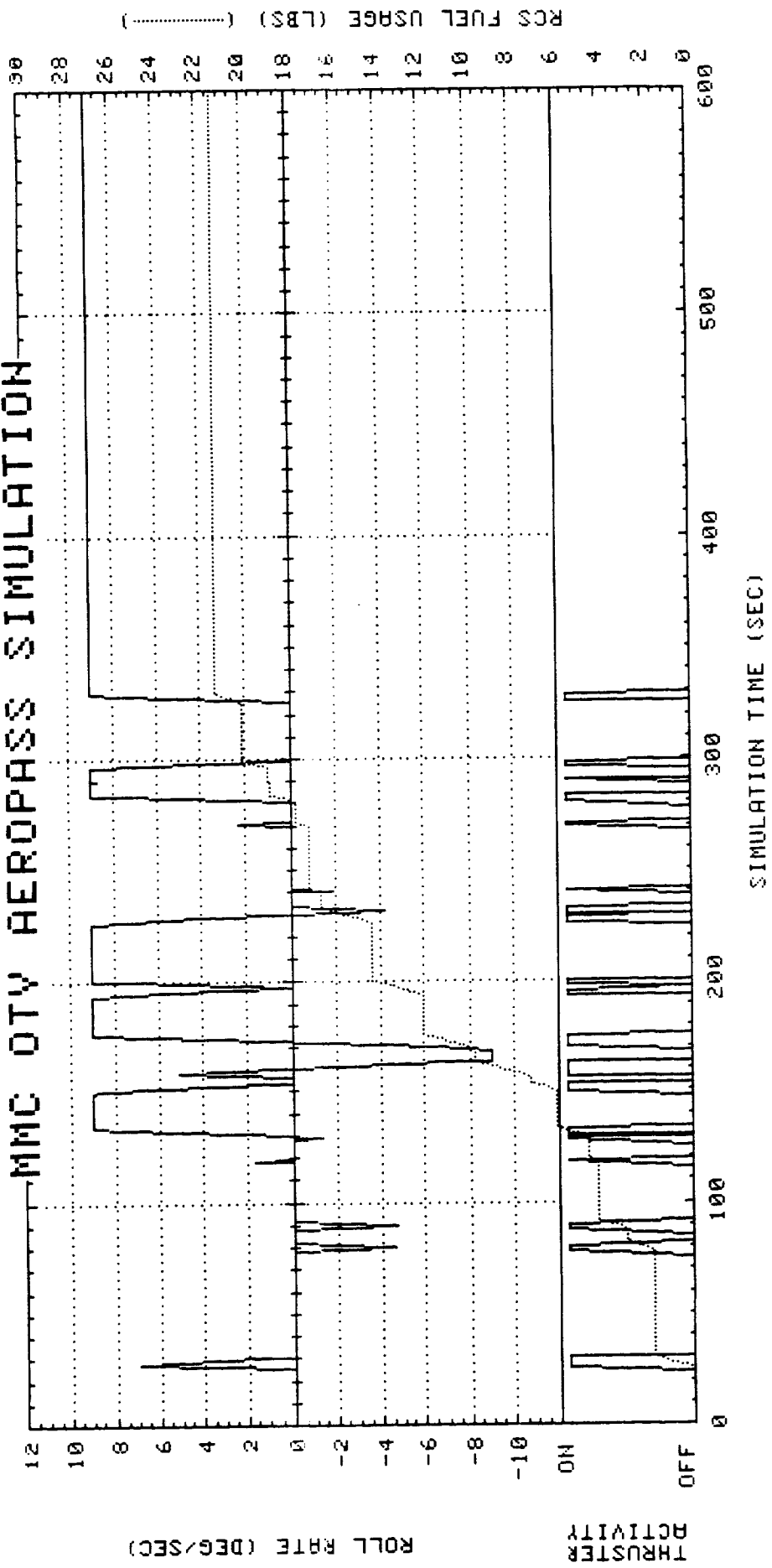


NOTE: DYNAMIC PRESSURE IS
FREE-STREAM VALUE

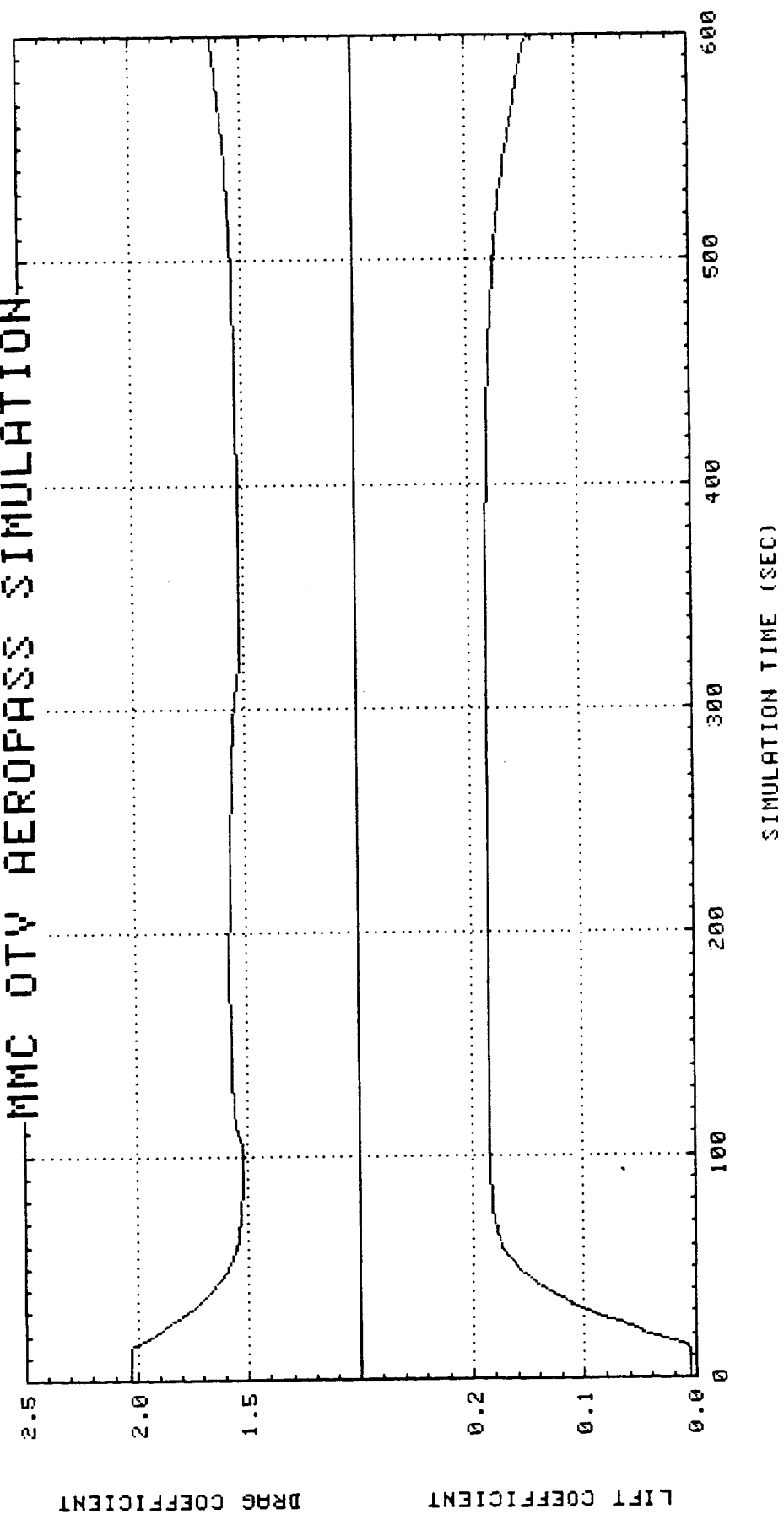
MMC QTY AEROPASS SIMULATION



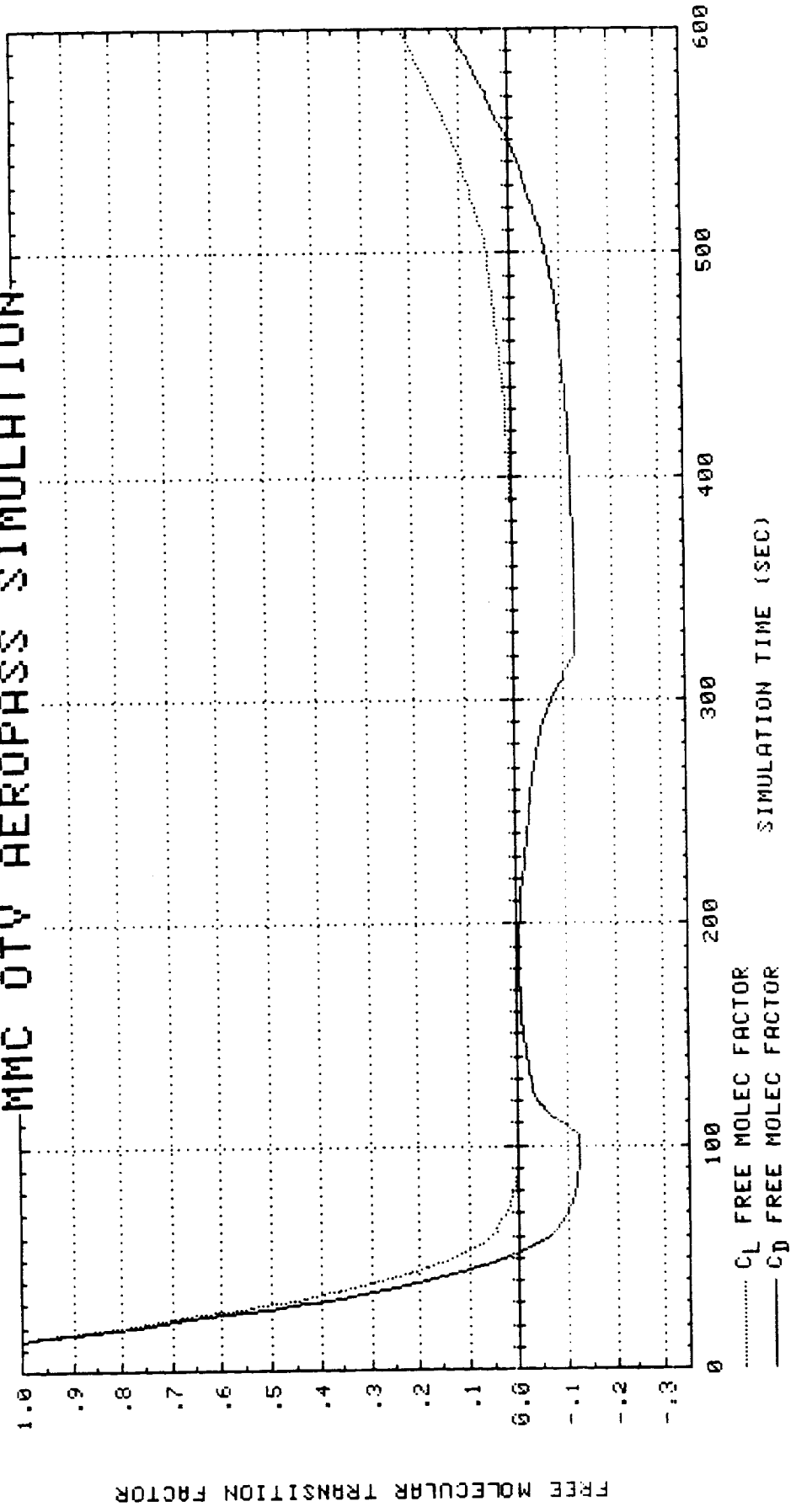
MMC OTY AEROPASS SIMULATION



MMC OTW AEROPASS SIMULATION



MMC OTV AEROPASS SIMULATION



APPENDIX E

OTV AEROPASS SIMULATION

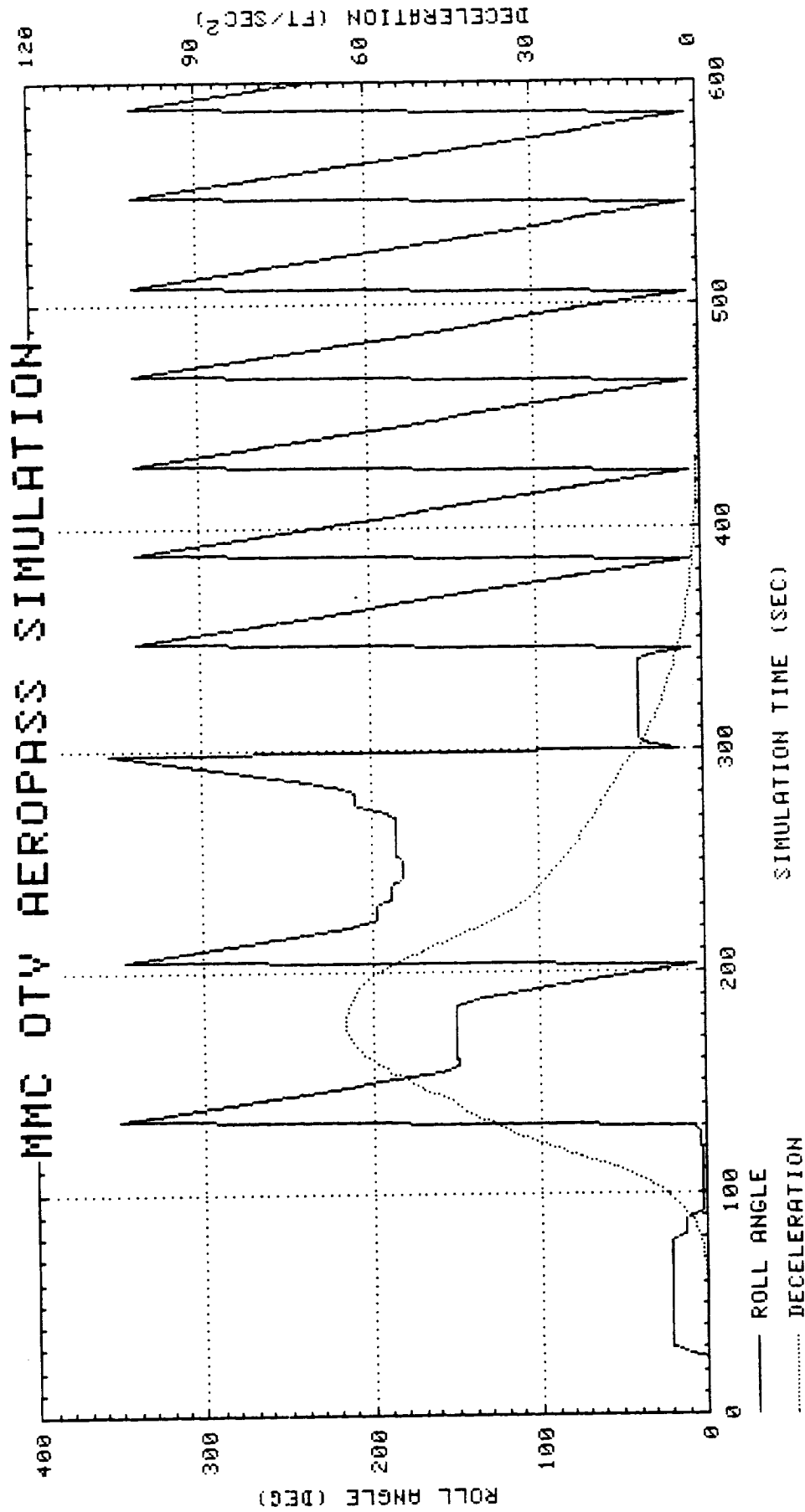
STS-6 ATMOSPHERE

ANGLE OF ATTACK ERROR = $+1^{\circ}$

EXIT APOGEE ERROR = 0.14 NM

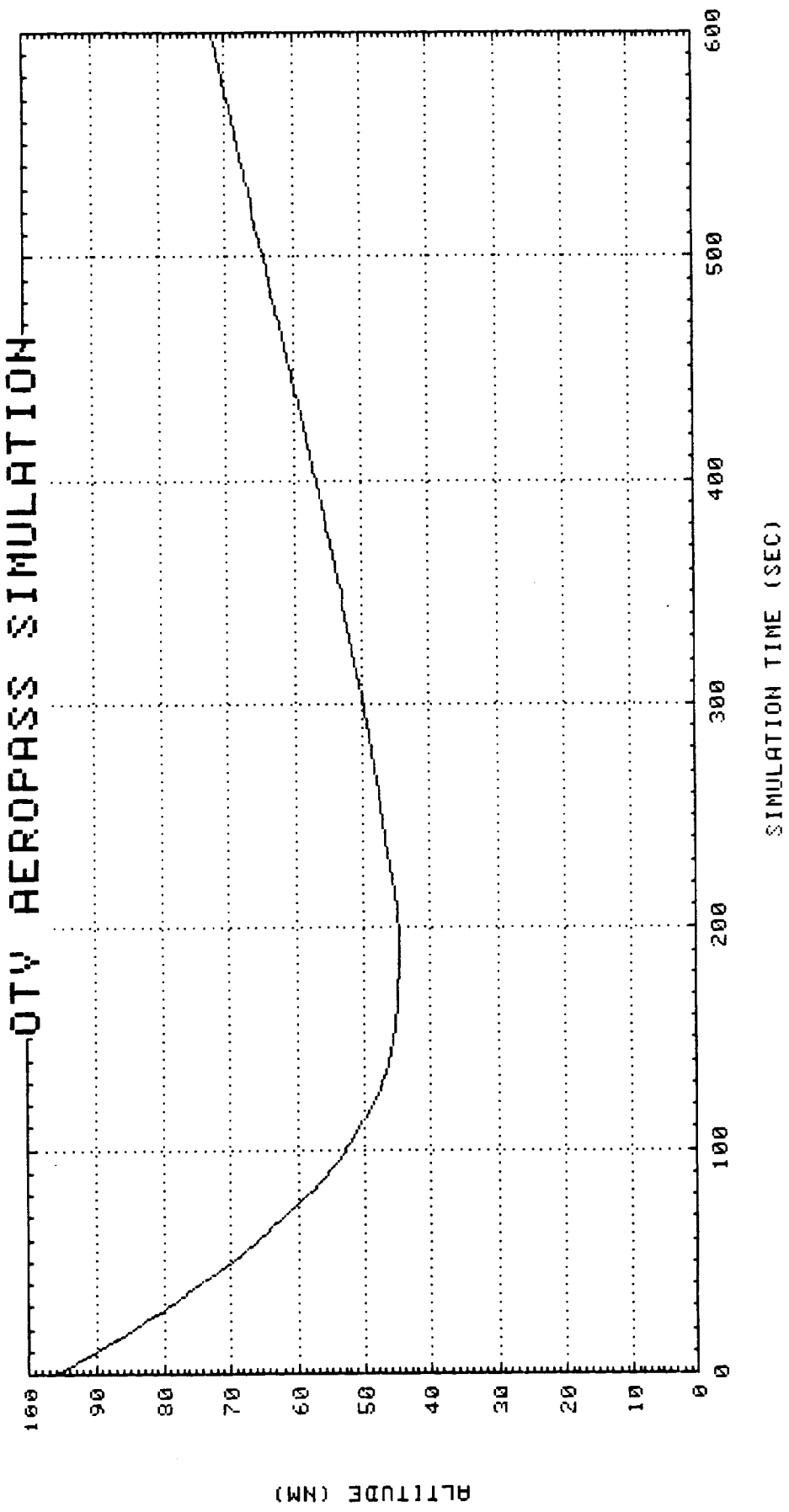
EXIT INCLINATION ERROR = $.0013^{\circ}$

THIS PAGE INTENTIONALLY LEFT BLANK

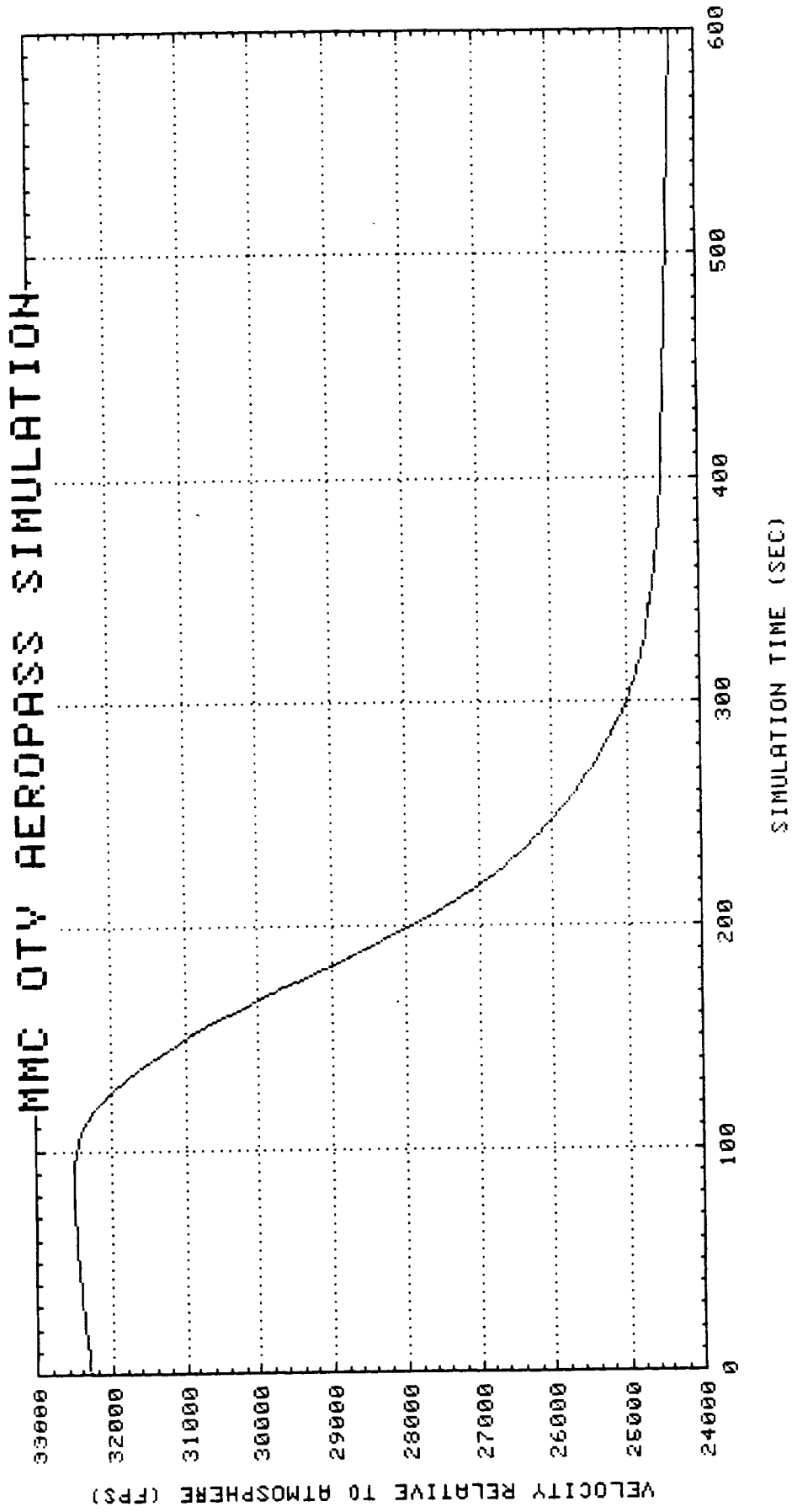


PRECEDING PAGE BLANK NOT FILMED

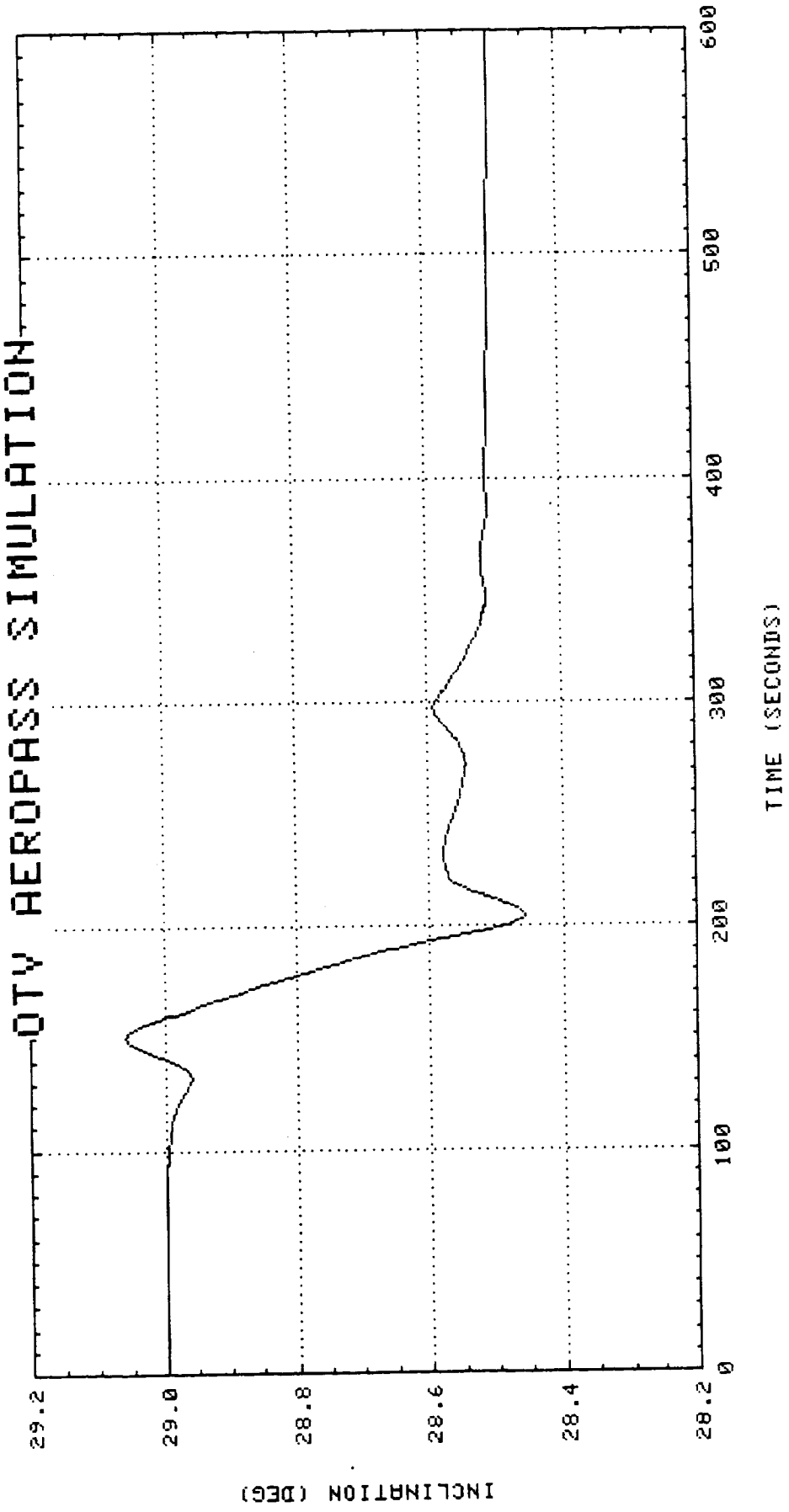
OTY AEROPASS SIMULATION

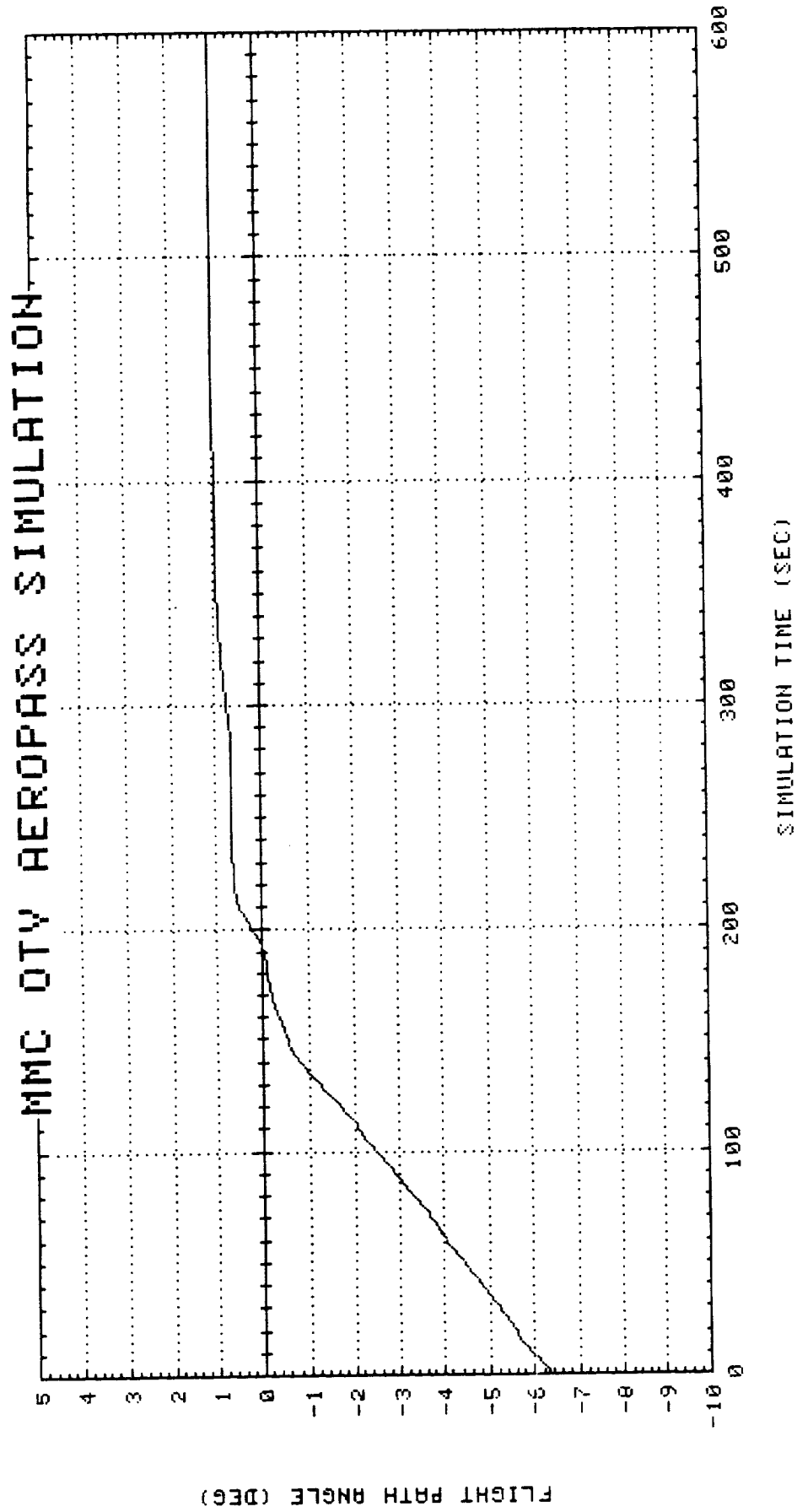


MMC OTV AEROPASS SIMULATION

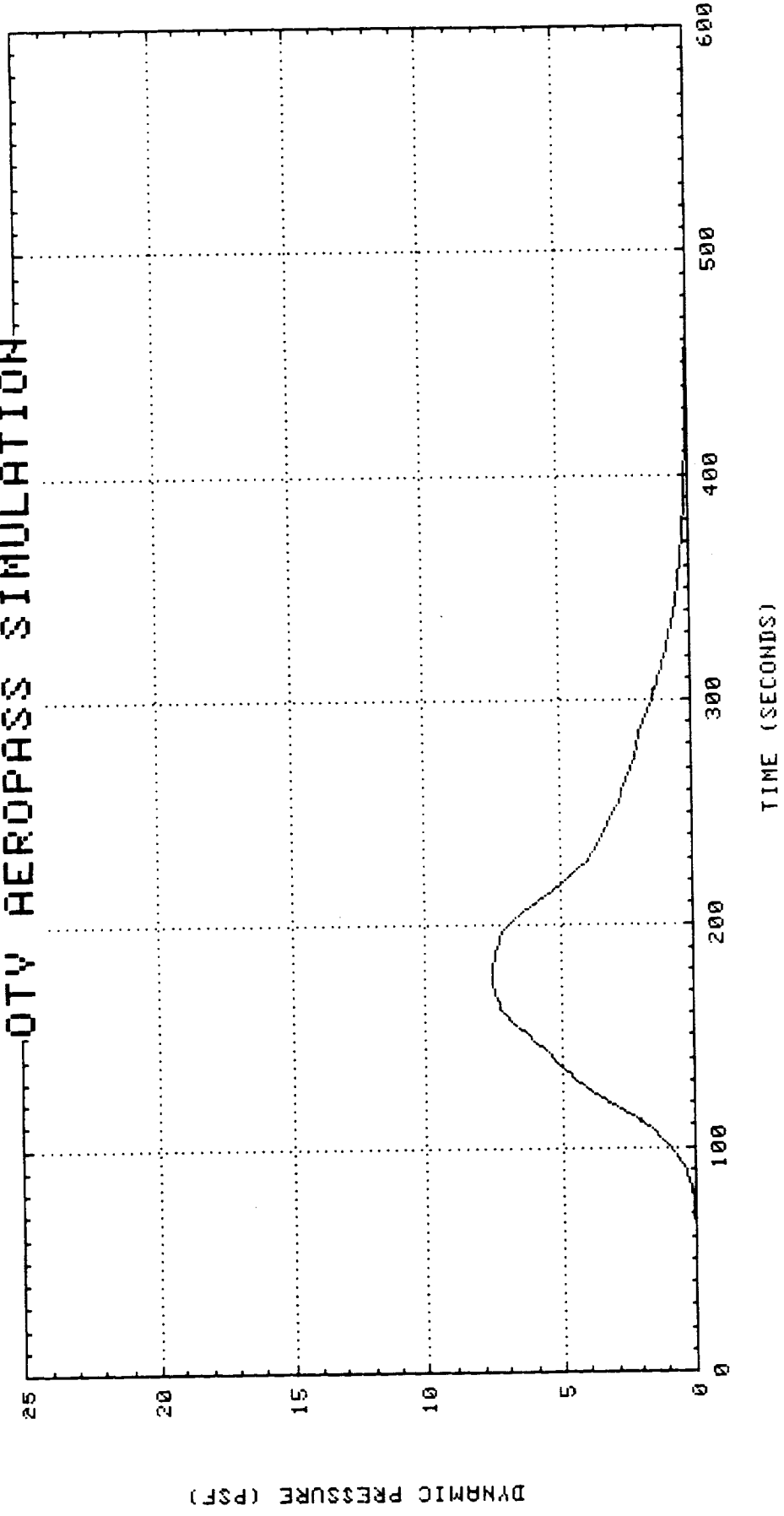


QTY AEROPASS SIMULATION



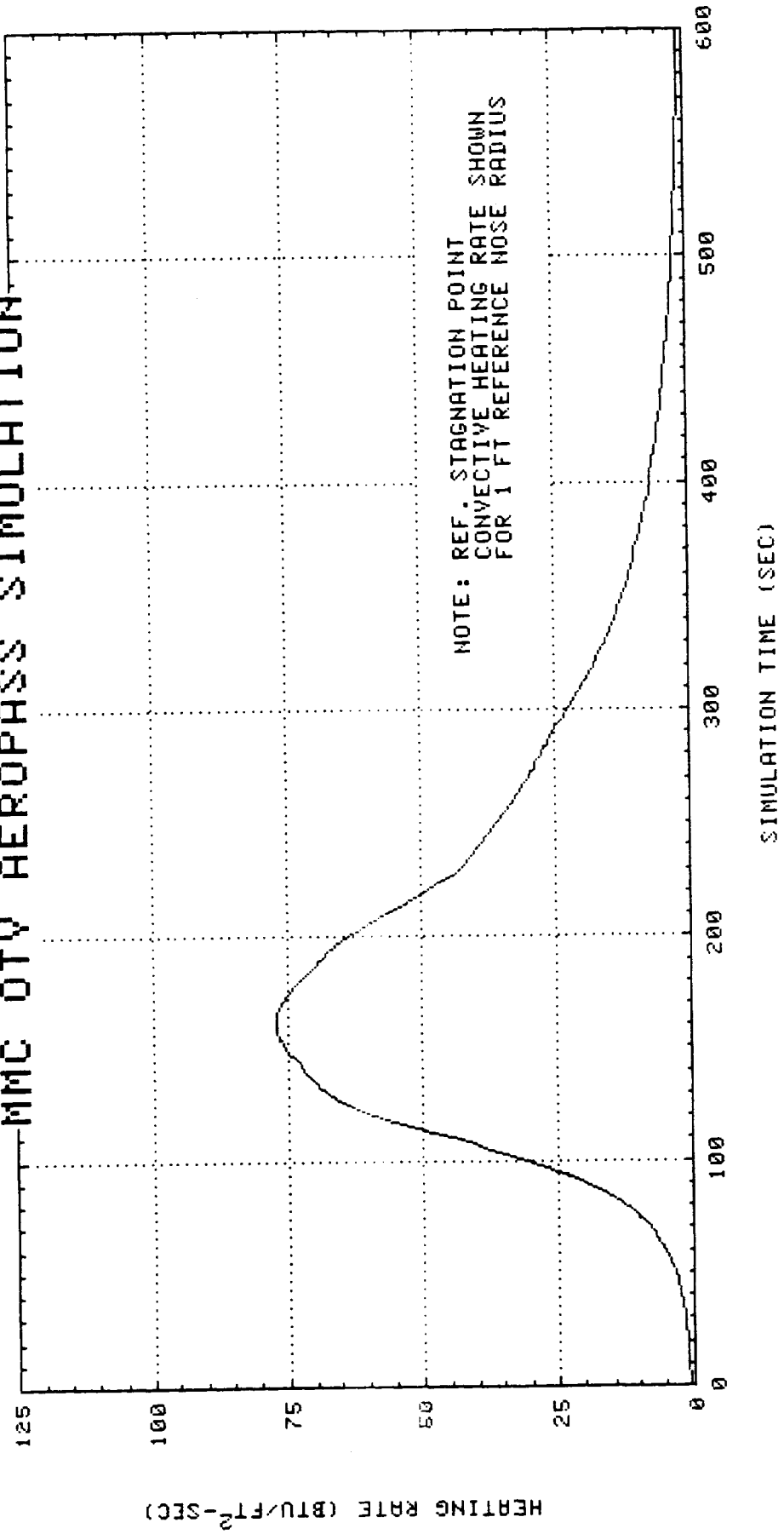


QTY AEROPASS SIMULATION

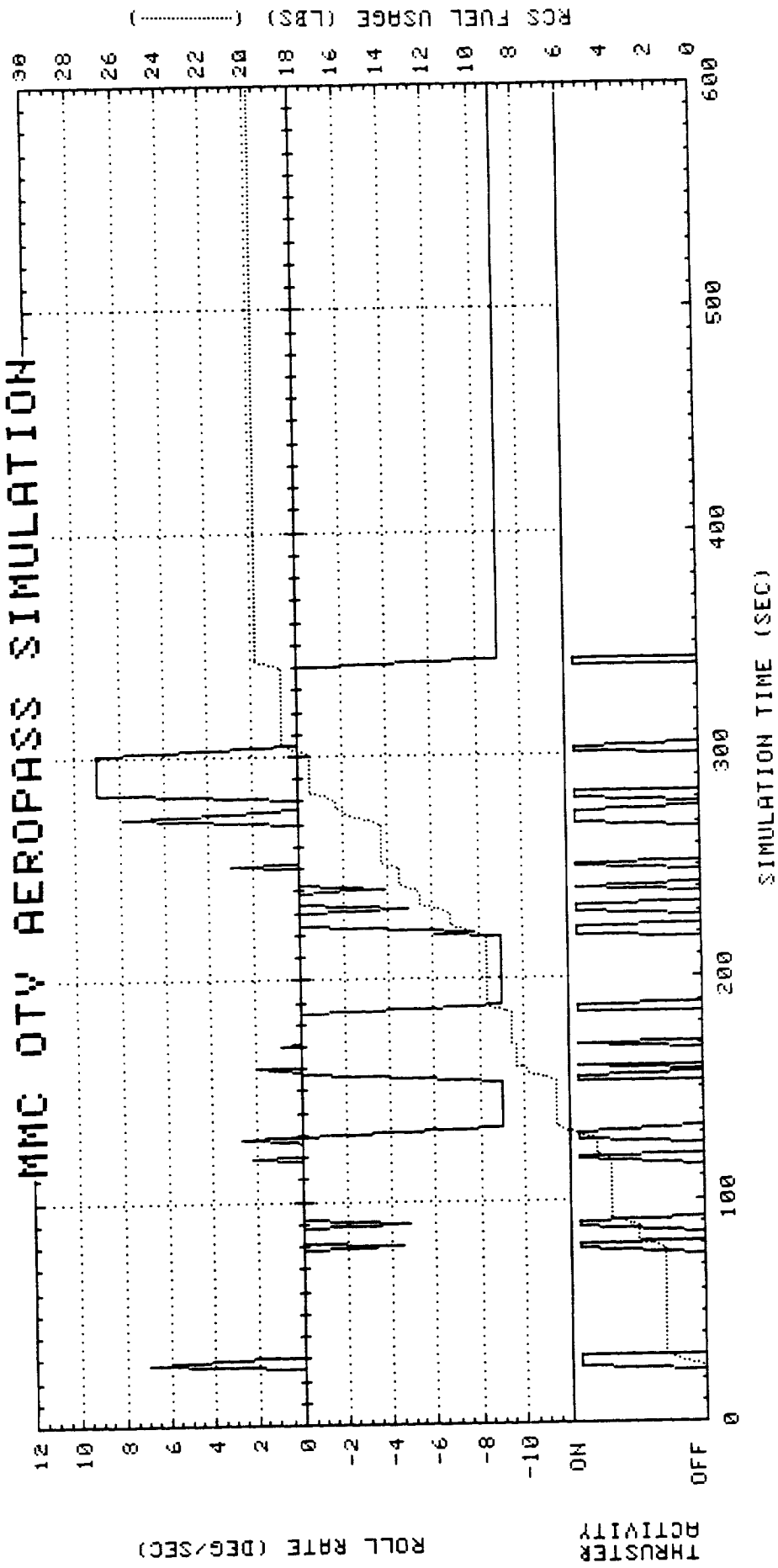


NOTE: DYNAMIC PRESSURE IS
FREE-STREAM VALUE

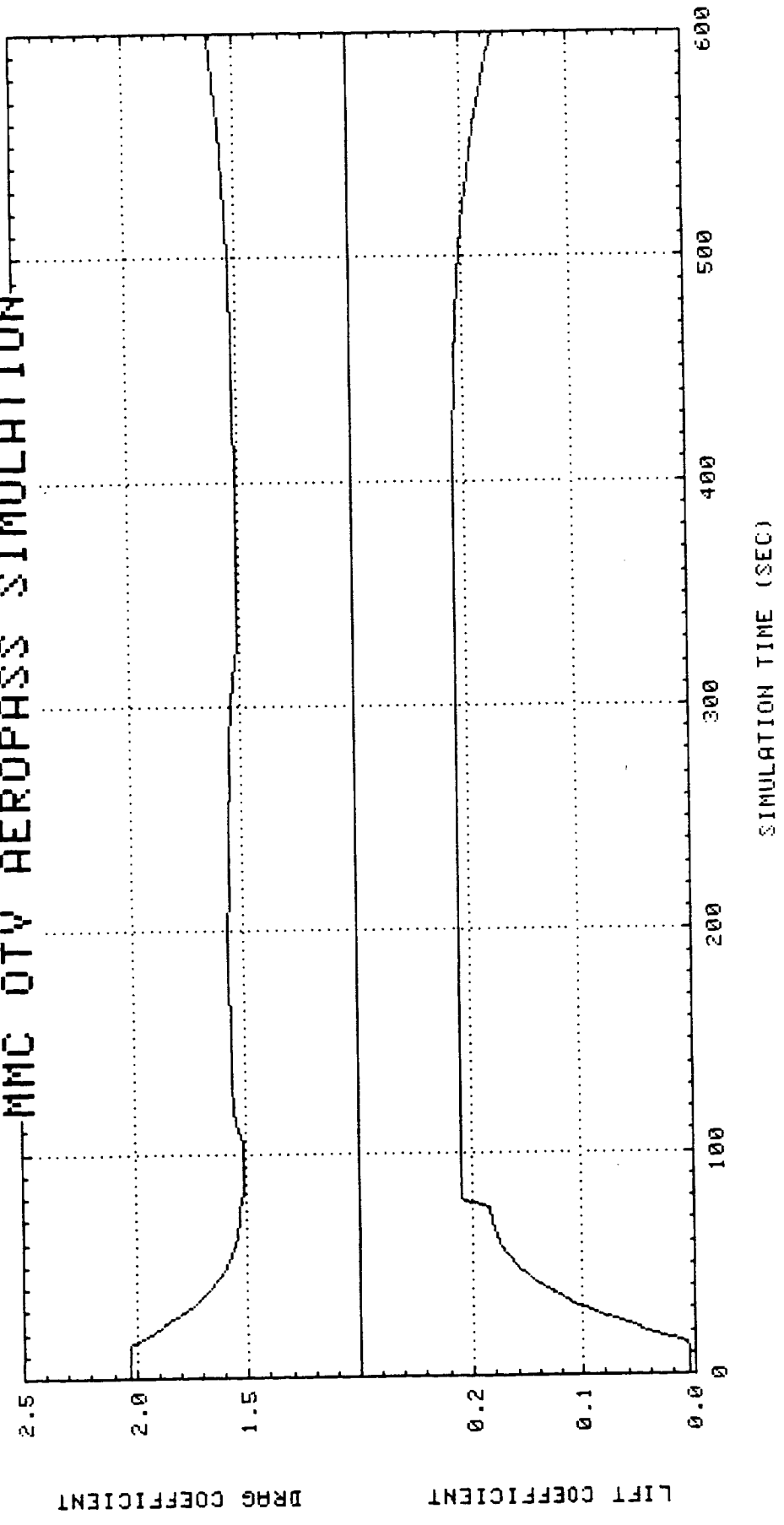
MMC QTY AEROPASS SIMULATION



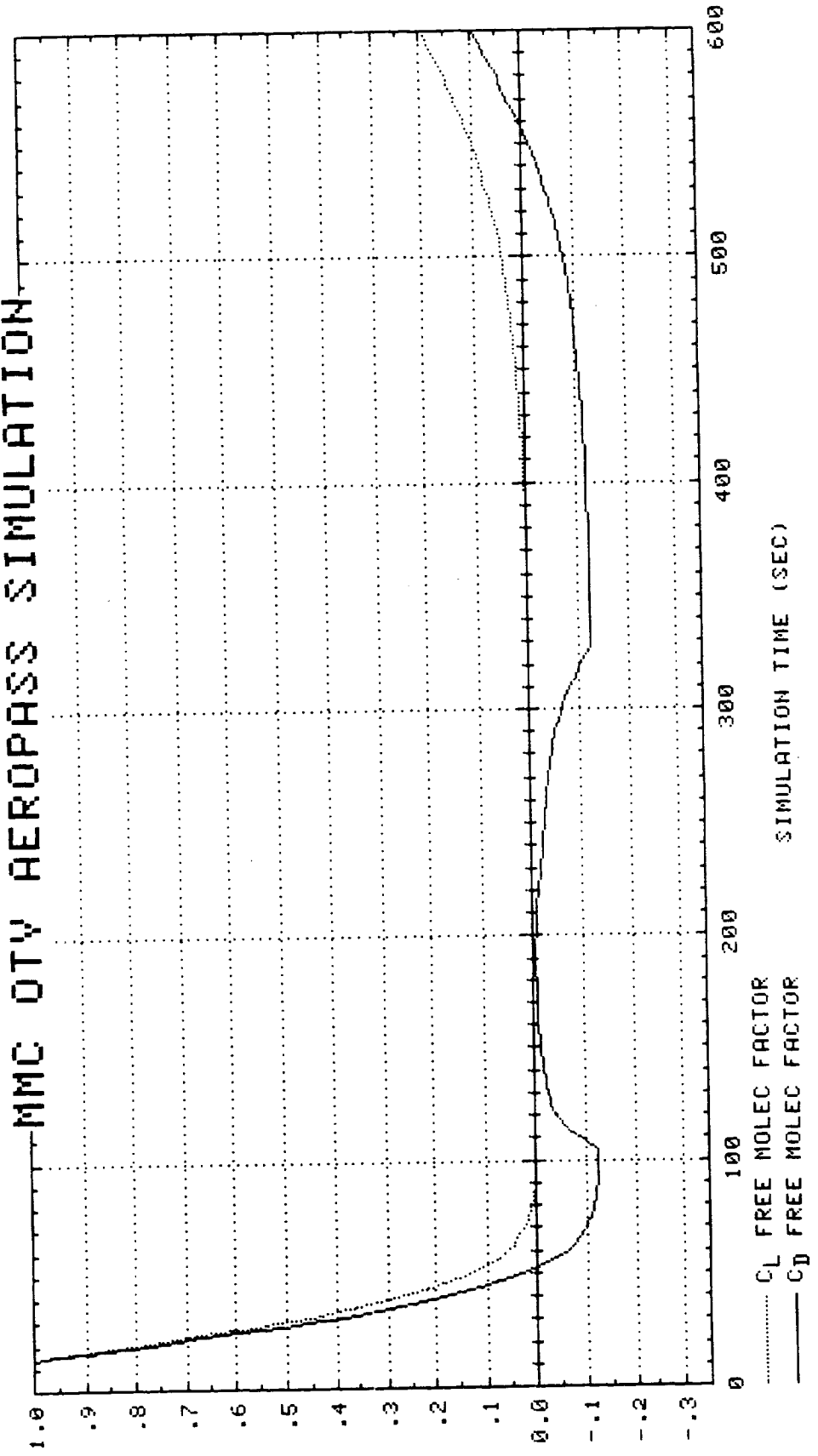
MMC OTV AEROPASS SIMULATION



MMC OTW AEROPASS SIMULATION



MMC OTY AEROPASS SIMULATION



APPENDIX F

OTV AEROPASS SIMULATION

STS-6 ATMOSPHERE

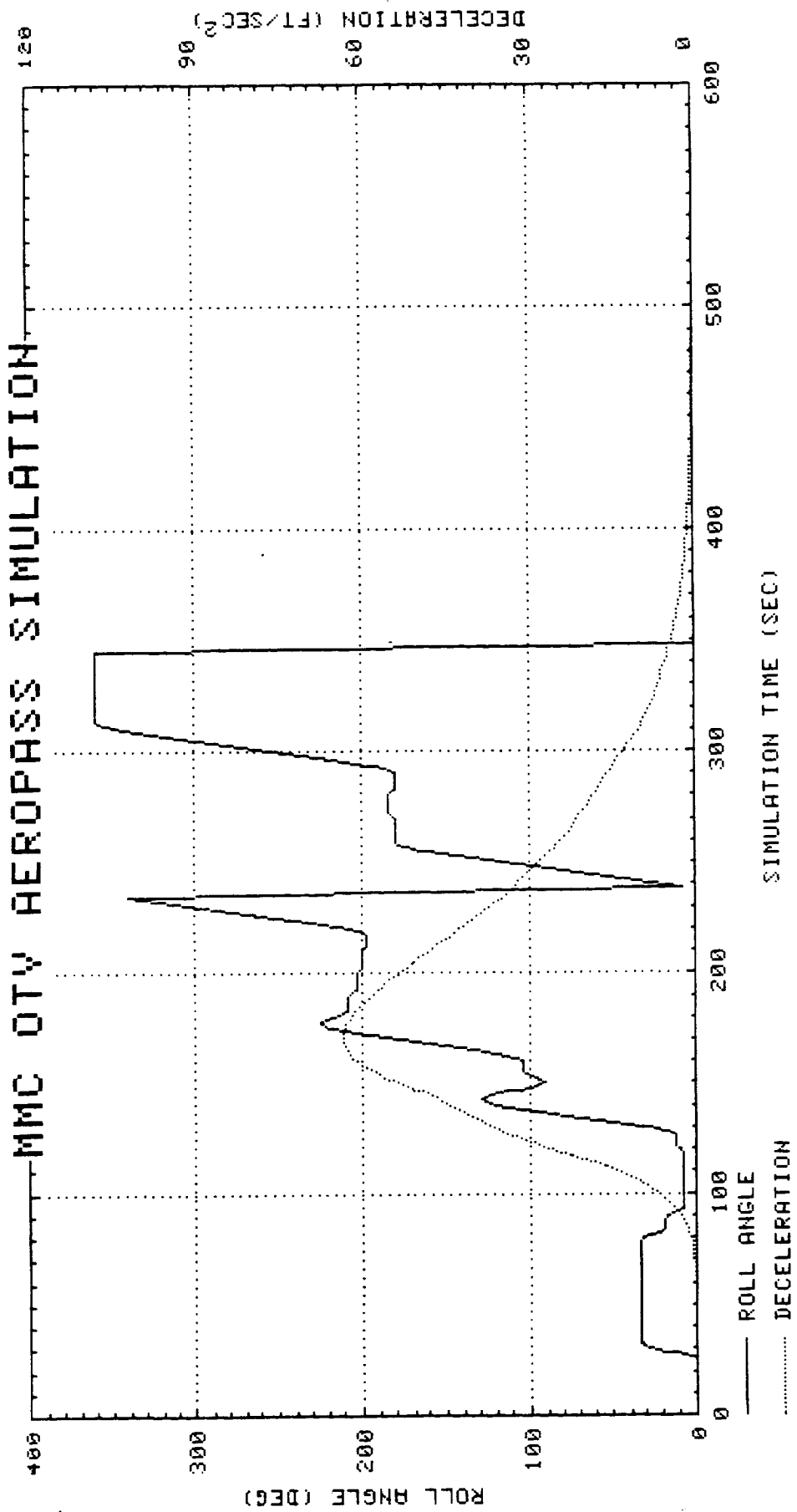
PERIGEE AIM ERROR = .2 NM

(EQUIVALENT TO A FLIGHT PATH ERROR OF .023°)

EXIT APOGEE ERROR = 6.40 NM

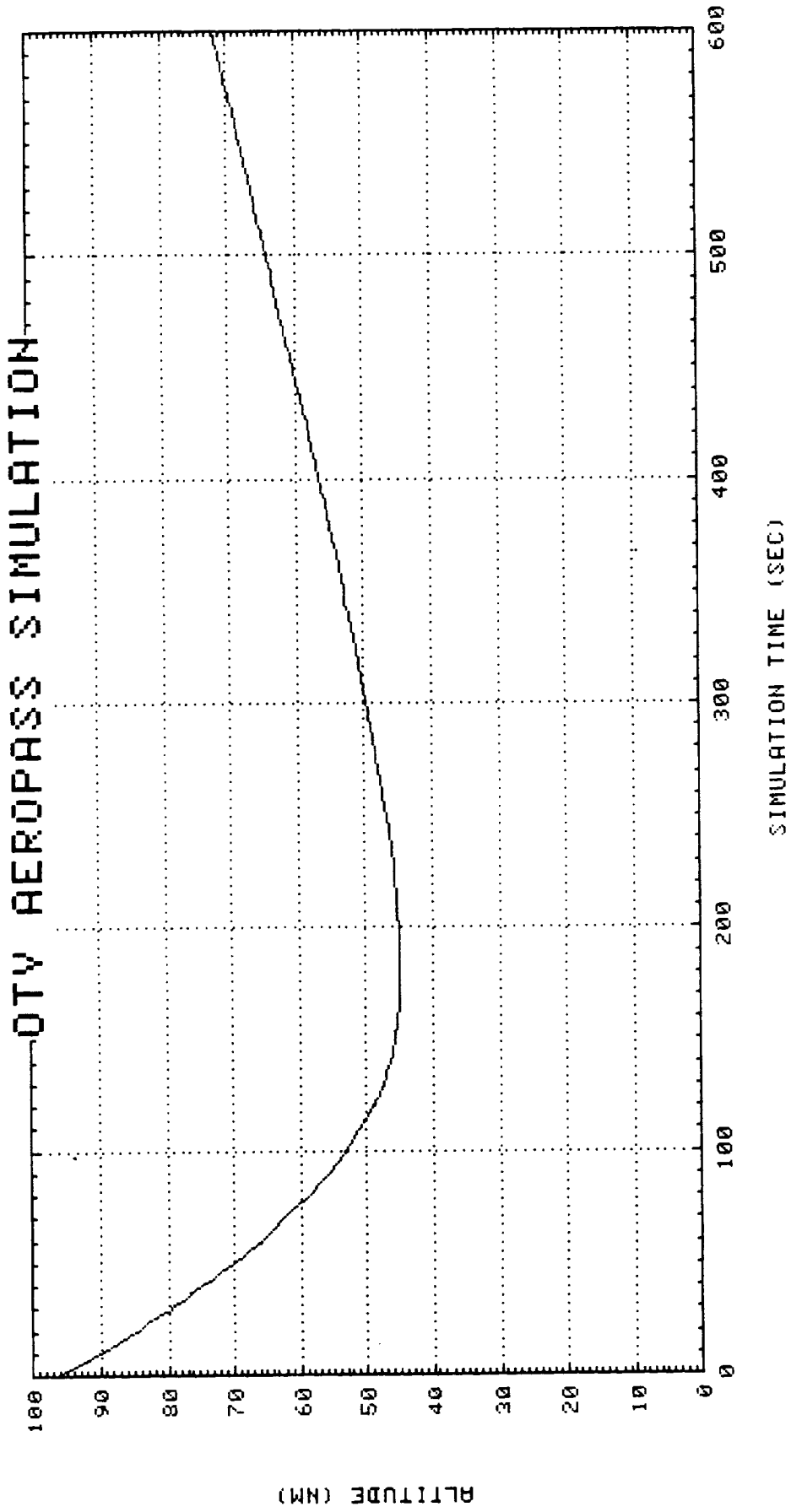
EXIT INCLINATION ERROR = .0166°

THIS PAGE INTENTIONALLY LEFT BLANK

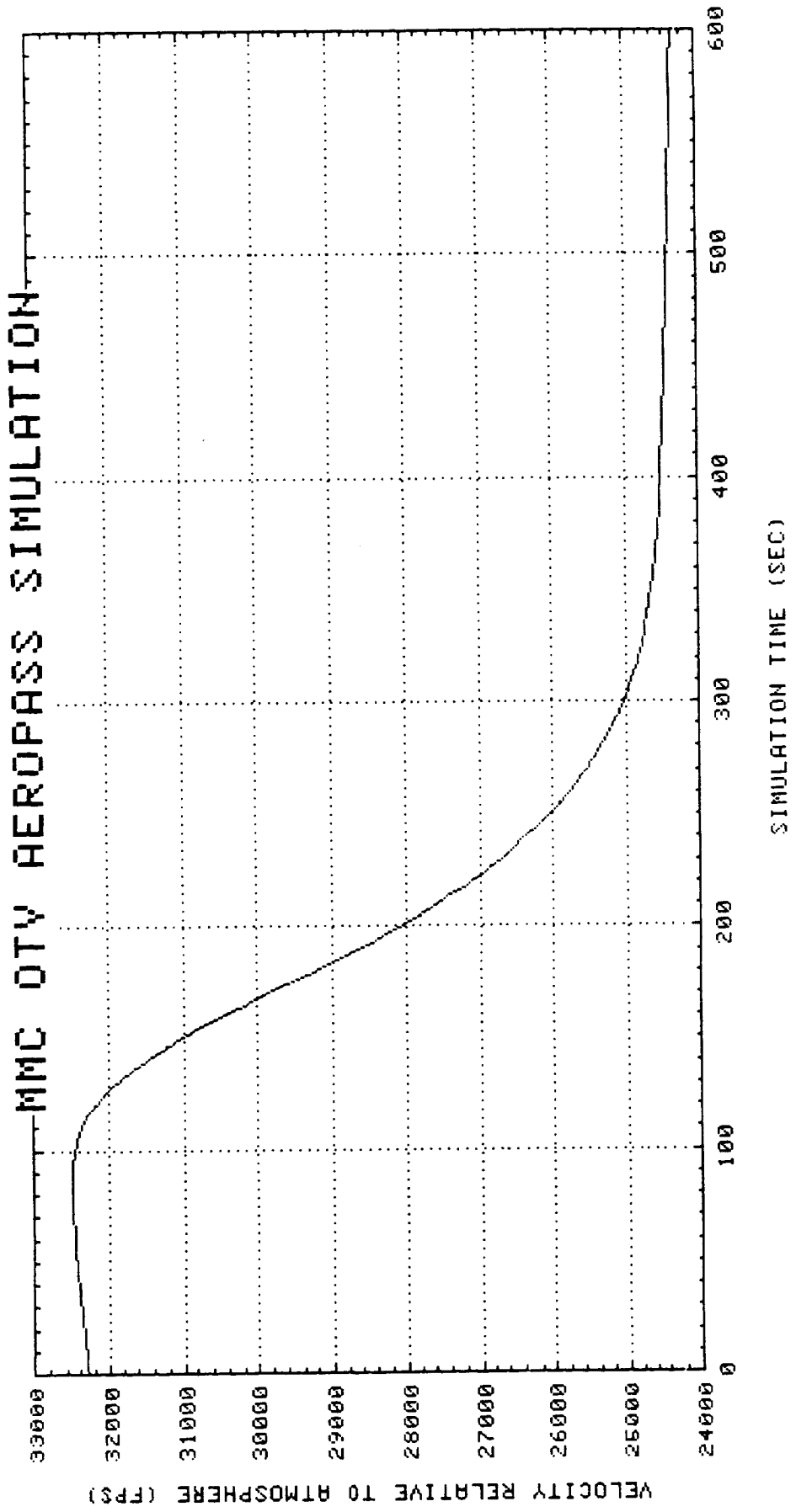


PRECEDING PAGE BLANK NOT FILMED

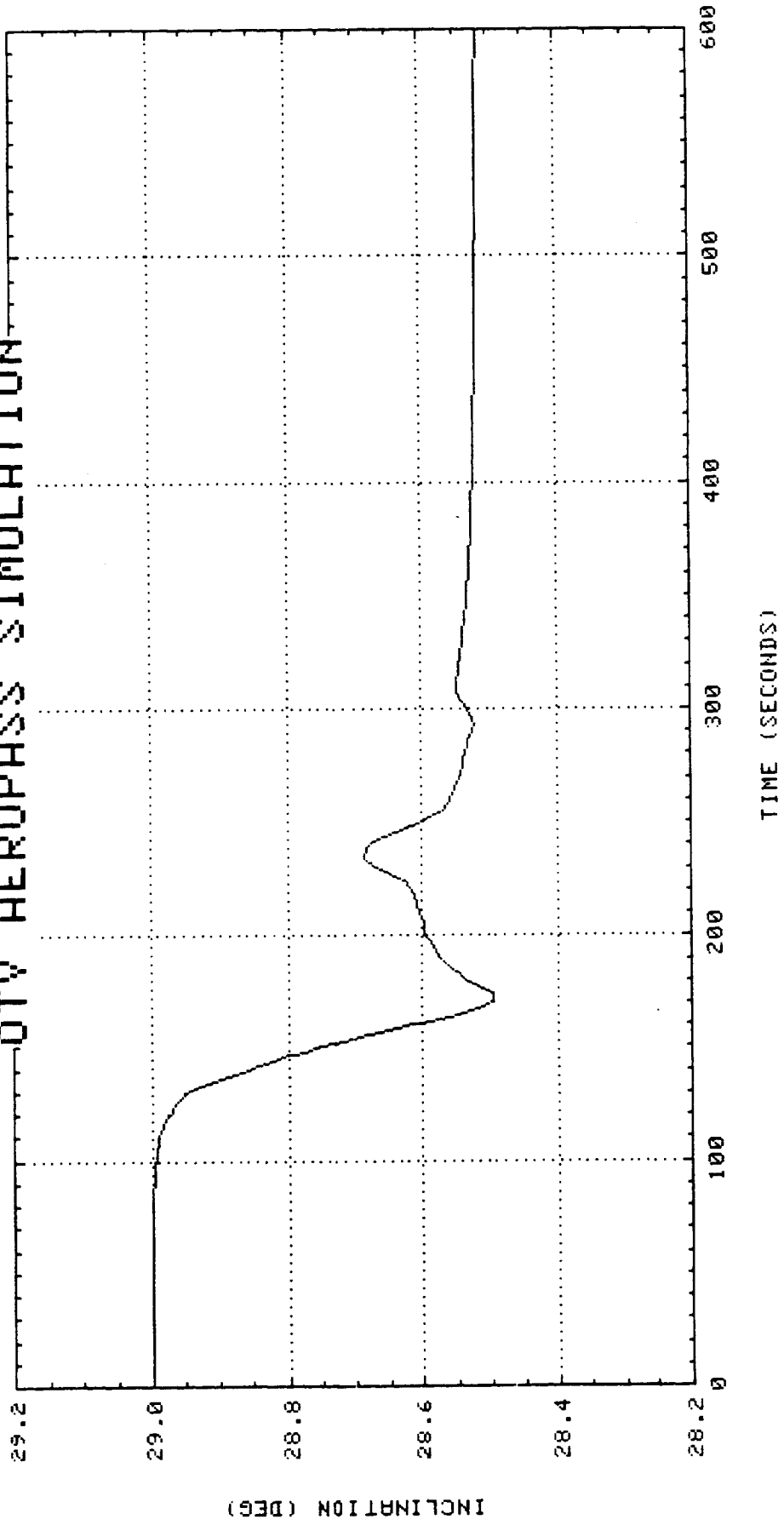
QTY AEROPASS SIMULATION



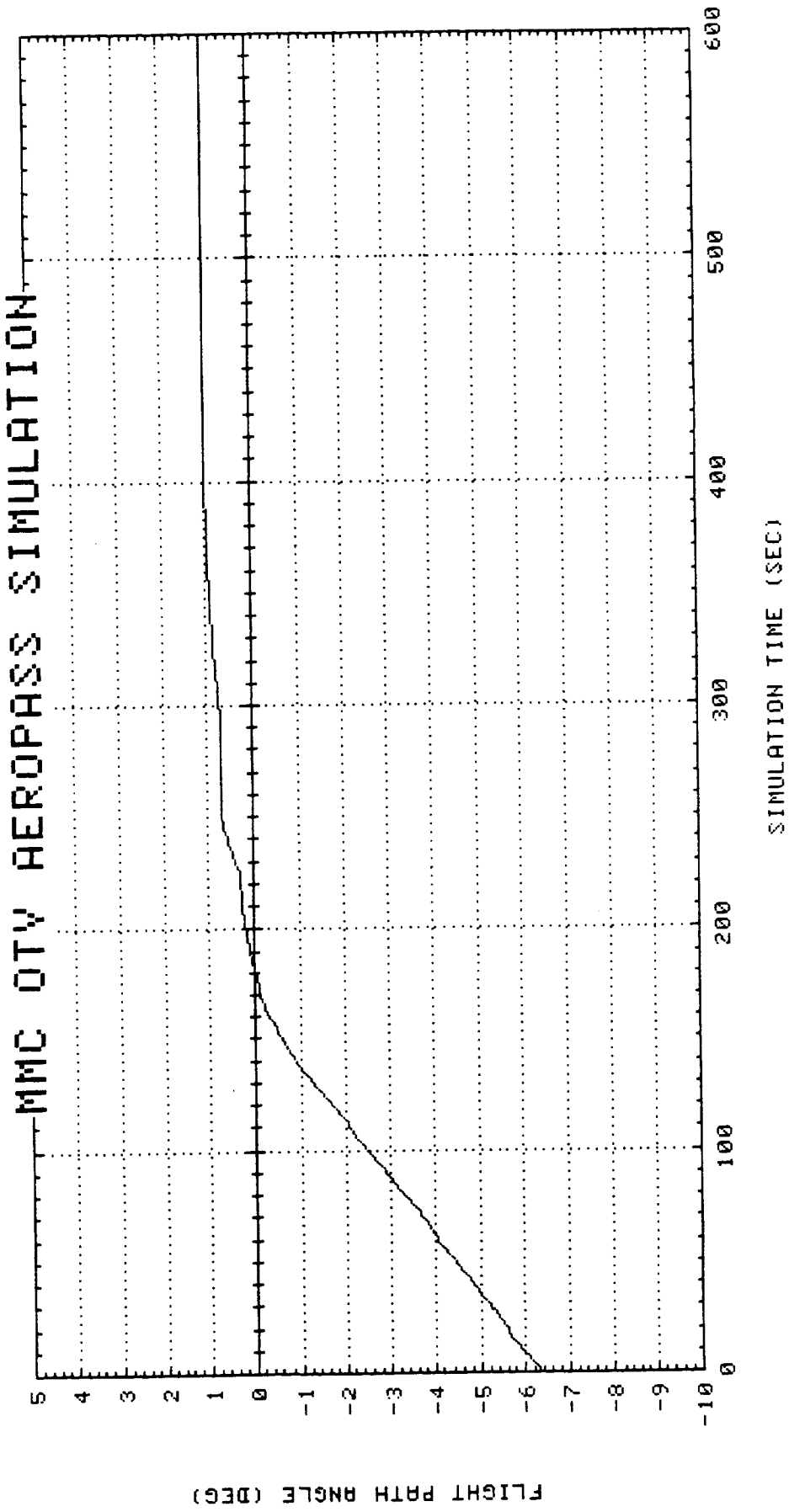
MMC DTV AEROPASS SIMULATION



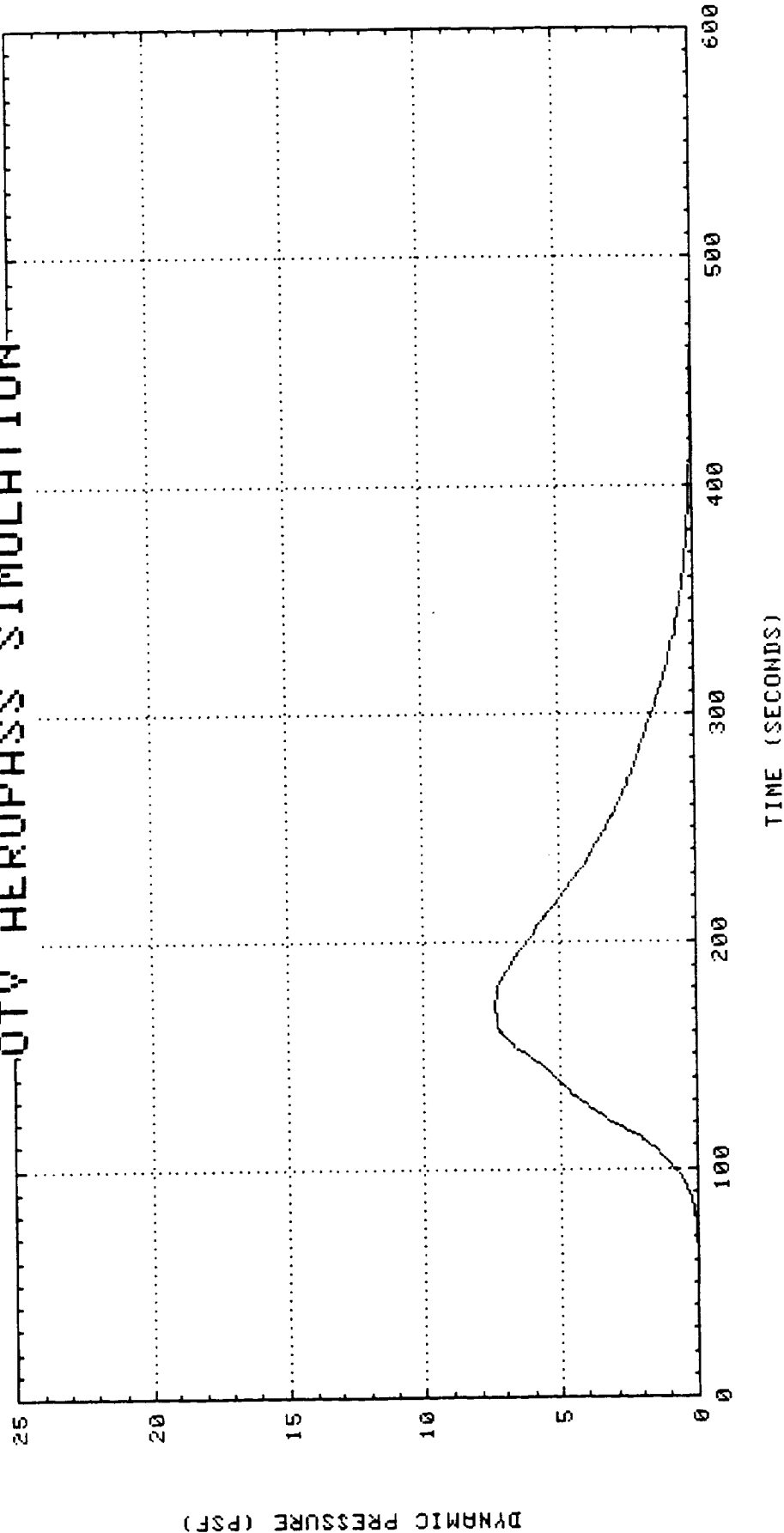
DTV AEROPASS SIMULATION



MMC OTV AEROPASS SIMULATION

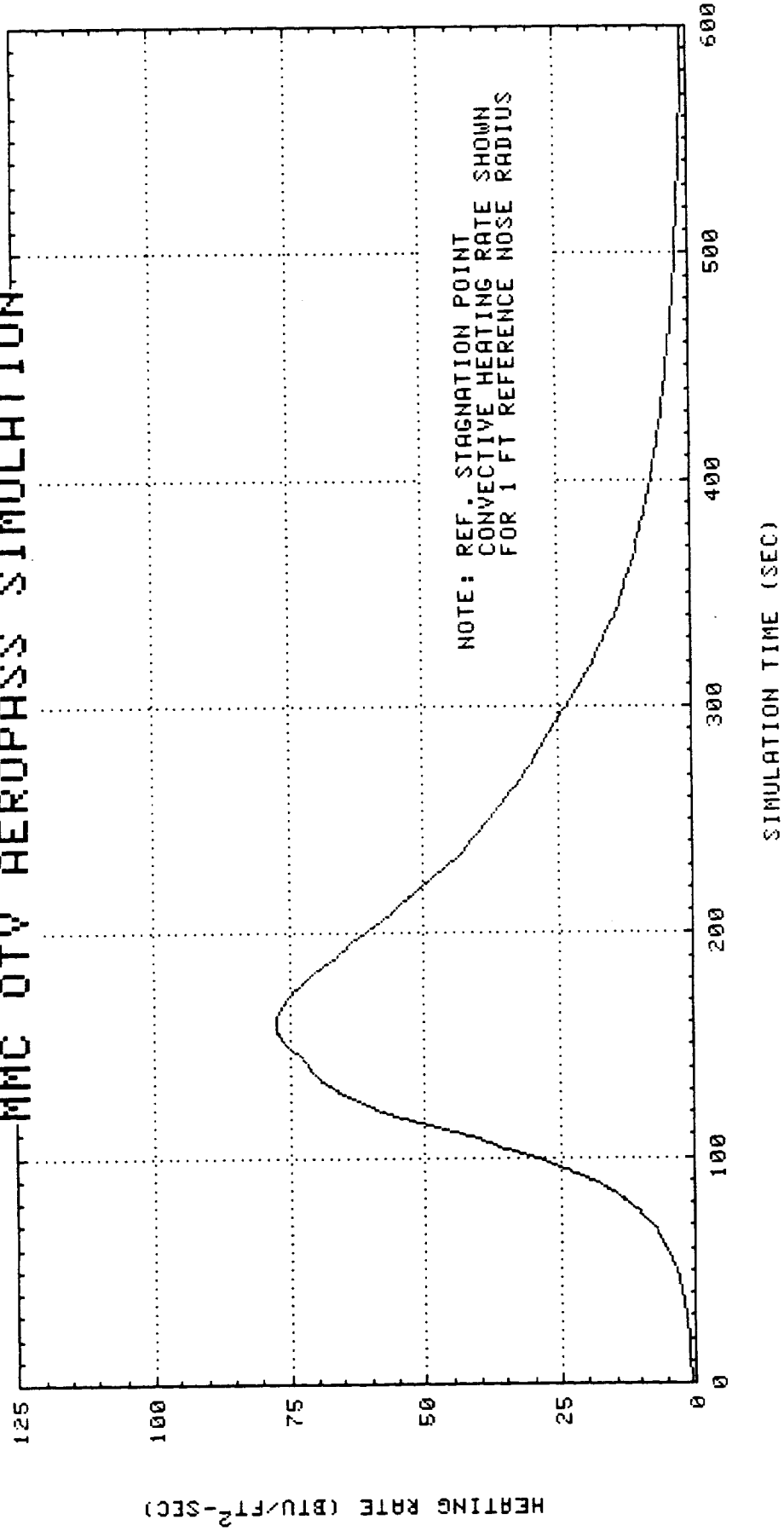


QTV AEROPASS SIMULATION

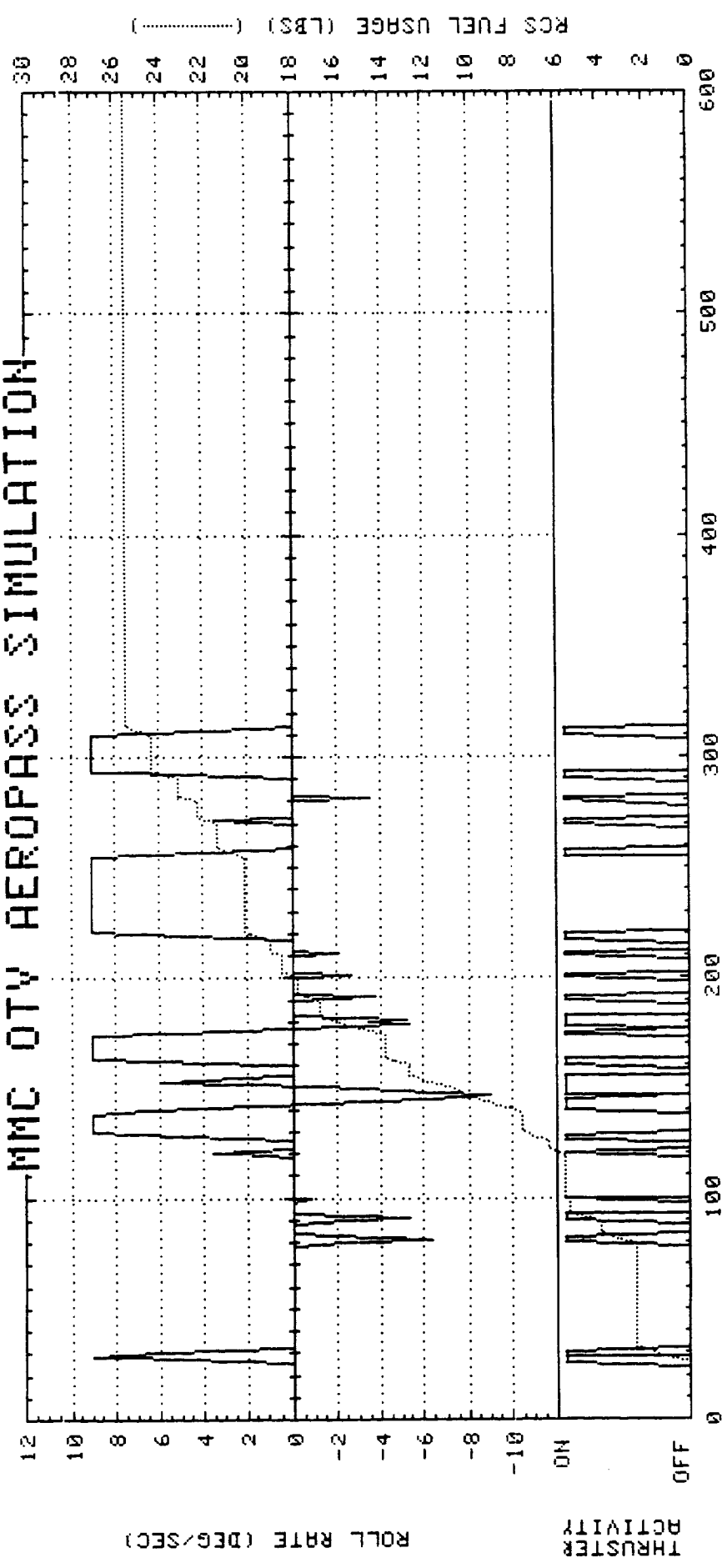


NOTE: DYNAMIC PRESSURE IS
FREE-STREAM VALUE

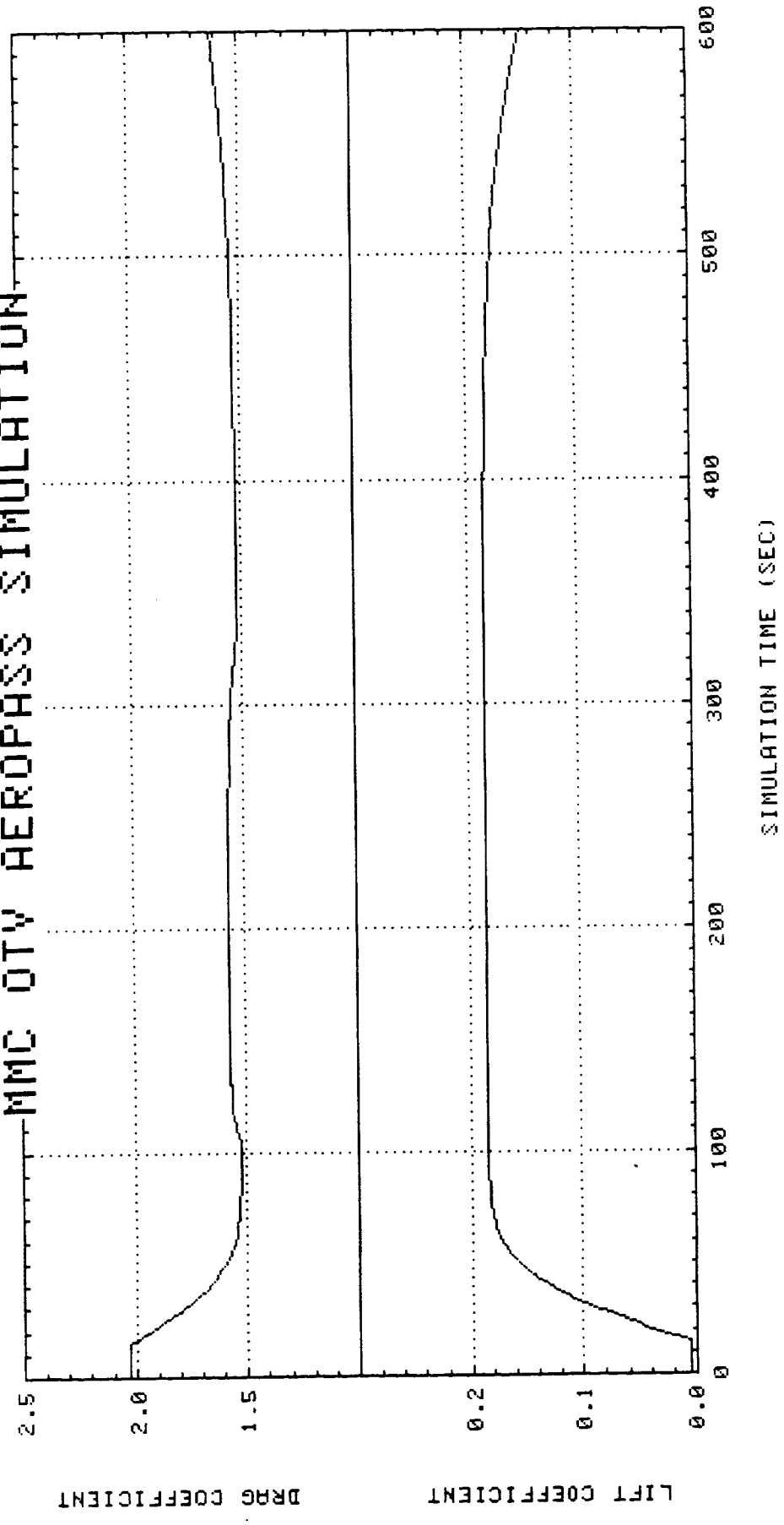
MMC OTV AEROPASS SIMULATION



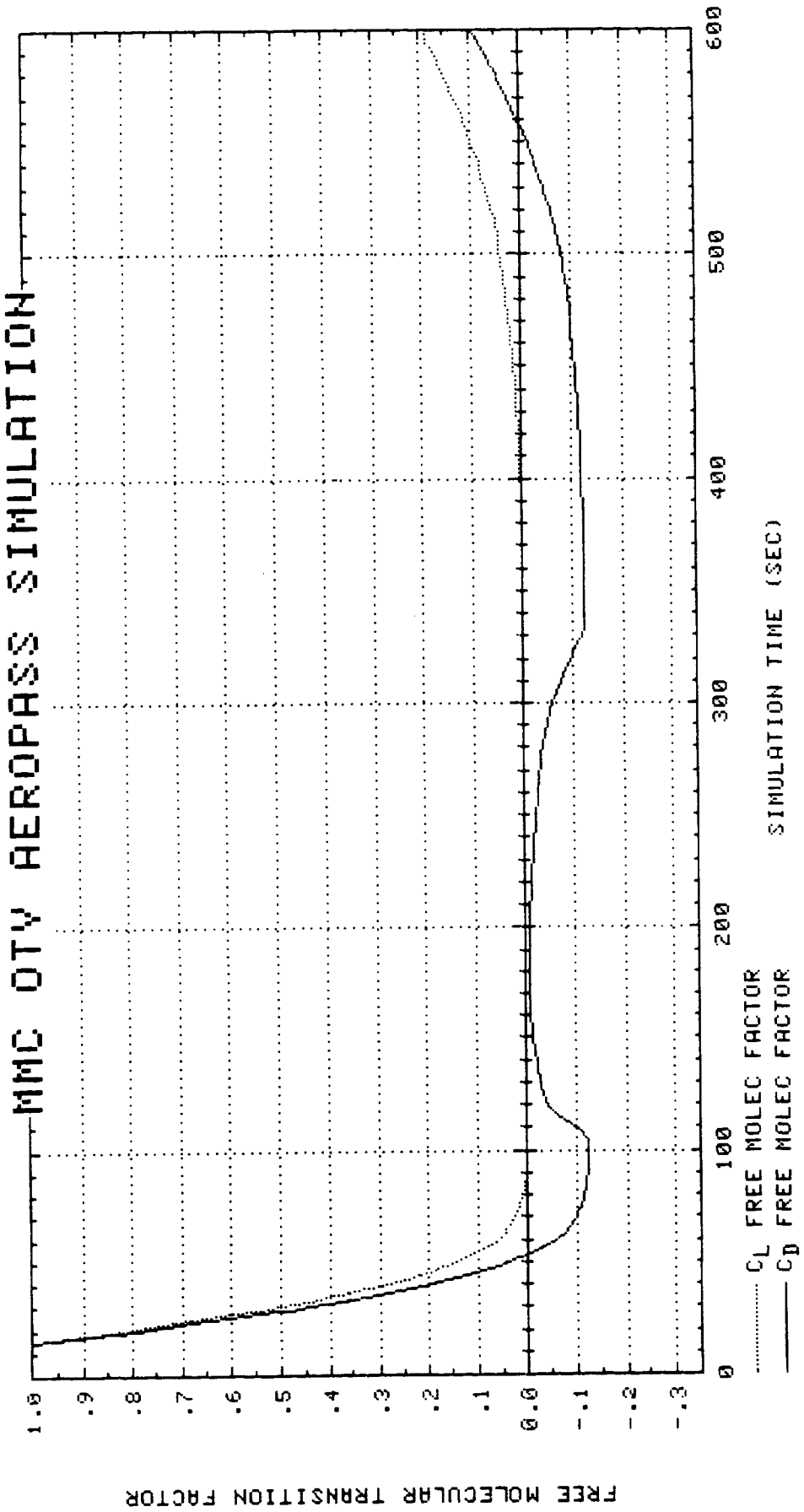
MMC OTV AEROPASS SIMULATION



MMC DTW AEROPASS SIMULATION



MMC OTY AEROPASS SIMULATION



APPENDIX C

OTV AEROPASS SIMULATION

STS-6 ATMOSPHERE

BULK DENSITY SHIFT = +22%
(EQUIVALENT TO A BALLISTIC COEFFICIENT SHIFT)

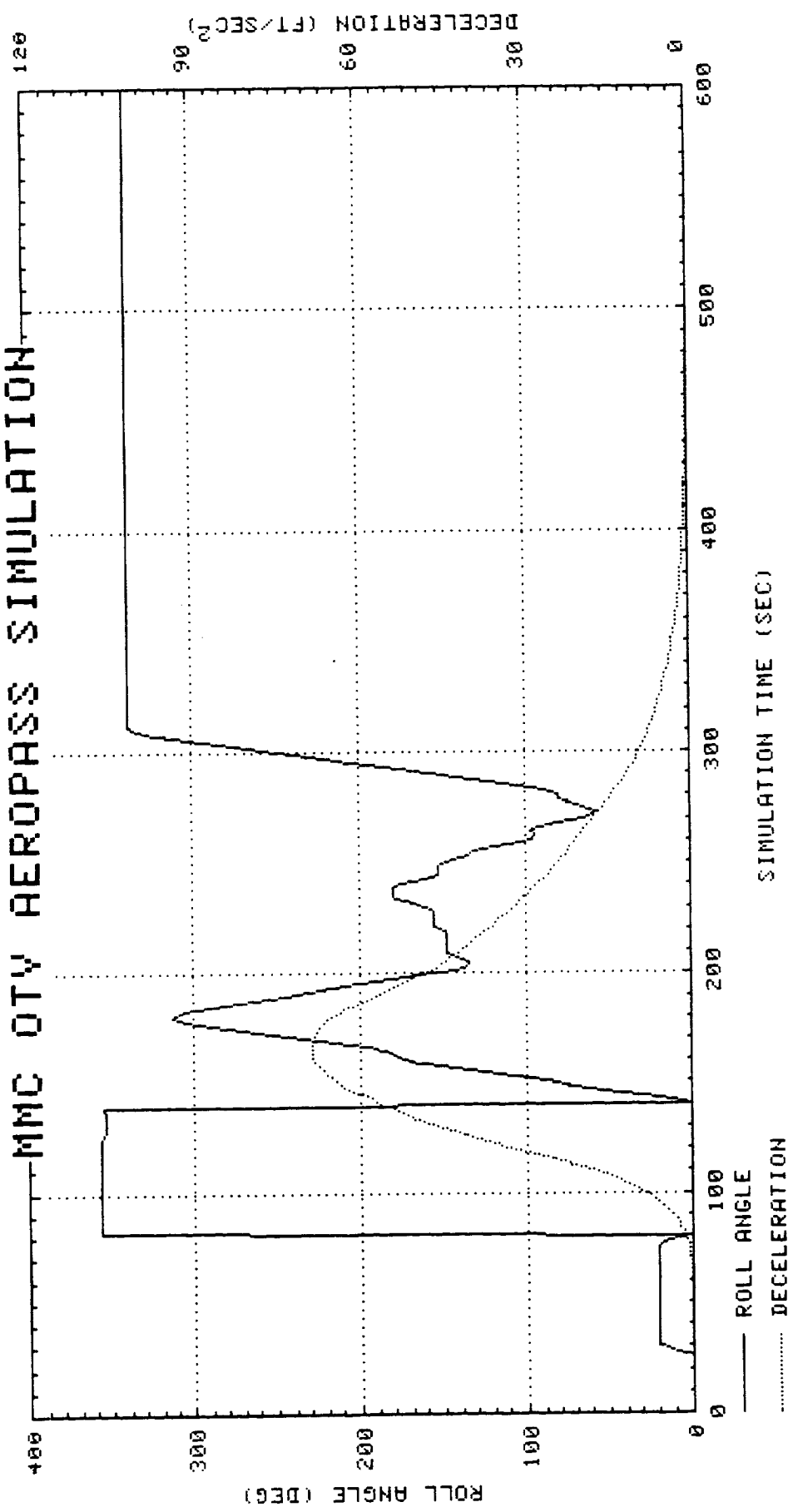
EXIT APOGEE ERROR = 2.77 NM

EXIT INCLINATION ERROR = .0030°

(

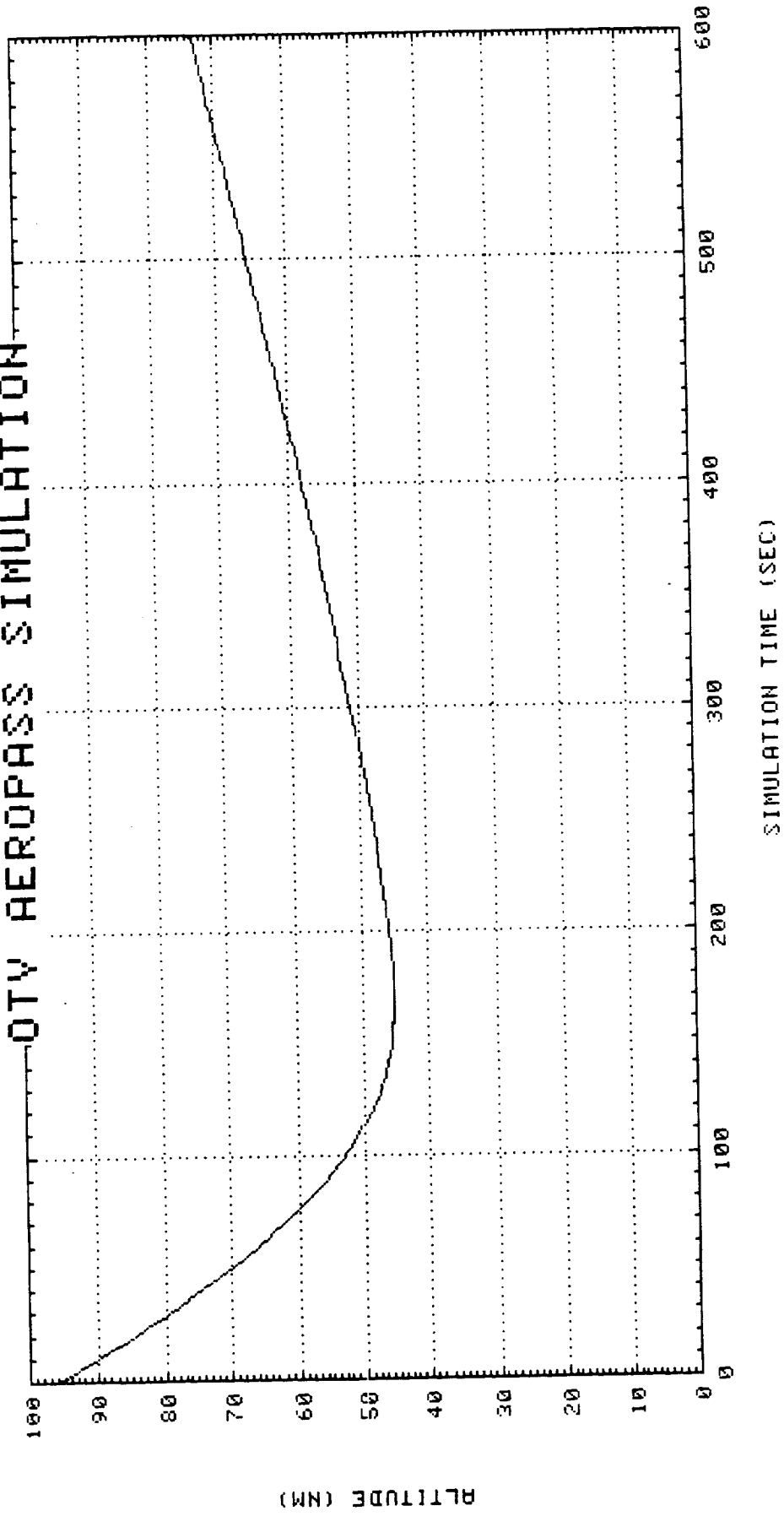
THIS PAGE INTENTIONALLY LEFT BLANK

MMC OTV AEROPASS SIMULATION

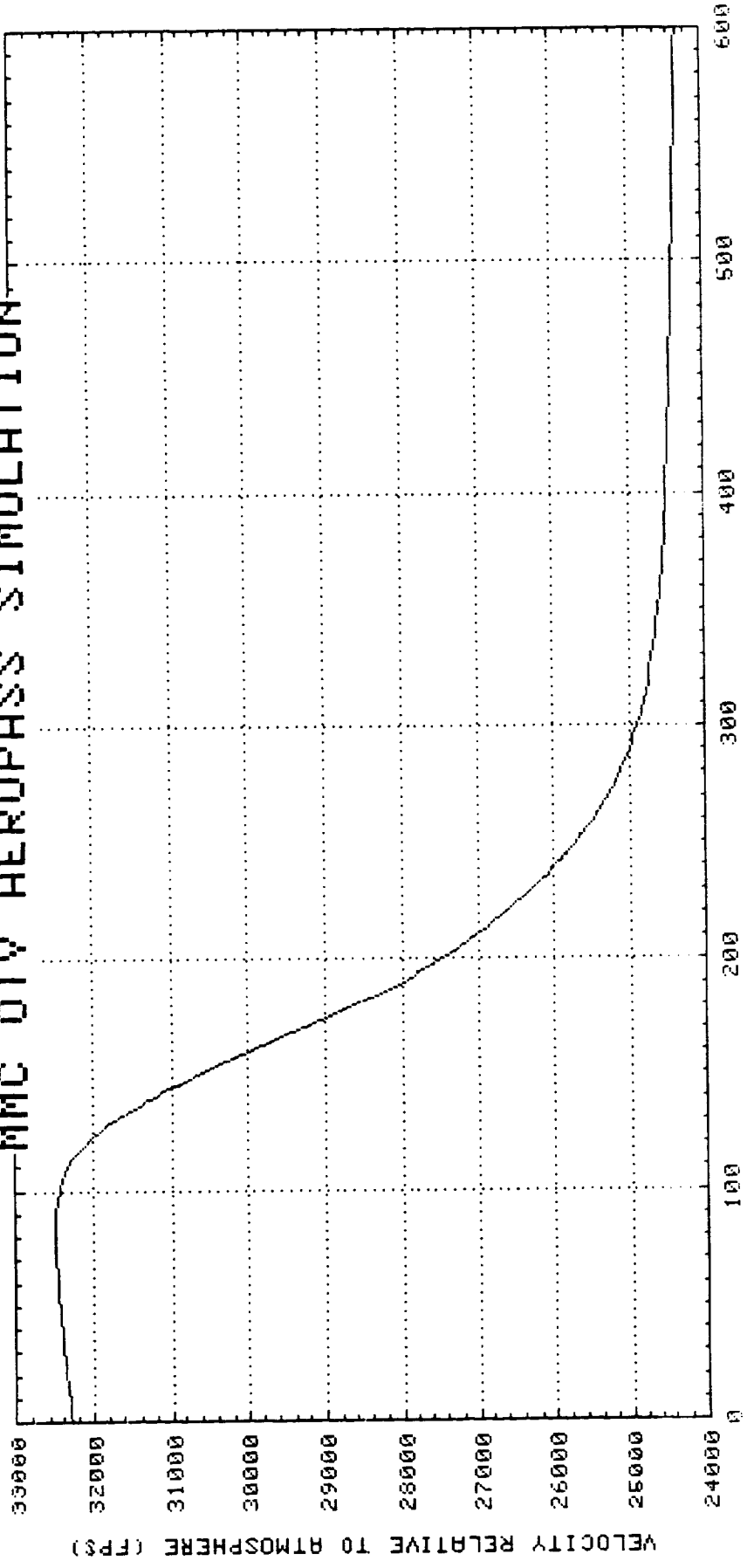


PRECEDING PAGE BLANK NOT FILMED

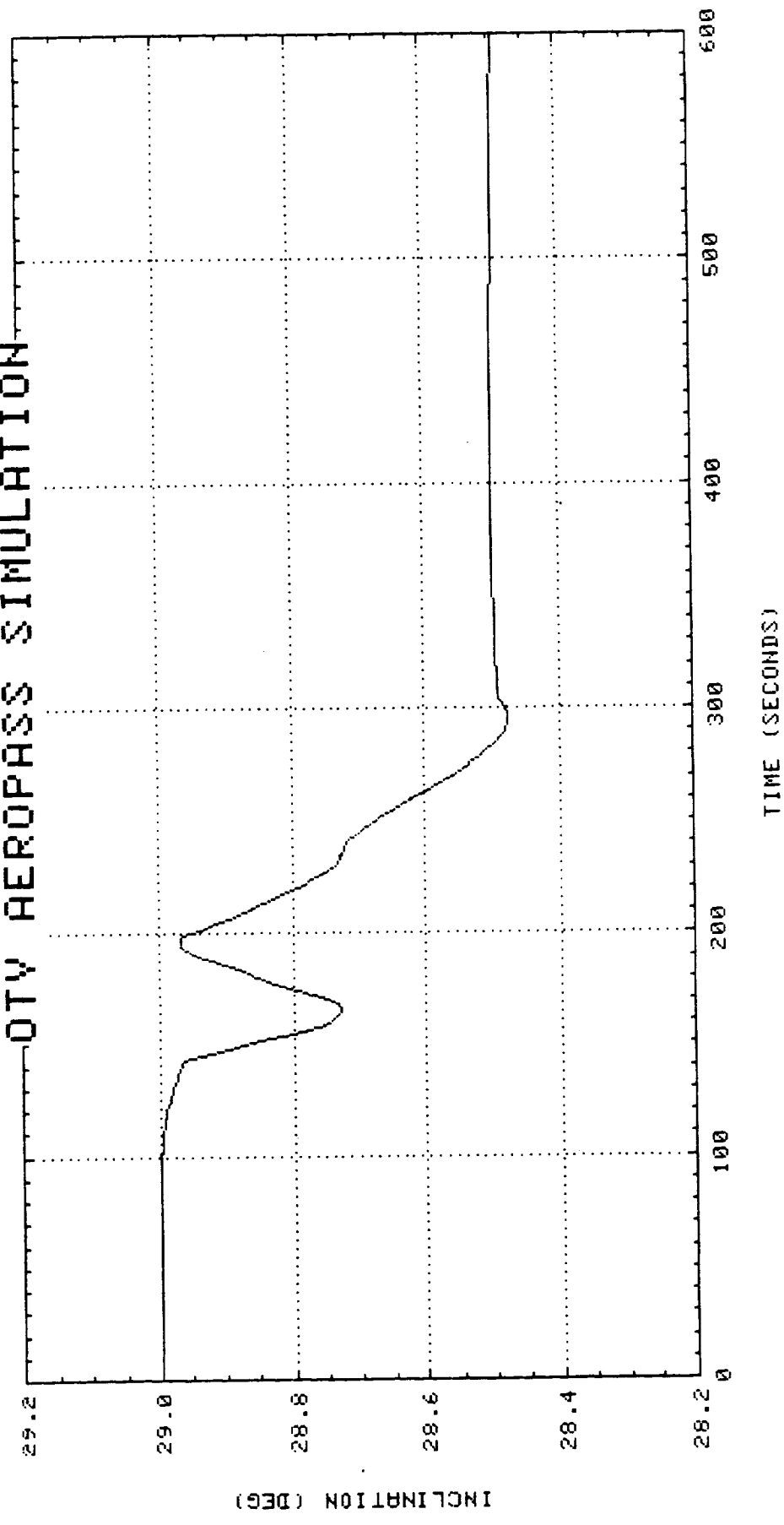
QTV AEROPASS SIMULATION



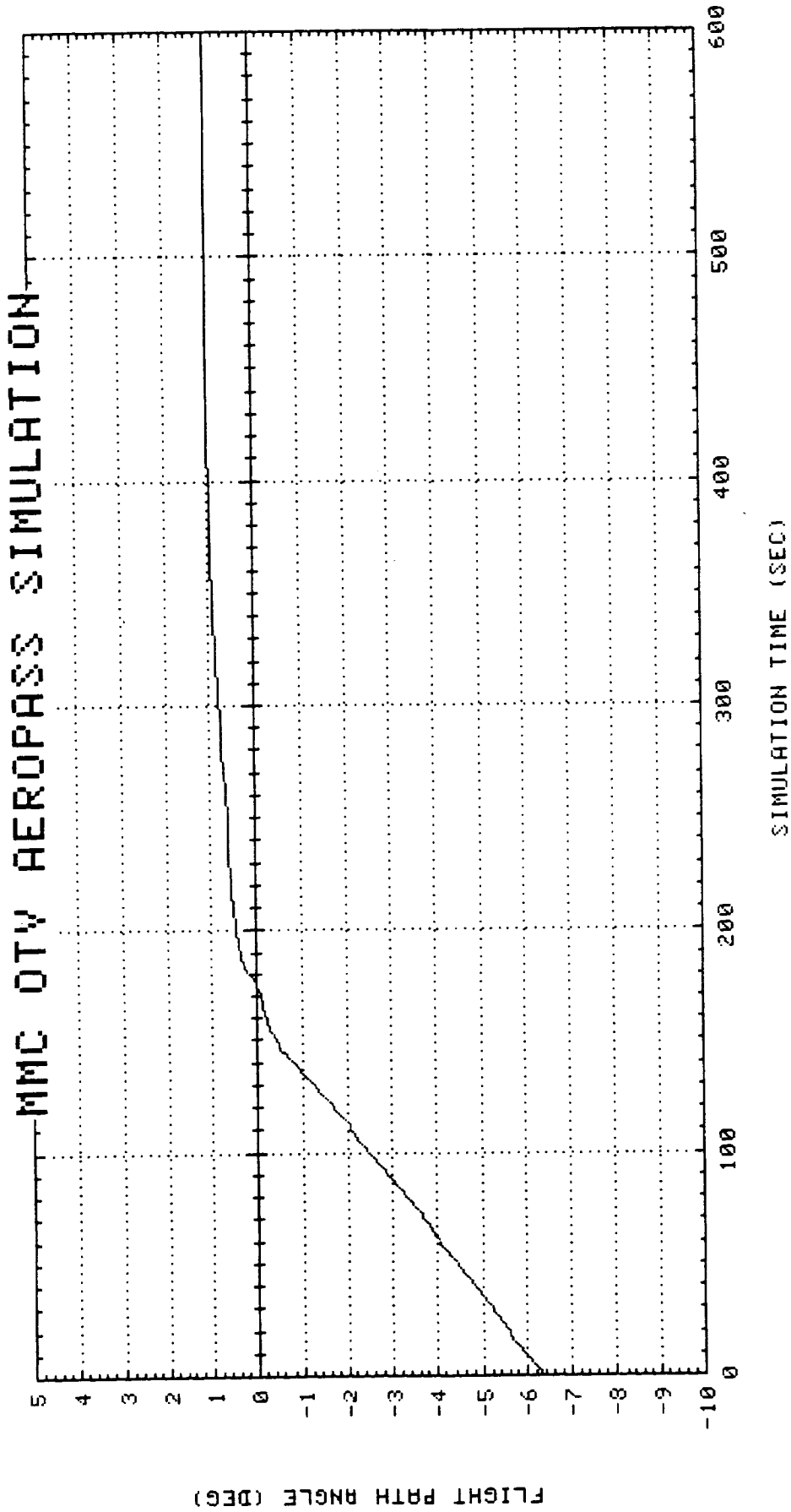
MMC DTV AEROPASS SIMULATION



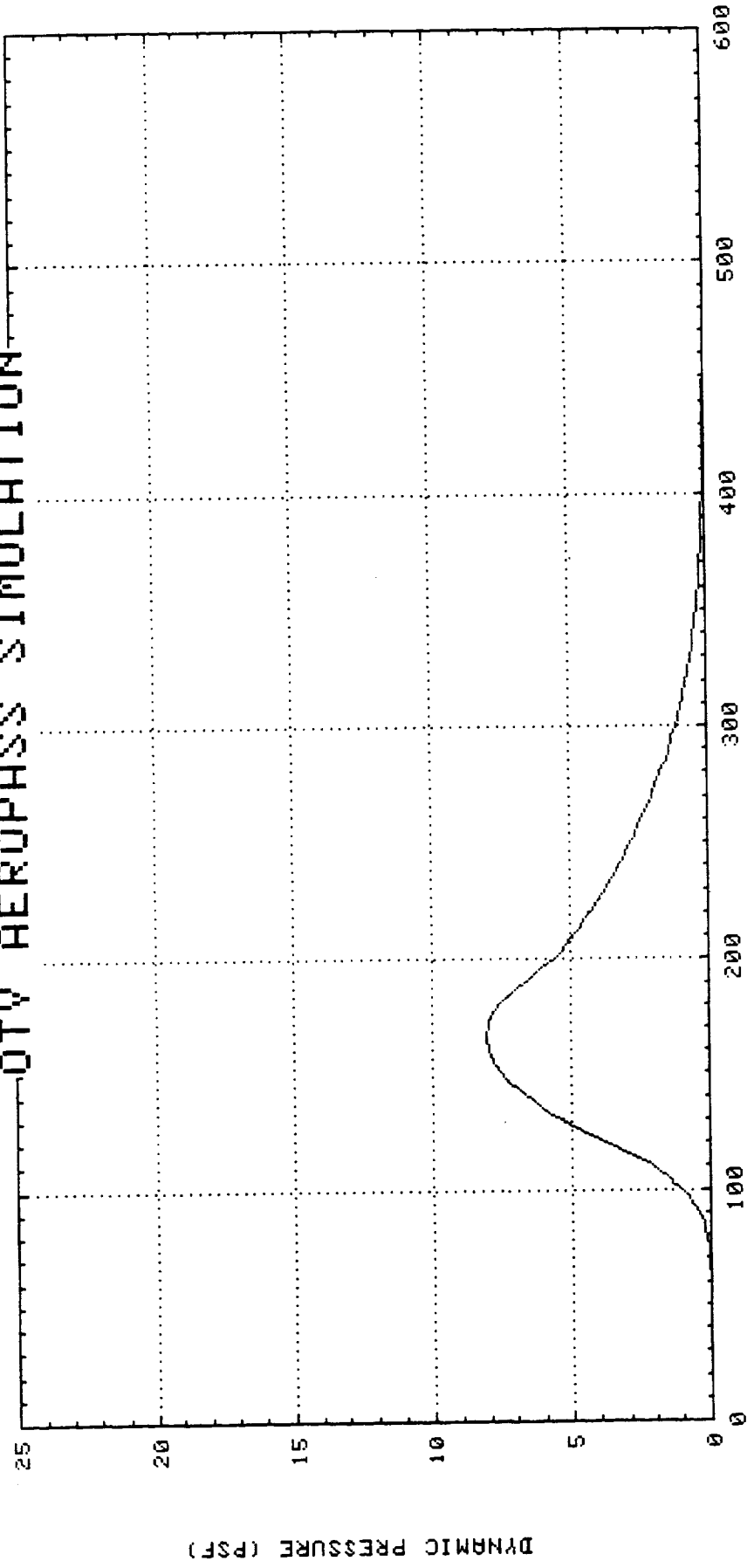
QTY AEROPASS SIMULATION



MMC OTV AEROPASS SIMULATION

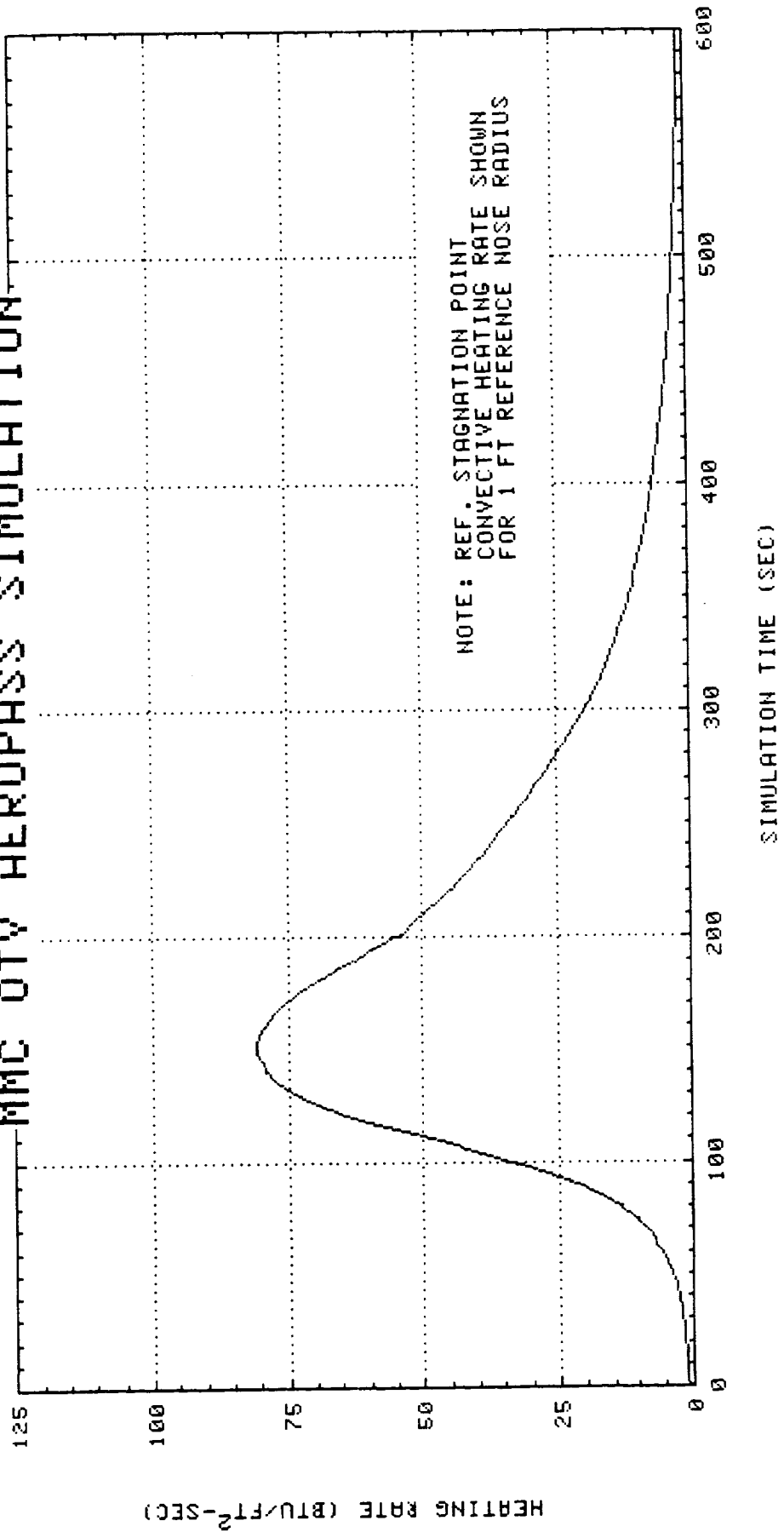


QTV AEROPASS SIMULATION

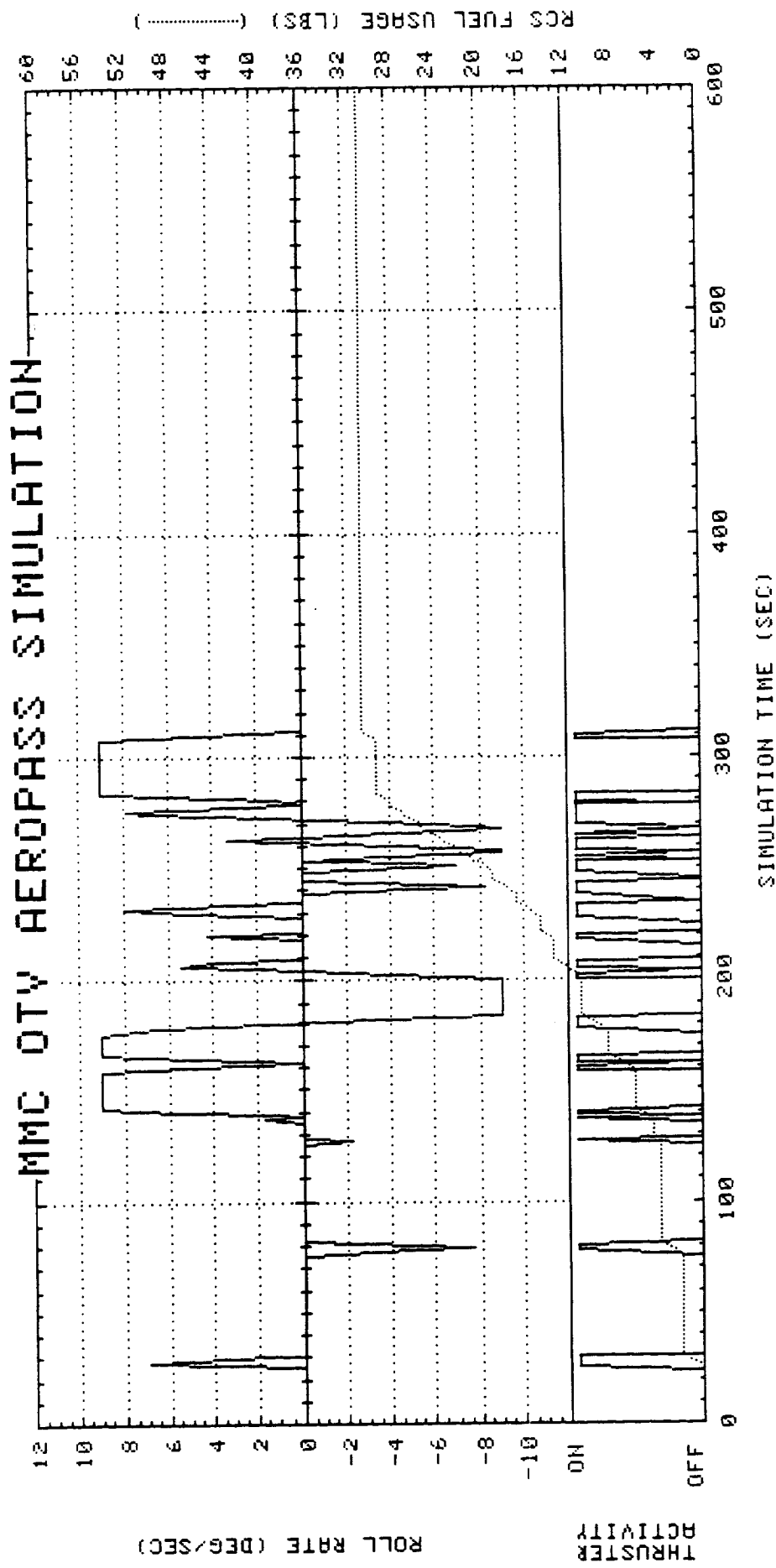


NOTE: DYNAMIC PRESSURE IS
FREE-STREAM VALUE

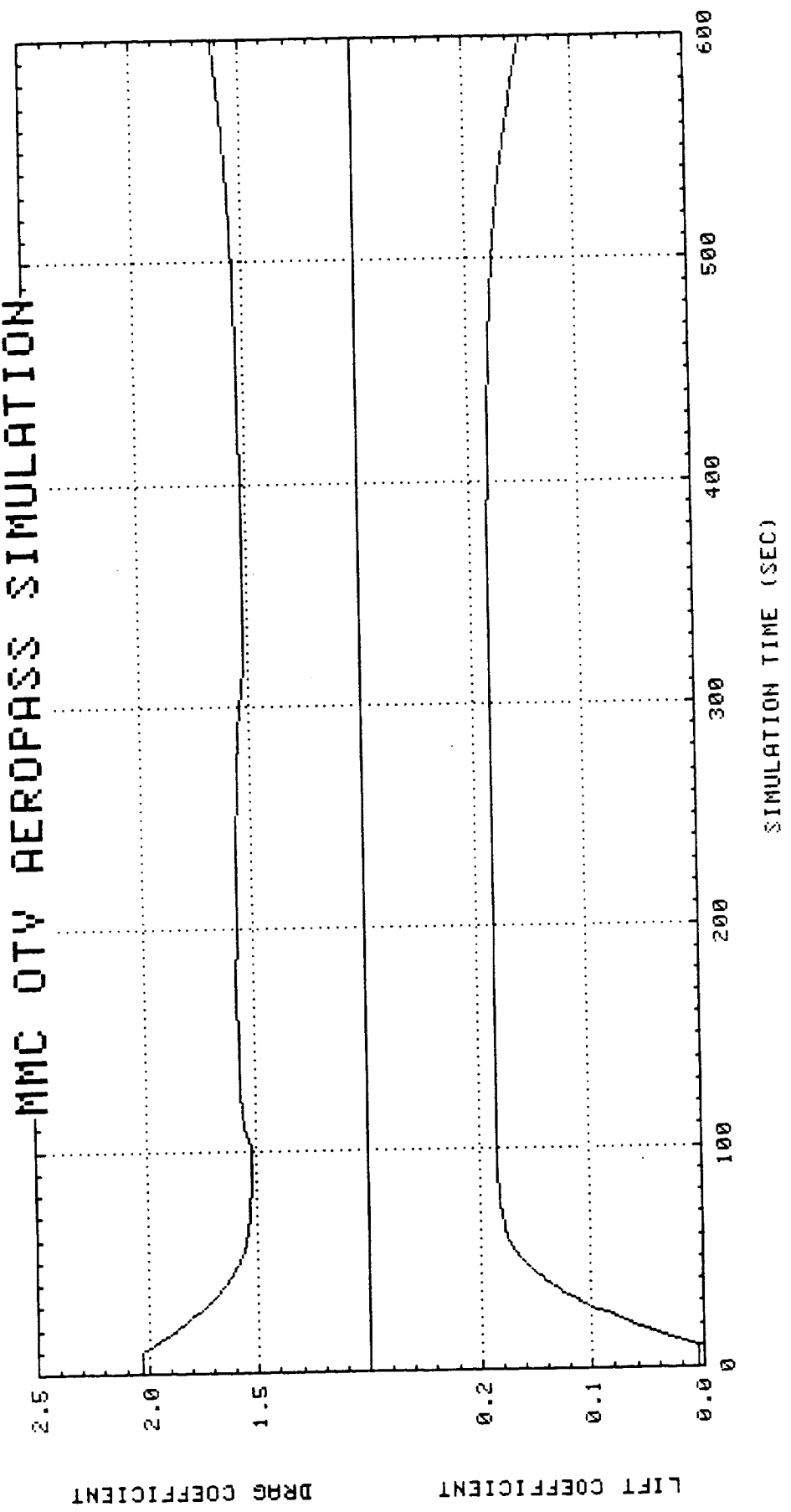
MMC OTV AEROPASS SIMULATION



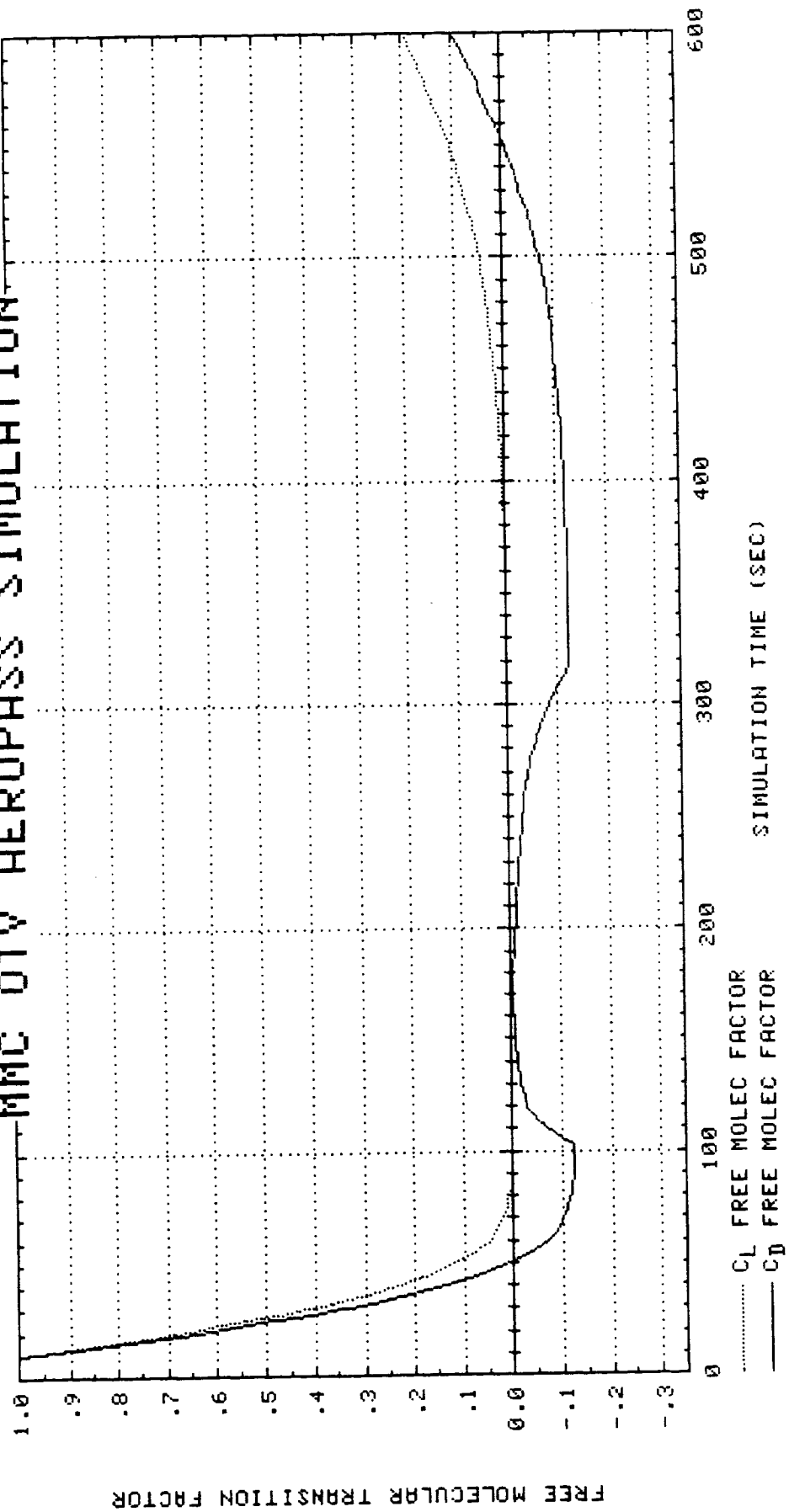
MMC OTV AEROPASS SIMULATION



MMC OTV AEROPASS SIMULATION



MMC OTV AEROPASS SIMULATION



APPENDIX H

OTV AEROPASS SIMULATION

STS-6 ATMOSPHERE

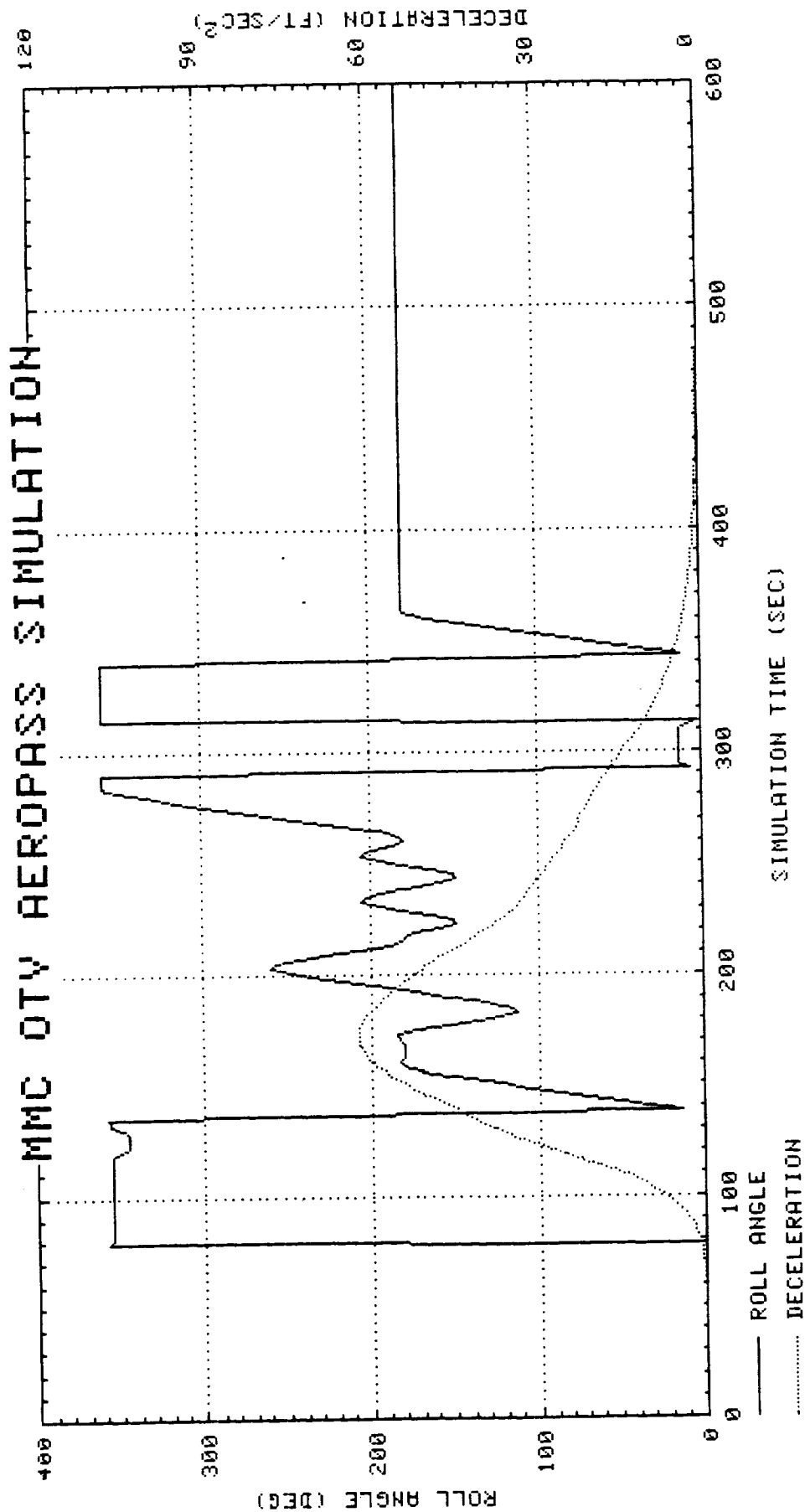
NAV ERROR: 2000' POS.

14 FPS VELOCITY

EXIT APOGEE ERROR = 1.88 NM

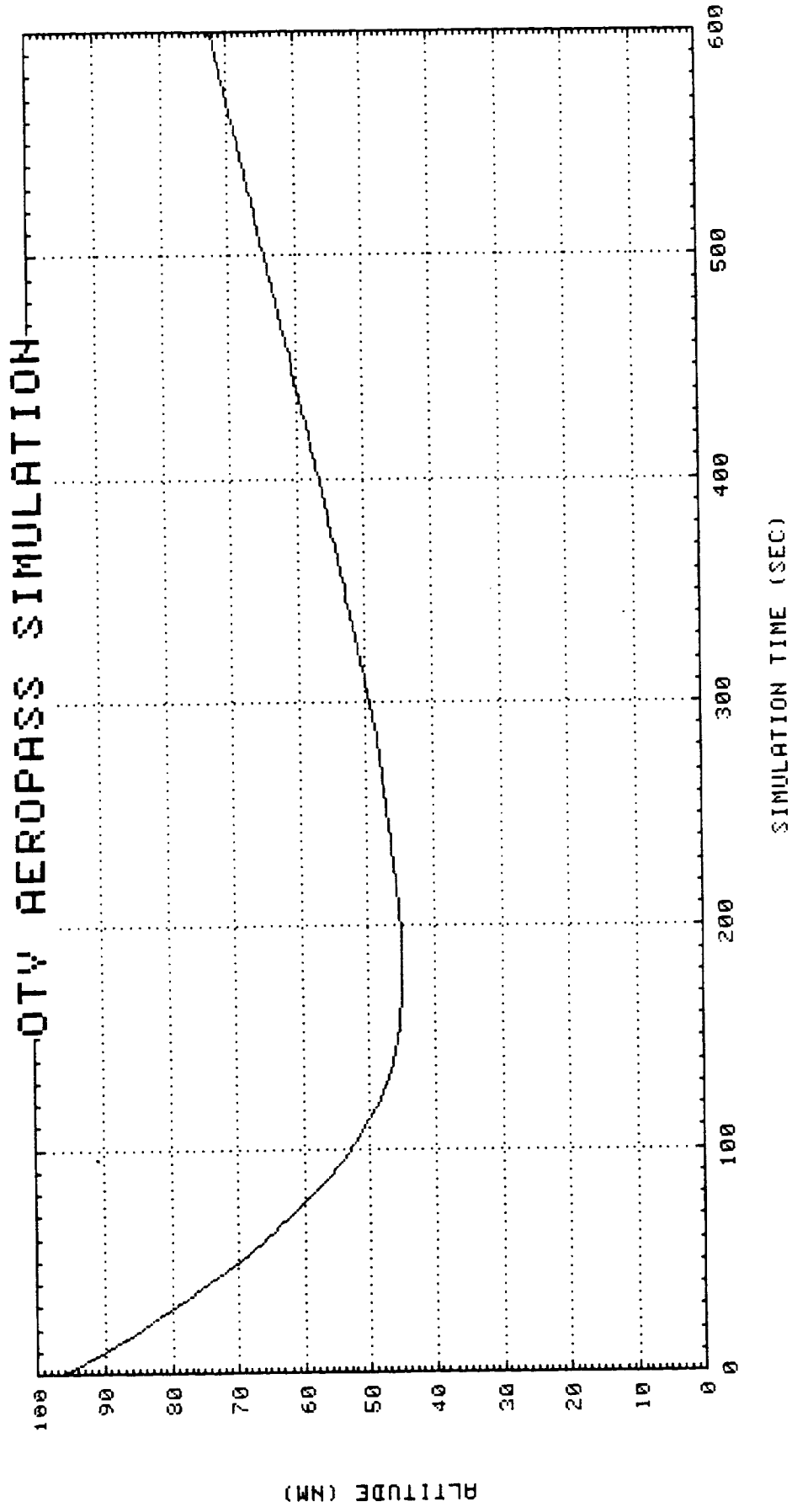
EXIT INCLINATION ERROR = .0161°

THIS PAGE INTENTIONALLY LEFT BLANK

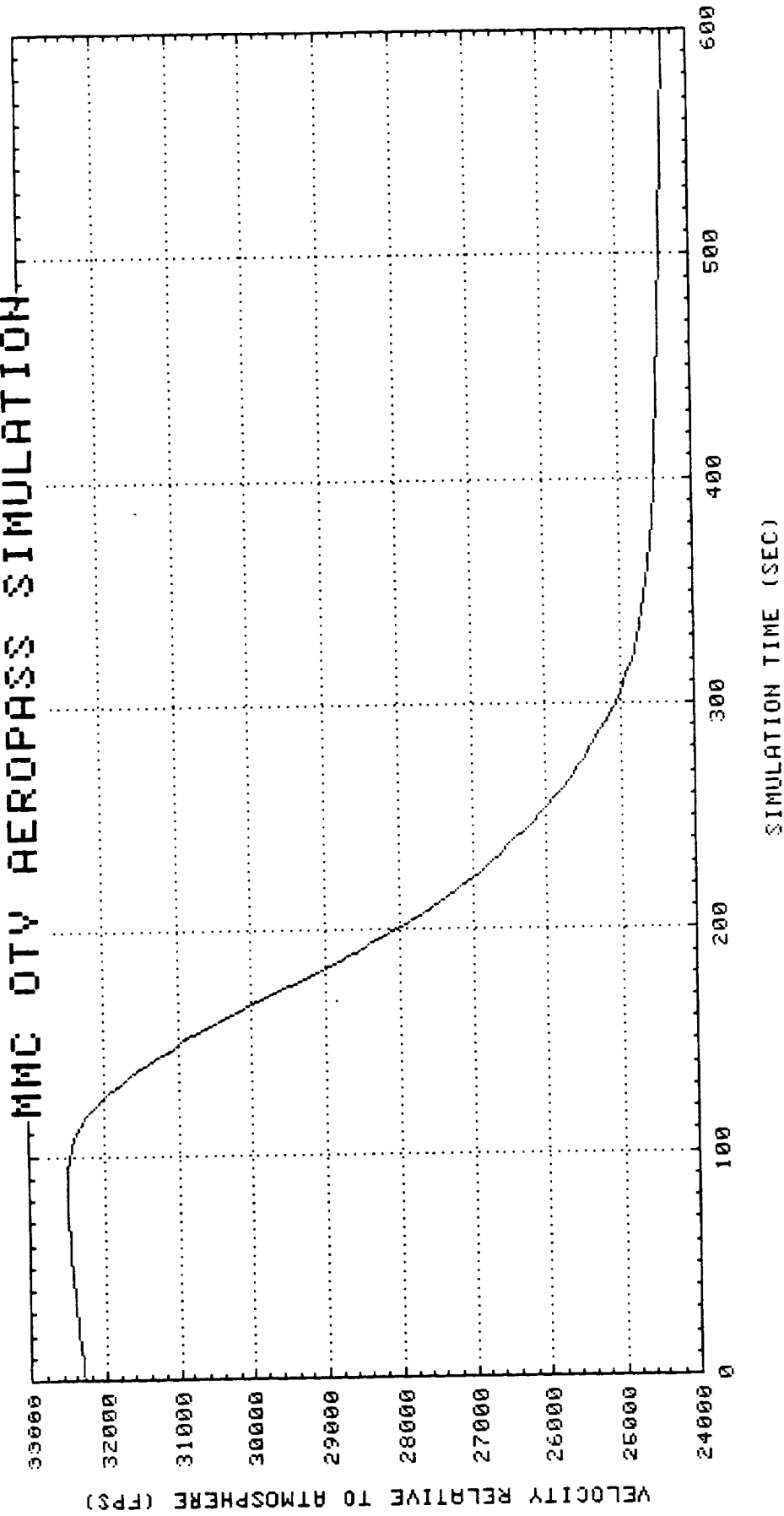


PRECEDING PAGE BLANK NOT FILMED

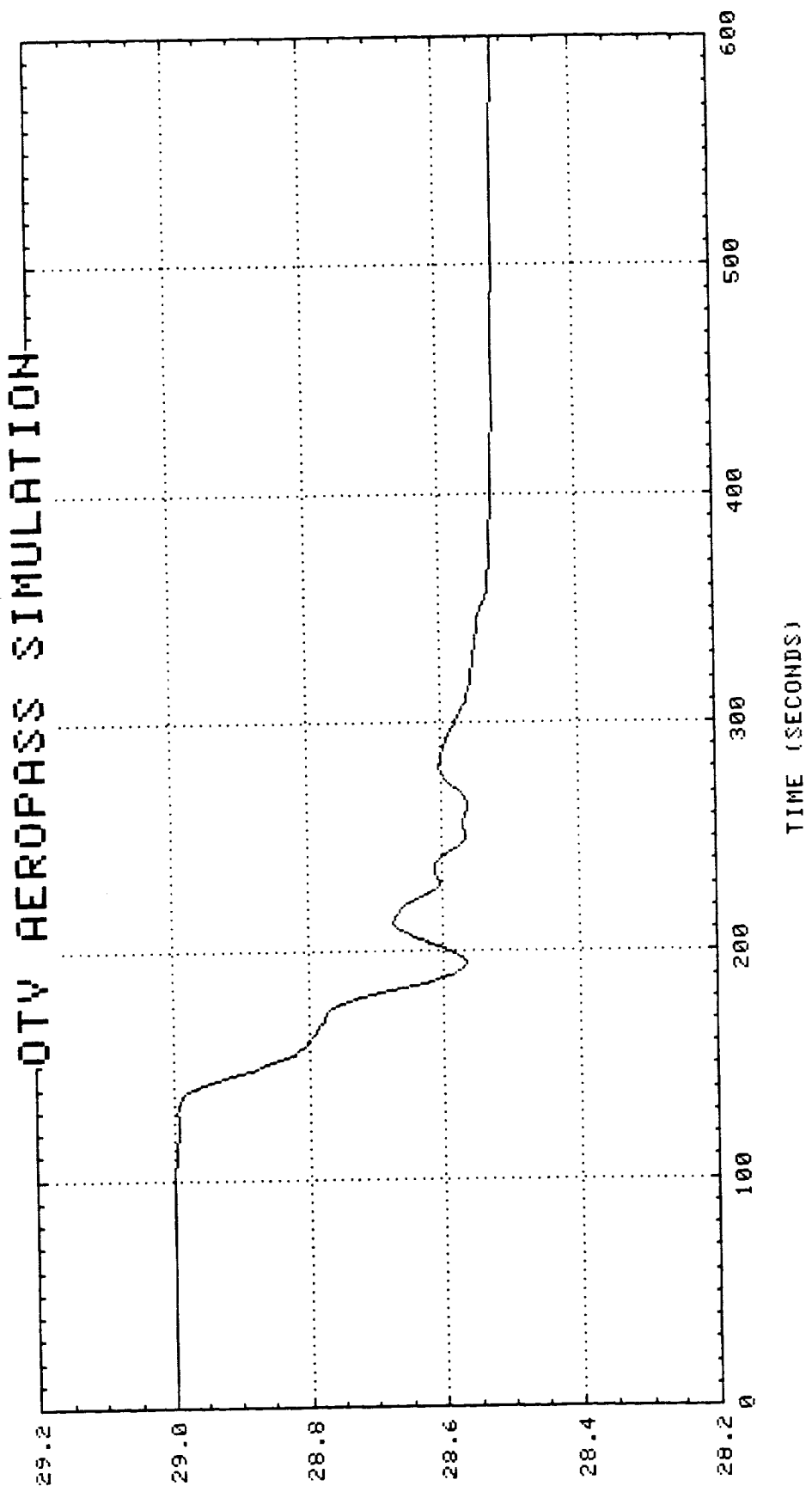
OTV AEROPASS SIMULATION



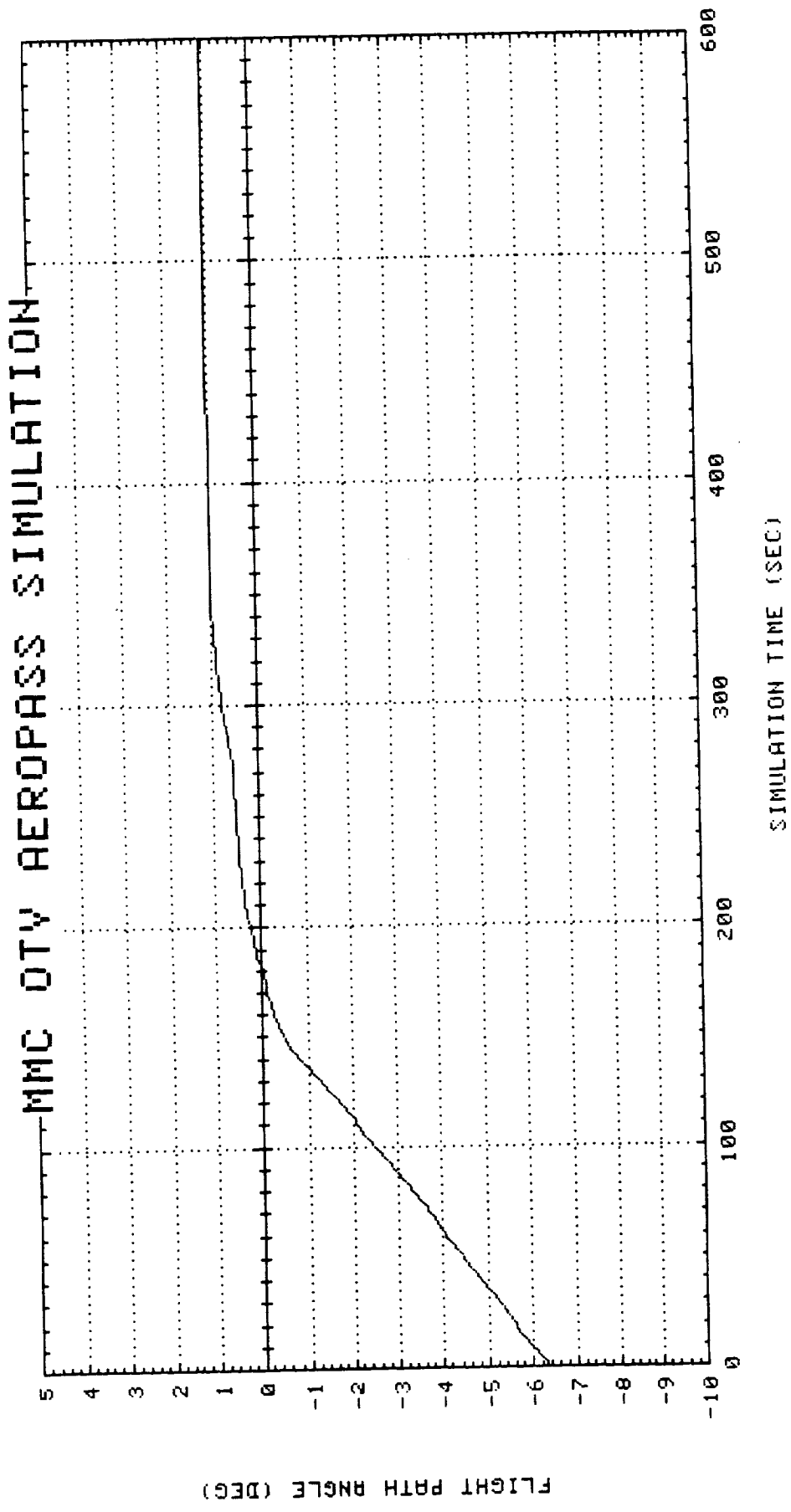
MMC OTV AEROPASS SIMULATION



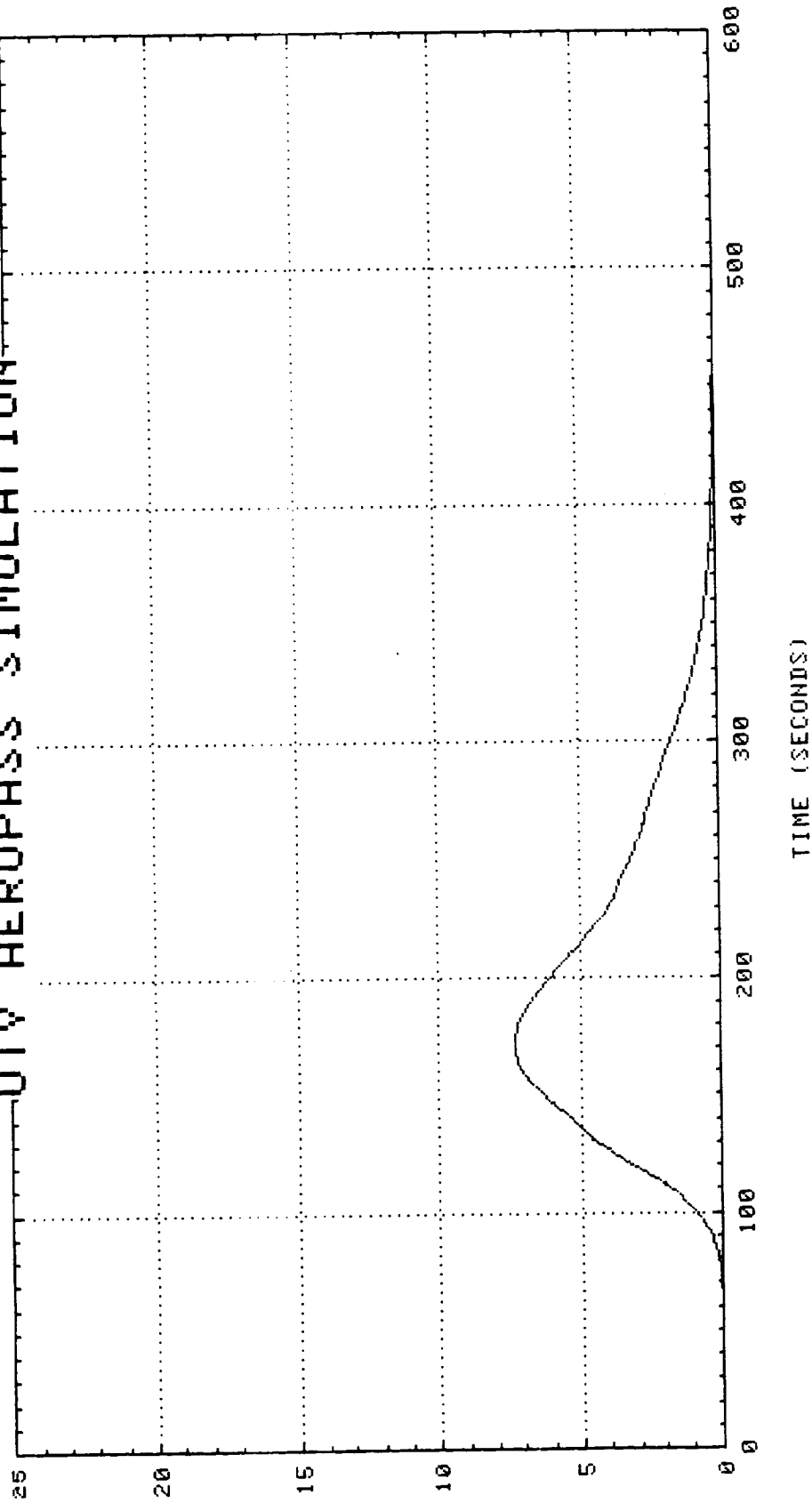
DTV AEROPASS SIMULATION



MMC DTW AEROPASS SIMULATION

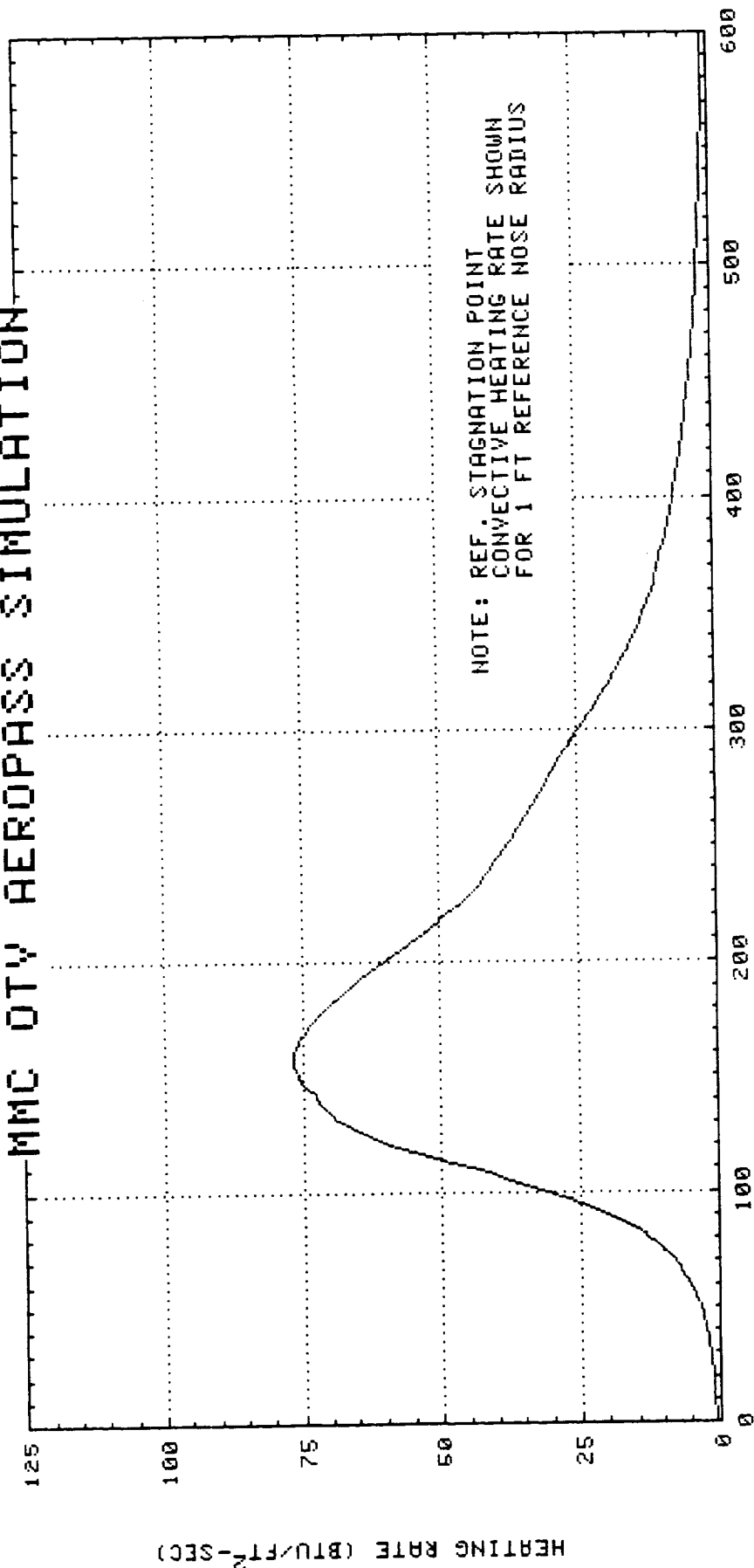


QTY AEROPASS SIMULATION



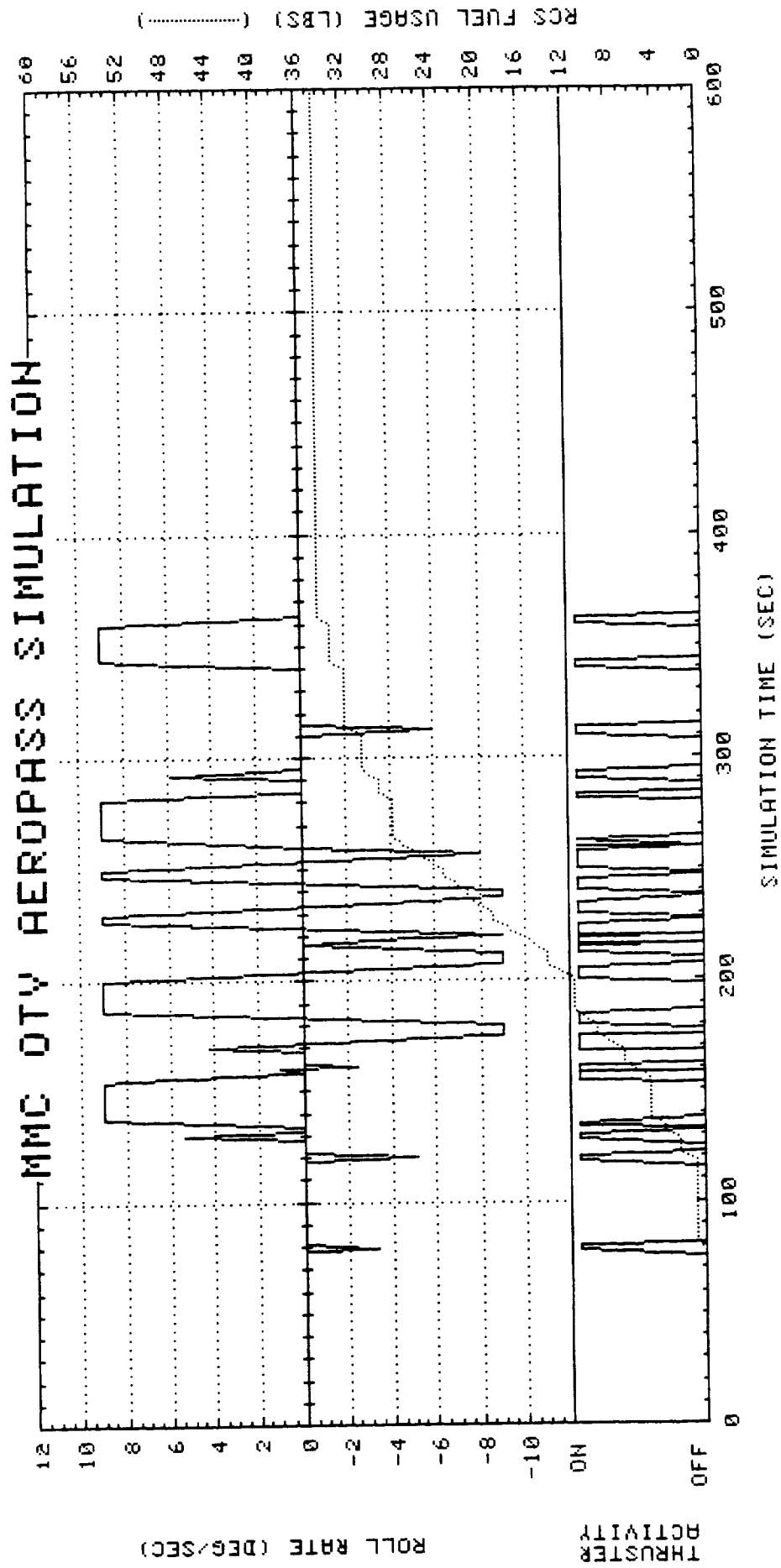
NOTE: DYNAMIC PRESSURE IS
FREE-STREAM VALUE

MMC OTV AEROPASS SIMULATION

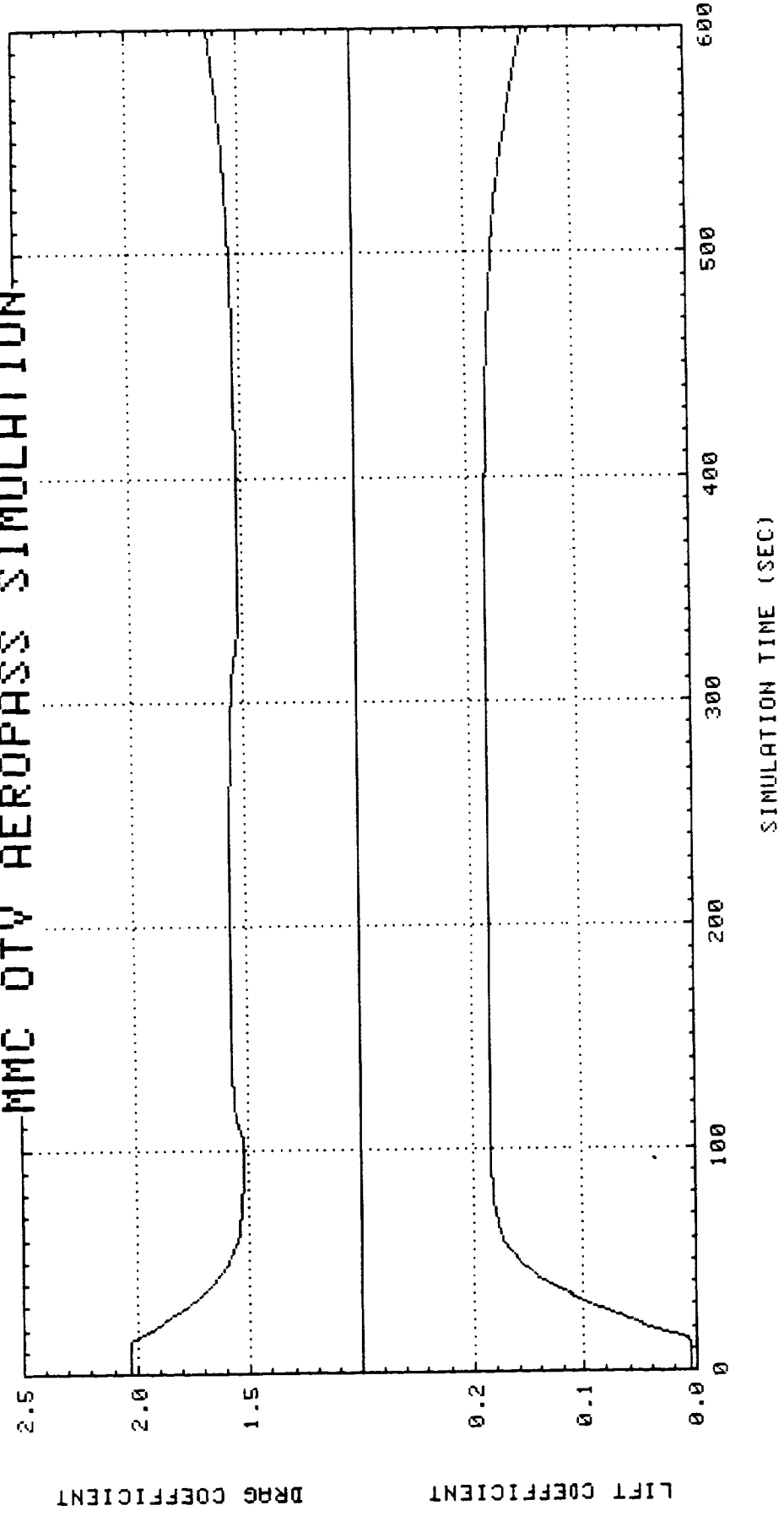


NOTE: REF. STAGNATION POINT
CONVECTIVE HEATING RATE SHOWN
FOR 1 FT REFERENCE NOSE RADIUS

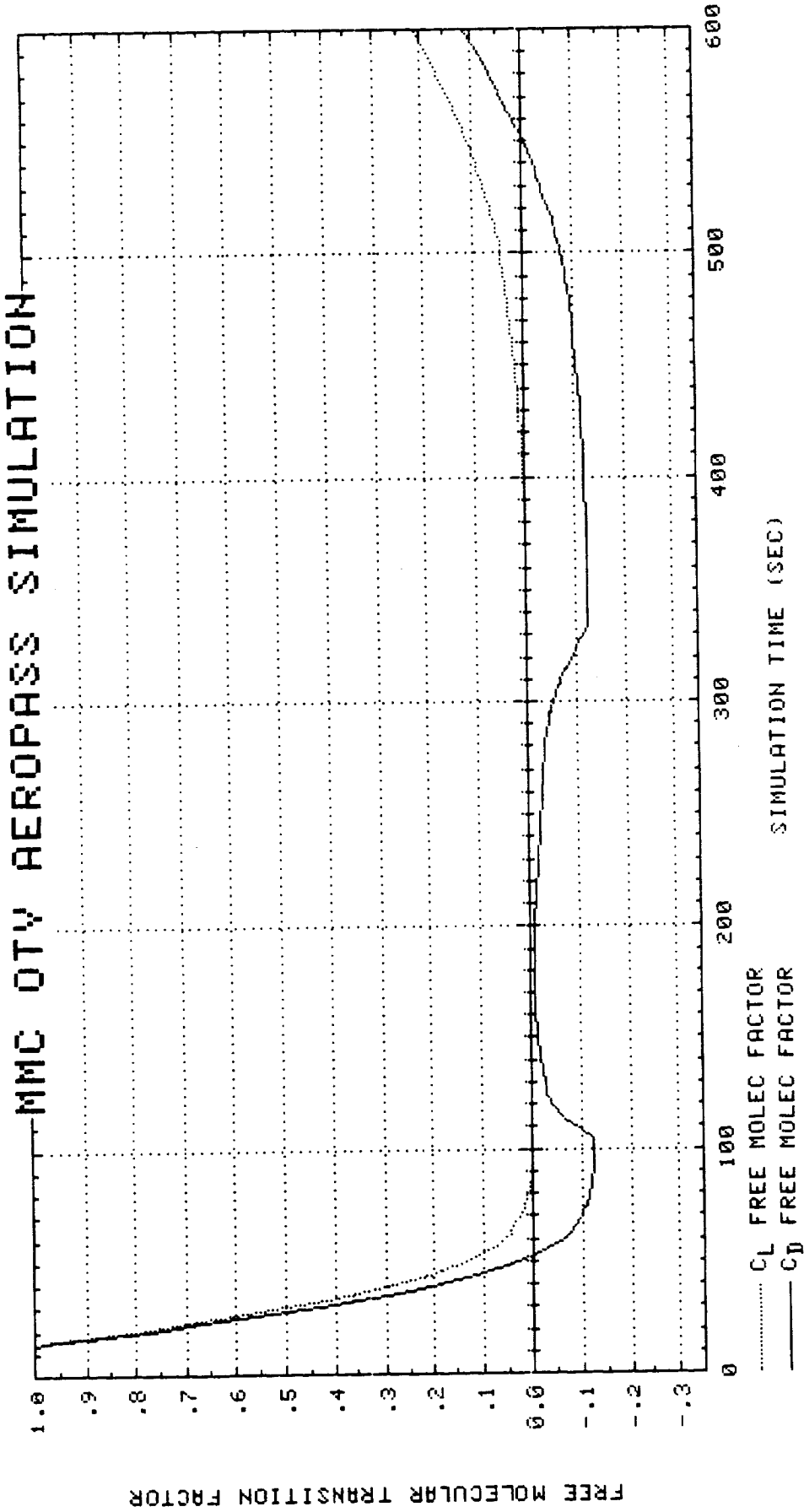
MMC DTY AEROPASS SIMULATION



MMC OTW AEROPASS SIMULATION



MMC OTV AEROPASS SIMULATION



APPENDIX I

OTV AEROPASS SIMULATION

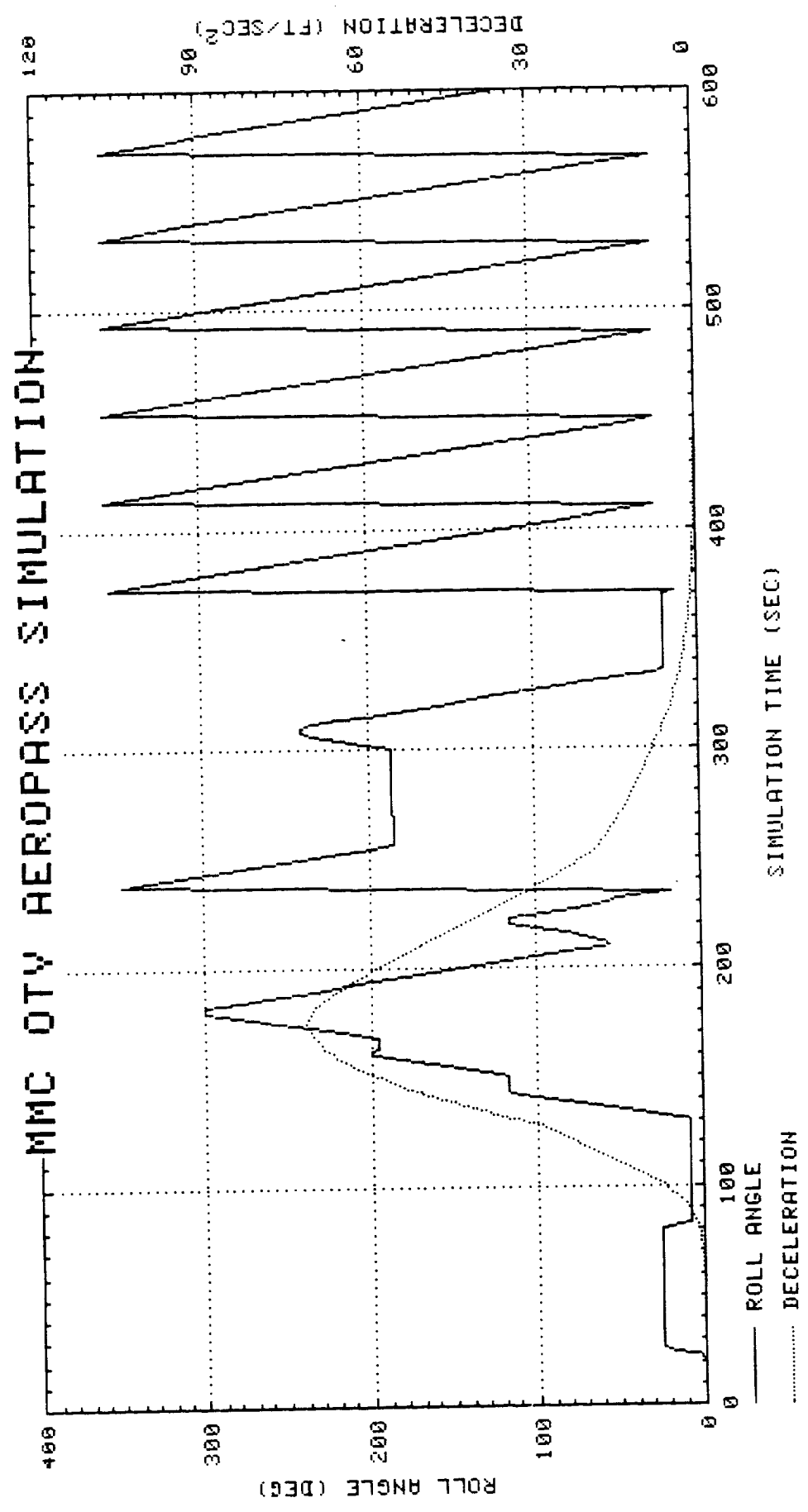
STS-6 ATMOSPHERE
SPACE-BASED OTV

EXIT APOGEE ERROR = 0.10 NM

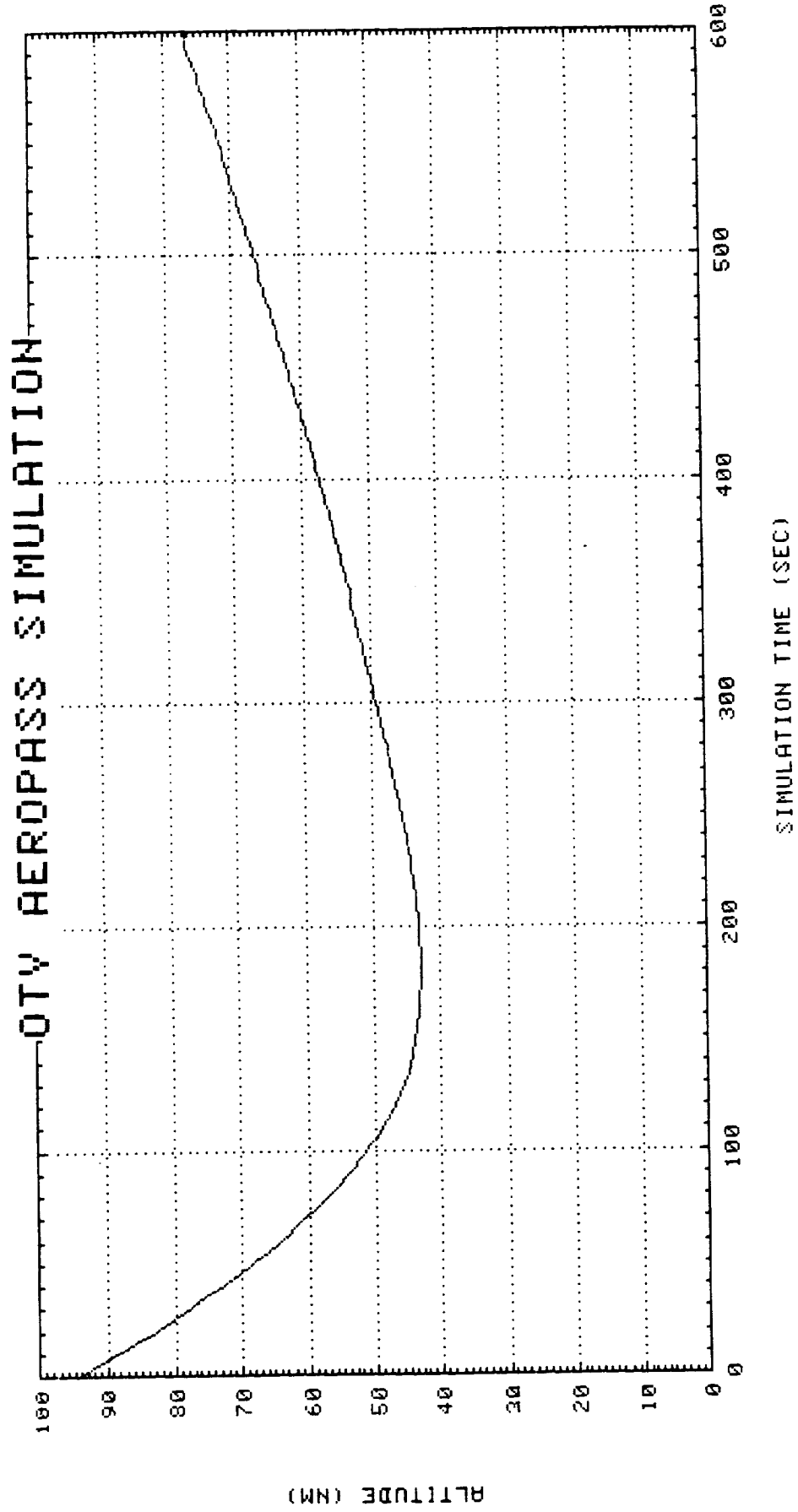
EXIT INCLINATION ERROR = .0131°

THIS PAGE INTENTIONALLY LEFT BLANK

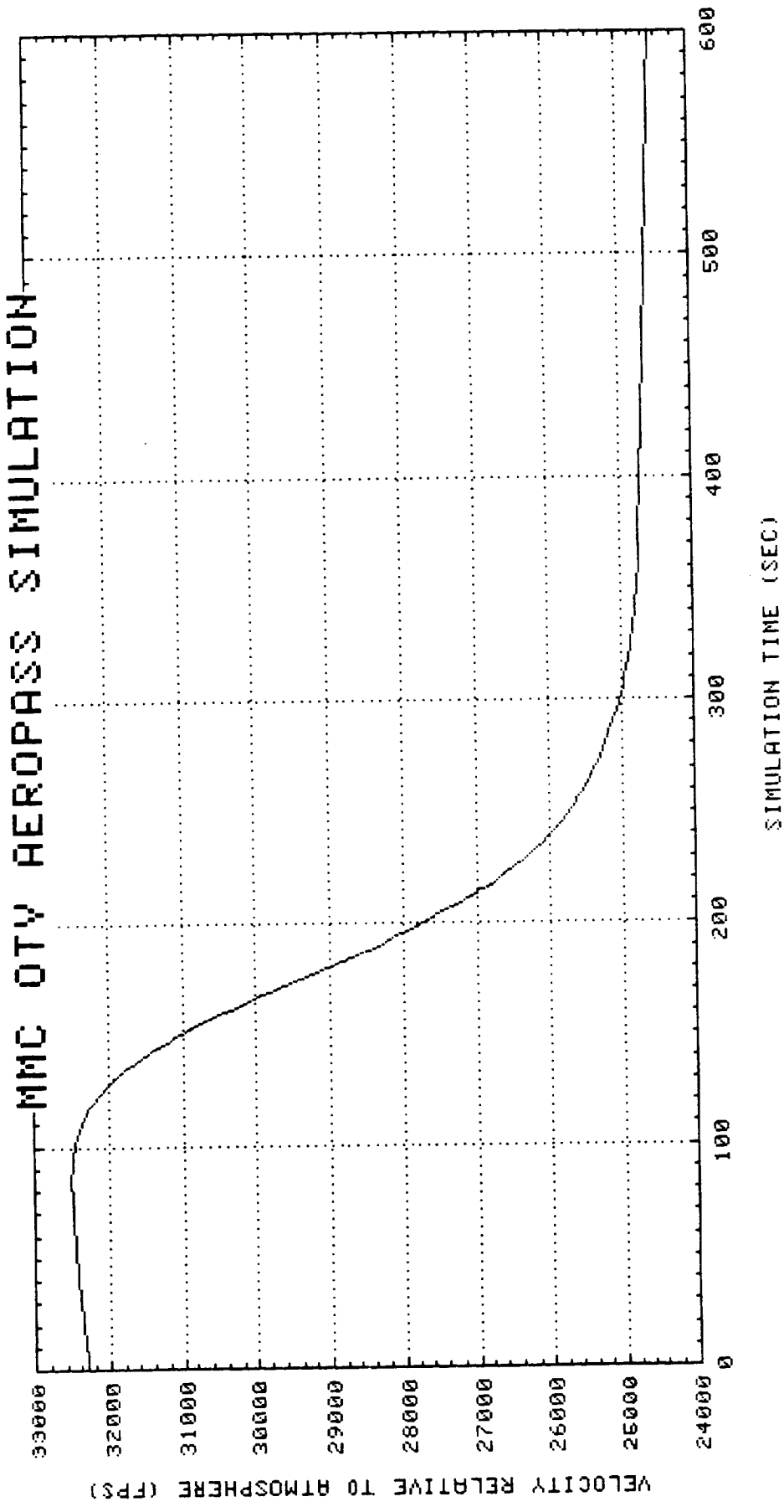
PRECEDING PAGE BLANK NOT FILMED



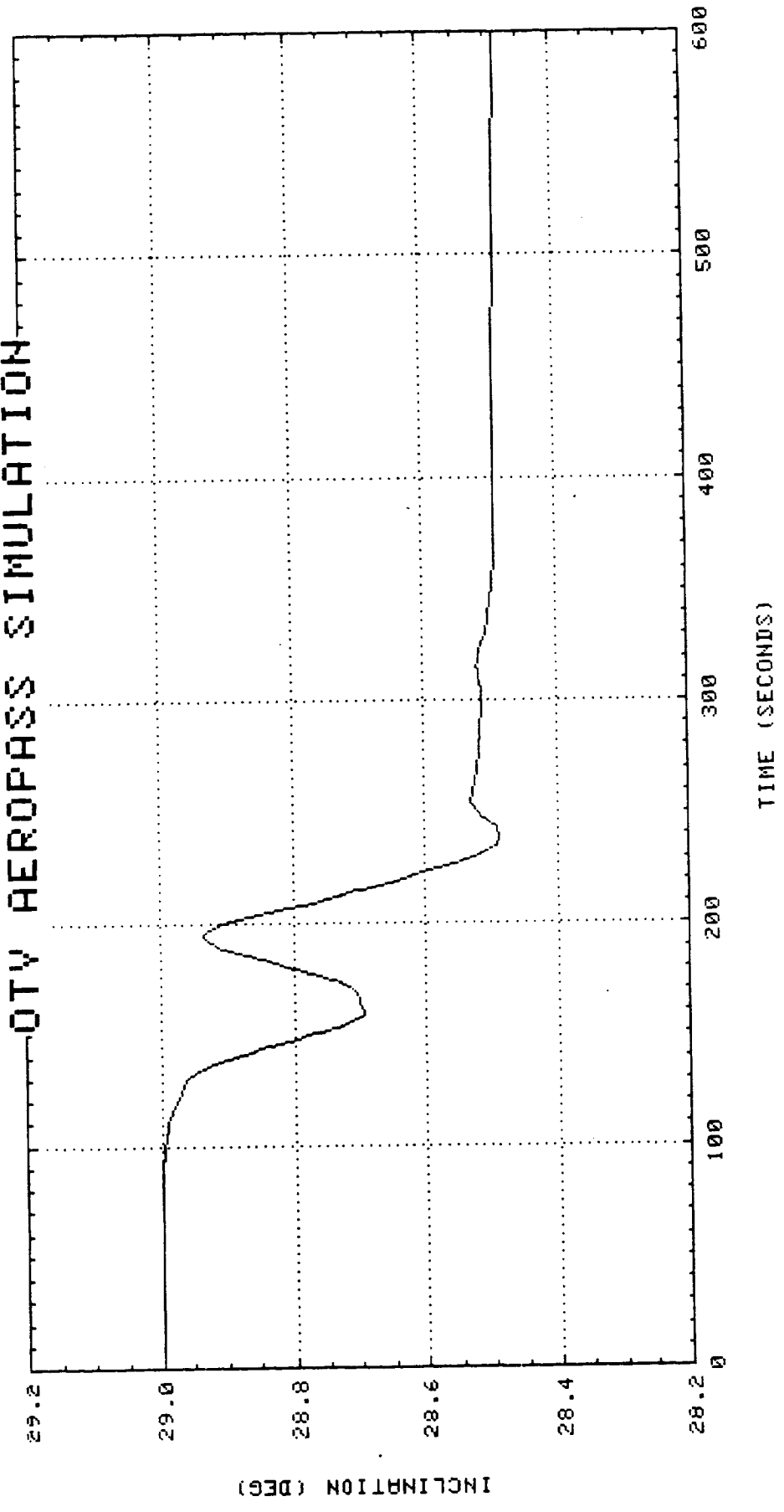
ORIGINAL PAGE IS
OF POOR QUALITY



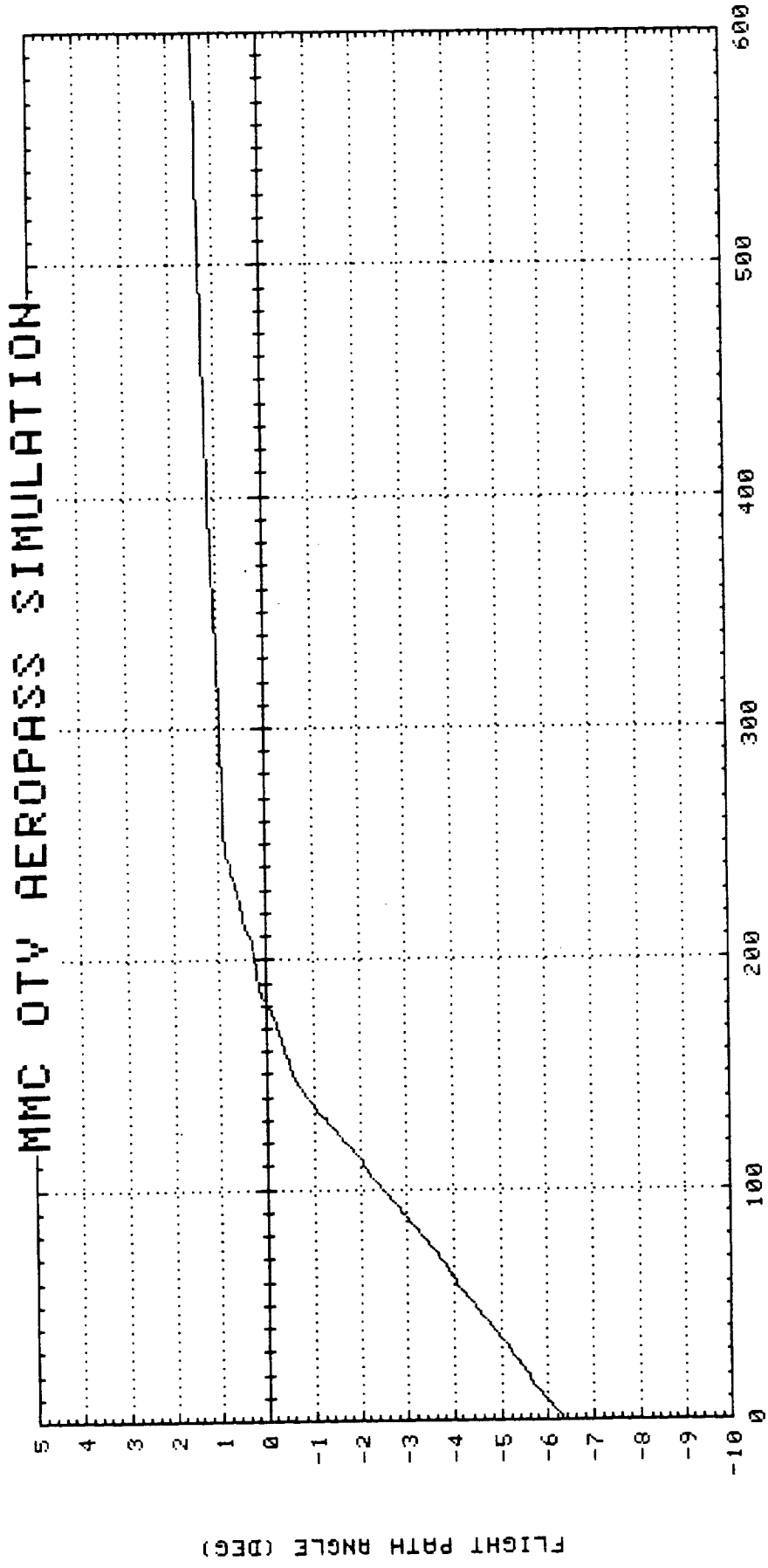
MMC OTV AEROPASS SIMULATION



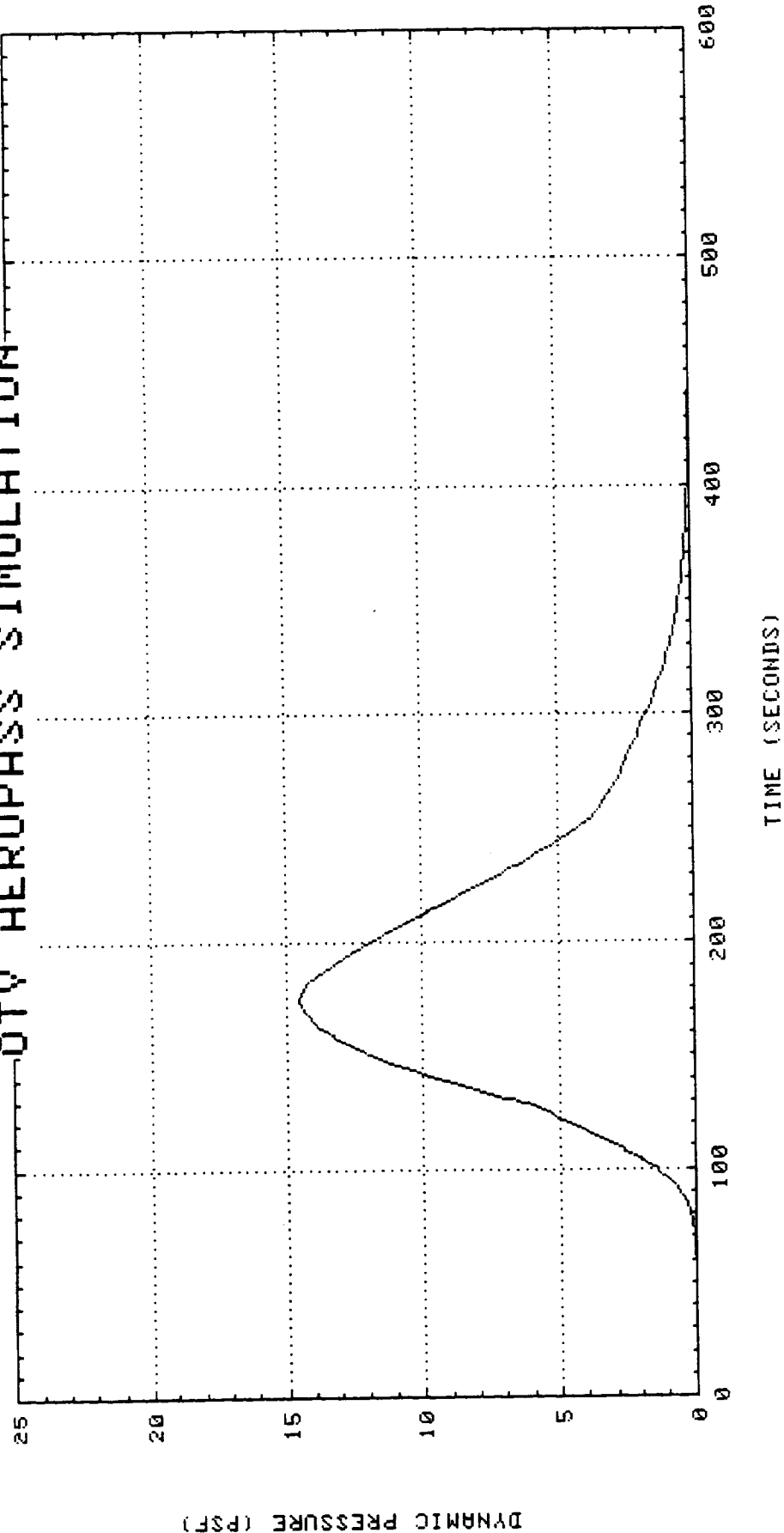
QTY AEROPASS SIMULATION



MMC OTV AEROPASS SIMULATION

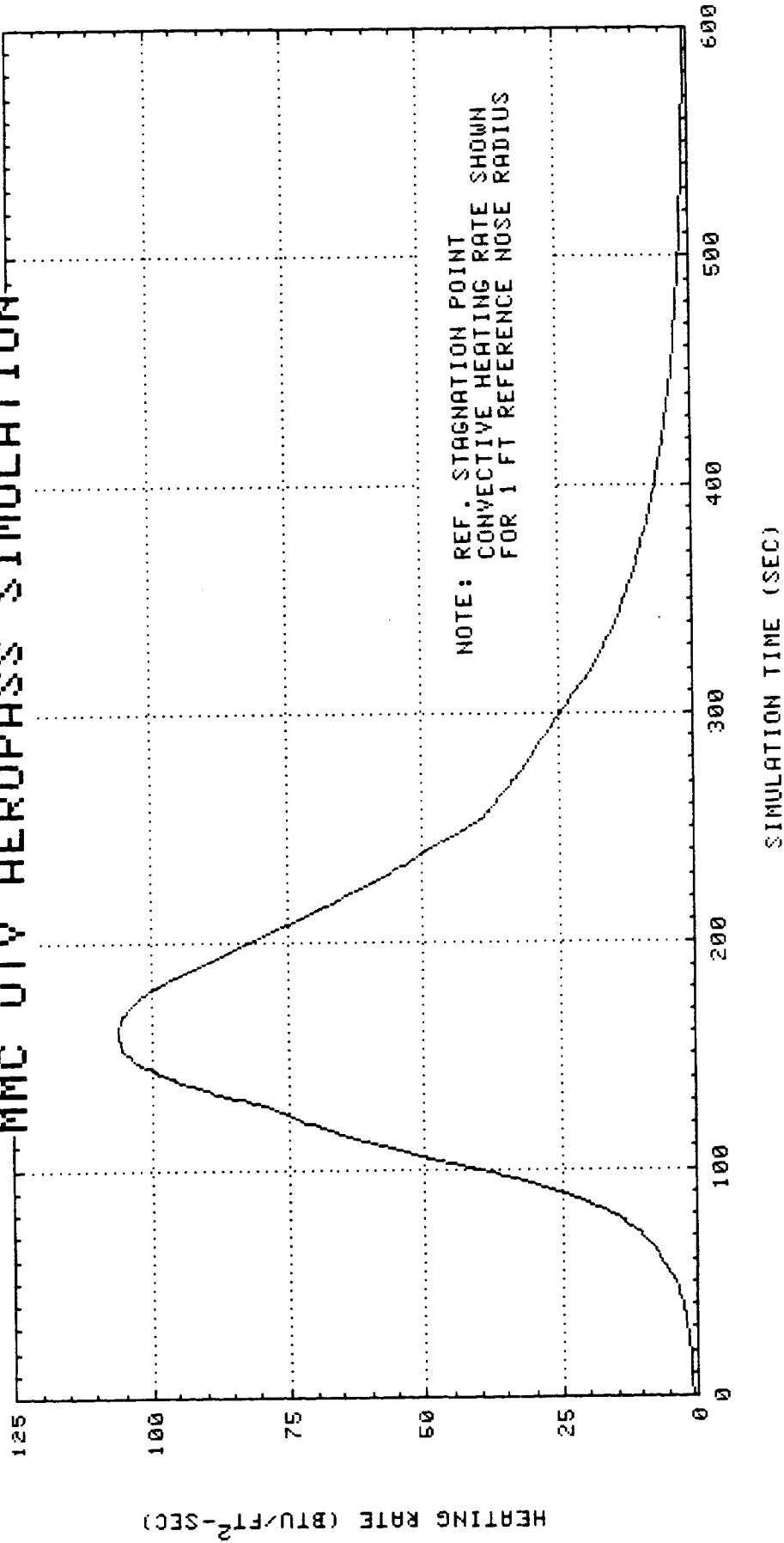


QTV AEROPASS SIMULATION

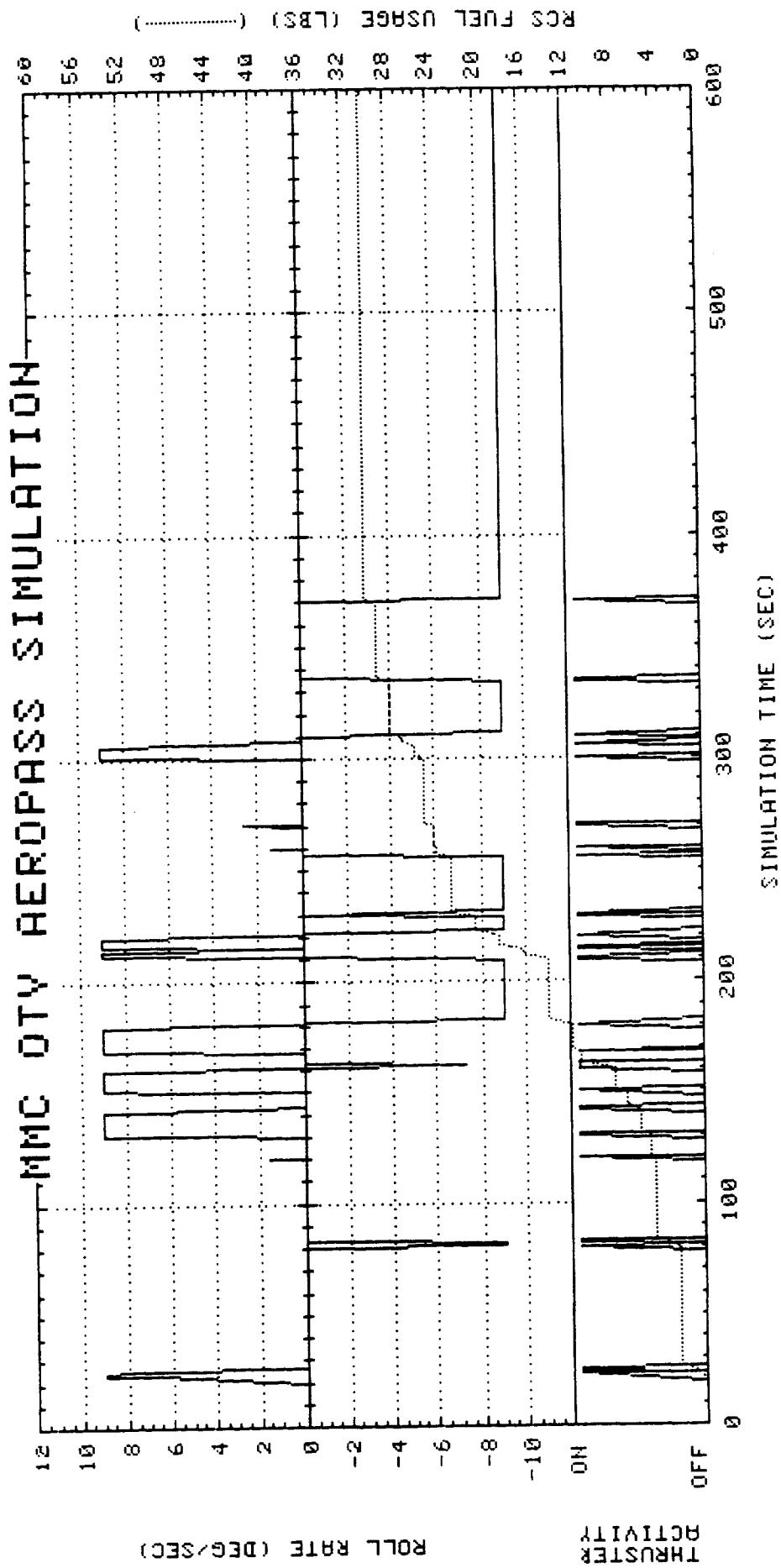


NOTE: DYNAMIC PRESSURE IS FREE-STREAM VALUE

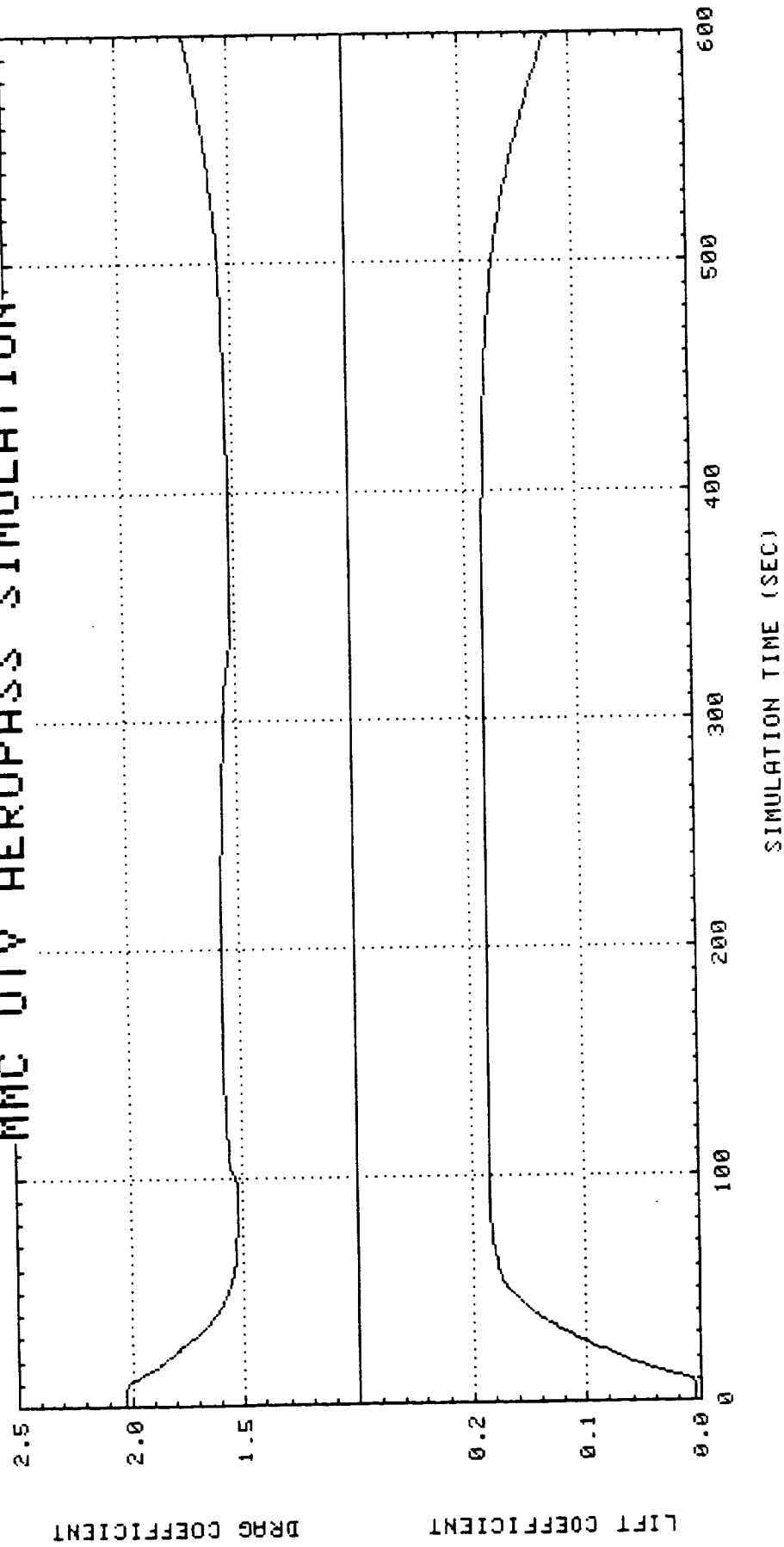
MMC OTV AEROPASS SIMULATION



MMC DTV AEROPASS SIMULATION



MMC QTY AEROPASS SIMULATION



MMC QTY AEROPASS SIMULATION

